

**Schriftenreihe des Instituts für  
Pflanzenbau und Pflanzenzüchtung  
Christian-Albrechts-Universität zu Kiel**

*Series of the Institute of  
Crop Science and Plant Breeding  
Kiel University*

---

**Grünland und Futterbau / Ökologischer Landbau**

*Grass and Forage Science / Organic Agriculture*



**Stephen Björn Wirth**

**The Role of Plant Functional Diversity in  
Productivity and Soil Organic Carbon Stocks of  
Managed Grasslands: Advancements Using a  
Dynamic Global Vegetation Model**

**119**

Schriftenreihe des Instituts für Pflanzenbau und Pflanzenzüchtung  
der Christian-Albrechts-Universität zu Kiel, Heft 119, 2025

Series of the Institute of Crop Science and Plant Breeding  
at Kiel University, No 119, 2025

*veröffentlicht mit Genehmigung  
der Agrar- und Ernährungswissenschaftlichen Fakultät*

Institut für Pflanzenbau und Pflanzenzüchtung  
Agrar- und Ernährungswissenschaftliche Fakultät  
Christian-Albrechts-Universität zu Kiel  
Christian-Albrechts-Platz 4  
24118 Kiel, Germany

**ISSN: 1435-2613**

CC-BY 4.0



---

Aus dem Institut für Pflanzenbau und Pflanzenzüchtung  
– Grünland und Futterbau/Ökologischer Landbau –  
der Christian-Albrechts-Universität zu Kiel

---

**THE ROLE OF PLANT FUNCTIONAL DIVERSITY IN PRODUCTIVITY  
AND SOIL ORGANIC CARBON STOCKS OF MANAGED GRASSLANDS:  
ADVANCEMENTS USING A DYNAMIC GLOBAL VEGETATION MODEL**

**DISSERTATION**

zur Erlangung des Doktorgrades  
der Agrar- und Ernährungswissenschaftlichen Fakultät  
der Christian-Albrechts-Universität zu Kiel

vorgelegt von

**M.Sc. Stephen Björn Wirth**

aus Landau in der Pfalz

Kiel, 2025

---

Dekan: Prof. Dr. Tim Diekötter

1. Berichterstatter: Prof. Dr. Friedhelm Taube

2. Berichterstatter: Prof. Dr. Hermann Lotze-Campen

Tag der mündlichen Prüfung: 02.07.2025

# Contents

<b>List of Figures</b>	<b>vi</b>
<b>List of Tables</b>	<b>xi</b>
<b>List of Abbreviations</b>	<b>xii</b>
<b>Zusammenfassung</b>	<b>xiii</b>
<b>Summary</b>	<b>xvi</b>
<b>1 General introduction</b>	<b>1</b>
1.1 Managed grasslands: An overview . . . . .	1
1.1.1 The role of managed grasslands for food security and the environment . . . . .	1
1.1.2 Managed grasslands under climate change . . . . .	2
1.1.3 Modelling managed grasslands at large spatial scales . . . . .	4
1.1.4 Functional diversity of managed grasslands . . . . .	4
1.2 Functional traits and ecological strategies . . . . .	6
1.2.1 Functional trait relationships . . . . .	6
1.2.2 The CSR theory . . . . .	8
1.3 The LPJmL model . . . . .	9
1.3.1 General model description . . . . .	9
1.3.2 The managed grassland module . . . . .	10
1.3.3 LPJmL-CSR . . . . .	10
1.4 Research justification and objectives . . . . .	11
1.5 Thesis outline . . . . .	12
1.6 References . . . . .	13
<b>2 Do details matter? Disentangling the processes related to plant species interactions in two grassland models of different complexity</b>	<b>24</b>
2.1 Introduction . . . . .	25
2.1.1 Drivers of grassland dynamics . . . . .	25
2.1.2 Plant species richness . . . . .	27
2.1.3 Biogeochemical models . . . . .	27
2.1.4 Model intercomparison studies . . . . .	28
2.1.5 Research question . . . . .	29

2.2	Methods . . . . .	29
2.2.1	Model description . . . . .	30
2.2.2	Site and scenario description . . . . .	35
2.3	Results . . . . .	37
2.3.1	Model calibration and evaluation . . . . .	38
2.3.2	Aboveground biomass dynamics and resource competition . . . . .	39
2.4	Discussion . . . . .	46
2.4.1	Above-ground biomass seasonality . . . . .	46
2.4.2	Species interaction and community assembly . . . . .	49
2.4.3	Limitations . . . . .	51
2.4.4	Fields of model development . . . . .	53
2.5	Conclusion . . . . .	54
2.6	References . . . . .	56
<b>3</b>	<b>Connecting competitor, stress-tolerator and ruderal (CSR) theory and Lund Potsdam Jena managed Land 5 (LPJmL 5) to assess the role of environmental conditions, management and functional diversity for grassland ecosystem functions</b>	<b>64</b>
3.1	Introduction . . . . .	65
3.1.1	The role of environmental conditions and management for grassland vegetation and SOC storage . . . . .	66
3.1.2	Functional diversity and ecological strategies . . . . .	67
3.1.3	Modelling ecosystem functions of permanent grasslands . . . . .	68
3.2	Methods . . . . .	68
3.2.1	Overview of managed grassland representations in LPJmL . . . . .	69
3.2.2	Site description . . . . .	70
3.2.3	Model development . . . . .	71
3.2.4	Defining the C, S and R PFTs . . . . .	74
3.2.5	Modelling protocol . . . . .	80
3.3	Results . . . . .	81
3.3.1	Evaluation of new PFTs . . . . .	82
3.3.2	Comparison of parameterisations between sites and different management intensities . . . . .	85
3.3.3	Effects of resource limitation . . . . .	86
3.3.4	Community composition . . . . .	89

3.4	Discussion . . . . .	91
3.4.1	Forage offtake, SOC and community composition under different management and resource limitations . . . . .	91
3.4.2	Stress and disturbance gradients across sites and management . . . . .	96
3.4.3	Limitations and further need for research . . . . .	98
3.5	Conclusions . . . . .	101
3.6	References . . . . .	102
<b>4</b>	<b>Biological nitrogen fixation of natural and agricultural vegetation simulated with LPJmL 5.7.9</b>	<b>109</b>
4.1	Introduction . . . . .	110
4.2	Methods . . . . .	112
4.2.1	Model description . . . . .	112
4.2.2	BNF-relevant nitrogen cycle components in LPJmL . . . . .	113
4.2.3	The C-costly approach . . . . .	113
4.2.4	Modelling protocol . . . . .	115
4.2.5	Model evaluation . . . . .	116
4.3	Results . . . . .	117
4.3.1	Comparison of the BNF approaches . . . . .	117
4.3.2	Effects on the nitrogen and carbon cycle and productivity . . . . .	121
4.4	Discussion . . . . .	124
4.5	Conclusions . . . . .	128
4.6	References . . . . .	129
<b>5</b>	<b>Global grassland productivity and carbon storage benefit from functional diversity already under moderate climate change</b>	<b>134</b>
5.1	Introduction . . . . .	135
5.2	Methods . . . . .	138
5.2.1	LPJmL-CSR . . . . .	138
5.2.2	Calibration and evaluation data . . . . .	139
5.2.3	Model calibration and evaluation . . . . .	142
5.2.4	Modelling protocol . . . . .	143
5.3	Results . . . . .	145
5.3.1	Evaluation of model performance . . . . .	145
5.3.2	Global productivity and SOC stocks under climate change . . . . .	148

5.3.3	Spatial patterns of productivity and SOC stocks at the end of the century . . . .	151
5.3.4	Representative example regions . . . . .	153
5.4	Discussion . . . . .	156
5.4.1	Highlights and limits of LPJmL-CSR . . . . .	156
5.4.2	The role of functional diversity . . . . .	158
5.5	Conclusions . . . . .	159
5.6	References . . . . .	160
<b>6</b>	<b>General discussion</b>	<b>167</b>
6.1	The contribution of grassland functional diversity to forage supply, soil organic carbon stocks and food security . . . . .	168
6.2	Implications for the dual challenge: biodiversity loss and climate change . . . . .	171
6.3	Advantages and disadvantages of using LPJmL-CSR to assess functional diversity . . .	173
6.4	Overall conclusion and future outlook . . . . .	175
6.5	References . . . . .	176
<b>A</b>	<b>Supplementary information for Chapter 2: "Do details matter? Disentangling the processes related to plant species interactions in two grassland models of different complexity"</b>	<b>i</b>
A.1	Information on empirical data, input parameter and calibration of the grassland models GRASSMIND and LPJmL . . . . .	i
A.2	Model parameterization . . . . .	ii
A.3	Model Calibration . . . . .	vii
A.4	Model evaluation . . . . .	x
A.5	Competition related processes of GRASSMIND and LPJmL . . . . .	xix
A.6	Additional Figures Baseline_Mow and NoMow . . . . .	xxii
A.7	Additional Figures ModD_Mow and ExtrD_Mow . . . . .	xl
A.8	Additional Figures Baseline_, ModD_and ExtrD_Mow and NoMow . . . . .	xliv
A.9	References . . . . .	xlviii
<b>B</b>	<b>Supplementary information for Chapter 3: "Connecting competitor stress-tolerator and ruderal (CSR) theory and Lund Potsdam Jena managed Land 5 (LPJmL 5) to assess the role of environmental conditions management and functional diversity for grassland ecosystem functions"</b>	<b>I</b>
B.1	Model description . . . . .	1
B.2	MSE components . . . . .	liv

## Contents

B.3	Additional figures . . . . .	liv
B.4	Additional tables . . . . .	lxviii
B.5	Model development . . . . .	lxviii
B.6	Input data and parameters . . . . .	lxix
B.7	R packages . . . . .	lxxii
B.8	References . . . . .	lxxiii
<b>C</b>	<b>Supplementary information for Chapter 4: "Biological nitrogen fixation of natural and agricultural vegetation simulated with LPJmL 5.7.9."</b>	<b>lxxvi</b>
C.1	Nitrogen demand and uptake . . . . .	lxxvi
C.2	Spin-up simulation carbon stocks . . . . .	lxxviii
C.3	Additional figures and tables . . . . .	lxxix
C.4	References . . . . .	lxxxix
<b>D</b>	<b>Supplementary information for Chapter 5: "Global grassland productivity and carbon storage benefit from functional diversity already under moderate climate change"</b>	<b>xc</b>
D.1	Additional figures . . . . .	xc
D.2	References . . . . .	cviii
	<b>Acknowledgements</b>	<b>cix</b>

# List of Figures

1.1	Ternary plot visualising the CSR theory. Main strategies (C, S and R) are displayed at the nodes of the triangle. Environmental conditions that lead to the emergence of different strategies are shown as the stress (blue) and disturbance (red) gradients. Intermediate strategies can be positioned anywhere within the triangle. . . . .	9
2.1	Processes and plant compartments simulated in GRASSMIND and LPJmL (see Fig. A.1 for an individual representation of each model) . . . . .	31
2.2	Simulated and observed AGB in $\text{gDM m}^{-2}$ for <i>P. pratensis</i> (a), <i>P. lanceolata</i> (b), <i>F. pratensis</i> (c) and <i>F. rubra</i> (d) for GRASSMIND (red) and LPJmL (blue). Coloured lines and labels show model results and RMSE, grey points show observations used for the evaluation. Observations are the median of samples for each date and error bars show one standard deviation. If three or less observations were available all observations were plotted and their range indicated with a line. Outliers are highlighted with labels and arrows. . . . .	40
2.3	Mean ( $\mu$ ) AGB in $\text{gDM m}^{-2}$ for GRASSMIND (red) and LPJmL (blue) averaged over all simulation years for each day of the year for monocultures (a,b,c,d) and two-species mixtures (e,f,g,h,i,j). For mixtures total AGB (top) and species specific AGB (bottom) are shown separately. Coloured ribbons show $\mu \pm \sigma$ . . . . .	41
2.4	Normalized parameter values for GRASSMIND (red) and LPJmL (blue) for parameters important for species competition. Full circles show parameters which are not comparable between the two models and half circles show parameters used similarly in both models. The different species are ranked by competitiveness with the label size, ranging from most competitive (large) to least competitive (small). . . . .	43
2.5	Simulated and observed (Fischer et al., 2019) fractional soil water content at the Jena Experiment site (a), relative changes of soil water content in $\text{m}^3 \text{m}^{-3}$ (b), absolute changes of soil water content in $\text{m}^3 \text{m}^{-3}$ as well as daily precipitation in mm with reduction for ModD (light grey) and ExtrD (light and dark grey) (c), absolute changes in AGB (d) in $\text{gDM m}^{-2}$ and relative changes in transpiration (e) caused by the moderate (dotted) and extreme (dashed) droughts for LPJmL (blue) and GRASSMIND (red). Simulation results of mixture of <i>P. pratensis</i> and <i>F. pratensis</i> using observed weather data (a) and average climate (b-e). . . . .	45

## List of Figures

2.6	Mean ( $\mu$ ) AGB in $\text{gDM m}^{-2}$ for GRASSMIND (red) and LPJmL (blue) for the sum of the two-species mixture of <i>P. pratensis</i> and <i>F. pratensis</i> (a). Coloured ribbons show $\mu \pm \sigma$ . Horizontal lines show overall mean for Baseline_Mow (dot-dashed) and Baseline_NoMow (solid). Difference between Baseline_Mow and ModD_Mow (dot-dashed) and ModD_NoMow (solid, b) and ExtrD_Mow (dot-dashed) and ExtrD_NoMow (solid, c) between April and October of the drought year. . . . .	46
3.1	Stress (blue) and disturbance (red) gradient and associated traits and their hierarchy (low, in between and high). . . . .	77
3.2	Mean square error (MSE) for the different management scenarios ( $x$ axis) for forage off-take/leaf biomass in $\text{Mg DM ha}^{-1} \text{ yr}^{-1}$ , SOC in $\text{Mg DM ha}^{-1} \text{ yr}^{-1}$ and FPC (columns, left to right) for the temperate grassland, hot steppe and cold steppe (rows, top to bottom). For forage offtake/leaf biomass and SOC, MSEs for the old (LPJmL 5) and new (LPJmL-CSR) model version are shown. For FPC, MSEs are shown for each PFT separately for LPJmL-CSR before and after the calibration. The colours separate the MSE into three components: the bias (grey) showing the systematic error for each variable; the phase (yellow), showing the temporal shift against observations; and the variance (blue), which is the random error not attributable to bias and phase compared to observations. . . . .	83
3.3	Spiderplots of normalised parameter values after calibration for each site (columns) and management scenario (rows). The centre and the edge represent the low and high ends of the stress (black labels) and disturbance (grey labels) gradients. The colours of the points distinguish the three PFTs. The tables show the mean of normalised parameter values for each PFT and the two trade-off dimensions. . . . .	84
3.4	Simulated forage offtake/leaf biomass ( <b>a, b, c</b> ) and SOC ( <b>d, e, f</b> ) for all sites, management levels and resource limitation scenarios. Bars show the annual forage offtake and coloured segments the forage offtake for each cut/month. Line colours differ between rainfed (prevailing conditions, black), rainfed fertilised (red) and irrigated unfertilised (blue), while line types show the grazing management intensity as low (ungrazed/C0 or extensively grazed/S1, solid) and high (grazed/C1 or intensively grazed/S6, dashed). . . . .	87
3.5	Ternary plots of the share of standing aboveground biomass of the C, S and R PFTs for the temperate grassland ( <b>a</b> ), the ungrazed ( <b>b</b> ) and grazed hot steppe ( <b>c</b> ), and the extensively ( <b>d</b> ) and intensively ( <b>e</b> ) grazed cold steppe. Colours differ between the rainfed (red), irrigated (blue) and fertilised (green) scenarios. Points with a black border show the mean composition of the time series. . . . .	90

*List of Figures*

4.1	Dimensionless temperature limitation function $f_T(T)$ <b>(a)</b> and soil water limitation function $f_W(\text{SWC})$ <b>(b)</b> . . . . .	114
4.2	Evaluation against global <b>(a)</b> and site-specific data <b>(b, c)</b> . Global evaluation plot inspired by Davies-Barnard and Friedlingstein (2020) showing global BNF (in $\text{TgN yr}^{-1}$ ) from different studies (black) compared to the Original (red) and C-costly (blue) BNF approach implemented in LPJmL. Studies are labelled by author names and whether they consider potential natural vegetation (PNV), actual natural vegetation (NV) or actual land use (LU). We assigned the Davies-Barnard and Friedlingstein (2020) data to the LU category because they consider cropland area as grasslands and not as potential forest areas. Percentage values give the overlap between the ranges of the simulation results and the literature estimates derived using Eq. (4.9). Simulated values are the median between 2001 and 2010, and the ranges show the minimum and maximum. Site-specific evaluation <b>(b, c)</b> comparing data from observations for soybean (green) and pulses (blue) for rainfed (RF) (circle) and irrigated (IR) (triangle) experiment and simulation results is shown using the Original <b>(b)</b> and C-costly <b>(c)</b> BNF approaches. Labels show the RMSE of the two approaches. . . . .	118
4.3	Simulated average annual BNF (in $\text{gN m}^{-2} \text{yr}^{-1}$ ) for the years 2001 to 2010 using the Original <b>(a)</b> and C-costly <b>(b)</b> approaches. The average (line) and 5th to 95th percentiles (shading) of simulated and observed BNF per latitude (in $\text{gN m}^{-2} \text{yr}^{-1}$ ), using the Original (red) and C-costly (blue) approaches and data from Davies-Barnard and Friedlingstein (2020) (DBF), are shown <b>(c)</b> . . . . .	119
4.4	Global terrestrial N balance. Scenarios include the Original approach, the C-costly approach for natural vegetation and actual land use. Net balance is denoted by the black line. N inputs include N from manure, synthetic fertiliser deposition, PFT establishment (Estab) and BNF. N losses include leaching, volatilisation, $\text{N}_2$ emissions, fire N, harvested N, land-use change emissions (deforestation and product turnover) and $\text{N}_2\text{O}$ emissions from nitrification and denitrification. . . . .	122
5.1	Overview of processing steps to prepare the calibration data and selection of grid cell subset for calibration. All data have a global coverage and a $0.05^\circ$ by $0.05^\circ$ resolution. Coloured boxes highlight preprocessing input (blue), temporal data of intermediate steps (white) and output data (red). Arrows show the information flow from input to output data and numbers reference specific steps described in 5.2.2 and 5.2.3 . . . . .	140

*List of Figures*

5.2	Boxplots (a,c), density plot (b) and latitudinal averages (d) of the difference between simulated and observed annual (a) and monthly (b) GPP between 2000 and 2016 and annual FPC (c,d) data for the parameter set before (prior, blue) and after (best, red) the calibration. For the latitude plot, lines show the differences to the 2000 to 2016 average of simulation results and shaded areas show the 5th to 95th percentiles. . . . .	146
5.3	Time series of global total GPP (a), PFT-specific GPP (b), dry matter intake (c) and SOC stocks (d) from 1901 until 2100. Panels a,c and d show historical data (purple, dashed) and projections for RCP 2.6 (yellow) and 7.0 (lightblue) for the FD+ (solid) and FD- (dotted) scenarios. Grassland areas are shown in panel a (dot-dashed). For the PFT-specific GPP, different scenarios (FD- and FD+) and SSPs (2.6 and 7.0) are shown in separate panels and colors distinguish the C- (darkblue), S- (red) and R-PFT (darkgreen). Lines show the median and shaded areas the 5th to 95th percentile across five GCMs. . . . .	149
5.4	Global distribution of gross primary production (GPP) and soil organic carbon (SOC) dependent on functional diversity. Left panels show the average GPP for the scenarios (a) FD+, (b) FD- and (c) their difference, i.e. the net effect of a higher functional diversity. Right panels (b,d,f) show the respective results for SOC. All distributions show the 2091 to 2100 average of the respective output variable simulated using climate data from the MRI-ESM2-0. . . . .	150
5.5	Global distribution of PFT-specific gross primary production (GPP) and foliage projective cover (FPC) dependent on functional diversity. All panels show the relative change between FD+ and FD- i.e. the net effect of a higher functional diversity. From left to right, panels show the distribution for the C- (a,d,g), S- (b,e,h) and R-PFTs (c,f,i). The first (a,b,c) and third (g,h,i) rows show the distribution using all PFTs present in FD+. The second row (d,e,f) shows the distribution using only the dominant PFT in FD+. Similar values (difference of 0) are shown in green, while white areas in d-f are grid cells in which the respective PFT is not dominant and no value is available. All distribution show the 2091 to 2100 average of the respective output variable simulated using climate data from the MRI-ESM2-0. . . . .	151
5.6	Locations of the three example regions Uganda and South Sudan (blue), Germany (yellow) and North and South Carolina (red). . . . .	153

*List of Figures*

5.7 Distribution of the relative change between FD+ and FD- for gross primary production (GPP, a,d,g) and soil organic carbon (SOC, b,e,h) and the absolute change of the number of PFT present (c,f,i) dependent on functional diversity for the three example regions (Uganda and South Sudan, Germany and North and South Carolina). From top to bottom, the rows show the data for Uganda and South Sudan (a,b,c), Germany (d,e,f) and North and South Carolina (g,h,i). From left to right, columns show the relative change in GPP (a,d,g) and SOC (b,e,h) and the absolute change in the number of PFTs (c,f,i). All distributions are based on the 2091 to 2100 average of the respective output variable simulated using climate data from the MRI-ESM2-0. . . . . 154

# List of Tables

2.1	Simulation scenario names, environmental conditions and management . . . . .	37
3.1	Overview of the environmental conditions and management of the investigated grasslands.	71
3.2	Parameter names, units, ranges, associated CSR gradient(s) and the hierarchy of the parameters for the C, S and R PFTs. . . . .	78
3.3	Variables used for parameterisation (para) and evaluation (eval) of the new PFTs at the study sites . . . . .	79
3.4	Scenario names and management (mowing/grazing intensity, irrigation, fertilisation) used for the simulations at the Lindhof (temperate grassland), Syferkuil (hot steppe) and Xilin (cold steppe) sites. . . . .	81
4.1	BNF-related PFT-specific parameter values for the tropical broadleaved evergreen tree (TrBE), tropical broadleaved raingreen tree (TrBR), temperate needleleaved evergreen tree (TeNE), temperate broadleaved evergreen tree (TeBE), temperate broadleaved summergreen tree (TeBS), boreal needleleaved evergreen tree (BoNE), boreal broadleaved summergreen tree (BoBS), boreal needleleaved summergreen tree (BoNS), tropical herbaceous (TrH), temperate herbaceous (TeH), polar herbaceous (PoH), soybean and pulses.	115
4.2	N balance values for 2001 to 2010 shown in the figures. LUC (land-use change) includes deforestation emissions, product turnover and negative N fluxes. . . . .	123
5.1	PFT-specific minimum, maximum default and optimised values for calibrated parameters.	144

# List of Abbreviations

<b>°C</b>	Degree Celsius
<b>BNF</b>	Biological Nitrogen Fixation
<b>C</b>	Competitive
<b>CH<sub>4</sub></b>	Methane
<b>CO<sub>2</sub></b>	Carbon dioxide
<b>CSR</b>	Competitor, Stress-tolerator, Ruderal
<b>DGVM</b>	Dynamic Global Vegetation Model
<b>GPP</b>	Gross Primary Productivity
<b>GRASSMIND</b>	Grassland Individual-based Dynamic Model
<b>IBC-grass</b>	Individual-Based plant Community-grass
<b>LAI</b>	Leaf Area Index
<b>LL</b>	Leaf Longevity
<b>LPJ-GUESS</b>	Lund-Potsdam-Jena General Ecosystem Simulator
<b>LPJmL</b>	Lund-Potsdam-Jena managed Land
<b>LPJmL-CSR</b>	Lund-Potsdam-Jena managed Land Competitor, Stress-Tolerator, Ruderal
<b>LPJmL-FIT</b>	Lund-Potsdam-Jena managed Land - Flexible Individual Traits
<b>MAgPIE</b>	Model of Agricultural Production and its Impacts on the Environment
<b>Mha</b>	Mega hectares
<b>N<sub>2</sub>O</b>	Nitrous oxide
<b>NPP</b>	Net Primary Productivity
<b>PFT</b>	Plant Functional Type
<b>R</b>	Ruderal
<b>S</b>	Stress-tolerant
<b>SDG</b>	Sustainable Development Goal
<b>SLA</b>	Specific Leaf Area
<b>SOC</b>	Soil Organic Carbon
<b>TgCO<sub>2</sub>eq yr<sup>-1</sup></b>	Teragrams of carbon dioxide equivalent per year

# Zusammenfassung

Bewirtschaftetes Grünland bedeckt einen erheblichen Teil der globalen Landoberfläche in verschiedenen Klimazonen. Gleichzeitig trägt es zur Nahrungs-/Existenzgrundlage vieler Menschen sowie zur Ernährungssicherheit durch die Produktion von Wiederkäuerfleisch und Milchprodukten bei. Die Produktivität — und damit die Tragfähigkeit für Vieh — von bewirtschaftetem Grünland hängt von den klimatischen Bedingungen und der Bewirtschaftung sowie der funktionalen Diversität der Pflanzenbestände ab. Während die funktionale Diversität durch klimatische Bedingungen und Bewirtschaftung beeinflusst wird, spielt sie auch eine direkte Rolle für die Produktivität des Ökosystems. Die Rolle der funktionalen Diversität wurde anhand von Feldversuchen und -beobachtungen umfassend untersucht. Diese Forschung hat gezeigt, dass funktionale Diversität die Anpassungsfähigkeit von bewirtschaftetem Grünland an den Klimawandel stärkt und dessen essenzielle Ökosystemdienstleistungen fördert. Dies ist wichtig, da der projizierte Klimawandel zahlreiche Ökosystemdienstleistungen von bewirtschaftetem Grünland beeinflussen wird.

Während funktionale Diversität in kleinräumlichen Computermodellen explizit berücksichtigt wird, fehlt eine entsprechende Darstellung in globalen Modellen. Allerdings sind globale Modelle — wie beispielsweise Dynamische Globale Vegetationsmodelle (DGVMs) — weit verbreitet, um die Auswirkungen des Klimawandels auf die Vegetation zu bewerten. Um die Projektionen der Ökosystemdienstleistungen von bewirtschaftetem Grünland verbessern zu können, ist es von großer Bedeutung, die Rolle der funktionalen Diversität in Modellen abzubilden. Die Hauptziele dieser Dissertation sind: (1) die Identifizierung wesentlicher Modellentwicklungsbereiche, um die funktionale botanische Diversität von bewirtschaftetem Grünland in einem DGVM abzubilden (Kapitel 2), (2) die Beschreibung der Implementierung notwendiger Modelländerungen (Kapitel 3 und 4) und (3) die Bewertung der Rolle von funktionaler Diversität für die Produktivität und den organischen Bodenkohlenstoffspeicher von bewirtschaftetem Grünland auf lokaler und globaler Skala (Kapitel 3 und 5) sowie unter Klimawandelbedingungen (Kapitel 5).

Um zentrale Bereiche der Modellentwicklung zu identifizieren, wurde das Lund-Potsdam-Jena managed Land (LPJmL)-Modell mit dem individuenbasierten Grassland Individual-based Dynamic Model (GRASSMIND) verglichen. Für diesen Vergleich wurden mit beiden Modellen Monokulturen und Pflanzengemeinschaften mit bis zu vier Arten des Jena Experiments, einem bekannten Biodiversitätsexperiment, simuliert. Die simulierten Szenarien umfassten verschiedene Niederschlagsniveaus sowohl mit als auch ohne Mahd. Eine detaillierte Analyse der Prozessabbildungen in LPJmL und GRASSMIND wurde durchgeführt, um die Stärken und Schwächen der Modelle hinsichtlich der Simulation artenreicher Pflanzengemeinschaften zu bewerten. Die Ergebnisse zeigen, dass die Simulationsergebnisse bei den Modellen moderat mit den Beobachtungen übereinstimmen. Sie heben jedoch auch die Notwendigkeit

für Verbesserungen hervor, insbesondere bei der Abbildung von Zielkonflikten zwischen ökologischen Strategien sowie der Konkurrenz um Ressourcen.

Auf Grundlage dieser Erkenntnisse beschreibt Kapitel 3 einen Ansatz zur Simulation der funktionalen Diversität von bewirtschaftetem Grünland im LPJmL-Modell. Dieser basiert auf der Competitor, Stress-Tolerant, Ruderal (CSR)-Theorie und funktionalen Pflanzeigenschaften. Funktionale Pflanzeigenschaften können verwendet werden, um wichtige Zielkonflikte zwischen ökologischen Strategien durch Beziehungen zwischen verschiedenen Pflanzeigenschaften zu beschreiben. Die CSR-Theorie ist ein bekanntes System zur Beschreibung ökologischer Strategien und wurde mit den Zielkonflikten verknüpft, die durch die Beziehungen zwischen Pflanzeigenschaften im globalen Spektrum der Pflanzenform und -funktion dargestellt werden. Durch die Nutzung dieser Verknüpfung kann das erweiterte LPJmL-CSR-Modell die funktionale Diversität von bewirtschaftetem Grünland unter verschiedenen Klima- und Bewirtschaftungsbedingungen simulieren. Die Weiterentwicklung von LPJmL zu LPJmL-CSR umfasst eine explizite Abbildung der im blattökonomischen Spektrum beschriebenen Beziehung zwischen spezifischer Blattfläche und Blattlebensdauer, die getrennte Darstellung der ober- und unterirdischen Ressourcenverteilung und eine verbesserte Abbildung der Etablierung und Mortalität.

Zusätzlich zu diesen Entwicklungen wurde LPJmL um eine neue Darstellung der biologischen Stickstofffixierung erweitert (Kapitel 4). Diese Entwicklung berücksichtigt explizit die Bodentemperatur und den Bodenwassergehalt als limitierende Faktoren der biologischen Stickstofffixierung sowie die mit ihr verbundenen Respirationkosten. Hierdurch wird die Fähigkeit von LPJmL, die Dynamik des Kohlenstoff- und Stickstoffkreislaufs zu simulieren, verbessert.

Zur Evaluierung von LPJmL-CSR wurden Simulationen für drei Grünlandstandorte mit unterschiedlichen Klima- und Bewirtschaftungsbedingungen durchgeführt. Diese ausgewählten Standorte umfassen ein Grünland mit gemäßigttem Klima, eine heiße und eine kalte Steppe. Für die Standorte lagen jeweils Beobachtungen zu Grünfütterentnahme, Blattbiomasse und/oder organischem Bodenkohlenstoff für mehrere Bewirtschaftungsintensitäten vor. Um die Dynamik der Pflanzengemeinschaft zu bewerten, wurden weitere Szenarien mit unterschiedlicher Ressourcenlimitierung simuliert. Im Vergleich zu LPJmL erzeugte LPJmL-CSR verbesserte Simulationsergebnisse für alle untersuchten Variablen. Weiterhin bildete LPJmL-CSR zentrale Zielkonflikte zwischen ökologischen Strategien ab und simulierte plausible Verschiebungen der Zusammensetzung der Pflanzengemeinschaft unter verschiedenen Ressourcenlimitierungen. Während diese Ergebnisse spezifisch für die untersuchten Standorte sind, zeigen sie den Erfolg der Modellentwicklung von LPJmL-CSR und ermöglichen eine Bewertung auf globaler Skala (Kapitel 5).

Um eine global anwendbare Version von LPJmL-CSR zu entwickeln, wurde das Modell gegen historische Daten zur Bruttoprimärproduktion (BPP) und den CSR-Anteilen von Pflanzengemeinschaften kalibriert. Anschließend wurden mehrere Simulationsexperimente durchgeführt, um die BPP und den

organischen Bodenkohlenstoffspeicher bis 2100 unter der Annahme von niedriger oder hoher funktionaler Diversität sowie unter moderatem und stärkerem Klimawandel zu bewerten. Die Simulationsergebnisse heben die Bedeutung von funktionaler Diversität für die BPP und den organischen Bodenkohlenstoffspeicher bereits unter moderatem Klimawandel hervor. Das Szenario mit niedriger funktionaler Diversität, in dem die Anpassungsfähigkeit der Pflanzengemeinschaft unterdrückt wurde, projizierte deutlich geringere globale BPP und organische Bodenkohlstoffspeicher. Allerdings zeigten die räumlichen Muster regional substanzielle Unterschiede und manche Gebiete wiesen eine erhöhte BPP sowie höhere organische Bodenkohlenstoffspeicher bei niedriger funktionaler Diversität auf. Eine detaillierte Auswertung von drei Beispielregionen — Uganda und Südsudan (Afrika), Deutschland (Europa) und North und South Carolina (Nordamerika) — zeigte, dass die tieferliegenden Gründe für die Unterschiede zwischen den Szenarien mit niedriger und hoher Diversität sowohl vom initialen als auch vom zukünftigen Klima abhängen. Die Ergebnisse von LPJmL-CSR sind im Einklang mit empirischen Erkenntnissen und betonen die Bedeutung von funktionaler Diversität für die Anpassung von Grünlandpflanzengemeinschaften an den Klimawandel.

Zusammenfassend führt diese Dissertation einen neuen Ansatz zur Simulation funktionaler Diversität von bewirtschaftetem Grünland in DGVMs ein. Dies ist entscheidend, um die Projektionen der Ökosystemdienstleistungen bewirtschafteten Grünlands unter Klimawandel zu verbessern. Die Ergebnisse demonstrieren, dass funktionale Diversität zur Produktivität und zum Bodenkohlenstoffspeicher bewirtschafteten Grünlands beiträgt und so zum Beispiel Effekte der durch Überbeweidung verursachten Einschränkung der Ernährungssicherheit und Kohlenstoffsequestrierung in Grünlandböden abbilden kann. Obwohl Feldexperimente diesen Zusammenhang bereits etabliert haben, bietet die Simulation funktionaler Diversität auf globaler Skala eine neue Perspektive, um die komplexen Interaktionen zwischen Klimabedingungen, Bewirtschaftung und funktionaler Diversität im bewirtschafteten Grünland zu erfassen.

LPJmL-CSR hat somit das Potenzial, zukünftig zu mehreren Forschungsbereichen beizutragen. Erstens könnte LPJmL-CSR zur Entwicklung nachhaltiger Bewirtschaftungspraktiken unter verschiedenen Klimawandelszenarien beitragen und somit politische Entscheidungsträger:innen über den Wert funktionaler Diversität informieren und einen Beitrag im Kampf gegen Biodiversitätsverlust leisten. Zweitens betrachtet diese Dissertation die Rolle von funktionaler Diversität auf der Basis vorgeschriebener Szenarien. Allerdings sind Klimawandel und Biodiversitätsverlust eng verknüpft und zukünftige Forschung sollte Rückkopplungsmechanismen untersuchen. Drittens projizieren Landnutzungsallokationsmodelle die Veränderung von Grünlandflächen auf Basis der sozioökonomischen Entwicklung und des Klimawandels. Explizite Informationen über die Rolle funktionaler Diversität für bewirtschaftetes Grünland könnten als zusätzliche Einschränkung bei der Reallokation von Landnutzung dienen und entsprechende Projektionen verbessern.

# Summary

Managed grasslands occupy a substantial share of the terrestrial area across different climates and contribute to many people's livelihoods and food security through ruminant meat and dairy production. The productivity — and in turn the livestock carrying capacity — of managed grasslands depends on climatic conditions and management and plant functional diversity. While plant functional diversity is shaped by climatic conditions and management, it also plays a direct role in the productivity of managed grasslands. The role of functional diversity has been extensively studied through field experiments and observations. This research has provided evidence that functional diversity supports essential ecosystem services in managed grasslands and enhances their adaptation to climate change.

While functional diversity has been incorporated into computer models at small spatial scales, at the global scale such a representation has been missing. However, global-scale models such as dynamic global vegetation models (DGVMs) are widely used to assess the impacts of climate change on vegetation, and enabling DGVMs to simulate the role of functional diversity is crucial for improving projections of ecosystem services in managed grasslands. Therefore, the main objectives of this thesis were to: (1) identify important areas of model development needed to represent functional diversity in managed grasslands in DGVMs (Chapter 2), (2) implement the necessary changes (Chapters 3 and 4) and (3) to assess the role of functional diversity in grassland productivity and soil organic carbon (SOC) stocks at the local and global scale (Chapters 3 and 5) and under climate change (Chapter 5).

To identify key areas for model development, the Lund-Potsdam-Jena managed Land (LPJmL) model was compared with the Grassland Individual-based Dynamic Model (GRASSMIND). For this comparison, both models were used to simulate monocultures and multi-species plant communities from the Jena Experiment, a well-known biodiversity experiment. The simulated scenarios included varying levels of precipitation both with and without mowing. An in-depth analysis of process representations in LPJmL and GRASSMIND was conducted to assess each model's strengths and weaknesses when simulating multi-species communities. The results showed that both models moderately matched observations of monoculture and multi-species communities but also highlighted the need to improve the representation of trade-offs between ecological strategies and competition for resources.

Based on these findings, Chapter 3 presents an approach to simulate the functional diversity of managed grasslands in the LPJmL model incorporating the competitor, stress-tolerant, ruderal (CSR) theory and functional traits. Functional plant traits describe key trade-offs between ecological strategies through trait-trait relationships. The CSR theory is a well-known framework describing ecological strategies and has been linked to the trade-offs described by the trait-trait relationships of the global spectrum of plant form and function. Leveraging this connection, the extended LPJmL-CSR model can simulate the functional diversity of managed grasslands across various climatic and management con-

ditions. The main differences between LPJmL and LPJmL-CSR include an explicit representation of the relationship between specific leaf area and leaf longevity as described by the leaf economic spectrum, the separation of above and belowground resource distribution and improved representations of establishment and mortality.

In addition to these developments, a new representation of biological nitrogen fixation was introduced in LPJmL (Chapter 4). This implementation explicitly accounts for soil temperature and soil water content limitations on biological nitrogen fixation as well as its associated respiratory costs thereby enhancing LPJmL's ability to simulate the carbon and nitrogen cycle dynamics.

To evaluate LPJmL-CSR, simulation experiments were conducted at three grassland sites with distinct climatic and management conditions. The selected sites consisted of a temperate grassland, a hot steppe and a cold steppe where observations of forage offtake, leaf biomass and/or SOC stocks for several management intensities were available. Additional resource limitation scenarios were simulated to assess community dynamics. Compared to LPJmL, LPJmL-CSR produced improved simulation results for all investigated variables. Furthermore, LPJmL-CSR captured key trade-offs between ecological strategies and simulated plausible shifts in community composition under varying resource limitations. While these results were specific to the investigated sites, they highlighted the success of LPJmL-CSR's model development and enabled a global scale assessment (Chapter 5).

To develop a globally applicable version of LPJmL-CSR, the model was calibrated using historical data on gross primary productivity (GPP) and CSR shares of plant communities. Subsequently, multiple simulation experiments were conducted to assess managed grassland GPP and SOC until 2100, assuming either low or high functional diversity under moderate and more severe climate change. The simulation results highlight the importance of functional diversity for managed grassland GPP and SOC stocks, even under moderate climate change. The low functional diversity scenario, in which community adaptation was suppressed, projected substantially lower global GPP and SOC stocks. However, the spatial patterns reveal substantial regional differences and indicate that some areas exhibit increased GPP and SOC stocks in the low functional diversity scenario. A detailed assessment of three example regions — Uganda and South Sudan (Africa), Germany (Europe) and North and South Carolina (North America) — showed that underlying reasons for differences between the high and low functional diversity scenarios depend on both initial and future climatic conditions. The results of LPJmL-CSR align with empirical findings and emphasize the importance of functional diversity for the adaptation of grassland communities to climate change.

In summary, this thesis introduces a novel approach to simulate the functional diversity of managed grasslands in DGVMs, which is crucial for improving projections of managed grassland ecosystem services under climate change. The results demonstrate that functional diversity contributes to managed grassland productivity and SOC stocks and food security. While field experiments have already

## *Summary*

established this relationship, simulating the role of functional diversity at a global scale offers a new perspective for disentangling the complex interactions between climatic conditions, management and functional diversity in managed grasslands.

LPJmL-CSR has the potential to contribute to multiple research areas in the future. First, LPJmL-CSR could be utilised to investigate sustainable management practices across various climate change scenarios. These assessments could provide policymakers with insights into the value of functional diversity and help to combat biodiversity loss. Second, this thesis includes only an assessment that prescribes both low- and high-functional-diversity scenarios. However, climate change and biodiversity loss are interconnected, and future research should examine feedback mechanisms between the two. Third, land-use allocation models project changes in grassland areas based on socio-economic development and climate change. Explicit information on the role of functional diversity in managed grasslands could serve as an additional constraint in land-use reallocation to improve the respective projections.

# Chapter 1

## General introduction

### 1.1 Managed grasslands: An overview

Managed grasslands cover approximately 40.5% of the terrestrial Earth surface (excluding Greenland and Antarctica) (Orwin et al., 2014; White et al., 2000) and contribute to the livelihoods of approximately one billion people (Suttie et al., 2005). Managed grasslands are areas dominated by herbaceous vegetation across different climates (Gibson, 2008) that are subject to a multitude of management practices, livestock grazing being the most common (Bai and Cotrufo, 2022). Managed grasslands are highly complex ecosystems providing a variety of ecosystem services, which can be exemplified by examining only two variables— water availability and livestock density:

In humid climates, managed grasslands can produce large amounts of biomass for livestock feed, sustaining high numbers of animals and supporting dairy or ruminant meat production (Smit et al., 2008). However, too intensive management may lead to soil organic carbon (SOC) loss and long-term degradation (McSherry and Ritchie, 2013). In dry climates, biomass production and animal numbers are limited, rendering managed grasslands especially vulnerable to overgrazing (Li et al., 2018). At the same time, livestock grazing is a primary source of income for farmers in dry climates as it is often the only agricultural land use possible (Blench, 2001; Steinfeld et al., 2006). Including additional variables such as temperature, nutrient availability or the vegetation composition increases the complexity (Li et al., 2018) but is necessary to identify sustainable management options. These management options are needed to ensure the continued contribution of managed grasslands to food security and support climate change mitigation and facilitate adaptation to its impacts (Reid et al., 2004; Soussana et al., 2014).

#### 1.1.1 The role of managed grasslands for food security and the environment

Managed grasslands are primarily used as a source of feed for ruminant livestock and contribute to the production of protein-rich food products such as ruminant meat and dairy (Herrero et al., 2013a; Herrero et al., 2013b). Their role in food security varies across world regions and depends on the local context (O'Mara, 2012; Peyraud and Peeters, 2016). Food security generally encompasses four dimensions: availability, access, utilisation and the stability of these three dimensions (World Food Summit, 1996). While this thesis only investigates the availability and stability dimensions, I provide a brief overview of the status of global food security as this was a key motivation for the doctoral program "Third Ways of Feeding the World" that provided the funding for this thesis.

The Sustainable Development Goal (SDG) on Zero Hunger (United Nations, 2015a) can only be

achieved if food security is ensured for everyone. However, globally, between 691 and 783 million people faced hunger in 2022, and nearly 200 million children under five years of age were stunted or wasted (FAO et al., 2023), which is evidence that further action to combat hunger is required. Managed grasslands provide protein-rich food such as dairy products and ruminant meat and can help to reduce malnutrition locally (FAO et al., 2020; Leroy et al., 2023). At the same time, as a consequence of unhealthy diets, approximately 2.5 billion adults (WHO, 2024) and 37 million children were overweight in 2022 (FAO et al., 2023), posing a threat to the SDG on Global Health and Well-Being (United Nations, 2015b). One contributing factor of these unhealthy diets is an overly high share of meat and dairy products (Abete et al., 2014; Song et al., 2016; Willett et al., 2019).

Looking beyond the health impacts, food systems are a major contributor to climate change accounting for approximately 34% of the total greenhouse gas emissions (Crippa et al., 2021). Of these, ruminant livestock production systems contribute to climate change with total emissions ranging from 5.6 to 7.5 TgCO<sub>2</sub>eq yr<sup>-1</sup> (estimates for 1995 to 2005; Herrero et al., 2016). The main sources include methane (CH<sub>4</sub>) from enteric fermentation (1.6 to 2.7 TgCO<sub>2</sub>eq yr<sup>-1</sup>), nitrous oxide (N<sub>2</sub>O) emissions from feed production (1.3 to 2.0 TgCO<sub>2</sub>eq yr<sup>-1</sup>) and land use for pastures and animal feed (approximately 1.6 TgCO<sub>2</sub>eq yr<sup>-1</sup>) (Gerber et al., 2013; Herrero et al., 2013b; Herrero et al., 2016; Popp et al., 2010; Tubiello et al., 2013; US EPA, 2006). In addition, ruminant livestock production systems are responsible for approximately 66% of total agricultural water consumption (Heinke et al., 2020) and, along with other livestock systems, account for 80% of agricultural land use (Steinfeld and Gerber, 2010; Weindl et al., 2017). Livestock production systems also threaten biodiversity, for example through their contribution to habitat change (Steinfeld et al., 2006) and rangeland degradation (Asner et al., 2004). However, it has to be noted that livestock grazing creates and maintains sward structural heterogeneity, which can also benefit biodiversity (Rook et al., 2004). Finally, livestock-related nitrogen emissions constitute approximately 35% of the total agricultural nitrogen emissions primarily from feed production and manure management (Bodirsky et al., 2014; Conijn et al., 2018; Uwizeye et al., 2020).

Achieving food security without compromising on climate change mitigation, biodiversity conservation and environmental pollution remains a challenge but is essential and a reduction in global livestock production is needed to achieve the goals of the Paris Agreement and the SDGs (Ruggeri Laderchi et al., 2024; Steinfeld et al., 2006; Willett et al., 2019).

### **1.1.2 Managed grasslands under climate change**

It is well established that climate change will lead to an increase in the land surface temperature, altered spatiotemporal precipitation patterns and an increased likelihood of extreme events such as droughts (Alexander et al., 2006; Alexander, 2016; Li et al., 2021). Regardless of whether we limit emissions and

global average temperature increase to 1.5°C or not, climate change will impact the terrestrial carbon (Frank et al., 2015), nitrogen (e.g., Lee et al., 2016; Sinha et al., 2017) and water cycles (Allan et al., 2020) and agriculture (Jägermeyr et al., 2021; Lange et al., 2020). In agriculture, rising atmospheric carbon dioxide (CO<sub>2</sub>) concentrations, the temperature increase and changes in precipitation patterns will impact plant growth (Franks et al., 2013; Kirschbaum, 2011; Rötter and van de Geijn, 1999). Negative impacts on yields should be minimised as they pose a threat to food security and achieving the Zero Hunger Sustainable Development Goal (e.g., Gregory et al., 2005; Schmidhuber and Tubiello, 2007).

While the impact on productivity is important for both croplands and grasslands, managed grasslands provide a variety of additional non-cultural ecosystem services. I focus on climate-change impacts on grassland productivity and soil organic carbon storage and did not investigate other ecosystem services of managed grasslands, such as erosion control, habitat provisioning (Tribot et al., 2018) and important cultural ecosystem services, such as their utilization for recreational activities (Van Oijen et al., 2020). For managed grasslands, climate change is expected to impact the amount and timing of grassland productivity, animal carrying capacity and periods suitable for grazing, the carbon balance and non-CO<sub>2</sub> emissions from CH<sub>4</sub> and N<sub>2</sub>O (Chang et al., 2017). Increased photosynthesis and greater leaf biomass likely result in increased productivity (e.g., Campbell and Stafford Smith, 2000) limited by leaf nitrogen content (Nowak et al., 2004) and water-use efficiency (Rötter and van de Geijn, 1999; Soussana and Lüscher, 2007). However, the interactions of temperature, water availability, nutrients, soil, vegetation and management intensity lead to a complex climate-change response in managed grasslands (Dumont et al., 2015; Jones and Donnelly, 2004; Roy et al., 2016; Soussana et al., 2013) and accelerated climate change may exceed the adaptation capacities of grassland communities (Cang et al., 2016).

Chang et al. (2017) project an increase of 6 to 20% in potential grassland yields and 10 to 25% in optimal stocking densities for Europe, compared to the 1981-2010 average depending on the level of climate change. They also project a carbon sink in European grasslands for a 1.5°C warming but regional carbon neutrality or a carbon source for a 3.5°C warming (Chang et al., 2017). However, while they reflect management adaptations to optimise productivity, they do not consider dietary changes, which may lead to further intensification in the livestock sector, cause grassland degradation and alter the carbon balance. As a matter of fact, when assessing the full greenhouse gas balance of grasslands, Chang et al. (2021) show that the carbon sink increases from CO<sub>2</sub> fertilisation and other climatic drivers in extensively grazed systems and the carbon losses from intensification and land-use change are almost balanced, making global grasslands nearly carbon neutral. This calls for sustainable management to enhance grassland carbon storage and prevent a shift to a carbon source (Bai and Cotrufo, 2022; Chang et al., 2021; Conant et al., 2017; Smith et al., 2007).

Ninety percent of the grassland carbon is stored in the soil, either as roots or soil organic matter, and is highly vulnerable to overgrazing and land conversion (Bai and Cotrufo, 2022; Bardgett et al., 2021;

White et al., 2000). Spatiotemporal changes in precipitation and an increase in severe droughts will affect community composition, carbon allocation and microbial processes, such as decomposition (Bai and Cotrufo, 2022). In savanna grasslands, increasing fire frequencies may modify long-term carbon storage by intensifying nutrient limitation (Bai and Cotrufo, 2022; Pellegrini et al., 2018; Zhou et al., 2022). To prevent SOC loss or even yield an increase, improved grazing management (Conant et al., 2017; Wilson et al., 2018; Wu et al., 2017), as well as maintaining (Bai and Cotrufo, 2022) and restoring (Chen et al., 2018; Prommer et al., 2020; Yang et al., 2019) biodiversity, are important.

### **1.1.3 Modelling managed grasslands at large spatial scales**

In addition to field experiments, computer models can be used to systematically assess the role of environmental conditions, management and functional diversity. A computer model is always a simplification of reality and the level of detail used to represent specific real-world features depends on the model's purpose. Grassland models have been developed at various spatial scales and for different purposes. I provide an overview of managed grassland models that were developed to simulate productivity and soil organic carbon storage in 2.1.3.

At large to global scales, Dynamic Global Vegetation Models (DGVMs) are commonly applied. These models have been developed to simulate global biogeochemical cycles and the dynamics of vegetation patterns (Quillet et al., 2010; Sitch et al., 2003). Historically, DGVMs modelled natural vegetation using a small set of plant functional types (PFTs) and a detailed representation of photosynthesis to simulate the carbon cycle across different biomes (e.g. Brovkin et al., 1997). To account for anthropogenic influences on the carbon cycle, these models were extended to also simulate croplands and grasslands (Bondeau et al., 2007) and over time additional management practices were implemented (e.g. Jägermeyr et al., 2017; Lutz et al., 2019; Rolinski et al., 2018).

However, while functional diversity is represented in several local- to regional-scale models such as the Grassland Individual-based Dynamic Model (GRASSMIND) (Taubert et al., 2012; Taubert et al., 2020a; Taubert et al., 2020b), the Individual-Based plant Community-grass (IBC-grass) model (May et al., 2009) and the GrasslandTraitSim model (Nößler et al., 2024), global-scale models such as the Lund-Potsdam-Jena managed Land (LPJmL) model (Rolinski et al., 2018; Schaphoff et al., 2018; von Bloh et al., 2018) lack such a representation.

### **1.1.4 Functional diversity of managed grasslands**

Empirical research from the world's major grassland biomes consistently shows that biodiversity supports productivity (Grace et al., 2016; Walde et al., 2021), forage supply (Schaub et al., 2020) and SOC stocks (Anacker et al., 2021; Spohn et al., 2023). However, historical productivity increases were

mainly driven by grassland expansion and intensification, which in turn led to species and biodiversity loss (Guo et al., 2023; Isbell et al., 2015b). For example, in the North American Great Plains as well as the Asian steppes, traditional grazing systems have been replaced by more intensive systems, and today these grasslands are at risk of large-scale degradation due to overgrazing (Batunacun et al., 2018; Weaver, 1954). As a consequence, precipitation infiltration (Wu et al., 2022) and soil fertility decline (Wu and Tiessen, 2002), leading to a reduction in the livestock carrying capacity of these grasslands (Piipponen et al., 2022) unless management practices are adapted (Akiyama and Kawamura, 2007; Augustine et al., 2021; Wilcox et al., 2012). While soil fertility loss can be counteracted to some extent with synthetic fertilisers or manure, such adaptations increase the production costs due to the need for additional labour, machinery and inputs (Holubek and Petrovic, 2011). Additionally, they may promote competitive or dominant species that can utilise the additional resources most efficiently, thereby accelerating biodiversity loss (Gaujour et al., 2012; Melts et al., 2018). Sustainable management practices should consider the role of biodiversity in managed grassland ecosystem services.

Biodiversity research is constantly evolving and the advent of large databases such as TRY (Kattge et al., 2020), combined with new artificial intelligence-based methods of data analysis (e.g., Schiller et al., 2021; Wolf et al., 2022), will likely provide additional insights in the future. However, it is already clear today that biodiversity underpins most ecosystem services (Cardinale et al., 2012; Costanza et al., 1997; Zhang et al., 2022). Biodiversity unifies taxonomic, ecological, morphological and functional diversity. While all four are important, the focus of this thesis is on plant functional diversity.

Functional diversity is a component of biodiversity that describes the range of functions provided by the flora (and/or fauna) of a community or ecosystem (Petchey and Gaston, 2006). A common measure of functional diversity is the value and range of traits associated with ecosystem functioning. For example, a grassland community that contains only species with a similar leaf longevity (LL) — a trait that describes the lifespan of a leaf — is less diverse than one containing species with different LLs. The concept of leaf economics can metaphorically be described as the time after which a leaf must be replaced by a new one to maintain the plant's leaf biomass. As the production of new leaves requires carbon, the plant must be able to assimilate the required amount of carbon within this time frame or it will lose leaf biomass. It is well known that the LL is not independent of the investment cost in terms of carbon to produce a leaf (Chabot and Hicks, 1982; Wright et al., 2004). Leaves with a short lifespan have lower investment costs compared to leaves with a long lifespan. Since a specific area of leaf contains a different amount of carbon depending on the investment, the investment can be expressed as leaf mass per area or its inverse, the Specific Leaf Area (SLA). In an environment with abundant resources, rapidly constructing new leaves and having to replace them more often is easy. However, if resources become scarce, such a strategy is not successful, and a plant community that only follows this strategy will suffer more — and lose for example biomass — than a community with a more

diverse strategy portfolio. This example illustrates two important features of functional diversity.

First, functional diversity underpins a range of ecosystem functions and services and extensive research has been conducted to quantify the role of functional diversity in individual and across functions and services (Hector and Bagchi, 2007; Isbell et al., 2011; Pasari et al., 2013; Zavaleta et al., 2010). That research includes extensive long-term field experiments, such as the well-known biodiversity experiments at Cedar Creek (Tilman et al., 2001) and the Jena experiment (Weisser et al., 2017). These and other experiments provided key insights into the role of functional diversity in productivity (diversity-productivity theory e.g., Craven et al., 2016; Schulze and Mooney, 1993; Tilman et al., 2012), resistance and resilience of productivity (diversity-stability theory e.g., Buzhdygan et al., 2020; Hoover et al., 2014; Isbell et al., 2015a) and the success of invading species (diversity-invasion theory e.g., Fargione et al., 2003; Petermann et al., 2010; Zavaleta and Hulvey, 2004). For a comprehensive overview I refer to Tilman et al. (2014).

Second, functional diversity can be expressed through traits and is representative of ecological strategies, which are key components of the methods used in this thesis.

## 1.2 Functional traits and ecological strategies

The term 'plant trait' is used broadly to describe various features of plants (Violle et al., 2007). Functional traits are traits that describe ecological strategies (Pérez-Harguindeguy et al., 2013). The concept of functional traits is well-established and the compilation of large trait databases, such as TRY (Kattge et al., 2020), forms the basis for quantifying relationships between multiple traits, relating them to ecological strategies and incorporating this knowledge into vegetation models (McMahon et al., 2011).

### 1.2.1 Functional trait relationships

A prominent example is the leaf economic spectrum (Wright et al., 2004), which provides power laws to describe the relationship between SLA, LL and leaf nitrogen content. This allows a quantitative description of the well-known trade-off between the fast-growing and short-lived and the slow-growing and long-lived strategies of leaf production (fast-slow leaf economics, Reich, 2014). Recently, the development of global databases such as TRY made trait data available to a wide range of researchers from different disciplines and provided the basis for a large body of literature on additional trait-trait relationships and their role in ecosystem services (Kattge et al., 2020). Using data from TRY, the global spectrum of plant form and function combines the leaf economic spectrum with phenological and morphological traits, which also allows for describing the strategy trade-off between tall plants with a limited number of large seeds and small plants with a high number of small seeds (Díaz et al., 2016).

Recently, the concept of leaf economics has been applied to roots as well, leading to the concept of

the root economic space, which includes two dimensions: the fast-slow dimension, which is similar to the fast-slow component of the leaf economic spectrum and can be described through a trade-off between root tissue density and root nitrogen content and the do-it-yourself-outsourcing dimension, which is described through a trade-off between specific root length and investment in a mycorrhizal partner (Bergmann et al., 2020).

A connection between the above- and below-ground trait trade-offs can be established via the fast-slow dimension, which is aligned between the above- and below-ground plant organs, providing an integrated framework (Weigelt et al., 2021). However, while such frameworks provide a high-level, holistic description relating plant form and function, they also have drawbacks. Foremost, genes are not the only determining factor for plant traits, and individuals of the same species already show a broad range of trait values depending on local environmental conditions (Mitchell et al., 2018; Roybal and Butterfield, 2019; Siefert et al., 2014). Therefore, applying the relationships to a specific plant community is difficult without also considering environmental conditions.

In vegetation modelling, trait-trait relationships have been incorporated into models at different scales, improving their capability to represent ecosystems. Such trait-based models often simulate a number of individuals for which trait values are randomly sampled from a prescribed distribution to represent the various plants in a community. For instance, the Lund-Potsdam-Jena managed Land-flexible individual traits (LPJmL-FIT) model represents the fast-slow leaf economics and a trade-off between wood density and tree mortality based on TRY data (Sakschewski et al., 2015). While originally developed to simulate vegetation dynamics in the Amazon, it has been extended to European forests (Thonicke et al., 2020). Compared to its sister model, LPJmL, which was used in this thesis, forest dynamics are better captured. However, LPJmL-FIT does not include managed grasslands.

The GRASSMIND model (Taubert et al., 2012; Taubert et al., 2020a; Taubert et al., 2020b) is an example of an individual-based grassland model that simulates the differences between individuals based on multiple traits. Similar to LPJmL-FIT and other trait-based models, it follows a gap approach (Botkin et al., 1972), assuming that disturbances or stochastic age mortality create gaps in the vegetative cover where new vegetation can establish. Due to the stochasticity of the approach, multiple realisations of the community with several thousand individuals of different species must be simulated, making such models computationally expensive. In contrast, the LPJmL model is computationally comparatively cheap but requires a more aggregated way of representing functional diversity through the grouping of similar species into PFTs. In the past, this grouping was done based on growth form (tree or grass), leaf type (broad- or needle-leaved), phenology (summer-, rain- or evergreen) and photosynthetic pathway (C3 or C4). This led to the development of a limited number of PFTs to represent managed grasslands, which do not distinguish different ecological strategies or functional diversity. To overcome this, I applied the competitor, stress-tolerator, ruderal (CSR) theory (Campbell and Grime, 1992; Grime, 1974; Grime,

1977) to introduce additional PFTs. The CSR theory is a simple concept for grouping species according to their ecological strategies and has been connected to the concept of functional traits (Pierce et al., 2013; Pierce et al., 2017).

### 1.2.2 The CSR theory

In 1974, Philip J. Grime developed the CSR theory based on a large set of field experiments in the United Kingdom. This theory distinguishes three main ecological strategies based on habitat conditions. The competitive (C) strategy predominates in habitats with abundant resources, where species that can utilise these resources most efficiently thrive and outcompete other species. This strategy is characterised by fast growth and the production of large amounts of leaves with a short lifespan. The stress-tolerant (S) strategy characterises species that invest resources in the ability to survive in resource-poor environments, where the competitive strategy is not successful. This strategy is characterised by slower growth and leaves with a long lifespan. While this strategy can also result in large plants, this takes considerably more time compared to the competitive strategy. The ruderal (R) strategy is characterised by short life cycles, completed during periods of beneficial conditions and a large number of seeds that lie dormant during uninhabitable periods. As a result of the short life cycle, this strategy does not support the growth of large plants. However, similar to the competitive strategy, it facilitates the growth of leaves with a short lifespan. While these three strategies are the ones that give the theory its name, they represent extremes, and in-between strategies are common. Visually, the CSR theory is typically depicted as a triangle, with the main strategies at its nodes and intermediate strategies positioned within the triangle (Fig. 1.1). For example, a competitive stress-tolerant strategy can be positioned at or near the edge between the competitive and the stress-tolerant nodes.

As mentioned earlier (see 1.2.1), ecological strategies can be expressed through functional traits. Pierce et al. (2013) use the functional traits SLA, leaf area, and leaf dry matter content to connect CSR theory and the global spectrum of plant form and function (Díaz et al., 2016), and to explain CSR variation across species and within communities. These and other connections between traits and strategies form the basis for the Lund-Potsdam-Jena managed Land Competitor, Stress-Tolerator, Ruderal (LPJmL-CSR) model developed in the context of this thesis.

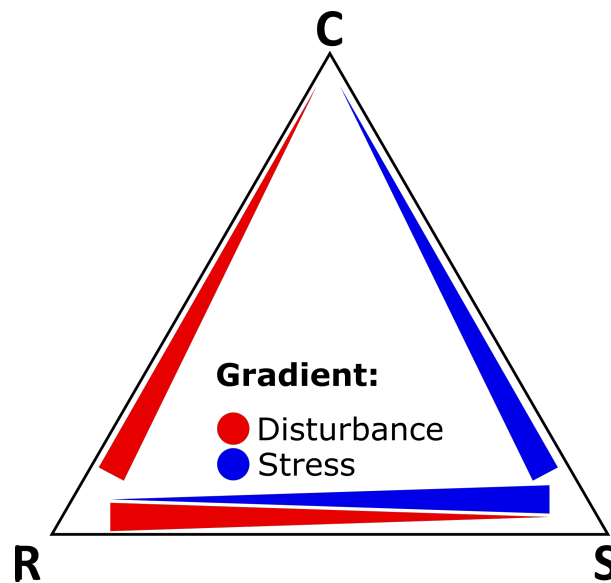


Figure 1.1: Ternary plot visualising the CSR theory. Main strategies (C, S and R) are displayed at the nodes of the triangle. Environmental conditions that lead to the emergence of different strategies are shown as the stress (blue) and disturbance (red) gradients. Intermediate strategies can be positioned anywhere within the triangle.

## 1.3 The LPJmL model

LPJmL is a DGVM that simulates the terrestrial carbon, nitrogen and water cycles of natural vegetation and managed land. The productivity of different vegetation types is calculated considering the co-limitation of temperature, light, water and nitrogen for photosynthesis. A detailed model description of LPJmL and the most recent developments are provided in von Bloh et al. (2018), Schaphoff et al. (2018), Heinke et al. (2023) and Wirth et al. (2024) (Chapter 4), and I provide a brief overview.

### 1.3.1 General model description

LPJmL simulates different vegetation types using the concept of PFTs, which group one or several species, depending on common traits, into one representative entity: the PFT. For example, LPJmL distinguishes only a tropical broadleaved evergreen and raingreen PFT to represent tropical forests. For each PFT, LPJmL simulates the dynamics of an average individual to represent the entire population, using several state variables. The most important state variables include the carbon and nitrogen pools of different plant organs (leaves and roots, but also sapwood and heartwood for trees), a labile nitrogen pool and the number of average individuals in the represented population. The dynamics are based on the processes of establishment and reproduction, turnover and mortality and allocation of net primary productivity (NPP) to different plant organs. NPP is the carbon accumulated by photosynthesis (gross primary productivity, GPP) minus the losses from autotrophic respiration. While these processes provide the basis for all vegetation types simulated by LPJmL, the simulation of managed grasslands includes

additional processes due to management.

### 1.3.2 The managed grassland module

Implemented grassland management options include irrigation, the application of synthetic fertiliser and manure, as well as different options for daily and rotational grazing and mowing. Irrigation options are described in (Jägermeyr et al., 2015) and the application of manure and synthetic fertiliser includes the amount and timing of the treatment (von Bloh et al., 2018). All grazing and mowing options are described in detail in Rolinski et al. (2018) and Heinke et al. (2023), and I briefly present the mowing and daily grazing options, as these are relevant for this thesis.

Mowing is implemented as a biomass removal on specified days of the year, after which only a predefined amount of stubble biomass remains. For daily grazing, two options for determining forage intake by the animals were developed. The main difference lies in the determination of the maximum and actual forage intake. The initial routine by Rolinski et al. (2018) calculates a fixed maximum forage intake based on a fixed feed demand per unit of metabolic body weight. If actual forage biomass is lower than the maximum forage intake, all forage biomass, except for a predefined amount of stubble, is removed. Otherwise, forage biomass is reduced by the maximum intake. In contrast, Heinke et al. (2023) calculate the maximum forage intake dynamically by additionally considering the crude protein content of forage dry matter, which they derive from the daily updated forage nitrogen content. Actual forage intake is a function of the leaf area index (LAI), following Herrero et al. (2000) and Johnson and Parsons (1985).

While multiple management options have been implemented in detail, less attention has been paid to the representation of the plant community. LPJmL generally represents managed grasslands using three herbaceous PFTs, which group together graminoids, forbs and herbs. While this is comparable to other DGVMs, this broad categorization has been criticised as insufficient to represent the global variation of grassland communities (Linstädter et al., 2014; Pfeiffer et al., 2019). The three herbaceous PFTs include a tropical C4 and a temperate and a polar C3 PFT. The simulated plant organs are leaves and roots, which grow and decay following the processes listed in 1.3. Additionally, while the number of average individuals in a community is a variable for the tree PFTs, it is a constant of one for the grass PFTs. Using functional traits and CSR theory, I extended the model to represent additional PFTs distinguishing different strategies.

### 1.3.3 LPJmL-CSR

A full description of LPJmL-CSR is provided in Chapters 3 and 4; here, I give only a brief overview. In LPJmL-CSR I use the connections between functional traits, which are used as parameters in LPJmL,

and CSR theory to extend the set of herbaceous PFTs. As a prerequisite, several parts of the model had to be refined.

First, I defined the SLA-LL relationship (Chabot and Hicks, 1982; Wright et al., 2004) as a power law based on data from the TRY database (Kattge et al., 2020) (Chapter 3). Second, I included the below-ground biomass in the competition for water using root functional traits (Chapter 3). Third, I implemented a new approach to represent biological nitrogen fixation (BNF) that explicitly considers the PFT-specific co-limitation of temperature and water availability, the respiration cost of nitrogen fixation and the potential fixation rate (Chapter 4). Fourth, to simulate the number of average individuals as a variable instead of a constant, I modified the reproduction and mortality routines to increase and decrease the number of average individuals (Chapter 3).

With these extensions, LPJmL-CSR is the fundamental tool I used for this thesis.

## 1.4 Research justification and objectives

My main goal was to provide a global assessment of the role of functional diversity in managed grasslands productivity and SOC storage under different climate-change scenarios. Increasing our understanding of the role of functional diversity for these variables is important for better comprehension of the dynamics of the land carbon cycle and to quantify climate-change impacts on forage supply in terms of quantity, quality and stability. Such knowledge can be used to inform policymakers, farmers and other stakeholders about the consequences of mismanagement and foster the development of sustainable management practices. While the extensive empirical research on the role of functional diversity of managed grasslands provides insight into the current state, it is not sufficient to project the future state of managed grasslands globally. For this purpose, dynamic global vegetation models that can simulate the effects of land-use change and different management practices on the global carbon and nitrogen cycles are used. In addition to projecting future productivity and soil organic carbon storage of managed grasslands, these models are used to calculate the overall net carbon flux of the land surface, which is a key component in determining the global carbon budget. Whether the land surface is a carbon sink or a source is at least to some extent determined by the carbon balance of managed grasslands. However, such models have so far neglected the role of functional diversity in managed grasslands. To achieve the main goal of this thesis, I incorporated a representation of functional diversity in managed grasslands into the LPJmL DGVM, which provides the basis to investigate the following overarching research questions:

1. How can dynamic global vegetation models be adapted to represent the functional diversity of managed grasslands?

2. What is the role of functional diversity for the productivity, forage supply and SOC stocks of managed grasslands at local to national scales under different management practices and climate conditions?
3. How important is functional diversity for managed grassland productivity and soil organic carbon storage at the global scale and under climate change?

## 1.5 Thesis outline

To achieve the objectives of this thesis, the development of the LPJmL-CSR model and simulation experiments were conducted. The findings are presented in separate chapters.

Chapter 2 aims to lay the foundation for the development of the LPJmL-CSR model. In this study, the LPJmL model is compared to the GRASSMIND model to identify key processes that need further development to represent functional diversity (research question 1). The two selected models differ in their resolution, purpose and detail of process representation. For example, while GRASSMIND focuses on the community dynamics but contains a less complex empirical photosynthesis model, LPJmL uses a more aggregated representation of the community but a more complex process-based photosynthesis model. Both models were calibrated to simulate different communities at the site of the Jena Experiment (Thuringia, Germany, 50°55'N, 11°35'E, 130 m above sea level) for which extensive data are available. My co-authors and I systematically compared simulated data on above-ground biomass, GPP, NPP, LAI, plant cover and water uptake from several precipitation scenarios with and without mowing.

Chapter 3 presents the model development of LPJmL-CSR, which was based on the findings of Chapter 2 and the CSR theory. Selected processes were altered to allow the representation of trade-offs between the main CSR strategies based on functional traits and their relationships (research question 1). The new model LPJmL-CSR was calibrated and evaluated for three managed grassland sites: a temperate grassland, a hot and a cold steppe, for several management scenarios using data on forage offtake or leaf biomass, SOC and cover share of C, S and R strategists. My co-authors and I compared the simulated leaf biomass, SOC and community position across the different sites and management scenarios and assessed the effect of removing water and/or nutrient limitation on leaf biomass, SOC and community composition (research question 2).

Chapter 4 describes the development of the carbon-costly biological nitrogen fixation (BNF) approach (research question 1). The carbon-costly BNF approach is based on Yu and Zhuang (2020) and Ma et al. (2022). The fundamental differences compared to the original approach include the distinction between temperature and water limitations for BNF as well as the introduction of a carbon cost for BNF. PFTs can only invest a certain amount of their NPP into fixation, limiting BNF. Finally, while in the original

approach fixed nitrogen was added to the soil mineral nitrogen pool, in the carbon-costly approach it is directly used by the fixing PFT.

For Chapter 5, I used LPJmL-CSR to assess the productivity and SOC stocks of managed grasslands globally under climate change (research question 3). For this purpose, I calibrated and evaluated LPJmL-CSR globally using remote sensing data on GPP and community composition data from citizen science-based trait maps. To assess the role of functional diversity, I simulated scenarios with high and low functional diversity using the presence or absence of different ecological strategies as a proxy. My results show that the GPP and SOC stocks of managed grasslands benefit from functional diversity even under moderate climate change. However, the level of this benefit differs across the Earth, and some areas even experience an increase in GPP and SOC stocks in the low functional diversity scenario. I selected three example regions: Uganda and South Sudan (Africa), Germany (Europe) and North and South Carolina (North America) which differ in the underlying reasons for the change in GPP, SOC stocks and community composition between the scenarios with and without functional diversity to discuss the regional pattern in detail (research question 2).

Chapter 6 presents and discusses the overall findings of this thesis, considering the current state of knowledge from scientific literature. Based on the findings for research questions 1 to 3 presented in Chapters 2 to 5, I discuss the insights on functional diversity, the implications for the dual challenge of climate change and biodiversity loss and the advantages and disadvantages of the LPJmL-CSR model. Finally, I lay out the potential impact of my findings for policymakers and the development of sustainable management practices and provide an outlook on future research applications of LPJmL-CSR.

As this is a cumulative thesis, Chapters 2, 3, 4 and 5 are separate manuscripts that may include redundancies in their introductions, method descriptions and discussions. Edited versions of Chapters 2, 3 and 4 have been published as original research articles in peer-reviewed scientific journals. Chapter 5 is currently in preparation for submission to a peer-reviewed scientific journal.

## 1.6 References

- Abete, I., D. Romaguera, A. R. Vieira, A. L. de Munain, and T. Norat (2014). "Association between Total, Processed, Red and White Meat Consumption and All-Cause, CVD and IHD Mortality: A Meta-Analysis of Cohort Studies". In: *Br. J. Nutr.* 112.5, pp. 762–775. ISSN: 0007-1145, 1475-2662. DOI: 10.1017/S000711451400124X. (Visited on 04/17/2024).
- Akiyama, T. and K. Kawamura (2007). "Grassland Degradation in China: Methods of Monitoring, Management and Restoration". In: *Grassl. Sci.* 53.1, pp. 1–17. ISSN: 1744-697X. DOI: 10.1111/j.1744-697X.2007.00073.x. (Visited on 11/20/2024).
- Alexander, L. V., X. Zhang, T. C. Peterson, J. Caesar, B. Gleason, A. M. G. Klein Tank, M. Haylock, D. Collins, B. Trewin, F. Rahimzadeh, A. Tagipour, K. Rupa Kumar, J. Revadekar, G. Griffiths, L. Vincent, D. B. Stephenson, J. Burn, E. Aguilar, M. Brunet, M. Taylor, M. New, P. Zhai, M. Rusticucci, and J. L. Vazquez-Aguirre (2006). "Global Observed Changes in Daily Climate Extremes of Temperature and Precipitation". In: *J. Geophys. Res. Atmospheres* 111.D5. ISSN: 2156-2202. DOI: 10.1029/2005JD006290. (Visited on 04/17/2024).
- Alexander, L. V. (2016). "Global Observed Long-Term Changes in Temperature and Precipitation Extremes: A Review of Progress and Limitations in IPCC Assessments and Beyond". In: *Weather and Climate Extremes*. Observed and Projected (Longer-term) Changes in Weather and Climate Extremes 11, pp. 4–16. ISSN: 2212-0947. DOI: 10.1016/j.wace.2015.10.007. (Visited on 04/17/2024).

- Allan, R. P., M. Barlow, M. P. Byrne, A. Cherchi, H. Douville, H. J. Fowler, T. Y. Gan, A. G. Pendergrass, D. Rosenfeld, A. L. S. Swann, L. J. Wilcox, and O. Zolina (2020). “Advances in Understanding Large-Scale Responses of the Water Cycle to Climate Change”. In: *Ann. N. Y. Acad. Sci.* 1472.1, pp. 49–75. ISSN: 1749-6632. DOI: 10.1111/nyas.14337. (Visited on 04/17/2024).
- Anacker, B. L., T. R. Seastedt, T. M. Halward, and A. L. Lezberg (2021). “Soil Carbon and Plant Richness Relationships Differ among Grassland Types, Disturbance History and Plant Functional Groups”. In: *Oecologia* 196.4, pp. 1153–1166. ISSN: 1432-1939. DOI: 10.1007/s00442-021-04992-x. (Visited on 11/20/2024).
- Asner, G. P., A. J. Elmore, L. P. Olander, R. E. Martin, and A. T. Harris (2004). “Grazing Systems, Ecosystem Responses, and Global Change”. In: *Annu. Rev. Environ. Resour.* 29. Volume 29, 2004, pp. 261–299. ISSN: 1543-5938, 1545-2050. DOI: 10.1146/annurev.energy.29.062403.102142. (Visited on 04/17/2024).
- Augustine, D., A. Davidson, K. Dickinson, and B. Van Pelt (2021). “Thinking Like a Grassland: Challenges and Opportunities for Biodiversity Conservation in the Great Plains of North America”. In: *Rangeland Ecology & Management*. Great Plains 78, pp. 281–295. ISSN: 1550-7424. DOI: 10.1016/j.rama.2019.09.001. (Visited on 11/20/2024).
- Bai, Y. and M. F. Cotrufo (2022). “Grassland Soil Carbon Sequestration: Current Understanding, Challenges, and Solutions”. In: *Science* 377.6606, pp. 603–608. DOI: 10.1126/science.abo2380. (Visited on 02/13/2023).
- Bardgett, R. D., J. M. Bullock, S. Lavorel, P. Manning, U. Schaffner, N. Ostle, M. Chomel, G. Durigan, E. L. Fry, D. Johnson, J. M. Lavelle, G. Le Provost, S. Luo, K. Png, M. Sankaran, X. Hou, H. Zhou, L. Ma, W. Ren, X. Li, Y. Ding, Y. Li, and H. Shi (2021). “Combating Global Grassland Degradation”. In: *Nat Rev Earth Environ* 2.10, pp. 720–735. ISSN: 2662-138X. DOI: 10.1038/s43017-021-00207-2. (Visited on 03/08/2022).
- Batunacun, C. Nendel, Y. Hu, and T. Lakes (2018). “Land-Use Change and Land Degradation on the Mongolian Plateau from 1975 to 2015—A Case Study from Xilingol, China”. In: *Land Degrad. Dev.* 29.6, pp. 1595–1606. ISSN: 1099-145X. DOI: 10.1002/ldr.2948. (Visited on 11/20/2024).
- Bergmann, J., A. Weigelt, F. van der Plas, D. C. Laughlin, T. W. Kuyper, N. Guerrero-Ramirez, O. J. Valverde-Barrantes, H. Bruelheide, G. T. Freschet, C. M. Iversen, J. Kattge, M. L. McCormack, I. C. Meier, M. C. Rillig, C. Roumet, M. Semchenko, C. J. Sweeney, J. van Ruijven, L. M. York, and L. Mommer (2020). “The Fungal Collaboration Gradient Dominates the Root Economics Space in Plants”. In: *Sci. Adv.* 6.27, eaba3756. DOI: 10.1126/sciadv.aba3756. (Visited on 03/08/2022).
- Blench, R. (2001). *'You Can't Go Home Again'. Extensive Pastoral Livestock Systems: Issues and Options for the Future*. ODI/FAO Report. London, UK: Overseas Development Institute.
- Bodirsky, B. L., A. Popp, H. Lotze-Campen, J. P. Dietrich, S. Rolinski, I. Weindl, C. Schmitz, C. Müller, M. Bonsch, F. Humpenöder, A. Biewald, and M. Stevanovic (2014). “Reactive Nitrogen Requirements to Feed the World in 2050 and Potential to Mitigate Nitrogen Pollution”. In: *Nat Commun* 5.1, p. 3858. ISSN: 2041-1723. DOI: 10.1038/ncomms4858. (Visited on 04/17/2024).
- Bondeau, A., P. C. Smith, S. Zaehle, S. Schaphoff, W. Lucht, W. Cramer, D. Gerten, H. Lotze-Campen, C. Müller, M. Reichstein, and B. Smith (2007). “Modelling the Role of Agriculture for the 20th Century Global Terrestrial Carbon Balance”. In: *Glob. Change Biol.* 13.3, pp. 679–706. ISSN: 1365-2486. DOI: 10.1111/j.1365-2486.2006.01305.x. (Visited on 05/31/2023).
- Botkin, D. B., J. F. Janak, and J. R. Wallis (1972). “Some Ecological Consequences of a Computer Model of Forest Growth”. In: *J. Ecol.* 60.3, pp. 849–872. ISSN: 0022-0477. DOI: 10.2307/2258570. (Visited on 07/17/2020).
- Brovkin, V., A. Ganopolski, and Y. Svirezhev (1997). “A Continuous Climate-Vegetation Classification for Use in Climate-Biosphere Studies”. In: *Ecol. Model.* 101, pp. 251–261. ISSN: 0304-3800. DOI: 10.1016/S0304-3800(97)00049-5.
- Buzhdygan, O. Y., S. T. Meyer, W. W. Weisser, N. Eisenhauer, A. Ebeling, S. R. Borrett, N. Buchmann, R. Cortois, G. B. De Deyn, H. de Kroon, G. Gleixner, L. R. Hertzog, J. Hines, M. Lange, L. Mommer, J. Ravenek, C. Scherber, M. Scherer-Lorenzen, S. Scheu, B. Schmid, K. Steinauer, T. Strecker, B. Tietjen, A. Vogel, A. Weigelt, and J. S. Petermann (2020). “Biodiversity Increases Multitrophic Energy Use Efficiency, Flow and Storage in Grasslands”. In: *Nat Ecol Evol* 4.3, pp. 393–405. ISSN: 2397-334X. DOI: 10.1038/s41559-020-1123-8. (Visited on 11/20/2023).
- Campbell, B. D. and D. M. Stafford Smith (2000). “A Synthesis of Recent Global Change Research on Pasture and Rangeland Production: Reduced Uncertainties and Their Management Implications”. In: *Agriculture, Ecosystems & Environment* 82.1, pp. 39–55. ISSN: 0167-8809. DOI: 10.1016/S0167-8809(00)00215-2. (Visited on 04/17/2024).
- Campbell, B. D. and J. P. Grime (1992). “An Experimental Test of Plant Strategy Theory”. In: *Ecology* 73.1, pp. 15–29. ISSN: 1939-9170. DOI: 10.2307/1938717. (Visited on 06/13/2022).
- Cang, F. A., A. A. Wilson, and J. J. Wiens (2016). “Climate Change Is Projected to Outpace Rates of Niche Change in Grasses”. In: *Biol. Lett.* 12.9, p. 20160368. DOI: 10.1098/rsbl.2016.0368. (Visited on 04/19/2024).
- Cardinale, B. J., J. E. Duffy, A. Gonzalez, D. U. Hooper, C. Perrings, P. Venail, A. Narwani, G. M. Mace, D. Tilman, D. A. Wardle, A. P. Kinzig, G. C. Daily, M. Loreau, J. B. Grace, A. Larigauderie, D. S. Srivastava, and S. Naeem (2012). “Biodiversity Loss and Its Impact on Humanity”. In: *Nature* 486.7401, pp. 59–67. ISSN: 1476-4687. DOI: 10.1038/nature11148. (Visited on 01/29/2021).
- Chabot, B. F. and D. J. Hicks (1982). “The Ecology of Leaf Life Spans”. In: *Annu. Rev. Ecol. Syst.* 13.1, pp. 229–259. ISSN: 0066-4162. DOI: 10.1146/annurev.es.13.110182.001305. (Visited on 04/19/2024).
- Chang, J., P. Ciais, T. Gasser, P. Smith, M. Herrero, P. Havlík, M. Obersteiner, B. Guenet, D. S. Goll, W. Li, V. Naipal, S. Peng, C. Qiu, H. Tian, N. Viovy, C. Yue, and D. Zhu (2021). “Climate Warming from Managed Grasslands Cancels the Cooling Effect of Carbon Sinks in Sparsely Grazed and Natural Grasslands”. In: *Nat Commun* 12.1, p. 118. ISSN: 2041-1723. DOI: 10.1038/s41467-020-20406-7. (Visited on 04/17/2024).

- Chang, J., P. Ciais, N. Viovy, J.-F. Soussana, K. Klumpp, and B. Sultan (2017). “Future Productivity and Phenology Changes in European Grasslands for Different Warming Levels: Implications for Grassland Management and Carbon Balance”. In: *Carbon Balance and Management* 12.1, p. 11. ISSN: 1750-0680. DOI: 10.1186/s13021-017-0079-8. (Visited on 04/17/2024).
- Chen, S., W. Wang, W. Xu, Y. Wang, H. Wan, D. Chen, Z. Tang, X. Tang, G. Zhou, Z. Xie, D. Zhou, Z. Shanguan, J. Huang, J.-S. He, Y. Wang, J. Sheng, L. Tang, X. Li, M. Dong, Y. Wu, Q. Wang, Z. Wang, J. Wu, F. S. Chapin, and Y. Bai (2018). “Plant Diversity Enhances Productivity and Soil Carbon Storage”. In: *Proc. Natl. Acad. Sci.* 115.16, pp. 4027–4032. DOI: 10.1073/pnas.1700298114. (Visited on 02/13/2023).
- Conant, R. T., C. E. P. Cerri, B. B. Osborne, and K. Paustian (2017). “Grassland Management Impacts on Soil Carbon Stocks: A New Synthesis”. In: *Ecol. Appl.* 27.2, pp. 662–668. ISSN: 1939-5582. DOI: 10.1002/eap.1473. (Visited on 02/13/2023).
- Conijn, J. G., P. S. Bindraban, J. J. Schröder, and R. E. E. Jongschaap (2018). “Can Our Global Food System Meet Food Demand within Planetary Boundaries?” In: *Agriculture, Ecosystems & Environment* 251, pp. 244–256. ISSN: 0167-8809. DOI: 10.1016/j.agee.2017.06.001. (Visited on 04/17/2024).
- Costanza, R., R. d’Arge, R. de Groot, S. Farber, M. Grasso, B. Hannon, K. Limburg, S. Naeem, R. V. O’Neill, J. Paruelo, R. G. Raskin, P. Sutton, and M. van den Belt (1997). “The Value of the World’s Ecosystem Services and Natural Capital”. In: *Nature* 387.6630, pp. 253–260. ISSN: 1476-4687. DOI: 10.1038/387253a0. (Visited on 04/19/2024).
- Craven, D., F. Isbell, P. Manning, J. Connolly, H. Bruelheide, A. Ebeling, C. Roscher, J. van Ruijven, A. Weigelt, B. Wilsey, C. Beierkuhnlein, E. de Luca, J. N. Griffin, Y. Hautier, A. Hector, A. Jentsch, J. Kreyling, V. Lanta, M. Loreau, S. T. Meyer, A. S. Mori, S. Naeem, C. Palmberg, H. W. Polley, P. B. Reich, B. Schmid, A. Siebenkäs, E. Seabloom, M. P. Thakur, D. Tilman, A. Vogel, and N. Eisenhauer (2016). “Plant Diversity Effects on Grassland Productivity Are Robust to Both Nutrient Enrichment and Drought”. In: *Philos. Trans. R. Soc. B Biol. Sci.* 371.1694. ISSN: 0962-8436. DOI: 10.1098/rstb.2015.0277. (Visited on 12/09/2019).
- Crippa, M., E. Solazzo, D. Guizzardi, F. Monforti-Ferrario, F. N. Tubiello, and A. Leip (2021). “Food Systems Are Responsible for a Third of Global Anthropogenic GHG Emissions”. In: *Nat Food* 2.3, pp. 198–209. ISSN: 2662-1355. DOI: 10.1038/s43016-021-00225-9. (Visited on 04/17/2024).
- Díaz, S., J. Kattge, J. H. C. Cornelissen, I. J. Wright, S. Lavorel, S. Dray, B. Reu, M. Kleyer, C. Wirth, I. C. Prentice, E. Garnier, G. Bönisch, M. Westoby, H. Poorter, P. B. Reich, A. T. Moles, J. Dickie, A. N. Gillison, A. E. Zanne, J. Chave, S. J. Wright, S. N. Sheremet’ev, H. Jactel, C. Baraloto, B. Cerabolini, S. Pierce, B. Shipley, D. Kirkup, F. Casanoves, J. S. Joswig, A. Günther, V. Falczuk, N. Rüger, M. D. Mahecha, and L. D. Gorné (2016). “The Global Spectrum of Plant Form and Function”. In: *Nature* 529.7585, pp. 167–171. ISSN: 1476-4687. DOI: 10.1038/nature16489. (Visited on 03/24/2020).
- Dumont, B., D. Andueza, V. Niderkorn, A. Lüscher, C. Porqueddu, and C. Picon-Cochard (2015). “A Meta-Analysis of Climate Change Effects on Forage Quality in Grasslands: Specificities of Mountain and Mediterranean Areas”. In: *Grass Forage Sci.* 70.2, pp. 239–254. ISSN: 1365-2494. DOI: 10.1111/gfs.12169. (Visited on 04/17/2024).
- FAO, GDP, and IFCN (2020). *Dairy’s Impact on Reducing Global Hungry*. Tech. rep. Chicago, Illinois, USA. (Visited on 01/24/2025).
- FAO, IFAD, UNICEF, WFP, and WHO (2023). *The State of Food Security and Nutrition in the World 2023. Urbanization, Agrifood Systems Transformation and Healthy Diets across the Rural–Urban Continuum*. Rome: FAO. ISBN: 978-92-5-137226-5. DOI: 10.4060/cc3017en. (Visited on 04/15/2024).
- Fargione, J., C. S. Brown, and D. Tilman (2003). “Community Assembly and Invasion: An Experimental Test of Neutral versus Niche Processes”. In: *Proc. Natl. Acad. Sci.* 100.15, pp. 8916–8920. DOI: 10.1073/pnas.1033107100. (Visited on 04/25/2024).
- Frank, D., M. Reichstein, M. Bahn, K. Thonicke, D. Frank, M. D. Mahecha, P. Smith, M. van der Velde, S. Vicca, F. Babst, C. Beer, N. Buchmann, J. G. Canadell, P. Ciais, W. Cramer, A. Ibrom, F. Miglietta, B. Poulter, A. Rammig, S. I. Seneviratne, A. Walz, M. Wattenbach, M. A. Zavala, and J. Zscheischler (2015). “Effects of Climate Extremes on the Terrestrial Carbon Cycle: Concepts, Processes and Potential Future Impacts”. In: *Glob. Change Biol.* 21.8, pp. 2861–2880. ISSN: 1365-2486. DOI: 10.1111/gcb.12916. (Visited on 04/17/2024).
- Franks, P. J., M. A. Adams, J. S. Amthor, M. M. Barbour, J. A. Berry, D. S. Ellsworth, G. D. Farquhar, O. Ghannoum, J. Lloyd, N. McDowell, R. J. Norby, D. T. Tissue, and S. von Caemmerer (2013). “Sensitivity of Plants to Changing Atmospheric CO<sub>2</sub> Concentration: From the Geological Past to the next Century”. In: *New Phytol.* 197.4, pp. 1077–1094. ISSN: 1469-8137. DOI: 10.1111/nph.12104. (Visited on 04/17/2024).
- Gaujour, E., B. Amiaud, C. Mignolet, and S. Plantureux (2012). “Factors and Processes Affecting Plant Biodiversity in Permanent Grasslands. A Review”. In: *Agron. Sustain. Dev.* 32.1, pp. 133–160. ISSN: 1773-0155. DOI: 10.1007/s13593-011-0015-3. (Visited on 11/20/2024).
- Gerber, P. J., H. Steinfeld, B. Henderson, A. Mottet, C. Opio, J. Dijkman, A. Falcucci, and G. Tempio, eds. (2013). *Tackling Climate Change through Livestock: A Global Assessment of Emissions and Mitigation Opportunities*. Rome: Food and Agriculture Organization of the United Nations (FAO). ISBN: 978-92-5-107920-1.
- Gibson, D. J. (2008). *Grasses and Grassland Ecology*. OUP Oxford. ISBN: 978-0-19-154609-9.
- Grace, J. B., T. M. Anderson, E. W. Seabloom, E. T. Borer, P. B. Adler, W. S. Harpole, Y. Hautier, H. Hillebrand, E. M. Lind, M. Pärtel, J. D. Bakker, Y. M. Buckley, M. J. Crawley, E. I. Damschen, K. F. Davies, P. A. Fay, J. Firn, D. S. Gruner, A. Hector, J. M. H. Knops, A. S. MacDougall, B. A. Melbourne, J. W. Morgan, J. L. Orrock, S. M. Prober, and M. D. Smith (2016). “Integrative Modelling Reveals Mechanisms Linking Productivity and Plant Species Richness”. In: *Nature* 529.7586, pp. 390–393. ISSN: 1476-4687. DOI: 10.1038/nature16524. (Visited on 03/11/2019).

- Gregory, P., J. Ingram, and M. Brklacich (2005). “Climate Change and Food Security”. In: *Philos. Trans. R. Soc. B Biol. Sci.* 360.1463, pp. 2139–2148. DOI: 10.1098/rstb.2005.1745. (Visited on 04/17/2024).
- Grime, J. P. (1974). “Vegetation Classification by Reference to Strategies”. In: *Nature* 250.5461, pp. 26–31. ISSN: 0028-0836, 1476-4687. DOI: 10.1038/250026a0. (Visited on 06/13/2022).
- Grime, J. P. (1977). “Evidence for the Existence of Three Primary Strategies in Plants and Its Relevance to Ecological and Evolutionary Theory”. In: *Am. Nat.* 111.982, pp. 1169–1194. ISSN: 0003-0147,1537-5323. DOI: 10.1086/283244. (Visited on 10/28/2021).
- Guo, Y., E. H. Boughton, S. Bohlman, C. Bernacchi, P. J. Bohlen, R. Boughton, E. DeLucia, J. E. Fauth, N. Gomez-Casanovas, D. G. Jenkins, G. Lollis, R. S. Miller, P. F. Quintana-Ascencio, G. Sonnier, J. Sparks, H. M. Swain, and J. Qiu (2023). “Grassland Intensification Effects Cascade to Alter Multifunctionality of Wetlands within Metaecosystems”. In: *Nat Commun* 14.1, p. 8267. ISSN: 2041-1723. DOI: 10.1038/s41467-023-44104-2. (Visited on 11/20/2024).
- Hector, A. and R. Bagchi (2007). “Biodiversity and Ecosystem Multifunctionality”. In: *Nature* 448.7150, pp. 188–190. ISSN: 1476-4687. DOI: 10.1038/nature05947. (Visited on 04/25/2024).
- Heinke, J., M. Lannerstad, D. Gerten, P. Havlík, M. Herrero, A. M. O. Notenbaert, H. Hoff, and C. Müller (2020). “Water Use in Global Livestock Production—Opportunities and Constraints for Increasing Water Productivity”. In: *Water Resour. Res.* 56.12, e2019WR026995. ISSN: 1944-7973. DOI: 10.1029/2019WR026995. (Visited on 04/17/2024).
- Heinke, J., S. Rolinski, and C. Müller (2023). “Modelling the Role of Livestock Grazing in C and N Cycling in Grasslands with LPJmL5.0-Grazing”. In: *Geosci. Model Dev.* 16.9, pp. 2455–2475. ISSN: 1991-959X. DOI: 10.5194/gmd-16-2455-2023. (Visited on 05/31/2023).
- Herrero, M., R. H. Fawcett, V. Silveira, J. Busqué, A. Bernués, and J. B. Dent (2000). “Modelling the Growth and Utilisation of Kikuyu Grass (*Pennisetum Clandestinum*) under Grazing. 1. Model Definition and Parameterisation”. In: *Agricultural Systems* 65.2, pp. 73–97. ISSN: 0308-521X. DOI: 10.1016/S0308-521X(00)00028-7. (Visited on 11/02/2021).
- Herrero, M., D. Grace, J. Njuki, N. Johnson, D. Enahoro, S. Silvestri, and M. C. Rufino (2013a). “The Roles of Livestock in Developing Countries”. In: *Animal* 7, pp. 3–18. ISSN: 1751-7311. DOI: 10.1017/S1751731112001954. (Visited on 04/15/2024).
- Herrero, M., P. Havlik, H. Valin, A. Notenbaert, M. C. Rufino, P. K. Thornton, M. Blummel, F. Weiss, D. Grace, and M. Obersteiner (2013b). “Biomass Use, Production, Feed Efficiencies, and Greenhouse Gas Emissions from Global Livestock Systems”. In: *Proc. Natl. Acad. Sci.* 110.52, pp. 20888–20893. ISSN: 0027-8424, 1091-6490. DOI: 10.1073/pnas.1308149110. (Visited on 03/06/2019).
- Herrero, M., B. Henderson, P. Havlík, P. K. Thornton, R. T. Conant, P. Smith, S. Wirsenius, A. N. Hristov, P. Gerber, M. Gill, K. Butterbach-Bahl, H. Valin, T. Garnett, and E. Stehfest (2016). “Greenhouse Gas Mitigation Potentials in the Livestock Sector”. In: *Nature Clim Change* 6.5, pp. 452–461. ISSN: 1758-6798. DOI: 10.1038/nclimate2925. (Visited on 04/17/2024).
- Holubek, I. and F. Petrovic (2011). “An Economic Analysis of Permanent and Oversown Grasslands Based on the Data from Research Experiments”. In: *Ekológia Slovak Repub.* 30.1. ISSN: 1335-342X. (Visited on 11/20/2024).
- Hoover, D. L., A. K. Knapp, and M. D. Smith (2014). “Resistance and Resilience of a Grassland Ecosystem to Climate Extremes”. In: *Ecology* 95.9, pp. 2646–2656. ISSN: 1939-9170. DOI: 10.1890/13-2186.1. (Visited on 01/13/2021).
- Isbell, F., V. Calcagno, A. Hector, J. Connolly, W. S. Harpole, P. B. Reich, M. Scherer-Lorenzen, B. Schmid, D. Tilman, J. van Ruijven, A. Weigelt, B. J. Wilsey, E. S. Zavaleta, and M. Loreau (2011). “High Plant Diversity Is Needed to Maintain Ecosystem Services”. In: *Nature* 477.7363, pp. 199–202. ISSN: 1476-4687. DOI: 10.1038/nature10282. (Visited on 04/25/2024).
- Isbell, F., D. Craven, J. Connolly, M. Loreau, B. Schmid, C. Beierkuhnlein, T. M. Bezemer, C. Bonin, H. Bruelheide, E. de Luca, A. Ebeling, J. N. Griffin, Q. Guo, Y. Hautier, A. Hector, A. Jentsch, J. Kreyling, V. Lanta, P. Manning, S. T. Meyer, A. S. Mori, S. Naeem, P. A. Niklaus, H. W. Polley, P. B. Reich, C. Roscher, E. W. Seabloom, M. D. Smith, M. P. Thakur, D. Tilman, B. F. Tracy, W. H. van der Putten, J. van Ruijven, A. Weigelt, W. W. Weisser, B. Wilsey, and N. Eisenhauer (2015a). “Biodiversity Increases the Resistance of Ecosystem Productivity to Climate Extremes”. In: *Nature* 526.7574, pp. 574–577. ISSN: 1476-4687. DOI: 10.1038/nature15374. (Visited on 05/22/2019).
- Isbell, F., D. Tilman, S. Polasky, and M. Loreau (2015b). “The Biodiversity-Dependent Ecosystem Service Debt”. In: *Ecol. Lett.* 18.2, pp. 119–134. ISSN: 1461-0248. DOI: 10.1111/ele.12393. (Visited on 11/20/2024).
- Jägermeyr, J., D. Gerten, J. Heinke, S. Schaphoff, M. Kummu, and W. Lucht (2015). “Water Savings Potentials of Irrigation Systems: Global Simulation of Processes and Linkages”. In: *Hydrol. Earth Syst. Sci.* 19.7, pp. 3073–3091. ISSN: 1027-5606. DOI: 10.5194/hess-19-3073-2015. (Visited on 06/19/2023).
- Jägermeyr, J., C. Müller, A. C. Ruane, J. Elliott, J. Balkovic, O. Castillo, B. Faye, I. Foster, C. Folberth, J. A. Franke, K. Fuchs, J. R. Guarin, J. Heinke, G. Hoogenboom, T. Iizumi, A. K. Jain, D. Kelly, N. Khabarov, S. Lange, T.-S. Lin, W. Liu, O. Mialyk, S. Minoli, E. J. Moyer, M. Okada, M. Phillips, C. Porter, S. S. Rabin, C. Scheer, J. M. Schneider, J. F. Schyns, R. Skalsky, A. Smerald, T. Stella, H. Stephens, H. Webber, F. Zabel, and C. Rosenzweig (2021). “Climate Impacts on Global Agriculture Emerge Earlier in New Generation of Climate and Crop Models”. In: *Nat Food* 2.11, pp. 873–885. ISSN: 2662-1355. DOI: 10.1038/s43016-021-00400-y. (Visited on 04/17/2024).
- Jägermeyr, J., A. Pastor, H. Biemans, and D. Gerten (2017). “Reconciling Irrigated Food Production with Environmental Flows for Sustainable Development Goals Implementation”. In: *Nat Commun* 8.1, p. 15900. ISSN: 2041-1723. DOI: 10.1038/ncomms15900. (Visited on 10/05/2023).
- Johnson, I. R. and A. J. Parsons (1985). “A Theoretical Analysis of Grass Growth under Grazing”. In: *Journal of Theoretical Biology* 112.2, pp. 345–367. ISSN: 0022-5193. DOI: 10.1016/S0022-5193(85)80292-7. (Visited on 04/25/2024).

- Jones, M. B. and A. Donnelly (2004). "Carbon Sequestration in Temperate Grassland Ecosystems and the Influence of Management, Climate and Elevated CO<sub>2</sub>". In: *New Phytol.* 164.3, pp. 423–439. ISSN: 1469-8137. DOI: 10.1111/j.1469-8137.2004.01201.x. (Visited on 04/19/2024).
- Kattge, J., G. Bönisch, S. Díaz, S. Lavorel, I. C. Prentice, P. Leadley, S. Tautenhahn, G. D. A. Werner, T. Aakala, M. Abedi, A. T. R. Acosta, G. C. Adamidis, K. Adamson, M. Aiba, C. H. Albert, J. M. Alcántara, C. Alcázar C, I. Aleixo, H. Ali, B. Amiaud, C. Ammer, M. M. Amoroso, M. Anand, C. Anderson, N. Anten, J. Antos, D. M. G. Apgaua, T.-L. Ashman, D. H. Asmara, G. P. Asner, M. Aspinwall, O. Atkin, I. Aubin, L. Baastrup-Spohr, K. Bahalkeh, M. Bahn, T. Baker, W. J. Baker, J. P. Bakker, D. Baldocchi, J. Baltzer, A. Banerjee, A. Baranger, J. Barlow, D. R. Barneche, Z. Baruch, D. Bastianelli, J. Battles, W. Bauerle, M. Bauters, E. Bazzato, M. Beckmann, H. Beeckman, C. Beierkuhnlein, R. Bekker, G. Belfry, M. Belluau, M. Beloiu, R. Benavides, L. Benomar, M. L. Berdugo-Lattke, E. Berenguer, R. Bergamin, J. Bergmann, M. Bergmann Carlucci, L. Berner, M. Bernhardt-Römermann, C. Bigler, A. D. Bjorkman, C. Blackman, C. Blanco, B. Blonder, D. Blumenthal, K. T. Bocanegra-González, P. Boeckx, S. Bohlman, K. Böhning-Gaese, L. Boisvert-Marsh, W. Bond, B. Bond-Lamberty, A. Boom, C. C. F. Boonman, K. Bordin, E. H. Boughton, V. Boukili, D. M. J. S. Bowman, S. Bravo, M. R. Brendel, M. R. Broadley, K. A. Brown, H. Bruelheide, F. Brunnich, H. H. Bruun, D. Bruy, S. W. Buchanan, S. F. Bucher, N. Buchmann, R. Buitenwerf, D. E. Bunker, J. Bürger, S. Burrascano, D. F. R. P. Burslem, B. J. Butterfield, C. Byun, M. Marques, M. C. Scalon, M. Caccianiga, M. Cadotte, M. Cailleret, J. Camac, J. J. Camarero, C. Company, G. Campetella, J. A. Campos, L. Cano-Arboleda, R. Canullo, M. Carbognani, F. Carvalho, F. Casanoves, B. Castagneyrol, J. A. Catford, J. Cavender-Bares, B. E. L. Cerabolini, M. Cervellini, E. Chacón-Madrigal, K. Chapin, F. S. Chapin, S. Chelli, S.-C. Chen, A. Chen, P. Cherubini, F. Chianucci, B. Choat, K.-S. Chung, M. Chytrý, D. Ciccarelli, L. Coll, C. G. Collins, L. Conti, D. Coomes, J. H. C. Cornelissen, W. K. Cornwell, P. Corona, M. Coyea, J. Craine, D. Craven, J. P. G. M. Cromsigt, A. Csecserits, K. Cufar, M. Cuntz, A. C. da Silva, K. M. Dahlin, M. Dainese, I. Dalke, M. Dalle Fratte, A. T. Dang-Le, J. Danihelka, M. Dannoura, S. Dawson, A. J. de Beer, A. De Frutos, J. R. De Long, B. Dechant, S. Delagrangue, N. Delpierre, G. Derroire, A. S. Dias, M. H. Diaz-Toribio, P. G. Dimitrakopoulos, M. Dobrowolski, D. Doktor, P. Dřevojan, N. Dong, J. Dransfield, S. Dressler, L. Duarte, E. Ducouret, S. Dullinger, W. Durka, R. Duursma, O. Dymova, A. E-Vojtkó, R. L. Eckstein, H. Ejtehadi, J. Elser, T. Emilio, K. Engemann, M. B. Erfanian, A. Erfmeier, A. Esquivel-Muelbert, G. Esser, M. Estiarte, T. F. Domingues, W. F. Fagan, J. Fagúndez, D. S. Falster, Y. Fan, J. Fang, E. Farris, F. Fazlioglu, Y. Feng, F. Fernandez-Mendez, C. Ferrara, J. Ferreira, A. Fidelis, B. Finegan, J. Firn, T. J. Flowers, D. F. B. Flynn, V. Fontana, E. Forey, C. Forgiarini, L. François, M. Frangipani, D. Frank, C. Frenette-Dussault, G. T. Freschet, E. L. Fry, N. M. Fyllas, G. G. Mazzochini, S. Gachet, M. Gallagher, G. Ganade, F. Ganga, P. García-Palacios, V. Gargaglione, E. Garnier, J. L. Garrido, A. L. de Gasper, G. Gea-Izquierdo, D. Gibson, A. N. Gillison, A. Giroldo, M.-C. Glasenhardt, S. Gleason, M. Gliesch, E. Goldberg, B. Gödel, E. Gonzalez-Akre, J. L. Gonzalez-Andujar, A. González-Melo, A. González-Robles, B. J. Graae, E. Granda, S. Graves, W. A. Green, T. Gregor, N. Gross, G. R. Guerin, A. Günther, A. G. Gutiérrez, L. Haddock, A. Haines, J. Hall, A. Hambuckers, W. Han, S. P. Harrison, W. Hattingh, J. E. Hawes, T. He, P. He, J. M. Heberling, A. Helm, S. Hempel, J. Hentschel, B. Hérault, A.-M. Hereş, K. Herz, M. Heuertz, T. Hickler, P. Hietz, P. Higuchi, A. L. Hipp, A. Hirons, M. Hock, J. A. Hogan, K. Holl, O. Honnay, D. Hornstein, E. Hou, N. Hough-Snee, K. A. Hovstad, T. Ichie, B. Igić, E. Illa, M. Isaac, M. Ishihara, L. Ivanov, L. Ivanova, C. M. Iversen, J. Izquierdo, R. B. Jackson, B. Jackson, H. Jactel, A. M. Jagodzinski, U. Jandt, S. Jansen, T. Jenkins, A. Jentsch, J. R. P. Jaspersen, G.-F. Jiang, J. L. Johansen, D. Johnson, E. J. Jokela, C. A. Joly, G. J. Jordan, G. S. Joseph, D. Junaedi, R. R. Junker, E. Justes, R. Kabzems, J. Kane, Z. Kaplan, T. Kattenborn, L. Kavelanova, E. Kearsley, A. Kempel, T. Kenzo, A. Kerkhoff, M. I. Khalil, N. L. Kinlock, W. D. Kissling, K. Kitajima, T. Kitzberger, R. Kjeller, T. Klein, M. Kleyer, J. Klimešová, J. Klipel, B. Kloeppel, S. Klotz, J. M. H. Knops, T. Kohyama, F. Koike, J. Kollmann, B. Komac, K. Komatsu, C. König, N. J. B. Kraft, K. Kramer, H. Kreft, I. Kühn, D. Kumarathunge, J. Kuppler, H. Kurokawa, Y. Kurosawa, S. Kuyah, J.-P. Laclau, B. Lafleur, E. Lallai, E. Lamb, A. Lamprecht, D. J. Larkin, D. Laughlin, Y. Le Bagousse-Pinguet, G. le Maire, P. C. le Roux, E. le Roux, T. Lee, F. Lens, S. L. Lewis, B. Lhotsky, Y. Li, X. Li, J. W. Lichstein, M. Liebergesell, J. Y. Lim, Y.-S. Lin, J. C. Linares, C. Liu, D. Liu, U. Liu, S. Livingstone, J. Llusà, M. Lohbeck, Á. López-García, G. Lopez-Gonzalez, Z. Lososová, F. Louault, B. A. Lukács, P. Lukeš, Y. Luo, M. Lussu, S. Ma, C. Maciel Rabelo Pereira, M. Mack, V. Maire, A. Mäkelä, H. Mäkinen, A. C. M. Malhado, A. Mallik, P. Manning, S. Manzoni, Z. Marchetti, L. Marchino, V. Marcilio-Silva, E. Marcon, M. Marignani, L. Markesteijn, A. Martin, C. Martínez-Garza, J. Martínez-Vilalta, T. Mašková, K. Mason, N. Mason, T. J. Massad, J. Masse, I. Mayrose, J. McCarthy, M. L. McCormack, K. McCulloh, I. R. McFadden, B. J. McGill, M. Y. McPartland, J. S. Medeiros, B. Medlyn, P. Meerts, Z. Mehrabi, P. Meir, F. P. L. Melo, M. Mencuccini, C. Meredieu, J. Messier, I. Mészáros, J. Metsaranta, S. T. Michaletz, C. Michelaki, S. Migalina, R. Milla, J. E. D. Miller, V. Minden, R. Ming, K. Mokany, A. T. Moles, A. Molnár V, J. Molofsky, M. Molz, R. A. Montgomery, A. Monty, L. Moravcová, A. Moreno-Martínez, M. Moretti, A. S. Mori, S. Mori, D. Morris, J. Morrison, L. Mucina, S. Mueller, C. D. Muir, S. C. Müller, F. Munoz, I. H. Myers-Smith, R. W. Myster, M. Nagano, S. Naidu, A. Narayanan, B. Natesan, L. Negoita, A. S. Nelson, E. L. Neuschulz, J. Ni, G. Niedrist, J. Nieto, Ü. Niinemets, R. Nolan, H. Nottebrock, Y. Nouvellon, A. Novakovskiy, T. N. Network, K. O. Nystuen, A. O'Grady, K. O'Hara, A. O'Reilly-Nugent, S. Oakley, W. Oberhuber, T. Ohtsuka, R. Oliveira, K. Öllerer, M. E. Olson, V. Onipchenko, Y. Onoda, R. E. Onstein, J. C. Ordonez, N. Osada, I. Ostonen, G. Ottaviani, S. Otto, G. E. Overbeck, W. A. Ozinga, A. T. Pahl, C. E. T. Paine, R. J. Pakeman, A. C. Papageorgiou, E. Parfionova, M. Pärtel, M. Patacca, S. Paula, J. Paule, H. Pauli, J. G. Pausas, B. Peco, J. Penuelas, A. Perea, P. L. Peri, A. C. Petisco-Souza, A. Petraglia, A. M. Petritan, O. L. Phillips, S. Pierce, V. D. Pillar, J. Pisek, A. Pomogaybin, H. Poorter, A. Portsmouth, P. Poschlod, C. Potvin, D. Pounds, A. S. Powell, S. A. Power, A. Prinzing, G. Puglielli, P. Pyšek, V. Raavel, A. Rammig, J. Ransijn, C. A. Ray, P. B. Reich, M. Reichstein, D. E. B. Reid, M. Réjou-Méchain, V. R. de Dios, S. Ribeiro, S. Richardson, K. Riibak, M. C. Rillig, F. Riviera, E. M. R. Robert, S. Roberts, B. Robroek, A. Roddy, A. V. Rodrigues, A. Rogers, E. Rollinson, V. Rolo,

- C. Römermann, D. Ronzhina, C. Roscher, J. A. Rosell, M. F. Rosenfield, C. Rossi, D. B. Roy, S. Royer-Tardif, N. Rüger, R. Ruiz-Peinado, S. B. Rumpf, G. M. Rusch, M. Ryo, L. Sack, A. Saldaña, B. Salgado-Negret, R. Salguero-Gomez, I. Santa-Regina, A. C. Santacruz-García, J. Santos, J. Sardans, B. Schamp, M. Scherer-Lorenzen, M. Schleuning, B. Schmid, M. Schmidt, S. Schmitt, J. V. Schneider, S. D. Schowanek, J. Schrader, F. Schrod, B. Schuldt, F. Schurr, G. Selaya Garvizu, M. Semchenko, C. Seymour, J. C. Sfair, J. M. Sharpe, C. S. Sheppard, S. Sheremetiev, S. Shiodera, B. Shipley, T. A. Shovon, A. Siebenkäs, C. Sierra, V. Silva, M. Silva, T. Sitzia, H. Sjöman, M. Slot, N. G. Smith, D. Sodhi, P. Soltis, D. Soltis, B. Somers, G. Sonnier, M. V. Sørensen, E. E. Sosinski Jr, N. A. Soudzilovskaia, A. F. Souza, M. Spasojevic, M. G. Sperandii, A. B. Stan, J. Stegen, K. Steinbauer, J. G. Stephan, F. Sterck, D. B. Stojanovic, T. Strydom, M. L. Suarez, J.-C. Svenning, I. Svitková, M. Svitok, M. Svoboda, E. Swaine, N. Swenson, M. Tabarelli, K. Takagi, U. Tappeiner, R. Tarifa, S. Tauougourdeau, C. Tavsanoğlu, M. te Beest, L. Tedersoo, N. Thiffault, D. Thom, E. Thomas, K. Thompson, P. E. Thornton, W. Thuiller, L. Tichý, D. Tissue, M. G. Tjoelker, D. Y. P. Tng, J. Tobias, P. Török, T. Tarin, J. M. Torres-Ruiz, B. Tóthmérész, M. Treurnicht, V. Trivellone, F. Trolliet, V. Trotsiuk, J. L. Tsakalos, I. Tsiripidis, N. Tysklind, T. Umehara, V. Usoltsev, M. Vadeboncoeur, J. Vaezi, F. Valladares, J. Vamosi, P. M. van Bodegom, M. van Breugel, E. Van Cleemput, M. van de Weg, S. van der Merwe, F. van der Plas, M. T. van der Sande, M. van Kleunen, K. Van Meerbeek, M. Vanderwel, K. A. Vanselow, A. Vårhammar, L. Varone, M. Y. Vasquez Valderrama, K. Vassilev, M. Vellend, E. J. Veneklaas, H. Verbeeck, K. Verheyen, A. Vibrans, I. Vieira, J. Villacís, C. Violle, P. Vivek, K. Wagner, M. Waldram, A. Waldron, A. P. Walker, M. Waller, G. Walther, H. Wang, F. Wang, W. Wang, H. Watkins, J. Watkins, U. Weber, J. T. Weedon, L. Wei, P. Weigelt, E. Weiher, A. W. Wells, C. Wellstein, E. Wenk, M. Westoby, A. Westwood, P. J. White, M. Whitten, M. Williams, D. E. Winkler, K. Winter, C. Womack, I. J. Wright, S. J. Wright, J. Wright, B. X. Pinho, F. Ximenes, T. Yamada, K. Yamaji, R. Yanai, N. Yankov, B. Yguel, K. J. Zanini, A. E. Zanne, D. Zelený, Y.-P. Zhao, J. Zheng, J. Zheng, K. Ziemińska, C. R. Zirbel, G. Zizka, I. C. Zo-Bi, G. Zotz, and C. Wirth (2020). “TRY Plant Trait Database – Enhanced Coverage and Open Access”. In: *Glob. Change Biol.* 26.1, pp. 119–188. ISSN: 1365-2486. DOI: 10.1111/gcb.14904. (Visited on 04/19/2024).
- Kirschbaum, M. U. (2011). “Does Enhanced Photosynthesis Enhance Growth? Lessons Learned from CO<sub>2</sub> Enrichment Studies”. In: *Plant Physiology* 155.1, pp. 117–124. ISSN: 0032-0889. DOI: 10.1104/pp.110.166819. (Visited on 04/17/2024).
- Lange, S., J. Volkholz, T. Geiger, F. Zhao, I. Vega, T. Veldkamp, C. P. O. Reyer, L. Warszawski, V. Huber, J. Jägermeyr, J. Schewe, D. N. Bresch, M. Büchner, J. Chang, P. Ciais, M. Dury, K. Emanuel, C. Folberth, D. Gerten, S. N. Gosling, M. Grillakis, N. Hanasaki, A.-J. Henrot, T. Hickler, Y. Honda, A. Ito, N. Khabarov, A. Koutroulis, W. Liu, C. Müller, K. Nishina, S. Ostberg, H. Müller Schmied, S. I. Seneviratna, T. Stacke, J. Steinkamp, W. Thiery, Y. Wada, S. Willner, H. Yang, M. Yoshikawa, C. Yue, and K. Frieler (2020). “Projecting Exposure to Extreme Climate Impact Events Across Six Event Categories and Three Spatial Scales”. In: *Earths Future* 8.12, e2020EF001616. ISSN: 2328-4277. DOI: 10.1029/2020EF001616. (Visited on 04/17/2024).
- Lee, M., E. Shevliakova, S. Malyshev, P. C. D. Milly, and P. R. Jaffé (2016). “Climate Variability and Extremes, Interacting with Nitrogen Storage, Amplify Eutrophication Risk”. In: *Geophys. Res. Lett.* 43.14, pp. 7520–7528. ISSN: 1944-8007. DOI: 10.1002/2016GL069254. (Visited on 04/17/2024).
- Leroy, F., N. W. Smith, A. T. Adesogan, T. Beal, L. Iannotti, P. J. Moughan, and N. Mann (2023). “The Role of Meat in the Human Diet: Evolutionary Aspects and Nutritional Value”. In: *Animal Frontiers* 13.2, pp. 11–18. ISSN: 2160-6056. DOI: 10.1093/af/vfac093. (Visited on 01/24/2025).
- Li, C., F. Zwiers, X. Zhang, G. Li, Y. Sun, and M. Wehner (2021). “Changes in Annual Extremes of Daily Temperature and Precipitation in CMIP6 Models”. In: *J. Clim.* 34.9, pp. 3441–3460. ISSN: 0894-8755, 1520-0442. DOI: 10.1175/JCLI-D-19-1013.1. (Visited on 04/17/2024).
- Li, W., X. Li, Y. Zhao, S. Zheng, and Y. Bai (2018). “Ecosystem Structure, Functioning and Stability under Climate Change and Grazing in Grasslands: Current Status and Future Prospects”. In: *Current Opinion in Environmental Sustainability. System Dynamics and Sustainability* 33, pp. 124–135. ISSN: 1877-3435. DOI: 10.1016/j.cosust.2018.05.008. (Visited on 04/17/2024).
- Linstädter, A., J. Schellberg, K. Brüser, C. A. M. García, R. J. Oomen, C. C. du Preez, J. C. Ruppert, and F. Ewert (2014). “Are There Consistent Grazing Indicators in Drylands? Testing Plant Functional Types of Various Complexity in South Africa’s Grassland and Savanna Biomes”. In: *PLOS ONE* 9.8, e104672. ISSN: 1932-6203. DOI: 10.1371/journal.pone.0104672. (Visited on 04/25/2024).
- Lutz, F., T. Herzfeld, J. Heinke, S. Rolinski, S. Schaphoff, W. von Bloh, J. J. Stoorvogel, and C. Müller (2019). “Simulating the Effect of Tillage Practices with the Global Ecosystem Model LPJmL (Version 5.0-Tillage)”. In: *Geosci. Model Dev.* 12.6, pp. 2419–2440. ISSN: 1991-959X. DOI: 10.5194/gmd-12-2419-2019. (Visited on 05/31/2023).
- Ma, J., S. Olin, P. Anthoni, S. S. Rabin, A. D. Bayer, S. S. Nyawira, and A. Arneith (2022). “Modeling Symbiotic Biological Nitrogen Fixation in Grain Legumes Globally with LPJ-GUESS (v4.0, R10285)”. In: *Geosci. Model Dev.* 15.2, pp. 815–839. ISSN: 1991-959X. DOI: 10.5194/gmd-15-815-2022. (Visited on 02/18/2022).
- May, F., V. Grimm, and F. Jeltsch (2009). “Reversed Effects of Grazing on Plant Diversity: The Role of below-Ground Competition and Size Symmetry”. In: *Oikos* 118.12, pp. 1830–1843. ISSN: 1600-0706. DOI: 10.1111/j.1600-0706.2009.17724.x. (Visited on 06/23/2021).
- McMahon, S. M., S. P. Harrison, W. S. Armbruster, P. J. Bartlein, C. M. Beale, M. E. Edwards, J. Kattge, G. Midgley, X. Morin, and I. C. Prentice (2011). “Improving Assessment and Modelling of Climate Change Impacts on Global Terrestrial Biodiversity”. In: *Trends in Ecology & Evolution* 26.5, pp. 249–259. ISSN: 0169-5347. DOI: 10.1016/j.tree.2011.02.012. (Visited on 04/25/2024).
- McSherry, M. E. and M. E. Ritchie (2013). “Effects of Grazing on Grassland Soil Carbon: A Global Review”. In: *Glob. Change Biol.* 19.5, pp. 1347–1357. ISSN: 1365-2486. DOI: 10.1111/gcb.12144. (Visited on 06/13/2022).

- Melts, I., K. Lanno, M. Sammuli, K. Uchida, K. Heinsoo, T. Kull, and L. Laanisto (2018). “Fertilising Semi-Natural Grasslands May Cause Long-Term Negative Effects on Both Biodiversity and Ecosystem Stability”. In: *J. Appl. Ecol.* 55.4, pp. 1951–1955. ISSN: 1365-2664. DOI: 10.1111/1365-2664.13129. (Visited on 11/20/2024).
- Mitchell, R. M., J. P. Wright, and G. M. Ames (2018). “Species’ Traits Do Not Converge on Optimum Values in Preferred Habitats”. In: *Oecologia* 186.3, pp. 719–729. ISSN: 1432-1939. DOI: 10.1007/s00442-017-4041-y. (Visited on 04/25/2024).
- Nöbfler, F., T. Moulin, O. Buzhdygan, B. Tietjen, and F. May (2024). “A Trait-Based Model to Describe Plant Community Dynamics in Managed Grasslands (GrasslandTraitSim.Jl v1.0.0)”. In: *EGUsphere*, pp. 1–46. DOI: 10.5194/egusphere-2024-3798. (Visited on 02/18/2025).
- Nowak, R. S., D. S. Ellsworth, and S. D. Smith (2004). “Functional Responses of Plants to Elevated Atmospheric CO<sub>2</sub>—Do Photosynthetic and Productivity Data from FACE Experiments Support Early Predictions?” In: *New Phytol.* 162.2, pp. 253–280. ISSN: 1469-8137. DOI: 10.1111/j.1469-8137.2004.01033.x. (Visited on 04/18/2024).
- O’Mara, F. P. (2012). “The Role of Grasslands in Food Security and Climate Change”. In: *Annals of Botany* 110.6, pp. 1263–1270. ISSN: 0305-7364. DOI: 10.1093/aob/mcs209. (Visited on 04/15/2024).
- Orwin, K. H., N. Ostle, A. Wilby, and R. D. Bardgett (2014). “Effects of Species Evenness and Dominant Species Identity on Multiple Ecosystem Functions in Model Grassland Communities”. In: *Oecologia* 174.3, pp. 979–992. ISSN: 1432-1939. DOI: 10.1007/s00442-013-2814-5. (Visited on 03/07/2025).
- Pasari, J. R., T. Levi, E. S. Zavaleta, and D. Tilman (2013). “Several Scales of Biodiversity Affect Ecosystem Multifunctionality”. In: *Proc. Natl. Acad. Sci.* 110.25, pp. 10219–10222. DOI: 10.1073/pnas.1220333110. (Visited on 04/25/2024).
- Pellegrini, A. F. A., A. Ahlström, S. E. Hobbie, P. B. Reich, L. P. Nieradzic, A. C. Staver, B. C. Scharenbroch, A. Jumpponen, W. R. L. Anderegg, J. T. Randerson, and R. B. Jackson (2018). “Fire Frequency Drives Decadal Changes in Soil Carbon and Nitrogen and Ecosystem Productivity”. In: *Nature* 553.7687, pp. 194–198. ISSN: 1476-4687. DOI: 10.1038/nature24668. (Visited on 04/19/2024).
- Pérez-Harguindeguy, N., S. Díaz, E. Garnier, S. Lavorel, H. Poorter, P. Jaureguiberry, M. S. Bret-Harte, W. K. Cornwell, J. M. Craine, D. E. Gurvich, C. Urcelay, E. J. Veneklaas, P. B. Reich, L. Poorter, I. J. Wright, P. Ray, L. Enrico, J. G. Pausas, A. C. De Vos, N. Buchmann, G. Funes, F. Quétier, J. G. Hodgson, K. Thompson, H. D. Morgan, H. Ter Steege, L. Sack, B. Blonder, P. Poschlod, M. V. Vaieretti, G. Conti, A. C. Staver, S. Aquino, and J. H. C. Cornelissen (2013). “New Handbook for Standardised Measurement of Plant Functional Traits Worldwide”. In: *Aust. J. Bot.* 61.3, p. 167. ISSN: 0067-1924. DOI: 10.1071/BT12225. (Visited on 04/25/2024).
- Petchey, O. L. and K. J. Gaston (2006). “Functional Diversity: Back to Basics and Looking Forward”. In: *Ecol. Lett.* 9.6, pp. 741–758. ISSN: 1461-0248. DOI: 10.1111/j.1461-0248.2006.00924.x. (Visited on 02/21/2018).
- Petermann, J. S., A. J. F. Fergus, C. Roscher, L. A. Turnbull, A. Weigelt, and B. Schmid (2010). “Biology, Chance, or History? The Predictable Reassembly of Temperate Grassland Communities”. In: *Ecology* 91.2, pp. 408–421. ISSN: 1939-9170. DOI: 10.1890/08-2304.1. (Visited on 04/25/2024).
- Peyraud, J.-L. and A. Peeters (2016). “The Role of Grassland Based Production System in the Protein Security”. In: *26 Gen. Meet. Eur. Grassl. Fed. EGF. Trondheim, Norway*.
- Pfeiffer, M., L. Langan, A. Linstädter, C. Martens, C. Gaillard, J. C. Ruppert, S. I. Higgins, E. I. Mudongo, and S. Scheiter (2019). “Grazing and Aridity Reduce Perennial Grass Abundance in Semi-Arid Rangelands – Insights from a Trait-Based Dynamic Vegetation Model”. In: *Ecological Modelling* 395, pp. 11–22. ISSN: 0304-3800. DOI: 10.1016/j.ecolmodel.2018.12.013. (Visited on 02/13/2023).
- Pierce, S., G. Brusa, I. Vagge, and B. E. L. Cerabolini (2013). “Allocating CSR Plant Functional Types: The Use of Leaf Economics and Size Traits to Classify Woody and Herbaceous Vascular Plants”. In: *Funct. Ecol.* 27.4, pp. 1002–1010. ISSN: 1365-2435. DOI: 10.1111/1365-2435.12095. (Visited on 09/26/2018).
- Pierce, S., D. Negreiros, B. E. L. Cerabolini, J. Kattge, S. Díaz, M. Kleyer, B. Shipley, S. J. Wright, N. A. Soudzilovskaia, V. G. Onipchenko, P. M. van Bodegom, C. Frenette-Dussault, E. Weiher, B. X. Pinho, J. H. C. Cornelissen, J. P. Grime, K. Thompson, R. Hunt, P. J. Wilson, G. Buffa, O. C. Nyakunga, P. B. Reich, M. Caccianiga, F. Mangili, R. M. Ceriani, A. Luzzaro, G. Brusa, A. Siefert, N. P. U. Barbosa, F. S. Chapin, W. K. Cornwell, J. Fang, G. W. Fernandes, E. Garnier, S. L. Stradic, J. Peñuelas, F. P. L. Melo, A. Slaviero, M. Tabarelli, and D. Tampucci (2017). “A Global Method for Calculating Plant CSR Ecological Strategies Applied across Biomes World-Wide”. In: *Funct. Ecol.* 31.2, pp. 444–457. ISSN: 1365-2435. DOI: 10.1111/1365-2435.12722. (Visited on 11/26/2020).
- Piipponen, J., M. Jalava, J. de Leeuw, A. Rizayeva, C. Godde, G. Cramer, M. Herrero, and M. Kummu (2022). “Global Trends in Grassland Carrying Capacity and Relative Stocking Density of Livestock”. In: *Glob. Change Biol.* 28.12, pp. 3902–3919. ISSN: 1365-2486. DOI: 10.1111/gcb.16174. (Visited on 02/02/2023).
- Popp, A., H. Lotze-Campen, and B. Bodirsky (2010). “Food Consumption, Diet Shifts and Associated Non-CO<sub>2</sub> Greenhouse Gases from Agricultural Production”. In: *Global Environmental Change. Governance, Complexity and Resilience* 20.3, pp. 451–462. ISSN: 0959-3780. DOI: 10.1016/j.gloenvcha.2010.02.001. (Visited on 04/17/2024).
- Prommer, J., T. W. N. Walker, W. Wanek, J. Braun, D. Zezula, Y. Hu, F. Hofhansl, and A. Richter (2020). “Increased Microbial Growth, Biomass, and Turnover Drive Soil Organic Carbon Accumulation at Higher Plant Diversity”. In: *Glob. Change Biol.* 26.2, pp. 669–681. ISSN: 1365-2486. DOI: 10.1111/gcb.14777. (Visited on 04/19/2024).
- Quillet, A., C. Peng, and M. Garneau (2010). “Toward Dynamic Global Vegetation Models for Simulating Vegetation–Climate Interactions and Feedbacks: Recent Developments, Limitations, and Future Challenges”. In: *Environ. Rev.* 18.NA, pp. 333–353. ISSN: 1181-8700, 1208-6053. DOI: 10.1139/A10-016. (Visited on 04/06/2018).
- Reich, P. B. (2014). “The World-Wide ‘Fast–Slow’ Plant Economics Spectrum: A Traits Manifesto”. In: *J. Ecol.* 102.2, pp. 275–301. ISSN: 1365-2745. DOI: 10.1111/1365-2745.12211. (Visited on 03/23/2020).

- Reid, R. S., P. K. Thornton, G. J. McCrabb, R. L. Kruska, F. Atieno, and P. G. Jones (2004). “Is It Possible to Mitigate Greenhouse Gas Emissions in Pastoral Ecosystems of the Tropics?” In: *Environment, Development and Sustainability* 6.1, pp. 91–109. ISSN: 1573-2975. DOI: 10.1023/B:ENVI.0000003631.43271.6b. (Visited on 04/15/2024).
- Rolinski, S., C. Müller, J. Heinke, I. Weindl, A. Biewald, B. L. Bodirsky, A. Bondeau, E. R. Boons-Prins, A. F. Bouwman, P. A. Leffelaar, J. A. te Roller, S. Schaphoff, and K. Thonicke (2018). “Modeling Vegetation and Carbon Dynamics of Managed Grasslands at the Global Scale with LPJmL 3.6”. In: *Geosci. Model Dev.* 11.1, pp. 429–451. ISSN: 1991-9603. DOI: 10.5194/gmd-11-429-2018. (Visited on 02/27/2018).
- Rook, A., B. Dumont, J. Isselstein, K. Osoro, M. WallisDeVries, G. Parente, and J. Mills (2004). “Matching Type of Livestock to Desired Biodiversity Outcomes in Pastures – a Review”. In: *Biological Conservation* 119.2, pp. 137–150. ISSN: 00063207. DOI: 10.1016/j.biocon.2003.11.010. (Visited on 04/17/2024).
- Rötter, R. and S. van de Geijn (1999). “Climate Change Effects on Plant Growth, Crop Yield and Livestock”. In: *Climatic Change* 43.4, pp. 651–681. ISSN: 1573-1480. DOI: 10.1023/A:1005541132734. (Visited on 04/17/2024).
- Roy, J., C. Picon-Cochard, A. Augusti, M.-L. Benot, L. Thiery, O. Darsonville, D. Landais, C. Piel, M. Defossez, S. Devidal, C. Escape, O. Ravel, N. Fromin, F. Volaire, A. Milcu, M. Bahn, and J.-F. Soussana (2016). “Elevated CO<sub>2</sub> Maintains Grassland Net Carbon Uptake under a Future Heat and Drought Extreme”. In: *Proc. Natl. Acad. Sci.* 113.22, pp. 6224–6229. DOI: 10.1073/pnas.1524527113. (Visited on 04/19/2024).
- Roybal, C. M. and B. J. Butterfield (2019). “Species-Specific Trait–Environment Relationships among Populations of Widespread Grass Species”. In: *Oecologia* 189.4, pp. 1017–1026. ISSN: 1432-1939. DOI: 10.1007/s00442-019-04372-6. (Visited on 04/25/2024).
- Ruggeri Laderchi, C., H. Lotze-Campen, F. DeClerck, B. L. Bodirsky, Q. Collignon, M. S. Crawford, S. Dietz, L. Fesenfeld, C. Hunecke, D. Leip, S. Lord, S. Lowder, S. Nagenborg, T. Pilditch, A. Popp, I. Wedl, F. Branca, S. Fan, J. Fanzo, J. Gosh, B. Harriss-White, N. Ishii, R. Kyte, W. Mathai, S. Chomba, S. Nordhagen, R. Nugent, J. Swinnen, M. Torero, D. Laborde Debouquet, P. Karfakis, J. Voegelé, G. Sethi, P. Winters, O. Edenhofer, R. Kanbur, and V. Songwe (2024). *The Economics of the Food System Transformation, Global Policy Report*. Tech. rep. Food System economics Commission (FSEC). (Visited on 04/15/2024).
- Sakschewski, B., W. von Bloh, A. Boit, A. Rammig, J. Kattge, L. Poorter, J. Peñuelas, and K. Thonicke (2015). “Leaf and Stem Economics Spectra Drive Diversity of Functional Plant Traits in a Dynamic Global Vegetation Model”. In: *Glob. Change Biol.* 21.7, pp. 2711–2725. ISSN: 1365-2486. DOI: 10.1111/gcb.12870. (Visited on 10/15/2018).
- Schaphoff, S., W. von Bloh, A. Rammig, K. Thonicke, H. Biemans, M. Forkel, D. Gerten, J. Heinke, J. Jägermeyr, J. Knauer, F. Langerwisch, W. Lucht, C. Müller, S. Rolinski, and K. Waha (2018). “LPJmL4 – a Dynamic Global Vegetation Model with Managed Land – Part 1: Model Description”. In: *Geosci. Model Dev.* 11.4, pp. 1343–1375. ISSN: 1991-959X. DOI: 10.5194/gmd-11-1343-2018. (Visited on 05/31/2023).
- Schaub, S., R. Finger, F. Leiber, S. Probst, M. Kreuzer, A. Weigelt, N. Buchmann, and M. Scherer-Lorenzen (2020). “Plant Diversity Effects on Forage Quality, Yield and Revenues of Semi-Natural Grasslands”. In: *Nat Commun* 11.1, p. 768. ISSN: 2041-1723. DOI: 10.1038/s41467-020-14541-4. (Visited on 11/20/2024).
- Schiller, C., S. Schmidlein, C. Boonman, A. Moreno-Martínez, and T. Kattenborn (2021). “Deep Learning and Citizen Science Enable Automated Plant Trait Predictions from Photographs”. In: *Sci Rep* 11.1, p. 16395. ISSN: 2045-2322. DOI: 10.1038/s41598-021-95616-0. (Visited on 01/10/2025).
- Schmidhuber, J. and F. N. Tubiello (2007). “Global Food Security under Climate Change”. In: *Proc. Natl. Acad. Sci.* 104.50, pp. 19703–19708. DOI: 10.1073/pnas.0701976104. (Visited on 04/17/2024).
- Schulze, E.-D. and H. A. Mooney, eds. (1993). *Biodiversity and Ecosystem Function*. Berlin, Heidelberg: Springer. ISBN: 978-3-540-58103-1 978-3-642-58001-7. DOI: 10.1007/978-3-642-58001-7. (Visited on 04/25/2024).
- Siefert, A., J. D. Fridley, and M. E. Ritchie (2014). “Community Functional Responses to Soil and Climate at Multiple Spatial Scales: When Does Intraspecific Variation Matter?” In: *PLOS ONE* 9.10, e111189. ISSN: 1932-6203. DOI: 10.1371/journal.pone.0111189. (Visited on 03/09/2018).
- Sinha, E., A. M. Michalak, and V. Balaji (2017). “Eutrophication Will Increase during the 21st Century as a Result of Precipitation Changes”. In: *Science* 357.6349, pp. 405–408. DOI: 10.1126/science.aan2409. (Visited on 04/17/2024).
- Sitch, S., B. Smith, I. C. Prentice, A. Arneth, A. Bondeau, W. Cramer, J. O. Kaplan, S. Levis, W. Lucht, M. T. Sykes, K. Thonicke, and S. Venevsky (2003). “Evaluation of Ecosystem Dynamics, Plant Geography and Terrestrial Carbon Cycling in the LPJ Dynamic Global Vegetation Model”. In: *Glob. Change Biol.* 9.2, pp. 161–185. ISSN: 1365-2486. DOI: 10.1046/j.1365-2486.2003.00569.x. (Visited on 03/03/2018).
- Smit, H. J., M. J. Metzger, and F. Ewert (2008). “Spatial Distribution of Grassland Productivity and Land Use in Europe”. In: *Agricultural Systems* 98.3, pp. 208–219. ISSN: 0308-521X. DOI: 10.1016/j.agsy.2008.07.004. (Visited on 04/15/2024).
- Smith, P., D. Martino, Z. Cai, D. Gwary, H. Janzen, P. Kumar, B. McCarl, S. Ogle, F. O’Mara, C. Rice, B. Scholes, O. Sirotenko, M. Howden, T. McAllister, G. Pan, V. Romanenkov, U. Schneider, S. Towprayoon, M. Wattenbach, and J. Smith (2007). “Greenhouse Gas Mitigation in Agriculture”. In: *Philos. Trans. R. Soc. B Biol. Sci.* 363.1492, pp. 789–813. DOI: 10.1098/rstb.2007.2184. (Visited on 04/19/2024).
- Song, M., T. T. Fung, F. B. Hu, W. C. Willett, V. D. Longo, A. T. Chan, and E. L. Giovannucci (2016). “Association of Animal and Plant Protein Intake With All-Cause and Cause-Specific Mortality”. In: *JAMA Internal Medicine* 176.10, pp. 1453–1463. ISSN: 2168-6106. DOI: 10.1001/jamainternmed.2016.4182. (Visited on 04/17/2024).
- Soussana, J.-F. and A. Lüscher (2007). “Temperate Grasslands and Global Atmospheric Change: A Review”. In: *Grass Forage Sci.* 62.2, pp. 127–134. ISSN: 1365-2494. DOI: 10.1111/j.1365-2494.2007.00577.x. (Visited on 04/17/2024).
- Soussana, J.-F., K. Klumpp, and F. Ehrhardt (2014). “The Role of Grassland in Mitigating Climate Change”. In: *Future Eur. Grassl.* 75, pp. 75–90. (Visited on 05/28/2019).

- Soussana, J.-F., L. G. Barioni, T. B. Ari, R. Conant, P. Gerber, P. Havlik, A. Ickowicz, and M. Howden (2013). “Managing Grassland Systems in a Changing Climate: The Search for Practical Solutions”. In: *Revitalising Grassl. Sustain Our Communities Proc. 22nd Int. Grassl. Congr.* Ed. by D. L. Michalk, G. D. Millar, W. B. Badgery, and K. M. Broadfoot. Vol. 22. Australia: CSIRO, pp. 10–27.
- Spohn, M., S. Bagchi, L. A. Biederman, E. T. Borer, K. A. Bråthen, M. N. Bugalho, M. C. Caldeira, J. A. Catford, S. L. Collins, N. Eisenhauer, N. Hagenah, S. Haider, Y. Hautier, J. M. H. Knops, S. E. Koerner, L. Laanisto, Y. Lekberg, J. P. Martina, H. Martinson, R. L. McCulley, P. L. Peri, P. Macek, S. A. Power, A. C. Risch, C. Roscher, E. W. Seabloom, C. Stevens, G. F. ( Veen, R. Virtanen, and L. Yahdjian (2023). “The Positive Effect of Plant Diversity on Soil Carbon Depends on Climate”. In: *Nat Commun* 14.1, p. 6624. ISSN: 2041-1723. DOI: 10.1038/s41467-023-42340-0. (Visited on 11/20/2024).
- Steinfeld, H. and P. Gerber (2010). “Livestock Production and the Global Environment: Consume Less or Produce Better?” In: *Proc. Natl. Acad. Sci.* 107.43, pp. 18237–18238. DOI: 10.1073/pnas.1012541107. (Visited on 04/17/2024).
- Steinfeld, H., P. Gerber, T. D. Wassenaar, V. Castel, M. Rosales M., and C. de Haan (2006). *Livestock’s Long Shadow: Environmental Issues and Options*. Rome: Food and Agriculture Organization of the United Nations. ISBN: 978-92-5-105571-7.
- Suttie, J., S. Reynolds, and C. Batello, eds. (2005). *Grasslands of the World*. Vol. No. 34. Plant Production and Protection Series. Rome: Food & Agriculture Organization of the United Nations. ISBN: 978-92-5-105337-9.
- Taubert, F., K. Frank, and A. Huth (2012). “A Review of Grassland Models in the Biofuel Context”. In: *Ecological Modelling*. 7th European Conference on Ecological Modelling (ECEM) 245, pp. 84–93. ISSN: 0304-3800. DOI: 10.1016/j.ecolmodel.2012.04.007. (Visited on 02/07/2019).
- Taubert, F., J. Hetzer, J. S. Schmid, and A. Huth (2020a). “The Role of Species Traits for Grassland Productivity”. In: *Ecosphere* 11.7, e03205. ISSN: 2150-8925. DOI: 10.1002/ecs2.3205. (Visited on 02/09/2023).
- Taubert, F., J. Hetzer, J. S. Schmid, and A. Huth (2020b). “Confronting an Individual-Based Simulation Model with Empirical Community Patterns of Grasslands”. In: *PLOS ONE* 15.7, e0236546. ISSN: 1932-6203. DOI: 10.1371/journal.pone.0236546. (Visited on 02/09/2023).
- Thonicke, K., M. Billing, W. von Bloh, B. Sakschewski, Ü. Niinemets, J. Peñuelas, J. H. C. Cornelissen, Y. Onoda, P. van Bodegom, M. E. Schaepman, F. D. Schneider, and A. Walz (2020). “Simulating Functional Diversity of European Natural Forests along Climatic Gradients”. In: *J. Biogeogr.* 47.5, pp. 1069–1085. ISSN: 1365-2699. DOI: 10.1111/jbi.13809. (Visited on 06/23/2023).
- Tilman, D., F. Isbell, and J. M. Cowles (2014). “Biodiversity and Ecosystem Functioning”. In: *Annu. Rev. Ecol. Evol. Syst.* 45.1, pp. 471–493. ISSN: 1543-592X. DOI: 10.1146/annurev-ecolsys-120213-091917. (Visited on 03/06/2019).
- Tilman, D., P. B. Reich, and F. Isbell (2012). “Biodiversity Impacts Ecosystem Productivity as Much as Resources, Disturbance, or Herbivory”. In: *PNAS* 109.26, pp. 10394–10397. ISSN: 0027-8424, 1091-6490. DOI: 10.1073/pnas.1208240109. (Visited on 12/16/2020).
- Tilman, D., P. B. Reich, J. Knops, D. Wedin, T. Mielke, and C. Lehman (2001). “Diversity and Productivity in a Long-Term Grassland Experiment”. In: *Science* 294.5543, pp. 843–845. DOI: 10.1126/science.1060391. (Visited on 01/06/2025).
- Tribot, A.-S., J. Deter, and N. Mouquet (2018). “Integrating the Aesthetic Value of Landscapes and Biological Diversity”. In: *Proc. R. Soc. B Biol. Sci.* 285.1886, p. 20180971. DOI: 10.1098/rspb.2018.0971. (Visited on 01/28/2020).
- Tubiello, F. N., M. Salvatore, S. Rossi, A. Ferrara, N. Fitton, and P. Smith (2013). “The FAOSTAT Database of Greenhouse Gas Emissions from Agriculture”. In: *Environ. Res. Lett.* 8.1, p. 015009. ISSN: 1748-9326. DOI: 10.1088/1748-9326/8/1/015009. (Visited on 04/17/2024).
- United Nations (2015a). *Goal 2 — Department of Economic and Social Affairs*. <https://sdgs.un.org/goals/goal2>. (Visited on 04/15/2024).
- United Nations (2015b). *Goal 3 — Department of Economic and Social Affairs*. <https://sdgs.un.org/goals/goal3>. (Visited on 04/15/2024).
- US EPA (2006). *Global Anthropogenic Non-CO2 Greenhouse Gas Emissions: 1990–2020*.
- Uwizeye, A., I. J. M. de Boer, C. I. Opio, R. P. O. Schulte, A. Falcucci, G. Tempio, F. Teillard, F. Casu, M. Rulli, J. N. Galloway, A. Leip, J. W. Erisman, T. P. Robinson, H. Steinfeld, and P. J. Gerber (2020). “Nitrogen Emissions along Global Livestock Supply Chains”. In: *Nat Food* 1.7, pp. 437–446. ISSN: 2662-1355. DOI: 10.1038/s43016-020-0113-y. (Visited on 04/17/2024).
- Van Oijen, M., Z. Barcza, R. Confalonieri, P. Korhonen, G. Kröel-Dulay, E. Lellei-Kovács, G. Louarn, F. Louault, R. Martin, T. Moulin, E. Moredi, C. Picon-Cochar, S. Rolinski, N. Viovy, S. B. Wirth, and G. Bellocchi (2020). “Incorporating Biodiversity into Biogeochemistry Models to Improve Prediction of Ecosystem Services in Temperate Grasslands: Review and Roadmap”. In: *Agronomy* 10.2, p. 259. DOI: 10.3390/agronomy10020259. (Visited on 02/13/2020).
- Violle, C., M.-L. Navas, D. Vile, E. Kazakou, C. Fortunel, I. Hummel, and E. Garnier (2007). “Let the Concept of Trait Be Functional!” In: *Oikos* 116.5, pp. 882–892. ISSN: 1600-0706. DOI: 10.1111/j.0030-1299.2007.15559.x. (Visited on 04/25/2024).
- von Bloh, W., S. Schaphoff, C. Müller, S. Rolinski, K. Waha, and S. Zaehle (2018). “Implementing the Nitrogen Cycle into the Dynamic Global Vegetation, Hydrology, and Crop Growth Model LPJmL (Version 5.0)”. In: *Geosci. Model Dev.* 11.7, pp. 2789–2812. ISSN: 1991-959X. DOI: 10.5194/gmd-11-2789-2018. (Visited on 05/31/2023).
- Walde, M., E. Allan, S. L. Cappelli, M. Didion-Gency, A. Gessler, M. M. Lehmann, N. A. Pichon, and C. Grossiord (2021). “Both Diversity and Functional Composition Affect Productivity and Water Use Efficiency in Experimental Temperate Grasslands”. In: *J. Ecol.* 109.11, pp. 3877–3891. ISSN: 1365-2745. DOI: 10.1111/1365-2745.13765. (Visited on 11/20/2024).

- Weaver, J. (1954). *North American Prairie*. Lincoln, Nebraska: JOHNSEN PUBLISHING COMPANY.
- Weigelt, A., L. Mommer, K. Andrzejak, C. M. Iversen, J. Bergmann, H. Bruelheide, Y. Fan, G. T. Freschet, N. R. Guerrero-Ramírez, J. Kattge, T. W. Kuyper, D. C. Laughlin, I. C. Meier, F. van der Plas, H. Poorter, C. Roumet, J. van Ruijven, F. M. Sabatini, M. Semchenko, C. J. Sweeney, O. J. Valverde-Barrantes, L. M. York, and M. L. McCormack (2021). “An Integrated Framework of Plant Form and Function: The Belowground Perspective”. In: *New Phytol.* 232.1, pp. 42–59. ISSN: 1469-8137. DOI: 10.1111/nph.17590. (Visited on 11/23/2021).
- Weindl, I., A. Popp, B. L. Bodirsky, S. Rolinski, H. Lotze-Campen, A. Biewald, F. Humpeöder, J. P. Dietrich, and M. Stevanović (2017). “Livestock and Human Use of Land: Productivity Trends and Dietary Choices as Drivers of Future Land and Carbon Dynamics”. In: *Global and Planetary Change* 159, pp. 1–10. ISSN: 0921-8181. DOI: 10.1016/j.gloplacha.2017.10.002. (Visited on 04/17/2024).
- Weisser, W. W., C. Roscher, S. T. Meyer, A. Ebeling, G. Luo, E. Allan, H. Beßler, R. L. Barnard, N. Buchmann, F. Buscot, C. Engels, C. Fischer, M. Fischer, A. Gessler, G. Gleixner, S. Halle, A. Hildebrandt, H. Hillebrand, H. de Kroon, M. Lange, S. Leimer, X. Le Roux, A. Milcu, L. Mommer, P. A. Niklaus, Y. Oelmann, R. Proulx, J. Roy, C. Scherber, M. Scherer-Lorenzen, S. Scheu, T. Tschardtke, M. Wachendorf, C. Wagg, A. Weigelt, W. Wilcke, C. Wirth, E.-D. Schulze, B. Schmid, and N. Eisenhauer (2017). “Biodiversity Effects on Ecosystem Functioning in a 15-Year Grassland Experiment: Patterns, Mechanisms, and Open Questions”. In: *Basic Appl. Ecol.* Biodiversity Effects on Ecosystem Functioning: The Jena Experiment 23, pp. 1–73. ISSN: 1439-1791. DOI: 10.1016/j.baee.2017.06.002. (Visited on 01/27/2020).
- White, R. P., S. Murray, and M. Rohweder (2000). “Pilot Analysis of Global Ecosystems: Grassland Ecosystems.” In: *Pilot Anal. Glob. Ecosyst. Grassl. Ecosyst.* (Visited on 02/13/2023).
- WHO (2024). *Obesity and Overweight*. <https://www.who.int/news-room/fact-sheets/detail/obesity-and-overweight>. (Visited on 04/15/2024).
- Wilcox, B. P., M. G. Sorice, J. Angerer, and C. L. Wright (2012). “Historical Changes in Stocking Densities on Texas Rangelands”. In: *Rangeland Ecology & Management* 65.3, pp. 313–317. ISSN: 1550-7424. DOI: 10.2111/REM-D-11-00119.1. (Visited on 11/20/2024).
- Willett, W., J. Rockström, B. Loken, M. Springmann, T. Lang, S. Vermeulen, T. Garnett, D. Tilman, F. DeClerck, A. Wood, M. Jonell, M. Clark, L. J. Gordon, J. Fanzo, C. Hawkes, R. Zurayk, J. A. Rivera, W. D. Vries, L. M. Sibanda, A. Afshin, A. Chaudhary, M. Herrero, R. Agustina, F. Branca, A. Lartey, S. Fan, B. Crona, E. Fox, V. Bignet, M. Troell, T. Lindahl, S. Singh, S. E. Cornell, K. S. Reddy, S. Narain, S. Nishtar, and C. J. L. Murray (2019). “Food in the Anthropocene: The EAT–Lancet Commission on Healthy Diets from Sustainable Food Systems”. In: *The Lancet* 393.10170, pp. 447–492. ISSN: 0140-6736, 1474-547X. DOI: 10.1016/S0140-6736(18)31788-4. (Visited on 04/15/2024).
- Wilson, C. H., M. S. Strickland, J. A. Hutchings, T. S. Bianchi, and S. L. Flory (2018). “Grazing Enhances Belowground Carbon Allocation, Microbial Biomass, and Soil Carbon in a Subtropical Grassland”. In: *Glob. Change Biol.* 24.7, pp. 2997–3009. ISSN: 1365-2486. DOI: 10.1111/gcb.14070. (Visited on 04/19/2024).
- Wirth, S. B., J. Braun, J. Heinke, S. Ostberg, S. Rolinski, S. Schaphoff, F. Stenzel, W. von Bloh, and C. Müller (2024). “Biological Nitrogen Fixation of Natural and Agricultural Vegetation Simulated with LPJmL 5.7.9”. In: *EGUsphere*, pp. 1–29. DOI: 10.5194/egusphere-2023-2946. (Visited on 03/18/2024).
- Wolf, S., M. D. Mahecha, F. M. Sabatini, C. Wirth, H. Bruelheide, J. Kattge, Á. Moreno Martínez, K. Mora, and T. Kattenborn (2022). “Citizen Science Plant Observations Encode Global Trait Patterns”. In: *Nat Ecol Evol* 6.12, pp. 1850–1859. ISSN: 2397-334X. DOI: 10.1038/s41559-022-01904-x. (Visited on 09/18/2023).
- World Food Summit (1996). *Declaration on World Food Security*. Rome: FAO. (Visited on 04/15/2024).
- Wright, I. J., P. B. Reich, M. Westoby, D. D. Ackerly, Z. Baruch, F. Bongers, J. Cavender-Bares, T. Chapin, J. H. C. Cornelissen, M. Diemer, J. Flexas, E. Garnier, P. K. Groom, J. Gulias, K. Hikosaka, B. B. Lamont, T. Lee, W. Lee, C. Lusk, J. J. Midgley, M.-L. Navas, U. Niinemets, J. Oleksyn, N. Osada, H. Poorter, P. Poot, L. Prior, V. I. Pyankov, C. Roumet, S. C. Thomas, M. G. Tjoelker, E. J. Veneklaas, and R. Villar (2004). “The Worldwide Leaf Economics Spectrum”. In: *Nature* 428.6985, pp. 821–827. ISSN: 1476-4687. DOI: 10.1038/nature02403.
- Wu, G.-L., Y. Liu, F.-P. Tian, and Z.-H. Shi (2017). “Legumes Functional Group Promotes Soil Organic Carbon and Nitrogen Storage by Increasing Plant Diversity”. In: *Land Degrad. Dev.* 28.4, pp. 1336–1344. ISSN: 1099-145X. DOI: 10.1002/ldr.2570. (Visited on 04/19/2024).
- Wu, R. and H. Tiessen (2002). “Effect of Land Use on Soil Degradation in Alpine Grassland Soil, China”. In: *Soil Sci. Soc. Am. J.* 66.5, pp. 1648–1655. ISSN: 1435-0661. DOI: 10.2136/sssaj2002.1648. (Visited on 11/20/2024).
- Wu, X., X. Dang, Z. Meng, D. Fu, W. Cong, F. Zhao, and J. Guo (2022). “Mechanisms of Grazing Management Impact on Preferential Water Flow and Infiltration Patterns in a Semi-Arid Grassland in Northern China”. In: *Science of The Total Environment* 813, p. 152082. ISSN: 0048-9697. DOI: 10.1016/j.scitotenv.2021.152082. (Visited on 11/20/2024).
- Yang, Y., D. Tilman, G. Furey, and C. Lehman (2019). “Soil Carbon Sequestration Accelerated by Restoration of Grassland Biodiversity”. In: *Nat. Commun.* 10.1, p. 718. ISSN: 2041-1723. DOI: 10.1038/s41467-019-08636-w. (Visited on 10/21/2020).
- Yu, T. and Q. Zhuang (2020). “Modeling Biological Nitrogen Fixation in Global Natural Terrestrial Ecosystems”. In: *Biogeosciences* 17.13, pp. 3643–3657. ISSN: 1726-4170. DOI: 10.5194/bg-17-3643-2020. (Visited on 02/18/2022).
- Zavaleta, E. S. and K. B. Hulvey (2004). “Realistic Species Losses Disproportionately Reduce Grassland Resistance to Biological Invaders”. In: *Science* 306.5699, pp. 1175–1177. DOI: 10.1126/science.1102643. (Visited on 04/25/2024).
- Zavaleta, E. S., J. R. Pasari, K. B. Hulvey, and G. D. Tilman (2010). “Sustaining Multiple Ecosystem Functions in Grassland Communities Requires Higher Biodiversity”. In: *Proc. Natl. Acad. Sci.* 107.4, pp. 1443–1446. DOI: 10.1073/pnas.0906829107. (Visited on 04/25/2024).

## Chapter 1 General introduction

- Zhang, Y., Z. Wang, Y. Lu, and L. Zuo (2022). “Editorial: Biodiversity, Ecosystem Functions and Services: Interrelationship with Environmental and Human Health”. In: *Front. Ecol. Evol.* 10. ISSN: 2296-701X. DOI: 10.3389/fevo.2022.1086408. (Visited on 04/19/2024).
- Zhou, Y., J. Singh, J. R. Butnor, C. Coetsee, P. B. Boucher, M. F. Case, E. G. Hockridge, A. B. Davies, and A. C. Staver (2022). “Limited Increases in Savanna Carbon Stocks over Decades of Fire Suppression”. In: *Nature* 603.7901, pp. 445–449. ISSN: 1476-4687. DOI: 10.1038/s41586-022-04438-1. (Visited on 04/19/2024).

# Chapter 2

## Do details matter? Disentangling the processes related to plant species interactions in two grassland models of different complexity

Stephen B. Wirth<sup>1,2</sup>, Franziska Taubert<sup>3</sup>, Britta Tietjen<sup>4,5</sup>, Christoph Müller<sup>1</sup> and Susanne Rolinski<sup>1</sup>

<sup>1</sup>Potsdam Institute for Climate Impact Research (PIK), Member of the Leibniz Association, P.O. Box 60 12 03, 14412 Potsdam, Germany

<sup>2</sup>Institute of Crop Science and Plant Breeding, Grass and Forage Science/Organic Agriculture, Kiel University, Hermann-Rodewald-Str. 9, 24118, Kiel, Germany

<sup>3</sup>Department of Ecological Modelling, Helmholtz Centre for Environmental Research–UFZ, Permoserstrasse 15, Leipzig 04318 Germany

<sup>4</sup>Freie Universität Berlin, Institute of Biology, Theoretical Ecology, Königin-Luise-Str. 2/4 Gartenhaus, 14195 Berlin, Germany

<sup>5</sup>Berlin-Brandenburg Institute of Advanced Biodiversity Research (BBIB), D-14195 Berlin, Germany

Status: Published

Journal: Ecological modelling

Received: 23 April 2021

Revised: 30 August 2021

Accepted: 31 August 2021

Published: 14 September 2021

DOI: <https://doi.org/10.1016/j.ecolmodel.2021.109737>

---

**Abstract:** Biogeochemical models of vegetation dynamics could potentially be used to complement empirical studies on the effect of plant species richness. A key precondition is the simulation of species coexistence. While community scale models regularly incorporate respective processes, models at the field or landscape scale used for larger scale assessments, require additional model development. However, it is unclear how the particular process description within these models affects simulations of species performance and resulting ecosystem functions.

We compare simulations of two grassland models of different complexity for monocultures and two-species mixtures in a grassland experiment in Jena, Germany. By providing an in-depth analysis of the models' process descriptions, we evaluate their ability to simulate the response of different species, their interactions and their joint performance to drought and mowing.

Both models simulated similar average above-ground biomass (AGB) but showed different intra-annual variability. Generally, the models had difficulties representing a balanced species composition in multiple species mixtures and competition for space was the main driver of community composition in both models. The resulting communities were dominated by the more competitive species, while the weak competitor was only marginally present in most mixtures independent of drought and mowing. The competitive strength which we derived from the calibrated parameter sets of the species differed between the models and the agreement on which species dominate specific mixtures was mixed. While both models simulated reduced soil water content and above-ground biomass in response to drought, the strength and duration of these responses differed. Despite these differences, simulated species interactions were barely affected, and strong competitors remained dominant. Mowing had opposing effects on the competition for space in the models, which could be attributed to the different representations of plants in the two models.

The models selected for the comparison are two representatives for local- and large-scale applications and use widely applied approaches for which our comparison highlighted strengths and weaknesses. To enable the investigated models (and those with similar complexity) to simulate coexistence of multiple species, niche differentiation needs to be improved. This requires a stricter separation of access to different resources and improved representation of different ecological strategies for which community scale models that are able to simulate coexistence may be an inspiration. Our approach may serve as an example for other modellers looking for ways to identify important model processes for further model development in the context of species interaction.

---

## 2.1 Introduction

Grasslands are a key element of ruminant livestock production systems and provide multiple ecosystem services like carbon sequestration (Chang et al., 2015), erosion control (Zhu et al., 2015) and habitats for pollinators and other fauna (Dass et al., 2018; Tribot et al., 2018). They strongly affect biogeochemical cycles at different scales (Moinet et al., 2017; Zhou et al., 2017) and lately, their carbon storage potential has been controversially discussed in the context of climate change mitigation (e.g. Godde et al., 2020; Lorenz and Lal, 2018; Yang et al., 2019). The functions and services provided by grasslands are strongly controlled by the prevailing environmental conditions, but also by the specific management (Tilman et al., 2012). The response of a grassland ecosystem to changes in these drivers was shown to be mediated by species richness and community composition (Craven et al., 2016; Vogel et al., 2012; Yin et al., 2017). Consequently, a good understanding of the mechanisms driving grassland dynamics is essential to assess and project future productivity, ecosystem services and functions under different stressors, such as climate change (Van Oijen et al., 2020).

### 2.1.1 Drivers of grassland dynamics

In this study, we focus on the effect of two important drivers of grassland dynamics: decreased water availability resulting from meteorological droughts, which can result from climate change, and biomass

removal by mowing, which is a common practice in livestock production.

### **2.1.1.1 Water**

Water availability results from the local balance of inputs through precipitation and losses by transpiration, evaporation, seepage and runoff. During drought, precipitation is absent or below water requirements for a longer period, either within one season or across multiple years. A decrease in precipitation can suppress ecosystem photosynthesis, soil respiration and carbon cycling (Beier et al., 2012; Wu et al., 2011) as well as key soil processes (Emmett et al., 2004). Additionally, an increase in inter-rainfall intervals can lead to reduced net primary production, flowering duration and soil CO<sub>2</sub> flux in grasslands (Fay et al., 2000). Other severe impacts on grassland ecosystems include a rapid loss of biomass, plant cover, and even species (Carroll et al., 2021; Tilman and El Haddi, 1992; Weaver, 1942). In addition, droughts were shown to influence community composition and diversity patterns of grasslands (Buckland et al., 1997; Jung et al., 2020; Knapp et al., 2008). The response of an ecosystem to periods of drought depends on characteristics of the drought itself, such as its duration, its intensity and its frequency (Denton et al., 2017; Felton et al., 2020). It also depends on the characteristics of the grassland community, as grassland species have developed several strategies to resist and survive droughts (Blair et al., 2014; Reich, 2014). While annual species often use an escape strategy by completing their life cycle outside the dry season (Kooyers, 2015; Norton et al., 2016), perennial species use dehydration avoidance or tolerance as a strategy (Zwicke et al., 2015) by regulating their leaf water potential (Ratzmann et al., 2019a; Ratzmann et al., 2019b). Dehydration avoidance is associated with an increase in water uptake or decrease of water losses, while dehydration tolerance ensures plant survival by maintaining cell integrity of meristematic tissue (Ludlow, 1989; Volaire et al., 2009; Zwicke et al., 2015). Additionally, species-rich communities often better buffer adverse effects of droughts in the long run than low-diverse communities, as they allow for shifts in their composition towards potentially better adapted species (Hoover et al., 2018; Isbell et al., 2015) but may also alter environmental conditions reducing drought stress of more vulnerable species (Wright et al., 2021). Species-rich communities may also benefit from complementarity effects that arise from the use of soil water stored in different soil depths by opposing rooting strategies (Guderle et al., 2018; Klaus et al., 2016; Kulmatiski and Beard, 2013).

### **2.1.1.2 Mowing**

In addition to drought, the frequent removal of above-ground plant biomass through mowing or cutting also affects the composition of grassland communities as well as their productivity, which in turn may affect the grassland's resilience to drought events. The intensity of mowing is a result of the frequency of

mowing and the applied cutting height. While the prevailing pedoclimatic conditions restrict grassland productivity via temperature, light, water and nutrient constraints, under similar conditions the highest grassland productivity has been found at intermediate mowing intensities, whereas very low or high mowing intensities often decrease productivity (Hopkins, 2000; Weigelt et al., 2009). At low mowing intensity, competition for limiting resources such as water and nutrients, drives the community dynamics, and thus more competitive species dominate the community (Smart et al., 2006). Therefore, the community is often shaped by fewer but larger plants compared to grasslands with higher mowing intensities. In contrast, in grasslands with a very high mowing intensity, biomass is removed so frequently, that fast growth and high stature traits associated with competitive species are not advantageous but lead to selective removal of these species instead (Yin et al., 2017; Yu et al., 2015). The resulting community often consists of a high number of small plants. This is accompanied by reduced shading and competition for nutrients and increased growth of less competitive species, promoting species richness (Pecháčková et al., 2010; Peltzer and Wilson, 2001; Williams et al., 2007).

### **2.1.2 Plant species richness**

The grassland ecosystems' responses to these two drivers, water availability and mowing, and the mechanisms involved, as well as the role of plant species richness of grassland communities, have been studied using field observations and experiments along a diversity gradient (e.g. Craven et al., 2016; Tilman et al., 2014). Despite the large number of experiments the mechanistic understanding of the processes regulating community responses to drought and mowing, especially in species-rich communities is still limited (Weisser et al., 2017). While the patterns can be reproduced using mathematical models (e.g. Han et al., 2019), to dissect the underlying processes of ecosystem dynamics, biogeochemical models (BGMs) have the potential to complement empirical studies, as they can mechanistically analyze the interacting responses of biotic and abiotic components of grasslands to changing environmental conditions (Van Oijen et al., 2020; Wilcox et al., 2020). However, this requires that two preconditions are met: First, the models need to represent all relevant processes that shape the community under specific environmental and management conditions reasonably well. Second, the models need to represent different ecological strategies enabling the communities to adapt if prevailing conditions change. However, BGMs have not yet been assessed sufficiently with respect to these two preconditions.

### **2.1.3 Biogeochemical models**

BGMs of grasslands have been developed and applied to determine grassland dynamics since the end of the 1980s (e.g. Coffin and Lauenroth, 1990; Duru et al., 2009; Hunt et al., 1991; Schapendonk et al., 1998; Siehoff et al., 2011; Thornley and Verberne, 1989). These models have been developed for

applications at multiple scales and with different levels of represented process detail. Models at the community scale simulating individual plants with different traits have been used to study the effect of resource availability and disturbance regimes on the community and its member species (e.g. May et al., 2009; Soussana et al., 2012). At the plot or field scale individual-based and other models distinguishing traits only between species or functional types have been used to assess productivity and yields for different environmental conditions and management (e.g. Höglind et al., 2016; Taubert et al., 2012). At the continental or global scale dynamic global vegetation models have been developed to assess element cycling commonly using only a small number of functional types to simulate grassland ecosystems (e.g. Rolinski et al., 2018; Vuichard et al., 2007). The level of detail and the number of resources that are considered for plant growth and competition vary not only with the spatial scale for which models have been developed, but also between models applied at similar scales (for an extensive review see Taubert et al., 2012).

At the community scale, models that simulate the effects of plant species richness and the interactions between species have been developed (e.g. Clark et al., 2018; Turnbull et al., 2013; Weiss et al., 2014). The high detail of the plant interactions is achieved at the expense of detail in biogeochemical process descriptions. We refer to these models as plant interaction models (PIM) to distinguish them from BGMs. The latter still need substantial development to incorporate plant species richness and species interaction. In order to enable these models to simulate differently diverse communities and quantitatively assess the effect of plant species richness, important processes need to be identified and the appropriateness of potential alternative approaches has to be evaluated. An in-depth analysis of the interactions between two species can be used to identify the important processes. Doing such an analysis for model representatives which exemplify a type of model (a number of models sharing similar approaches) and comparing the performance of multiple model representatives, may be used to identify the limitations of current model implementations as well as general knowledge gaps that can inform the next steps of model development. The approach can also uncover similarities and differences regarding the strengths and weaknesses of specific approaches. This knowledge can be used to inform on potential development options for the assessed models as well as other models of the same type.

#### **2.1.4 Model intercomparison studies**

While comparison studies are more common for models of cereal crops (e.g. Asseng et al., 2019; Durand et al., 2018; Müller et al., 2017) only comparably few studies for forage grasses have been published (Korhonen et al., 2018). Of these few grassland model intercomparison studies, some have used a large model ensemble and cover multiple sites (e.g. Ehrhardt et al., 2018; Sándor et al., 2017; Sándor et al., 2020). While they quantify and discuss the uncertainty within the ensemble, a detailed analy-

sis of the processes within each model is beyond their scope. In contrast, other studies have used a small number of models allowing for a more detailed analysis of model differences at one or multiple sites (e.g. Hurtado-Uria et al., 2013; Korhonen et al., 2018; Persson et al., 2019). These studies are, however, limited to one specific species, neglecting inter-specific competition and differences between parametrizations obtained for multiple species, which to our knowledge have only been assessed using PIMs (Crawford et al., 2021).

### **2.1.5 Research question**

To expand on this for BGMs of different scales and to assess the role of how processes are represented in different models, we compared simulated grassland properties for two biogeochemical grassland models (GRASSMIND: Taubert et al. 2012; Taubert et al. 2020a; Taubert et al. 2020b; LPJmL: Rolinski et al. 2018; Schaphoff et al. 2018; von Bloh et al. 2018) using different scenarios of water availability and management using simulations of monocultures and two-species mixtures. The GRASSMIND model follows an individual-based approach using fixed traits for each species and simulates photosynthesis using light response curves (Thornley and Johnson, 1990), while the LPJmL model follows an average individual approach and simulates photosynthesis using an adapted Farquhar approach (Haxeltine and Prentice, 1996; Prentice et al., 2000). Using data from a long-term biodiversity experiment (Weisser et al., 2017) — the Jena Experiment — we first calibrated and evaluated the models for four species for observed climatic conditions and management. Subsequently, we compared the models for scenarios with no, moderate and extreme drought conditions in combination with and without mowing. With this study we pursue the following objectives:

- (i) identify the relevant processes to explain the main similarities and differences between the models outcomes for our scenarios,
- (ii) assess the effects of mowing and drought in relation to calibrated parameters for the monocultures and the two-species mixtures and explain the differences using the processes identified in (i) and
- (iii) discuss our findings from (i) and (ii) in the context of other modelling approaches.

## **2.2 Methods**

We used the vegetation models LPJmL (Rolinski et al. 2018; Schaphoff et al. 2018; von Bloh et al. 2018, see 2.2.1.1) and GRASSMIND (Taubert et al. 2012; Taubert et al. 2020a; Taubert et al. 2020b, see 2.2.1.2) for our comparison. The models were first calibrated and evaluated for four monocultures and subsequently grassland dynamics were assessed for multiple scenarios of management and drought conditions for the monocultures as well as two-species mixtures (see 2.2.2).

### 2.2.1 Model description

The GRASSMIND and the LPJmL models both simulate daily dynamics of grassland vegetation. While LPJmL is usually applied at large spatial scales, for this study, it is used as a point model, simulating small plots with no further spatial distinction. This plot level is the smallest spatial unit for which all dynamics represented in LPJmL are simulated, whereas in GRASSMIND the smallest spatial units are the single plants, which simulate the dynamics on  $1 \text{ m}^2$  to represent the plot. In both models, at each daily timestep, the amount of biomass gained by photosynthesis is calculated and allocated to the leaves and roots after subtracting losses from growth and maintenance respiration. Subsequently, the biomass losses from mortality and turnover of biomass into the litter layer are determined. The amount of new biomass gained depends on available space, soil and climate conditions and management. At optimal temperatures, sufficiently available space to grow and under adequate radiation, water and nitrogen supply, higher photosynthesis rates can be achieved, while suboptimal resource supply or high vegetation density limit photosynthesis and thus growth. This can result in altered competition and community composition. Both models can account for management measures by irrigation and application of fertilizer, can increase biomass gains. Biomass removal by mowing can be carried out at fixed dates, reducing the tissue available for photosynthesis after the mowing event.

Each model considers the environmental factors space not already occupied by vegetation, temperature, radiation, water and nitrogen availability, and simulates similar processes to describe biomass gains and losses. Fig. 2.1 provides a condensed overview of the similarities and differences while a separate depiction is provided in Fig. A.1. However, the process implementations differ in specific aspects, e.g., in LPJmL overcrowding reduces the above-ground biomass depending on the excess *cover*, while in GRASSMIND the excess *cover* determines the number of individuals killed which are then randomly selected (Tab. A.8). While we use the term *cover* for the comparison of the models throughout this paper, it is defined differently. In LPJmL, plant geometry is not simulated and cannot be used to calculate the *cover*. Here, *cover* is the foliage projected cover (*FPC*) which is calculated from the leaf area index (*LAI*). In GRASSMIND, where plant geometry is simulated, *cover* is calculated as the sum of the individual plants' base area. This is an important difference between the models and has to be kept in mind when reading sections 2.3 and 2.4.

In addition, a key difference of the models is the representation of the vegetation itself. Grassland communities consist of several taxonomic groups, however, only graminoids, small, and tall herbs are represented in the two models. For each modelled species or functional type, LPJmL simulates one average individual with a given set of traits. The dynamics of the average individual are then scaled up to the plot scale, neglecting differences between individuals of the same species. In contrast, GRASSMIND follows an individual-based approach explicitly simulating multiple individuals of the same species that

have the same set of traits but can differ in size (e.g. plant height and base area). Both models distinguish the plant compartments leaves and roots, but in GRASSMIND leaf tissue is further divided into living and standing senescent tissue, while in LPJmL senescent tissue is directly added to the litter layer of the soil. For a detailed description we refer to Rolinski et al. (2018), Schaphoff et al. (2018), and von Bloh et al. (2018) for the LPJmL model and to Taubert et al. (2020a) and Taubert et al. (2020b) and Taubert et al. (2012) for the GRASSMIND model.

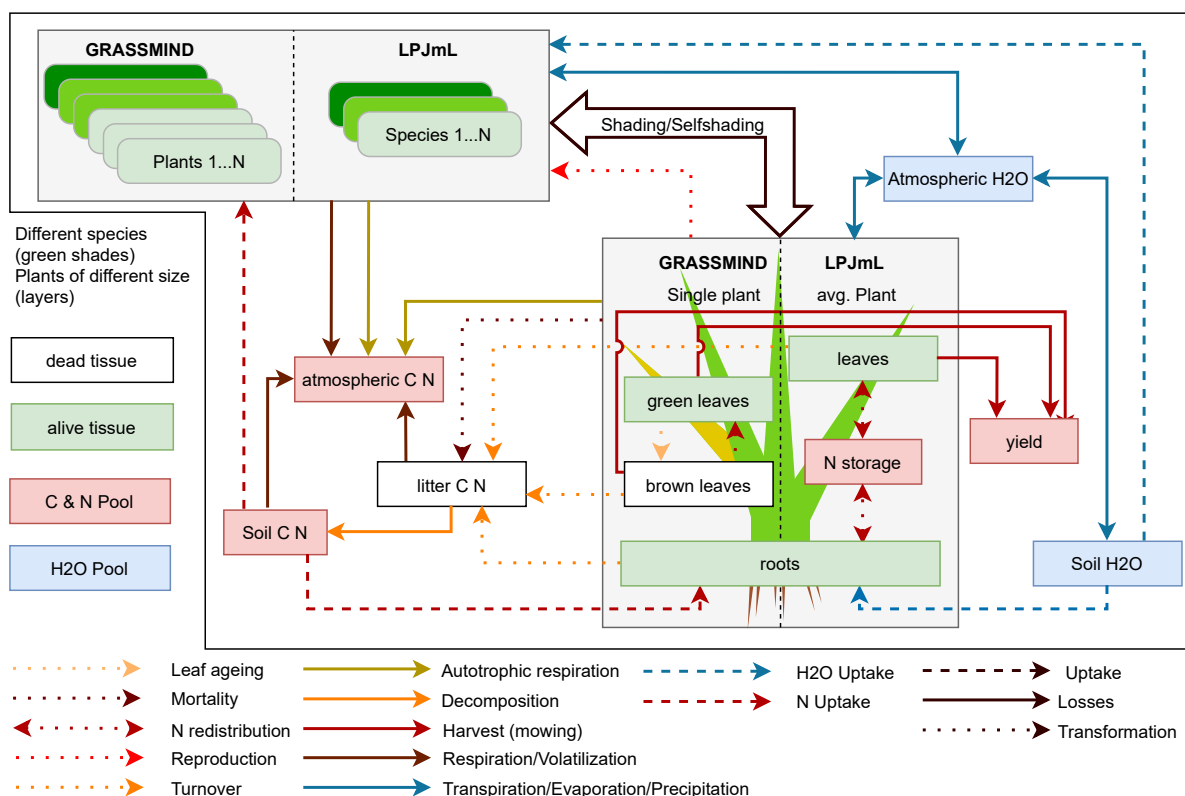


Figure 2.1: Processes and plant compartments simulated in GRASSMIND and LPJmL (see Fig. A.1 for an individual representation of each model)

### 2.2.1.1 LPJmL

LPJmL is a process-based BGM of the carbon, water and nitrogen cycle, developed mainly for global-scale applications (Schaphoff et al., 2018; von Bloh et al., 2018) and has been extended to simulate different grassland management routines (Rolinski et al., 2018). However, as the model simulates processes for representative points without an explicit reference to space, it is also applicable at the plot scale (e.g Ehrhardt et al., 2018). LPJmL is representative for several related models (e.g. LPJ-GUESS Smith et al. 2001, LPJFit Sakschewski et al. 2015 or LPX Prentice et al. 2000) but also other DGVMs (e.g. JULES Clark et al. 2011 or ORCHIDEE Vuichard et al. 2007). The model simulates the dynamics of an average individual of a species or a plant functional type (PFT) with daily timesteps based on the following processes: (a) establishment of new species and reproduction of present species, (b)

plant turnover, (c) biomass accumulation based on gross primary production (GPP) and autotrophic respiration, which is limited by environmental conditions and competition for resources between species. Direct biotic interactions are not simulated.

**Photosynthesis** LPJmL simulates GPP based on a simplification of the Farquhar approach in combination with a big leaf approach for which the optimum photosynthetic activity as a trade-off between light energy and RuBisCO availability is derived numerically (Collatz et al., 1991; Collatz et al., 1992; Farquhar and Caemmerer, 1982; Prentice et al., 2000; von Bloh et al., 2018). A crucial part of the photosynthesis is the fraction of absorbed photosynthetically active radiation (FAPAR) which is determined using a factor depending on snowcover, a biome-specific scaling factor and the PFT's *FPC*, which is defined as the fraction of ground area covered by a vertical projection of the vegetation's foliage, and determines how much of the photosynthetically active radiation (PAR) can actually be intercepted by the canopy. The *FPC* of each PFT is calculated from the PFT's specific LAI and light extinction coefficient. Afterwards, the realised *FPC* of each PFT is weighted depending on LAI and *FPC* of all other PFTs present in the plot. Additionally, limitations due to water and nitrogen stress are accounted for by comparing resource demand and supply.

**Water and nitrogen stress** LPJmL simulates soil water dynamics in six distinct layers, to which plants have access, depending on their root distribution (Schaphoff et al., 2018). Here, we focus on plant water demand, supply, and uptake, to analyse the impacts these processes have on each PFT and the entire community. In the computation of GPP, an estimated canopy conductance under unlimited water supply is used to calculate the atmospheric water demand following Monteith (1995). Even though plants share the same soil water supply on the plot, plant available soil water is calculated separately for each PFT, depending on its maximum water transport capacity, vertical root distribution, and *FPC*. If the atmospheric demand is not met, canopy conductance is reduced in accordance to the water supply. This reduced conductance rate is used to determine actual GPP.

A similar approach is applied for the nitrogen stress in which the plant-available nitrogen supply is compared to the plant's demand. In case the leaf nitrogen content is below a threshold, the carboxylation capacity is reduced to match the actual nitrogen supply in the leaves. Since the carboxylation capacity is also used to determine water limitation, the actual water demand is updated and GPP is updated to account for both water and nitrogen limitations (see von Bloh et al., 2018, for a detailed description of the nitrogen cycle in LPJmL).

**Allocation, establishment and mortality** The assimilated carbon is distributed between leaves and roots, considering the discrepancy between the actual and the aspired leaf-to-root-ratio of carbon.

If the actual leaf-to-root ratio is larger than the aspired (more leaf carbon than root carbon) more carbon is allocated to the roots and the other way around. Under water limited conditions, additional carbon is allocated to the roots. Subsequently, the assimilated nitrogen is distributed considering the prescribed range of carbon-to-nitrogen-ratios of leaves and roots. If the allocation of nitrogen would exceed the lower limit of these ranges, a part of the nitrogen is stored so it can be distributed at a later time. If not enough nitrogen is available and the upper limit of the ranges would be exceeded, leaf and/or root carbon is reduced and the excess added to the litter layer. Afterwards, the *FPC* of all PFTs is updated. Each day, the model evaluates the present species and allows for establishment of new species if these can grow under simulated conditions. For all species (already present and newly established) reproduction is calculated based on the equal distribution of available space. The more space is available the more reproduction is possible. If the total *FPC* exceeds 1.0, overcrowding mortality reduces the leaf biomass until the *FPC* is smaller 1.0.

All these processes interact and lead to daily changes in the PFTs' carbon and nitrogen pools. The process rates depend on a set of PFT specific parameters that resemble plant functional traits. It is possible to represent different strategies of particular species using observations of multiple functional-traits or measurements from experiments, that correspond to a subset of the parameters to calibrate the model. A full model description is available in Schaphoff et al. (2018) and von Bloh et al. (2018) and the open source version of the model is available at <https://github.com/PIK-LPJmL/LPJmL>. We use a consolidated version of LPJmL5 (von Bloh et al., 2018) extended to simulate daily establishment.

### **2.2.1.2 GRASSMIND**

GRASSMIND is an individual- and process-based grassland model (Taubert et al., 2012; Taubert et al., 2020a; Taubert et al., 2020b) where plant growth is based on the concept of light response curves that is also used in several other models (e.g. Seib-DGVM Sato et al. 2007). The model simulates the daily dynamics of individual plants of different species or PFTs at the plot scale (e.g., 1 to 100 m<sup>2</sup>) based on the following processes: (a) recruitment and emergence of plant seedlings, (b) plant senescence and mortality, (c) growth of plants (based on GPP and autotrophic respiration), which can be (d) limited by environmental conditions or reduced due to competition between plants. Interactions between plants encompass competition for the resources light, space, water and nitrogen. Plant competition depends on plant size and species identity, but does not account for the particular spatial locations of a plant ('gap approach'; Botkin et al., 1972; Fischer et al., 2016; Köhler and Huth, 2004; Shugart, 1998). Each plant species is described by a set of plant traits, which determines its performance in the above-mentioned processes and its growth form.

**Photosynthesis** GRASSMIND first calculates a plant's potential GPP using the concept of light response curves (Thornley and Johnson, 1990), which is subsequently reduced to account for water, nitrogen and temperature limitations. The potential GPP is predominantly determined by the photosynthetically active radiation (PAR) that the plant receives, which is comparable to FAPAR in LPJmL. In GRASSMIND, this depends on the LAI and other factors such as shading by larger plants. Competition for light is modelled asymmetrically, which means that larger plants receive more non-attenuated light than smaller plants. Dependent on species-specific traits, some species can cope better with lower light levels than others. Large plants with large leaf area can reach their potential GPP limit as a result of self-shading. The response of potential GPP to air temperature is similar for all plants, but reductions of potential GPP due to soil water deficits, nitrogen stress or competition are dependent on species-specific traits that control resource demand and supply.

**Water and nitrogen stress** Water, carbon and nitrogen dynamics are modelled in 20 equally large soil layers in GRASSMIND using a daily version of the Century soil model (Parton et al., 1988). Soil water stress is modelled using a linear reduction dependent on soil water content, permanent wilting point and field capacity (Granier et al., 1999). Species-specific differences in water uptake are a result of the water demand of plants (using the concept of water use efficiency) and their rooting depth in relation to the availability of water in different soil layers.

A similar approach is used for plant nitrogen stress. Based on the potential NPP, which is a balance between possibly limited GPP and autotrophic respiration (modelled proportional to plant biomass), the plant nitrogen demand is calculated using C:N ratios of green and brown leaves and roots (species-specific model parameters). Again, the potential NPP of a plant is reduced linearly dependent on the ratio of nitrogen supply and demand. Leave senescence can add nitrogen resources to the supply via retranslocation from yellowing to still green leaves. The actual GPP is calculated from the potential GPP by accounting for the limitations from temperature, water and nitrogen stress using multiplicative factors. Subsequently the autotrophic respiration is accounted for to obtain the actual NPP.

**Allocation, recruitment and mortality** The actual NPP is then distributed between shoots (stems and leaves), roots and reproductive biomass. A species-specific fraction is allocated to the shoots and the root biomass is updated dependent on this fraction and the shoot-root ratio. The remaining NPP is allocated to the reproduction pool. Corresponding nitrogen fluxes are calculated according to the respective C:N ratios. The growth of plants based on an increased net productivity results in an increased plant biomass, leaf area, rooting depth and root branch length, plant height and width, dependent on species-specific traits.

Recruitment and mortality of plants determine, in turn, the density of plants on the simulated area.

Recruitment can occur from three sources: migration from a surrounding meta-community as a constant inflow, sowing of seeds at specific times and local reproduction of plants depending on their fitness. Plants of a higher fitness are able to invest more of their NPP into reproduction and can produce more seeds. In this study, seed ingrowth from a meta-community and local recruitment are summarized in one model parameter. While seedlings can grow at any time and establish dependent on species traits (e.g. germination rate), plant mortality is modelled in terms of a background mortality and a crowding mortality. The background mortality is constant (but differs between seedlings and mature plants) and independent of environmental conditions and overcrowding. Plants that have reached their expected maximum age die immediately. If the total vegetation cover, which is calculated based on all plant's width or lateral expansion, exceeds an area size (of one m<sup>2</sup>), crowding mortality reduces the number of individual plants (irrespective of size or plant age). A full model description of GRASSMIND can be found in Taubert et al. (2012) and Taubert et al. (2020a) and Taubert et al. (2020b) and on [www.formind.org/downloads](http://www.formind.org/downloads).

### 2.2.2 Site and scenario description

Both models were applied to plots of the Jena Experiment, which is situated at the northern edge of Jena (Thuringia, Germany) on the floodplain of the Saale river (50°55'N, 11°35'E, 130 m a.s.l. Weisser et al., 2017). The annual mean temperature and mean annual precipitation between 1980 and 2010 were 9.9 °C and 610 mm/year, respectively (Hoffmann et al., 2014), and the soil is classified as Eutric Fluvisol (Roscher et al., 2004).

For our simulations, we used gap filled daily weather data for temperature, precipitation, and shortwave radiation from 2002 to 2014 (MPI, 2019; Taubert et al., 2020b). Within this period, annual precipitation ranged from 368 to 784 mm/year with a mean of 526 mm/year which is below the 1980 to 2010 average. For the use in LPJmL we had to normalize leap years (2004, 2008, and 2012) to 365 days. We chose to remove December 31st in leap years to maintain the seasonality within the years. Since data on harvest events were only available at monthly resolution (Weigelt et al., 2010), we assumed harvests to occur in the middle of the month (15<sup>th</sup>). Data on soil bulk density, field capacity and permanent wilting point were measured in four blocks set up along a soil texture gradient perpendicular to the river Saale (Roscher et al., 2004). In addition to the measurements we derived porosity from soil texture. For our simulations we always used the data on soil properties from the block in which our selected species plots were located.

### 2.2.2.1 Species selection

At the Jena site, several experiments were conducted in parallel. We use data from two experiments, the main experiment (Roscher et al., 2004), which was designed to compare the different diversity levels and the monoculture experiment (Heisse et al., 2007), which was established as a control, for example to compare mixture and monoculture yields. The species pool of the Jena Experiment consists of 64 species from four functional groups (grasses, small herbs, tall herbs, and legumes), that grow well under the site conditions (Weisser et al., 2017). Monocultures of all 64 species were established in the monoculture experiment, while in the main experiment monocultures of only 16 (four from each functional group) species were sown, limiting the number of species available for our study. We excluded the tall herb and legume species from our selection because we assumed the small herbs and grasses to be more suitable for usage in both models. Of the eight remaining species we excluded *B. perennis* because the experimental plots were strongly affected by the rust fungi *Puccinia coronata* and *P. graminis*, which led to a decrease in productivity and the abandonment of the plots in later years (Weisser et al., 2017). To reduce the complexity of our comparison we selected only four of the remaining seven species for our simulations. We selected three common fodder grasses (*Poa pratensis*, *Festuca pratensis* and *Festuca rubra*) and one very common small herb (*Plantago lanceolata*). For all selected species data was available in the two experiments allowing us to use the data of the main experiment for the calibration while evaluating the models against the data from the monoculture experiments.

### 2.2.2.2 Calibration and evaluation

For model calibration we used the data from the monoculture plots of the main experiment on above-ground biomass (AGB), leaf area index (LAI) and vegetation cover for both models, as well as vegetation height in addition for GRASSMIND (see 2.2.2.2). We evaluated the performance of both models, by using data on AGB from the monoculture experiment which consisted of small plots of monocultures of all species used in the main experiment (Heisse et al., 2007). For both calibration and evaluation, we used the daily weather data from 2002 to 2014 and the mowing frequency that was reported for the Jena Experiment, where plots were mown twice a year, usually in May and September. Plots of the main and the monoculture experiments were not fertilized, therefore, we did not add any fertilizer and excluded nitrogen deposition in our simulations.

The model specific calibration procedures as well as the parameters selected for calibration are described in A.1. The observed data sets used for the calibration and the evaluation both show a decrease of monoculture productivity over time (Marquard et al., 2013), which results in substantially lower values of AGB in the later years. Additionally, for some AGB observations, the variability of data for one sampling period was large, which was also found in other grassland experiments (e.g. Vuichard et al.,

2007). For LPJmL, a spinup run was conducted, to obtain soil carbon, nitrogen, water and temperature values to initialize the calibration and evaluation simulations (spinup conditions are described in A.1).

### 2.2.2.3 Simulation scenarios

As we were interested in the effects of drought and mowing on modelled processes and on the performance of species in monocultures and the two-species mixtures, we run three precipitation scenarios (baseline, moderate drought, extreme drought), each with and without mowing. Each scenario was run for 28 years: for the first 14 years the baseline scenario was used in all scenarios as a spinup to obtain an equilibrium state of the plant community. In GRASSMIND, the scenario simulations could be started right away, while for LPJmL they were based on the initial spinup run also used for calibration and evaluation. For the baseline treatment, we simply repeated these 14 years. For our drought treatments, we excluded parts of the rain (see below) in year 16, but returned to the baseline scenario for years 17-28. All evaluations refer to the years 15 to 28 of our simulations. We first generated our baseline scenario, in which we reduced the effects of intra-annual rainfall variability that could otherwise mask the effects of droughts. To obtain the baseline scenario (Baseline\_Mow) time-series we grouped the data based on annual and spring precipitation sums into three clusters using euclidean distances and a Ward clustering algorithm (Murtagh and Legendre, 2014). The hierarchical cluster analysis was performed with R Version 3.5.3 using the `hclust` function from the `stats`-package (R Core Team, 2019). We selected the cluster with the medium annual and spring precipitation which contained seven years. For the moderate drought scenario (ModD\_Mow) we used the same time-series but excluded precipitation in April and May of year 16. We extended the exclusion to March and June for the extreme drought (ExtrD\_Mow). By this, we reduced the annual precipitation by approximately 20 and 40%, respectively. We ran simulations for Scenarios Baseline\_Mow, ModD\_Mow and ExtrD\_Mow with limited nitrogen supply and with mowing. Additionally, we ran simulations with the same environmental conditions but without mowing (Baseline\_NoMow, ModD\_NoMow and ExtrD\_NoMow).

Table 2.1: Simulation scenario names, environmental conditions and management

<b>Scenario</b>	<b>weather data</b>	<b>precipitation reduction</b>	<b>management</b>
calibration/evaluation	observed	none	with mowing
Baseline/ModD/ExtrD_Mow	medium cluster	none/moderate/extreme	with mowing
Baseline/ModD/ExtrD_NoMow,	medium cluster	none/moderate/extreme	without mowing

## 2.3 Results

We analysed model outputs on above-ground biomass (AGB), GPP, NPP, LAI, Losses (litterfall and mortality), *cover* and water uptake. We present the results for AGB in the main text and for the other

variables (only for our baseline scenario Baseline\_Mow) in appendix A. In Section 2.3.1, we briefly present the results of the calibration and model evaluation. Subsequently, we analyze our results of AGB dynamics for monocultures and mixtures for both models for our scenarios in Section 2.3.2.

### 2.3.1 Model calibration and evaluation

Model calibration was successfully conducted for both models following the procedures described in A.1. Overall both calibrated models reproduced the observed data from monocultures of the main experiment well for AGB (described as organic dry matter), LAI and (for GRASSMIND) height, but not for *cover*. Agreement with the experimental data varied between the models and for different species (Fig. A.2-4).

We were able to calibrate LPJmL and represent four different species modifying only four parameters. The parameter sets of the four species were derived during the calibration starting from the same initial parameter values for all species. LPJmL showed good agreement with data on LAI (RMSE 0.53 to 1.18  $\text{m}^2 \text{m}^{-2}$ ) and moderate agreement with AGB observations (RMSE 46.4 to 245.8  $\text{gDM m}^{-2}$ ), but data on *cover* did not agree well (RMSE 0.24 to 0.59  $\text{m}^2 \text{m}^{-2}$ ). Simulated *cover* values of monocultures in the calibration of LPJmL were low compared to observations. In LPJmL, plant size is not explicitly simulated and *cover* is calculated as foliage projected cover (FPC) from the LAI assuming a strong connection of the two (see 2.2.1.1). Using both LAI and *cover* in the calibration results in a trade-off in favour of the one that leads to better results for AGB. Furthermore, since observed *cover* was estimated visually, we assume LAI observations to be more reliable and attribute only minor importance to the fit of *cover* for LPJmL.

The calibration of GRASSMIND for the four monocultures required the fit of 13 species-specific parameters and also included the vegetation height, in addition to the observed LAI, *cover* and AGB. Good agreement of GRASSMIND was achieved for LAI (RMSE 0.47 to 0.71  $\text{m}^2 \text{m}^{-2}$ ) as well as for vegetation height (RMSE 0.083 to 0.218 m) and AGB results agreed moderately with observations (RMSE 34.0 to 236.6  $\text{gDM m}^{-2}$ ). As in LPJmL, GRASSMIND simulations did not agree well with the observed data on *cover* (RMSE 0.22 to 0.46  $\text{m}^2 \text{m}^{-2}$ ), but in contrast to LPJmL, GRASSMIND overestimated vegetation cover. In the simulation of GRASSMIND, vegetation cover is derived from individual plant sizes and allowed to settle around 100%. For the model calibration, observed vegetation cover (excluding weeds and dead material) is therefore compared only with the cover of green leaves of the simulated plants (excluding standing senescent leaves). Note, that the calibration here differs from previous calibrations of GRASSMIND (Taubert et al., 2020b) to harmonize the study design and simplify the comparison of the two models (see section A.1 for a detailed description of the calibration procedure).

### 2.3.1.1 Deviations from observations

Although AGB values agreed only moderately with the observations, the agreement with the majority of the data is significantly better, because a major share (LPJmL: 51 to 81% and GRASSMIND: 57 to 87%) of the sum of square errors SE can be attributed to only two of the twelve observation dates for each species (Fig. A.5-7). The observations can be partitioned into high AGB and low AGB observations. For all the plots we used, high AGB observations were sampled in the early years (2002 to 2004) of the experiment, while observations from the later years showed substantially lower AGB because of a decrease in productivity (Marquard et al., 2013). A large share of the sum of SEs is related to the high AGB observations in the early years. This high productivity at the beginning of the experiment cannot be reproduced by either model. This may be a result of the uncertain initial soil conditions (e.g. soil fertility) because of the unknown management history prior to the experiment in Jena but may also be related to the obtained parameterizations. For both models, selected parameter values are static and cannot change over time, therefore as long as the environmental conditions and management remain similar, the models do not simulate any temporal trends. To adequately simulate the high AGB levels in the early years of the experiment a different set of parameter values would be needed. However, since the majority of the data consists of low AGB samples collected after the decrease in productivity the calibration procedure returns a set of parameter values which reproduce this subset of the observations well. We were able to confirm this with our evaluation (Fig. 2.2) where we used the AGB observations from the monoculture experiments (Heisse et al., 2007). Here, the RMSEs of both models were very similar (e.g.: 81.7 gDM m<sup>-2</sup> for LPJmL and 77.8 gDM m<sup>-2</sup> for GRASSMIND for *P. pratensis*). The data from the monoculture experiment show the same productivity decrease as the main experiment and similar to the calibration, a major share of the SE (55 and 82 %) can be attributed to only two observations (Fig. A.8).

### 2.3.2 Aboveground biomass dynamics and resource competition

In our comparison we focus on the differences and similarities in the AGB dynamics of both models for the different scenarios. We ordered the description of the results so that differences in climatic conditions and management to the baseline scenario increase step by step. First, we present results for our baseline scenario, Baseline\_Mow (see 2.3.2.1), which — while already using climate data with reduced variability (see 2.2.2.3) — is not subject to additional precipitation reduction and uses the standard management (as also used in the calibration and evaluation). Second, we compare the result from Baseline\_Mow to the drought scenarios (ModD\_Mow and ExtrD\_Mow see 2.3.2.2) in which precipitation reductions are prescribed. Third, we compare Baseline\_Mow, ModD\_Mow and ExtrD\_Mow to the scenarios without mowing Baseline\_NoMow, ModD\_NoMow and ExtrD\_NoMow (see 2.3.2.3).

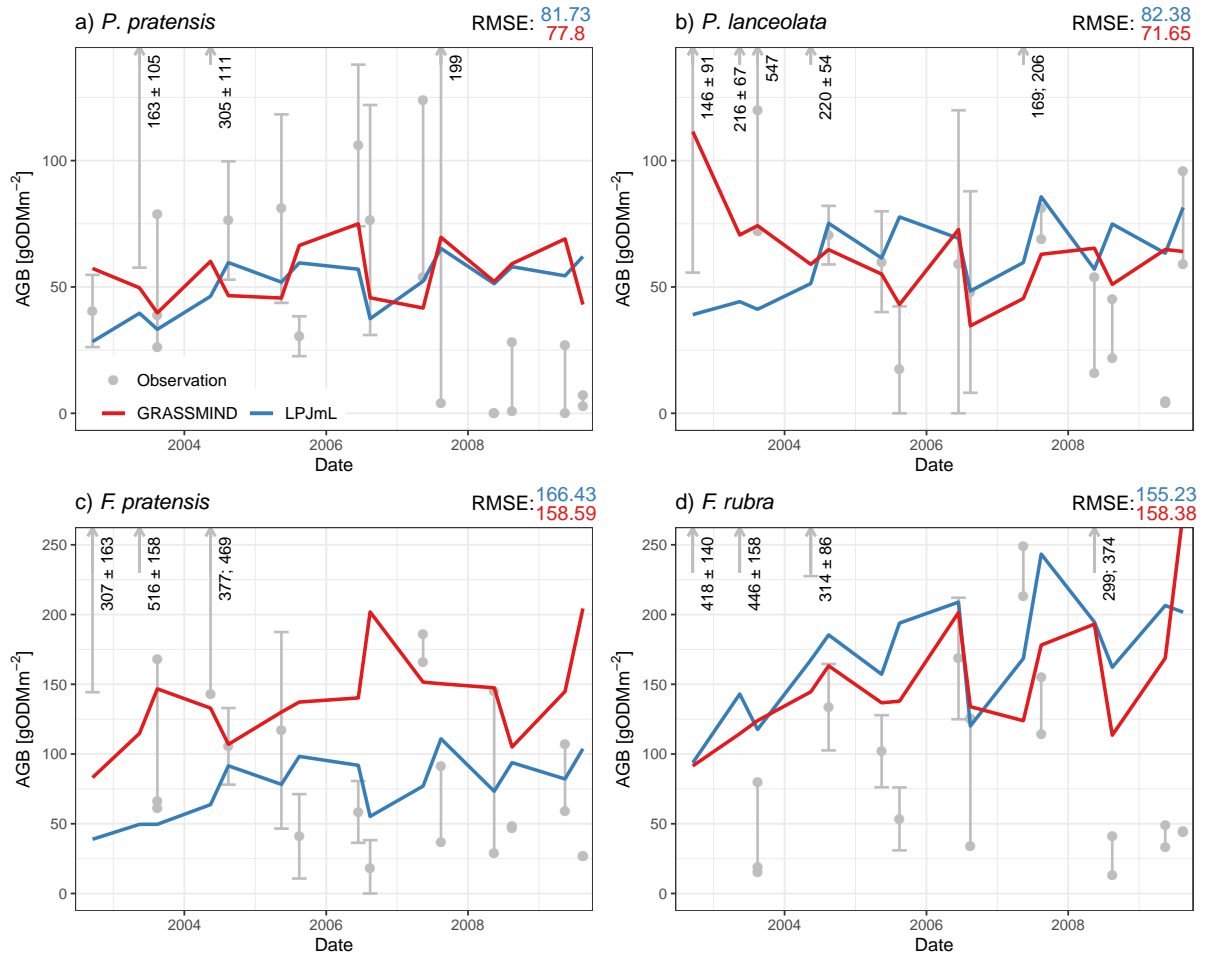


Figure 2.2: Simulated and observed AGB in  $\text{gDM m}^{-2}$  for *P. pratensis* (a), *P. lanceolata* (b), *F. pratensis* (c) and *F. rubra* (d) for GRASSMIND (red) and LPJmL (blue). Coloured lines and labels show model results and RMSE, grey points show observations used for the evaluation. Observations are the median of samples for each date and error bars show one standard deviation. If three or less observations were available all observations were plotted and their range indicated with a line. Outliers are highlighted with labels and arrows.

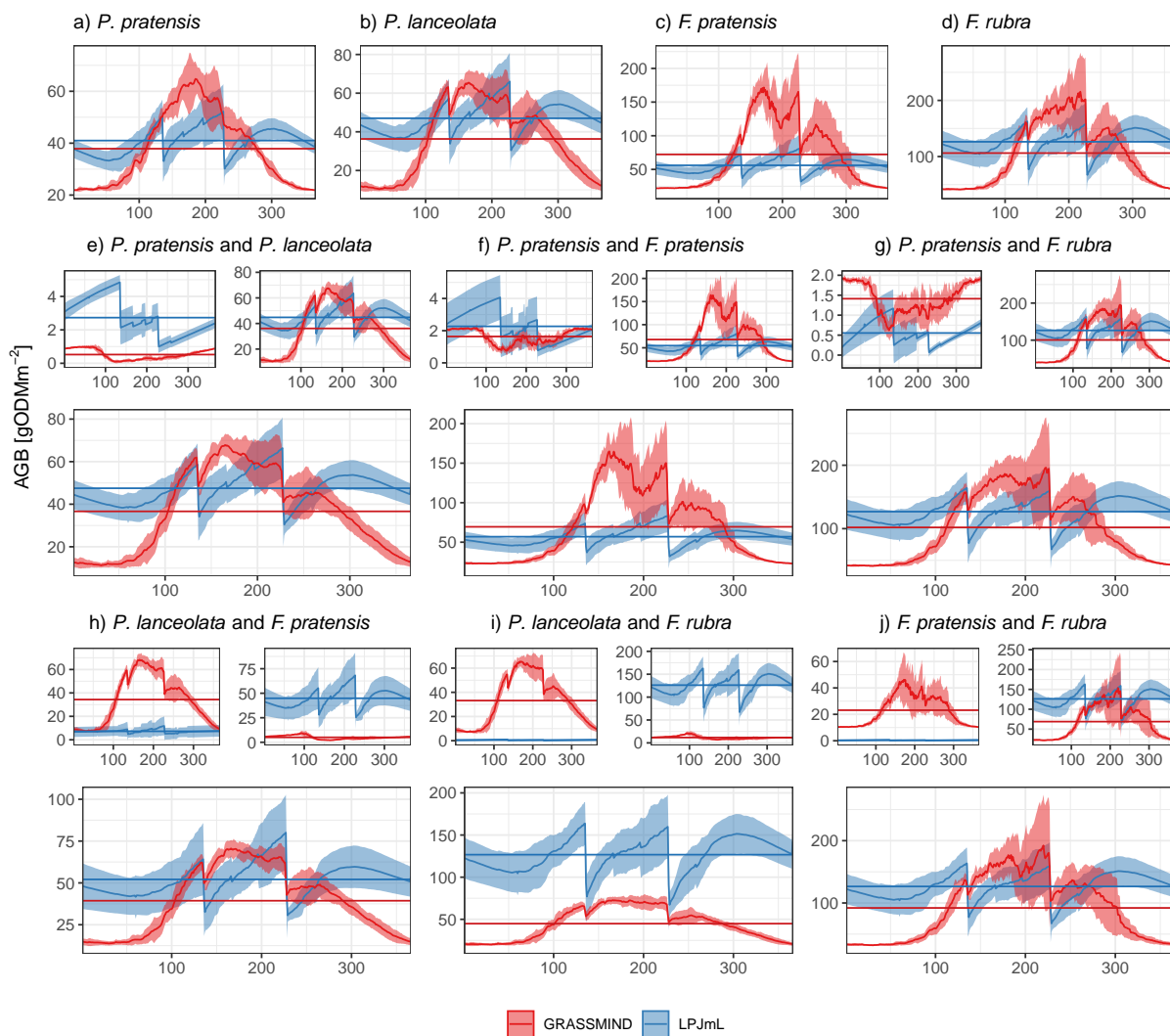


Figure 2.3: Mean ( $\mu$ ) AGB in  $\text{gDM m}^{-2}$  for GRASSMIND (red) and LPJmL (blue) averaged over all simulation years for each day of the year for monocultures (a,b,c,d) and two-species mixtures (e,f,g,h,i,j). For mixtures total AGB (top) and species specific AGB (bottom) are shown separately. Coloured ribbons show  $\mu \pm \sigma$ .

### 2.3.2.1 Simulated dynamics in the baseline scenario with mowing

The monoculture simulation experiments under the baseline rainfall treatment with mowing (Fig. 2.3 a-d) show similar overall means in AGB in both models. AGB values are highest for *F. rubra* (LPJmL: 126 gDM m<sup>-2</sup> and GRASSMIND: 106 gDM m<sup>-2</sup>) and lowest for *P. pratensis* (LPJmL: 41 gDM m<sup>-2</sup>) and *P. lanceolata* (GRASSMIND: 36 gDM m<sup>-2</sup>). However, the intra-annual dynamics indicate strong differences between LPJmL and GRASSMIND: The variation of AGB between seasons is much more pronounced for GRASSMIND than for LPJmL, with lower AGB in winter but for most species higher AGB during the summer months. This is connected to the different process implementations in both models that are used to derive NPP from GPP and autotrophic respiration and AGB losses in the form of turnover and mortality (see 2.2.1 and 2.4.1). For the two-species mixture experiments (Fig. 2.3 e-j) the AGB dynamics are driven by the dominant species. The dominant species can either be the same (Fig. 2.3 e-g) with similar differences in mean values as in the monocultures or different (Fig. 2.3 h-j) with larger discrepancies in mean values. In addition to NPP and AGB loss from turnover and mortality, competition between species affects the AGB dynamics. While these processes are sufficient to explain the off-season AGB dynamics, the additional reduction from mowing has to be considered for the dynamics within the growing season. The effect of mowing strongly differs between the two models (Fig. 2.3a-j) and is the underlying reason for the different AGB peaks during the growing season. In LPJmL, 47.6 to 207.0 gDM m<sup>-2</sup> is on average removed by mowing. This amount is significantly smaller in GRASSMIND (1.4 to 31.3 gDM m<sup>-2</sup>). The large differences in biomass reduction are related to the different implementations of the mowing routines and the representation of the plants themselves.

In both models, the dominant species exploit available resources more efficiently, which is related to the parameterization of the species. Higher parameter values for important traits are directly related to a higher competitive strength (Fig. 2.4). In LPJmL, this is related to the calibrated parameters via specific processes. While all parameters (Fig. 2.4) are important to calibrate the simulated AGB to the observations, the leaf to root ratio ( $lr$ ) and stubble density ( $\rho_{veg}$ ) are of minor importance for competition. Here, the light extinction coefficient ( $k_{beer}$ ) and the specific leaf area ( $SLA$ ) which are used to calculate  $FPC$  are most important. Higher values of these two parameters result in higher  $FPC$  values and the species utilize space more effectively.  $k_{beer}$  is highest for the most competitive species (*F. rubra*) and lowest for the least competitive species (*P. pratensis*).  $SLA$  is less important and only influences competitive strength for species with similar  $k_{beer}$  values (*F. pratensis* and *P. lanceolata*). In GRASSMIND, benefits of a species in the fast and successful establishment of seedlings, high germination rate ( $germ$ ), short time of emergence ( $t_{em}$ ) and low seedling mortality ( $m_{seed}$ ), also determine the competitive strength of that species in mixtures (as for *P. lanceolata*). In this case, the larger mature plant mortality ( $m_{basic}$ ) weighs less than the favourably low seedling mortality ( $m_{seed}$ ) because plants

mature later (higher  $age_{rep}$ ). Highly productive species (higher maximum gross leaf photosynthesis  $p_{max}$ , higher  $SLA$ , higher shoot-root ratio  $sr$ ) can be more competitive in mixtures which, however, can be altered by self-shading (high height-width ratio  $hw$ ) or shading by other plants (low  $hw$ ), by fast leaf senescence (low  $lls$ ) or waterstress-related attributes. The latter are of specific importance as we show in Section 2.3.2.2, while water use efficiency ( $WUE$ ) and allocation rate of net productivity to shoot biomass ( $alloc_{shoot}$ ) are only of minor importance (as for *P. pratensis*).

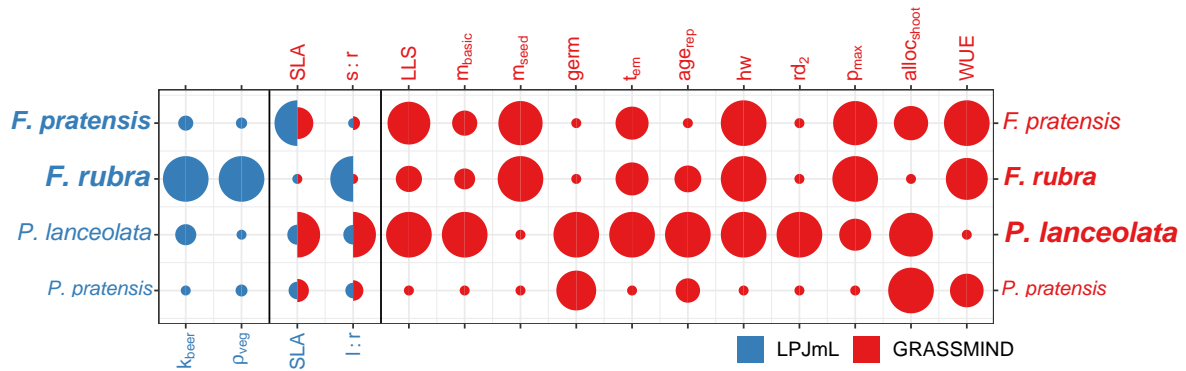


Figure 2.4: Normalized parameter values for GRASSMIND (red) and LPJmL (blue) for parameters important for species competition. Full circles show parameters which are not comparable between the two models and half circles show parameters used similarly in both models. The different species are ranked by competitiveness with the label size, ranging from most competitive (large) to least competitive (small).

### 2.3.2.2 Effects of rainfall reduction

In both models, the AGB decreased during the drought treatments with mowing (Fig. 2.5d and A.27-31d). Overall, effects were qualitatively the same for both the moderate and the extreme drought and just differed in their order of magnitude for both models. We compared the lowest AGB values during the drought (Fig. 2.5e and A.27-31e i.e. the maximum difference between the baseline and the drought scenarios) for both models. While the smallest differences between the baseline and drought scenarios are similar between the two models during the moderate and the extreme drought (LPJmL: -13.9 and -23.1  $gDM m^{-2}$ ; GRASSMIND: -11.5 and -12.0  $gDM m^{-2}$ ), in GRASSMIND the largest differences are more extensive (-130.5 and -170.7  $gDM m^{-2}$ ) than in LPJmL (-77.2 and -110.5  $gDM m^{-2}$ ). The decrease of AGB under drought is a result of the reduced water uptake (Fig. 2.5e and A.27-31e) after soil water resources in the first 20 cm of the soil are depleted. This depletion of soil water content is stronger in GRASSMIND (-20% Fig. 2.5b and A.27-31b). Here, the permanent wilting point is reached and no water is available for transpiration, leading to no plant growth (i.e. GPP) at all and a fast decline of AGB, caused by continued mortality and turnover. In LPJmL, the soil water depletion is less

severe (-13 to -14%) but the reduced water supply also limits GPP. The balance of the reduced GPP, the respiration (which is not affected by the drought) and turnover becomes negative and AGB decreases. Compared to GRASSMIND, this results in a smaller and slower decline of AGB.

After the end of the drought treatment, soil water resources are replenished. In both drought scenarios a similar soil water content compared to the baseline scenarios is reached shortly after the end of the drought (Fig. 2.5b and A.27-31b). However, in all scenarios, the soil water content remains below field capacity because of the low July precipitation which results in additional water stress (Fig. 2.5c and A.27-31c).

After the end of the treatment, vegetation recovers at different speed in both models. In GRASSMIND, the recovery is fast and the AGB reaches a pre-treatment level soon after the soil water is replenished (Fig. 2.5d and A.27-31d). In LPJmL, recovery is slower and AGB two years after the treatment can still be substantially lower than the pre-treatment AGB. After a complete recovery, the AGB of the scenarios with rainfall reduction treatments and the baseline scenario are the same, because of identical environmental and management conditions. In LPJmL, all simulated species suffer from the drought and only start recovering after the end of the drought. In GRASSMIND, this is similar except for *P. lanceolata* which after a short period of AGB losses, already gains biomass (i.e. positive GPP) during the drought. This is the only deep rooting species with higher values of the parameters of the rooting depth power law relationship ( $rd_1$  and  $rd_2$ ). These ensure a good species performance and competition even during the precipitation reduction were *P. lanceolata* takes advantage of water in deeper soil layers (Fig. A.27,29 and 30) and benefits from the reduced crowding mortality.

### 2.3.2.3 Comparison of mowing effects

Mowing has very different effects in the two models in the monoculture and mixture simulations for the baseline scenario (Fig. 2.6a and A.32-36a). In GRASSMIND, mean AGB values are barely higher in the baseline scenario without mowing than with mowing (-1.5 to +4.5 gDM m<sup>-2</sup>), while in LPJmL these are considerably larger (+90.6 to +210.7 gDM m<sup>-2</sup>). As established in Section 2.3.2.1, mowing plays an important role for AGB dynamics. In GRASSMIND, the amount of biomass reduced is not pre-determined but linked to the plant height structure of the community (i.e., frequency of large and small plants). Because only a few individuals exceed the mowing height (here 0.1 m) the reductions from mowing are small. In contrast, in LPJmL vegetation height is not simulated and mowing directly reduces AGB to a predefined threshold.

The effect of mowing on mean AGB also alters the effect of the moderate and extreme precipitation reduction, increasing the differences between the models (Fig. 2.6b,c and A.32-36 b,c). Losses during the reduction treatment are similar to those in the scenarios with mowing in GRASSMIND (-7.2 to

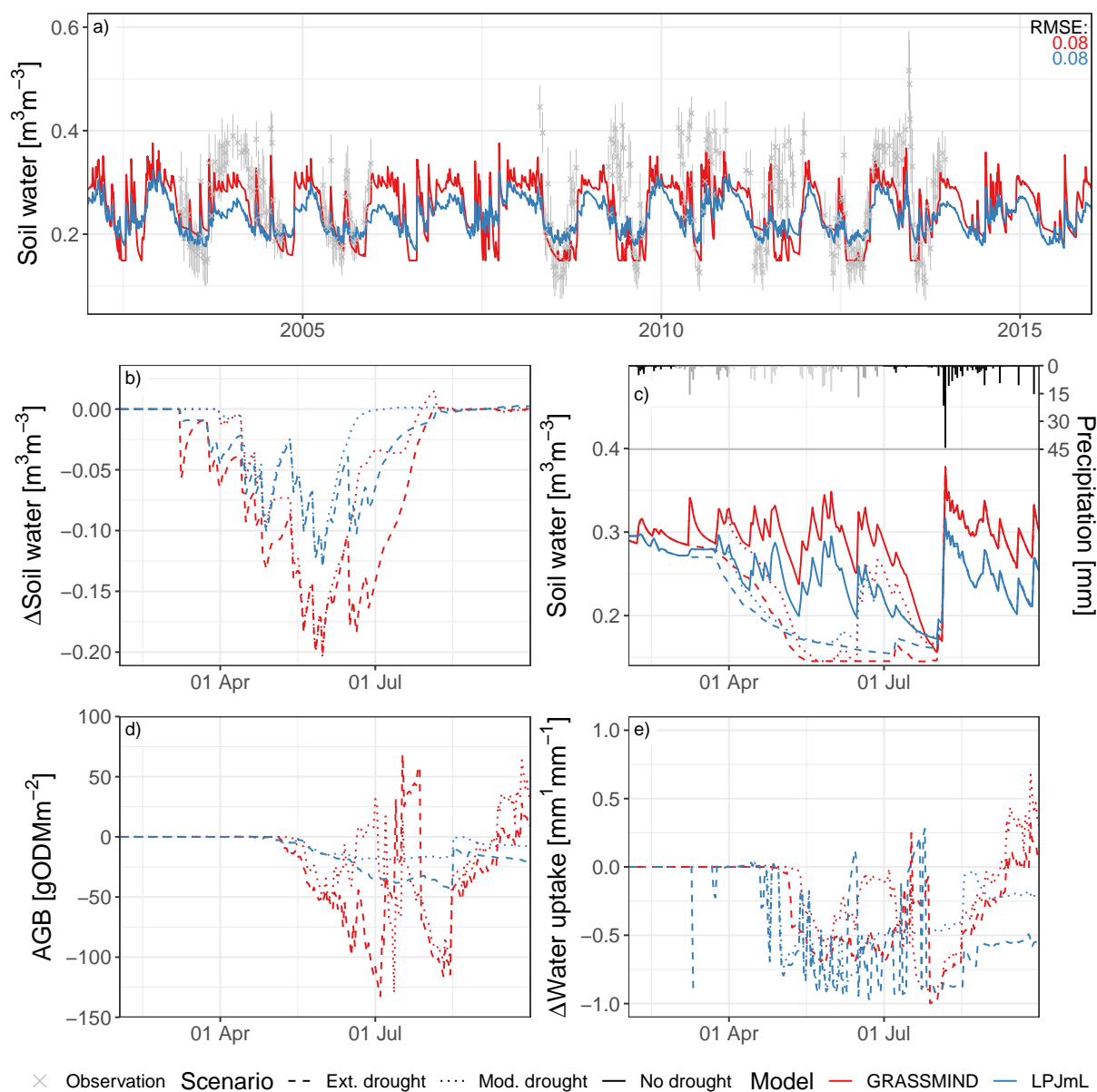


Figure 2.5: Simulated and observed (Fischer et al., 2019) fractional soil water content at the Jena Experiment site (a), relative changes of soil water content in  $\text{m}^3 \text{m}^{-3}$  (b), absolute changes of soil water content in  $\text{m}^3 \text{m}^{-3}$  as well as daily precipitation in mm with reduction for ModD (light grey) and ExtrD (light and dark grey) (c), absolute changes in AGB (d) in  $\text{gDM m}^{-2}$  and relative changes in transpiration (e) caused by the moderate (dotted) and extreme (dashed) droughts for LPJmL (blue) and GRASSMIND (red). Simulation results of mixture of *P. pratensis* and *F. pratensis* using observed weather data (a) and average climate (b-e).

-160.1 gDM m<sup>-2</sup>), but strongly increase in LPJmL (-70.8 to 156.5 gDM m<sup>-2</sup>), because the generally higher AGB leads to higher turnover and respiration (Fig. A.19). As in the scenarios with mowing, community composition was barely affected in the scenarios without mowing, regardless of the precipitation reduction treatment (Fig A.14,22,23).

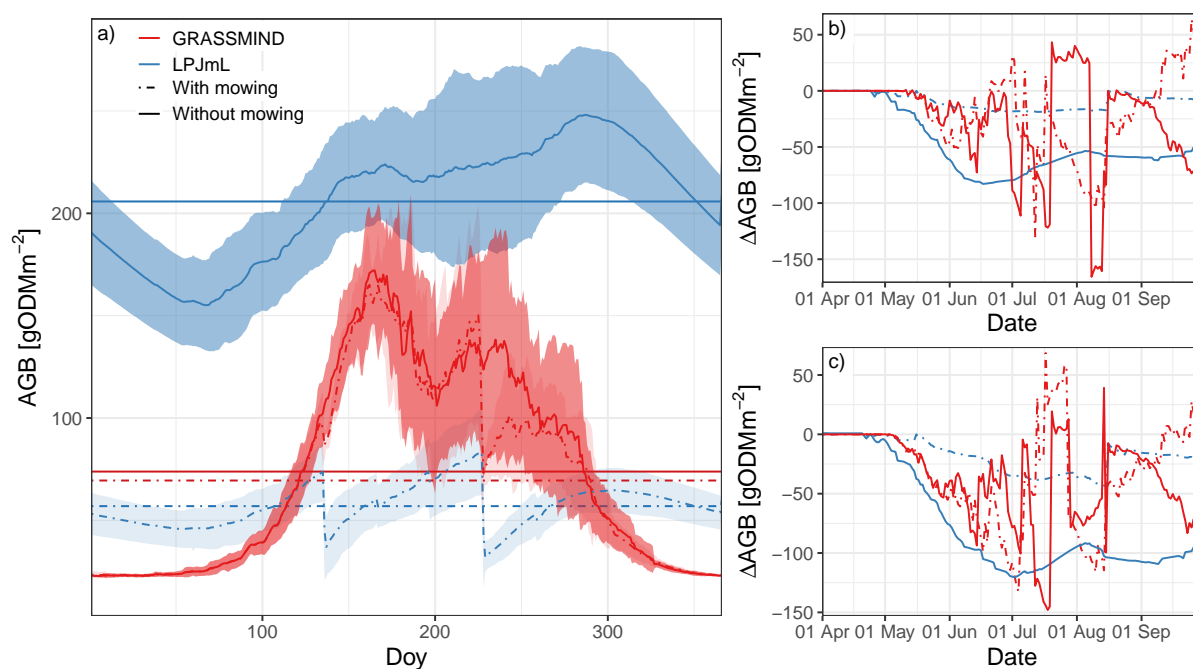


Figure 2.6: Mean ( $\mu$ ) AGB in gDM m<sup>-2</sup> for GRASSMIND (red) and LPJmL (blue) for the sum of the two-species mixture of *P. pratensis* and *F. pratensis* (a). Coloured ribbons show  $\mu \pm \sigma$ . Horizontal lines show overall mean for Baseline\_Mow (dot-dashed) and Baseline\_NoMow (solid). Difference between Baseline\_Mow and ModD\_Mow (dot-dashed) and ModD\_NoMow (solid, b) and ExtrD\_Mow (dot-dashed) and ExtrD\_NoMow (solid, c) between April and October of the drought year.

## 2.4 Discussion

Differences in simulated responses of monocultures and two-species mixtures to drought and mowing can be related to process representations of above- and below-ground resource competition, as well as of water dynamics and community representation. Even though we could not test the relevance of individual processes, the differences between model results and implemented features can shed some light on the importance of different mechanisms and model features for simulated dynamics.

### 2.4.1 Above-ground biomass seasonality

The two models show substantially different intra-annual AGB dynamics for which we identified several underlying mechanisms. Strongest differences were found during the off-season, where no data is available from the Jena Experiment for calibration or evaluation of the models, suggesting that the

calibration process helped to reduce differences between models.

#### 2.4.1.1 Processes determining AGB

Our simulations show that GPP and NPP have higher average and peak values for GRASSMIND (Fig. A.9,10). Gains in biomass are resulting from NPP, which is dependent on GPP. Both are controlled by LAI and *cover*, which also show higher average and peak values for GRASSMIND (Fig. A.11,12), and together with the amount of absorbed radiation determine the rate of photosynthesis. Here, the models use different process realisations: In GRASSMIND, vegetation height and LAI of each individual determine its GPP from which respiration losses are subtracted to obtain NPP. In LPJmL, *cover* (calculated as *FPC* using LAI) is used to determine the amount of absorbed radiation and resulting GPP. Similar to GRASSMIND, autotrophic respiration is subtracted to obtain NPP. Both models account for the effect of shading differently: GRASSMIND directly via interactions between individuals and LPJmL indirectly within the calculation of *cover*. While the high LAI values for GRASSMIND result in high productivity, the lower LAI values for LPJmL lead to low *cover* values and lower productivity. The higher productivity of GRASSMIND can only lead to the similar average value of AGB we observed for the two models, if it is counteracted by higher losses. These result from age- and overcrowding-related mortality and turnover, as well as mowing during the growing season (Fig. A.13). Turnover and in the case of GRASSMIND also age mortality constantly contribute to these losses (independent of environmental conditions and management), but with different magnitudes in both models. Losses from overcrowding are linked to total plant *cover* and describe competition for space, which can lead to decreased establishment and increased mortality in both models. In GRASSMIND, *cover* includes alive and standing senescent biomass. Here, available space is always fully occupied, leading to a constant loss of biomass from overcrowding. This loss arises from the number of individuals that die from overcrowding which is dependent on the number of individuals present and the total *cover* of the plot (Tab. A.8). In GRASSMIND, competition for space occurs between conspecifics (individuals of the same species) and heterospecifics (individuals of different species) and is therefore also effective in monocultures, whereas in LPJmL competition for space occurs only between different species, so that losses due to overcrowding do not occur in monocultures and observed losses result from turnover (Fig. A.12 a-d).

#### 2.4.1.2 AGB dynamics outside and during the growing season

The higher winter AGB in LPJmL compared to GRASSMIND originates in the model-specific representation of the leaves. In both models, AGB is the entire amount of standing biomass. In LPJmL, a distinction between photosynthetically active (green) and already senescent leaves (yellow) is not made,

but a constant proportion of the total leaf biomass is transferred to the litter pools each day of the year. In GRASSMIND, such a distinction is made, but yellow AGB is constantly transferred to the litter so that AGB consists predominantly of green leaf biomass. This results in a larger reduction of the AGB during the off-season. Therefore, AGB shows high values during the growing season, but low values during the off-season in GRASSMIND, while in LPJmL despite similar GPP and NPP, AGB values are higher.

These differences are sufficient to explain the off-season deviations between the models, where biomass losses from overcrowding lead to the lower AGB of GRASSMIND. However, to fully explain the differences within the growing season, the additional reduction of AGB from mowing has to be considered. The effect of mowing strongly differs between the two models (Fig. 2.3a-j). In GRASSMIND, the vegetative height of the individuals is explicitly simulated, and during mowing events only larger individuals are reduced. Because the simulated height distribution of the community is often skewed towards smaller individuals, biomass reductions are small. In LPJmL, height is not simulated explicitly and the amount of extracted biomass is determined as the difference between total AGB and a predefined residual biomass. This results in the different AGB during the peak growing season.

We are aware that monocultures and two species mixtures are not representative for the diversity of grassland communities and are thus difficult to compare to observations from other grassland ecosystems. Nevertheless, empirical studies that support both types of AGB seasonality exist. AGB dynamics of LPJmL are comparable to observations of total AGB (e.g. Poyda et al., 2020) while the dynamics in GRASSMIND are similar to observations of green AGB (e.g. Inoue et al., 2015).

#### **2.4.1.3 Processes controlling drought response**

The comparison to the scenarios with a moderate and extreme drought showed an effect of the drought on AGB during and after. Although water became limiting during the drought, competition for space remained strong and the community compositions of the two-species mixtures were barely affected. In none of the mixtures the subordinate species gained a substantial advantage in either of the models (Fig. A.20,21). Both the moderate and the extreme drought lead to short term reductions of AGB followed by a full recovery. The drought effect was stronger in GRASSMIND, where water uptake is only limited by the available soil water. If this falls below a threshold, water stress occurs regardless of plant water demand, which in reality might still be fulfilled even under a reduced water supply. On the contrary, in LPJmL plant water demand is calculated depending on the potential canopy conductance (which is derived from the productivity of the AGB) and compared to the supply. Therefore, even if the soil water content is low, especially species with a low AGB may not suffer from water stress even under a reduced soil water content. The water stress during the drought directly inhibited growth

of new biomass. However, the losses depicted in Section 2.4.1.1 are only indirectly affected by the environmental conditions through the reduced amount of available biomass or covered area and remain substantial (Fig. A.24-26). This changes the balance between biomass gains and losses and leads to an overall decline of above-ground biomass.

In GRASSMIND, the drought affects the community structure which consists of different individuals, leading to different productivity and mortality patterns compared to the baseline scenario. In contrast, in LPJmL the average individuals adjust to the changing conditions and become similar to the baseline scenario after a full recovery.

#### **2.4.1.4 Recovery after drought**

While recovery from drought in GRASSMIND was fast, it took up to two years in LPJmL. Drought recovery depends on a number of factors and evidence from observational studies exists, supporting the fast recovery (e.g. Hofer et al., 2016) as well as the slow recovery (e.g. Sala et al., 2012). However, the different model responses to similar conditions suggest drought recovery is not well captured by the models and additional research is needed. For this, we provide some insight on the mechanisms implemented in both models: In GRASSMIND, the fast recovery is possible, firstly because water stress is only dependent on supply. As soon as the soil water supply is replenished, while the demand is still lower than before the drought, the water stress penalty is removed which allows optimal growth of newly established seedlings. Secondly, plants in GRASSMIND do not change or adapt specific traits in response to drought events, like the allocation of NPP to above- or below-ground biomass or the water-use efficiency. In LPJmL, recovery takes longer because of two reasons. First, the loss of vegetation during drought reduces the water demand and limits productivity even after soil water is replenished. Second, water stress triggers an increased resource allocation to the roots, i.e. below-ground biomass (BGB), which is not reversed instantaneously when carbon assimilation or vegetation carbon is low. The additional allocation to BGB during and shortly after the drought results in a lower AGB implying also reductions of *FPC*. As *FPC* is used as an estimate of the covered part of the plot and therefore controls the access to resources, the calculation of plant-available water is reduced to the covered share of the plot.

#### **2.4.2 Species interaction and community assembly**

We identified competition for space as the main driver of species interactions in both models (see 2.4.1). Despite the differences in AGB, the competition for space shows a weak seasonality in both models. In LPJmL, this depends on the LAI, which shows a weak seasonality and therefore, the competition for space is similar within and outside the growing season. In GRASSMIND, the AGB and LAI seasonality

are more pronounced but both have no effect on the competition for space, which is determined from the *cover*. This is high within and outside the growing season and so is competition for space. Coexistence between species without one species being strongly dominant occurred in GRASSMIND and LPJmL only in rare cases of mixtures, when species showed similar competitiveness. Stable coexistence has to be achieved to assess the effects of plant species richness, because it is a precondition for long-term maintenance of diversity (Turnbull et al., 2013). To achieve this, fitness as well as niche differences have to be simulated appropriately (Chesson, 2000) and process representations need to be improved. For GRASSMIND, additional insights on community dynamics could be gained through the extraction of density dependence functions of the different species mixtures (Han et al., 2019). However, for LPJmL the density dependence functions would always be constant because only one average individual is simulated to represent an entire species. Therefore, we did not pursue this further but instead focused on identifying key processes by assessing the role of specific parameters (2.4.2.1) and responses to changes in environmental or management conditions (2.4.2.2).

#### **2.4.2.1 The role of specific model parameters**

In both models, the species that grow fast (higher SLA) and intercept light more efficiently (higher  $k_{beer}$ ) are more competitive. These two parameters have a strong influence on simulation results which is in line with findings from sensitivity analyses (see A.1 and Forkel et al., 2014; Hetzer et al., 2021; Schmid et al., 2021; Taubert et al., 2020a; Zaehle et al., 2005). Even though the different shoot:root ratios between species lead to different overall root carbon, competition for below-ground resources does not play a major role. However, in LPJmL only the assumed species-specific vertical distribution of roots and in GRASSMIND the maximum rooting depth, are considered for water uptake, neglecting the horizontal branching of root networks. In LPJmL, the vertical root distributions are similar for the simulated species, as is the maximum rooting depth in GRASSMIND, except for *P. lanceolata* which had access to deeper soil layers than the other species. Nevertheless, competition for space outweighed that for below-ground resources.

#### **2.4.2.2 The effect of drought and mowing on competition**

A moderate or extreme drought leads to major reductions in biomass but does not or only barely change the interaction between the species. In neither model, root biomass is considered for the calculation of water supply. Instead LPJmL determines the access to soil layers based on the vertical root distribution and uses *cover* to distribute available water between species. GRASSMIND determines access depending on rooting depth assuming roots are equally distributed among accessed layers and uses potential GPP to calculate the individual plants' water demand which is reduced by a multiplicative factor under

water stress to determine uptake. This underpins that competition is driven by above-ground processes and emphasizes the necessity to focus future model development on below-ground plant organs and processes. This may be a challenging task since knowledge on root traits, below-ground processes and driving forces are distinctively harder to obtain from field experiments and observations (Delory et al., 2017; Polomski and Kuhn, 2002). Recent efforts to build a global database for root traits (Guerrero-Ramírez et al., 2021) may help to better inform parametrization of root distributions and access to soil resources. Comparing the scenarios with and without mowing revealed not only substantial differences in the effect of mowing on AGB but controversially showed that mowing affects competition for space differently for both models. In LPJmL, mowing increases the competition for space. This is best illustrated using the mixture of *P. lanceolata* and *F. pratensis*. Here, stable coexistence of two species emerges in the scenarios without mowing, but *F. pratensis* dominates in the mown scenarios. In LPJmL, these two species have similar competitive strength (see 2.3.2.1). Following this, we hypothesize that mowing increases competitive pressure in LPJmL and the stronger competitor is dominant even at small differences between two species. Mowing in LPJmL reduces the AGB to a species specific residual. However, this residual is scaled with the species *FPC* to constrain the total residual biomass of the community. When the species have similar AGB, they constitute a similar *FPC* and the species with the higher species specific residual ( $\rho_{veg}$ ) has an advantage in the scenario with mowing but not in the scenario without mowing. If the competitive strength of the two species differs, the dominant species with the higher *FPC* always has an advantage. In GRASSMIND on the other hand, competition for space is stronger in the scenarios without mowing, because mowing shifts the individuals' height to width relationship, which leads to increased investments into height growth after a mowing event and a reduced investment into area growth and competition for space between conspecifics and heterospecifics. Without mowing, the individuals can continuously invest more of their productivity into expansion leading to an increased competition for space and overcrowding mortality. While we did not observe any changes in community composition in our simulations, these can occur if the species have different geometrical properties. For example, a species producing smaller and wider individuals would outcompete a species producing tall and thin individuals in the scenario with mowing and vice versa in the scenario without mowing.

### 2.4.3 Limitations

Our model comparison focused on differences and similarities of two grassland models. To compare the models, we developed a calibration setup using only observation data from monocultures. The rare emergence of coexistence between two species in GRASSMIND simulations results from this constraint to monoculture observations included in the calibration and the fixed non-adaptive behaviour of plant traits. Results from a recent study with GRASSMIND (Taubert et al., 2020a) showed coexistence of

*P. pratensis* and *P. lanceolata* similar to observations, calibrating on observational data of monocultures and mixed patches. In contrast, we only used monoculture data for calibration. As plant traits in GRASSMIND are fixed and do not change in response to species interactions, the calibration of this study captures predominantly intra-specific plant interactions rather than inter-specific interactions. Further, we here prescribed similar seed recruitment rates for the analysed monocultures and mixtures which already changes the competitive strength of some species (in contrast to Taubert et al., 2020a). The better reproduction of coexistence of species in Taubert et al. (2020a) in comparison to our setup suggests that calibration should be done against data that include inter-species interactions, which may otherwise be lost in the simulations. The more balanced species composition in GRASSMIND may emerge because the individual based approach and the explicit simulations of plant geometry generally allows a broader representation of different ecological strategies. Competition for space between conspecifics and heterospecifics is simulated depending on the geometry, while competition for other resources is more dependent on functional traits. In LPJmL, plant geometry is not simulated and the *FPC* is extensively used, not only in the competition for space, but also for other resources such as light and water. This contains the assumption that an investment in increased AGB (leading to an increased *FPC*) will improve both above- and below-ground resource exploitation similarly, while investments in BGB do not yield any advantage. This assumption may be valid for productive habitats, where only radiation but not below-ground resources are limiting and increased investment in BGB has no advantages. In these habitats, species following a competitive strategy with a fast exploitation of available resources are dominant. In other habitats (e.g. where below-ground resources are limited) a mix of species following different ecological strategies may emerge. However, controlling the resource exploitation for multiple resources using the same traits, precludes the trade-offs between different strategies and leads to the dominance of competitive species in all habitats. Here, different resource exploitation strategies and the trade-off between resource exploitation and stress tolerance have to be considered. The data available from observations additionally limited the calibration setup (see 2.3.1). Only two observations per year, both within the growing season, were available and therefore the seasonality can not be inferred from the data. Data for all monocultures show a strong decrease in soil fertility and AGB a few years after the start of the experiment (Weisser et al., 2017). This decrease cannot be captured by the models, which only capture the low values well.

Additional limitations were introduced by our scenarios. First, the simulated drought does not consider changes in radiation, humidity, wind speed and temperature which covary (Mishra and Singh, 2010; Wilhite, 2000) and is therefore comparable to a rainfall exclusion experiment (Reynolds et al., 1999; Yahdjian and Sala, 2002) instead of a real world drought. Second, mowing was conducted at a height of 10 cm at the Jena Experiment. However, while in GRASSMIND the height is explicitly simulated and, therefore, the mowing height can be defined as an input, in LPJmL this is not possible,

and the residual biomass after mowing is used as a proxy for mowing height. Since no data on residual biomass was available from the Jena Experiment, we cannot evaluate whether the mowing simulated in the models is a realistic approximation of the mowing conducted at the Jena Experiment.

Both models did not reproduce the variability of the observed soil water content (see Fig. 2.5a and Fig. S2.1), which for LPJmL is in line with a recent study on nitrogen emissions (Lutz et al., 2020). However, the importance of these discrepancies for the observed responses of AGB and community composition remains unclear and we see the need for an in-depth study of soil water dynamics, especially considering that other recent studies suggest that the drought response is not well captured in terrestrial biosphere models (Bastos et al., 2020; Paschalis et al., 2020).

#### 2.4.4 Fields of model development

Our comparison highlighted fields to consider for future model development. While the inclusion of other models of grassland dynamics was beyond the scope of our analysis, GRASSMIND and LPJmL are representative of specific types of models (see 2.1.3) for which comparable model representatives may show similar or additional challenges but also potential solutions when applied to the same research questions and settings as pointed out here. The core of numerous models is the productivity in the form of photosynthesis. The simplified Farquhar photosynthesis model (e.g. in LPJmL, Farquhar and Caemmerer, 1982) has a great depth of biochemical detail, while the single-leaf photosynthesis model (e.g. in GRASSMIND, Thornley and Johnson, 1990) uses a more aggregated calculation integrated over the individuals projected area (Taubert et al., 2012). An even simpler approach just uses light-use efficiency (e.g. LINGRA, Schapendonk et al., 1998). In all of these approaches, water stress is considered by a reduction of productivity at optimal water supply by either a reduction factor (GRASSMIND, LINGRA) or an adjustment of the maximum carboxylation rate  $V_{max}$  (LPJmL). Our study shows that both options simulate a response to drought, however this is mediated by the interaction with the representation of soil water dynamics, which can strongly impact onset, duration and recovery time of the drought response. Additionally, the current representation of photosynthesis is aggravating realistic simulations of rainfall exclusion experiments or droughts and future model development should include non-stomatal limitation of photosynthesis (e.g. reduced RuBisCo activity, Medrano et al., 1997; Parry et al., 2002) during drought (Zhou et al., 2017).

Furthermore, in both models, transpiration response to water stress is modelled linearly and transpiration reduction is overestimated for soil water levels close to field capacity. Experimental data however suggest a nonlinear relationship (see Verhoef and Egea, 2014, for a collection of experiments). A variety of nonlinear approaches exist, however since we did not test their suitability for the different model types, we do not give a recommendation but refer to Dewar (2002) and Egea et al. (2011) and Verhoef

and Egea (2014) for further reading.

Competition was focused on space and light, while below-ground processes played a minor role. So far, only the distribution but not the amount of BGB is used for resource competition and trade-offs between higher investments in AGB or BGB cannot be represented. This may be attributed to the original development for a temperate climate. However, this missing strategy trade-off is one reason why the simulated drought had little impact on competition dynamics. Additionally, drought response could be improved by systematically testing and incorporating drought escape (Kooyers, 2015; Norton et al., 2016) and tolerance (Ratzmann et al., 2019a; Ratzmann et al., 2019b; Zwicke et al., 2015) strategies in the existing model structures or implement hydraulic failure of severely stressed vegetation (see e.g. Kennedy et al., 2019; Sperry et al., 2016). The Hurley pasture model (Thornley, 1997; Thornley, 1998) follows a resistance approach considering root mass, root density and the resistance in the bulk soil (Thornley, 1996; Thornley and Verberne, 1989) that could be feasible for models using a light-response function and can likely be adapted for a Farquhar approach. Drought response is not only dependent on the soil hydrology models used but also depends on the models capacity to simulate specific strategies for (i) water use efficiency, (ii) carbon allocation, (iii) root distribution and (iv) regeneration of different species after drought (van der Molen et al., 2011). While numerous approaches to improve soil hydrology exist (Deckmyn et al., 2020; Vereecken et al., 2016; Vereecken et al., 2019), the simulation of coexistence of multiple species and their specific strategies remains challenging (see 2.4.2). To further improve the models and enable the simulation of stable coexistence and therefore plant species richness, plant interaction models, which were explicitly designed to assess biodiversity effects may serve as additional inspiration for model development. A key limitation was the simulation of niche differences, which are a necessary condition for stable coexistence. In addition to the process improvements suggested above, adding a hierarchy that determined resource access for each species and resources was shown to be a feasible approach (Clark et al., 2018). To separate above and below-ground niches, the below-ground space has to be distributed between species or individuals in addition to the above-ground space. In GRASSMIND, a refinement of the below-ground geometry (non-uniform vertical root distribution per plant) and hierarchically modelled resource access could be beneficial. For LPJmL, the root biomass within each soil layer and a species specific lateral distribution could be combined to distribute below-ground resources.

## 2.5 Conclusion

Recently, empiricists as well as modellers have suggested biogeochemical models as a potential tool to complement empirical research to increase the knowledge on interacting responses of biotic and abiotic components of grasslands to changing environmental conditions and the underlying mechanisms (Van

Oijen et al., 2020; Wilcox et al., 2020). Currently, approaches that prescribe the species' share within the community based on environmental factors, phenology and management exist (Confalonieri, 2014; Movedi et al., 2019). However, these do not consider the underlying mechanisms explicitly. To enable process-based models to simulate differently diverse communities and quantitatively assess the effect of plant species richness, substantial model development is needed. We compared two grassland models that have been developed at different scales, under different assumptions and for different purposes but which are representative of several other models. Despite the differences, the models showed similar weaknesses. Already at low diversity levels (monocultures and two-species mixtures), the models had difficulties to simulate a balanced community. In the majority of our scenarios, one species contributed almost the entire biomass of the mixture. While this can partially be attributed to the study design, a considerable part is related to the process representations in the models. Substantial improvement of these processes is needed to enable models to also simulate communities that are only weakly dominated by one species. We identified several responsible processes and suggested potential solutions based on our findings and available literature. Additionally, we found that the outcome of competition in the models was determined by the same processes independent of resource availability (Drought did barely affect species presence), which shows that the representation of trade-offs between different ecological strategies also needs improvement. As LPJmL and GRASSMIND can be seen as typical representations for particular types of models, this reveals potential pathways of model development to improve the interaction between species and drought response for similar models. For other model types, our study may serve as an example for a structured assessment of implemented processes, that can be used to identify and address the key parts of the model hindering a more realistic representation of multi-species communities or species interaction in a structured way. In cases where empirical data is needed to improve the models, knowing the specific processes that should be developed further is useful to inform field researchers.

**Code and data availability:** The model output data used for this study are openly available at <https://doi.org/10.5281/zenodo.4720262>.

**Author contributions:** **Stephen B. Wirth:** Conceptualization, Methodology, Software, Validation, Formal analysis, Investigation, Writing - Original Draft, Visualization **Fraziska Taubert:** Conceptualization, Methodology, Software, Validation, Formal analysis, Investigation, Writing - Review & Editing, Visualization **Britta Tietjen:** Conceptualization, Methodology, Writing - Review & Editing **Christoph Müller:** Writing - Review & Editing, Resources, Supervision **Susanne Rolinski:** Conceptualization, Methodology, Writing - Review & Editing, Supervision

**Acknowledgements:** SBW acknowledges financial support from the Evangelisches Studienwerk Villigst foundation, under the research program: "Third Ways of Feeding The World" and the German Federal Ministry for Education and Research (BMBF) within the projects Climasteppe (grant 01DJ18012) and POLISES (grant 01LN1315A). BT acknowledges financial support from the BMBF within the Collaborative Project "Bridging in Biodiversity Science-BIBS" (funding number 01LC1501A1). SR acknowledges financial support from the BMBF for funding of the projects MACMIT (grant 01LN1317A) and Climasteppe (grant 01DJ18012). We thank Anke Hildebrandt for providing the soil water content data collected during the Jena Experiment. We enjoyed discussions and help from Kirsten Thonicke, Birgit Müller, Marcel van Oijen, Thorsten Reinsch, Arne Poyda, Friedhelm Taube and the Landuse Working Group at PIK.

## 2.6 References

- Asseng, S., P. Martre, A. Maiorano, R. P. Rötter, G. J. O’Leary, G. J. Fitzgerald, C. Girousse, R. Motzo, F. Giunta, M. A. Babar, M. P. Reynolds, A. M. S. Kheir, P. J. Thorburn, K. Waha, A. C. Ruane, P. K. Aggarwal, M. Ahmed, J. Balkovič, B. Basso, C. Biernath, M. Bindi, D. Cammarano, A. J. Challinor, G. D. Sanctis, B. Dumont, E. E. Rezaei, E. Fereres, R. Ferrise, M. Garcia-Vila, S. Gayler, Y. Gao, H. Horan, G. Hoogenboom, R. C. Izaurralde, M. Jabloun, C. D. Jones, B. T. Kassie, K.-C. Kersebaum, C. Klein, A.-K. Koehler, B. Liu, S. Minoli, M. M. S. Martin, C. Müller, S. N. Kumar, C. Nendel, J. E. Olesen, T. Palosuo, J. R. Porter, E. Priesack, D. Ripoche, M. A. Semenov, C. Stöckle, P. Stratonovitch, T. Streck, I. Supit, F. Tao, M. V. der Velde, D. Wallach, E. Wang, H. Webber, J. Wolf, L. Xiao, Z. Zhang, Z. Zhao, Y. Zhu, and F. Ewert (2019). “Climate Change Impact and Adaptation for Wheat Protein”. In: *Glob. Change Biol.* 25.1, pp. 155–173. ISSN: 1365-2486. DOI: 10.1111/gcb.14481. (Visited on 03/18/2021).
- Bastos, A., Z. Fu, P. Ciais, P. Friedlingstein, S. Sitch, J. Pongratz, U. Weber, M. Reichstein, P. Anthoni, A. Arneth, V. Haverd, A. Jain, E. Joetzjer, J. Knauer, S. Lienert, T. Loughran, P. C. McGuire, W. Obermeier, R. S. Padrón, H. Shi, H. Tian, N. Viovy, and S. Zaehle (2020). “Impacts of Extreme Summers on European Ecosystems: A Comparative Analysis of 2003, 2010 and 2018”. In: *Philos. Trans. R. Soc. B Biol. Sci.* 375.1810, p. 20190507. ISSN: 0962-8436, 1471-2970. DOI: 10.1098/rstb.2019.0507. (Visited on 09/14/2020).
- Beier, C., C. Beierkuhnlein, T. Wohlgemuth, J. Penuelas, B. Emmett, C. Körner, H. de Boeck, J. H. Christensen, S. Leuzinger, I. A. Janssens, and K. Hansen (2012). “Precipitation Manipulation Experiments – Challenges and Recommendations for the Future”. In: *Ecol. Lett.* 15.8, pp. 899–911. ISSN: 1461-0248. DOI: 10.1111/j.1461-0248.2012.01793.x. (Visited on 01/28/2020).
- Blair, J., J. Nippert, and J. Briggs (2014). “Grassland Ecology”. In: *Ecology and the Environment*. Ed. by R. K. Monson. New York, NY: Springer New York, pp. 389–423. ISBN: 978-1-4614-7500-2 978-1-4614-7501-9. DOI: 10.1007/978-1-4614-7501-9\_14. (Visited on 05/21/2019).
- Botkin, D. B., J. F. Janak, and J. R. Wallis (1972). “Some Ecological Consequences of a Computer Model of Forest Growth”. In: *J. Ecol.* 60.3, pp. 849–872. ISSN: 0022-0477. DOI: 10.2307/2258570. (Visited on 07/17/2020).
- Buckland, S. M., J. P. Grime, J. G. Hodgson, and K. Thompson (1997). “A Comparison of Plant Responses to the Extreme Drought of 1995 in Northern England”. In: *J. Ecol.* 85.6, pp. 875–882. ISSN: 0022-0477. DOI: 10.2307/2960608. (Visited on 12/16/2020).
- Carroll, C. J. W., I. J. Slette, R. J. Griffin-Nolan, L. E. Baur, A. M. Hoffman, E. M. Denton, J. E. Gray, A. K. Post, M. K. Johnston, Q. Yu, S. L. Collins, Y. Luo, M. D. Smith, and A. K. Knapp (2021). “Is a Drought a Drought in Grasslands? Productivity Responses to Different Types of Drought”. In: *Oecologia*. ISSN: 1432-1939. DOI: 10.1007/s00442-020-04793-8. (Visited on 01/13/2021).
- Chang, J., P. Ciais, N. Viovy, N. Vuichard, B. Sultan, and J.-F. Soussana (2015). “The Greenhouse Gas Balance of European Grasslands”. In: *Glob. Change Biol.* 21.10, pp. 3748–3761. ISSN: 1365-2486. DOI: 10.1111/gcb.12998. (Visited on 06/15/2020).
- Chesson, P. (2000). “Mechanisms of Maintenance of Species Diversity”. In: *Annu. Rev. Ecol. Syst.* 31.1, pp. 343–366. ISSN: 0066-4162. DOI: 10.1146/annurev.ecolsys.31.1.343. (Visited on 06/28/2021).
- Clark, A. T., C. Lehman, and D. Tilman (2018). “Identifying Mechanisms That Structure Ecological Communities by Snapping Model Parameters to Empirically Observed Tradeoffs”. In: *Ecol. Lett.* 21.4, pp. 494–505. ISSN: 1461-0248. DOI: 10.1111/ele.12910. (Visited on 06/23/2021).
- Clark, D. B., L. M. Mercado, S. Sitch, C. D. Jones, N. Gedney, M. J. Best, M. Pryor, G. G. Rooney, R. L. H. Essery, E. Blyth, O. Boucher, R. J. Harding, C. Huntingford, and P. M. Cox (2011). “The Joint UK Land Environment Simulator (JULES), Model Description – Part 2: Carbon Fluxes and Vegetation Dynamics”. In: *Geosci. Model Dev.* 4.3, pp. 701–722. ISSN: 1991-9603. DOI: 10.5194/gmd-4-701-2011. (Visited on 06/28/2021).
- Coffin, D. P. and W. K. Lauenroth (1990). “A Gap Dynamics Simulation Model of Succession in a Semiarid Grassland”. In: *Ecological Modelling* 49.3, pp. 229–266. ISSN: 0304-3800. DOI: 10.1016/0304-3800(90)90029-G. (Visited on 09/02/2020).
- Collatz, G. J., J. T. Ball, C. Grivet, and J. A. Berry (1991). “Physiological and Environmental Regulation of Stomatal Conductance, Photosynthesis and Transpiration: A Model That Includes a Laminar Boundary Layer”. In: *Agric. For. Meteorol.* 54.2, pp. 107–136. ISSN: 0168-1923. DOI: 10.1016/0168-1923(91)90002-8. (Visited on 06/01/2018).
- Collatz, G., M. Ribas-Carbo, and J. Berry (1992). “Coupled Photosynthesis-Stomatal Conductance Model for Leaves of C 4 Plants”. In: *Funct. Plant Biol.* 19. DOI: 10.1071/PP9920519.
- Confalonieri, R. (2014). “CoSMo: A Simple Approach for Reproducing Plant Community Dynamics Using a Single Instance of Generic Crop Simulators”. In: *Ecological Modelling* 286, pp. 1–10. ISSN: 0304-3800. DOI: 10.1016/j.ecolmodel.2014.04.019. (Visited on 06/30/2021).
- Craven, D., F. Isbell, P. Manning, J. Connolly, H. Bruelheide, A. Ebeling, C. Roscher, J. van Ruijven, A. Weigelt, B. Wilsey, C. Beierkuhnlein, E. de Luca, J. N. Griffin, Y. Hautier, A. Hector, A. Jentsch, J. Kreyling, V. Lanta, M. Loreau, S. T. Meyer, A. S. Mori, S. Naeem, C. Palmberg, H. W. Polley, P. B. Reich, B. Schmid, A. Siebenkäs, E. Seabloom, M. P. Thakur, D. Tilman, A. Vogel, and N. Eisenhauer (2016). “Plant Diversity Effects on Grassland Productivity Are Robust to Both Nutrient Enrichment and Drought”. In: *Philos. Trans. R. Soc. B Biol. Sci.* 371.1694. ISSN: 0962-8436. DOI: 10.1098/rstb.2015.0277. (Visited on 12/09/2019).
- Crawford, M. S., K. E. Barry, A. T. Clark, C. E. Farrow, J. Hines, E. Ladouceur, J. W. Lichstein, I. Maréchaux, F. May, A. S. Mori, B. Reineking, L. A. Turnbull, C. Wirth, and N. Rürger (2021). “The Function-Dominance Correlation Drives

- the Direction and Strength of Biodiversity–Ecosystem Functioning Relationships”. In: *Ecol. Lett.* 00, pp. 1–14. ISSN: 1461-0248. DOI: 10.1111/ele.13776. (Visited on 06/23/2021).
- Dass, P., B. Z. Houlton, Y. Wang, and D. Warlind (2018). “Grasslands May Be More Reliable Carbon Sinks than Forests in California”. In: *Environ. Res. Lett.* 13.7, p. 074027. ISSN: 1748-9326. DOI: 10.1088/1748-9326/aac39. (Visited on 01/28/2020).
- Deckmyn, G., O. Flores, M. Mayer, X. Domene, A. Schnepf, K. Kuka, K. Van Looy, D. P. Rasse, M. J. Briones, S. Barot, M. Berg, E. Vanguelova, I. Ostonen, H. Vereecken, L. M. Suz, B. Frey, A. Frossard, A. Tiunov, J. Frouz, T. Grebenc, M. Öpik, M. Javaux, A. Uvarov, O. Vindušková, P. Henning Krogh, O. Franklin, J. Jiménez, and J. Curiel Yuste (2020). “KEYLINK: Towards a More Integrative Soil Representation for Inclusion in Ecosystem Scale Models. I. Review and Model Concept”. In: *PeerJ* 8, e9750. ISSN: 2167-8359. DOI: 10.7717/peerj.9750. (Visited on 11/23/2020).
- Delory, B. M., E. W. A. Weidlich, L. Meder, A. Lütje, R. van Duijnen, R. Weidlich, and V. M. Temperton (2017). “Accuracy and Bias of Methods Used for Root Length Measurements in Functional Root Research”. In: *Methods Ecol. Evol.* 8.11, pp. 1594–1606. ISSN: 2041-210X. DOI: 10.1111/2041-210X.12771. (Visited on 01/29/2021).
- Denton, E. M., J. D. Dietrich, M. D. Smith, and A. K. Knapp (2017). “Drought Timing Differentially Affects Above- and Belowground Productivity in a Mesic Grassland”. In: *Plant Ecol.* 218.3, pp. 317–328. ISSN: 1573-5052. DOI: 10.1007/s11258-016-0690-x. (Visited on 01/13/2021).
- Dewar, R. C. (2002). “The Ball–Berry–Leuning and Tardieu–Davies Stomatal Models: Synthesis and Extension within a Spatially Aggregated Picture of Guard Cell Function”. In: *Plant Cell Environ.* 25.11, pp. 1383–1398. ISSN: 1365-3040. DOI: 10.1046/j.1365-3040.2002.00909.x. (Visited on 03/23/2021).
- Durand, J.-L., K. Delusca, K. Boote, J. Lizaso, R. Manderscheid, H. J. Weigel, A. C. Ruane, C. Rosenzweig, J. Jones, L. Ahuja, S. Anapalli, B. Basso, C. Baron, P. Bertuzzi, C. Biernath, D. Deryng, F. Ewert, T. Gaiser, S. Gayler, F. Heinlein, K. C. Kersebaum, S.-H. Kim, C. Müller, C. Nendel, A. Olioso, E. Priesack, J. R. Villegas, D. Ripoche, R. P. Rötter, S. I. Seidel, A. Srivastava, F. Tao, D. Timlin, T. Twine, E. Wang, H. Webber, and Z. Zhao (2018). “How Accurately Do Maize Crop Models Simulate the Interactions of Atmospheric CO<sub>2</sub> Concentration Levels with Limited Water Supply on Water Use and Yield?” In: *Eur. J. Agron.* Recent Advances in Crop Modelling to Support Sustainable Agricultural Production and Food Security under Global Change 100, pp. 67–75. ISSN: 1161-0301. DOI: 10.1016/j.eja.2017.01.002. (Visited on 03/18/2021).
- Duru, M., M. Adam, P. Cruz, G. Martin, P. Ansquer, C. Ducourtieux, C. Jouany, J. P. Theau, and J. Viegas (2009). “Modelling Above-Ground Herbage Mass for a Wide Range of Grassland Community Types”. In: *Ecol. Model.* 220.2, pp. 209–225. ISSN: 0304-3800. DOI: 10.1016/j.ecolmodel.2008.09.015. (Visited on 10/20/2020).
- Egea, G., A. Verhoef, and P. L. Vidale (2011). “Towards an Improved and More Flexible Representation of Water Stress in Coupled Photosynthesis–Stomatal Conductance Models”. In: *Agric. For. Meteorol.* 151.10, pp. 1370–1384. ISSN: 0168-1923. DOI: 10.1016/j.agrformet.2011.05.019. (Visited on 03/23/2021).
- Ehrhardt, F., J.-F. Soussana, G. Bellocchi, P. Grace, R. McAuliffe, S. Recous, R. Sándor, P. Smith, V. Snow, M. d. A. Migliorati, B. Basso, A. Bhatia, L. Brilli, J. Doltra, C. D. Dorich, L. Doro, N. Fitton, S. J. Giacomini, B. Grant, M. T. Harrison, S. K. Jones, M. U. F. Kirschbaum, K. Klumpp, P. Laville, J. Léonard, M. Liebig, M. Lieffering, R. Martin, R. S. Massad, E. Meier, L. Merbold, A. D. Moore, V. Myrtilis, P. Newton, E. Pattey, S. Rolinski, J. Sharp, W. N. Smith, L. Wu, and Q. Zhang (2018). “Assessing Uncertainties in Crop and Pasture Ensemble Model Simulations of Productivity and N<sub>2</sub>O Emissions”. In: *Glob. Change Biol.* 24.2, e603–e616. ISSN: 1365-2486. DOI: 10.1111/gcb.13965. (Visited on 12/17/2020).
- Emmett, B. A., C. Beier, M. Estiarte, A. Tietema, H. L. Kristensen, D. Williams, J. Peñuelas, I. Schmidt, and A. Sowerby (2004). “The Response of Soil Processes to Climate Change: Results from Manipulation Studies of Shrublands Across an Environmental Gradient”. In: *Ecosystems* 7.6, pp. 625–637. ISSN: 1435-0629. DOI: 10.1007/s10021-004-0220-x. (Visited on 01/28/2021).
- Farquhar, G. D. and S. von Caemmerer (1982). “Modelling of Photosynthetic Response to Environmental Conditions”. In: *Physiological Plant Ecology II*. Encyclopedia of Plant Physiology. Springer, Berlin, Heidelberg, pp. 549–587. ISBN: 978-3-642-68152-3 978-3-642-68150-9. DOI: 10.1007/978-3-642-68150-9\_17. (Visited on 06/01/2018).
- Fay, P. A., J. D. Carlisle, A. K. Knapp, J. M. Blair, and S. L. Collins (2000). “Altering Rainfall Timing and Quantity in a Mesic Grassland Ecosystem: Design and Performance of Rainfall Manipulation Shelters”. In: *Ecosystems* 3.3, pp. 308–319. ISSN: 1432-9840, 1435-0629. DOI: 10.1007/s100210000028. (Visited on 01/28/2021).
- Felton, A. J., I. J. Slette, M. D. Smith, and A. K. Knapp (2020). “Precipitation Amount and Event Size Interact to Reduce Ecosystem Functioning during Dry Years in a Mesic Grassland”. In: *Glob. Change Biol.* 26.2, pp. 658–668. ISSN: 1365-2486. DOI: 10.1111/gcb.14789. (Visited on 01/13/2021).
- Fischer, C., S. Leimer, C. Roscher, J. Ravenek, H. de Kroon, Y. Kreutziger, J. Baade, H. Beßler, N. Eisenhauer, A. Weigelt, L. Mommer, M. Lange, G. Gleixner, W. Wilcke, B. Schröder, and A. Hildebrandt (2019). “Plant Species Richness and Functional Groups Have Different Effects on Soil Water Content in a Decade-Long Grassland Experiment”. In: *J. Ecol.* 107.1, pp. 127–141. ISSN: 1365-2745. DOI: 10.1111/1365-2745.13046. (Visited on 08/27/2020).
- Fischer, R., F. Bohn, M. Dantas de Paula, C. Dislich, J. Groeneveld, A. G. Gutiérrez, M. Kazmierczak, N. Knapp, S. Lehmann, S. Paulick, S. Pütz, E. Rödiger, F. Taubert, P. Köhler, and A. Huth (2016). “Lessons Learned from Applying a Forest Gap Model to Understand Ecosystem and Carbon Dynamics of Complex Tropical Forests”. In: *Ecol. Model.* Next Generation Ecological Modelling, Concepts, and Theory: Structural Realism, Emergence, and Predictions 326, pp. 124–133. ISSN: 0304-3800. DOI: 10.1016/j.ecolmodel.2015.11.018. (Visited on 07/17/2020).

- Forkel, M., N. Carvalhais, S. Schaphoff, W. v. Bloh, M. Migliavacca, M. Thurner, and K. Thonicke (2014). "Identifying Environmental Controls on Vegetation Greenness Phenology through Model–Data Integration". In: *Biogeosciences* 11.23, pp. 7025–7050. ISSN: 1726-4170. DOI: 10.5194/bg-11-7025-2014. (Visited on 06/29/2021).
- Godde, C. M., I. J. M. de Boer, E. zu Ermgassen, M. Herrero, C. E. van Middelaar, A. Muller, E. Rööös, C. Schader, P. Smith, H. H. E. van Zanten, and T. Garnett (2020). "Soil Carbon Sequestration in Grazing Systems: Managing Expectations". In: *Clim. Change* 161.3, pp. 385–391. ISSN: 1573-1480. DOI: 10.1007/s10584-020-02673-x. (Visited on 10/21/2020).
- Granier, A., N. Bréda, P. Biron, and S. Villette (1999). "A Lumped Water Balance Model to Evaluate Duration and Intensity of Drought Constraints in Forest Stands". In: *Ecological Modelling* 116.2, pp. 269–283. ISSN: 0304-3800. DOI: 10.1016/S0304-3800(98)00205-1. (Visited on 07/17/2020).
- Guderle, M., D. Bachmann, A. Milcu, A. Gockele, M. Bechmann, C. Fischer, C. Roscher, D. Landais, O. Ravel, S. Devidal, J. Roy, A. Gessler, N. Buchmann, A. Weigelt, and A. Hildebrandt (2018). "Dynamic Niche Partitioning in Root Water Uptake Facilitates Efficient Water Use in More Diverse Grassland Plant Communities". In: *Funct. Ecol.* 32.1, pp. 214–227. ISSN: 1365-2435. DOI: 10.1111/1365-2435.12948. (Visited on 01/29/2021).
- Guerrero-Ramírez, N. R., L. Mommer, G. T. Freschet, C. M. Iversen, M. L. McCormack, J. Kattge, H. Poorter, F. van der Plas, J. Bergmann, T. W. Kuyper, L. M. York, H. Bruelheide, D. C. Laughlin, I. C. Meier, C. Roumet, M. Semchenko, C. J. Sweeney, J. van Ruijven, O. J. Valverde-Barrantes, I. Aubin, J. A. Catford, P. Manning, A. Martin, R. Milla, V. Minden, J. G. Pausas, S. W. Smith, N. A. Soudzilovskaia, C. Ammer, B. Butterfield, J. Craine, J. H. C. Cornelissen, F. T. de Vries, M. E. Isaac, K. Kramer, C. König, E. G. Lamb, V. G. Onipchenko, J. Peñuelas, P. B. Reich, M. C. Rillig, L. Sack, B. Shipley, L. Tedersoo, F. Valladares, P. van Bodegom, P. Weigelt, J. P. Wright, and A. Weigelt (2021). "Global Root Traits (GRooT) Database". In: *Glob. Ecol. Biogeogr.* 30.1, pp. 25–37. ISSN: 1466-8238. DOI: 10.1111/geb.13179. (Visited on 01/29/2021).
- Han, Z.-Q., T. Liu, H.-F. Liu, X.-R. Hao, W. Chen, and B.-L. Li (2019). "Derivation of Species Interactions Strength in a Plant Community with Game Theory". In: *Ecological Modelling* 394, pp. 27–33. ISSN: 0304-3800. DOI: 10.1016/j.ecolmodel.2018.12.018. (Visited on 06/28/2021).
- Haxeltine, A. and I. C. Prentice (1996). "BIOME3: An Equilibrium Terrestrial Biosphere Model Based on Ecophysiological Constraints, Resource Availability, and Competition among Plant Functional Types". In: *Glob. Biogeochem. Cycles* 10.4, pp. 693–709. ISSN: 1944-9224. DOI: 10.1029/96GB02344. (Visited on 06/17/2020).
- Heisse, K., C. Roscher, J. Schumacher, and E.-D. Schulze (2007). "Establishment of Grassland Species in Monocultures: Different Strategies Lead to Success". In: *Oecologia* 152.3, pp. 435–447. ISSN: 1432-1939. DOI: 10.1007/s00442-007-0666-6. (Visited on 12/22/2020).
- Hetzer, J., A. Huth, and F. Taubert (2021). "The Importance of Plant Trait Variability in Grasslands: A Modelling Study". In: *Ecological Modelling* 453, p. 109606. ISSN: 0304-3800. DOI: 10.1016/j.ecolmodel.2021.109606. (Visited on 07/14/2021).
- Hofer, D., M. Suter, E. Haughey, J. A. Finn, N. J. Hoekstra, N. Buchmann, and A. Lüscher (2016). "Yield of Temperate Forage Grassland Species Is Either Largely Resistant or Resilient to Experimental Summer Drought". In: *J. Appl. Ecol.* 53.4, pp. 1023–1034. ISSN: 1365-2664. DOI: 10.1111/1365-2664.12694. (Visited on 01/08/2021).
- Hoffmann, K., W. Bivour, B. Früh, M. Koßmann, and P.-H. Voß (2014). *Klimauntersuchungen in Jena für die Anpassung an den Klimawandel und seine erwarteten Folgen: ein Ergebnisbericht*. DWD. ISBN: 978-3-88148-471-8. (Visited on 02/06/2020).
- Höglind, M., M. Van Oijen, D. Cameron, and T. Persson (2016). "Process-Based Simulation of Growth and Overwintering of Grassland Using the BASGRA Model". In: *Ecol. Model.* 335, pp. 1–15. ISSN: 0304-3800. DOI: 10.1016/j.ecolmodel.2016.04.024. (Visited on 08/21/2020).
- Hoover, D. L., K. R. Wilcox, and K. E. Young (2018). "Experimental Droughts with Rainout Shelters: A Methodological Review". In: *Ecosphere* 9.1, e02088. ISSN: 2150-8925. DOI: 10.1002/ecs2.2088. (Visited on 09/01/2020).
- Hopkins, A. (2000). "Herbage Production". In: *Grass: Its Production and Utilization*. Oxford: Blackwell Publishing, pp. 99–110. ISBN: 978-0-632-05017-8.
- Hunt, H. W., M. J. Trlica, E. F. Redente, J. C. Moore, J. K. Detling, T. G. F. Kittel, D. E. Walter, M. C. Fowler, D. A. Klein, and E. T. Elliott (1991). "Simulation Model for the Effects of Climate Change on Temperate Grassland Ecosystems". In: *Ecol. Model.* 53, pp. 205–246. ISSN: 0304-3800. DOI: 10.1016/0304-3800(91)90157-V. (Visited on 10/20/2020).
- Hurtado-Uria, C., D. Hennessy, L. Shalloo, R. P. O. Schulte, L. Delaby, and D. O'connor (2013). "Evaluation of Three Grass Growth Models to Predict Grass Growth in Ireland". In: *J. Agric. Sci.* 151.1, pp. 91–104. ISSN: 0021-8596, 1469-5146. DOI: 10.1017/S0021859612000317. (Visited on 11/23/2020).
- Inoue, T., S. Nagai, H. Kobayashi, and H. Koizumi (2015). "Utilization of Ground-Based Digital Photography for the Evaluation of Seasonal Changes in the Aboveground Green Biomass and Foliage Phenology in a Grassland Ecosystem". In: *Ecol. Inform.* 25, pp. 1–9. ISSN: 1574-9541. DOI: 10.1016/j.ecoinf.2014.09.013. (Visited on 01/29/2021).
- Isbell, F., D. Craven, J. Connolly, M. Loreau, B. Schmid, C. Beierkuhnlein, T. M. Bezemer, C. Bonin, H. Bruelheide, E. de Luca, A. Ebeling, J. N. Griffin, Q. Guo, Y. Hautier, A. Hector, A. Jentsch, J. Kreyling, V. Lanta, P. Manning, S. T. Meyer, A. S. Mori, S. Naeem, P. A. Niklaus, H. W. Polley, P. B. Reich, C. Roscher, E. W. Seabloom, M. D. Smith, M. P. Thakur, D. Tilman, B. F. Tracy, W. H. van der Putten, J. van Ruijven, A. Weigelt, W. W. Weisser, B. Wilsey, and N. Eisenhauer (2015). "Biodiversity Increases the Resistance of Ecosystem Productivity to Climate Extremes". In: *Nature* 526.7574, pp. 574–577. ISSN: 1476-4687. DOI: 10.1038/nature15374. (Visited on 05/22/2019).
- Jung, E.-Y., J. Gaviria, S. Sun, and B. M. J. Engelbrecht (2020). "Comparative Drought Resistance of Temperate Grassland Species: Testing Performance Trade-Offs and the Relation to Distribution". In: *Oecologia* 192.4, pp. 1023–1036. ISSN: 1432-1939. DOI: 10.1007/s00442-020-04625-9. (Visited on 12/16/2020).

- Kennedy, D., S. Swenson, K. W. Oleson, D. M. Lawrence, R. Fisher, A. C. L. da Costa, and P. Gentine (2019). “Implementing Plant Hydraulics in the Community Land Model, Version 5”. In: *J. Adv. Model. Earth Syst.* 11.2, pp. 485–513. ISSN: 1942-2466. DOI: 10.1029/2018MS001500. (Visited on 03/12/2021).
- Klaus, V. H., N. Hölzel, D. Prati, B. Schmitt, I. Schöning, M. Schruppf, E. F. Solly, F. Hänsel, M. Fischer, and T. Kleinebecker (2016). “Plant Diversity Moderates Drought Stress in Grasslands: Implications from a Large Real-World Study on 13C Natural Abundances”. In: *Sci. Total Environ.* 566–567, pp. 215–222. ISSN: 0048-9697. DOI: 10.1016/j.scitotenv.2016.05.008. (Visited on 01/29/2021).
- Knapp, A. K., C. Beier, D. D. Briske, A. T. Classen, Y. Luo, M. Reichstein, M. D. Smith, S. D. Smith, J. E. Bell, P. A. Fay, J. L. Heisler, S. W. Leavitt, R. Sherry, B. Smith, and E. Weng (2008). “Consequences of More Extreme Precipitation Regimes for Terrestrial Ecosystems”. In: *BioScience* 58.9, pp. 811–821. ISSN: 0006-3568. DOI: 10.1641/B580908. (Visited on 01/28/2021).
- Köhler, P. and A. Huth (2004). “Simulating Growth Dynamics in a South-East Asian Rainforest Threatened by Recruitment Shortage and Tree Harvesting”. In: *Clim. Change* 67.1, pp. 95–117. ISSN: 1573-1480. DOI: 10.1007/s10584-004-0713-9. (Visited on 07/17/2020).
- Kooyers, N. J. (2015). “The Evolution of Drought Escape and Avoidance in Natural Herbaceous Populations”. In: *Plant Sci.* 234, pp. 155–162. ISSN: 0168-9452. DOI: 10.1016/j.plantsci.2015.02.012. (Visited on 03/23/2020).
- Korhonen, P., T. Palosuo, T. Persson, M. Höglind, G. Jégo, M. Van Oijen, A.-M. Gustavsson, G. Bélanger, and P. Virkajärvi (2018). “Modelling Grass Yields in Northern Climates – a Comparison of Three Growth Models for Timothy”. In: *Field Crops Res.* 224, pp. 37–47. ISSN: 0378-4290. DOI: 10.1016/j.fcr.2018.04.014. (Visited on 11/23/2020).
- Kulmatiski, A. and K. H. Beard (2013). “Root Niche Partitioning among Grasses, Saplings, and Trees Measured Using a Tracer Technique”. In: *Oecologia* 171.1, pp. 25–37. ISSN: 1432-1939. DOI: 10.1007/s00442-012-2390-0. (Visited on 01/29/2021).
- Lorenz, K. and R. Lal (2018). “Carbon Sequestration in Grassland Soils”. In: *Carbon Sequestration in Agricultural Ecosystems*. Ed. by K. Lorenz and R. Lal. Cham: Springer International Publishing, pp. 175–209. ISBN: 978-3-319-92318-5. DOI: 10.1007/978-3-319-92318-5\_4. (Visited on 03/19/2019).
- Ludlow, M. M. (1989). “Strategies of Response to Water Stress”. In: *Struct. Funct. Responses Environ. Stress. Water Short*. Ed. by K. Kreeb, H. Richter, and T. M. Hinckley. Berlin, July 24–August 1, 1987: The Hague, SPB Academic Publishers, pp. 269–281. (Visited on 01/14/2021).
- Lutz, F., S. Del Grosso, S. Ogle, S. Williams, S. Minoli, S. Rolinski, J. Heinke, J. J. Stoorvogel, and C. Müller (2020). “The Importance of Management Information and Soil Moisture Representation for Simulating Tillage Effects on N<sub>2</sub>O Emissions in LPJmL5.0-Tillage”. In: *Geosci. Model Dev.* 13.9, pp. 3905–3923. ISSN: 1991-959X. DOI: 10.5194/gmd-13-3905-2020. (Visited on 03/23/2021).
- Marquard, E., B. Schmid, C. Roscher, E. De Luca, K. Nadrowski, W. W. Weisser, and A. Weigelt (2013). “Changes in the Abundance of Grassland Species in Monocultures versus Mixtures and Their Relation to Biodiversity Effects”. In: *PLoS ONE* 8.9. Ed. by J. Moen, e75599. ISSN: 1932-6203. DOI: 10.1371/journal.pone.0075599. (Visited on 03/24/2020).
- May, F., V. Grimm, and F. Jeltsch (2009). “Reversed Effects of Grazing on Plant Diversity: The Role of below-Ground Competition and Size Symmetry”. In: *Oikos* 118.12, pp. 1830–1843. ISSN: 1600-0706. DOI: 10.1111/j.1600-0706.2009.17724.x. (Visited on 06/23/2021).
- Medrano, H., M. a. J. Parry, X. Socias, and D. W. Lawlor (1997). “Long Term Water Stress Inactivates Rubisco in Subterranean Clover”. In: *Ann. Appl. Biol.* 131.3, pp. 491–501. ISSN: 1744-7348. DOI: 10.1111/j.1744-7348.1997.tb05176.x. (Visited on 03/22/2021).
- Mishra, A. K. and V. P. Singh (2010). “A Review of Drought Concepts”. In: *Journal of Hydrology* 391.1, pp. 202–216. ISSN: 0022-1694. DOI: 10.1016/j.jhydrol.2010.07.012. (Visited on 01/08/2021).
- Moinet, G. Y. K., E. Cieraad, M. H. Turnbull, and D. Whitehead (2017). “Effects of Irrigation and Addition of Nitrogen Fertiliser on Net Ecosystem Carbon Balance for a Grassland”. In: *Sci. Total Environ.* 579, pp. 1715–1725. ISSN: 0048-9697. DOI: 10.1016/j.scitotenv.2016.11.199. (Visited on 12/15/2020).
- Monteith, J. L. (1995). “Accommodation between Transpiring Vegetation and the Convective Boundary Layer”. In: *Journal of Hydrology. Atmospheric and Hydrological Processes at the Soil-Vegetation-Atmosphere Interface* 166.3, pp. 251–263. ISSN: 0022-1694. DOI: 10.1016/0022-1694(94)05086-D. (Visited on 06/04/2018).
- Movedi, E., G. Bellocchi, G. Argenti, L. Paleri, F. Vesely, N. Staglianò, C. Dibari, and R. Confalonieri (2019). “Development of Generic Crop Models for Simulation of Multi-Species Plant Communities in Mown Grasslands”. In: *Ecological Modelling* 401, pp. 111–128. ISSN: 0304-3800. DOI: 10.1016/j.ecolmodel.2019.03.001. (Visited on 06/28/2021).
- MPI (2019). *Max-Planck-Institute for Biogeochemistry*. <https://www.bgc-jena.mpg.de/wetter/>. (Visited on 12/22/2020).
- Müller, C., J. Elliott, J. Chryssanthacopoulos, A. Arneth, J. Balkovic, P. Ciais, D. Deryng, C. Folberth, M. Glotter, S. Hoek, T. Iizumi, R. C. Izaurralde, C. Jones, N. Khabarov, P. Lawrence, W. Liu, S. Olin, T. A. M. Pugh, D. K. Ray, A. Reddy, C. Rosenzweig, A. C. Ruane, G. Sakurai, E. Schmid, R. Skalsky, C. X. Song, X. Wang, A. de Wit, and H. Yang (2017). “Global Gridded Crop Model Evaluation: Benchmarking, Skills, Deficiencies and Implications”. In: *Geosci. Model Dev.* 10.4, pp. 1403–1422. ISSN: 1991-959X. DOI: 10.5194/gmd-10-1403-2017. (Visited on 03/18/2021).
- Murtagh, F. and P. Legendre (2014). “Ward’s Hierarchical Agglomerative Clustering Method: Which Algorithms Implement Ward’s Criterion?” In: *J. Classif.* 31.3, pp. 274–295. ISSN: 1432-1343. DOI: 10.1007/s00357-014-9161-z. (Visited on 08/24/2020).
- Norton, M. R., D. P. Malinowski, and F. Voltaire (2016). “Plant Drought Survival under Climate Change and Strategies to Improve Perennial Grasses. A Review”. In: *Agron. Sustain. Dev.* 36.2, p. 29. ISSN: 1773-0155. DOI: 10.1007/s13593-016-0362-1. (Visited on 01/13/2021).

- Parry, M. A. J., P. J. Andralojc, S. Khan, P. J. Lea, and A. J. Keys (2002). “Rubisco Activity: Effects of Drought Stress”. In: *Ann. Bot.* 89.7, pp. 833–839. ISSN: 0305-7364. DOI: 10.1093/aob/mcf103. (Visited on 03/22/2021).
- Parton, W. J., J. W. B. Stewart, and C. V. Cole (1988). “Dynamics of C, N, P and S in Grassland Soils: A Model”. In: *Biogeochemistry* 5.1, pp. 109–131. ISSN: 1573-515X. DOI: 10.1007/BF02180320. (Visited on 07/17/2020).
- Paschalis, A., S. Fatichi, J. Zscheischler, P. Ciais, M. Bahn, L. Boysen, J. Chang, M. D. Kauwe, M. Estiarte, D. Goll, P. J. Hanson, A. B. Harper, E. Hou, J. Kigel, A. K. Knapp, K. S. Larsen, W. Li, S. Lienert, Y. Luo, P. Meir, J. E. M. S. Nabel, R. Ogaya, A. J. Parolari, C. Peng, J. Peñuelas, J. Pongratz, S. Rambal, I. K. Schmidt, H. Shi, M. Sternberg, H. Tian, E. Tschumi, A. Ukkola, S. Vicca, N. Viovy, Y.-P. Wang, Z. Wang, K. Williams, D. Wu, and Q. Zhu (2020). “Rainfall Manipulation Experiments as Simulated by Terrestrial Biosphere Models: Where Do We Stand?” In: *Glob. Change Biol.* 26.6, pp. 3336–3355. ISSN: 1365-2486. DOI: 10.1111/gcb.15024. (Visited on 09/01/2020).
- Pecháčková, S., V. Hadincová, Z. Münzbergová, T. Herben, and F. Krahulec (2010). “Restoration of Species-Rich, Nutrient-Limited Mountain Grassland by Mowing and Fertilization”. In: *Restor. Ecol.* 18.s1, pp. 166–174. ISSN: 1526-100X. DOI: 10.1111/j.1526-100X.2009.00615.x. (Visited on 01/15/2021).
- Peltzer, D. A. and S. D. Wilson (2001). “Variation in Plant Responses to Neighbors at Local and Regional Scales.” In: *Am. Nat.* 157.6, pp. 610–625. ISSN: 0003-0147. DOI: 10.1086/320623. (Visited on 01/15/2021).
- Persson, T., M. Höglind, M. Van Oijen, P. Korhonen, T. Palosuo, G. Jégo, P. Virkajärvi, G. Bélanger, and A. -. Gustavsson (2019). “Simulation of Timothy Nutritive Value: A Comparison of Three Process-Based Models”. In: *Field Crops Res.* 231, pp. 81–92. ISSN: 0378-4290. DOI: 10.1016/j.fcr.2018.11.008. (Visited on 11/23/2020).
- Polomski, J. and N. Kuhn (2002). “Root Research Methods”. In: *Plant Roots – the Hidden Half*. Dekker, pp. 295–321. ISBN: 978-0-8247-0631-9. (Visited on 01/29/2021).
- Poyda, A., T. Reinsch, I. J. Struck, R. H. Skinner, C. Kluß, and F. Taube (2020). “Low Assimilate Partitioning to Root Biomass Is Associated with Carbon Losses at an Intensively Managed Temperate Grassland”. In: *Plant Soil*. ISSN: 1573-5036. DOI: 10.1007/s11104-020-04771-2. (Visited on 01/29/2021).
- Prentice, C., M. Heimann, and S. Sitch (2000). “The Carbon Balance of the Terrestrial Biosphere: Ecosystem Models and Atmospheric Observations”. In: *Ecol. Appl.* 10.6, pp. 1553–1573. ISSN: 1051-0761. DOI: 10.2307/2641224. (Visited on 06/01/2018).
- R Core Team (2019). *A Language and Environment for Statistical Computing*. R Foundation for Statistical Computing. Vienna, Austria.
- Ratzmann, G., F. C. Meinzer, and B. Tietjen (2019a). “Iso/Anisohydry: Still a Useful Concept”. In: *Trends Plant Sci.* 24.3, pp. 191–194. ISSN: 1360-1385. DOI: 10.1016/j.tplants.2019.01.001. (Visited on 03/02/2021).
- Ratzmann, G., L. Zakharova, and B. Tietjen (2019b). “Optimal Leaf Water Status Regulation of Plants in Drylands”. In: *Sci. Rep.* 9.1, p. 3768. ISSN: 2045-2322. DOI: 10.1038/s41598-019-40448-2. (Visited on 03/02/2021).
- Reich, P. B. (2014). “The World-Wide ‘Fast–Slow’ Plant Economics Spectrum: A Traits Manifesto”. In: *J. Ecol.* 102.2, pp. 275–301. ISSN: 1365-2745. DOI: 10.1111/1365-2745.12211. (Visited on 03/23/2020).
- Reynolds, J. F., R. A. Virginia, P. R. Kemp, A. G. de Souza, and D. C. Tremmel (1999). “Impact of Drought on Desert Shrubs: Effects of Seasonality and Degree of Resource Island Development”. In: *Ecol. Monogr.* 69.1, pp. 69–106. ISSN: 1557-7015. DOI: 10.1890/0012-9615(1999)069[0069:IODODS]2.0.CO;2. (Visited on 09/01/2020).
- Rolinski, S., C. Müller, J. Heinke, I. Weindl, A. Biewald, B. L. Bodirsky, A. Bondeau, E. R. Boons-Prins, A. F. Bouwman, P. A. Leffelaar, J. A. te Roller, S. Schaphoff, and K. Thonicke (2018). “Modeling Vegetation and Carbon Dynamics of Managed Grasslands at the Global Scale with LPJmL 3.6”. In: *Geosci. Model Dev.* 11.1, pp. 429–451. ISSN: 1991-9603. DOI: 10.5194/gmd-11-429-2018. (Visited on 02/27/2018).
- Roscher, C., J. Schumacher, J. Baade, W. Wilcke, G. Gleixner, W. W. Weisser, B. Schmid, and E.-D. Schulze (2004). “The Role of Biodiversity for Element Cycling and Trophic Interactions: An Experimental Approach in a Grassland Community”. In: *Basic Appl. Ecol.* 5.2, pp. 107–121. ISSN: 1439-1791. DOI: 10.1078/1439-1791-00216. (Visited on 02/06/2020).
- Sakschewski, B., W. von Bloh, A. Boit, A. Rammig, J. Kattge, L. Poorter, J. Peñuelas, and K. Thonicke (2015). “Leaf and Stem Economics Spectra Drive Diversity of Functional Plant Traits in a Dynamic Global Vegetation Model”. In: *Glob. Change Biol.* 21.7, pp. 2711–2725. ISSN: 1365-2486. DOI: 10.1111/gcb.12870. (Visited on 10/15/2018).
- Sala, O. E., L. A. Gherardi, L. Reichmann, E. Jobbágy, and D. Peters (2012). “Legacies of Precipitation Fluctuations on Primary Production: Theory and Data Synthesis”. In: *Philos. Trans. R. Soc. B Biol. Sci.* 367.1606, pp. 3135–3144. DOI: 10.1098/rstb.2011.0347. (Visited on 09/01/2020).
- Sándor, R., Z. Barcza, M. Acutis, L. Doro, D. Hidy, M. Köchy, J. Minet, E. Lellei-Kovács, S. Ma, A. Perego, S. Rolinski, F. Ruget, M. Sanna, G. Seddaiu, L. Wu, and G. Bellocchi (2017). “Multi-Model Simulation of Soil Temperature, Soil Water Content and Biomass in Euro-Mediterranean Grasslands: Uncertainties and Ensemble Performance”. In: *Eur. J. Agron. Uncertainty in Crop Model Predictions* 88, pp. 22–40. ISSN: 1161-0301. DOI: 10.1016/j.eja.2016.06.006. (Visited on 11/23/2020).
- Sándor, R., F. Ehrhardt, P. Grace, S. Recous, P. Smith, V. Snow, J.-F. Soussana, B. Basso, A. Bhatia, L. Brilli, J. Doltra, C. D. Dorich, L. Doro, N. Fitton, B. Grant, M. T. Harrison, M. U. F. Kirschbaum, K. Klumpp, P. Laville, J. Léonard, R. Martin, R.-S. Massad, A. Moore, V. Myrriotis, E. Pattey, S. Rolinski, J. Sharp, U. Skiba, W. Smith, L. Wu, Q. Zhang, and G. Bellocchi (2020). “Ensemble Modelling of Carbon Fluxes in Grasslands and Croplands”. In: *Field Crops Res.* 252, p. 107791. ISSN: 0378-4290. DOI: 10.1016/j.fcr.2020.107791. (Visited on 11/23/2020).
- Sato, H., A. Itoh, and T. Kohyama (2007). “SEIB–DGVM: A New Dynamic Global Vegetation Model Using a Spatially Explicit Individual-Based Approach”. In: *Ecological Modelling* 200.3, pp. 279–307. ISSN: 0304-3800. DOI: 10.1016/j.ecolmodel.2006.09.006. (Visited on 06/28/2021).

- Schapendonk, A. H. C. M., W. Stol, D. W. G. van Kraalingen, and B. A. M. Bouman (1998). “LINGRA, a Sink/Source Model to Simulate Grassland Productivity in Europe”. In: *Eur. J. Agron.* 9.2, pp. 87–100. ISSN: 1161-0301. DOI: 10.1016/S1161-0301(98)00027-6. (Visited on 09/02/2020).
- Schaphoff, S., W. von Bloh, A. Rammig, K. Thonicke, H. Biemans, M. Forkel, D. Gerten, J. Heinke, J. Jägermeyr, J. Knauer, F. Langerwisch, W. Lucht, C. Müller, S. Rolinski, and K. Waha (2018). “LPJmL4 – a Dynamic Global Vegetation Model with Managed Land – Part 1: Model Description”. In: *Geosci. Model Dev.* 11.4, pp. 1343–1375. ISSN: 1991-959X. DOI: 10.5194/gmd-11-1343-2018. (Visited on 05/31/2023).
- Schmid, J. S., A. Huth, and F. Taubert (2021). “Influences of Traits and Processes on Productivity and Functional Composition in Grasslands: A Modeling Study”. In: *Ecological Modelling* 440, p. 109395. ISSN: 0304-3800. DOI: 10.1016/j.ecolmodel.2020.109395. (Visited on 02/13/2023).
- Shugart, H. H. (1998). *Terrestrial Ecosystems in Changing Environments*. Cambridge; New York: Cambridge University Press.
- Siehoff, S., G. Lennartz, I. C. Heilburg, M. Roß-Nickoll, H. T. Ratte, and T. G. Preuss (2011). “Process-Based Modeling of Grassland Dynamics Built on Ecological Indicator Values for Land Use”. In: *Ecol. Model.* 222.23, pp. 3854–3868. ISSN: 0304-3800. DOI: 10.1016/j.ecolmodel.2011.10.003. (Visited on 12/11/2020).
- Smart, S. M., K. Thompson, R. H. Marrs, M. G. Le Duc, L. C. Maskell, and L. G. Firbank (2006). “Biotic Homogenization and Changes in Species Diversity across Human-Modified Ecosystems”. In: *Proc. R. Soc. B Biol. Sci.* 273.1601, pp. 2659–2665. DOI: 10.1098/rspb.2006.3630. (Visited on 03/12/2021).
- Smith, B., I. C. Prentice, and M. T. Sykes (2001). “Representation of Vegetation Dynamics in the Modelling of Terrestrial Ecosystems: Comparing Two Contrasting Approaches within European Climate Space”. In: *Glob. Ecol. Biogeogr.* 10.6, pp. 621–637. ISSN: 1466-8238. DOI: 10.1046/j.1466-822X.2001.t01-1-00256.x. (Visited on 06/28/2021).
- Soussana, J.-F., V. Maire, N. Gross, B. Bachelet, L. Pagès, R. Martin, D. Hill, and C. Wirth (2012). “Gemini: A Grassland Model Simulating the Role of Plant Traits for Community Dynamics and Ecosystem Functioning. Parameterization and Evaluation”. In: *Ecol. Model.* 231, pp. 134–145. ISSN: 0304-3800. DOI: 10.1016/j.ecolmodel.2012.02.002. (Visited on 12/17/2020).
- Sperry, J. S., Y. Wang, B. T. Wolfe, D. S. Mackay, W. R. L. Anderegg, N. G. McDowell, and W. T. Pockman (2016). “Pragmatic Hydraulic Theory Predicts Stomatal Responses to Climatic Water Deficits”. In: *New Phytol.* 212.3, pp. 577–589. ISSN: 1469-8137. DOI: 10.1111/nph.14059. (Visited on 03/12/2021).
- Taubert, F., K. Frank, and A. Huth (2012). “A Review of Grassland Models in the Biofuel Context”. In: *Ecological Modelling. 7th European Conference on Ecological Modelling (ECEM)* 245, pp. 84–93. ISSN: 0304-3800. DOI: 10.1016/j.ecolmodel.2012.04.007. (Visited on 02/07/2019).
- Taubert, F., J. Hetzer, J. S. Schmid, and A. Huth (2020a). “The Role of Species Traits for Grassland Productivity”. In: *Ecosphere* 11.7, e03205. ISSN: 2150-8925. DOI: 10.1002/ecs2.3205. (Visited on 02/09/2023).
- Taubert, F., J. Hetzer, J. S. Schmid, and A. Huth (2020b). “Confronting an Individual-Based Simulation Model with Empirical Community Patterns of Grasslands”. In: *PLOS ONE* 15.7, e0236546. ISSN: 1932-6203. DOI: 10.1371/journal.pone.0236546. (Visited on 02/09/2023).
- Thornley, J. (1996). “Modelling Water in Crops and Plant Ecosystems”. In: *Ann. Bot.* 77.3, pp. 261–275. ISSN: 03057364. DOI: 10.1006/anbo.1996.0030. (Visited on 09/02/2020).
- Thornley, J. (1997). “Temperate Grassland Responses to Climate Change: An Analysis Using the Hurley Pasture Model”. In: *Ann. Bot.* 80.2, pp. 205–221. ISSN: 03057364. DOI: 10.1006/anbo.1997.0430. (Visited on 09/02/2020).
- Thornley, J. H. M. (1998). *Grassland Dynamics: An Ecosystem Simulation Model*. CAB International. ISBN: 978-0-85199-227-3.
- Thornley, J. H. M. and E. L. J. Verberne (1989). “A Model of Nitrogen Flows in Grassland”. In: *Plant Cell Environ.* 12.9, pp. 863–886. ISSN: 1365-3040. DOI: 10.1111/j.1365-3040.1989.tb01967.x. (Visited on 09/02/2020).
- Thornley, J. and I. Johnson (1990). *Plant and Crop Modelling: A Mathematical Approach to Plant and Crop Physiology*. Oxford: Clarendon Press.
- Tilman, D. and A. El Haddi (1992). “Drought and Biodiversity in Grasslands”. In: *Oecologia* 89.2, pp. 257–264. ISSN: 1432-1939. DOI: 10.1007/BF00317226. (Visited on 12/16/2020).
- Tilman, D., F. Isbell, and J. M. Cowles (2014). “Biodiversity and Ecosystem Functioning”. In: *Annu. Rev. Ecol. Evol. Syst.* 45.1, pp. 471–493. ISSN: 1543-592X. DOI: 10.1146/annurev-ecolsys-120213-091917. (Visited on 03/06/2019).
- Tilman, D., P. B. Reich, and F. Isbell (2012). “Biodiversity Impacts Ecosystem Productivity as Much as Resources, Disturbance, or Herbivory”. In: *PNAS* 109.26, pp. 10394–10397. ISSN: 0027-8424, 1091-6490. DOI: 10.1073/pnas.1208240109. (Visited on 12/16/2020).
- Tribot, A.-S., J. Deter, and N. Mouquet (2018). “Integrating the Aesthetic Value of Landscapes and Biological Diversity”. In: *Proc. R. Soc. B Biol. Sci.* 285.1886, p. 20180971. DOI: 10.1098/rspb.2018.0971. (Visited on 01/28/2020).
- Turnbull, L. A., J. M. Levine, M. Loreau, and A. Hector (2013). “Coexistence, Niches and Biodiversity Effects on Ecosystem Functioning”. In: *Ecol. Lett.* 16.s1, pp. 116–127. ISSN: 1461-0248. DOI: 10.1111/ele.12056. (Visited on 06/23/2021).
- van der Molen, M. K., A. J. Dolman, P. Ciais, T. Eglin, N. Gobron, B. E. Law, P. Meir, W. Peters, O. L. Phillips, M. Reichstein, T. Chen, S. C. Dekker, M. Doubková, M. A. Friedl, M. Jung, B. J. J. M. van den Hurk, R. A. M. de Jeu, B. Kruijt, T. Ohta, K. T. Rebel, S. Plummer, S. I. Seneviratne, S. Sitch, A. J. Teuling, G. R. van der Werf, and G. Wang (2011). “Drought and Ecosystem Carbon Cycling”. In: *Agric. For. Meteorol.* 151.7, pp. 765–773. ISSN: 0168-1923. DOI: 10.1016/j.agrformet.2011.01.018. (Visited on 11/23/2020).
- Van Oijen, M., Z. Barcza, R. Confalonieri, P. Korhonen, G. Kröel-Dulay, E. Lellei-Kovács, G. Louarn, F. Louault, R. Martin, T. Moulin, E. Moredi, C. Picon-Cochard, S. Rolinski, N. Viovy, S. B. Wirth, and G. Bellocchi (2020). “Incorporat-

- ing Biodiversity into Biogeochemistry Models to Improve Prediction of Ecosystem Services in Temperate Grasslands: Review and Roadmap”. In: *Agronomy* 10.2, p. 259. DOI: 10.3390/agronomy10020259. (Visited on 02/13/2020).
- Vereecken, H., A. Schnepf, J. W. Hopmans, M. Javaux, D. Or, T. Roose, J. Vanderborght, M. H. Young, W. Amelung, M. Aitkenhead, S. D. Allison, S. Assouline, P. Baveye, M. Berli, N. Brüggemann, P. Finke, M. Flury, T. Gaiser, G. Govers, T. Ghezzehei, P. Hallett, H. J. H. Franssen, J. Heppell, R. Horn, J. A. Huisman, D. Jacques, F. Jonard, S. Kollet, F. Lafolie, K. Lamorski, D. Leitner, A. McBratney, B. Minasny, C. Montzka, W. Nowak, Y. Pachepsky, J. Padarian, N. Romano, K. Roth, Y. Rothfuss, E. C. Rowe, A. Schwen, J. Šimůnek, A. Tiktak, J. V. Dam, S. E. A. T. M. van der Zee, H. J. Vogel, J. A. Vrugt, T. Wöhling, and I. M. Young (2016). “Modeling Soil Processes: Review, Key Challenges, and New Perspectives”. In: *Vadose Zone J.* 15.5, vzj2015.09.0131. ISSN: 1539-1663. DOI: 10.2136/vzj2015.09.0131. (Visited on 01/08/2021).
- Vereecken, H., L. Weihermüller, S. Assouline, J. Šimůnek, A. Verhoef, M. Herbst, N. Archer, B. Mohanty, C. Montzka, J. Vanderborght, G. Balsamo, M. Bechtold, A. Boone, S. Chadburn, M. Cuntz, B. Decharme, A. Ducharne, M. Ek, S. Garrigues, K. Goergen, J. Ingwersen, S. Kollet, D. M. Lawrence, Q. Li, D. Or, S. Swenson, P. de Vrese, R. Walko, Y. Wu, and Y. Xue (2019). “Infiltration from the Pedon to Global Grid Scales: An Overview and Outlook for Land Surface Modeling”. In: *Vadose Zone J.* 18.1, p. 180191. ISSN: 1539-1663. DOI: 10.2136/vzj2018.10.0191. (Visited on 11/23/2020).
- Verhoef, A. and G. Egea (2014). “Modeling Plant Transpiration under Limited Soil Water: Comparison of Different Plant and Soil Hydraulic Parameterizations and Preliminary Implications for Their Use in Land Surface Models”. In: *Agric. For. Meteorol.* 191, pp. 22–32. ISSN: 0168-1923. DOI: 10.1016/j.agrformet.2014.02.009. (Visited on 01/28/2021).
- Vogel, A., M. Scherer-Lorenzen, and A. Weigelt (2012). “Grassland Resistance and Resilience after Drought Depends on Management Intensity and Species Richness”. In: *PLOS ONE* 7.5, e36992. ISSN: 1932-6203. DOI: 10.1371/journal.pone.0036992. (Visited on 12/09/2019).
- Volaire, F., M. R. Norton, and F. Lelièvre (2009). “Summer Drought Survival Strategies and Sustainability of Perennial Temperate Forage Grasses in Mediterranean Areas”. In: *Crop Sci.* 49.6, pp. 2386–2392. ISSN: 1435-0653. DOI: 10.2135/cropsci2009.06.0317. (Visited on 01/13/2021).
- von Bloh, W., S. Schaphoff, C. Müller, S. Rolinski, K. Waha, and S. Zaehle (2018). “Implementing the Nitrogen Cycle into the Dynamic Global Vegetation, Hydrology, and Crop Growth Model LPJmL (Version 5.0)”. In: *Geosci. Model Dev.* 11.7, pp. 2789–2812. ISSN: 1991-959X. DOI: 10.5194/gmd-11-2789-2018. (Visited on 05/31/2023).
- Vuichard, N., P. Ciais, N. Viovy, P. Calanca, and J.-F. Soussana (2007). “Estimating the Greenhouse Gas Fluxes of European Grasslands with a Process-Based Model: 2. Simulations at the Continental Level”. In: *Glob. Biogeochem. Cycles* 21.1. ISSN: 1944-9224. DOI: 10.1029/2005GB002612. (Visited on 08/13/2018).
- Weaver, J. E. (1942). “Competition of Western Wheat Grass with Relict Vegetation of Prairie”. In: *Am. J. Bot.* 29.5, pp. 366–372.
- Weigelt, A., W. W. Weisser, N. Buchmann, and M. Scherer-Lorenzen (2009). “Biodiversity for Multifunctional Grasslands: Equal Productivity in High-Diversity Low-Input and Low-Diversity High-Input Systems”. In: *Biogeosciences* 6.8, pp. 1695–1706. ISSN: 1726-4170. DOI: 10.5194/bg-6-1695-2009. (Visited on 11/20/2024).
- Weigelt, A., E. Marquard, V. M. Temperton, C. Roscher, C. Scherber, P. N. Mwangi, S. Felten, N. Buchmann, B. Schmid, E.-D. Schulze, and W. W. Weisser (2010). “The Jena Experiment: Six Years of Data from a Grassland Biodiversity Experiment”. In: *Ecology* 91.3, pp. 930–931. ISSN: 1939-9170. DOI: 10.1890/09-0863.1. (Visited on 12/22/2020).
- Weiss, L., H. Pfestorf, F. May, K. Körner, S. Boch, M. Fischer, J. Müller, D. Prati, S. A. Socher, and F. Jeltsch (2014). “Grazing Response Patterns Indicate Isolation of Semi-Natural European Grasslands”. In: *Oikos* 123.5, pp. 599–612. ISSN: 1600-0706. DOI: 10.1111/j.1600-0706.2013.00957.x. (Visited on 06/23/2021).
- Weisser, W. W., C. Roscher, S. T. Meyer, A. Ebeling, G. Luo, E. Allan, H. Beßler, R. L. Barnard, N. Buchmann, F. Buscot, C. Engels, C. Fischer, M. Fischer, A. Gessler, G. Gleixner, S. Halle, A. Hildebrandt, H. Hillebrand, H. de Kroon, M. Lange, S. Leimer, X. Le Roux, A. Milcu, L. Mommer, P. A. Niklaus, Y. Oelmann, R. Proulx, J. Roy, C. Scherber, M. Scherer-Lorenzen, S. Scheu, T. Tschardtke, M. Wachendorf, C. Wagg, A. Weigelt, W. Wilcke, C. Wirth, E.-D. Schulze, B. Schmid, and N. Eisenhauer (2017). “Biodiversity Effects on Ecosystem Functioning in a 15-Year Grassland Experiment: Patterns, Mechanisms, and Open Questions”. In: *Basic Appl. Ecol.* Biodiversity Effects on Ecosystem Functioning: The Jena Experiment 23, pp. 1–73. ISSN: 1439-1791. DOI: 10.1016/j.baae.2017.06.002. (Visited on 01/27/2020).
- Wilcox, K. R., K. J. Komatsu, and M. L. Avolio (2020). “Improving Collaborations between Empiricists and Modelers to Advance Grassland Community Dynamics in Ecosystem Models”. In: *New Phytol.* 228.5, pp. 1467–1471. ISSN: 1469-8137. DOI: 10.1111/nph.16900. (Visited on 12/07/2020).
- Wilhite, D. A. (2000). “Drought as a Natural Hazard: Concepts and Definitions”. In: *Drought: A Global Assessment*. Vol. 1. London: Routledge, pp. 3–18.
- Williams, D. W., L. L. Jackson, and D. D. Smith (2007). “Effects of Frequent Mowing on Survival and Persistence of Forbs Seeded into a Species-Poor Grassland”. In: *Restor. Ecol.* 15.1, pp. 24–33. ISSN: 1526-100X. DOI: 10.1111/j.1526-100X.2006.00186.x. (Visited on 01/15/2021).
- Wright, A. J., L. Mommer, K. Barry, and J. van Ruijven (2021). “Stress Gradients and Biodiversity: Monoculture Vulnerability Drives Stronger Biodiversity Effects during Drought Years”. In: *Ecology* 102.1, e03193. ISSN: 1939-9170. DOI: 10.1002/ecy.3193. (Visited on 03/24/2021).
- Wu, Z., P. Dijkstra, G. W. Koch, J. Peñuelas, and B. A. Hungate (2011). “Responses of Terrestrial Ecosystems to Temperature and Precipitation Change: A Meta-Analysis of Experimental Manipulation”. In: *Glob. Change Biol.* 17.2, pp. 927–942. ISSN: 1365-2486. DOI: 10.1111/j.1365-2486.2010.02302.x. (Visited on 01/28/2020).

- Yahdjian, L. and O. E. Sala (2002). "A Rainout Shelter Design for Intercepting Different Amounts of Rainfall". In: *Oecologia* 133.2, pp. 95–101. ISSN: 1432-1939. DOI: 10.1007/s00442-002-1024-3. (Visited on 09/01/2020).
- Yang, Y., D. Tilman, G. Furey, and C. Lehman (2019). "Soil Carbon Sequestration Accelerated by Restoration of Grassland Biodiversity". In: *Nat. Commun.* 10.1, p. 718. ISSN: 2041-1723. DOI: 10.1038/s41467-019-08636-w. (Visited on 10/21/2020).
- Yin, X., W. Qi, and G. Du (2017). "Diversity Effects under Different Nutrient Addition and Cutting Frequency Environments in Experimental Plant Communities". In: *Ecol. Res.* 32.4, pp. 611–619. ISSN: 1440-1703. DOI: 10.1007/s11284-017-1474-z. (Visited on 12/16/2020).
- Yu, Q., H. Wu, Z. Wang, D. F. B. Flynn, H. Yang, F. Lü, M. Smith, and X. Han (2015). "Long Term Prevention of Disturbance Induces the Collapse of a Dominant Species without Altering Ecosystem Function". In: *Sci Rep* 5.1, p. 14320. ISSN: 2045-2322. DOI: 10.1038/srep14320. (Visited on 06/13/2022).
- Zaehle, S., S. Sitch, B. Smith, and F. Hatterman (2005). "Effects of Parameter Uncertainties on the Modeling of Terrestrial Biosphere Dynamics". In: *Glob. Biogeochem. Cycles* 19.3. ISSN: 1944-9224. DOI: 10.1029/2004GB002395. (Visited on 07/02/2021).
- Zhou, G., X. Zhou, Y. He, J. Shao, Z. Hu, R. Liu, H. Zhou, and S. Hosseinibai (2017). "Grazing Intensity Significantly Affects Belowground Carbon and Nitrogen Cycling in Grassland Ecosystems: A Meta-Analysis". In: *Glob. Change Biol.* 23.3, pp. 1167–1179. ISSN: 1365-2486. DOI: 10.1111/gcb.13431. (Visited on 12/15/2020).
- Zhu, H., B. Fu, S. Wang, L. Zhu, L. Zhang, L. Jiao, and C. Wang (2015). "Reducing Soil Erosion by Improving Community Functional Diversity in Semi-Arid Grasslands". In: *J. Appl. Ecol.* 52.4, pp. 1063–1072. ISSN: 1365-2664. DOI: 10.1111/1365-2664.12442. (Visited on 04/13/2021).
- Zwicke, M., C. Picon-Cochard, A. Morvan-Bertrand, M.-P. Prud'homme, and F. Volaire (2015). "What Functional Strategies Drive Drought Survival and Recovery of Perennial Species from Upland Grassland?" In: *Ann. Bot.* 116.6, pp. 1001–1015. ISSN: 0305-7364. DOI: 10.1093/aob/mcv037. (Visited on 01/13/2021).

# Chapter 3

## Connecting competitor, stress-tolerator and ruderal (CSR) theory and Lund Potsdam Jena managed Land 5 (LPJmL 5) to assess the role of environmental conditions, management and functional diversity for grassland ecosystem functions

Stephen B. Wirth<sup>1,2</sup>, Arne Poyda<sup>2</sup>, Friedhelm Taube<sup>2</sup>, Britta Tietjen<sup>3,4</sup>, Christoph Müller<sup>1</sup>, Kirsten Thonicke<sup>1</sup>, Anja Linstädter<sup>5,6</sup>, Kai Behn<sup>5,6</sup>, Sibyll Schaphoff<sup>1</sup>, Werner von Bloh<sup>1</sup> and Susanne Rolinski<sup>1</sup>

<sup>1</sup>Potsdam Institute for Climate Impact Research (PIK), Member of the Leibniz Association, P.O. Box 60 12 03, 14412 Potsdam, Germany

<sup>2</sup>Institute of Crop Science and Plant Breeding, Grass and Forage Science/Organic Agriculture, Kiel University, Hermann-Rodewald-Str. 9, 24118, Kiel, Germany

<sup>3</sup>Freie Universität Berlin, Institute of Biology, Theoretical Ecology, Königin-Luise-Str. 2/4 Gartenhaus, 14195 Berlin, Germany

<sup>4</sup>Berlin-Brandenburg Institute of Advanced Biodiversity Research (BBIB), D-14195 Berlin, Germany

<sup>5</sup>University of Potsdam, Institute of Biochemistry and Biology, Potsdam, Germany

<sup>6</sup>Institute of Crop Science and Resource Conservation, University of Bonn, Bonn, Germany

Status: Published

Journal: Biogeosciences

Received: 13 March 2023

Revised: 29 November 2023

Accepted: 29 November 2023

Published: 22 January 2024

DOI: <https://doi.org/10.5194/bg-21-381-2024>

---

**Abstract:** Forage offtake, leaf biomass and soil organic carbon storage are important ecosystem services of permanent grasslands, which are determined by climatic conditions, management and functional diversity. However, functional diversity is not independent of climate and management, and it is important to understand the role of functional diversity and these dependencies for ecosystem services of permanent grasslands, since functional

diversity may play a key role in mediating impacts of changing conditions. Large-scale ecosystem models are used to assess ecosystem functions within a consistent framework for multiple climate and management scenarios. However, large-scale models of permanent grasslands rarely consider functional diversity. We implemented a representation of functional diversity based on the competitor, stress-tolerator and ruderal (CSR) theory and the global spectrum of plant form and function into the Lund Potsdam Jena managed Land (LPJmL) dynamic global vegetation model (DGVM) forming LPJmL-CSR. Using a Bayesian calibration method, we parameterised new plant functional types (PFTs) and used these to assess forage offtake, leaf biomass, soil organic carbon storage and community composition of three permanent grassland sites. These are a temperate grassland and a hot and a cold steppe for which we simulated several management scenarios with different defoliation intensities and resource limitations. LPJmL-CSR captured the grassland dynamics well under observed conditions and showed improved results for forage offtake, leaf biomass and/or soil organic carbon (SOC) compared to the original LPJmL 5 version at the three grassland sites. Furthermore, LPJmL-CSR was able to reproduce the trade-offs associated with the global spectrum of plant form and function, and similar strategies emerged independent of the site-specific conditions (e.g. the C and R PFTs were more resource exploitative than the S PFT). Under different resource limitations, we observed a shift in the community composition. At the hot steppe, for example, irrigation led to a more balanced community composition with similar C, S and R PFT shares of aboveground biomass. Our results show that LPJmL-CSR allows for explicit analysis of the adaptation of grassland vegetation to changing conditions while explicitly considering functional diversity. The implemented mechanisms and trade-offs are universally applicable, paving the way for large-scale application. Applying LPJmL-CSR for different climate change and functional diversity scenarios may generate a range of future grassland productivities.

---

### 3.1 Introduction

Permanent grasslands deliver multiple ecosystem services, one of which is their role as a source of feed for livestock across the globe (White et al., 2000). Another service is their soil organic carbon (SOC) storage, which has the potential to contribute to climate change mitigation (e.g. Godde et al., 2020; Yang et al., 2019). These two important ecosystem services depend on the climatic conditions, soil properties, management and functional diversity. The climatic conditions and soil properties determine the availability of important resources for photosynthesis and plant growth. While irrigation and fertiliser management are applied to increase the availability of specific resources and thereby productivity, grazing or mowing removes biomass, which can affect leaf and root growth and SOC stocks (Bai and Cotrufo, 2022; Conant et al., 2017). Even though functional diversity of the vegetation is not an independent factor but depends on environmental conditions (Fei et al., 2018; Grime, 2001) and management (Guo, 2007), it also affects forage supply and SOC (Chen et al., 2018; Yang et al., 2019). Furthermore, functional diversity plays an important role for the resistance and resilience of an ecosystem towards the impacts of changing conditions and might be essential to maintain the ecosystem functioning and ecosystem service provision of permanent grasslands under climate change (Guuroh et al., 2018; Isbell

et al., 2015). Therefore, it is important to understand the role of functional diversity in permanent grasslands and its role for ecosystem services such as the amount of biomass removed through mowing or grazing (in the following referred to as forage offtake), aboveground biomass, and SOC storage.

### **3.1.1 The role of environmental conditions and management for grassland vegetation and SOC storage**

Forage offtake, leaf biomass, SOC and plant community composition are dependent on environmental conditions and management. Important factors for plant growth are atmospheric CO<sub>2</sub> concentration, radiation, temperature, water and nutrient supply. Atmospheric CO<sub>2</sub> constitutes the basic resource for photosynthesis, and its rising concentration as well as rainfall patterns can shift the competitive balance between C<sub>3</sub> and C<sub>4</sub> grassland species (Schimel et al., 2015; Xie et al., 2022). Provided with sufficient water and nutrients, grasslands can produce large amounts of biomass, while drought and nutrient stress lead to lower productivity. Since large amounts of biomass can lead to high carbon sequestration, this highlights the importance of temperature and precipitation for SOC storage (Wiesmeier et al., 2019). High precipitation also favours the formation of SOC-stabilising mineral surfaces (Chaplot et al., 2010; Doetterl et al., 2016) and affects decomposition rates (Meier and Leuschner, 2010). On the other hand, high temperatures can lead to an increase in microbial decomposition and a decrease in SOC stock (e.g. Koven et al., 2017; Sleutel et al., 2007) if soil moisture levels are sufficient to permit the formation of active microbial communities. Highest SOC stocks are generally found in cool humid climates but decrease towards warmer and drier climates (Jobbágy and Jackson, 2000). Additionally, removal of aboveground biomass through grazing or mowing may be beneficial for grassland productivity depending on its intensity (Ruppert et al., 2015) by removing moribund plant material and triggering growth (over-)compensation. However, mowing and grazing also affect the belowground biomass, and highly intensive management may lead to overgrazing and cause SOC loss (McSherry and Ritchie, 2013). Still, global meta-analyses of grazing effects on SOC did not find consistent trends (McSherry and Ritchie, 2013; Piñeiro et al., 2010).

Together, the environmental factors and the management act as filters for the plant functional types (PFTs) representative of species that are best suited for the specific conditions. Changes in management or climatic and soil conditions may alter this filtering process and lead to the selection of different strategies either indirectly through alterations of the resource limitations that can cause shifts in the competitive balance between functional types (e.g. Tilman and El Haddi, 1992; Yu et al., 2015) or directly in the case of management by manipulating the species pool through reseeding and weeding (Weisser et al., 2017) or selective grazing (e.g. Wan et al., 2015).

### 3.1.2 Functional diversity and ecological strategies

Functionally diverse ecosystems contain species that follow different ecological strategies and can be described through a representation of these strategies. We define ecological strategy as the traits a plant or species uses to occupy a certain habitat. Plants have evolved a range of different ecological strategies that influence the performance of different species in different habitats. Functional diversity which underpins robustness against environmental and management change of certain ecosystem functions is related to the presence or absence of specific strategies. For example, a community in which multiple strategies are present is less vulnerable to fluctuations or changes in environmental conditions or management (Buzhdygan et al., 2020). To distinguish between different ecological strategies, several classification schemes have been developed. The competitor, stress-tolerator and ruderal (CSR) theory (Campbell and Grime, 1992; Grime, 1977; Grime, 2001) distinguishes three main strategies: competitive (C), stress-tolerant (S) and ruderal (R) strategies can be placed at the nodes of a triangle, while intermediate strategies are placed in between. This scheme can be used to classify the average strategy of a community (e.g. Caccianiga et al., 2006) as well as the strategies of single species (e.g. Grime, 1974). The main strategies are associated with different plant behaviours. C species are efficient resource users and grow fast but do not deal well with resource limitations or frequent disturbances. Opposite are S species which invest resources into more robust tissue that grows slower but enables them to cope with resource limitations. While both C and S species are vulnerable towards disturbance, R species use periods between disturbances to complete their life cycle and have an advantage in disturbance-prone environments. This different behaviour is expressed through different trait values which in turn can be used to classify plants according to the CSR theory. A prominent example is the “global spectrum of plant form and function” which explains differences in ecosystem function using traits related to growth economics, stature and life cycle (Díaz et al., 2016) and has been combined with the CSR theory and applied to single-species communities but also multi-species communities (Pierce et al., 2013; Pierce et al., 2017). Additionally, several other CSR analysis methods have been developed (Grime et al., 1988; Hodgson et al., 1999) and applied to compare vegetation function (e.g. Hunt et al., 2004; Schmidtlein et al., 2012) and to assess various community processes (Pierce et al., 2017), e.g. resistance, resilience, and coexistence (Lepš et al., 1982); succession (Caccianiga et al., 2006); and the biodiversity–productivity relationship (Cerabolini et al., 2016). Pierce et al. (2017) provided a method to classify and compare the CSR strategies of different vascular plants at the global scale, which is useful to assess community assembly in different environments. However, additional methods are needed to also predict ecosystem functioning and ecosystem service provision of the assembled communities.

### 3.1.3 Modelling ecosystem functions of permanent grasslands

To assess forage offtake or leaf biomass and SOC storage of permanent grasslands under different environmental conditions and management, models of grassland dynamics can be useful tools (e.g. Chang et al., 2021; Jebari et al., 2022; Rolinski et al., 2018). Models at the community and plot scale that incorporate very detailed approaches to simulate functional diversity in a specific context already exist (e.g. May et al., 2009; Schmid et al., 2021). In contrast, large-scale vegetation models generally use a very simple representation of the community and do not consider the trade-offs described by the global spectrum of plant form and function (Díaz et al., 2016) at all or only partially (e.g. Pfeiffer et al., 2019; Sakschewski et al., 2015). However, large-scale models provide the means to assess functional diversity in a wide range of environmental conditions and management interventions to improve projections of ecosystems functions under future climate change (e.g. Herzfeld et al., 2021; Sitch et al., 2008). In addition, such models could be useful to improve knowledge on the mechanisms underlying the global spectrum of plant form and function and help better distinguish local variability from large-scale patterns. To overcome current limitations of large-scale models, simplifications such as the CSR theory provide the opportunity to incorporate ecological strategies and functional diversity into large-scale models.

The dynamic global vegetation model (DGVM) Lund Potsdam Jena managed Land (LPJmL) is able to simulate different grazing or mowing management (Rolinski et al., 2018), irrigation (Schaphoff et al., 2018), application of manure and synthetic fertiliser (von Bloh et al., 2018), and tillage (Lutz et al., 2019). The CSR strategies and their relationship to specific plant traits provide a simple way to incorporate functional diversity into the LPJmL model to include its effects in the assessment of forage offtake or leaf biomass and SOC storage of grasslands for different environmental conditions and management scenarios. To this end, we implemented the trade-off associated with the three main strategies of the CSR theory (Grime, 1977) for managed grasslands in LPJmL using the global spectrum of plant form and function (Díaz et al., 2016) to assess

- how important functional diversity is for forage offtake or leaf biomass and SOC dynamics in different climates and under different management regimes;
- how changing resource limitations affect forage offtake or leaf biomass, SOC, and community composition.

## 3.2 Methods

We conducted our assessment at three permanent grassland sites in different climates: a temperate meadow in northern Germany with favourable climatic conditions for grassland productivity, as well

as a savanna rangeland in South Africa and a cold steppe pasture in Inner Mongolia (China) with less favourable climatic conditions. Throughout the rest of the paper, we refer to the sites as temperate grassland, hot steppe, and cold steppe, respectively, following the Köppen–Geiger climate classification (Kottek et al., 2006). At each site, we assessed two levels of management intensity which either differed with respect to the amount of fertiliser applied (temperate grassland) or the defoliation intensity (hot and cold steppe).

We extended LPJmL to account for trade-offs between C, S and R plant species as described by the CSR theory (Grime, 1977) using functional traits. We used two strategy axes to distinguish these three strategies. First, we distinguished between acquisitive (C and R) and conservative (S) strategies using resource economics. Second, we used reproduction strategies and stature to distinguish between plant species with large investments in reproduction but a small stature (R) from plant species with small investments in reproduction with a wide range of statures (C and S). Both strategy axes are expressed through several model parameters (Sect. 3.2.4).

To represent the different strategies, we parameterised three herbaceous PFTs – one competitive (C PFT), one stress-tolerant (S PFT) and one ruderal (R PFT) – for each site and management intensity (see Sect. 3.2.3 for details). Strategies that are in between these three main strategies (e.g. competitive ruderal or stress-tolerant ruderal) were not reflected by additional PFTs but should be reflected in the fractional cover of the main strategy (e.g. if a competitive ruderal strategy is advantageous in an environment, this results in a higher share of the competitive and the ruderal PFT). We evaluated the new implementation in the following, referred to as LPJmL-CSR, against forage offtake or leaf biomass and SOC observations for the different sites.

### 3.2.1 Overview of managed grassland representations in LPJmL

We extended the LPJmL model version 5 (LPJmL 5), which already included the representation of managed grasslands using a daily allocation scheme (Schaphoff et al., 2018), four different management options (Rolinski et al., 2018) and the nitrogen cycle (von Bloh et al., 2018). In this model version, the dynamics of a grassland were simulated using three herbaceous PFTs that do not distinguish between forbs and graminoids: one polar C<sub>3</sub>, one temperate C<sub>3</sub> and one tropical C<sub>4</sub> herbaceous PFT, which were constrained to the respective climatic regions by bio-climatic limits. Tree PFTs, which are also part of LPJmL, were not allowed to establish on managed grasslands, and all further descriptions provided here of or related to PFTs only concern herbaceous PFTs. As a consequence, all grasslands that are not located at the border between climatic regions were simulated using only one of these PFTs to represent herbaceous vegetation. In theory, however, the number of PFTs that could coexist within a grid cell is not limited. In LPJmL, each PFT represents an entire population of adult plants using the concept of

average individuals. The PFT describes the carbon and nitrogen stocks of the leaves and roots of an average individual and the number of average individuals in a population. It follows that the carbon and nitrogen stocks of the population can be determined by multiplying the average individual stocks with the number of average individuals. Carbon and nitrogen stocks as well as the number of average individuals are dynamically calculated each day from the simulated processes: (1) establishment of new PFTs and reproduction of established PFTs (Sect. 3.2.3.3), (2) biomass accumulation calculated from gross primary production (GPP) and autotrophic respiration limited by environmental conditions, and (3) plant turnover. LPJmL represents the response of the vegetation to temperature, water and nitrogen stress but disregards additional causes of stress such as other nutrient deficiencies, salt, heavy metals, ozone or UV radiation. At the core of the model is the representation of growth dynamics including the assimilation and allocation of new biomass through photosynthesis and turnover of senescent tissue. Each day, the GPP is calculated dependent on radiation, temperature, water and nitrogen limitations for each PFT. Subsequently, net primary productivity (NPP) is computed by subtracting growth and maintenance respiration from GPP. In a third step, the assimilated carbon is distributed between leaves and roots to approach the prescribed optimal leaf mass to root mass ratio. Finally, senescent leaf and root tissue is transferred to the litter layer.

In LPJmL 5, each herbaceous PFT is represented by one average plant individual. The initial community composition is not prescribed. Instead, upon initialisation, each PFT is established based on the PFT-specific establishment rate and offspring biomass (Sect. 3.2.3.3 and 3.2.4.1). The community composition during each time step emerges from the competition for resources, dependent on the processes described above. Different management options are available for irrigation, fertilisation, and grazing or mowing. In this study, we use the mowing and the daily grazing option to determine forage offtake. While mowing removes all biomass above a threshold of  $50 \text{ gC m}^{-2}$ , the forage offtake from daily grazing depends on the livestock unit's feed demand (details in Appendix B.1.4 and Rolinski et al., 2018). The daily grazing option does not account for animal preferences (Rolinski et al., 2018). Irrigation options used here are no irrigation (rainfed) or potential irrigation (no water limitation; Jägermeyr et al., 2015). Manure fertilisation options were adapted from the crop module (see the Supplement) and include the amount and timing of manure application. Manure application can be split over several treatments. In grazed grasslands, 25 % of the grazed carbon (Rolinski et al., 2018) and 50 % of the nitrogen are returned to the soil as dung or urine of the grazing animals (Huhtanen et al., 2008).

### 3.2.2 Site description

We conducted our assessment at three different sites (Fig. B.2) which are located in different biomes with substantial differences in precipitation and temperature, covering the warm temperate fully humid

Table 3.1: Overview of the environmental conditions and management of the investigated grasslands.

Site	Temperate grassland		Hot steppe		Cold steppe	
Location	Lindhof, Germany		Syferkuil, South Africa		Xilin, China	
Coordinates	54°27'N, 9°57'E		23°85'S, 29°7'E		43°38'N, 116°42'E	
Mean annual temperature [°C]	9.4		20.5		0.9	
Mean annual precipitation [mm]	746		432		329	
Köppen–Geiger class	Cfb		BSh		BSk	
Soil type	Sandy loam		Loamy sand		Sandy clay loam	
Management	Fertilisation		Cattle grazing		Sheep grazing	
Experiment	unfertilised	fertilised	ungrazed	grazed	low intensity	high intensity
Forage offtake [Mg DM ha <sup>-1</sup> yr <sup>-1</sup> ]	7.9 ± 1.6	9.2 ± 2.0	–	–	0.4 ± 0.3	0.6 ± 0.2
Leaf biomass [Mg DM ha <sup>-1</sup> yr <sup>-1</sup> ]	–	–	1.1 ± 0.6	1.5 ± 0.6	–	–
SOC depth [m]	0.3		0.3		1	
SOC value [Mg C ha <sup>-1</sup> ]	69.7 ± 3.7	71.9 ± 3.4	36 ± 20		273 ± 60	
Literature	(DWD, 2021, Reinsch et al., 2018a, Reinsch et al., 2018b)		(Munjonji et al., 2020, Scheiter et al., 2023)		(Hoffmann et al., 2016, Ren et al., 2017, Wiesmeier et al., 2011)	

(temperate grassland), the arid hot steppe (hot steppe) and the arid cold steppe climates (cold steppe) (Kottek et al., 2006), and are subject to different management intensities (Table 3.1).

The temperate grassland is located in favourable climatic conditions and provides high forage supply. The vegetation is dominated by C strategists with marginal shares of S and R. It is cut four times each year in May, July, August and September. Data on two experiments were available: an unfertilised (N0) control and a fertilised (N1) treatment with 240 kg N ha<sup>-1</sup> yr<sup>-1</sup> in the form of cattle manure split over four applications at the beginning of the growing season and after the first three cuts (Reinsch et al., 2018a; Reinsch et al., 2018b).

Arid conditions lead to a lower forage supply for the hot steppe. S strategists dominate the vegetation, while the R strategy is subordinate and the C strategy is only marginally present. Data for an ungrazed (C0) control and a rotationally (C1) grazed experiment with a livestock density of 0.1 cows per hectare with a body weight of around 450 kg were available (Munjonji et al., 2020).

As a result of the low precipitation and temperatures, the cold steppe is least productive. Similar to the hot steppe, the S strategy is dominant and C as well as R strategists have marginal shares. We used data of experiments with two different livestock densities of grazing sheep with a body weight of around 35 kg: the low grazing intensity (S1) of 1.5 sheep ha<sup>-1</sup> and the high grazing intensity (S6) with 9 sheep ha<sup>-1</sup> (Hoffmann et al., 2016).

### 3.2.3 Model development

To extend the LPJmL model to simulate different communities in which different ecological strategies are dominant, we focused on three aspects. First, we adapted resource uptake and distribution (Sect. 3.2.3.1) to improve niche differentiation (see Hardin, 1960). Second, we implemented the trade-off between fast tissue growth at low construction cost and longevity versus slow tissue growth at high construction cost and longevity described by the leaf economics spectrum (LES) (Sect. 3.2.3.2; Wright et al., 2004). Third, we altered the representation of the plants' lifecycle (Sect. 3.2.3.3) to distinguish

different reproductive strategies. We provide a qualitative description of the aspects of recent model development that are important for LPJmL-CSR in the main text and refer to Appendix B for the technical details and other minor improvements compared to the original code.

### 3.2.3.1 Resource uptake and distribution

In the LPJmL model, the different PFTs compete for space/light, water and nitrogen. In past model versions, these resources were distributed between PFTs based on foliage projective cover (FPC). The FPC is used as a proxy for actual cover, which would require the explicit simulation of the plant geometries. Distributing these different resources based on one variable neglected the importance of different traits for the uptake of different resources. In particular, water uptake should also be dependent on root traits such as the extent of the root network and the amount of fine root biomass (Tron et al., 2015). Using root traits to determine access to water enables the model to simulate different strategies for water-resource use. Therefore, we adapted the implementation of water supply to make it dependent on root biomass instead of FPC to provide a distinction between the criteria for aboveground and belowground resource uptake and distribution. Based on the concept of the FPC, we implemented a belowground equivalent based on root instead of leaf biomass (Appendix B.1). First, the PFT's access to water from different soil layers is calculated as described in Schaphoff et al. (2018). Second, the amount of water available for the PFT is determined by considering its root biomass and the new parameter ( $k_{\text{root}}$ ), which is a proxy for root properties associated with morphological properties of the root network (e.g. branching and spread).

### 3.2.3.2 The leaf economic spectrum

The LES describes correlations between several plant functional traits. Among these are the specific leaf area (SLA) and the leaf longevity, which can be used to express the differences between resource acquisitive vs. resource conservative growth strategies (Wright et al., 2004). The resource acquisitive strategy is associated with fast growth of leaves at low construction costs with a high SLA and a short longevity. In contrast, the resource conservative strategy promotes slow growth of long-lived leaves with low SLA. Therefore, to represent the trade-offs associated with the differences between these strategies, a functional relationship between SLA and leaf longevity can be used.

Despite the importance of SLA and leaf longevity for several processes within LPJmL, the SLA vs. leaf longevity trade-off has not been implemented for managed grasslands in LPJmL before. SLA is used to calculate the leaf area index (LAI) of a given grassland area from the dynamically computed leaf biomass, which is important for the interception of light energy and thus for photosynthesis. The leaf longevity was represented through turnover rates, which determine the amount of leaf biomass trans-

ferred to the litter layer (Schaphoff et al., 2018). As long as differences between ecological strategies were not considered and only one PFT was used to simulate a managed grassland, this approach was sufficient. However, this means that grasslands along a resource stress gradient only differed in their productivity but not in other aspects of the community. Yet in reality, slow-growing, resource-conservative plants in stress-prone ecosystems are not only less productive but also supply less forage with a lower nutrient content (Lee, 2018; Onoda et al., 2017). Such ecosystems are also more vulnerable to overgrazing (Liu et al., 2013) and recover more slowly from disturbances (Teng et al., 2020). Incorporating the SLA vs. leaf longevity trade-off is essential to account for the differences between ecological strategies, which are important to adequately represent ecosystem functions of managed grasslands under different climatic conditions and management.

The SLA vs. leaf longevity trade-off has already been implemented in the related LPJmL-FIT model and applied to tropical (Sakschewski et al., 2015) and European forests (Thonicke et al., 2020). For this study, we implemented the SLA vs. leaf longevity trade-off for managed grasslands using a functional relationship between the two based on trait observations. Similar to Sakschewski et al. (2015), we derived a power law for SLA and leaf longevity from trait data retrieved from the TRY database (Boensch and Kattge, 2018). This power law provides a functional relationship between SLA and leaf longevity, which is used to calculate the PFT-specific leaf longevity from predefined SLA values within LPJmL-CSR (Appendix B.1.1). Based on the alignment of the resource conservation axis of the root economic space (Bergmann et al., 2020) and the LES (Weigelt et al., 2021), we assume that leaf and root longevity are not independent from each other and maintain a fixed ratio of the two in LPJmL-CSR.

### 3.2.3.3 Reproduction and mortality

Herbaceous plants are adapted to different growing conditions and therefore have different reproduction strategies and whole plant – or for graminoids phytomere – longevity. In LPJmL, each herbaceous PFT was simulated using only one average individual with specified properties. Age mortality was implicitly included in the representation of turnover of leaves and roots and not as a separate process. The only additional cause of mortality was negative leaf and/or root biomass after allocation as a result of prolonged stress. While this may be caused by water stress, additional causes of mortality from water stress such as embolism (Jacobsen et al., 2019) or heat stress were not considered.

LPJmL does not simulate seed bank formation, and reproduction is not limited by the amount of seeds available in a seed bank. Instead, the establishment depends on the bare-ground area and the PFT-specific establishment rate. Furthermore, in LPJmL 5, reproduction was simulated as a biomass increase of the average individual. We argue that this was not sufficient to simulate different reproduction strategies, which differ in the amount of seeds, seed survival and germination rates, and germination

requirements (Brown and Venable, 1986; Thompson, 1987).

In the representation of CSR strategies in LPJmL-CSR, we retained the approach of establishing seedlings instead of seeds but allowed PFTs to establish different numbers of seedlings in agreement with their reproductive strategy. To achieve this, we abandoned the approach of using only one average individual to simulate each PFT and introduced a dynamic number of average individuals assuming a homogeneous population (i.e. individuals of the same PFT share the same properties) but form the community together. Based on the existing implementation, we modified the reproduction so that additional individuals are established and thereby increase the number of average individuals simulated. Each day, the number of average individuals of each PFT is increased if there was bare-ground area available. The bare-ground area is distributed between established PFTs depending on their establishment rate  $k_{\text{est}}$ . The total amount of seedlings established is calculated based on  $k_{\text{est}}$ , accounting for the bare-ground area. Subsequently, the number of average individuals is increased and the individual-specific carbon and nitrogen stocks are adjusted. LPJmL-CSR does not consider trait plasticity or evolutionary processes and therefore does not account for phenotypic adaptation. This also means that already established and newly established average individuals share the same traits. Since space for plant establishment is limited and age-related mortality is common in natural grasslands (Zimmermann et al., 2010), we prohibit an infinite increase in the number of average individuals by adding an age mortality based on the growth efficiency to reduce the number of average individuals (Appendix B.1.2). The growth efficiency is the ratio of the net change in the individual carbon stocks (the result of net photosynthesis and turnover) and the individual carbon stocks. Assuming that old plants grow more slowly, this is used as a proxy for population age and resulting age mortality. We did not implement additional causes of mortality such as drought or fire (Zimmermann et al., 2010). While the new approach does not simulate individual or phytomere morphology explicitly, it provides some implicit information on community structure and plant size through the number of average individuals, the area covered by them and their biomass. It can be assumed that few individuals that maintain a high cover and biomass must be larger than more individuals that provide a similar cover and biomass.

### 3.2.4 Defining the C, S and R PFTs

We based our new PFTs on the already existing herbaceous PFTs (Schaphoff et al., 2018), from which we retained the majority of parameter values. We used the temperate herbaceous PFT for the temperate grassland, we used the tropical herbaceous PFT for the hot steppe, and we used the polar herbaceous PFT for the cold steppe. To design the new C, S and R PFTs for each of these environments and given management scenarios, we assessed a subset of parameters that represent functional traits inspired by the global spectrum of plant form and function (Díaz et al., 2016) and define our trait space using the

stress and disturbance gradient to distinguish the CSR strategies. Based on past sensitivity analyses (Forkel et al., 2019; Zaehle et al., 2005) and expected behaviour of newly implemented trade-offs, we selected four parameters for each dimension to distinguish the CSR strategies (Table 3.2).

### 3.2.4.1 The stress and disturbance gradients

We assumed that the position of a PFT within the CSR triangle can be determined through trade-offs between plant functional traits along the stress and the disturbance gradients according to the relations described below. Names, descriptions and usage of the model parameters are based on the model versions LPJmL 4 (Schaphoff et al., 2018) and 5 (von Bloh et al., 2018).

According to CSR theory, stress is defined as constrained metabolic efficiency limiting biomass production and can be caused by a variety of factors (Grime, 1977). The stress gradient expresses the intensity of stress a species is exposed to in a certain habitat. It ranges from unstressed to severely stressed and can include the combined impacts of several stressors. Different traits and their values are associated with the ability of a plant to cope with the different stress levels. The traits of the LES (Wright et al., 2004) together with different strategies for resource use can be used to distinguish C and R strategists (low stress tolerance) from S strategists (high stress tolerance).

Since the LPJmL model only represents a subset of possible stress factors (Sect. 3.2.1), only stress arising from temperature and water as well as nitrogen availability can be considered. Within LPJmL-CSR, some traits are linked to a general response to stress independent of the stressor, while others are used to represent adaptation to specific stressors. Since the grassland steppe sites simulated by us are predominantly limited by water, we decided to focus on water stress. This allows for a better understanding of the underlying processes and the resulting patterns. To represent the stress gradient, we used functional traits associated with the growth rate and water-resource use. We selected the maximum transpiration rate ( $E_{\max}$ ), the minimum canopy conductance ( $g_{\min}$ ), the specific leaf area (SLA) and the leaf-to-root mass ratio ( $l_{\text{mro}}$ ).

**SLA** The specific leaf area is the ratio of leaf area to leaf dry mass and a measure of the amount of biomass required to produce a unit of leaf area. It is predominantly associated with the stress gradient in the CSR theory. SLA is used in four processes of LPJmL-CSR. First, it is used to calculate the LAI, which controls light interception and thus productivity determining the area occupied by a PFT in competition with other PFTs. Second, SLA is used to determine the aboveground biomass of newly established seedlings from the seedling LAI (see explanation of  $LAI_{\text{sapl}}$ ). Third, it is used to determine the actual mortality rate (Appendix B.1.2). Fourth, it is used to calculate the leaf longevity controlling tissue turnover and litterfall (Sect. 3.2.3.2). The SLA can be used to determine the trade-off between short-lived, acquisitive (high SLA) and long-lived, conservative

(low SLA) leaves. In contrast, in LPJmL 5 it was only used in the first and second processes.

**Imro** The leaf mass to root mass ratio (Imro) is the target ratio of aboveground and belowground biomass. It is predominantly associated with the CSR stress gradient, but since it controls investments into above vs. belowground biomass, it also affects the PFTs response to the removal of aboveground biomass. Imro is used within two processes of LPJmL 5 and LPJmL-CSR. First, it is used to determine the allocation of the current day's productivity to aboveground and belowground biomass pools to approach Imro. Second, it is used to calculate the belowground biomass of newly established seedlings from the aboveground biomass of newly established seedlings (Appendix B.1.2). The Imro can be used to differentiate between strategies on investing assimilates for aboveground (high Imro) or belowground (low Imro) growth and the resulting access to resources.

**$E_{\max}$**  The maximum transpiration rate defines the upper limit of transpiration per day. It is predominantly associated with the CSR stress gradient. In LPJmL 5 and LPJmL-CSR,  $E_{\max}$  is used to calculate the water supply. Here,  $E_{\max}$  presents the upper limit and actual transpiration is reduced depending on the PFT-specific root distribution and the soil water content.  $E_{\max}$  can be used to distinguish more (low  $E_{\max}$ ) and less (high  $E_{\max}$ ) water-saving strategies.

**$g_{\min}$**  This defines the minimum canopy conductance (in mm per second) that is independent of photosynthesis and a result of other processes controlling the lower limit of transpiration. It is predominantly associated with the stress gradient. In LPJmL 5 and LPJmL-CSR,  $g_{\min}$  is used in the calculation of the total canopy conductance as a part of the photosynthesis routine.  $g_{\min}$  can be used to distinguish more (low  $g_{\min}$ ) and less (high  $g_{\min}$ ) water-saving strategies.

Similar to the stress gradient, the disturbance gradient ranges from undisturbed to severely disturbed. Reproductive traits and plant stature (Grime, 1974; Salisbury, 1943; Westoby et al., 1996) can be used to distinguish C and S strategists (low disturbance tolerance) from R strategists (high disturbance tolerance). Functional traits associated with reproduction and plant geometry can be used to represent the trade-off associated with the disturbance gradient. We selected the following functional traits involved in the direct interaction of the different PFTs: the root efficiency coefficient ( $k_{\text{root}}$ ), the light extinction coefficient ( $k_{\text{beer}}$ ), the establishment rate ( $k_{\text{est}}$ ) and the leaf area index of a seedling ( $\text{LAI}_{\text{sapl}}$ ). While seedling is the more intuitive term for herbaceous plants and we will use it throughout the paper, the subscript in the parameter name refers to saplings because it was adopted from the tree PFTs in the past.

**$k_{\text{beer}}$**  The light extinction coefficient is a parameter describing the amount of light absorbed by a vegetation layer. It is predominantly associated with the CSR disturbance gradient, but since it is used in the calculation of the FPC, which also determines resource access, it is also associated with the

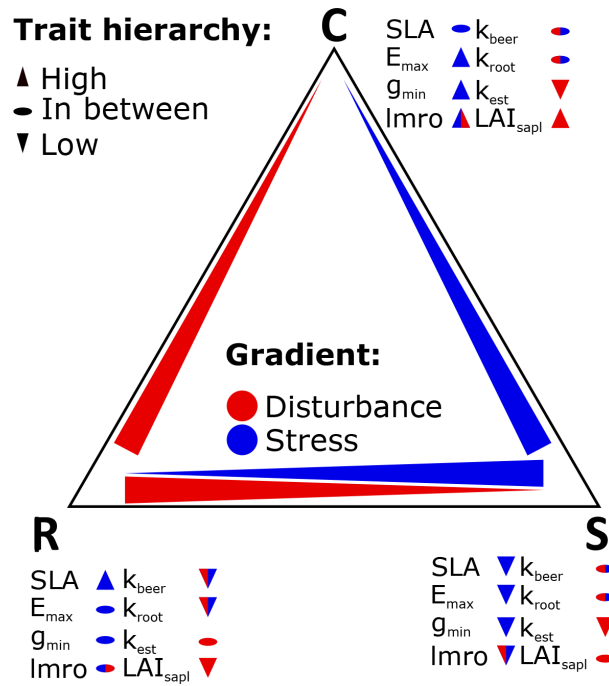


Figure 3.1: Stress (blue) and disturbance (red) gradient and associated traits and their hierarchy (low, in between and high).

CSR stress gradient. In LPJmL 5 and LPJmL-CSR,  $k_{\text{beer}}$  is used to determine FPC controlling the PFT-specific area share and its access to light.  $k_{\text{beer}}$  can be used as a proxy to distinguish large (high  $k_{\text{beer}}$  – rarely shaded by competitors and have high light absorption capacity) from small (low  $k_{\text{beer}}$  – potentially shaded by competitors and have high light absorption capacity only if dominant) stature plants and is essential for the competition for light and space.

$k_{\text{root}}$  The root efficiency coefficient is a parameter used as a proxy for root functional traits such as branching and density of the root network. It is predominantly associated with the CSR disturbance gradient, but it also affects PFT-specific water access.  $k_{\text{root}}$  was introduced in LPJmL-CSR and is used to represent the belowground morphology controlling the PFT-specific share of the belowground and its access to respective resources.  $k_{\text{root}}$  can be used as a proxy to distinguish sparse and constrained (low  $k_{\text{root}}$ ) from dense and spread root networks (high  $k_{\text{root}}$ ) and is important for the competition for water.

$k_{\text{est}}$  The establishment rate describes the maximum amount of seedlings established per day. It is predominantly associated with the CSR disturbance gradient. While in LPJmL 5  $k_{\text{est}}$  was used to determine the increase of the biomass of the average individual, in LPJmL-CSR  $k_{\text{est}}$  is used to calculate the increase of the number of average individuals per square metre ( $\text{Ind. m}^{-2}$ ) from establishment on bare-ground area.  $k_{\text{est}}$  can be used to distinguish the number of offspring and thus strategies with low (low  $k_{\text{est}}$ ) and high (high  $k_{\text{est}}$ ) reproductive capacity.

$LAI_{sapl}$  The seedling LAI is the leaf area index of a newly established seedling. It is predominantly associated with the CSR disturbance gradient. In LPJmL 5 and LPJmL-CSR, it is used to calculate the aboveground biomass of a seedling using the PFT-specific SLA. It can be used to distinguish the biomass of offspring (low/high  $LAI_{sapl}$  lead to low/high offspring biomass) which we use as a proxy for the competitive strength of the offspring of different strategies.

In total, we used eight parameters to distinguish the PFTs and defined plausible ranges for their parameterisation so that different CSR strategies can be represented by the extended set of PFTs. The selected traits affect a variety of processes within the model and differentiate the C, S and R PFTs along the stress and disturbance gradients. We assumed all parameters to be independent from each other. While we are aware that SLA and the light extinction coefficient  $k_{beer}$  are correlated in reality because the transmissivity of leaves increases with SLA we have to treat them as independent because in LPJmL, the light extinction coefficient does not describe the transmissivity of a single leaf but of the entire vegetation layer. Stacking a high number of high transmissivity leaves may result in the same light extinction compared to a lower number of low transmissivity leaves. In LPJmL-CSR, a similar  $k_{beer}$  would be assigned for both cases because it represents the light extinction coefficient of the entire vegetation layer.

Table 3.2: Parameter names, units, ranges, associated CSR gradient(s) and the hierarchy of the parameters for the C, S and R PFTs.

Parameter	Abbreviation	Unit	Min	Max	Predominant gradient	Subsidiary gradient	Hierarchy
Specific leaf area	SLA	$[m^2 gC^{-1}]$	0.01	0.1	stress	–	$S < C < R$
Light extinction coefficient	$k_{beer}$	$[-]$	0.2	0.8	disturbance	stress	$R < C \& S$
Establishment rate	$k_{est}$	$[Ind. m^{-2} d^{-1}]$	3000	6000	disturbance	–	$R > C \& S$
Root efficiency coefficient	$k_{root}$	$[-]$	0.005	0.025	disturbance	stress	$R < S < C$
Leaf to root mass ratio	$lmro$	$[-]$	0.6	1	stress	disturbance	$S < R < C$
Maximum transpiration rate	$E_{max}$	$[mm d^{-1}]$	4	12	stress	–	$S < R < C$
Seedling leaf area index	$LAI_{sapl}$	$[-]$	0.01	0.15	disturbance	–	$R < S < C$
Minimum canopy conductance	$g_{min}$	$[mm s^{-1}]$	0.3	2	stress	–	$S < R < C$

### 3.2.4.2 Parameterisation and evaluation of new PFTs

To parameterise the new PFTs, we had to assess the model performance for different parameter sets. We included several variables in the calculation of a likelihood (logLI): forage offtake or leaf biomass; SOC, and C, S, and R strategy covers (Table 3.3). Data on forage offtake, leaf biomass and SOC were available from several field experiments conducted at the respective sites. For C, S and R PFT covers, data were only available for the hot steppe and we defined values based on our knowledge of the site-specific conditions to agree with CSR theory for the other sites.

We optimised the logLI using a Markov chain Monte Carlo (MCMC) method with a Metropolis algorithm (Van Oijen et al., 2005; Wirth et al., 2021). This method evaluates the performance of a

Table 3.3: Variables used for parameterisation (para) and evaluation (eval) of the new PFTs at the study sites

Site	Variable	Resolution	Usage	Source	Literature
Temp. grassland	Dry matter yield	per cut	para/eval	field observations	Reinsch et al. (2018b)
Temp. grassland	Soil carbon	annual	para/eval	field observations	Reinsch et al. (2018b)
Temp. grassland	Cover of C, S and R PFTs	constant	para	expert estimate	–
Hot steppe	Leaf biomass	annual	para/eval	field observations	Munjonji et al. (2020)
Hot steppe	Soil carbon	monthly	eval	field observations	Munjonji et al. (2020)
Hot steppe	Cover of C, S and R PFTs	constant	para	expert estimate	–
Cold steppe	Leaf biomass	monthly	para	field observations	Schönbach et al. (2012)
Cold steppe	Grazing offtake	monthly	eval	field observations	Schönbach et al. (2012)
Cold steppe	Soil carbon	constant	para	field observations	Wiesmeier et al. (2011)
Cold steppe	Cover of C, S and R PFTs	constant	para	expert estimate	–

sequence of sampled parameter sets. In the following, we refer to a sequence as a *chain* and to an iteration as a *link*. At the beginning of the chain, a first parameter set is drawn from a multivariate Gaussian distribution with its modes at the centre of the parameter ranges for each parameter and its variances as a fraction of the parameter ranges. A fraction of the ranges is used to limit the difference between parameter sets of subsequent links which improves the performance of the algorithm. The width of this fraction is controlled through a tuning parameter and is fixed for the entire chain, while the modes of the Gaussian distribution are updated throughout the chain if the model performance calculated as the total likelihood (logLI, Eq. 3.1) improves.

$$\log\text{LI}_i = \log\text{Prior}_i + \log\text{Link}_i \quad (3.1)$$

The total likelihood logLI is calculated for each link  $i$ . It consists of a prior likelihood (logPrior $_i$ , Eq. 3.2) and the likelihood of the current link (logLink $_i$ , Eq. 3.3).

$$\log\text{Prior}_i = \sum_j B(\theta_{i,j}, p, q) \quad (3.2)$$

The prior likelihood, logPrior, is calculated from the prior distribution, which represents an initial guess on the resulting posterior distribution. We chose a geometrical prior distribution (B) with the shape parameters  $p = 1 + 4 \cdot (\hat{\theta}_{\text{centre}} - \hat{\theta}_{\text{min}} / \hat{\theta}_{\text{max}} - \hat{\theta}_{\text{min}})$  and  $q = 6 - p$ . Here,  $\theta_{i,j}$  represents the parameter values of each parameter  $j$  of the current link  $i$ ,  $\hat{\theta}_{\text{centre}}$  represents the values at the centre of the parameter space, and  $\hat{\theta}_{\text{min}}$  and  $\hat{\theta}_{\text{max}}$  are the lower and upper limits of the parameter space, respectively.

$$\log\text{Link}_i = \sum_k -0.5 \cdot \frac{y_{\text{sim},i,k} - y_{\text{obs},k}}{\sigma_{\text{obs},k}}^2 - 0.5 \cdot \log(2\pi) - \log(\sigma_{\text{obs},k}) \quad (3.3)$$

The likelihood of the current link, logLink $_i$ , is a measure of the model performance of a simulation using  $\theta_{i,j}$ . The logLink $_i$  incorporates the difference between simulation results ( $y_{\text{sim}}$ ) and observations ( $y_{\text{obs}}$ ) for all variables  $k$ , also including the uncertainty of the observations ( $\sigma_{\text{obs}}$ ). The overall likelihood

( $\log LI_i$ ) is compared to the highest likelihood that was achieved so far ( $\log LI$ ) to decide about the acceptance of the current parameter set. If the difference between the current likelihood and the highest likelihood ( $\Delta \log LI = \log LI_{\max} - \log LI_i$ ) is positive, the parameter set is always accepted. For negative  $\Delta \log LI$ , it is only accepted if it exceeds the natural logarithm of a random number between 0 and 1. This mechanism prohibits the outcome that the algorithm is trapped in local optima. At the end of the chain, the algorithm returns a posterior parameter distributions whose modes are the parameter values with the best model performance.

We used the same parameter space for all three new PFTs but ensured that we select parameter values consistent with the traits associated with CSR theory. We prescribed a hierarchy based on our expertise (Table 3.2) for each parameter that defines whether a PFT has to obtain a higher or lower value compared to the other PFTs. For example, S PFTs must have a lower SLA than C and R PFTs, because the S strategy is associated with slower growth and longer-living tissue than the C and R strategies.

Our approach included two steps represented by two subsequent chains. The first chain was short and used a large tuning parameter so that the sampling covered the entire parameter space and an area of good model performance could be identified. The second chain started in the area discovered by the first chain, was longer and used a smaller tuning parameter to find the optimal parameter values within the area.

We evaluated the new PFTs using the mean square error (MSE) and its components (see Appendix B.2). For the evaluation, we either used a different data set or split the data into different sets for parameterisation and evaluation if the number of replicates was at least eight for the majority of observations (Table 3.3). Observations with less than eight replicates were only used for the parameterisation. For the hot steppe, we used the difference in SOC between the ungrazed and grazed scenario for the evaluation because the current representation of the processes listed in Sect. 3.4.1.2 made it impossible to simulate the overall SOC level adequately. For the cold steppe, SOC data were only available for 1 year and the common management for the examined region (Wiesmeier et al., 2011). While this is comparable to our extensive grazing intensity, for the intensive grazing intensity we assumed a 25 % lower SOC level. We based this assumption on Kölbl et al. (2011) who reported around 25 % lower SOC content of the topsoil under heavy grazing compared to areas without or with periods of moderate grazing.

### 3.2.5 Modelling protocol

Simulations with LPJmL are driven by data on climate variables and management. If available, we used climate data obtained at the sites (see the Supplement). For missing climate variables, we supplemented data from the GSWP3-ERA5 data set for the temperate grassland and bias-adjusted data from the MRI-ESM2-0 (Lange and Büchner, 2022) for the hot and cold steppe. To design the new PFTs and evaluate

Table 3.4: Scenario names and management (mowing/grazing intensity, irrigation, fertilisation) used for the simulations at the Lindhof (temperate grassland), Syferkuil (hot steppe) and Xilin (cold steppe) sites.

Name	Mowing/grazing	Irrigation	Fertiliser application
Temperate grassland N0	Mowing (4 cuts)	rainfed	unfertilised
Temperate grassland N1	Mowing (4 cuts)	rainfed	fertilised 240 kg N ha <sup>-1</sup> yr <sup>-1</sup>
Hot steppe C0 R U	Grazing (0.0 cows ha <sup>-1</sup> )	rainfed	unfertilised
Hot steppe C1 R U	Grazing (0.1 cows ha <sup>-1</sup> )	rainfed	unfertilised
Hot steppe C0 I U	Grazing (0.0 cows ha <sup>-1</sup> )	irrigated	unfertilised
Hot steppe C1 I U	Grazing (0.1 cows ha <sup>-1</sup> )	irrigated	unfertilised
Cold steppe S1 R U	Grazing (1.5 sheep ha <sup>-1</sup> )	rainfed	unfertilised
Cold steppe S6 R U	Grazing (9 sheep ha <sup>-1</sup> )	rainfed	unfertilised
Cold steppe S1 I U	Grazing (1.5 sheep ha <sup>-1</sup> )	irrigated	unfertilised
Cold steppe S6 I U	Grazing (9 sheep ha <sup>-1</sup> )	irrigated	unfertilised
Cold steppe S1 I F	Grazing (1.5 sheep ha <sup>-1</sup> )	irrigated	fertilised
Cold steppe S6 I F	Grazing (9 sheep ha <sup>-1</sup> )	irrigated	fertilised

the model development, we reproduced the management under which the experiments were conducted (Sect. 3.2.2 and Table 3.1).

LPJmL-CSR simulates all processes and provides all outputs with a daily resolution. If necessary, outputs are aggregated to a monthly or annual resolution in the postprocessing. Before simulating managed grasslands, the model was run for 30 000 years with natural vegetation to obtain an equilibrium of the carbon and nitrogen cycle during a spin-up simulation. Afterwards, a second spin-up of 390 years was conducted to account for the effects of historical land-use change on soil conditions. For none of the sites, data on the land use history were available, and we assumed livestock grazing with a moderate density for the second spin-up period to account for the transition from natural vegetation to managed land. A detailed list of all inputs and settings to reproduce the conditions of the sites and experiments is provided in the Supplement.

In addition to the simulations done for the parameterisation of the new PFTs, we simulated several scenarios to analyse forage offtake, leaf biomass and SOC for different water or nitrogen limitation levels. For each site, we simulated the two management schemes also used to derive the new PFTs. To evaluate the changes of forage offtake, leaf biomass, SOC and community composition in response to different resource limitations, we simulated our three sites additionally without the prevailing site-specific limitations. For this, we removed water limitation for the hot steppe and water and nitrogen limitation separately for the cold steppe (Table 3.4).

Pre- and postprocessing of the data and figure creation were conducted using R (R Core Team, 2019). A list of all R packages used is provided in the Supplement.

### 3.3 Results

We evaluated LPJmL-CSR for the selected variables (Sect. 3.3.1) – results of the parameterisation are shown in the Supplement. Afterwards, we assessed the effect of removing the resource limitations

(Sect. 3.3.3), compared the traits and trade-offs within and across sites (Sect. 3.3.2) and analysed the community composition (Sect. 3.3.4).

### 3.3.1 Evaluation of new PFTs

For each site and management scenario, the new PFTs led to improved model results for forage off-take/leaf biomass and a reduced mean square error (MSE) compared to a simulation using LPJmL 5 (Fig. 3.2a, d and g), which did not include the changes described in Sect. 3.2.3. A major improvement was the capability of LPJmL-CSR to distinguish between CSR strategies using different PFTs. For all sites and strategies, we were able to find parameter sets for the new PFTs that enable LPJmL-CSR to represent the community well. Annual averages of the C, S and R PFT covers simulated by LPJmL-CSR compared well to the expected cover which we used for the parameterisation. MSEs for the FPC were below 0.02 (Fig. 3.2c, f and g) across sites and scenarios. Simulation results for forage off-take/leaf biomass improved at all sites (Fig. 3.2a, d and g). For the temperate grassland and the extensive grazing scenario in the cold steppe, the MSE of SOC was lower in LPJmL-CSR (Fig. 3.2b and h) but similar for the hot steppe and moderately higher for the intensively grazed cold steppe (Fig. 3.2e and h).

#### 3.3.1.1 Temperate grassland

Forage off-take of the temperate grassland for the unfertilised scenario was strongly underestimated by LPJmL 5 (Fig. B.3a), and the MSE improved from 431.7 to 112.2 (Mg DM ha<sup>-1</sup>)<sup>2</sup> in LPJmL-CSR (Fig. 3.2a). For the fertilised scenario, LPJmL 5 underestimated forage off-take less severely (Fig. B.3b), and the MSE was similar with 96.4 (Mg DM ha<sup>-1</sup>)<sup>2</sup> in LPJmL 5 to 105.3 (Mg DM ha<sup>-1</sup>)<sup>2</sup> in LPJmL-CSR. For the unfertilised scenario, the representation of SOC improved as well. For the unfertilised scenario, LPJmL 5 strongly underestimated SOC stocks (Fig. B.4a), and the MSE was reduced from 1262 to 21.4 (Mg C ha<sup>-1</sup>)<sup>2</sup>. However, it remained similar with 11 and 37.9 (Mg C ha<sup>-1</sup>)<sup>2</sup> for the fertilised scenario (Figs. 3.2b and B.4b).

#### 3.3.1.2 Hot steppe

Simulation results for the hot steppe presented a mixed picture showing lower MSEs for leaf biomass but higher MSEs for SOC in LPJmL-CSR compared to LPJmL 5. For the ungrazed (C0) scenario, the MSE of leaf biomass improved from 10154.1 to 1.9 (Mg DM ha<sup>-1</sup>)<sup>2</sup> (Fig. 3.2d). Similarly, for the grazed (C1) scenario, the MSE of leaf biomass improved from 9522.5 to 40.1 (Mg DM ha<sup>-1</sup>)<sup>2</sup>. The MSE for the difference in SOC between the ungrazed and grazed scenario was lower in LPJmL 5 and increased from 6.3 to 251.2 (Mg C ha<sup>-1</sup>)<sup>2</sup> (Fig. 3.2e). LPJmL 5 already simulated the SOC difference between the scenarios well impeding improvements through LPJmL-CSR. Furthermore, improvements in leaf

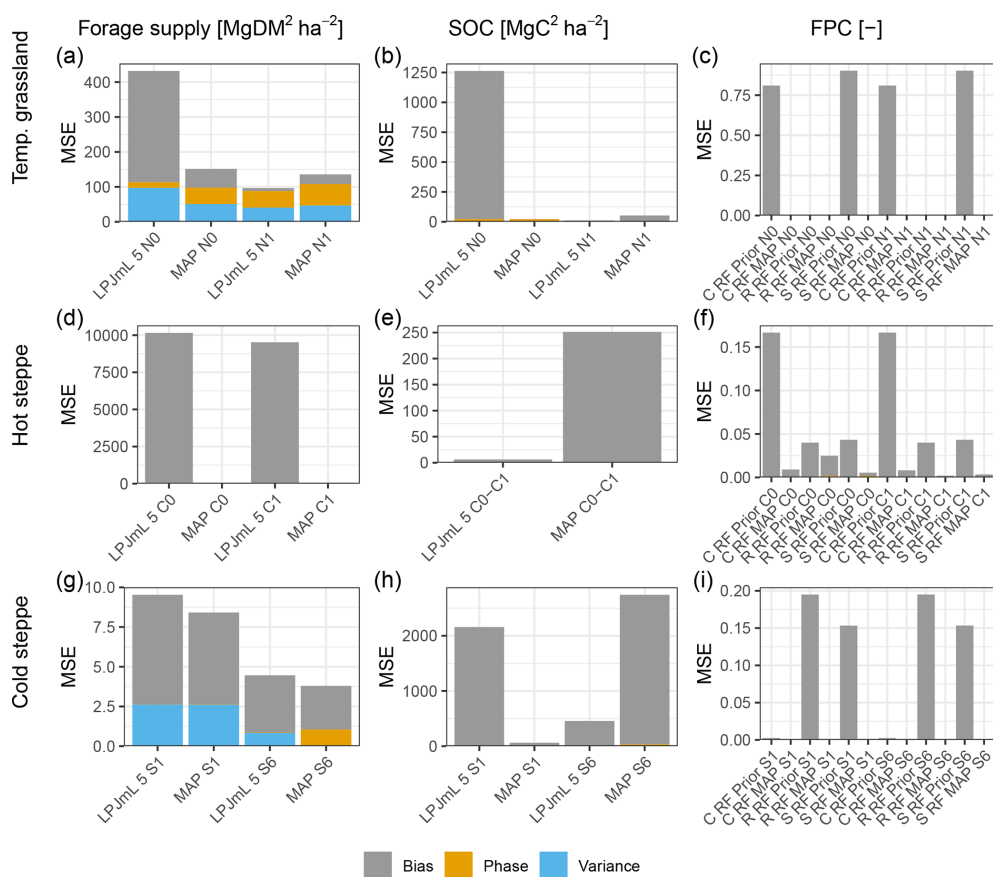


Figure 3.2: Mean square error (MSE) for the different management scenarios ( $x$  axis) for forage off-take/leaf biomass in  $\text{Mg DM ha}^{-1} \text{ yr}^{-1}$ , SOC in  $\text{Mg DM ha}^{-1} \text{ yr}^{-1}$  and FPC (columns, left to right) for the temperate grassland, hot steppe and cold steppe (rows, top to bottom). For forage off-take/leaf biomass and SOC, MSEs for the old (LPJmL 5) and new (LPJmL-CSR) model version are shown. For FPC, MSEs are shown for each PFT separately for LPJmL-CSR before and after the calibration. The colours separate the MSE into three components: the bias (grey) showing the systematic error for each variable; the phase (yellow), showing the temporal shift against observations; and the variance (blue), which is the random error not attributable to bias and phase compared to observations.

biomass outweighed degradation in SOC stocks and LPJmL-CSR fits the observations better overall. However, compared to observations, LPJmL 5 severely overestimated leaf biomass and LPJmL-CSR underestimated leaf biomass (Fig. B.5) and both model versions overestimated SOC in the ungrazed and grazed scenario (Fig. B.6).

### 3.3.1.3 Cold steppe

For the cold steppe, animal feed demand was met in both model versions for the low grazing intensity (S1). Still, the MSE for forage off-take improved from 9.5 to 8.4 ( $\text{Mg DM ha}^{-1}$ )<sup>2</sup> (Fig. 3.2g). For the high grazing intensity (S6), the feed demand was not always met in both models versions. Here, the MSE improved from 4.5 in LPJmL 5 to 3.8 ( $\text{Mg DM ha}^{-1}$ )<sup>2</sup>. Both LPJmL 5 and CSR underestimated observed forage off-take for both grazing intensities but the dynamics at the high grazing intensity were

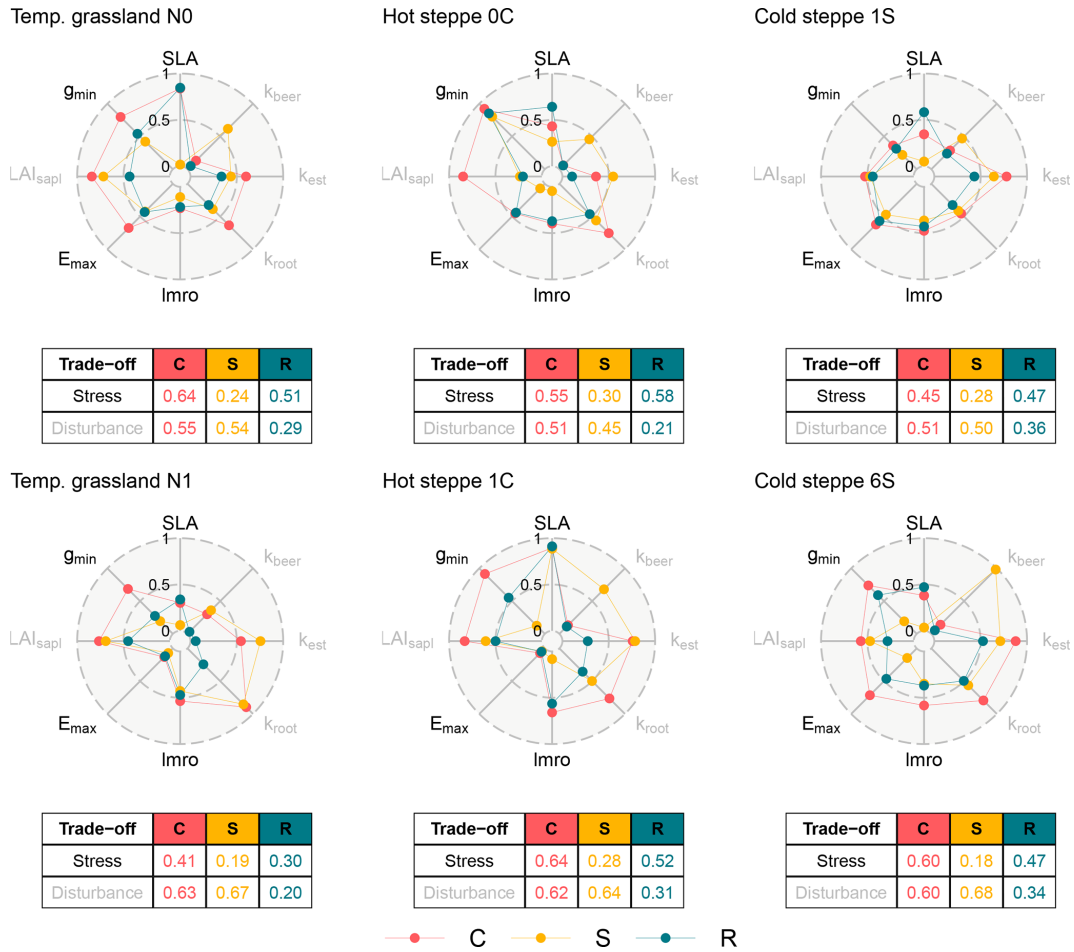


Figure 3.3: Spiderplots of normalised parameter values after calibration for each site (columns) and management scenario (rows). The centre and the edge represent the low and high ends of the stress (black labels) and disturbance (grey labels) gradients. The colours of the points distinguish the three PFTs. The tables show the mean of normalised parameter values for each PFT and the two trade-off dimensions.

captured better by LPJmL-CSR (Fig. B.7). Unfortunately, replicates for forage offtake were not sufficient to split the data and no additional data were available for evaluation. Similarly, only data on SOC for 1 year, which did not distinguish between areas of different grazing intensity, were available. Since these data were already used for the parameterisation, we were not able to properly evaluate SOC. While LPJmL 5 strongly underestimated SOC for the low grazing intensity (S1), LPJmL-CSR captured the observations better but still underestimated observations (Fig. B.8). Values were within the standard deviation of the observations for the low grazing intensity. For the high grazing intensity (S6), we assumed that 75 % of the observed SOC to be an appropriate estimate for calibration (Sect. 3.2.4.2). However, both LPJmL 5 and LPJmL-CSR overestimate this reduced calibration estimate (Sect. 3.4.1.3). The MSE was reduced from  $2157.5$  to  $60.5$  ( $\text{Mg C ha}^{-1}$ )<sup>2</sup> for the low grazing intensity and increased from  $456.7$  to  $2741.5$  ( $\text{Mg C ha}^{-1}$ )<sup>2</sup> for the high grazing intensity (Fig. 3.2h).

### 3.3.2 Comparison of parameterisations between sites and different management intensities

The environmental conditions, the management and the communities at the examined sites were different, and each site and management could be placed at a different location within the CSR triangle. Therefore, we expected different parameterisations across and within the sites for our new PFTs reflected through the PFT positions along the stress and disturbance gradients. Throughout this study, we focus on the two dimensions and discuss parameters in the context of these dimensions.

#### 3.3.2.1 Management intensities

At all sites, the different management scenarios resulted in different parameter values for the three PFTs. For the temperate grassland, the calibration selected a less resource-exploitative strategy for the C and R PFT in the fertilised scenario indicated by the lower value for the stress gradient which resulted from higher leaf longevity (lower SLA), while the S PFT's strategy remained similar (Fig. 3.3). Additionally, all PFTs showed a lower maximum transpiration rate ( $E_{\max}$ ) and higher investments into aboveground biomass (higher  $lmro$ ). For the disturbance gradient, the C and S PFTs had a higher value in the fertilised scenario. For the C and S PFTs, this indicated that the calibration selected a strategy with less offspring (lower  $k_{\text{est}}$ ) and a more efficient root network (higher  $k_{\text{root}}$ ). The R PFT had a lower value caused by an increase in number of offspring (higher  $k_{\text{est}}$ ).

For the hot steppe, the S and R PFTs showed a lower value for the stress gradient for the grazed scenario (C1), and the calibration selected a more water-saving (lower  $E_{\max}$  and/or  $g_{\min}$ ) strategy. These differences were counteracted to some extent by an increased investment in aboveground biomass (higher  $lmro$ ) and a more resource-exploitative strategy (higher SLA). The C PFT showed similar differences except for the reduction of the minimum canopy conductance ( $g_{\min}$ ). However, this is likely an artefact of the parameterisation. As stated in Sect. 3.2.4.1, both SLA and  $lmro$  not only underpin the compensation of defoliation but also play a role for resource uptake and distribution. In the ungrazed scenario (C0), no defoliation has to be compensated and both parameters only play a role for resource uptake and distribution, which likely affected the selection of  $g_{\min}$ . In contrast in the grazed scenario (C1),  $g_{\min}$  and  $E_{\max}$  become more important for resource uptake and distribution. For the disturbance gradient, all PFTs had higher values from different causes: the C PFT established less offspring (lower  $k_{\text{est}}$ ), the S PFT increased its stature (higher  $k_{\text{beer}}$ ) and seedling size (higher  $LAI_{\text{sapl}}$ ), and the R PFT only increased its seedling size (higher  $LAI_{\text{sapl}}$ ).

Consistent with the findings for the other sites, for the cold steppe all PFTs showed different strategies for the different management intensities. While the value for the stress gradient was the same for the R PFT and only differed for the C and S PFTs, the calibration selected different trait values for all PFTs.

For the C PFT, the calibration selected a less water-saving strategy (higher  $E_{\max}$  and  $g_{\min}$ ) and for the S PFT a more water-saving strategy (lower  $E_{\max}$  and  $g_{\min}$ ). For the disturbance gradient, the C and S PFT showed a higher value, and the R PFT showed a lower value in the intensively grazed scenario (S6). While for the C PFT this was the result of an increase in the efficiency of its root network (higher  $k_{\text{root}}$ ), for the S PFT this was a result of an increase in stature (higher  $k_{\text{beer}}$ ; Sect. 3.2.4.1). In contrast, the R PFT had a smaller stature (lower  $k_{\text{beer}}$ ) and seedling size (lower  $\text{LAI}_{\text{sapl}}$ ).

### 3.3.2.2 Site-specific conditions

Across sites, we found a large variation within both dimensions which ranged from 0.30 to 0.64 for the stress and from 0.18 to 0.68 for the disturbance gradient (Fig. 3.3). As a consequence of our assumptions for the parameterisation, the sorting of the parameter values for the three PFTs had to match the hierarchy defined in Table 3.2 (Sect. 3.2.4.2) for each site. Between sites however, we did not make any assumptions that would predetermine an order, meaning that each site could occupy a different area of the two dimensions. For example, an R PFT had to have a higher value for the stress gradient compared to the S PFT for the same site, but could have a lower value compared to the S PFT of another site, as is the case when comparing the temperate grassland to the hot steppe. For the disturbance gradient, the same case can be made.

However, if averaged over all sites and management scenarios, the C PFT still was the most resource exploitative with a value of 0.55 for the stress gradient, while the R and S PFT were more resource conservative with values of 0.48 and 0.25. Similarly, the R PFT produced most offspring and had the smallest stature with a value of 0.29 compared to 0.57 and 0.58 for the C and S PFTs. While this general pattern emerged clearly for the two dimensions, there were substantial differences between the sites when comparing the contributing parameters. Most similar was the  $\text{Imro}$  determining investments into aboveground versus belowground biomass, which contributed to high values of the C and R PFTs for the stress gradient for several scenarios. For the steppe sites, there was some alignment within the S PFTs, which all had a larger stature (higher  $k_{\text{beer}}$ ). The remaining parameters were not discernibly aligned across sites.

### 3.3.3 Effects of resource limitation

To assess the effect of resource limitation, we compared different scenarios with LPJmL-CSR. In addition to the scenarios using the prevailing climatic conditions (resource limited), we simulated scenarios where we removed the limitation of water or nitrogen supply. For the temperate grassland and the hot steppe, the different management scenarios of the unfertilised and fertilised as well as ungrazed and grazed scenario led to differences in soil carbon before the first year shown in Fig. 3.3.

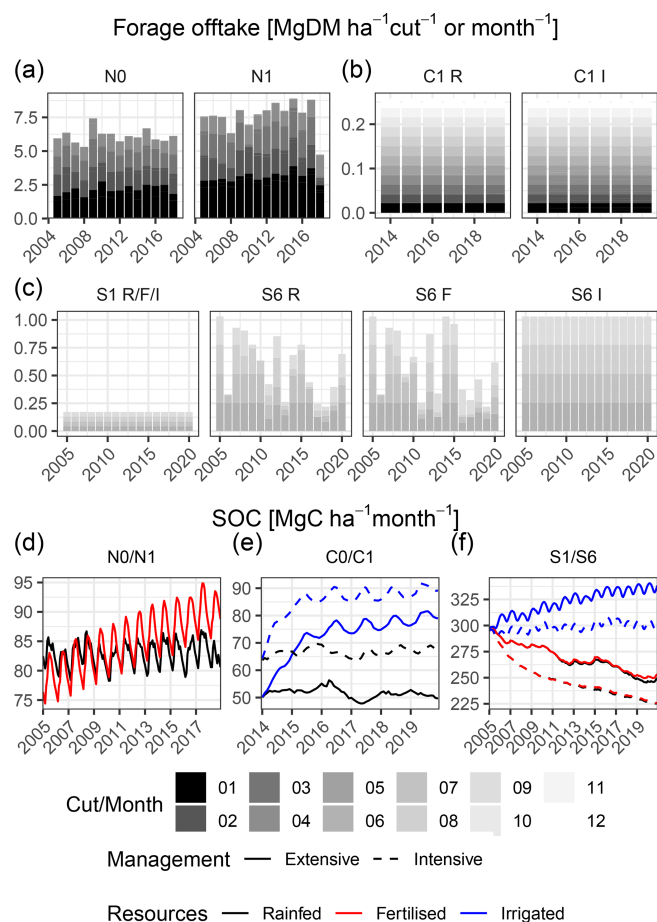


Figure 3.4: Simulated forage offtake/leaf biomass (**a, b, c**) and SOC (**d, e, f**) for all sites, management levels and resource limitation scenarios. Bars show the annual forage offtake and coloured segments the forage offtake for each cut/month. Line colours differ between rainfed (prevailing conditions, black), rainfed fertilised (red) and irrigated unfertilised (blue), while line types show the grazing management intensity as low (ungrazed/C0 or extensively grazed/S1, solid) and high (grazed/C1 or intensively grazed/S6, dashed).

### 3.3.3.1 Temperate grassland

The temperate grassland already is a productive site where water and nitrogen are not limiting productivity, and we did not simulate any additional scenarios but focused on comparing the two fertilisation levels (N0 and N1). For both scenarios, total annual forage offtake was similar and between  $5.3$  and  $7.4 \text{ Mg DM ha}^{-1} \text{ yr}^{-1}$  for the unfertilised and between  $4.7$  and  $8.9 \text{ Mg DM ha}^{-1} \text{ yr}^{-1}$  for the fertilised scenario (Fig. 3.4a). The first cut was the most productive, yielding between  $1.8$  and  $2.8 \text{ Mg DM ha}^{-1} \text{ yr}^{-1}$  for the unfertilised and between  $2.5$  and  $3.9 \text{ Mg DM ha}^{-1} \text{ yr}^{-1}$  for the fertilised scenario. The subsequent cuts contributed substantially to the overall forage offtake except in 2018, which was a drought year. Here, the forage offtake from all cuts was reduced. In all cuts, the dominant C PFT contributed the majority of the forage offtake. In both scenarios, the S and R PFTs barely contributed (2% and 8% share of forage offtake on average) in all cuts (Fig. B.9). Overall, dry matter yield (DMY) was more stable between years (except 2018) in the fertilised scenario because of higher

yields during the regrowth stages (cuts 2 to 4). These compensated the slightly lower DMY of the first cut compared to the unfertilised scenario.

The SOC showed no significant trend for the unfertilised scenario, where the annual average decreased by  $0.02 \text{ Mg C ha}^{-1} \text{ yr}^{-1}$  on average ( $\tau = 0.09$ ,  $p$  value 0.1). In contrast, SOC in the fertilised scenario increased by  $0.96 \text{ Mg C ha}^{-1} \text{ yr}^{-1}$  on average ( $\tau = 0.56$ ,  $p$  value  $< 0.001$ ), respectively (Fig. 3.4d). Intra-annual SOC dynamics, which are driven by the litter production and C input from manure, were stronger in the fertilised scenario.

### 3.3.3.2 Hot steppe

For the hot steppe, we simulated an irrigated (I) scenario in addition to the rainfed (R) scenario which was used for the calibration of our PFTs for the ungrazed (C0) and grazed (C1) management. Annual forage offtake was  $0.26 \text{ Mg DM ha}^{-1} \text{ yr}^{-1}$  in the rainfed scenario (Fig. 3.4b), and animal feed demand was always met (Fig. B.10a). Similarly, the feed demand was always met in the irrigated scenario (Fig. B.10b). However, between the two scenarios the composition of forage offtake strongly differed. In the rainfed scenario, the S PFT contributed the majority in most years, whereas in the irrigated scenario the community composition changed, and all PFTs contributed to forage offtake similarly. A shift also occurred in the ungrazed scenario, which was still dominated by the S PFT but showed a higher share of the C and R PFTs after several years as well. This change was related to the changing community composition (Sect. 3.3.4.2) and increased leaf biomass in the irrigated scenario. In the ungrazed scenario, 55 % of the leaf biomass increase from irrigation resulted from elevated growth of the S PFT, 21 % from the C PFT and 23 % from the R PFT. This was different in the grazed scenario, with -18 % (S PFT), 82 % (C PFT) and 37 % (R PFT), respectively.

The SOC of the rainfed scenarios did not show strong trends (Fig. 3.4e). However, the negative trend in the ungrazed scenario (C0) was still significant ( $\tau = -0.27$ ,  $p$  value  $< 0.001$ ). In the irrigated scenario, SOC increased strongly with little differences between the grazing scenarios – on average by  $4.9 \text{ Mg C ha}^{-1} \text{ yr}^{-1}$  in the ungrazed and  $4.2 \text{ Mg C ha}^{-1} \text{ yr}^{-1}$  in the grazed scenario. However, SOC did not increase linearly but showed a much stronger increase which was unrealistically high in the first 1 to 2 years after the start of irrigation ( $10.4 \text{ Mg C ha}^{-1} \text{ yr}^{-1}$  in the ungrazed and  $10.6 \text{ Mg C ha}^{-1} \text{ yr}^{-1}$  in the grazed scenario) than in the remaining time series ( $2.1 \text{ Mg C ha}^{-1} \text{ yr}^{-1}$  in the ungrazed and  $1.0 \text{ Mg C ha}^{-1} \text{ yr}^{-1}$  in the grazed scenario).

### 3.3.3.3 Cold steppe

For the cold steppe, we simulated an irrigated (I) and a fertilised (F) scenario in addition to the rainfed (R) scenario used for the parameterisation for both the low (S1) and high (S6) grazing intensities. Total

forage offtake was  $0.17 \text{ Mg DM ha}^{-1} \text{ yr}^{-1}$  for all scenarios with low grazing intensity because the feed demand of the animals was always met (Fig. 3.4c). In all scenarios, the forage offtake was almost entirely attributed to the dominant S PFT, (Fig. B.11a–c). For the high grazing intensity, total forage offtake was  $1.03 \text{ Mg DM ha}^{-1} \text{ yr}^{-1}$  if the feed demand was met. This was always the case in the irrigated scenario but not in the rainfed and fertilised scenarios. In the latter two, the model simulated very similar forage offtake, indicating that nitrogen addition was not sufficient to increase productivity because water was the main limiting factor. In all three scenarios, the S PFT was dominant (Fig. B.11d–f). However, in the rainfed and fertilised scenarios the share of the S PFT decreased in months when the feed demand could not be met and mainly the share of the C PFT increased. In the irrigated scenario, only the S PFT contributed to the forage offtake (for an explanation, see Sect. 3.4.1.3).

SOC was similar for the rainfed and fertilised but differed for the irrigated low- and high-grazing-intensity scenarios (Fig. 3.4f). Both the rainfed and fertilised scenarios showed a significant negative trend for SOC, which was similar between the high grazing intensity where SOC decreased by roughly  $4 \text{ Mg C ha}^{-1} \text{ yr}^{-1}$  on average ( $\tau = -0.99$ ,  $p$  value  $< 0.001$ ) and the low grazing intensity with SOC losses of  $3 \text{ Mg C ha}^{-1} \text{ yr}^{-1}$  on average ( $\tau = -0.87$ ,  $p$  value  $< 0.001$ ). For the irrigated scenarios, SOC increased by  $2.5 \text{ Mg C ha}^{-1} \text{ yr}^{-1}$  on average ( $\tau = 0.79$ ,  $p$  value  $< 0.001$ ) for low grazing intensity and  $0.4 \text{ Mg C ha}^{-1} \text{ yr}^{-1}$  on average ( $\tau = 0.47$ ,  $p$  value  $< 0.001$ ) for high grazing intensity.

### 3.3.4 Community composition

We compared expected and realised shares of the C, S and R PFTs for the three sites using leaf biomass and explored seasonal and inter-annual dynamics, and we analysed shifts under different resource limitations.

As already evidenced by the low MSE values for the FPCs of all PFTs after calibration (Fig. 3.2), LPJmL-CSR captured our expert estimates on C, S and R PFT covers, which defined the position of the ecosystem within the CSR triangle well. However, these were annual averages and did not prescribe any intra-annual variability. Since aboveground biomass and FPC are directly related and aboveground biomass is the less abstract variable to interpret, we present results based on aboveground biomass from here on.

#### 3.3.4.1 Intra-annual variability

Each site showed substantial intra-annual dynamics of total aboveground biomass (Fig. B.12a, b, B.13a, c, B.14a, g) and the monthly average of the aboveground biomass share of the C, S and R PFTs (Fig. 3.5). However, the intra-annual dynamics were different between sites. In the temperate grassland, the C PFT was dominant throughout the year; however, after the end of a growing season, the marginal PFTs had

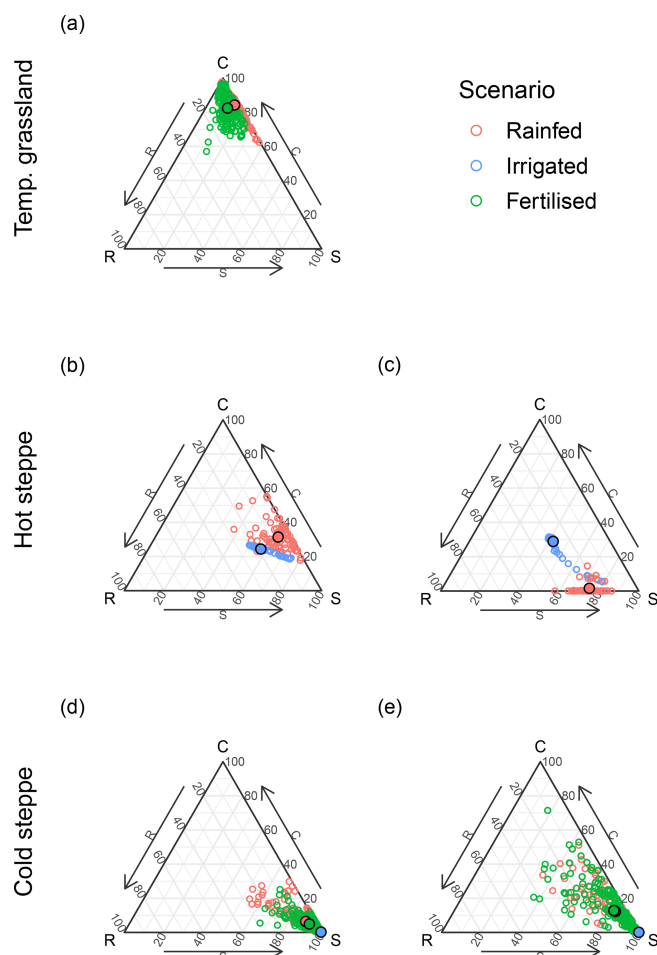


Figure 3.5: Ternary plots of the share of standing aboveground biomass of the C, S and R PFTs for the temperate grassland (a), the ungrazed (b) and grazed hot steppe (c), and the extensively (d) and intensively (e) grazed cold steppe. Colours differ between the rainfed (red), irrigated (blue) and fertilised (green) scenarios. Points with a black border show the mean composition of the time series.

an increasing share until after the first cut (Fig. B.12c, d). While in the unfertilised (N0) scenario the share of the S PFT increased, the share of the S and R PFTs increased in the fertilised (N1) scenario (Fig. 3.5a).

In the hot steppe, the community was dominated by the S PFT in both management scenarios (Fig. 3.5b and d). In the ungrazed (C0) scenario, the C PFT made up almost the entire remainder of the aboveground biomass (Fig. B.13a). However, the C PFT was replaced by the R PFT in the grazed (C1) scenario (Fig. B.13c).

For the cold steppe, PFT shares of aboveground biomass did not show strong intra-annual variation for the extensive (S1) grazing scenario (Fig. 3.5c). However, for the intensive (S6) grazing scenario, the C and R PFTs strongly contributed to the overall leaf biomass, and the C PFT was even dominant during and after the grazing period (Fig. B.14h).

### 3.3.4.2 Effects of irrigation and fertilisation

Removing resource limitations led to a shift in the community composition for the hot and cold steppe.

The hot steppe transitioned from an S-dominated community to a community with more balanced CSR shares that was still dominated by the S PFT (Fig. 3.5b and d). This transition occurred within the first 1 to 2 years after the beginning of irrigation for both scenarios (Fig. B.13e–g), which was reflected through the shift in the community average in Fig. 3.5b and d. Whether or not this is the new equilibrium state or the community is still transitioning is crucial (Sect. 3.4.1.2).

While removing the nitrogen limitation did not alter the community composition of the cold steppe under extensive (S1) and intensive (S6) grazing, irrigation had an effect (Fig. 3.5c and e). The S PFT out-competed the other PFTs entirely in the both grazing scenarios throughout the time series (Figs. 3.5c and e and B.14e, f, k, l).

## 3.4 Discussion

### 3.4.1 Forage offtake, SOC and community composition under different management and resource limitations

At all sites, forage offtake, SOC and community composition differed between the different management intensity and resource limitation scenarios. The implemented model extension enabled the model to successfully simulate differences between C, S and R strategists (Sect. 3.4.2). We were able to define new PFTs using a Bayesian calibration method that led to improved simulation of forage offtake and/or SOC at three sites under different environmental conditions and management. Our implementation is a major advancement because of the following:

1. It allows for explicit analyses of the adaptation of the vegetation to changing conditions compared to the model version in which only productivity changed.
2. Changes in the productivity of the community caused by changing conditions are the result of a changing community composition and should therefore not only be quantitatively different to those in LPJmL 5 but also more reliable.
3. This allows for assessment of the adaptive capacity under different levels of functional diversity by adding or removing specific strategies.

Furthermore, in LPJmL-CSR the initial community composition is not dependent on additional data, which facilitates the application at different sites or at larger scales.

### 3.4.1.1 Temperate grassland

While the fertilised scenario for the temperate grassland was already well simulated in LPJmL 5, the unfertilised scenario underestimated forage offtake (Sect. 3.3.1.1). In LPJmL-CSR, growth of the vegetation was faster than in LPJmL 5 which led to higher yields for all cuts. We identified two reasons for the faster growth. First, the new implementation for biological nitrogen fixation (Appendix B.1.3) reduced nitrogen stress and promoted higher photosynthesis rates. Second, while the parameters used for LPJmL-CSR were tuned for performance under the site-specific environmental conditions and management, the parameters used in LPJmL 5 were defined for large-scale simulations with different management scenarios.

The temperate grassland is neither water nor nutrient limited, and since we only assessed scenarios with reduced resource limitations, we only compared the fertilised and unfertilised scenarios. Despite the additional nitrogen input in the fertilised scenario, the unfertilised scenario achieved a similar forage offtake. Missing nutrients were acquired through biological nitrogen fixation, which was much higher in the unfertilised scenario, which is in line with the higher share of legumes observed in the field experiments (Reinsch et al., 2020). Despite the higher share of legumes in the unfertilised experiments, the share of C, S and R strategists was similar, and both fertilisation levels were dominated by C species, which was well-represented by the model.

The simulated SOC was strongly dependent on the land use history for which available data were limited. For simplicity, we did not simulate crop rotations for the land use history but selected a livestock density of 1.0 LSU ha<sup>-1</sup> (where LSU represents livestock unit) for the land use spin-up simulation (see Sect. 3.2.5 and the Supplement) to prescribe a fixed grazing pressure, which led to an underestimation of observations in the unfertilised scenario in LPJmL 5. This indicated that carbon inputs into the soil were too low in LPJmL 5. LPJmL-CSR showed smaller deviations from observations and an adequate representation of the trends (Sect. 3.3.1.1). The increased soil carbon input had three reasons. First, the trade-off between SLA and leaf longevity led to higher turnover rates and in turn higher litterfall compared to LPJmL 5. Second, accounting for mortality explicitly constituted an additional input into the litter layer. Third, our simulation included manure application which provided an additional carbon input into the system.

The community composition showed some intra-annual variability, and higher shares of the marginal PFTs at the end and the beginning of a growing season in the unfertilised and fertilised scenarios (Sect. 3.3.4.1). The S PFT gained higher shares in the unfertilised scenario, showing an advantage of the S over the R PFT despite the fact that strong nitrogen stress was avoided through biological nitrogen fixation. In contrast, if nitrogen stress was removed entirely, the S PFT lost its advantage and the R PFT could increase its share. After the first cut, these shares of the S and R PFTs became smaller,

because a cut is a disturbance that directly removes part of the aboveground biomass. One strategy to cope with this is grazing (or in this case mowing) tolerance (Briske, 1986; Stuart-Hill and Mentis, 1982), which requires fast regrowth of the leaves to compensate for the removed biomass as is typical for a C strategist (Grime, 1977, and Sect. 3.4.2.2).

### 3.4.1.2 Hot steppe

For the hot steppe, LPJmL 5 performed better for SOC, while LPJmL-CSR performed better for forage offtake. We identified several reasons for these inconsistent results. First, LPJmL does not distinguish between leaves of different age classes and therefore not between alive, senescent or moribund tissue (Schaphoff et al., 2018). All tissue is either alive and associated with the plant or moribund and part of the litter layer. However, observed forage offtake also included senescent biomass (Munjonji et al., 2020). This predisposed the model to underestimate forage offtake when accounting for realistic turnover rates, which was observed in the low biomass values simulated in LPJmL-CSR. Second, litter decomposition is a function of soil moisture, temperature and litter composition (Schaphoff et al., 2018). However, the PFTs do not differ in their persistence of the litter, which is the case for different plant species and across ecological strategies (Brovkin et al., 2012). Considering this may help to improve the simulation of SOC dynamics in the future. Third, the vegetation was described as an open thornbush savanna (Acocks, 1988; Scheiter et al., 2023) which includes a woody component. However, in LPJmL managed grassland vegetation does not include bushes or trees and therefore only partially represents the observed community.

The S PFT was dominant in the grazed and ungrazed scenarios, while the remainder of the aboveground biomass was contributed by different PFTs depending on the scenario (Sect. 3.3.2.1). The dominance of the S PFT independent of grazing is plausible considering the pronounced dry vs. wet season dynamics at the site that impose water stress (Scheiter et al., 2023) and potentially also nitrogen stress. The R PFT was more tolerant towards grazing disturbances and gained dominance in the grazed scenario, replacing the C PFT which had a lower ability to deal with disturbance. Removing the water limitation led to an increase in forage offtake and SOC, which can be expected when removing the main resource limitation. However, the majority of the SOC increase occurred in the first 2 years after the start of irrigation, which is not realistic. This can be explained by the missing representation of senescent tissue in combination with the adaptation of the community composition: removing the water limitation led to a strong increase in leaf biomass, which was substantially higher than the feed demand of the simulated grazing intensity and increased the input to the litter layer. Furthermore, the share of the R and C PFTs which have a lower leaf longevity than the S PFT increased, leading to faster inputs into the litter layer. After 1 to 2 years, the community composition reached a new equilibrium, and inputs into

the litter layer decreased. Introducing senescent tissue would increase the competition for light due to self-shading effects (Zimmermann et al., 2010) and likely slow down this transition.

In addition, irrigation led to a shift in the community composition (Sect. 3.3.4.2) and an increase in leaf biomass to which the C and R PFT together contributed more than the S PFT (Sect. 3.3.3.2). We cannot determine whether or not increases under irrigation would be lower for an S-PFT monoculture, which does not contain other ecological strategies, but we strongly suspect so.

In both the ungrazed and the grazed scenario, the community transitioned from strongly S-dominated to a community with higher shares of the C and R PFTs that were still S-dominated. According to the CSR theory, this type of community emerges in somewhat stressed and disturbed habitats (Grime, 1977). While this case can easily be made for the grazed scenario, where the disturbance is caused by the animals, the ungrazed scenario does not include such a clear disturbance. The success of both the C and the R PFTs is likely determined by the similarity of their SLA,  $k_{\text{beer}}$  and  $l_{\text{mro}}$ , which become more important compared to  $E_{\text{max}}$  and  $g_{\text{min}}$  if there is no water limitation. Potentially larger differences in these parameter would lead to the success of one of the two instead.

Less than 2 years is a very fast transition, and while the shares of the leaf biomass seem to have reached a new equilibrium after 1 or 2 years of irrigation, it is likely that the soil carbon and nitrogen pools are not in equilibrium yet. This is especially interesting when considering that the overall increase in leaf biomass may promote litterfall and the formation of inorganic nitrogen. This in turn may lead to reduced nitrogen limitation and additional changes in the community composition. Furthermore, biological nitrogen fixation is dependent on soil moisture and may therefore also contribute to decreasing nitrogen stress under irrigation. However, irrigation also leads to increased leaching and could therefore also decrease inorganic nitrogen availability. Future analysis considering longer timescales may help to identify intermediate and final transition states.

Regardless of the equilibrium state of the transition, its velocity is likely overestimated by LPJmL for two reasons. First, the C and R PFTs can establish quickly despite their limited presence before the onset of irrigation because LPJmL does not simulate a seed bank which would in reality be small at least for the C PFT limiting its establishment. Second, in reality growth of established individuals is limited and a transition as simulated is strongly controlled by reproduction and dispersal, which slow down population biomass increase. In LPJmL, already established individuals continue to grow and the population biomass increases even without additional establishment.

### 3.4.1.3 Cold steppe

LPJmL 5 underestimated the observed forage offtake of the cold steppe, because the feed demand, which was originally designed to represent large cattle (Rolinski et al., 2018), was scaled down linearly

with animal body weight. This led to an unrealistically low feed demand because the feed demand body weight relationship is not linear but follows a power law (Cordova et al., 1978). Our new calculation of feed demand (Appendix B.1.4) led to a higher feed demand and forage offtake simulations were improved for low and high grazing intensities.

Under observed conditions, the high grazing intensity severely reduced aboveground biomass, and feed demand was not met in all years except the year directly after the increase in stocking density, indicating overgrazing. The reduced biomass availability was also observed by Schönbach et al. (2012) in their field experiment. Additionally, LPJmL simulates a different community composition compared to the low grazing intensity. The relative share of the C and to some extent also the R PFT is higher for the high grazing intensity (Figs. B.11b and B.14h) because such strategies are better suited to tolerate grazing.

During and after the grazing period, the C and R PFTs had a higher share of the community aboveground biomass. Both these PFTs can regrow faster and invest more into aboveground biomass, which gave them an advantage over the S PFT under grazing. In addition to the observed environmental conditions, we simulated two scenarios where we removed the water and nitrogen limitations separately. Removing the nitrogen limitation barely affected biomass availability, and forage offtake was similar compared to the rainfed scenario (Sect. 3.3.3.3). The additional soil nitrogen could not be utilised by the plants, because water was the main limiting factor (Bai et al., 2004; Li et al., 2011). In contrast, removing the water limitation led to an increase in leaf biomass, and forage offtake met the demand in all years even for the high grazing intensity. This is in line with irrigation and fertilisation experiments conducted in the cold steppe (Li et al., 2011) and other sites with similar conditions (e.g. Shi et al., 2022). Contrary to the results of Li et al. (2011), who reported a lower share of annuals and bi-annuals – that are more likely C than S strategists – in the rainfed treatments, the S PFT was dominant in the irrigated scenarios. One reason for this could be that LPJmL does not simulate seed banks, which play a major role for the establishment and success of the annuals and bi-annuals (Brown and Venable, 1986; Thompson, 1987). Instead, LPJmL simulates establishment of additional seedlings dependent on available space, assuming that resources for reproduction are available at any time and not dependent on past investments into seed production.

Despite the fact that we did not have separate data on SOC under the two grazing intensities, our results showed a lower SOC storage for the high grazing intensity typical for overgrazed steppes (e.g. Wiesmeier et al., 2012) compared to the low grazing intensity which constituted the typical livestock density for the region (Hoffmann et al., 2016). Wiesmeier et al. (2012) investigated the effect of high grazing intensities on the SOC, observing significant SOC losses within 3 years of increased grazing, which is in line with our simulation results. Fertilisation had no effect on SOC, because leaf biomass and in turn carbon inputs into the soil did not increase. In contrast, irrigation led to an increase of SOC,

which was stronger for the low grazing intensity. This is likely because more biomass was produced, and the surplus of the feed demand was not removed but contributes to the litter layer. However, these gains would not justify the effort that would be necessary to irrigate large areas.

Removing the water limitation led to a transition from S-dominated to an S-monoculture community under both grazing intensities (Sect. 3.3.4.2). Since the site was still severely nutrient-limited and exposed to low temperatures, it seems that an S strategy remained advantageous. Furthermore, the S PFT showed trait values associated with large investments in roots and more persistent root tissue (Sect. 3.3.2.1), which provides a likely explanation for its increased dominance: it had an advantage in the competition for the additional water. Similar to the hot steppe, it is possible that our time frame is too short for the soil pools to have reached a new equilibrium. As described in Sect. 3.4.1.2, irrigation alone already affects processes that could increase nitrogen supply by biological nitrogen fixation and litterfall, but it could also decrease it by leaching. Both biological nitrogen fixation and mineralisation are dependent on soil moisture as well as on temperature, which is low in the cold steppe limiting the increase of inorganic nitrogen. Therefore, it is possible that only an intermediate state emerges during our simulation period. Especially when also considering the increased leaching, we expect that the cold steppe is still nitrogen limited under irrigation; therefore, combining irrigation with fertilisation could further reduce nitrogen limitation, leading to increased productivity and changes in the community composition. However, the leaf biomass increase may also be limited by higher maintenance respiration which is connected to leaf nitrogen content. Additional analysis is needed to enhance the understanding of these complex interactions.

## **3.4.2 Stress and disturbance gradients across sites and management**

### **3.4.2.1 Across sites**

We used a Bayesian calibration method to find suitable parameter values of eight parameters assigned to two trade-off dimensions for the new PFTs. Due to lacking data on starting values and ranges for the three new PFTs, we used the same ranges and starting values for each PFT but prescribed an order of the parameters. Within a site and management scenario, the prescribed hierarchy for specific parameters also predefined the ranking of the PFTs along the stress and disturbance gradients. Across sites and management, we did not constrain the PFTs to positions within the two dimensions. Theoretically, all PFTs of the temperate grassland could have been associated with a more conservative strategy for the stress gradient compared to the PFTs of the hot steppe. However, while there were some differences between the sites and management; on average, the C and R PFTs occupied a more resource-exploitative position for the stress gradient and the S PFTs a more conservative one (Sect. 3.3.2.2). Similarly, for the disturbance gradient the C and S PFTs occupied a position associated with less but larger offspring and

a larger stature compared to the R PFT. It is an emergent property of the model that not only the relative position of the PFTs of a site and management scenario determined community composition but also the overall positions along the stress and disturbance gradients (which we derived from the global spectrum of plant form and function Díaz et al., 2016) were important. Our experiences from these three sites showed similar strategies that are independent of environmental conditions, indicating that LPJmL-CSR is capable of reproducing the empirically derived trade-offs associated with the global spectrum of plant form and function (Díaz et al., 2016). However, LPJmL-CSR will benefit from additional testing on larger scales in the future.

### 3.4.2.2 Across management

While missing processes such as the representation of seed banks as at the hot steppe (Sect. 3.4.1.2) and poor data as at the cold steppe (Sect. 3.4.1.3) may have led to biased model dynamics to some extent, we clearly demonstrated the importance of representing different ecological strategies.

The calibration selected different strategies along the stress and disturbance gradients for the different management intensities (Sect. 3.3.2.1), which were related to changes in resource limitations or disturbance level: in LPJmL-CSR, a change in resource availability only changes the conditions for the establishment of a community but does not directly affect the established vegetation (changes in environmental filters; Bazzaz, 1991; Woodward and Diament, 1991). In reality, however, a change in resource availability may also increase the mortality for specific strategy types, affecting the already established community as well. In temperate grasslands, manure application increases N supply and reduces the number of available niches that can be occupied by different ecological strategies. In the unfertilised experiment, species could satisfy their N demand through two different strategies: competition for the limited resource in the soil or biological N fixation (BNF). In the fertilised experiment, only the first strategy was advantageous as BNF creates additional costs. In the field experiment, this was evidenced through the substantially different amounts of legumes between the two experiments (Reinisch et al., 2020). In the model, N-fixing and non-N-fixing species are both collated within each PFT. Therefore, in the unfertilised scenario, a PFT had to apply a strategy combining N uptake and fixation, whereas it could focus on N uptake in the fertilised scenario. Since we calibrated the unfertilised and fertilised scenarios separately using the same data for C, S and R PFT covers, the difference in strategy between the two scenarios is expressed through the different positions of the PFTs along the stress and disturbance gradients: higher investments into belowground biomass ( $lmro$ ) provide an advantage in the competition for plant-available nitrogen (Johnson and Biondini, 2001). In the model, this led to a reduced need of fixing additional nitrogen and in turn a reduction of the investment costs associated with biological nitrogen fixation (Sect. 3.3.2.1).

In contrast to resource availability, a disturbance directly affects the vegetation. In the case of grazing, it also influences resource availability indirectly through removal of nutrients from and spatial redistribution within the system (Chuan et al., 2018; Liu et al., 2023; Wan et al., 2015). In LPJmL, the grazing of the animals at the steppe sites constituted a direct reduction of leaf biomass proportional to the cover of each PFT (Rolinski et al., 2018). Under intensive grazing, strategies of grazing tolerance or avoidance are essential (Briske, 1986; Stuart-Hill and Mentis, 1982). While grazing tolerance is mainly associated with fast regrowth (Briske, 1986; Hyder, 1972, stress gradient), grazing avoidance strategies can operate in time and space. Grazing avoidance in time is possible through the completion of the lifecycle between grazing intervals (Noy-Meir, 1990, disturbance gradient). Grazing avoidance in space is contingent on reducing plant size (Branson, 1953; Rechenthin, 1956). However, since plant size is not explicitly represented in LPJmL, we do not discuss this strategy further (Sect. 3.2.3.3). In the hot steppe, we simulated a daily grazing system, which makes grazing avoidance through the lifecycle impossible, and the PFTs had to follow a grazing-tolerance strategy. This was expressed through changes in the stress gradient: all PFTs increased their investment into aboveground biomass and faster tissue growth (Sect. 3.3.2.1). Because LPJmL does not account for differences in the palatability of different strategy types the parameterisation could not select for such likely successful strategies, leading to a potentially biased community composition.

At the cold steppe site, grazing only happened during the growing season, and both grazing tolerance and avoidance could be useful strategies. However, grazing avoidance in time, which is the only type simulated by LPJmL, will not be successful as it would mean shifting biomass production to the non-growing season where the environmental conditions do not allow growth. Still, between the extensive and intensive grazing scenarios, the differences between the PFTs in both dimensions do support different strategy adjustments (Sect. 3.3.2.1). The C PFT increased its investment into aboveground biomass to tolerate grazing, while the S and R PFTs did not show any adjustment. However, since the high grazing pressure caused degradation of the aboveground biomass, differences between the two management scenarios not only reflect different strategies to deal with the disturbance but also reflect different strategies for survival outside the grazed period. As such, all PFTs constructed long-living tissue to survive unproductive conditions outside the growing season in the intensive grazing scenario. This was not necessary in the extensive grazing scenario, because the PFTs retained substantial aboveground biomass at the end of the growing season and did not need to be as resource conservative.

### **3.4.3 Limitations and further need for research**

The representation of different CSR strategies is a new feature in LPJmL, a model which is mainly used at large to global spatial scales. Past explorations have pointed out the difficulties of adding new

PFTs to DGVMs in general (Yang et al., 2015) and also to LPJmL (Wirth et al., 2021). We therefore decided to only add a small number of PFTs which should represent the three main CSR strategies and no sub-strategies. We used expert estimates to determine the shares of the three strategies. These three strategy shares sum up to 100 % and also encompass species that would be added to a sub-strategy in a less coarse approach. Consequently, our results show a very simplified representation of the different strategies within a community and across sites, which might be better represented using a small-scale model such as IBC GRASS (May et al., 2009) or GRASSMIND (Taubert et al., 2012; Taubert et al., 2020a; Taubert et al., 2020b). However, large-scale applications also benefit from the inclusion of universally applicable trade-offs between different ecological strategies and the improved representation of productivity changes.

Furthermore, we reduced the trade-offs between C, S and R strategists to fit into two dimensions and used a limited amount of parameters to express these. While this simplification was necessary, this also means that we do not represent all effects, advantages or trade-offs of functional diversity. However, as LPJmL is a global model, our aim was not to optimise performance for specific sites, but to evaluate and test an approach which can easily be applied at the global scale without the need of a global data set on community composition of grasslands. Keeping this in mind, and considering the difficulties of adding PFTs to a DGVM as well as the global heritage of the model, we find that representing even just the three main CSR strategies constitutes a major improvement of LPJmL.

Generally, the approach of using a small number of PFTs with a fixed set of parameters has been criticised (Quillet et al., 2010), leading to the development of next-generation DGVMs that apply an individual-based approach such as LPJmL-FIT (Sakschewski et al., 2015) or aDGVM (Scheiter et al., 2013). These models simulate the competition between individual plants for which parameter values are drawn from predefined ranges upon establishment. Given sufficient time, only successful strategies will survive. Such models provide a much more nuanced representation of functional diversity compared to classic DGVMs with their coarse division into fixed PFTs but are also computationally substantially more expensive because of the high number of individuals for which all processes have to be calculated. Past studies have therefore often focused on specific regions such as the Amazon rainforest (Sakschewski et al., 2015), European forests (Thonicke et al., 2020) or South African semi-arid rangelands (Pfeiffer et al., 2019). In contrast, classic DGVMs are still widely applied on the global scale, e.g. to calculate the global carbon budget (Friedlingstein et al., 2022), and we see the need to continue their development for the foreseeable future. Combining our approach of distinguishing between PFTs that follow the main strategies of the CSR theory with an individual-based approach, making use of the full parameter range instead of single points, provides an interesting opportunity for future research of diverse grasslands.

For this study, we only assessed three sites at which our approach worked well. We did not include

a site dominated by R strategists since this is not common for managed grasslands, but we also did not include CS and CSR habitats which are typical for unfertilised and fertilised pastures, respectively (Grime, 1974). Additional research including these intermediate habitats might provide more insight into the newly implemented strategies and trade-offs. While separate calibrations are feasible for a small number of sites and scenarios, for large-scale or global assessments the lack of data and the computational requirement for the calibration make a site-specific calibration infeasible. However, using a more efficient calibration method and remote sensing data instead of on-site experiments can be used to derive a set of PFTs which are representative of the entire globe or at least climatic regions. For LPJmL, a genetic optimisation algorithm has been used to successfully calibrate the phenology (Forkel et al., 2014) and vegetation dynamics (Forkel et al., 2019) of natural ecosystems. Following this approach, we believe it is possible to identify C, S and R PFTs for the tropical, temperate and polar regions, ending up with nine PFTs in total.

In LPJmL, herbaceous plants are represented as average individuals of a number of different PFTs, without an explicit representation of geometry. Therefore, we used the light extinction coefficient as a proxy for stature, assuming that small-stature plants would be less competitive for light. We here deviate from the common interpretation of the light extinction coefficient, which is usually defined as the light absorption of a layer of leaves. However, as explained in Sect. 3.2.4, LPJmL represents the entire vegetation as a single layer, and we therefore define the light extinction coefficient not for a single leaf but a stack of leaves. Taller plants likely produce more layers of leaves, corresponding to a larger stack and a thicker vegetation layer with a higher light extinction. However, thickness of the vegetation layer is not explicitly represented in LPJmL, and we represent the described differences by using lower light extinction coefficients for small-stature plants for which we assume a lower thickness of the vegetation layer and higher light extinction coefficients for large-stature plants. However, this is not sufficient to simulate grazing avoidance in space (Sect. 3.4.2.2), and an explicit representation of plant height and area could further improve the representation of ecological strategies (Wirth et al., 2021). Furthermore, the coexistence of trees and grass species, which is typical for savanna sites, is not implemented in the LPJmL model. However, this is crucial to adequately represent such ecosystems (Rolinski et al., 2021) and should be a focus of future model development. Another important aspect in savanna and other dryland ecosystems is the distinction between annual and perennial plants. In LPJmL, this distinction is not explicitly made. While the R PFT has a higher replacement rate of average individuals, it is not constrained to a specific growing season, after which it is completely killed to be re-established the following growing season. Incorporating this distinction into the model is an option to add additional functional diversity and will likely improve model results.

LPJmL-CSR only represents age mortality; that is, the effects of mortality from other causes such as frost, heat and embolism are not represented. Especially under changing climatic conditions, specific

strategy types may show increased mortality and lose their advantage to the advantage of other strategy types. Including additional causes of mortality may introduce additional trade-offs and enhance the differentiation between strategy types.

Plant species have adapted to grazers in many ways, one of which is grazing avoidance by being less or even unpalatable. This is a successful strategy in grazing systems because, in contrast to mowing, which is indiscriminate, grazing animals show preferences for plants with a higher palatability (Hardison et al., 1954; Tribe and Gordon, 1950). Selective grazing and grazing avoidance through palatability are currently not represented in LPJmL but can have a strong effect on the community composition (Newman et al., 1995; Parsons et al., 1994). Including preferences, e.g. for high SLA PFTs, may improve simulation results further. Additionally, LPJmL-CSR does not consider mechanical stress caused by trampling of animals and potential strategy dependent damage. Incorporating this may add another dimension of stress to distinguish different PFTs.

Data coverage for the temperate grassland site was good, and observations were available for multiple years and with sufficient replicates. For the two steppe sites, data on SOC were scarce. Especially additional data on trends and equilibria under specific management conditions might promote further improvement of the model and help with the parameterisation of new PFTs. We based our parameterisation of the new PFTs on expert estimates for the C, S, and R PFT covers. While we are confident that these estimates were adequate, data on a small number of traits would be sufficient to calculate the shares for each PFT following Pierce et al. (2013), and we would like to encourage including such data as a standard in sampling procedures for future experiments.

The scenarios we examined here only involved the reduction of stress by removing either water or nitrogen limitations. Additional insight might be gained from doing the opposite and imposing additional limitations or looking into gradual changes in environmental conditions.

### 3.5 Conclusions

We presented a new approach for large-scale models and DGVMs to simulate the three main CSR strategies of managed grassland PFTs. In addition to improving the simulation of forage offtake or leaf biomass and SOC at three different sites, the approach successfully simulated the dynamic community composition at these sites and reproduced the spectrum of plant form and function (Díaz et al., 2016). This is a major improvement, allowing researchers to explicitly assess how the presence or absence of specific plant strategies affects ecosystem functioning and thus ecosystem service provision of managed grasslands. Using this new feature, scenarios for projections of forage offtake, leaf biomass and SOC under climate change can be complemented with different constraints on the adaptive capacity of the vegetation. Such projections can provide a range of future grassland productivity as decision-support

for policy-makers. To further improve these projections, extending the sites by considering habitats with intermediate environmental conditions as well as the scenarios by including additional resource limitations (e.g. droughts) or gradual changes of environmental conditions (e.g. temperature increase) could be useful to gain additional insights into the model and to study the complex interactions of climate change, management and functional diversity.

**Code and data availability:** The source code is publicly available under the GNU AGPL version 3 license. An exact version of the code described here and the data used to create the figures is archived under <https://zenodo.org/records/10217244> (Wirth et al., 2023).

**Author contributions:** SBW, SR and AP designed the study in discussion with AL, BT, FT and CM. SBW designed and conducted the model implementation with inputs from SR and AP. WvB and SSch contributed to general model development and evaluation. SBW conducted the model simulations and wrote the original draft of the manuscript. All authors discussed the simulation results and the original draft. AL, BT, SR, CM, AP, SSch, FT, and KB reviewed and edited the manuscript. AL, KB, AP and FT contributed unpublished empirical data from grassland sites and experiments. SR, AP and FT supervised this study.

**Acknowledgements:** SBW acknowledges financial support from the Evangelisches Studienwerk Villigst foundation, under the research program: "Third Ways of Feeding The World", the Global Commons Stewardship (GCS) project funded by the University of Tokyo / Institute for Future Initiatives and the German Federal Ministry for Education and Research (BMBF) within the projects CLIMASTEPE (grant no. 01DJ8012), EXIMO (grant no. 01LP1903D) and ABCDR (grant no. 01LS2105A). SR acknowledges financial support from the BMBF within the projects CLIMASTEPE (grant no. 01DJ8012), AGrEc (grant no. 01DG21039), MAPPY (grant no. 01LS1903A) and ABCDR (grant no. 01LS2105A). BT acknowledges funding by the BMBF in the framework of the ValuGaps project (grant no. 01UT2103C). AL and KB acknowledge funding by the BMBF within projects of the SPACES initiative ("Limpopo Living Landscapes" project – grant no. 01LL1304D; "SALLnet" grant no. 01LL1802C). We thank Stefan Lange for providing the GSWP3-ERA5 data set and Edwin Mudongo, Vincent Mokoka, and the Risk and Vulnerability Center at the University of Limpopo, South Africa, for data acquisition at the hot steppe site.

### 3.6 References

- Acocks, J. P. H. (1988). *Veld Types of South Africa*. 3rd ed. Vol. 57. Memoirs of the Botanical Survey of South Africa. Cape Town, South Africa: Botanical Research Institute. ISBN: 978-0-621-11394-5.
- Bai, Y. and M. F. Cotrufo (2022). "Grassland Soil Carbon Sequestration: Current Understanding, Challenges, and Solutions". In: *Science* 377.6606, pp. 603–608. DOI: 10.1126/science.abo2380. (Visited on 02/13/2023).
- Bai, Y., X. Han, J. Wu, Z. Chen, and L. Li (2004). "Ecosystem Stability and Compensatory Effects in the Inner Mongolia Grassland". In: *Nature* 431.7005, pp. 181–184. ISSN: 1476-4687. DOI: 10.1038/nature02850. (Visited on 02/14/2023).
- Bazzaz, F. A. (1991). "Habitat Selection in Plants". In: *Am. Nat.* 137, S116–S130. ISSN: 0003-0147. JSTOR: 2462291. (Visited on 02/14/2023).
- Bergmann, J., A. Weigelt, F. van der Plas, D. C. Laughlin, T. W. Kuyper, N. Guerrero-Ramirez, O. J. Valverde-Barrantes, H. Bruelheide, G. T. Freschet, C. M. Iversen, J. Kattge, M. L. McCormack, I. C. Meier, M. C. Rillig, C. Roumet, M. Semchenko, C. J. Sweeney, J. van Ruijven, L. M. York, and L. Mommer (2020). "The Fungal Collaboration Gradient Dominates the Root Economics Space in Plants". In: *Sci. Adv.* 6.27, eaba3756. DOI: 10.1126/sciadv.aba3756. (Visited on 03/08/2022).
- Boenisch, G. and J. Kattge (2018). *TRY Plant Trait Database*. <https://www.try-db.org/TryWeb/Home.php>. (Visited on 03/08/2018).
- Branson, F. A. (1953). "Two New Factors Affecting Resistance of Grasses to Grazing". In: *Journal of Range Management* 6.3, p. 165. ISSN: 0022409X. DOI: 10.2307/3893839. JSTOR: 3893839. (Visited on 02/13/2023).
- Briske, D. D. (1986). "Plant Response to Defoliation: Morphological Considerations and Allocation Priorities". In: *Rangelands: A Resource under Siege*. Ed. by Joss, P. J., Lynch P. W., and Williams O. B. Canberra: Aust. Acad. Sci., pp. 425–427.
- Brovkin, V., P. M. van Bodegom, T. Kleinen, C. Wirth, W. K. Cornwell, J. H. C. Cornelissen, and J. Kattge (2012). "Plant-Driven Variation in Decomposition Rates Improves Projections of Global Litter Stock Distribution". In: *Biogeosciences* 9.1, pp. 565–576. ISSN: 1726-4189. DOI: 10.5194/bg-9-565-2012. (Visited on 12/04/2022).
- Brown, J. S. and D. L. Venable (1986). "Evolutionary Ecology of Seed-Bank Annuals in Temporally Varying Environments". In: *Am. Nat.* 127.1, pp. 31–47. ISSN: 0003-0147. DOI: 10.1086/284465. (Visited on 06/13/2022).

- Buzhdygan, O. Y., S. T. Meyer, W. W. Weisser, N. Eisenhauer, A. Ebeling, S. R. Borrett, N. Buchmann, R. Cortois, G. B. De Deyn, H. de Kroon, G. Gleixner, L. R. Hertzog, J. Hines, M. Lange, L. Mommer, J. Ravenek, C. Scherber, M. Scherer-Lorenzen, S. Scheu, B. Schmid, K. Steinauer, T. Strecker, B. Tietjen, A. Vogel, A. Weigelt, and J. S. Petermann (2020). “Biodiversity Increases Multitrophic Energy Use Efficiency, Flow and Storage in Grasslands”. In: *Nat Ecol Evol* 4.3, pp. 393–405. ISSN: 2397-334X. DOI: 10.1038/s41559-020-1123-8. (Visited on 11/20/2023).
- Caccianiga, M., A. Luzzaro, S. Pierce, R. M. Ceriani, and B. Cerabolini (2006). “The Functional Basis of a Primary Succession Resolved by CSR Classification”. In: *Oikos* 112.1, pp. 10–20. ISSN: 1600-0706. DOI: 10.1111/j.0030-1299.2006.14107.x. (Visited on 06/13/2022).
- Campbell, B. D. and J. P. Grime (1992). “An Experimental Test of Plant Strategy Theory”. In: *Ecology* 73.1, pp. 15–29. ISSN: 1939-9170. DOI: 10.2307/1938717. (Visited on 06/13/2022).
- Cerabolini, B. E. L., S. Pierce, A. Verginella, G. Brusa, R. M. Ceriani, and S. Armiraglio (2016). “Why Are Many Anthropogenic Agroecosystems Particularly Species-Rich?” In: *Plant Biosyst. - Int. J. Deal. Asp. Plant Biol.* 150.3, pp. 550–557. ISSN: 1126-3504. DOI: 10.1080/11263504.2014.987848. (Visited on 10/17/2022).
- Chang, J., P. Ciais, T. Gasser, P. Smith, M. Herrero, P. Havlík, M. Obersteiner, B. Guenet, D. S. Goll, W. Li, V. Naipal, S. Peng, C. Qiu, H. Tian, N. Viovy, C. Yue, and D. Zhu (2021). “Climate Warming from Managed Grasslands Cancels the Cooling Effect of Carbon Sinks in Sparsely Grazed and Natural Grasslands”. In: *Nat Commun* 12.1, p. 118. ISSN: 2041-1723. DOI: 10.1038/s41467-020-20406-7. (Visited on 04/17/2024).
- Chaplot, V., B. Bouahom, and C. Valentin (2010). “Soil Organic Carbon Stocks in Laos: Spatial Variations and Controlling Factors”. In: *Glob. Change Biol.* 16.4, pp. 1380–1393. ISSN: 1365-2486. DOI: 10.1111/j.1365-2486.2009.02013.x. (Visited on 10/12/2022).
- Chen, S., W. Wang, W. Xu, Y. Wang, H. Wan, D. Chen, Z. Tang, X. Tang, G. Zhou, Z. Xie, D. Zhou, Z. Shangguan, J. Huang, J.-S. He, Y. Wang, J. Sheng, L. Tang, X. Li, M. Dong, Y. Wu, Q. Wang, Z. Wang, J. Wu, F. S. Chapin, and Y. Bai (2018). “Plant Diversity Enhances Productivity and Soil Carbon Storage”. In: *Proc. Natl. Acad. Sci.* 115.16, pp. 4027–4032. DOI: 10.1073/pnas.1700298114. (Visited on 02/13/2023).
- Chuan, X., C. N. Carlyle, E. W. Bork, S. X. Chang, and D. B. Hewins (2018). “Long-Term Grazing Accelerated Litter Decomposition in Northern Temperate Grasslands”. In: *Ecosystems* 21.7, pp. 1321–1334. ISSN: 1435-0629. DOI: 10.1007/s10021-018-0221-9. (Visited on 02/14/2023).
- Conant, R. T., C. E. P. Cerri, B. B. Osborne, and K. Paustian (2017). “Grassland Management Impacts on Soil Carbon Stocks: A New Synthesis”. In: *Ecol. Appl.* 27.2, pp. 662–668. ISSN: 1939-5582. DOI: 10.1002/eap.1473. (Visited on 02/13/2023).
- Cordova, F. J., J. D. Wallace, and R. D. Pieper (1978). “Forage Intake by Grazing Livestock: A Review”. In: *J. Range Manag.* 31.6, pp. 430–438. ISSN: 0022-409X. DOI: 10.2307/3897201. JSTOR: 3897201. (Visited on 06/14/2022).
- Díaz, S., J. Kattge, J. H. C. Cornelissen, I. J. Wright, S. Lavorel, S. Dray, B. Reu, M. Kleyer, C. Wirth, I. C. Prentice, E. Garnier, G. Bönlisch, M. Westoby, H. Poorter, P. B. Reich, A. T. Moles, J. Dickie, A. N. Gillison, A. E. Zanne, J. Chave, S. J. Wright, S. N. Sheremet’ev, H. Jactel, C. Baraloto, B. Cerabolini, S. Pierce, B. Shipley, D. Kirkup, F. Casanoves, J. S. Joswig, A. Günther, V. Falczuk, N. Rüger, M. D. Mahecha, and L. D. Gorné (2016). “The Global Spectrum of Plant Form and Function”. In: *Nature* 529.7585, pp. 167–171. ISSN: 1476-4687. DOI: 10.1038/nature16489. (Visited on 03/24/2020).
- Doetterl, S., A. A. Berhe, E. Nadeu, Z. Wang, M. Sommer, and P. Fiener (2016). “Erosion, Deposition and Soil Carbon: A Review of Process-Level Controls, Experimental Tools and Models to Address C Cycling in Dynamic Landscapes”. In: *Earth-Science Reviews* 154, pp. 102–122. ISSN: 0012-8252. DOI: 10.1016/j.earscirev.2015.12.005. (Visited on 10/12/2022).
- DWD (2021). *Wetter Und Klima - Deutscher Wetterdienst - Leistungen - Klimadaten Deutschland - Monats- Und Tageswerte (Archiv)*. <https://www.dwd.de/DE/leistungen/klimadatendeutschland/klarchivtagmonat.html>. (Visited on 06/16/2022).
- Fei, S., I. Jo, Q. Guo, D. A. Wardle, J. Fang, A. Chen, C. M. Oswalt, and E. G. Brockerhoff (2018). “Impacts of Climate on the Biodiversity-Productivity Relationship in Natural Forests”. In: *Nat Commun* 9.1, p. 5436. ISSN: 2041-1723. DOI: 10.1038/s41467-018-07880-w. (Visited on 02/13/2023).
- Forkel, M., N. Carvalhais, S. Schaphoff, W. v. Bloh, M. Migliavacca, M. Thurner, and K. Thonicke (2014). “Identifying Environmental Controls on Vegetation Greenness Phenology through Model–Data Integration”. In: *Biogeosciences* 11.23, pp. 7025–7050. ISSN: 1726-4170. DOI: 10.5194/bg-11-7025-2014. (Visited on 06/29/2021).
- Forkel, M., M. Druke, M. Thurner, W. Dorigo, S. Schaphoff, K. Thonicke, W. von Bloh, and N. Carvalhais (2019). “Constraining Modelled Global Vegetation Dynamics and Carbon Turnover Using Multiple Satellite Observations”. In: *Sci Rep* 9.1, p. 18757. ISSN: 2045-2322. DOI: 10.1038/s41598-019-55187-7. (Visited on 06/29/2021).
- Friedlingstein, P., M. O’Sullivan, M. W. Jones, R. M. Andrew, L. Gregor, J. Hauck, C. Le Quéré, I. T. Luijckx, A. Olsen, G. P. Peters, W. Peters, J. Pongratz, C. Schwingshackl, S. Sitch, J. G. Canadell, P. Ciais, R. B. Jackson, S. R. Alin, R. Alkama, A. Arneth, V. K. Arora, N. R. Bates, M. Becker, N. Bellouin, H. C. Bittig, L. Bopp, F. Chevallier, L. P. Chini, M. Cronin, W. Evans, S. Falk, R. A. Feely, T. Gasser, M. Gehlen, T. Gkritzalis, L. Gloege, G. Grassi, N. Gruber, Ö. Gürses, I. Harris, M. Hefner, R. A. Houghton, G. C. Hurtt, Y. Iida, T. Ilyina, A. K. Jain, A. Jersild, K. Kadono, E. Kato, D. Kennedy, K. Klein Goldewijk, J. Knauer, J. I. Korsbakken, P. Landschützer, N. Lefèvre, K. Lindsay, J. Liu, Z. Liu, G. Marland, N. Mayot, M. J. McGrath, N. Metzl, N. M. Monacci, D. R. Munro, S.-I. Nakaoka, Y. Niwa, K. O’Brien, T. Ono, P. I. Palmer, N. Pan, D. Pierrot, K. Pockock, B. Poulter, L. Resplandy, E. Robertson, C. Rödenbeck, C. Rodriguez, T. M. Rosan, J. Schwinger, R. Séférian, J. D. Shutler, I. Skjelvan, T. Steinhoff, Q. Sun, A. J. Sutton, C. Sweeney, S. Takao, T. Tanhua, P. P. Tans, X. Tian, H. Tian, B. Tilbrook, H. Tsujino, F. Tubiello, G. R. van der Werf, A. P. Walker, R. Wanninkhof, C. Whitehead, A. Willstrand Wranne, R. Wright, W. Yuan, C. Yue, X. Yue, S. Zaehle, J. Zeng, and B.

- Zheng (2022). “Global Carbon Budget 2022”. In: *Earth Syst. Sci. Data* 14.11, pp. 4811–4900. ISSN: 1866-3508. DOI: 10.5194/essd-14-4811-2022. (Visited on 11/14/2023).
- Godde, C. M., I. J. M. de Boer, E. zu Ermgassen, M. Herrero, C. E. van Middelaar, A. Muller, E. Rös, C. Schader, P. Smith, H. H. E. van Zanten, and T. Garnett (2020). “Soil Carbon Sequestration in Grazing Systems: Managing Expectations”. In: *Clim. Change* 161.3, pp. 385–391. ISSN: 1573-1480. DOI: 10.1007/s10584-020-02673-x. (Visited on 10/21/2020).
- Grime, J. P. (1974). “Vegetation Classification by Reference to Strategies”. In: *Nature* 250.5461, pp. 26–31. ISSN: 0028-0836, 1476-4687. DOI: 10.1038/250026a0. (Visited on 06/13/2022).
- Grime, J. P. (1977). “Evidence for the Existence of Three Primary Strategies in Plants and Its Relevance to Ecological and Evolutionary Theory”. In: *Am. Nat.* 111.982, pp. 1169–1194. ISSN: 0003-0147,1537-5323. DOI: 10.1086/283244. (Visited on 10/28/2021).
- Grime, J. P. (2001). *Plant Strategies, Vegetation Processes, and Ecosystem Properties*. 2nd ed. Wiley. (Visited on 06/13/2022).
- Grime, J. P., J. G. Hodgson, and R. Hunt (1988). *Comparative Plant Ecology: A Functional Approach to Common British Species*. Springer Dordrecht. ISBN: 978-94-017-1094-7.
- Guo, Q. (2007). “The Diversity–Biomass–Productivity Relationships in Grassland Management and Restoration”. In: *Basic and Applied Ecology* 8.3, pp. 199–208. ISSN: 1439-1791. DOI: 10.1016/j.baae.2006.02.005. (Visited on 02/13/2023).
- Guuroh, R. T., J. C. Ruppert, J. Ferner, K. Čanak, S. Schmidlein, and A. Linstädter (2018). “Drivers of Forage Provision and Erosion Control in West African Savannas—A Macroecological Perspective”. In: *Agriculture, Ecosystems & Environment* 251, pp. 257–267. ISSN: 0167-8809. DOI: 10.1016/j.agee.2017.09.017. (Visited on 11/20/2023).
- Hardin, G. (1960). “The Competitive Exclusion Principle”. In: *Science* 131.3409, pp. 1292–1297. ISSN: 0036-8075, 1095-9203. DOI: 10.1126/science.131.3409.1292. (Visited on 08/14/2018).
- Hardison, W. A., J. T. Reid, C. M. Martin, and P. G. Woolfolk (1954). “Degree of Herbage Selection by Grazing Cattle”. In: *Journal of Dairy Science* 37.1, pp. 89–102. ISSN: 0022-0302. DOI: 10.3168/jds.S0022-0302(54)91236-9. (Visited on 04/25/2024).
- Herzfeld, T., J. Heinke, S. Rolinski, and C. Müller (2021). “Soil Organic Carbon Dynamics from Agricultural Management Practices under Climate Change”. In: *Earth Syst. Dyn.* 12.4, pp. 1037–1055. ISSN: 2190-4979. DOI: 10.5194/esd-12-1037-2021. (Visited on 05/31/2023).
- Hodgson, J. G., P. J. Wilson, R. Hunt, J. P. Grime, and K. Thompson (1999). “Allocating C-S-R Plant Functional Types: A Soft Approach to a Hard Problem”. In: *Oikos* 85.2, pp. 282–294. ISSN: 0030-1299. DOI: 10.2307/3546494. JSTOR: 3546494. (Visited on 03/25/2020).
- Hoffmann, C., M. Giese, U. Dickhoefer, H. Wan, Y. Bai, M. Steffens, C. Liu, K. Butterbach-Bahl, and X. Han (2016). “Effects of Grazing and Climate Variability on Grassland Ecosystem Functions in Inner Mongolia: Synthesis of a 6-Year Grazing Experiment”. In: *Journal of Arid Environments* 135, pp. 50–63. ISSN: 0140-1963. DOI: 10.1016/j.jaridenv.2016.08.003. (Visited on 12/09/2021).
- Huhtanen, P., J. I. Nousiainen, M. Rinne, K. Kytölä, and H. Khalili (2008). “Utilization and Partition of Dietary Nitrogen in Dairy Cows Fed Grass Silage-Based Diets”. In: *Journal of Dairy Science* 91.9, pp. 3589–3599. ISSN: 0022-0302. DOI: 10.3168/jds.2008-1181. (Visited on 02/13/2023).
- Hunt, R., J. Hodgson, K. Thompson, P. Bungener, N. Dunnett, and A. Askew (2004). “A New Practical Tool for Deriving a Functional Signature for Herbaceous Vegetation”. In: *Appl. Veg. Sci.* 7.2, pp. 163–170. ISSN: 1654-109X. DOI: 10.1111/j.1654-109X.2004.tb00607.x. (Visited on 10/17/2022).
- Hyder, D. N. (1972). “Defoliation in Relation to Vegetative Growth”. In: *The Biology and Utilization of Grasses*. Ed. by Youngner V. B. and McKell, C. M. New York: Academic Press, pp. 302–317.
- Isbell, F., D. Craven, J. Connolly, M. Loreau, B. Schmid, C. Beierkuhnlein, T. M. Bezemer, C. Bonin, H. Bruehlheide, E. de Luca, A. Ebeling, J. N. Griffin, Q. Guo, Y. Hautier, A. Hector, A. Jentsch, J. Kreyling, V. Lanta, P. Manning, S. T. Meyer, A. S. Mori, S. Naeem, P. A. Niklaus, H. W. Polley, P. B. Reich, C. Roscher, E. W. Seabloom, M. D. Smith, M. P. Thakur, D. Tilman, B. F. Tracy, W. H. van der Putten, J. van Ruijven, A. Weigelt, W. W. Weisser, B. Wilsey, and N. Eisenhauer (2015). “Biodiversity Increases the Resistance of Ecosystem Productivity to Climate Extremes”. In: *Nature* 526.7574, pp. 574–577. ISSN: 1476-4687. DOI: 10.1038/nature15374. (Visited on 05/22/2019).
- Jacobsen, A. L., R. B. Pratt, M. D. Venturas, and U. G. Hacke (2019). “Large Volume Vessels Are Vulnerable to Water-Stress-Induced Embolism in Stems of Poplar”. In: *IAWA J.* 40.1, 4–S4. ISSN: 0928-1541, 2294-1932. DOI: 10.1163/22941932-40190233. (Visited on 06/08/2023).
- Jägermeyr, J., D. Gerten, J. Heinke, S. Schaphoff, M. Kummu, and W. Lucht (2015). “Water Savings Potentials of Irrigation Systems: Global Simulation of Processes and Linkages”. In: *Hydrol. Earth Syst. Sci.* 19.7, pp. 3073–3091. ISSN: 1027-5606. DOI: 10.5194/hess-19-3073-2015. (Visited on 06/19/2023).
- Jebari, A., J. Álvaro-Fuentes, G. Pardo, I. Batalla, J. A. R. Martín, and A. Del Prado (2022). “Effect of Dairy Cattle Production Systems on Sustaining Soil Organic Carbon Storage in Grasslands of Northern Spain”. In: *Reg Environ Change* 22.2, p. 67. ISSN: 1436-378X. DOI: 10.1007/s10113-022-01927-x. (Visited on 06/13/2022).
- Jobbágy, E. G. and R. B. Jackson (2000). “The Vertical Distribution of Soil Organic Carbon and Its Relation to Climate and Vegetation”. In: *Ecol. Appl.* 10.2, pp. 423–436. ISSN: 1939-5582. DOI: 10.1890/1051-0761(2000)010[0423:TVDOSO]2.0.CO;2. (Visited on 10/12/2022).
- Johnson, H. A. and M. E. Biondini (2001). “Root Morphological Plasticity and Nitrogen Uptake of 59 Plant Species from the Great Plains Grasslands, U.S.A.” In: *Basic and Applied Ecology* 2.2, pp. 127–143. ISSN: 1439-1791. DOI: 10.1078/1439-1791-00044. (Visited on 02/14/2023).
- Kölbl, A., M. Steffens, M. Wiesmeier, C. Hoffmann, R. Funk, J. Krümmelbein, A. Reszkowska, Y. Zhao, S. Peth, R. Horn, M. Giese, and I. Kögel-Knabner (2011). “Grazing Changes Topography-Controlled Topsoil Properties and Their Interaction

- on Different Spatial Scales in a Semi-Arid Grassland of Inner Mongolia, P.R. China”. In: *Plant Soil* 340.1, pp. 35–58. ISSN: 1573-5036. DOI: 10.1007/s11104-010-0473-4. (Visited on 02/07/2023).
- Kottek, M., J. Grieser, C. Beck, B. Rudolf, and F. Rubel (2006). “World Map of the Köppen-Geiger Climate Classification Updated”. In: *metz* 15.3, pp. 259–263. ISSN: 0941-2948. DOI: 10.1127/0941-2948/2006/0130. (Visited on 11/29/2022).
- Koven, C. D., G. Hugelius, D. M. Lawrence, and W. R. Wieder (2017). “Higher Climatological Temperature Sensitivity of Soil Carbon in Cold than Warm Climates”. In: *Nature Clim Change* 7.11, pp. 817–822. ISSN: 1758-6798. DOI: 10.1038/nclimate3421. (Visited on 10/12/2022).
- Lange, S. and M. Büchner (2022). *Secondary ISIMIP3b Bias-Adjusted Atmospheric Climate Input Data*. DOI: 10.48364/ISIMIP.581124.1. (Visited on 02/16/2023).
- Lee, M. A. (2018). “A Global Comparison of the Nutritive Values of Forage Plants Grown in Contrasting Environments”. In: *J Plant Res* 131.4, pp. 641–654. ISSN: 1618-0860. DOI: 10.1007/s10265-018-1024-y. (Visited on 02/13/2023).
- Lepš, J., J. Osbornová-Kosinová, and M. Rejmánek (1982). “Community Stability, Complexity and Species Life History Strategies”. In: *Vegetatio* 50.1, pp. 53–63. ISSN: 0042-3106. DOI: 10.1007/BF00120678. (Visited on 10/17/2022).
- Li, J., S. Lin, F. Taube, Q. Pan, and K. Dittert (2011). “Above and Belowground Net Primary Productivity of Grassland Influenced by Supplemental Water and Nitrogen in Inner Mongolia”. In: *Plant Soil* 340.1, pp. 253–264. ISSN: 1573-5036. DOI: 10.1007/s11104-010-0612-y. (Visited on 12/09/2021).
- Liu, J., L. Li, L. Ji, Y. Li, J. Liu, and F. Y. Li (2023). “Divergent Effects of Grazing versus Mowing on Plant Nutrients in Typical Steppe Grasslands of Inner Mongolia”. In: *Journal of Plant Ecology* 16.1, rtac032. ISSN: 1752-993X. DOI: 10.1093/jpe/rtac032. (Visited on 02/14/2023).
- Liu, Y. Y., J. P. Evans, M. F. McCabe, R. A. M. de Jeu, A. I. J. M. van Dijk, A. J. Dolman, and I. Saizen (2013). “Changing Climate and Overgrazing Are Decimating Mongolian Steppes”. In: *PLOS ONE* 8.2, e57599. ISSN: 1932-6203. DOI: 10.1371/journal.pone.0057599. (Visited on 02/13/2023).
- Lutz, F., T. Herzfeld, J. Heinke, S. Rolinski, S. Schaphoff, W. von Bloh, J. J. Stoorvogel, and C. Müller (2019). “Simulating the Effect of Tillage Practices with the Global Ecosystem Model LPJmL (Version 5.0-Tillage)”. In: *Geosci. Model Dev.* 12.6, pp. 2419–2440. ISSN: 1991-959X. DOI: 10.5194/gmd-12-2419-2019. (Visited on 05/31/2023).
- May, F., V. Grimm, and F. Jeltsch (2009). “Reversed Effects of Grazing on Plant Diversity: The Role of below-Ground Competition and Size Symmetry”. In: *Oikos* 118.12, pp. 1830–1843. ISSN: 1600-0706. DOI: 10.1111/j.1600-0706.2009.17724.x. (Visited on 06/23/2021).
- McSherry, M. E. and M. E. Ritchie (2013). “Effects of Grazing on Grassland Soil Carbon: A Global Review”. In: *Glob. Change Biol.* 19.5, pp. 1347–1357. ISSN: 1365-2486. DOI: 10.1111/gcb.12144. (Visited on 06/13/2022).
- Meier, I. C. and C. Leuschner (2010). “Variation of Soil and Biomass Carbon Pools in Beech Forests across a Precipitation Gradient”. In: *Glob. Change Biol.* 16.3, pp. 1035–1045. ISSN: 1365-2486. DOI: 10.1111/j.1365-2486.2009.02074.x. (Visited on 10/12/2022).
- Munjonji, L., K. K. Ayisi, E. I. Mudongo, T. P. Mafeo, K. Behn, M. V. Mokoka, and A. Linstädter (2020). “Disentangling Drought and Grazing Effects on Soil Carbon Stocks and CO<sub>2</sub> Fluxes in a Semi-Arid African Savanna”. In: *Front. Environ. Sci.* 8. ISSN: 2296-665X. (Visited on 06/13/2022).
- Newman, J. A., A. J. Parsons, J. H. M. Thornley, P. D. Penning, and J. R. Krebs (1995). “Optimal Diet Selection by a Generalist Grazing Herbivore”. In: *Funct. Ecol.* 9.2, pp. 255–268. ISSN: 0269-8463. DOI: 10.2307/2390572. JSTOR: 2390572. (Visited on 08/07/2023).
- Noy-Meir, I. (1990). “Responses of Two Semiarid Rangeland Communities to Protection from Grazing”. In: *Isr. J. Plant Sci.* 39.4, pp. 431–442. ISSN: 0792-9978, 2223-8980. DOI: 10.1080/0021213X.1990.10677166. (Visited on 02/13/2023).
- Onoda, Y., I. J. Wright, J. R. Evans, K. Hikosaka, K. Kitajima, Ü. Niinemets, H. Poorter, T. Tosens, and M. Westoby (2017). “Physiological and Structural Tradeoffs Underlying the Leaf Economics Spectrum”. In: *New Phytol.* 214.4, pp. 1447–1463. ISSN: 1469-8137. DOI: 10.1111/nph.14496. (Visited on 02/13/2023).
- Parsons, A., J. Newman, P. Penning, A. Harvey, and R. Orr (1994). “Diet Preference of Sheep: Effects of Recent Diet, Physiological State and Species Abundance”. In: *J. Anim. Ecol.* 63.2, pp. 465–478. ISSN: 0021-8790. DOI: 10.2307/5563. JSTOR: 5563. (Visited on 08/07/2023).
- Pfeiffer, M., L. Langan, A. Linstädter, C. Martens, C. Gaillard, J. C. Ruppert, S. I. Higgins, E. I. Mudongo, and S. Scheiter (2019). “Grazing and Aridity Reduce Perennial Grass Abundance in Semi-Arid Rangelands – Insights from a Trait-Based Dynamic Vegetation Model”. In: *Ecological Modelling* 395, pp. 11–22. ISSN: 0304-3800. DOI: 10.1016/j.ecolmodel.2018.12.013. (Visited on 02/13/2023).
- Pierce, S., G. Brusa, I. Vagge, and B. E. L. Cerabolini (2013). “Allocating CSR Plant Functional Types: The Use of Leaf Economics and Size Traits to Classify Woody and Herbaceous Vascular Plants”. In: *Funct. Ecol.* 27.4, pp. 1002–1010. ISSN: 1365-2435. DOI: 10.1111/1365-2435.12095. (Visited on 09/26/2018).
- Pierce, S., D. Negreiros, B. E. L. Cerabolini, J. Kattge, S. Díaz, M. Kleyer, B. Shipley, S. J. Wright, N. A. Soudzilovskaia, V. G. Onipchenko, P. M. van Bodegom, C. Frenette-Dussault, E. Weiher, B. X. Pinho, J. H. C. Cornelissen, J. P. Grime, K. Thompson, R. Hunt, P. J. Wilson, G. Buffa, O. C. Nyakunga, P. B. Reich, M. Caccianiga, F. Mangili, R. M. Ceriani, A. Luzzaro, G. Brusa, A. Siefert, N. P. U. Barbosa, F. S. Chapin, W. K. Cornwell, J. Fang, G. W. Fernandes, E. Garnier, S. L. Stradic, J. Peñuelas, F. P. L. Melo, A. Slaviero, M. Tabarelli, and D. Tampucci (2017). “A Global Method for Calculating Plant CSR Ecological Strategies Applied across Biomes World-Wide”. In: *Funct. Ecol.* 31.2, pp. 444–457. ISSN: 1365-2435. DOI: 10.1111/1365-2435.12722. (Visited on 11/26/2020).
- Piñeiro, G., J. M. Paruelo, M. Oesterheld, and E. G. Jobbágy (2010). “Pathways of Grazing Effects on Soil Organic Carbon and Nitrogen”. In: *Rangeland Ecology & Management* 63.1, pp. 109–119. ISSN: 1550-7424. DOI: 10.2111/08-255.1. (Visited on 10/12/2022).

- Quillet, A., C. Peng, and M. Garneau (2010). “Toward Dynamic Global Vegetation Models for Simulating Vegetation–Climate Interactions and Feedbacks: Recent Developments, Limitations, and Future Challenges”. In: *Environ. Rev.* 18.NA, pp. 333–353. ISSN: 1181-8700, 1208-6053. DOI: 10.1139/A10-016. (Visited on 04/06/2018).
- R Core Team (2019). *A Language and Environment for Statistical Computing*. R Foundation for Statistical Computing, Vienna, Austria.
- Rechenthin, C. A. (1956). “Elementary Morphology of Grass Growth and How It Affects Utilization”. In: *Range Management* 9, pp. 167–170. (Visited on 02/13/2023).
- Reinsch, T., R. Loges, C. Kluß, and F. Taube (2018a). “Effect of Grassland Ploughing and Reseeding on CO<sub>2</sub> Emissions and Soil Carbon Stocks”. In: *Agriculture, Ecosystems & Environment* 265, pp. 374–383. ISSN: 0167-8809. DOI: 10.1016/j.agee.2018.06.020. (Visited on 06/24/2019).
- Reinsch, T., R. Loges, C. Kluß, and F. Taube (2018b). “Renovation and Conversion of Permanent Grass-Clover Swards to Pasture or Crops: Effects on Annual N<sub>2</sub>O Emissions in the Year after Ploughing”. In: *Soil and Tillage Research* 175, pp. 119–129. ISSN: 0167-1987. DOI: 10.1016/j.still.2017.08.009. (Visited on 06/24/2019).
- Reinsch, T., C. Malisch, R. Loges, and F. Taube (2020). “Nitrous Oxide Emissions from Grass–Clover Swards as Influenced by Sward Age and Biological Nitrogen Fixation”. In: *Grass Forage Sci.* 75.4, pp. 372–384. ISSN: 1365-2494. DOI: 10.1111/gfs.12496. (Visited on 12/07/2021).
- Ren, H., F. Taube, C. Stein, Y. Zhang, Y. Bai, and S. Hu (2017). “Grazing Weakens Temporal Stabilizing Effects of Diversity in the Eurasian Steppe”. In: *Ecol Evol* 8.1, pp. 231–241. ISSN: 2045-7758. DOI: 10.1002/ece3.3669. (Visited on 12/09/2021).
- Rolinski, S., C. Müller, J. Heinke, I. Weindl, A. Biewald, B. L. Bodirsky, A. Bondeau, E. R. Boons-Prins, A. F. Bouwman, P. A. Leffelaar, J. A. te Roller, S. Schaphoff, and K. Thonicke (2018). “Modeling Vegetation and Carbon Dynamics of Managed Grasslands at the Global Scale with LPJmL 3.6”. In: *Geosci. Model Dev.* 11.1, pp. 429–451. ISSN: 1991-9603. DOI: 10.5194/gmd-11-429-2018. (Visited on 02/27/2018).
- Rolinski, S., S. B. Wirth, C. Müller, and B. Tietjen (2021). “Strategies for Assessing Grassland Degradation”. In: *Jt. XXIV Int. Grassl. XI Int. Rangel. Kenya 2021 Virtual Congr. Oral Pap. Proc.* Vol. 1. Nairobi, Kenya: Kenya Agricultural and Livestock Research Organisation, pp. 383–387. ISBN: 978-996-30-093-5. (Visited on 06/22/2023).
- Ruppert, J. C., K. Harmony, Z. Henkin, H. A. Snyman, M. Sternberg, W. Willms, and A. Linstädter (2015). “Quantifying Drylands’ Drought Resistance and Recovery: The Importance of Drought Intensity, Dominant Life History and Grazing Regime”. In: *Glob. Change Biol.* 21.3, pp. 1258–1270. ISSN: 1365-2486. DOI: 10.1111/gcb.12777. (Visited on 11/20/2023).
- Sakschewski, B., W. von Bloh, A. Boit, A. Rammig, J. Kattge, L. Poorter, J. Peñuelas, and K. Thonicke (2015). “Leaf and Stem Economics Spectra Drive Diversity of Functional Plant Traits in a Dynamic Global Vegetation Model”. In: *Glob. Change Biol.* 21.7, pp. 2711–2725. ISSN: 1365-2486. DOI: 10.1111/gcb.12870. (Visited on 10/15/2018).
- Salisbury, E. J. (1943). “The Reproductive Capacity of Plants”. In: *Nature* 151.3829, pp. 319–320. ISSN: 1476-4687. DOI: 10.1038/151319a0. (Visited on 06/13/2022).
- Schaphoff, S., W. von Bloh, A. Rammig, K. Thonicke, H. Biemans, M. Forkel, D. Gerten, J. Heinke, J. Jägermeyr, J. Knauer, F. Langerwisch, W. Lucht, C. Müller, S. Rolinski, and K. Waha (2018). “LPJmL4 – a Dynamic Global Vegetation Model with Managed Land – Part 1: Model Description”. In: *Geosci. Model Dev.* 11.4, pp. 1343–1375. ISSN: 1991-959X. DOI: 10.5194/gmd-11-1343-2018. (Visited on 05/31/2023).
- Scheiter, S., L. Langan, and S. I. Higgins (2013). “Next-Generation Dynamic Global Vegetation Models: Learning from Community Ecology”. In: *New Phytol.* 198.3, pp. 957–969. ISSN: 1469-8137. DOI: 10.1111/nph.12210.
- Scheiter, S., M. Pfeiffer, K. Behn, K. K. Ayisi, F. Siebert, and A. Linstädter (2023). “Managing Southern African Rangeland Systems in the Face of Drought - a Synthesis of Observation, Experimentation, and Modelling for Policy and Decision Support”. In: *Sustainability of Southern African Ecosystems under Global Change*. Ed. by G. P. von Maltitz, G. F. Midgley, J. Veitch, C. Brümmer, R. P. Rötter, F. A. Viehberg, and M. Veste. Vol. 248. Ecological Studies. Springer.
- Schimel, D., B. B. Stephens, and J. B. Fisher (2015). “Effect of Increasing CO<sub>2</sub> on the Terrestrial Carbon Cycle”. In: *Proc. Natl. Acad. Sci.* 112.2, pp. 436–441. DOI: 10.1073/pnas.1407302112. (Visited on 08/07/2023).
- Schmid, J. S., A. Huth, and F. Taubert (2021). “Influences of Traits and Processes on Productivity and Functional Composition in Grasslands: A Modeling Study”. In: *Ecological Modelling* 440, p. 109395. ISSN: 0304-3800. DOI: 10.1016/j.ecolmodel.2020.109395. (Visited on 02/13/2023).
- Schmidtlein, S., H. Feilhauer, and H. Bruehlheide (2012). “Mapping Plant Strategy Types Using Remote Sensing”. In: *J. Veg. Sci.* 23.3, pp. 395–405. ISSN: 1654-1103. DOI: 10.1111/j.1654-1103.2011.01370.x. (Visited on 10/17/2022).
- Schönbach, P., H. Wan, M. Gierus, R. Loges, K. Müller, L. Lin, A. Susenbeth, and F. Taube (2012). “Effects of Grazing and Precipitation on Herbage Production, Herbage Nutritive Value and Performance of Sheep in Continental Steppe”. In: *Grass Forage Sci.* 67.4, pp. 535–545. ISSN: 1365-2494. DOI: 10.1111/j.1365-2494.2012.00874.x. (Visited on 06/09/2022).
- Shi, Y., Y. Ao, B. Sun, J. M. H. Knops, J. Zhang, Z. Guo, X. De, J. Han, Y. Yang, X. Jiang, C. Mu, and J. Wang (2022). “Productivity of *Leymus Chinensis* Grassland Is Co-Limited by Water and Nitrogen and Resilient to Climate Change”. In: *Plant Soil* 474.1, pp. 411–422. ISSN: 1573-5036. DOI: 10.1007/s11104-022-05344-1. (Visited on 06/13/2022).
- Sitch, S., C. Huntingford, N. Gedney, P. E. Levy, M. Lomas, S. L. Piao, R. Betts, P. Ciais, P. Cox, P. Friedlingstein, C. D. Jones, I. C. Prentice, and F. I. Woodward (2008). “Evaluation of the Terrestrial Carbon Cycle, Future Plant Geography and Climate–Carbon Cycle Feedbacks Using Five Dynamic Global Vegetation Models (DGVMs)”. In: *Glob. Change Biol.* 14.9, pp. 2015–2039. ISSN: 1365-2486. DOI: 10.1111/j.1365-2486.2008.01626.x. (Visited on 01/12/2023).

- Sleutel, S., S. De Neve, and G. Hofman (2007). “Assessing Causes of Recent Organic Carbon Losses from Cropland Soils by Means of Regional-Scaled Input Balances for the Case of Flanders (Belgium)”. In: *Nutr Cycl Agroecosyst* 78.3, pp. 265–278. ISSN: 1573-0867. DOI: 10.1007/s10705-007-9090-x. (Visited on 10/12/2022).
- Stuart-Hill, G. and M. Mentis (1982). “Coevolution of African Grasses and Large Herbivores”. In: *Proc. Annu. Congr. Grassl. Soc. South. Afr.* 17.1, pp. 122–128. ISSN: 0072-5560. DOI: 10.1080/00725560.1982.9648969. (Visited on 02/13/2023).
- Taubert, F., K. Frank, and A. Huth (2012). “A Review of Grassland Models in the Biofuel Context”. In: *Ecological Modelling*. 7th European Conference on Ecological Modelling (ECEM) 245, pp. 84–93. ISSN: 0304-3800. DOI: 10.1016/j.ecolmodel.2012.04.007. (Visited on 02/07/2019).
- Taubert, F., J. Hetzer, J. S. Schmid, and A. Huth (2020a). “The Role of Species Traits for Grassland Productivity”. In: *Ecosphere* 11.7, e03205. ISSN: 2150-8925. DOI: 10.1002/ecs2.3205. (Visited on 02/09/2023).
- Taubert, F., J. Hetzer, J. S. Schmid, and A. Huth (2020b). “Confronting an Individual-Based Simulation Model with Empirical Community Patterns of Grasslands”. In: *PLOS ONE* 15.7, e0236546. ISSN: 1932-6203. DOI: 10.1371/journal.pone.0236546. (Visited on 02/09/2023).
- Teng, Y., J. Zhan, F. B. Agyemang, and Y. Sun (2020). “The Effects of Degradation on Alpine Grassland Resilience: A Study Based on Meta-Analysis Data”. In: *Global Ecology and Conservation* 24, e01336. ISSN: 2351-9894. DOI: 10.1016/j.gecco.2020.e01336. (Visited on 02/13/2023).
- Thompson, K. (1987). “Seeds and Seed Banks”. In: *New Phytol.* 106.s1, pp. 23–34. ISSN: 1469-8137. DOI: 10.1111/j.1469-8137.1987.tb04680.x. (Visited on 06/13/2022).
- Thonicke, K., M. Billing, W. von Bloh, B. Sakschewski, Ü. Niinemets, J. Peñuelas, J. H. C. Cornelissen, Y. Onoda, P. van Bodegom, M. E. Schaepman, F. D. Schneider, and A. Walz (2020). “Simulating Functional Diversity of European Natural Forests along Climatic Gradients”. In: *J. Biogeogr.* 47.5, pp. 1069–1085. ISSN: 1365-2699. DOI: 10.1111/jbi.13809. (Visited on 06/23/2023).
- Tilman, D. and A. El Haddi (1992). “Drought and Biodiversity in Grasslands”. In: *Oecologia* 89.2, pp. 257–264. ISSN: 1432-1939. DOI: 10.1007/BF00317226. (Visited on 12/16/2020).
- Tribe, D. E. and J. G. Gordon (1950). “An experimental study of palatability.” In: *Agric. Progr.* 25, pp. 94–101. (Visited on 09/04/2023).
- Tron, S., G. Bodner, F. Laio, L. Ridolfi, and D. Leitner (2015). “Can Diversity in Root Architecture Explain Plant Water Use Efficiency? A Modeling Study”. In: *Ecological Modelling* 312, pp. 200–210. ISSN: 0304-3800. DOI: 10.1016/j.ecolmodel.2015.05.028. (Visited on 02/13/2023).
- Van Oijen, M., J. Rougier, and R. Smith (2005). “Bayesian Calibration of Process-Based Forest Models: Bridging the Gap between Models and Data”. In: *Tree Physiol* 25.7, pp. 915–927. ISSN: 0829-318X. DOI: 10.1093/treephys/25.7.915. (Visited on 02/04/2020).
- von Bloh, W., S. Schaphoff, C. Müller, S. Rolinski, K. Waha, and S. Zaehle (2018). “Implementing the Nitrogen Cycle into the Dynamic Global Vegetation, Hydrology, and Crop Growth Model LPJmL (Version 5.0)”. In: *Geosci. Model Dev.* 11.7, pp. 2789–2812. ISSN: 1991-959X. DOI: 10.5194/gmd-11-2789-2018. (Visited on 05/31/2023).
- Wan, H., Y. Bai, D. U. Hooper, P. Schönbach, M. Gierus, A. Schiborra, and F. Taube (2015). “Selective Grazing and Seasonal Precipitation Play Key Roles in Shaping Plant Community Structure of Semi-Arid Grasslands”. In: *Landscape Ecol* 30.9, pp. 1767–1782. ISSN: 1572-9761. DOI: 10.1007/s10980-015-0252-y. (Visited on 02/13/2023).
- Weigelt, A., L. Mommer, K. Andraczek, C. M. Iversen, J. Bergmann, H. Bruelheide, Y. Fan, G. T. Freschet, N. R. Guerrero-Ramírez, J. Kattge, T. W. Kuyper, D. C. Laughlin, I. C. Meier, F. van der Plas, H. Poorter, C. Roumet, J. van Ruijven, F. M. Sabatini, M. Semchenko, C. J. Sweeney, O. J. Valverde-Barrantes, L. M. York, and M. L. McCormack (2021). “An Integrated Framework of Plant Form and Function: The Belowground Perspective”. In: *New Phytol.* 232.1, pp. 42–59. ISSN: 1469-8137. DOI: 10.1111/nph.17590. (Visited on 11/23/2021).
- Weisser, W. W., C. Roscher, S. T. Meyer, A. Ebeling, G. Luo, E. Allan, H. Beßler, R. L. Barnard, N. Buchmann, F. Buscot, C. Engels, C. Fischer, M. Fischer, A. Gessler, G. Gleixner, S. Halle, A. Hildebrandt, H. Hillebrand, H. de Kroon, M. Lange, S. Leimer, X. Le Roux, A. Milcu, L. Mommer, P. A. Niklaus, Y. Oelmann, R. Proulx, J. Roy, C. Scherber, M. Scherer-Lorenzen, S. Scheu, T. Tschantke, M. Wachendorf, C. Wagg, A. Weigelt, W. Wilcke, C. Wirth, E.-D. Schulze, B. Schmid, and N. Eisenhauer (2017). “Biodiversity Effects on Ecosystem Functioning in a 15-Year Grassland Experiment: Patterns, Mechanisms, and Open Questions”. In: *Basic Appl. Ecol.* Biodiversity Effects on Ecosystem Functioning: The Jena Experiment 23, pp. 1–73. ISSN: 1439-1791. DOI: 10.1016/j.baae.2017.06.002. (Visited on 01/27/2020).
- Westoby, M., M. Leishman, and J. Lord (1996). “Comparative Ecology of Seed Size and Dispersal”. In: *Philos. Trans. R. Soc. Lond. B. Biol. Sci.* DOI: 10.1098/rstb.1996.0114. (Visited on 06/13/2022).
- White, R. P., S. Murray, and M. Rohweder (2000). “Pilot Analysis of Global Ecosystems: Grassland Ecosystems.” In: *Pilot Anal. Glob. Ecosyst. Grassl. Ecosyst.* (Visited on 02/13/2023).
- Wiesmeier, M., F. Barthold, B. Blank, and I. Kögel-Knabner (2011). “Digital Mapping of Soil Organic Matter Stocks Using Random Forest Modeling in a Semi-Arid Steppe Ecosystem”. In: *Plant Soil* 340.1, pp. 7–24. ISSN: 1573-5036. DOI: 10.1007/s11104-010-0425-z. (Visited on 02/16/2022).
- Wiesmeier, M., O. Kreyling, M. Steffens, P. Schoenbach, H. Wan, M. Gierus, F. Taube, A. Kölbl, and I. Kögel-Knabner (2012). “Short-Term Degradation of Semiarid Grasslands—Results from a Controlled-Grazing Experiment in Northern China”. In: *J. Plant Nutr. Soil Sci.* 175.3, pp. 434–442. ISSN: 1522-2624. DOI: 10.1002/jpln.201100327. (Visited on 01/03/2022).
- Wiesmeier, M., L. Urbanski, E. Hobbey, B. Lang, M. von Lützwow, E. Marin-Spiotta, B. van Wesemael, E. Rabot, M. Ließ, N. Garcia-Franco, U. Wollschläger, H.-J. Vogel, and I. Kögel-Knabner (2019). “Soil Organic Carbon Storage as a Key Function of Soils - A Review of Drivers and Indicators at Various Scales”. In: *Geoderma* 333, pp. 149–162. ISSN: 0016-7061. DOI: 10.1016/j.geoderma.2018.07.026. (Visited on 10/12/2022).

- Wirth, S. B., C. Müller, and S. Rolinski (2023). “Code and Data for Connecting CSR Theory and LPJmL 5 to Assess the Role of Environmental Conditions, Management and Functional Diversity for Grassland Ecosystem Functions”. In: (). DOI: 10.5281/zenodo.10217244. (Visited on 11/30/2023).
- Wirth, S. B., F. Taubert, B. Tietjen, C. Müller, and S. Rolinski (2021). “Do Details Matter? Disentangling the Processes Related to Plant Species Interactions in Two Grassland Models of Different Complexity”. In: *Ecological Modelling* 460, p. 109737. ISSN: 0304-3800. DOI: 10.1016/j.ecolmodel.2021.109737. (Visited on 09/16/2021).
- Woodward, F. I. and A. D. Diament (1991). “Functional Approaches to Predicting the Ecological Effects of Global Change”. In: *Funct. Ecol.* ISSN: 0269-8463. (Visited on 02/14/2023).
- Wright, I. J., P. B. Reich, M. Westoby, D. D. Ackerly, Z. Baruch, F. Bongers, J. Cavender-Bares, T. Chapin, J. H. C. Cornelissen, M. Diemer, J. Flexas, E. Garnier, P. K. Groom, J. Gulias, K. Hikosaka, B. B. Lamont, T. Lee, W. Lee, C. Lusk, J. J. Midgley, M.-L. Navas, U. Niinemets, J. Oleksyn, N. Osada, H. Poorter, P. Poot, L. Prior, V. I. Pyankov, C. Roumet, S. C. Thomas, M. G. Tjoelker, E. J. Veneklaas, and R. Villar (2004). “The Worldwide Leaf Economics Spectrum”. In: *Nature* 428.6985, pp. 821–827. ISSN: 1476-4687. DOI: 10.1038/nature02403.
- Xie, Q., A. Huete, C. C. Hall, B. E. Medlyn, S. A. Power, J. M. Davies, D. E. Medek, and P. J. Beggs (2022). “Satellite-Observed Shifts in C3/C4 Abundance in Australian Grasslands Are Associated with Rainfall Patterns”. In: *Remote Sensing of Environment* 273, p. 112983. ISSN: 0034-4257. DOI: 10.1016/j.rse.2022.112983. (Visited on 11/20/2023).
- Yang, Y., Q. Zhu, C. Peng, H. Wang, and H. Chen (2015). “From Plant Functional Types to Plant Functional Traits: A New Paradigm in Modelling Global Vegetation Dynamics”. In: *Progress in Physical Geography: Earth and Environment* 39.4, pp. 514–535. ISSN: 0309-1333. DOI: 10.1177/0309133315582018. (Visited on 04/06/2018).
- Yang, Y., D. Tilman, G. Furey, and C. Lehman (2019). “Soil Carbon Sequestration Accelerated by Restoration of Grassland Biodiversity”. In: *Nat. Commun.* 10.1, p. 718. ISSN: 2041-1723. DOI: 10.1038/s41467-019-08636-w. (Visited on 10/21/2020).
- Yu, Q., H. Wu, Z. Wang, D. F. B. Flynn, H. Yang, F. Lü, M. Smith, and X. Han (2015). “Long Term Prevention of Disturbance Induces the Collapse of a Dominant Species without Altering Ecosystem Function”. In: *Sci Rep* 5.1, p. 14320. ISSN: 2045-2322. DOI: 10.1038/srep14320. (Visited on 06/13/2022).
- Zaehle, S., S. Sitch, B. Smith, and F. Hatterman (2005). “Effects of Parameter Uncertainties on the Modeling of Terrestrial Biosphere Dynamics”. In: *Glob. Biogeochem. Cycles* 19.3. ISSN: 1944-9224. DOI: 10.1029/2004GB002395. (Visited on 07/02/2021).
- Zimmermann, J., S. I. Higgins, V. Grimm, J. Hoffmann, and A. Linstädter (2010). “Grass Mortality in Semi-Arid Savanna: The Role of Fire, Competition and Self-Shading”. In: *Perspectives in Plant Ecology, Evolution and Systematics* 12.1, pp. 1–8. ISSN: 1433-8319. DOI: 10.1016/j.ppees.2009.09.003. (Visited on 11/20/2023).

# Chapter 4

## Biological nitrogen fixation of natural and agricultural vegetation simulated with LPJmL 5.7.9

Stephen B. Wirth<sup>1,2</sup>, Johanna Braun<sup>1</sup>, Jens Heinke<sup>1</sup>, Sebastian Ostberg<sup>1</sup>, Susanne Rolinski<sup>1</sup>, Sibyll Schaphoff<sup>1</sup>, Fabian Stenzel<sup>1</sup>, Werner von Bloh<sup>1</sup>, Friedhelm Taube<sup>2</sup> and Christoph Müller<sup>1</sup>

<sup>1</sup>Potsdam Institute for Climate Impact Research (PIK), Member of the Leibniz Association, P.O. Box 60 12 03, 14412 Potsdam, Germany

<sup>2</sup>Institute of Crop Science and Plant Breeding, Grass and Forage Science/Organic Agriculture, Kiel University, Hermann-Rodewald-Str. 9, 24118, Kiel, Germany

Status: Published

Journal: Geoscientific Model Development

Received: 7 December 2023

Revised: 11 July 2024

Accepted: 21 August 2024

Published: 7 November 2024

DOI: <https://doi.org/10.5194/gmd-17-7889-2024>

---

**Abstract:** Biological nitrogen fixation (BNF) by symbiotic and free-living bacteria is an important source of plant-available nitrogen (N) in terrestrial ecosystems supporting carbon (C) sequestration and food production worldwide. Dynamic global vegetation models (DGVMs) are frequently used to assess the N and C cycles under dynamic land use and climate. BNF plays an important role in the components of both these cycles, making a robust representation of the processes and variables that BNF depends on important to reduce uncertainty within the C and N cycles and improve the ability of DGVMs to project future ecosystem productivity, vegetation patterns or the land C sink. Still, BNF is often modelled as a function of net primary productivity or evapotranspiration, and the actual drivers are neglected. We implemented plant-functional-type-specific limitations for BNF dependent on soil temperature and soil water content, as well as a cost of BNF, in the Lund–Potsdam–Jena managed Land (LPJmL) DGVM and compared the new (“C-costly”) against the previous (“Original”) approach and data from the scientific literature. For our comparison, we simulated a potential natural vegetation scenario and one including anthropogenic land use for the period from 1901 to 2016 for which we evaluate BNF and legume crop yields. Our results show stronger agreement with BNF observations for the C-costly than the Original approach for natural vegetation and agricultural areas. The C-costly approach reduced the overestimation of BNF, especially in hot

spots of legume crop production. Despite the reduced BNF in the C-costly approach, yields of legume crops were similar to the Original approach. While the net C and N balances were similar between the two approaches, the reduced BNF in the C-costly approach results in a slight underestimation of N losses from leaching, emissions and harvest compared to the values in the literature, supporting further investigation of the underlying reasons, such as processes represented in DGVMs and scenario assumptions. While we see the potential for further model development, for example, to separate symbiotic and free-living BNF, the C-costly approach is a major improvement over the simple Original approach because of the separate representation of important drivers and limiting factors of BNF, and the C-costly approach also improves the ability of LPJmL to project future C and N cycle dynamics.

---

## 4.1 Introduction

Biological nitrogen fixation (BNF) is an important source of plant-available nitrogen (N) in terrestrial ecosystems (Galloway et al., 1995). It can be separated into symbiotic (Granhall, 1981) and free-living (Reed et al., 2011) BNF, which account for the total BNF with different shares in different ecosystems (Davies-Barnard and Friedlingstein, 2020b). In natural terrestrial ecosystems, N deposition, N fixation through lightning, and BNF are the only processes that introduce additional reactive N into the system (Yu and Zhuang, 2020). In agricultural systems, increased N inputs are – together with extensive manure recycling – a major source of nitrous oxide (N<sub>2</sub>O) and ammonium (NH<sub>4</sub><sup>+</sup>) emissions (Reay et al., 2012; Tian et al., 2020) and nitrate (NO<sub>3</sub><sup>-</sup>) pollution (Moss, 2007). These inputs result from increased BNF and the deposition of additional anthropogenic N inputs, which originate mainly from synthetic fertiliser application (Lu and Tian, 2017). Promoting N-fixing crops such as forage and grain legumes for usage as green manure has been discussed (Becker et al., 1995; Fageria, 2007; Northup and Rao, 2016) to reduce N losses from nitrification, volatilisation, denitrification and leaching on agricultural land. Generally, symbiotic BNF, as well as free-living BNF, can be important for plant growth in N-limited ecosystems, and this supports carbon (C) sequestration and food production across the globe.

Briefly, BNF describes the transformation of atmospheric N<sub>2</sub> to ammonia (NH<sub>4</sub><sup>+</sup>) by a variety of soil microorganisms providing a source of mineral N for plants at the expense of C (Yu and Zhuang, 2020). The underlying mechanisms of BNF, as well as its role within the C and N cycles and for ecosystem productivity, have been described in detail in multiple studies (e.g. Cleveland et al., 1999; Davies-Barnard and Friedlingstein, 2020b; Yu and Zhuang, 2020). Here, we focus on the representation of BNF in the Lund–Potsdam–Jena managed Land (LPJmL) dynamic global vegetation model (DGVM) (Heinke et al., 2023; Herzfeld et al., 2021; Lutz et al., 2019; Porwollik et al., 2022; Schaphoff et al., 2018; von Bloh et al., 2018). We do not distinguish between symbiotic and free-living BNF throughout this study but only consider the total BNF as the sum of both forms.

DGVMs such as LPJmL can be used to assess the role of BNF for the productivity of natural and

agricultural ecosystems and its effects on the N and C cycles under dynamic land use and climate. A solid representation of the processes behind BNF is important to reduce uncertainty and improve the model results of DGVMs, which are frequently used in impact assessments and to inform policy-makers. A variety of approaches of different complexity to model BNF have been developed. A key difference between approaches is the selection of variables that control BNF and the accounting of the C cost of BNF. For example, Cleveland et al. (1999) use actual evapotranspiration as a single explanatory variable, while Yu and Zhuang (2020) consider soil temperature, soil water content, soil mineral N and soil C content. Both of these approaches do not consider the cost of BNF neglecting the reduced C assimilation (Cleveland et al., 1999; Yu and Zhuang, 2020), while others explicitly consider a cost per amount of N fixed and a maximum amount of C that can be invested in BNF (e.g. Ma et al., 2022). Even more complex approaches consider the different pathways of N uptake that are associated with a cost (active N uptake, retranslocation and BNF) and optimise for the minimum cost (e.g. Fisher et al., 2010). Depending on the considered variables, the simulated BNF and how it is affected by climate change may strongly differ, which in turn can have strong effects on the simulated C and N fluxes and pools.

A comparison to data published by Davies-Barnard and Friedlingstein (2020a) suggests that the approach that was implemented in LPJmL (von Bloh et al., 2018) based on Cleveland et al. (1999) – in the following defined as the “Original” approach – overestimates global BNF. In addition, we identified several shortcomings of the Original approach in LPJmL. In the Original approach, BNF is a function of actual evapotranspiration, which leads to an overestimation of BNF in moist but not necessarily N-limited ecosystems and an underestimation in dry but N-limited ecosystems. In this simplified implementation, BNF is not constrained by the availability of reactive forms of N, and additional N is fixed even if the reactive soil N is sufficient to fulfil the N demand, which potentially leads to an overestimation of the ammonia pool and N losses. For cultivated grain legumes, the approach assumes no limitation of BNF at all but simply supplies all N requested by the plant that cannot be fulfilled through N uptake from mineral N pools in the soil. This leads to an overestimation of cropland BNF. In order to overcome these deficiencies, here we describe a revision of the Original approach in LPJmL with a more complex approach, referred to as “C-costly” approach in the following. The C-costly approach is inspired by Ma et al. (2022) and Yu and Zhuang (2020) and introduces plant-functional-type (PFT)-specific limitations for BNF dependent on soil temperature and soil water content, as well as a C cost of BNF. In the following, we present the C-costly BNF approach and evaluate its performance against global and site-specific data. We discuss the differences between the Original and the C-costly BNF approach for the N cycle and plant productivity.

## 4.2 Methods

### 4.2.1 Model description

LPJmL is a dynamic global vegetation model (DGVM) with the full terrestrial hydrology and explicit representation of agricultural management systems for cropland and pastures. We have implemented the BNF module in the most recent development branch, which is based on a consolidated version of the carbon-only model (LPJmL4, Schaphoff et al., 2018), the N cycle (LPJmL5, von Bloh et al., 2018), tillage (Lutz et al., 2019), manure (Herzfeld et al., 2021), cover crop (Porwollik et al., 2022) and grazing management (Heinke et al., 2023) modules. There have been further model improvements that have not been described in publications elsewhere, including improved online coupling options with other models such as IMAGE (Müller et al., 2016) or copan:CORE (Donges et al., 2020). For a better representation of crops that are not explicitly represented (referred to as “others”), these are no longer assumed to be identical to managed grassland (Bondeau et al., 2007) but can be simulated as separate stands with distinct management inputs (e.g. fertiliser amounts).

The original spin-up protocol for LPJmL4, described in Schaphoff et al. (2013), was modified to account for the interaction between soils and plants through N supply in LPJmL5. The principal technique to accelerate the spin-up by calculating the equilibrium soil C stocks from litter decomposition (i.e. the flux of C into the soil C pools) and soil C turnover rates (or residence time) remains the same as in Schaphoff et al. (2013). However, the original code was refactored to improve the accuracy of estimates of equilibrium stocks and to apply the technique to soil C and N pools simultaneously.

In LPJmL5, an adjustment of N pools can lead to a change in plant productivity through a change in N supply from mineralisation. To account for this feedback, the C and N stock adjustments need to be repeated multiple times until the soil and the vegetation reach equilibria. The revised spin-up procedure starts with an initial period of 300 years, during which vegetation is allowed to establish. This is followed by a 2400-year period, during which soil C and N pools are updated every 15 years based on the litter decomposition and soil pool turnover rates of the preceding 10 years. This long period with repeated adjustment (160 times) of C and N pools is required to reach an equilibrium in regions with very low turnover rates (e.g. in the boreal zone). To reduce the effect of inter-annual variability on estimates of equilibrium stocks, a final adjustment is applied after 300 simulation years, using the litter decomposition and soil pool turnover rates over that period. Finally, the model is allowed to adjust to the new C and N stocks for another 500 simulation years.

To assess the effectiveness of the spin-up procedure, we conducted a 1000-year model run under the same conditions as during the spin-up period (i.e. stable pre-industrial atmospheric CO<sub>2</sub> concentration, atmospheric N deposition and climate) for which we present results in Appendix C.3.

Further changes to the code since the last published version (see Porwollik et al., 2022) include vari-

our bug fixes concerning fertiliser and manure application, data output, environmental flow requirements (Jägermeyr et al., 2017), soil temperature (Schaphoff et al., 2013) and bioenergy plantations (Beringer et al., 2011). The latest code changes are now also documented in a `CHANGELOG.md` file as part of the code repository (Wirth et al., 2023).

### 4.2.2 BNF-relevant nitrogen cycle components in LPJmL

While we refer to von Bloh et al. (2018) for a detailed description and evaluation of the N cycle in LPJmL, we briefly describe the main processes that determine N deficit – which is the prerequisite for N fixation in the C-costly approach – and the Original approach here and provide the full equations in Appendix C.1. An N deficit is defined as the difference between the plant N demand (Eq. C.4) and the active and passive N-uptake (Eq. C.5) and labile-N reserves (Eq. C.11).

$$N_{\text{deficit},t} = N_{\text{demand},t} - (N_{\text{uptake},t} + N_{\text{labile},t}) \quad (4.1)$$

The N demand accounts for N required to produce RuBisCo, depending on the maximum carboxylation capacity and the leaf area index (LAI) of the respective PFT (Eq. C.1, first summand) and the structural N demand, depending on the current N content of the different plant compartments (Eq. C.1, second summand, and Eq. C.4). N reserves are included using a PFT-specific parameter (Eq. C.4).

The N uptake is calculated as a combination of passive and active N uptake from the soil and is a function of the potential N uptake of the root system (Eq. C.5), which is reduced to account for soil mineral N availability (Eq. C.8), soil temperature (Eq. C.9) and plant N starvation (Eq. C.10). Labile N reserves represent the N currently available from past N uptake, BNF or retranslocation (Eq. C.11).

In the Original approach, BNF was calculated from the 20-year average of annual evapotranspiration (etp) for tree and herbaceous PFTs, following the function from Cleveland et al. (1999):

$$\text{BNF} = \begin{cases} \max(0, (0.0234 \cdot \text{etp} - 0.172)/10/365) & \text{if } C_{\text{root}} > 20 \text{ gC m}^{-2} \\ 0 & \text{otherwise.} \end{cases} \quad (4.2)$$

The resulting BNF is added to the  $\text{NH}_4^+$  pool of the first soil layer. For crop PFTs, BNF equals  $N_{\text{deficit}}$  and is directly added to  $N_{\text{labile}}$ .

### 4.2.3 The C-costly approach

A key feature is the connection of BNF to an associated cost represented as a reduction in the net primary production (NPP). The C-costly approach calculates actual BNF ( $N_{\text{fix}}$ ) from the potential BNF ( $N_{\text{fix,pot}}$ ) using several reduction factors. First, the N fixation rate for the environmental conditions  $N_{\text{fix,env}}$  is

calculated from  $N_{\text{fix,pot}}$  for the first two soil layers,  $l = 1, 2$ , accounting for reductions by dimensionless soil temperature and soil water content (SWC) limitation functions ( $f_T$ ,  $f_W$ ) and the root distribution rootdist in the interval  $[0, 1]$  (Ma et al., 2022):

$$N_{\text{fix,env}} = \sum_{l=1}^2 N_{\text{fix,pot}} \cdot f_T(T_{\text{soil},l}) \cdot f_W(\text{SWC}_l) \cdot \text{rootdist}_l. \quad (4.3)$$

The soil temperature limitation is increasing linearly outside the optimal temperature interval,  $[T_{\text{opt,low}}, T_{\text{opt,high}}]$  (Eq. 4.4; Fig. 4.1a), and it prohibits BNF if outside the tolerable temperature interval,  $[T_{\text{min}}, T_{\text{max}}]$ , while the soil water limitation is linearly dependent on the relative soil water content, SWC (Eq. 4.5; Fig. 4.1b).

$$f_T(T_{\text{soil}}) = \begin{cases} 0, & \text{if } T_{\text{soil}} < T_{\text{min}} \text{ or } T_{\text{soil}} > T_{\text{max}} \\ \frac{T_{\text{soil}} - T_{\text{min}}}{T_{\text{opt,low}} - T_{\text{min}}}, & \text{if } T_{\text{min}} \leq T_{\text{soil}} < T_{\text{opt,low}} \\ 1, & \text{if } T_{\text{opt,low}} \leq T_{\text{soil}} \leq T_{\text{opt,high}} \\ \frac{T_{\text{max}} - T_{\text{soil}}}{T_{\text{max}} - T_{\text{opt,high}}}, & \text{if } T_{\text{opt,high}} < T_{\text{soil}} \leq T_{\text{max}}. \end{cases} \quad (4.4)$$

$$f_W(\text{SWC}) = \begin{cases} 0, & \text{if } \text{SWC} \leq \text{SWC}_{\text{low}} \\ \varphi_1 + \text{SWC} \cdot \varphi_2, & \text{if } \text{SWC}_{\text{low}} < \text{SWC} < \text{SWC}_{\text{high}} \\ 1, & \text{if } \text{SWC} \geq \text{SWC}_{\text{high}}. \end{cases} \quad (4.5)$$

The root distribution is calculated as in Eq. (C.7). Since only the fraction of roots in the first two soil layers is used for BNF, shallow root profiles lead to a higher BNF compared to deep root profiles.  $N_{\text{fix,pot}}$ ,  $T_{\text{min}}$ ,  $T_{\text{opt,low}}$ ,  $T_{\text{opt,high}}$ ,  $T_{\text{max}}$ ,  $\text{SWC}_{\text{low}}$ ,  $\text{SWC}_{\text{high}}$ ,  $\varphi_1$  and  $\varphi_2$  are PFT-specific parameters (Table 4.1), and their values are adopted from Yu and Zhuang (2020) for the natural vegetation PFTs and from Ma et al. (2022) for soybean and pulses.

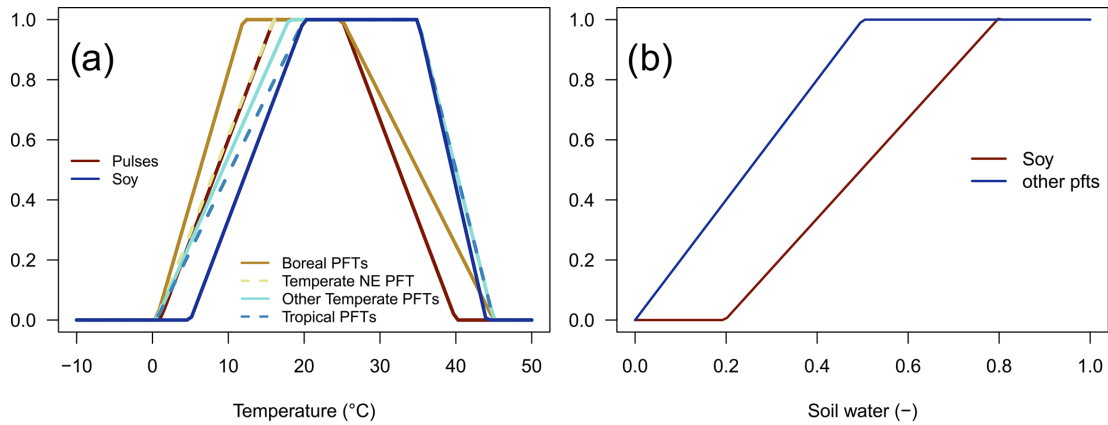


Figure 4.1: Dimensionless temperature limitation function  $f_T(T)$  (a) and soil water limitation function  $f_W(\text{SWC})$  (b).

Table 4.1: BNF-related PFT-specific parameter values for the tropical broadleaved evergreen tree (TrBE), tropical broadleaved raingreen tree (TrBR), temperate needleleaved evergreen tree (TeNE), temperate broadleaved evergreen tree (TeBE), temperate broadleaved summergreen tree (TeBS), boreal needleleaved evergreen tree (BoNE), boreal broadleaved summergreen tree (BoBS), boreal needleleaved summergreen tree (BoNS), tropical herbaceous (TrH), temperate herbaceous (TeH), polar herbaceous (PoH), soybean and pulses.

PFT	$N_{\text{fix,pot}}$ gN m <sup>-2</sup> d <sup>-1</sup>	$T_{\text{min}}$ °C	$T_{\text{opt,low}}$ °C	$T_{\text{opt,high}}$ °C	$T_{\text{max}}$ °C	SWC <sub>low</sub> m <sup>3</sup> m <sup>-3</sup>	SWC <sub>high</sub> m <sup>3</sup> m <sup>-3</sup>	$\varphi_1$ –	$\varphi_2$ –	$f_{\text{NPP}}$ –	cost <sub>BNF</sub> gC gN <sup>-1</sup>	$f_{\text{fixer}}$ –
TrBE	0.01	0.5	20	35	45	0	0.5	0	2.0	0.14	6	0.05
TrBR	0.01	0.5	20	35	45	0	0.5	0	2.0	0.14	6	0.05
TeNE	0.01	0.5	16	35	45	0	0.5	0	2.0	0.14	6	0.01
TeBE	0.01	0.5	18	35	45	0	0.5	0	2.0	0.14	6	0.01
TeBS	0.01	0.5	18	35	45	0	0.5	0	2.0	0.14	6	0.01
BoNE	0.01	0.5	12	25	45	0	0.5	0	2.0	0.14	6	0.03
BoBS	0.01	0.5	12	25	45	0	0.5	0	2.0	0.14	6	0.03
BoNS	0.01	0.5	12	25	45	0	0.5	0	2.0	0.14	6	0.03
TrH	0.01	0.5	20	35	45	0	0.5	0	2.0	0.14	6	0.05
TeH	0.01	0.5	18	35	45	0	0.5	0	2.0	0.14	6	0.01
PoH	0.01	0.5	12	25	45	0	0.5	0	2.0	0.14	6	0.03
Soybean	0.1	5	20	35	44	0.2	0.8	-0.33	1.67	0.25	6	1
Pulses	0.1	1	16	25	40	0	0.5	0	2.0	0.25	6	1

If  $N_{\text{fix,env}}$  exceeds the amount of N missing to fulfil the N demand of the current day (the N deficit  $N_{\text{deficit}}$ ), the N fixation is reduced as follows:

$$N_{\text{fix,need}} = \min(N_{\text{deficit}}, N_{\text{fix,env}}). \quad (4.6)$$

Finally, if the cost of the N fixation exceeds the NPP available for BNF, then the N fixation is further reduced to match the maximum amount that can be fixed with the current day's NPP share available for BNF.

$$N_{\text{fix}}(\text{NPP}) = \begin{cases} N_{\text{fix,need}}, & \text{if } \text{cost}_{\text{BNF}} \cdot N_{\text{fix,need}} < f_{\text{fixer}} \cdot f_{\text{NPP}} \cdot \text{NPP} \\ f_{\text{fixer}} \cdot f_{\text{NPP}} \cdot \text{NPP} / \text{cost}_{\text{BNF}}, & \text{otherwise,} \end{cases} \quad (4.7)$$

where  $f_{\text{NPP}}$  is the maximum share (dimensionless) of NPP available for BNF, which is set to 0.14 (Kull, 2002) for the natural PFTs and to 0.25 for soybean and pulses. The average N fixer fraction ( $f_{\text{fixer}}$ ) is set to 0.05 for the tropical, to 0.01 for the temperate and to 0.03 for the boreal zone (Yu and Zhuang, 2020). PFTs only fix additional N if the N uptake from other sources is insufficient and the net primary productivity (NPP) is larger than zero. The costs of BNF are set at a moderate constant value of 6 gC gN<sup>-1</sup> (Boote et al., 2009; Kaschuk et al., 2009; Patterson and Larue, 1983; Ryle et al., 1979).

#### 4.2.4 Modelling protocol

To compare the two BNF approaches, we simulated two scenarios. The first is a potential natural vegetation (PNV) scenario, which does not include anthropogenic land use or agricultural production systems. The second is a scenario that includes agricultural land use (LU). The same input data sets were

used for all scenarios. We used the climate data from the GSWP3-W5E5 data set (Cucchi et al., 2020; Kim, 2017; Lange et al., 2022), historical atmospheric N deposition (Yang and Tian, 2020), historical atmospheric CO<sub>2</sub> concentrations (Büchner and Reyer, 2022), historical land-use patterns (Ostberg et al., 2023) and grazing management data (Stenzel et al., 2023). For both BNF approaches, we conducted spin-up simulations of 3500 years using a random permutation of the climate data from 1901 to 1930. These spin-up simulations ensure that the C and N balances are in equilibrium. Afterwards, land use is introduced, and a second spin-up period of 390 years is run to capture the effects of historical land-use change on the C and N cycle. Following the two spin-up simulations, the model is run from 1901 until 2016 using the transient input data.

#### 4.2.5 Model evaluation

We compared simulated total global BNF for both approaches against several estimates which were derived empirically or reported in other modelling studies. Data on these estimates are available from Davies-Barnard and Friedlingstein (2020a). The global BNF is calculated as the sum of BNF per area times grid cell area over all grid cells:

$$\text{BNF}_{\text{glob}} = \sum_{\text{cell}}^{n_{\text{cell}}} \text{BNF}_{\text{cell}} \cdot \text{area}_{\text{cell}}. \quad (4.8)$$

For the evaluation we calculate the median, minimum and maximum between 2001 and 2010 and qualitatively compare these values against past estimates. We calculated the overlap between our results and the reported data if minimum and maximum values were available.

$$\text{Overlap} = \begin{cases} 0 & \text{if } x_{\min} > y_{\max} \text{ or } x_{\max} < y_{\min} \\ (\min(x_{\max}, y_{\max}) - \max(x_{\min}, y_{\min})) / (y_{\max} - y_{\min}) & \text{otherwise,} \end{cases} \quad (4.9)$$

where  $x_{\min}$  and  $x_{\max}$  are the simulated minimum and maximum, and  $y_{\min}$  and  $y_{\max}$  are the minimum and maximum values from the literature.

In addition, we compared our results to data obtained at several sites for the natural vegetation (Davies-Barnard and Friedlingstein, 2020a) and legume crops (Ma et al., 2022). To evaluate legume crop BNF and yields, we conducted additional local simulations matching the coordinates of the experiments following the protocol described in Sect. 4.2.4 but ensured that the respective crops (soybean or pulses) were grown under the reported water management (rainfed or irrigated). We calculated the root

mean square error (RMSE) as follows:

$$\text{RMSE} = \sqrt{\sum_n^N (x_n - y_n)^2 / N}, \quad (4.10)$$

where  $N$  is the number of observations, and  $x_n$  and  $y_n$  are the simulated and observed values.

## 4.3 Results

### 4.3.1 Comparison of the BNF approaches

Comparing the simulated BNF of both approaches to data from the literature and experiments showed a substantial improvement of the global BNF (Sect. 4.3.1.1), as well as the latitudinal and spatial patterns (Sect. 4.3.1.2).

#### 4.3.1.1 Comparison to data and other models

The two approaches show large differences in the simulated BNF. While the median global BNF between 2001 and 2010 was 191 TgN yr<sup>-1</sup> for the Original approach, for the C-costly approach it was substantially lower, with a value of 109 TgN yr<sup>-1</sup> (Fig. 4.2a). Comparing the global BNF of both approaches to estimates from the scientific literature shows the agreement of the C-costly values with several other data sources, while the Original approach overestimates most of the literature values. In particular, the recent estimate by Davies-Barnard and Friedlingstein (2020a) was closely matched by the C-costly approach, and 60 % of the simulated data were within the range of the Davies-Barnard and Friedlingstein (2020a) data (Fig. 4.2a). Despite the fact that the Original approach was not derived from the empirical relationship of Cleveland et al. (1999) for the legume crops, the data from Cleveland et al. (1999) are well matched by the Original approach, and only the spread of the Cleveland et al. (1999) data is underestimated. In comparison to the data of Xu-Ri and Prentice (2017), who reported much higher values compared to the other studies, BNF is underestimated by both approaches implemented in LPJmL. However, large differences are to be expected, considering that their approach does not calculate the actual BNF but rather the BNF needed to sustain global NPP (Xu-Ri and Prentice, 2017).

Comparing the spatial patterns of the two approaches to those of Davies-Barnard and Friedlingstein (2020a) shows that the Original approach generally overestimated BNF in large areas of the tropics and temperate zones (Fig. C.5c). The C-costly approach still overestimates BNF in the tropics and the production areas of soybean and/or pulses in India and the United States of America (USA), but the values are substantially smaller than in the Original approach (Fig. C.5f). In both approaches, observed BNF is slightly underestimated in the central to western part of the USA, Canada, China, Kazakhstan,

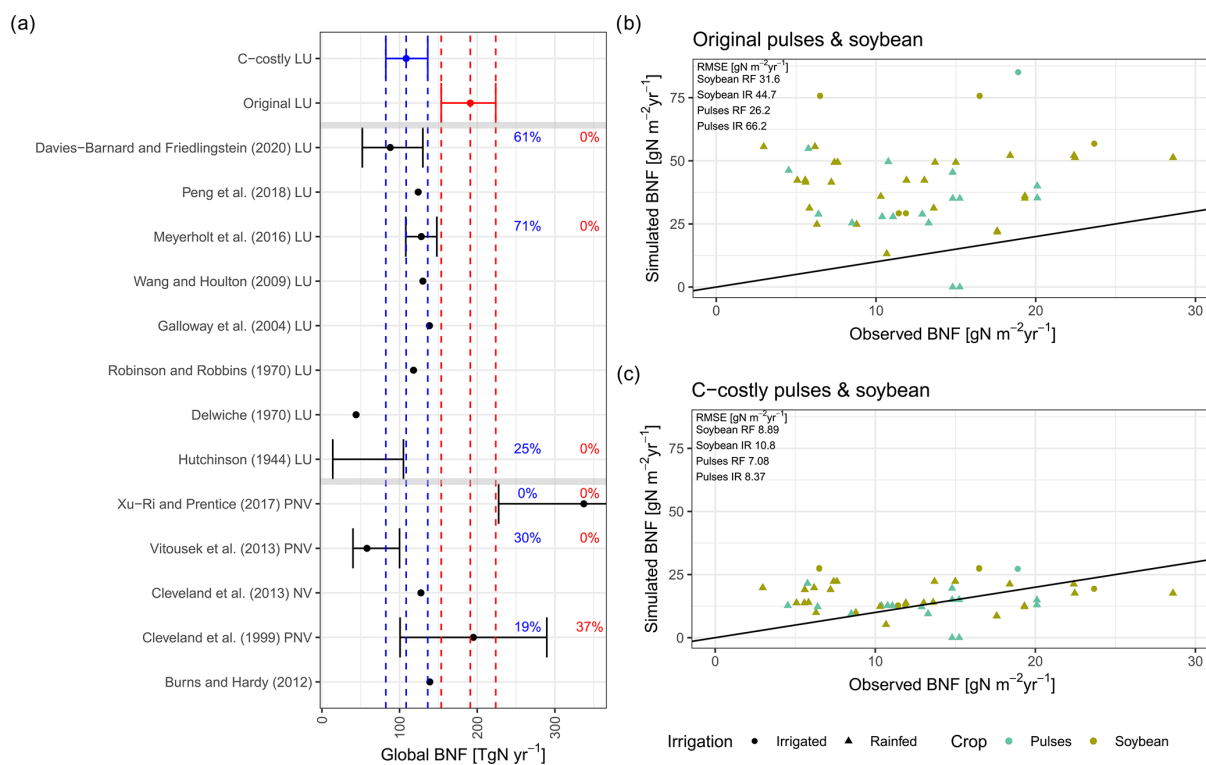


Figure 4.2: Evaluation against global (a) and site-specific data (b, c). Global evaluation plot inspired by Davies-Barnard and Friedlingstein (2020a) showing global BNF (in TgN yr<sup>-1</sup>) from different studies (black) compared to the Original (red) and C-costly (blue) BNF approach implemented in LPJmL. Studies are labelled by author names and whether they consider potential natural vegetation (PNV), actual natural vegetation (NV) or actual land use (LU). We assigned the Davies-Barnard and Friedlingstein (2020a) data to the LU category because they consider cropland area as grasslands and not as potential forest areas. Percentage values give the overlap between the ranges of the simulation results and the literature estimates derived using Eq. (4.9). Simulated values are the median between 2001 and 2010, and the ranges show the minimum and maximum. Site-specific evaluation (b, c) comparing data from observations for soybean (green) and pulses (blue) for rainfed (RF) (circle) and irrigated (IR) (triangle) experiment and simulation results is shown using the Original (b) and C-costly (c) BNF approaches. Labels show the RMSE of the two approaches.

Russia and Mongolia.

On croplands, BNF was 21 TgN yr<sup>-1</sup> with the C-costly approach, which is within the range of 17 to 31 TgN yr<sup>-1</sup> reported by a recent review (Zhang et al., 2021) and other studies (Bodirsky et al., 2012; Chang et al., 2021). This contrasts with the overestimation of cropland BNF in the Original approach, which was 68 TgN yr<sup>-1</sup>. For the two legume crop functional types representing soybean and pulses, we compared the simulation results to BNF and yield data from experiments (Figs. 4.2b and c and C.2a and b). For all except two experiments, the Original approach strongly overestimated BNF independent of the crop and the irrigation management. Using the C-costly approach, the cropland BNF was strongly reduced by a factor of approximately 2, leading to substantially lower RMSEs. While simulation results were closer to observations, some deviations remain. Pulses generally showed lower BNF for both approaches compared to soybean, while irrigated simulations generally showed a higher

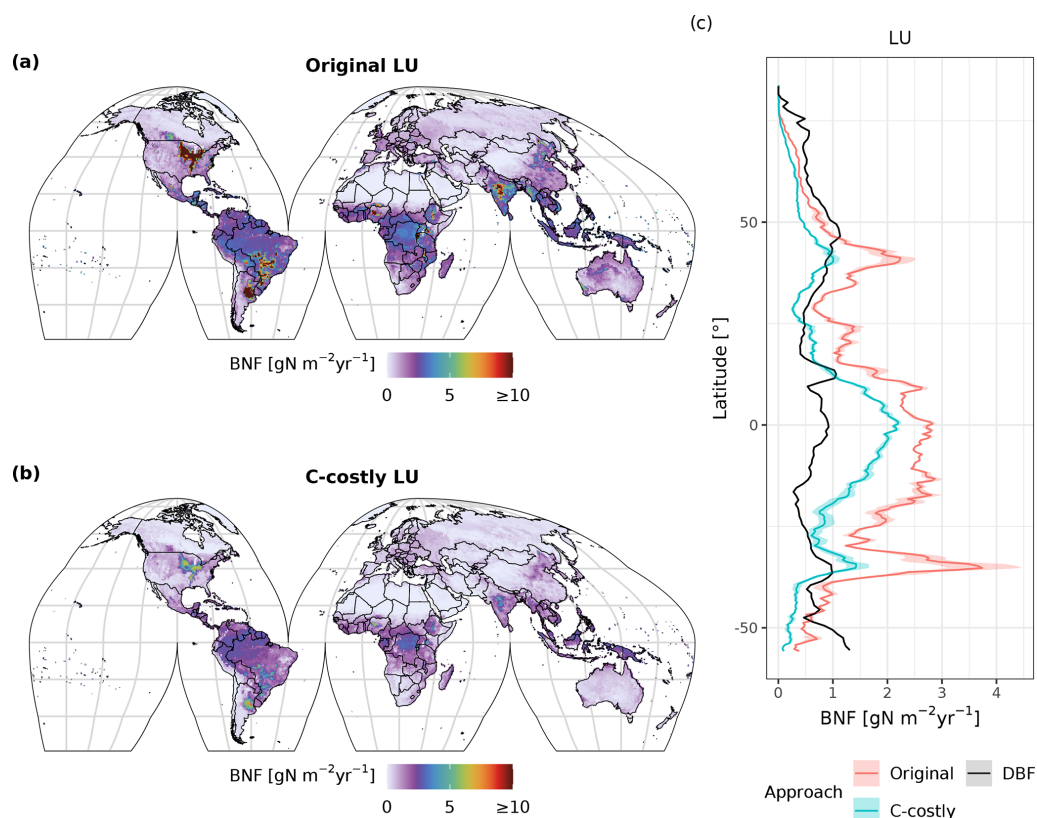


Figure 4.3: Simulated average annual BNF (in  $\text{gN m}^{-2} \text{yr}^{-1}$ ) for the years 2001 to 2010 using the Original (a) and C-costly (b) approaches. The average (line) and 5th to 95th percentiles (shading) of simulated and observed BNF per latitude (in  $\text{gN m}^{-2} \text{yr}^{-1}$ ), using the Original (red) and C-costly (blue) approaches and data from Davies-Barnard and Friedlingstein (2020a) (DBF), are shown (c).

BNF and overestimated BNF compared to observations for all experiments in the Original approach and for the vast majority in the C-costly approach. Crop yields barely differed between the two approaches and were comparable to observations (Fig. C.2a and b).

#### 4.3.1.2 Global variation in BNF

Generally, BNF decreases from low to high latitudes with similar gradients but from different levels for the two approaches (Fig. 4.3). In latitudes with a high share of crop legumes (e.g. 30 to 40° S), the reduction in the BNF in the C-costly approach is especially large. Both the Original and the C-costly approaches underestimate BNF at high latitudes (the Original more strongly so) compared to Davies-Barnard and Friedlingstein (2020a). The C-costly approach shows a good performance in the mid-latitudes, but both approaches overestimate BNF compared to observations in the tropics (Fig. 4.3). In the Original approach, especially the high BNF of cropland contributes to the overestimation. For the low latitudes, both approaches exceed the values from Davies-Barnard and Friedlingstein (2020b). However, the higher BNF in the tropics is comparable to the median of the TRENDY-N ensemble (see Sect. 4.4 and Kou-Giesbrecht et al., 2023).

With the Original approach, mineral N was added to the first soil layer and subsequently incorporated by the PFTs via the passive and active N-uptake pathway. This did not allow a separate identification of N to be taken up via BNF from the total N uptake, except for the legume crops which fixed their entire N deficit. Using the C-costly BNF, the model separates N uptake by BNF from passive and active N uptake against N concentration gradients (Fisher et al., 2010; Marschner et al., 1991), facilitating the analysis of the share of BNF in total N uptake subsequently referred to as  $\%N_{\text{dfa}}$ , which is commonly used to refer to this variable in the empirical literature (e.g. Herridge et al., 2008). In the PNV simulation, values for  $\%N_{\text{dfa}}$  were between 0% and 20% for most of the grid cells (Figs. C.8 and C.9b). The distribution is bimodal, showing a peak below 5% and one at approximately 10%. For the dynamic land-use simulation, the values for  $\%N_{\text{dfa}}$  are similar, but the second peak is barely distinguishable because of a higher share of  $\%N_{\text{dfa}}$  values between 5% and 10% (Figs. C.8 and C.9a). For the crop legumes,  $\%N_{\text{dfa}}$  is substantially higher, with the peak at around 80% (Fig. C.8d). The highest values are simulated at low latitudes, especially in India, sub-Saharan Africa and South America, while the lowest values are simulated in Canada, Russia and southern China (Fig. C.9d). In the Original approach,  $\%N_{\text{dfa}}$  of legume crops was almost exclusively 100% (Fig. C.8e).

In both approaches, BNF per area is higher for agricultural land than for natural vegetation (Fig. C.4d and f). BNF is especially high in hot spots of legume crop production such as Argentina, Brazil, India and the USA (Fig. 4.3a and b). While the spatial pattern is similar between the two approaches, in the Original approach, the cropland BNF leads to prominent peaks in the latitudinal distribution (Fig. 4.3c). These peaks correspond to hot spots of legume crop production, where the C-costly approach is up to  $15 \text{ gN m}^{-2} \text{ yr}^{-1}$  lower (Fig. C.5).

For natural vegetation, the differences are smaller. Here, the BNF in the Original approach is up to  $4 \text{ gN m}^{-2} \text{ yr}^{-1}$  higher compared to the C-costly approach (Fig. C.5). Here, the spatial patterns differ and show a stronger reduction in the BNF in dry regions (e.g. central Australia, the Eurasian steppe regions, southeast China and parts of Africa).

The various natural PFTs contribute differently to the lower overall BNF in the C-costly approach (Figs. C.6 and C.7). To some extent, this reflects changes in the PFT distribution (Figs. C.11 and C.12 in the Appendix). For the tropical PFTs, BNF is lower for the broadleaved raingreen tree ( $\Delta 5.25 \text{ TgN yr}^{-1}$ ; Fig. C.6b) and the herbaceous PFT ( $\Delta 14.1 \text{ TgN yr}^{-1}$ ; Fig. C.6i) and higher for the broadleaved evergreen tree ( $\Delta 7.3 \text{ TgN yr}^{-1}$ ; Fig. C.6a). While the temperate needleleaved evergreen tree PFT contributed to BNF in low latitudes outside its expected habitat (e.g. in India and Brazil) in the Original approach, this issue was resolved with the C-costly approach (Fig. C.6c). The temperate PFTs all fix less N in the C-costly approach than in the Original approach. The reductions are smaller for the broadleaved evergreen ( $\Delta 3.6 \text{ TgN yr}^{-1}$ ; Fig. C.6d) and summergreen ( $\Delta 3.8 \text{ TgN yr}^{-1}$ ; Fig. C.6e) tree and the herbaceous PFT ( $\Delta 4.7 \text{ TgN yr}^{-1}$ ; Fig. C.6j) compared to the needleleaved evergreen tree

( $\Delta 9.1 \text{ TgN yr}^{-1}$ ; Fig. C.6c). The BNF of boreal PFTs is similar ( $\Delta$  around  $0.5 \text{ TgN yr}^{-1}$ ; Fig. C.6f, g, and k) for all PFTs, except the needleleaved summergreen tree ( $\Delta 1.2 \text{ TgN yr}^{-1}$ ; Fig. C.6h), which fixes less N in the C-costly approach. In the Original approach, the temperate herbaceous PFT contributed twice as much as in the C-costly approach to the biological N fixation of the polar vegetation (Fig. C.6j). For pulses, the BNF was  $14.6 \text{ TgN yr}^{-1}$ , and for soybean, the BNF was  $6.4 \text{ TgN yr}^{-1}$  lower with the C-costly approach.

### 4.3.2 Effects on the nitrogen and carbon cycle and productivity

In LPJmL the C and N cycles are coupled via, for example, the N limitation of gross primary productivity (GPP), which controls the amount of assimilated C, the role of plant organ carbon-to-nitrogen (C : N) ratios for maintenance respiration and the availability of the resulting NPP for BNF. Additionally, the N content of the different plant organs (leaves, roots, sapwood, heartwood and storage organs) is derived dependent on the respective C content ensuring that their C : N ratios remain within a prescribed range. As a result, the N balance components presented in the following section are strongly shaped by their C cycle counterparts as the overall C and N balances represented by LPJmL are intimately linked.

We describe the N balance as the sum over in- and outfluxes of the vegetation and the soil. Therefore, the overall balance contains a change in vegetation and soil N stocks, including organic and mineral forms of N.

#### 4.3.2.1 Potential natural vegetation

Simulating only natural vegetation resulted in a positive terrestrial N balance with an average sink of  $52 \text{ TgN yr}^{-1}$  for the Original approach and  $54 \text{ TgN yr}^{-1}$  for the C-costly approach between 2001 and 2010 (Fig. 4.4a and b and Table 4.2). In 1901, N in- and outputs were almost balanced, and the sink remained small until the 1950s when N inputs from deposition increased, resulting in an increased sink. While the overall N balance was similar for both BNF approaches, the size of several components was different. The total BNF simulated with the Original approach was approximately double that of the C-costly BNF, leading to higher soil mineral N and organic C and N stocks. However, mineral N stocks were not utilised by the vegetation but instead lost to the atmosphere and waterbodies, leading to higher N emissions and leaching using the Original approach. Here,  $112 \text{ TgN yr}^{-1}$  were emitted and  $56 \text{ TgN yr}^{-1}$  were leached on average between 2001 and 2010, while for the C-costly approach, only  $79 \text{ TgN yr}^{-1}$  were emitted and  $39 \text{ TgN yr}^{-1}$  were leached (Table 4.2). All types of emissions are lower with the C-costly approach.  $\text{NH}_3$  emissions from volatilisation decrease by  $14 \text{ TgN yr}^{-1}$ ,  $\text{N}_2$  emissions by  $12 \text{ TgN yr}^{-1}$ ,  $\text{N}_2\text{O}$  emissions by  $3 \text{ TgN yr}^{-1}$  and fire emissions by  $5 \text{ TgN yr}^{-1}$ . Synchronised with the increase in deposition over time, emissions and leaching also increase in both approaches, with

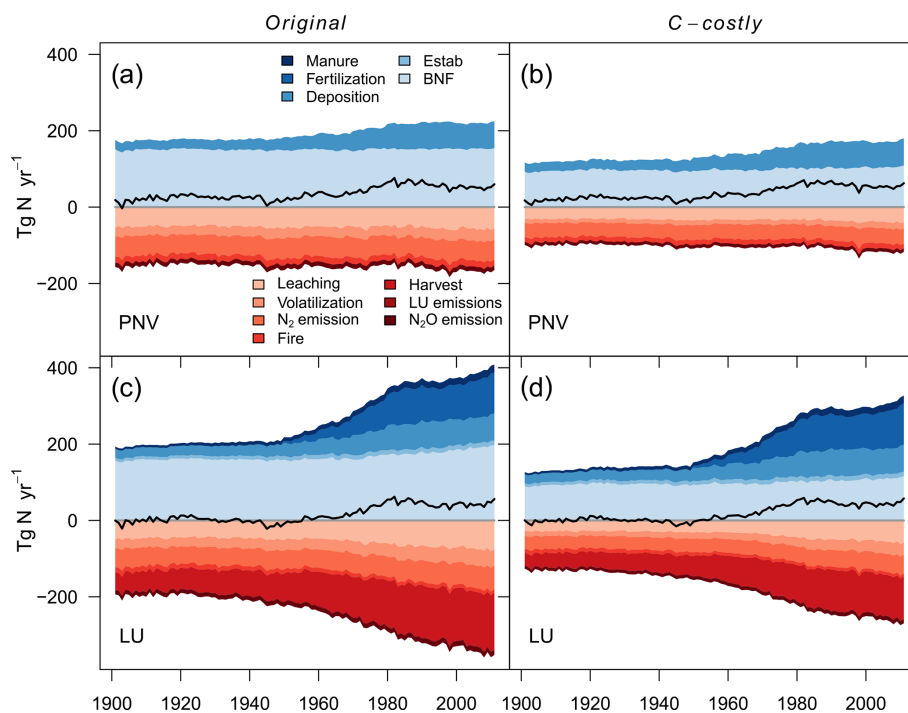


Figure 4.4: Global terrestrial N balance. Scenarios include the Original approach, the C-costly approach for natural vegetation and actual land use. Net balance is denoted by the black line. N inputs include N from manure, synthetic fertiliser deposition, PFT establishment (Estab) and BNF. N losses include leaching, volatilisation,  $N_2$  emissions, fire N, harvested N, land-use change emissions (deforestation and product turnover) and  $N_2O$  emissions from nitrification and denitrification.

stronger increases in the C-costly approach. Overall, N inputs increased by 35 TgN in total from 1950 to 2000 in the Original approach and by 42 TgN in the C-costly approach, while N losses from emissions and leaching increased by 1 and 4 TgN, respectively (Table 4.2).

In addition to the changes in several N cycle components, we expected changes in C cycle components. Overall, the C balance was similar for both approaches (Fig. C.10a and b). For the PNV simulations, the only C input into the system was the NPP. The NPP was 2.2 PgC  $yr^{-1}$  lower with the C-costly approach compared to the Original approach. However, C losses from heterotrophic respiration and fire were also lower by 1.9 and 0.3 PgC  $yr^{-1}$ , respectively.

#### 4.3.2.2 Dynamic land use

The simulations with dynamic land use include agricultural production and related additional N in- and outputs. Additional inputs are N from the application of manure and synthetic fertilisers, and additional outputs are N removed through crop harvesting, grazing and emissions from land-use change. The differences in the total BNF, soil mineral N and organic C and N stocks are similar to the PNV simulations. Between 2001 and 2010, LPJmL simulated an average N sink of 44 TgN  $yr^{-1}$  for the Original and 45 TgN  $yr^{-1}$  for the C-costly approach (Fig. 4.4c and d and Table 4.2). Already in 1901, the N

Table 4.2: N balance values for 2001 to 2010 shown in the figures. LUC (land-use change) includes deforestation emissions, product turnover and negative N fluxes.

	Original	C-costly	Literature	Original PNV	C-costly PNV	Literature
N losses (TgN yr <sup>-1</sup> )	344	263		168	118	
Leaching	74	55	93 <sup>a</sup> , 68 <sup>b</sup>	56	39	28.6 <sup>c</sup>
Volatilisation	43	32	21.4 <sup>d,e</sup>	31	17	–
N <sub>2</sub> emissions	60	47	68 <sup>a</sup> , 64.2 <sup>b</sup>	52	40	–
N <sub>2</sub> O emissions	13	10	10.9 <sup>f</sup> , 13 <sup>g</sup> , 10 <sup>h</sup> , 7.4–12.3 <sup>i</sup> , 12.9 <sup>j</sup>	12	9	–
Fire	10	8	–	17	13	–
Harvest	142	108	–	0	0	–
LUC	2	2	–	0	0	–
N gains (TgN yr <sup>-1</sup> )	388	307	–	220	172	–
BNF	191	110	See Fig. 4.2	153	104	19.8–107.9 <sup>k</sup>
Establishment fluxes	12	12	–	0	0	–
Deposition	67	67	–	67	67	–
Fertilisation	99	99	–	0	0	–
Manure	19	19	–	0	0	–
Net balance (TgN yr <sup>-1</sup> )	44	45		52	54	

<sup>a</sup> Bouwman et al. (2013). <sup>b</sup> Zaehle et al. (2010). <sup>c</sup> Braakhekke et al. (2017). <sup>d</sup> Volatilisation from natural soils (2.4 TgN yr<sup>-1</sup>) from Bouwman et al. (2002). <sup>e</sup> Volatilisation from manure and synthetic fertiliser on croplands and grasslands (19 TgN yr<sup>-1</sup>) from Bouwman et al. (1997). <sup>f</sup> Galloway et al. (2004). <sup>g</sup> Sutton et al. (2013). <sup>h</sup> Tian et al. (2019). <sup>i</sup> Tian et al. (2020). <sup>j</sup> Scheer et al. (2020). <sup>k</sup> Yu and Zhuang (2020).

balances of the PNV and dynamic land-use simulations diverge. Since there are no synthetic fertiliser inputs in 1901, only the relatively small additional inputs from establishment and manure were counteracted by N removal through crop harvesting and land use change emissions, shifting the total N balance towards a smaller source. This persists even after inputs from manure and fertiliser were increased from the 1950s onwards, which not only resulted in higher crop yields, and therefore N removed through harvesting, but also increased N losses from emissions and leaching. As was shown for the PNV simulations, the overall N balance is similar for both approaches but with different in- and output terms driven by the higher BNF in the Original approach. N emissions and leaching for the Original approach (128 and 74 TgN yr<sup>-1</sup>, respectively) were higher than for the C-costly approach (99 and 55 TgN yr<sup>-1</sup>, respectively) (Table 4.2). Similar to the PNV scenario, all types of emissions are lower with the C-costly approach. NH<sub>3</sub> emissions from volatilisation decrease by 11 TgN yr<sup>-1</sup>, N<sub>2</sub> emissions by 13 TgN yr<sup>-1</sup>, N<sub>2</sub>O emissions by 3 TgN yr<sup>-1</sup> and fire emissions by 2 TgN yr<sup>-1</sup>. N removal from harvesting was 142 TgN yr<sup>-1</sup> on average between 2001 and 2010 for the Original approach and 108 TgN yr<sup>-1</sup> for the C-costly approach. This indicates a stronger N limitation of agricultural areas in the C-costly approach. The majority of this reduction can be attributed to managed grassland and not croplands (Figs. C.13 and C.14).

Similar to the PNV simulations, the overall C balance barely differed between the two approaches (Fig. C.10c and d). While the C input from manure and establishment was similar for both approaches, NPP was 1.8 PgC yr<sup>-1</sup> lower in the C-costly approach. C lost from land-use change was similar. Fire emissions and C removed through harvesting only differed by 0.1 PgC yr<sup>-1</sup>, while heterotrophic respiration was 1.4 PgC yr<sup>-1</sup> lower in the C-costly approach than in the Original approach.

## 4.4 Discussion

While the Original approach only indirectly accounts for temperature and water limitation, as these also limit evapotranspiration and NPP, the C-costly approach explicitly considers the limitation of BNF from soil temperature, water content and NPP separately. These have long been established as limiting factors for BNF. Depending on the prevailing conditions, BNF may be limited more strongly by temperature or soil moisture or a combination of both. The role of temperature was explored early on by Meyer and Anderson (1959) and was followed by numerous studies for different plant species or legume crop varieties and temperature ranges (e.g. Montañez et al., 1995). Such studies allowed the quantification of optimal temperature ranges and limits facilitating the development of functions such as  $f_T(T_{\text{soil}})$ , which are based on empirically derived temperature curves (e.g. Halliday and Pate, 1976). A similarly large literature body exists on the role of soil moisture (e.g. Rousk et al., 2018; Serraj et al., 1999). Valentine et al. (2018), describing the different pathways with respect to how drought stress inhibits BNF, with an important aspect being the change in nodule water potential that indicates a strong connection to soil water content. While flooding of soils can also inhibit BNF through  $O_2$  limitation, nitrogenase was shown to be more active in waterlogged environments (Jiang et al., 2021). Therefore, we are confident that our linear function for  $f_W(\text{SWC})$ , assuming that only soil moisture levels that are too low limit BNF (Wu and McGechan, 1999), reflects empirical observations well. As BNF is associated with a respiratory loss of C, the net amount of C assimilated via photosynthesis (NPP) available for BNF, as well as the fixation efficiency (respiratory loss of C per gained N), forms an additional important controlling factor. A recent meta-analysis by Yao et al. (2024) highlights the importance of plant taxa for BNF in addition to abiotic factors. This is in line with early experimental work that quantified the respiratory loss of C per N fixed (Patterson and Larue, 1983; Reed et al., 2011; Voisin et al., 2003) and the total amount of NPP spent on fixation (Kaschuk et al., 2009) for different N-fixing plants and already showed that functional traits have to be considered when assessing BNF. Therefore, including NPP and a cost of fixation, as we did with the C-costly approach, is an important conceptual improvement.

The C-costly approach is not only conceptually superior to the simplistic Original approach in LPJmL, it also performs better in comparison to external data. Still, some mismatches with reference data remain, such as an overestimation of BNF in the tropics (Fig. 4.3c). However, the ensemble mean of a recent study evaluating the N cycle of 11 DGVMs shows a similar overestimation in the tropics and a large bias, indicating little agreement between models (Kou-Giesbrecht et al., 2023). They attributed this to the fact that BNF is typically modelled as a function of vegetation activity expressed either through NPP or evapotranspiration. Our results show that the overestimation of tropical BNF is reduced if temperature and water availability are considered separate limitations, which supports their interpretation. Furthermore, the NPP that can be used for BNF depends on the overall productivity, which certainly

is higher in the tropics. It is likely that additional variables not considered in our approach constrain BNF there, such as phosphorus limitation (Lee et al., 2019; Vitousek, 1984). However, it has also been suggested that as a result of higher N losses, tropical BNF should be higher than observations imply (Hedin et al., 2009). This could be a result of uncertainties inherent to BNF measurements (Soper et al., 2021) or the limited amount of data available from tropical ecosystems.

Furthermore, simulated BNF was at the higher end of the range reported by Davies-Barnard and Friedlingstein (2020b) for the C-costly approach. One explanation is that Davies-Barnard and Friedlingstein (2020b) aggregate cropland and grassland areas, assuming that their BNF rates are identical. However, a recent study provides evidence that the BNF of crop legumes might actually be substantially higher than that of forage legumes (Herridge et al., 2022; Peoples et al., 2021), and therefore, the BNF of croplands and grassland cannot be assumed to be similar. Consistent with this, we also had to select much higher potential N fixation rates for the crop PFTs compared to the other PFTs to achieve sufficient cropland BNF (Table 4.1).

We expected that limiting BNF of legume crops would result in stronger N stress and reduced yields. However, yields for the legume crops were similar between the two approaches. One explanation is the direct link that the maintenance respiration of a plant organ has to its N content. Reducing the N that is taken up via BNF results in a lower organ N content and maintenance respiration and thus similar NPP. Indeed, C : N ratios are higher for the C-costly approach compared to the Original approach, indicating a lower plant N content (Fig. C.3).

The average  $\%N_{dfa}$  of legume crops was between approximately 30 % and 100 % for the C-costly approach and 100 % for the Original approach. Comparing the distribution (Fig. C.8d) to  $\%N_{dfa}$  observations shows that the values of the C-costly approach are possible but at the upper end of observations, while those of the Original approach are not supported by observations. For soybean, experimental values range from 0 % to 98 %, with an average of 52 % (Salvagiotti et al., 2008). Herridge et al. (2008) report average values between 40 % and 75 % on average and up to 97 % for experiments but only 36 % and 68 % for farmers' fields, depending on the cultivated legume crop.  $\%N_{dfa}$  is strongly related to soil mineral N content and thus fertilisation levels. The high  $\%N_{dfa}$  may be an indication that either fertiliser levels or active and passive N uptake and retranslocation of N at leaf senescence are underestimated by LPJmL, and respective processes should be re-evaluated. We found a higher  $\%N_{dfa}$  for both the natural vegetation and the cropland in warm and dry areas (Fig. C.9) where mineralisation of organic N is limited (Dessureault-Rompré et al., 2010).

We expected that the differences in the BNF between the two approaches would be reflected by differences in the C stocks and fluxes due to the close link of the C and N cycles in LPJmL. Both the C inflow into terrestrial C stocks from NPP and outflows from harvest, heterotrophic respiration and fire were lower in the C-costly approach, leading to a similar net C balance for the two approaches

(Figs. C.10 and C.15). Accounting for the cost of BNF in the form of respiratory losses of NPP leads to lower NPP, which limited biomass accumulation and in turn harvest, as well as biomass available for burning and heterotrophic respiration via reduced litter accumulation. Because of the close link of the C and N cycles, the net N balance is also similar for the two approaches. The lower BNF in the C-costly approach results in lower N outfluxes, i.e. leaching, emissions and harvests. The Original approach added mineral N to the soils of the natural vegetation and managed grassland even if the vegetation was not N limited. Legume crops that received all the N that they demanded, as in the Original approach, returned high N content residues to the soil, increasing N inputs and mineral N stocks. As a result, the mineral N content of soils was higher in the Original approach, explaining the differences in yields and leaching. Similarly, soil mineral N content influences N emissions except fire emissions, which are controlled by the N content of the burned vegetation and litter. Since this also decreased, fire emissions were lower with the C-costly approach. In contrast to the lower BNF, which is in line with observations, N losses from leaching and emissions (from volatilisation, denitrification, nitrification, fire and land-use change) are underestimated by LPJmL simulations compared to observational data (see Table 4.2) in both approaches. The overestimation of emissions from volatilisation of soil  $\text{NH}_4^+$  is strongly reduced with the C-costly approach because the soil  $\text{NH}_4^+$  pool is lower in the C-costly approach compared to the Original approach, where BNF is directly added to the soil  $\text{NH}_4^+$  (see Sect. 4.2.2). While  $\text{N}_2\text{O}$  emissions compare well to literature estimates,  $\text{N}_2$  emissions are more strongly underestimated with the C-costly approach. Similar to the soil  $\text{NH}_4^+$  pool, the soil  $\text{NO}_3^-$  is reduced because less  $\text{NH}_4^+$  is available for nitrification, resulting in reduced  $\text{N}_2$  emissions. Overall, the reduction shifts emissions from an over- to an underestimation of the literature values. While one source of differences is the missing representation of  $\text{NO}_x$  emissions in LPJmL, this is not sufficient to fully explain the difference. However, the models of the TRENDY-N ensemble also underestimated N losses from emissions of  $\text{NH}_3$ ,  $\text{N}_2\text{O}$ ,  $\text{NO}_x$ , and  $\text{N}_2$ , as well as leaching (Kou-Giesbrecht et al., 2023), suggesting that processes within DGVMs and scenario assumptions need to be revised. For LPJmL, we identified several potential causes. First, the manure input accounts only for manure applied to cropland, and the total amount is in line with other sources reporting cropland manure (Zhang et al., 2021), but does not account for manure added to grasslands other than the internal recycling by grazing animals (Heinke et al., 2023). Second, N losses and emissions strongly vary between different agricultural production systems whose representation would require not only the implementation of more detailed management options but also data sets on the spatial patterns of the application of different management specifics of these systems. Third, we conducted our simulations assuming cover cropping outside the growing season on all croplands, which overestimates the extent of cover cropping and reduces N losses. However, data on cover cropping systems are not available (e.g. Porwollik et al., 2022).

While the C-costly approach improved simulation results for BNF, as well as other components of the

N balance, and model results are in line with other DGVMs that represent the N cycle, we see potential for further improvement. The C-costly approach depends on multiple parameters, some of which are not well constrained. Values for the potential N fixation rate vary between species and across sites (Ma et al., 2022), and selecting one value to be representative of one PFT or even all PFTs of an entire climate zone is a strong simplification. Furthermore, experiments have shown a large variation in the respiratory cost of BNF (Patterson and Larue, 1983; Reed et al., 2011; Voisin et al., 2003), as well as the amount of NPP that different plant species invest (Kaschuk et al., 2009), which is not well reflected by the current parameterisation.

In addition, we assume a constant fraction of N fixers present in a community. However, the number of N fixers changes over time, dependent on N stress (Herben et al., 2017; Taylor et al., 2019). N fixation, the share of fixers and/or nodule abundance is low in undisturbed N-rich environments, and nodules need to be produced to increase N fixation if N availability decreases (Crews, 1999; Fisher et al., 2010). Similarly, N fixation does not cease instantaneously when N becomes more abundant but is only reduced after the share of fixers and/or nodule abundance has decreased (Herben et al., 2017; Thornley et al., 1995). In contrast, fixers are always present in LPJmL and can instantly fix N if necessary. Therefore, LPJmL likely simulates an adaptation response that is too quick for the changing N availability and overestimates the short-term capability of the community to buffer changes in N availability.

While our approach simulates the total amount of BNF well, it does not distinguish the symbiotic from free-living or heterotrophic N fixation. However, these are two different sources of N, and their share of total BNF shows large spatial heterogeneity (Davies-Barnard and Friedlingstein, 2020b). In contrast to symbiotic BNF, free-living BNF does not require NPP expenditures, and separating the two may further improve simulation results for NPP and its dependent variables.

In the following, we qualitatively compare our approach to common approaches used in crop models and DGVMs. A synthesis of nine crop models by Liu et al. (2011) showed that soil water status and N supply were the most widely considered control variables. Soil temperature was only considered by four models and plant C supply only by two models, despite their importance for limiting BNF. The C-costly approach also uses empirical factors to account for soil temperature and soil water status, whereas the role of N supply, plant C supply and plant growth stage are simulated mechanistically in LPJmL, which is a clear distinction from the models assessed by Liu et al. (2011).

Our approach is at the higher end of the complexity when compared to 11 TRENDY-N DGVMs that include the N cycle. As shown in Kou-Giesbrecht et al. (2023), five DGVMs follow an approach similar to the Original approach, calculating BNF based on evapotranspiration or NPP; three models calculate BNF as a function of N limitation; two models assume a constant BNF; and in one model BNF is derived in post-processing to close the N cycle. The remaining three models use more complex approaches which can be compared to the C-costly approach. The Community Land Model (CLM)

version 5.0 (Lawrence et al., 2019) uses an approach based on Fisher et al. (2010), explicitly minimising the cost of active N uptake, retranslocation and BNF and distinguishes asymbiotic from symbiotic N fixation. In the Canadian Terrestrial Ecosystem Model (CTEM), BNF is a function of temperature, vegetation cover, soil nitrate and plant structural C pools (Arain et al., 2006; Dickinson et al., 2002). The Dynamic Land Ecosystem Model (DLEM) considers soil temperature, soil moisture status, soil C and soil N (Tian et al., 2015). While the approach used in CLM5.0 is more complex compared to the C-costly approach and addresses some of the conceptual shortcomings of the C-costly approach discussed earlier, the approach used in CTEM is of similar complexity and simulates values at the upper end of the recent literature estimates (Kou-Giesbrecht et al., 2023). However, global BNF values and latitudinal distribution simulated by CLM5.0, as shown by Kou-Giesbrecht et al. (2023) in Figs. 3 and A6, are comparable to those simulated with C-costly approach. To fully assess the advantages of such a complex approach over the C-costly approach or that of CTEM or DLEM, a comparison of the spatial patterns or of simulations at higher spatial resolution could be a worthwhile future endeavour.

## 4.5 Conclusions

Compared to the simplistic Original BNF implementation in LPJmL, the more complex C-costly approach, as described here, presents a substantial improvement of the representation of BNF in LPJmL. While the Original approach led to an overestimation of BNF and was insensitive to soil temperature and soil water conditions, the C-costly approach overcomes these issues and can help to better project future BNF and its effects on N limitation of the terrestrial biosphere, as well as losses of reactive N to the environment, including the greenhouse gas nitrous oxide ( $N_2O$ ). Further research is needed, especially with respect to balancing different in- and outfluxes and internal recycling rates. The current improvement of BNF simulations with LPJmL and the associated underestimation of loss terms exemplifies the scope of this problem. Our study highlights the importance of a detailed implementation of the processes controlling BNF for N cycling in DGVMs. While the C-costly approach already improved simulation results, we think that additional benefits would be gained by explicitly separating BNF by symbiotic and free-living bacteria and from accounting for the costs of other N-uptake sources, except passive N uptake.

**Code availability:** The source code of LPJmL in the exact form described here is available at 10.5281/zenodo.14012503 (Wirth et al., 2023) and at <https://github.com/PIK-LPJmL/LPJmL> (last access: 30 October 2024).

**Data availability:** The historical climate data from the GSWP3-W5E5 data set are available from 10.48364/ISIMIP.982724 (Lange et al., 2022). The historical data of atmospheric N deposition and atmospheric  $CO_2$  concentrations can be obtained from 10.48364/ISIMIP.600567 (Yang and Tian, 2020) and 10.48364/ISIMIP.664235.2 (Büchner and Reyer, 2022), respectively. All input data, model code, model outputs and scripts that have been used to produce the results presented in this paper are archived at the Potsdam Institute for Climate Impact Research and are available upon request.

**Author contributions:** SBW, CM, FS, SR, SiS and WvB designed the study. SBW designed and conducted the model implementation with inputs from CM, JB, SR, SiS and WvB. SBW, CM, FS, SR, SiS, WvB, SO, JH and JB contributed to the general model development and evaluation. SBW conducted the model simulations and wrote the original draft, with inputs from CM, FS, SR, SiS and WvB. SBW, CM, FS, SR, SiS, WvB, SO, JH and JB reviewed and edited the original draft. All authors discussed the simulation results and reviewed and edited the paper.

**Acknowledgements:** Fabian Stenzel acknowledges funding by the Global Challenges Foundation via Future Earth. We thank the two anonymous reviewers for their valuable feedback.

**Financial support:** This research has been supported by the Bundesministerium für Bildung und Forschung (grant nos. 01LP1903D and 01LS2105A), the European Union’s Horizon 2020 (grant nos. 101003536 and 869192), the Evangelisches Studienwerk Villigst (grant no. 851291) and Conservation International (grant no. CI-114129). The publication of this article was funded by the Open Access Fund of the Leibniz Association.

## 4.6 References

- Arain, M. A., F. Yuan, and T. Andrew Black (2006). “Soil–Plant Nitrogen Cycling Modulated Carbon Exchanges in a Western Temperate Conifer Forest in Canada”. In: *Agricultural and Forest Meteorology*. The Fluxnet-Canada Research Network: Influence of Climate and Disturbance on Carbon Cycling in Forests and Peatlands 140.1, pp. 171–192. ISSN: 0168-1923. DOI: 10.1016/j.agrformet.2006.03.021. (Visited on 06/14/2024).
- Becker, M., J. K. Ladha, and M. Ali (1995). “Green Manure Technology: Potential, Usage, and Limitations. A Case Study for Lowland Rice”. In: *Management of Biological Nitrogen Fixation for the Development of More Productive and Sustainable Agricultural Systems: Extended Versions of Papers Presented at the Symposium on Biological Nitrogen Fixation for Sustainable Agriculture at the 15th Congress of Soil Science, Acapulco, Mexico, 1994*. Ed. by J. K. Ladha and M. B. Peoples. Developments in Plant and Soil Sciences. Dordrecht: Springer Netherlands, pp. 181–194. ISBN: 978-94-011-0053-3. DOI: 10.1007/978-94-011-0053-3\_8. (Visited on 05/31/2023).
- Beringer, T., W. Lucht, and S. Schaphoff (2011). “Bioenergy Production Potential of Global Biomass Plantations under Environmental and Agricultural Constraints”. In: *GCB Bioenergy* 3.4, pp. 299–312. ISSN: 1757-1707. DOI: 10.1111/j.1757-1707.2010.01088.x. (Visited on 05/31/2023).
- Bodirsky, B. L., A. Popp, I. Weindl, J. P. Dietrich, S. Rolinski, L. Scheiffele, C. Schmitz, and H. Lotze-Campen (2012). “N<sub>2</sub>O Emissions from the Global Agricultural Nitrogen Cycle – Current State and Future Scenarios”. In: *Biogeosciences* 9.10, pp. 4169–4197. ISSN: 1726-4170. DOI: 10.5194/bg-9-4169-2012. (Visited on 11/15/2023).
- Bondeau, A., P. C. Smith, S. Zaehle, S. Schaphoff, W. Lucht, W. Cramer, D. Gerten, H. Lotze-Campen, C. Müller, M. Reichstein, and B. Smith (2007). “Modelling the Role of Agriculture for the 20th Century Global Terrestrial Carbon Balance”. In: *Glob. Change Biol.* 13.3, pp. 679–706. ISSN: 1365-2486. DOI: 10.1111/j.1365-2486.2006.01305.x. (Visited on 05/31/2023).
- Boote, K. J., G. Hoogenboom, J. W. Jones, and K. T. Ingram (2009). “Modeling Nitrogen Fixation and Its Relationship to Nitrogen Uptake in the CROPGRO Model”. In: *Quantifying and Understanding Plant Nitrogen Uptake for Systems Modeling*. CRC Press. ISBN: 978-0-429-14053-2.
- Bouwman, A. F., A. H. W. Beusen, J. Griffioen, J. W. Van Groenigen, M. M. Hefting, O. Oenema, P. J. T. M. Van Puijenbroek, S. Seitzinger, C. P. Slomp, and E. Stehfest (2013). “Global Trends and Uncertainties in Terrestrial Denitrification and N<sub>2</sub>O Emissions”. In: *Philos. Trans. R. Soc. B Biol. Sci.* 368.1621, p. 20130112. DOI: 10.1098/rstb.2013.0112. (Visited on 11/15/2023).
- Bouwman, A. F., L. J. M. Boumans, and N. H. Batjes (2002). “Estimation of Global NH<sub>3</sub> Volatilization Loss from Synthetic Fertilizers and Animal Manure Applied to Arable Lands and Grasslands”. In: *Glob. Biogeochem. Cycles* 16.2, pp. 8-1-8-14. ISSN: 1944-9224. DOI: 10.1029/2000GB001389. (Visited on 05/29/2024).
- Bouwman, A. F., D. S. Lee, W. a. H. Asman, F. J. Dentener, K. W. Van Der Hoek, and J. G. J. Olivier (1997). “A Global High-Resolution Emission Inventory for Ammonia”. In: *Glob. Biogeochem. Cycles* 11.4, pp. 561–587. ISSN: 1944-9224. DOI: 10.1029/97GB02266. (Visited on 05/29/2024).
- Braakhekke, M. C., K. T. Rebel, S. C. Dekker, B. Smith, A. H. W. Beusen, and M. J. Wassen (2017). “Nitrogen Leaching from Natural Ecosystems under Global Change: A Modelling Study”. In: *Earth Syst. Dyn.* 8.4, pp. 1121–1139. ISSN: 2190-4979. DOI: 10.5194/esd-8-1121-2017. (Visited on 11/15/2023).
- Büchner, M. and C. P. O. Reyer (2022). *ISIMIP3a Atmospheric Composition Input Data (v1.2)*. DOI: 10.48364/ISIMIP.664235.2. (Visited on 09/05/2023).
- Chang, J., P. Havlík, D. Leclère, W. de Vries, H. Valin, A. Deppermann, T. Hasegawa, and M. Obersteiner (2021). “Reconciling Regional Nitrogen Boundaries with Global Food Security”. In: *Nat Food* 2.9, pp. 700–711. ISSN: 2662-1355. DOI: 10.1038/s43016-021-00366-x. (Visited on 11/15/2023).
- Cleveland, C. C., A. R. Townsend, D. S. Schimel, H. Fisher, R. W. Howarth, L. O. Hedin, S. S. Perakis, E. F. Latty, J. C. Von Fischer, A. Elsegaard, and M. F. Wasson (1999). “Global Patterns of Terrestrial Biological Nitrogen (N<sub>2</sub>) Fixation in Natural Ecosystems”. In: *Glob. Biogeochem. Cycles* 13.2, pp. 623–645. ISSN: 1944-9224. DOI: 10.1029/1999GB900014. (Visited on 02/18/2022).

- Crews, T. E. (1999). “The Presence of Nitrogen Fixing Legumes in Terrestrial Communities: Evolutionary vs Ecological Considerations”. In: *Biogeochemistry* 46.1, pp. 233–246. ISSN: 1573-515X. DOI: 10.1007/BF01007581. (Visited on 11/07/2023).
- Cucchi, M., G. P. Weedon, A. Amici, N. Bellouin, S. Lange, H. Müller Schmied, H. Hersbach, and C. Buontempo (2020). “WFDE5: Bias-Adjusted ERA5 Reanalysis Data for Impact Studies”. In: *Earth Syst. Sci. Data* 12.3, pp. 2097–2120. ISSN: 1866-3508. DOI: 10.5194/essd-12-2097-2020. (Visited on 09/05/2023).
- Davies-Barnard, T. and P. Friedlingstein (2020a). *Data: The Global Distribution of Biological Nitrogen Fixation in Terrestrial Natural Ecosystems*. DOI: 10.24378/exe.2063. (Visited on 02/06/2023).
- Davies-Barnard, T. and P. Friedlingstein (2020b). “The Global Distribution of Biological Nitrogen Fixation in Terrestrial Natural Ecosystems”. In: *Glob. Biogeochem. Cycles* 34.3, e2019GB006387. ISSN: 1944-9224. DOI: 10.1029/2019GB006387. (Visited on 02/06/2023).
- Dessureault-Rompré, J., B. J. Zebarth, A. Georgallas, D. L. Burton, C. A. Grant, and C. F. Drury (2010). “Temperature Dependence of Soil Nitrogen Mineralization Rate: Comparison of Mathematical Models, Reference Temperatures and Origin of the Soils”. In: *Geoderma* 157.3, pp. 97–108. ISSN: 0016-7061. DOI: 10.1016/j.geoderma.2010.04.001. (Visited on 11/07/2023).
- Dickinson, R. E., J. A. Berry, G. B. Bonan, G. J. Collatz, C. B. Field, I. Y. Fung, M. Goulden, W. A. Hoffmann, R. B. Jackson, R. Myneni, P. J. Sellers, and M. Shaikh (2002). “Nitrogen Controls on Climate Model Evapotranspiration”. In: *J. Clim.* 15.3, pp. 278–295. ISSN: 0894-8755, 1520-0442. DOI: 10.1175/1520-0442(2002)015<0278:NCOCME>2.0.CO;2. (Visited on 06/14/2024).
- Donges, J. F., J. Heitzig, W. Barfuss, M. Wiedermann, J. A. Kassel, T. Kittel, J. J. Kolb, T. Kolster, F. Müller-Hansen, I. M. Otto, K. B. Zimmerer, and W. Lucht (2020). “Earth System Modeling with Endogenous and Dynamic Human Societies: The Copan: CORE Open World–Earth Modeling Framework”. In: *Earth Syst. Dyn.* 11.2, pp. 395–413. ISSN: 2190-4979. DOI: 10.5194/esd-11-395-2020. (Visited on 09/26/2023).
- Fageria, N. K. (2007). “Green Manuring in Crop Production”. In: *J. Plant Nutr.* 30.5, pp. 691–719. ISSN: 0190-4167. DOI: 10.1080/01904160701289529. (Visited on 05/31/2023).
- Fisher, J. B., S. Sitch, Y. Malhi, R. A. Fisher, C. Huntingford, and S.-Y. Tan (2010). “Carbon Cost of Plant Nitrogen Acquisition: A Mechanistic, Globally Applicable Model of Plant Nitrogen Uptake, Retranslocation, and Fixation”. In: *Glob. Biogeochem. Cycles* 24.1. ISSN: 1944-9224. DOI: 10.1029/2009GB003621. (Visited on 11/26/2019).
- Galloway, J. N., F. J. Dentener, D. G. Capone, E. W. Boyer, R. W. Howarth, S. P. Seitzinger, G. P. Asner, C. C. Cleveland, P. A. Green, E. A. Holland, D. M. Karl, A. F. Michaels, J. H. Porter, A. R. Townsend, and C. J. Vöösmary (2004). “Nitrogen Cycles: Past, Present, and Future”. In: *Biogeochemistry* 70.2, pp. 153–226. ISSN: 1573-515X. DOI: 10.1007/s10533-004-0370-0. (Visited on 05/26/2023).
- Galloway, J. N., W. H. Schlesinger, H. Levy II, A. Michaels, and J. L. Schnoor (1995). “Nitrogen Fixation: Anthropogenic Enhancement–Environmental Response”. In: *Glob. Biogeochem. Cycles* 9.2, pp. 235–252. ISSN: 1944-9224. DOI: 10.1029/95GB00158. (Visited on 05/31/2023).
- Granhall, U. (1981). “Biological Nitrogen Fixation in Relation to Environmental Factors and Functioning of Natural Ecosystems [Tundra Mires, Temperate Forests].” In: *Ecol. Bull.* 33, pp. 131–144. ISSN: 0346-6868. (Visited on 05/31/2023).
- Halliday, J. and J. S. Pate (1976). “The Acetylene Reduction Assay as a Means of Studying Nitrogen Fixation in White Clover under Sward and Laboratory Conditions”. In: *Grass Forage Sci.* 31.1, pp. 29–35. ISSN: 1365-2494. DOI: 10.1111/j.1365-2494.1976.tb01112.x. (Visited on 05/30/2024).
- Hedin, L. O., E. J. Brookshire, D. N. Menge, and A. R. Barron (2009). “The Nitrogen Paradox in Tropical Forest Ecosystems”. In: *Annu. Rev. Ecol. Evol. Syst.* 40.1, pp. 613–635. DOI: 10.1146/annurev.ecolsys.37.091305.110246. (Visited on 08/24/2023).
- Heinke, J., S. Rolinski, and C. Müller (2023). “Modelling the Role of Livestock Grazing in C and N Cycling in Grasslands with LPJmL5.0-Grazing”. In: *Geosci. Model Dev.* 16.9, pp. 2455–2475. ISSN: 1991-959X. DOI: 10.5194/gmd-16-2455-2023. (Visited on 05/31/2023).
- Herben, T., H. Mayerová, H. Skálová, V. Hadincová, S. Pecháčková, and F. Krahulec (2017). “Long-Term Time Series of Legume Cycles in a Semi-Natural Montane Grassland: Evidence for Nitrogen-Driven Grass Dynamics?” In: *Funct. Ecol.* 31.7, pp. 1430–1440. ISSN: 1365-2435. DOI: 10.1111/1365-2435.12844. (Visited on 11/07/2023).
- Herridge, D. F., K. E. Giller, E. S. Jensen, and M. B. Peoples (2022). “Quantifying Country-to-Global Scale Nitrogen Fixation for Grain Legumes II. Coefficients, Templates and Estimates for Soybean, Groundnut and Pulses”. In: *Plant Soil* 474.1, pp. 1–15. ISSN: 1573-5036. DOI: 10.1007/s11104-021-05166-7. (Visited on 08/24/2023).
- Herridge, D. F., M. B. Peoples, and R. M. Boddey (2008). “Global Inputs of Biological Nitrogen Fixation in Agricultural Systems”. In: *Plant Soil* 311.1, pp. 1–18. ISSN: 1573-5036. DOI: 10.1007/s11104-008-9668-3. (Visited on 04/26/2024).
- Herzfeld, T., J. Heinke, S. Rolinski, and C. Müller (2021). “Soil Organic Carbon Dynamics from Agricultural Management Practices under Climate Change”. In: *Earth Syst. Dyn.* 12.4, pp. 1037–1055. ISSN: 2190-4979. DOI: 10.5194/esd-12-1037-2021. (Visited on 05/31/2023).
- Jägermeyr, J., A. Pastor, H. Biemans, and D. Gerten (2017). “Reconciling Irrigated Food Production with Environmental Flows for Sustainable Development Goals Implementation”. In: *Nat Commun* 8.1, p. 15900. ISSN: 2041-1723. DOI: 10.1038/ncomms15900. (Visited on 10/05/2023).
- Jiang, S., M.-F. Jardinaud, J. Gao, Y. Pecrix, J. Wen, K. Mysore, P. Xu, C. Sanchez-Canizares, Y. Ruan, Q. Li, M. Zhu, F. Li, E. Wang, P. S. Poole, P. Gamas, and J. D. Murray (2021). “NIN-like Protein Transcription Factors Regulate Leghemoglobin Genes in Legume Nodules”. In: *Science* 374.6567, pp. 625–628. DOI: 10.1126/science.abg5945. (Visited on 05/30/2024).

- Kaschuk, G., T. W. Kuyper, P. A. Leffelaar, M. Hungria, and K. E. Giller (2009). “Are the Rates of Photosynthesis Stimulated by the Carbon Sink Strength of Rhizobial and Arbuscular Mycorrhizal Symbioses?” In: *Soil Biology and Biochemistry* 41.6, pp. 1233–1244. ISSN: 0038-0717. DOI: 10.1016/j.soilbio.2009.03.005. (Visited on 03/07/2022).
- Kim, H. (2017). *Global Soil Wetness Project Phase 3 Atmospheric Boundary Conditions (Experiment 1), Data Integration and Analysis System (DIAS)*. DOI: 10.20783/DIAS.501.
- Kou-Giesbrecht, S., V. K. Arora, C. Seiler, A. Arneeth, S. Falk, A. K. Jain, F. Joos, D. Kennedy, J. Knauer, S. Sitch, M. O’Sullivan, N. Pan, Q. Sun, H. Tian, N. Vuichard, and S. Zaehle (2023). “Evaluating Nitrogen Cycling in Terrestrial Biosphere Models: A Disconnect between the Carbon and Nitrogen Cycles”. In: *Earth Syst. Dynam.* 14.4, pp. 767–795. ISSN: 2190-4987. DOI: 10.5194/esd-14-767-2023. (Visited on 08/24/2023).
- Kull, O. (2002). “Acclimation of Photosynthesis in Canopies: Models and Limitations”. In: *Oecologia* 133.3, pp. 267–279. ISSN: 1432-1939. DOI: 10.1007/s00442-002-1042-1. (Visited on 03/07/2022).
- Lange, S., M. Mengel, S. Treu, and M. Büchner (2022). *ISIMIP3a Atmospheric Climate Input Data (v1.0)*. DOI: 10.48364/ISIMIP.982724. (Visited on 09/05/2023).
- Lawrence, D. M., R. A. Fisher, C. D. Koven, K. W. Oleson, S. C. Swenson, G. Bonan, N. Collier, B. Ghimire, L. van Kampenhout, D. Kennedy, E. Kluzek, P. J. Lawrence, F. Li, H. Li, D. Lombardozzi, W. J. Riley, W. J. Sacks, M. Shi, M. Vertenstein, W. R. Wieder, C. Xu, A. A. Ali, A. M. Badger, G. Bisht, M. van den Broeke, M. A. Brunke, S. P. Burns, J. Buzan, M. Clark, A. Craig, K. Dahlin, B. Drewniak, J. B. Fisher, M. Flanner, A. M. Fox, P. Gentine, F. Hoffman, G. Keppel-Aleks, R. Knox, S. Kumar, J. Lenaerts, L. R. Leung, W. H. Lipscomb, Y. Lu, A. Pandey, J. D. Pelletier, J. Perket, J. T. Randerson, D. M. Ricciuto, B. M. Sanderson, A. Slater, Z. M. Subin, J. Tang, R. Q. Thomas, M. Val Martin, and X. Zeng (2019). “The Community Land Model Version 5: Description of New Features, Benchmarking, and Impact of Forcing Uncertainty”. In: *J. Adv. Model. Earth Syst.* 11.12, pp. 4245–4287. ISSN: 1942-2466. DOI: 10.1029/2018MS001583. (Visited on 06/14/2024).
- Lee, M., E. Shevliakova, C. A. Stock, S. Malyshev, and P. C. D. Milly (2019). “Prominence of the Tropics in the Recent Rise of Global Nitrogen Pollution”. In: *Nat Commun* 10, p. 1437. ISSN: 2041-1723. DOI: 10.1038/s41467-019-09468-4. (Visited on 12/05/2023).
- Liu, Y., L. Wu, J. A. Baddeley, and C. A. Watson (2011). “Models of Biological Nitrogen Fixation of Legumes. A Review”. In: *Agronomy Sust. Developm.* 31.1, pp. 155–172. ISSN: 1773-0155. DOI: 10.1051/agro/2010008. (Visited on 04/26/2024).
- Lu, C. and H. Tian (2017). “Global Nitrogen and Phosphorus Fertilizer Use for Agriculture Production in the Past Half Century: Shifted Hot Spots and Nutrient Imbalance”. In: *Earth Syst. Sci. Data* 9.1, pp. 181–192. ISSN: 1866-3508. DOI: 10.5194/essd-9-181-2017. (Visited on 05/31/2023).
- Lutz, F., T. Herzfeld, J. Heinke, S. Rolinski, S. Schaphoff, W. von Bloh, J. J. Stoorvogel, and C. Müller (2019). “Simulating the Effect of Tillage Practices with the Global Ecosystem Model LPJmL (Version 5.0-Tillage)”. In: *Geosci. Model Dev.* 12.6, pp. 2419–2440. ISSN: 1991-959X. DOI: 10.5194/gmd-12-2419-2019. (Visited on 05/31/2023).
- Ma, J., S. Olin, P. Anthoni, S. S. Rabin, A. D. Bayer, S. S. Nyawira, and A. Arneeth (2022). “Modeling Symbiotic Biological Nitrogen Fixation in Grain Legumes Globally with LPJ-GUESS (v4.0, R10285)”. In: *Geosci. Model Dev.* 15.2, pp. 815–839. ISSN: 1991-959X. DOI: 10.5194/gmd-15-815-2022. (Visited on 02/18/2022).
- Marschner, H., M. Häussling, and E. George (1991). “Ammonium and Nitrate Uptake Rates and Rhizosphere pH in Non-Mycorrhizal Roots of Norway Spruce [*Picea Abies* (L.) Karst.]” In: *Trees* 5.1, pp. 14–21. ISSN: 1432-2285. DOI: 10.1007/BF00225330. (Visited on 12/05/2023).
- Meyer, D. R. and A. J. Anderson (1959). “Temperature and Symbiotic Nitrogen Fixation”. In: *Nature* 183.4653, pp. 61–61. ISSN: 1476-4687. DOI: 10.1038/183061a0. (Visited on 04/26/2024).
- Montañez, A., S. K. A. Danso, and G. Hardarson (1995). “The Effect of Temperature on Nodulation and Nitrogen Fixation by Five *Bradyrhizobium Japonicum* Strains”. In: *Applied Soil Ecology* 2.3, pp. 165–174. ISSN: 0929-1393. DOI: 10.1016/0929-1393(95)00052-M. (Visited on 04/26/2024).
- Moss, B. (2007). “Water Pollution by Agriculture”. In: *Philos. Trans. R. Soc. B Biol. Sci.* 363.1491, pp. 659–666. DOI: 10.1098/rstb.2007.2176. (Visited on 05/31/2023).
- Müller, C., E. Stehfest, J. G. van Minnen, B. Strengers, W. von Bloh, A. H. W. Beusen, S. Schaphoff, T. Kram, and W. Lucht (2016). “Drivers and Patterns of Land Biosphere Carbon Balance Reversal”. In: *Environ. Res. Lett.* 11.4, p. 044002. ISSN: 1748-9326. DOI: 10.1088/1748-9326/11/4/044002. (Visited on 05/31/2023).
- Northup, B. K. and S. C. Rao (2016). “Effects of Legume Green Manures on Forage Produced in Continuous Wheat Systems”. In: *Agron. J.* 108.1, pp. 101–108. ISSN: 1435-0645. DOI: 10.2134/agronj15.0031. (Visited on 05/31/2023).
- Ostberg, S., C. Müller, J. Heinke, and S. Schaphoff (2023). “LandInG 1.0: A Toolbox to Derive Input Datasets for Terrestrial Ecosystem Modelling at Variable Resolutions from Heterogeneous Sources”. In: *Geosci. Model Dev.* 16.11, pp. 3375–3406. ISSN: 1991-959X. DOI: 10.5194/gmd-16-3375-2023. (Visited on 09/05/2023).
- Patterson, T. G. and T. A. Larue (1983). “Root Respiration Associated with Nitrogenase Activity (C<sub>2</sub>H<sub>2</sub>) of Soybean, and a Comparison of Estimates 1”. In: *Plant Physiology* 72.3, pp. 701–705. ISSN: 0032-0889. DOI: 10.1104/pp.72.3.701. (Visited on 03/07/2022).
- Peoples, M. B., K. E. Giller, E. S. Jensen, and D. F. Herridge (2021). “Quantifying Country-to-Global Scale Nitrogen Fixation for Grain Legumes: I. Reliance on Nitrogen Fixation of Soybean, Groundnut and Pulses”. In: *Plant Soil* 469.1, pp. 1–14. ISSN: 1573-5036. DOI: 10.1007/s11104-021-05167-6. (Visited on 08/24/2023).
- Porwollik, V., S. Rolinski, J. Heinke, W. von Bloh, S. Schaphoff, and C. Müller (2022). “The Role of Cover Crops for Cropland Soil Carbon, Nitrogen Leaching, and Agricultural Yields – a Global Simulation Study with LPJmL (V. 5.0-Tillage-Cc)”. In: *Biogeosciences* 19.3, pp. 957–977. ISSN: 1726-4170. DOI: 10.5194/bg-19-957-2022. (Visited on 05/31/2023).

- Reay, D. S., E. A. Davidson, K. A. Smith, P. Smith, J. M. Melillo, F. Dentener, and P. J. Crutzen (2012). “Global Agriculture and Nitrous Oxide Emissions”. In: *Nature Clim Change* 2.6, pp. 410–416. ISSN: 1758-6798. DOI: 10.1038/nclimate1458. (Visited on 05/31/2023).
- Reed, S. C., C. C. Cleveland, and A. R. Townsend (2011). “Functional Ecology of Free-Living Nitrogen Fixation: A Contemporary Perspective”. In: *Annu. Rev. Ecol. Evol. Syst.* 42.1, pp. 489–512. DOI: 10.1146/annurev-ecolsys-102710-145034. (Visited on 05/31/2023).
- Xu-Ri and I. C. Prentice (2017). “Modelling the Demand for New Nitrogen Fixation by Terrestrial Ecosystems”. In: *Biogeosciences* 14.7, pp. 2003–2017. ISSN: 1726-4170. DOI: 10.5194/bg-14-2003-2017. (Visited on 05/26/2023).
- Rousk, K., P. L. Sorensen, and A. Michelsen (2018). “What Drives Biological Nitrogen Fixation in High Arctic Tundra: Moisture or Temperature?” In: *Ecosphere* 9.2, e02117. ISSN: 2150-8925. DOI: 10.1002/ecs2.2117. (Visited on 04/26/2024).
- Ryle, G. J. A., C. E. Powell, and A. J. Gordon (1979). “The Respiratory Costs of Nitrogen Fixation in Soyabean, Cowpea, and White Clover: I. Nitrogen Fixation and the Respiration of the Nodulated Root”. In: *Journal of Experimental Botany* 30.1, pp. 135–144. ISSN: 0022-0957. DOI: 10.1093/jxb/30.1.135. (Visited on 03/07/2022).
- Salvagiotti, F., K. G. Cassman, J. E. Specht, D. T. Walters, A. Weiss, and A. Dobermann (2008). “Nitrogen Uptake, Fixation and Response to Fertilizer N in Soybeans: A Review”. In: *Field Crops Research* 108.1, pp. 1–13. ISSN: 0378-4290. DOI: 10.1016/j.fcr.2008.03.001. (Visited on 04/26/2024).
- Schaphoff, S., U. Heyder, S. Ostberg, D. Gerten, J. Heinke, and W. Lucht (2013). “Contribution of Permafrost Soils to the Global Carbon Budget”. In: *Environ. Res. Lett.* 8.1, p. 014026. ISSN: 1748-9326. DOI: 10.1088/1748-9326/8/1/014026. (Visited on 05/31/2023).
- Schaphoff, S., W. von Bloh, A. Rammig, K. Thonicke, H. Biemans, M. Forkel, D. Gerten, J. Heinke, J. Jägermeyr, J. Knauer, F. Langerwisch, W. Lucht, C. Müller, S. Rolinski, and K. Waha (2018). “LPJmL4 – a Dynamic Global Vegetation Model with Managed Land – Part 1: Model Description”. In: *Geosci. Model Dev.* 11.4, pp. 1343–1375. ISSN: 1991-959X. DOI: 10.5194/gmd-11-1343-2018. (Visited on 05/31/2023).
- Scheer, C., K. Fuchs, D. E. Pelster, and K. Butterbach-Bahl (2020). “Estimating Global Terrestrial Denitrification from Measured N<sub>2</sub>O:(N<sub>2</sub>O+N<sub>2</sub>) Product Ratios”. In: *Current Opinion in Environmental Sustainability*. Climate Change, Reactive Nitrogen, Food Security and Sustainable Agriculture 47, pp. 72–80. ISSN: 1877-3435. DOI: 10.1016/j.cosust.2020.07.005. (Visited on 04/30/2024).
- Serraj, R., T. R. Sinclair, and L. C. Purcell (1999). “Symbiotic N<sub>2</sub> Fixation Response to Drought”. In: *Journal of Experimental Botany* 50.331, pp. 143–155. ISSN: 0022-0957. DOI: 10.1093/jxb/50.331.143. (Visited on 04/26/2024).
- Soper, F. M., B. N. Taylor, J. B. Winbourne, M. Y. Wong, K. A. Dynarski, C. R. G. Reis, M. B. Peoples, C. C. Cleveland, S. C. Reed, D. N. L. Menge, and S. S. Perakis (2021). “A Roadmap for Sampling and Scaling Biological Nitrogen Fixation in Terrestrial Ecosystems”. In: *Methods Ecol. Evol.* 12.6, pp. 1122–1137. ISSN: 2041-210X. DOI: 10.1111/2041-210X.13586. (Visited on 08/24/2023).
- Stenzel, F., J. Braun, J. Breier, K. Erb, D. Gerten, J. Heinke, S. Matej, S. Ostberg, S. Schaphoff, and W. Lucht (2023). “Biospheremetrics v1.0.1: An R Package to Calculate Two Complementary Terrestrial Biosphere Integrity Indicators: Human Colonization of the Biosphere (BioCol) and Risk of Ecosystem Destabilization (EcoRisk)”. In: *EGUsphere*, pp. 1–36. DOI: 10.5194/egusphere-2023-2503. (Visited on 11/03/2023).
- Sutton, M. A., A. Bleeker, C. M. Howard, M. Bekunda, B. Grizzetti, W. de Vries, H. J. M. van Grinsven, Y. P. Abrol, T. K. Adhya, G. Billen, E. A. Davidson, A. Datta, R. Diaz, J. W. Erisman, X. J. Liu, O. Oenema, C. Palm, N. Raghuram, S. Reis, R. W. Scholz, T. Sims, H. Westhoek, and F. S. Zhang (2013). *Our Nutrient World: The Challenge to Produce More Food and Energy with Less Pollution*. Edinburgh: NERC/Centre for Ecology & Hydrology. ISBN: 978-1-906698-40-9. (Visited on 11/15/2023).
- Taylor, B. N., R. L. Chazdon, and D. N. L. Menge (2019). “Successional Dynamics of Nitrogen Fixation and Forest Growth in Regenerating Costa Rican Rainforests”. In: *Ecology* 100.4, e02637. ISSN: 1939-9170. DOI: 10.1002/ecy.2637. (Visited on 11/07/2023).
- Thornley, J. H. M., J. Bergelson, and A. J. Parsons (1995). “Complex Dynamics in a Carbon-Nitrogen Model of a Grass-Legume Pasture”. In: *Annals of Botany* 75.1, pp. 79–84. ISSN: 0305-7364. DOI: 10.1016/S0305-7364(05)80012-5. (Visited on 11/07/2023).
- Tian, H., G. Chen, C. Lu, X. Xu, D. J. Hayes, W. Ren, S. Pan, D. N. Huntzinger, and S. C. Wofsy (2015). “North American Terrestrial CO<sub>2</sub> Uptake Largely Offset by CH<sub>4</sub> and N<sub>2</sub>O Emissions: Toward a Full Accounting of the Greenhouse Gas Budget”. In: *Climatic Change* 129.3, pp. 413–426. ISSN: 1573-1480. DOI: 10.1007/s10584-014-1072-9. (Visited on 06/14/2024).
- Tian, H., R. Xu, J. G. Canadell, R. L. Thompson, W. Winiwarter, P. Suntharalingam, E. A. Davidson, P. Ciais, R. B. Jackson, G. Janssens-Maenhout, M. J. Prather, P. Regnier, N. Pan, S. Pan, G. P. Peters, H. Shi, F. N. Tubiello, S. Zaehle, F. Zhou, A. Arneth, G. Battaglia, S. Berthet, L. Bopp, A. F. Bouwman, E. T. Buitenhuis, J. Chang, M. P. Chipperfield, S. R. S. Dangal, E. Dlugokencky, J. W. Elkins, B. D. Eyre, B. Fu, B. Hall, A. Ito, F. Joos, P. B. Krummel, A. Landolfi, G. G. Laruelle, R. Lauerwald, W. Li, S. Lienert, T. Maavara, M. MacLeod, D. B. Millet, S. Olin, P. K. Patra, R. G. Prinn, P. A. Raymond, D. J. Ruiz, G. R. van der Werf, N. Vuichard, J. Wang, R. F. Weiss, K. C. Wells, C. Wilson, J. Yang, and Y. Yao (2020). “A Comprehensive Quantification of Global Nitrous Oxide Sources and Sinks”. In: *Nature* 586.7828, pp. 248–256. ISSN: 1476-4687. DOI: 10.1038/s41586-020-2780-0. (Visited on 11/15/2023).
- Tian, H., J. Yang, R. Xu, C. Lu, J. G. Canadell, E. A. Davidson, R. B. Jackson, A. Arneth, J. Chang, P. Ciais, S. Gerber, A. Ito, F. Joos, S. Lienert, P. Messina, S. Olin, S. Pan, C. Peng, E. Saikawa, R. L. Thompson, N. Vuichard, W. Winiwarter, S. Zaehle, and B. Zhang (2019). “Global Soil Nitrous Oxide Emissions since the Preindustrial Era Estimated by an Ensemble

- of Terrestrial Biosphere Models: Magnitude, Attribution, and Uncertainty”. In: *Glob. Change Biol.* 25.2, pp. 640–659. ISSN: 1365-2486. DOI: 10.1111/gcb.14514. (Visited on 11/15/2023).
- Valentine, A. J., V. A. Benedito, and Y. Kang (2018). “Legume Nitrogen Fixation and Soil Abiotic Stress: From Physiology to Genomics and Beyond”. In: *Annual Plant Reviews Online*. John Wiley & Sons, Ltd. Chap. 9, pp. 207–248. ISBN: 978-1-119-31299-4. DOI: 10.1002/9781119312994.apr0456. (Visited on 04/26/2024).
- Vitousek, P. M. (1984). “Litterfall, Nutrient Cycling, and Nutrient Limitation in Tropical Forests”. In: *Ecology* 65.1, pp. 285–298. ISSN: 1939-9170. DOI: 10.2307/1939481. (Visited on 12/05/2023).
- Voisin, A. S., C. Salon, C. Jeudy, and F. R. Warembourg (2003). “Symbiotic N<sub>2</sub> Fixation Activity in Relation to C Economy of *Pisum Sativum* L. as a Function of Plant Phenology”. In: *Journal of Experimental Botany* 54.393, pp. 2733–2744. ISSN: 0022-0957. DOI: 10.1093/jxb/erg290. (Visited on 04/26/2024).
- von Bloh, W., S. Schaphoff, C. Müller, S. Rolinski, K. Waha, and S. Zaehle (2018). “Implementing the Nitrogen Cycle into the Dynamic Global Vegetation, Hydrology, and Crop Growth Model LPJmL (Version 5.0)”. In: *Geosci. Model Dev.* 11.7, pp. 2789–2812. ISSN: 1991-959X. DOI: 10.5194/gmd-11-2789-2018. (Visited on 05/31/2023).
- Wirth, S. B., C. Müller, W. von Bloh, S. Schaphoff, and S. Rolinski (2023). “Model Code for LPJmL5.7.9-Ccostly-Bnf”. In: DOI: 10.5281/zenodo.10257030. (Visited on 12/07/2023).
- Wu and McGechan (1999). “Simulation of Nitrogen Uptake, Fixation and Leaching in a Grass/White Clover Mixture”. In: *Grass Forage Sci.* 54.1, pp. 30–41. ISSN: 1365-2494. DOI: 10.1046/j.1365-2494.1999.00145.x. (Visited on 05/30/2024).
- Yang, J. and H. Tian (2020). *ISIMIP3b N-deposition Input Data (v1.0)*. DOI: 10.48364/ISIMIP.600567. (Visited on 09/05/2023).
- Yao, Y., B. Han, X. Dong, Y. Zhong, S. Niu, X. Chen, and Z. Li (2024). “Disentangling the Variability of Symbiotic Nitrogen Fixation Rate and the Controlling Factors”. In: *Glob. Change Biol.* 30.3, e17206. ISSN: 1365-2486. DOI: 10.1111/gcb.17206. (Visited on 04/26/2024).
- Yu, T. and Q. Zhuang (2020). “Modeling Biological Nitrogen Fixation in Global Natural Terrestrial Ecosystems”. In: *Biogeosciences* 17.13, pp. 3643–3657. ISSN: 1726-4170. DOI: 10.5194/bg-17-3643-2020. (Visited on 02/18/2022).
- Zaehle, S., A. D. Friend, P. Friedlingstein, F. Dentener, P. Peylin, and M. Schulz (2010). “Carbon and Nitrogen Cycle Dynamics in the O-CN Land Surface Model: 2. Role of the Nitrogen Cycle in the Historical Terrestrial Carbon Balance”. In: *Global Biogeochem. Cycles* 24.1, GB1006. ISSN: 1944-9224. DOI: 10.1029/2009GB003522. (Visited on 03/12/2018).
- Zhang, X., T. Zou, L. Lassaletta, N. D. Mueller, F. N. Tubiello, M. D. Lisk, C. Lu, R. T. Conant, C. D. Dorich, J. Gerber, H. Tian, T. Bruulsema, T. M. Maaz, K. Nishina, B. L. Bodirsky, A. Popp, L. Bouwman, A. Beusen, J. Chang, P. Havlík, D. Leclère, J. G. Canadell, R. B. Jackson, P. Heffer, N. Wanner, W. Zhang, and E. A. Davidson (2021). “Quantification of Global and National Nitrogen Budgets for Crop Production”. In: *Nat Food* 2.7, pp. 529–540. ISSN: 2662-1355. DOI: 10.1038/s43016-021-00318-5. (Visited on 11/15/2023).

# Chapter 5

## Global grassland productivity and carbon storage benefit from functional diversity already under moderate climate change

Stephen B. Wirth<sup>1,2</sup>, Christoph Müller<sup>1</sup>, Friedhelm Taube<sup>2</sup>, Jens Heinke<sup>1</sup>, Britta Tietjen<sup>3,4</sup> and Susanne Rolinski<sup>1</sup>

<sup>1</sup>Potsdam Institute for Climate Impact Research (PIK), Member of the Leibniz Association, P.O. Box 60 12 03, 14412 Potsdam, Germany

<sup>2</sup>Institute of Crop Science and Plant Breeding, Grass and Forage Science/Organic Agriculture, Kiel University, Hermann-Rodewald-Str. 9, 24118, Kiel, Germany

<sup>3</sup>Freie Universität Berlin, Institute of Biology, Theoretical Ecology, Königin-Luise-Str. 2/4 Gartenhaus, 14195 Berlin, Germany

<sup>4</sup>Berlin-Brandenburg Institute of Advanced Biodiversity Research (BBIB), D-14195 Berlin, Germany

Status: In preparation

---

**Abstract:** Field experiments have provided extensive evidence that functional diversity plays an important role for ecosystem services of managed grasslands such as their gross primary productivity (GPP) and soil organic carbon (SOC) stocks. Despite extensive empirical research, the application of vegetation models has been limited to assess the role of functional diversity at small spatial scales.

We used the Lund-Potsdam-Jena managed land (LPJmL) competitor stress-tolerant ruderal (CSR) model to assess the role of functional diversity in managed grassland GPP and SOC under climate change at the global scale. LPJmL-CSR simulates functional diversity using plant functional types to represent different ecological strategies based on functional traits connected to CSR strategies. The model was calibrated and evaluated against historical data on CSR shares of plant communities and GPP. Subsequently, we performed simulation experiments assuming low and high functional diversity levels and moderate and strong climate change.

Our results show that functional diversity plays an important role for managed grassland GPP and SOC stocks already under moderate climate change. A strong loss of functional diversity prohibits communities' adaptation to climate change, resulting in loss of GPP and SOC. Furthermore, spatial patterns of GPP and SOC stocks show substantial differences between the low and high functional diversity scenarios and depend on regional conditions. For GPP, the spatial patterns show a loss of up to 40% in the low functional diversity scenario in large areas but also an increase of up to 20% in other areas. For example, in North and South Carolina, increasing temperatures

lead to an increasing competitiveness for C4 plants and a change in community composition.

Generally, our results are consistent with empirical findings and support the importance of functional diversity as an insurance against climate change. To our knowledge, this is the first global-scale assessment, and it shows once more that preventing the loss of functional diversity is crucial for many livelihoods and underpins the need for the development and application of management practices that support the functional diversity of managed grasslands.

---

## 5.1 Introduction

Approximately 40% of the terrestrial ice-free Earth surface is covered by grassland ecosystems (White et al., 2000) which provide important ecosystem services supporting the livelihoods of at least a billion people (Suttie et al., 2005). However, as a consequence of too intensive use as well as land-use abandonment, already today grassland ecosystems are at risk of degradation which will likely increase under climate change (Prangel et al., 2023; Yan et al., 2023). Additionally, climate change may increase grassland ecosystems' vulnerability to overgrazing and ecosystem services may decline (Lee et al., 2021). To prevent further grassland degradation, management adaptations need to be developed based on improved understanding of the processes underpinning ecosystem service provisioning. Climatic conditions, soil health and management are all important factors for grassland ecosystem services. Temperature, soil water and nutrient availability directly control the amount of carbon grassland ecosystems can assimilate. While management in the form of irrigation or fertilizer application can be used to increase carbon assimilation by reducing water or nutrient stress, grazing or mowing reduces above-ground biomass (Bai and Cotrufo, 2022; Conant et al., 2017). However, the effect of grazing or mowing on carbon assimilation is complex. Although low to intermediate grazing or mowing intensities can have a positive effect on above-ground biomass, for example through the reduction of inter- and intraspecific competition for space and light and self-shading, higher intensities lead to a decline of above-ground biomass and ecosystem carbon assimilation in the long term (e.g., McSherry and Ritchie, 2013; Wang et al., 2022b) assuming the removed biomass is used as feed for livestock. In addition to climatic, soil and management conditions, the functional diversity of a grassland ecosystem also contributes to ecosystem service provision in rainfed and unfertilised grasslands and has been discussed as a means to increase resilience and/or resistance against climate change impacts (Hoover et al., 2014; Isbell et al., 2015).

The role of functional diversity has been extensively researched at small spatial scales using field experiments and observations (e.g. Buzhdygan et al., 2020; Pasari et al., 2013; Tilman et al., 2001) and synthesised in meta-analyses (e.g. Brose and Hillebrand, 2016; Cheng et al., 2024). At the local to landscape scales the role of functional diversity has also been incorporated into simulation models. Individual-based models such as GRASSMIND (e.g. Taubert et al., 2012; Taubert et al., 2020),

IBC-grass (e.g. Reeg et al., 2018; Reeg et al., 2020) or aDGVM2 (e.g. Pfeiffer et al., 2019; Scheiter et al., 2023) simulate functional diversity via competition between individual plants for which key functional traits are sampled from a distribution. Such models have successfully been applied to simulate the importance of functional diversity for several ecosystem services under different climatic and management conditions. While these studies provide important insight and advance research on universal relationships explaining observed benefits of functional diversity (Crawford et al., 2021), large- or global-scale studies that quantify the role of functional diversity in global grassland ecosystem services have not been conducted. For such large-scale analyses, dynamic global vegetation models (DGVMs) are widely applied. However, functional diversity of managed grasslands is not represented in state-of-the-art DGVMs despite the extent of grassland areas.

DGVMs are widely applied to study the effect of climate change on vegetation dynamics and the carbon cycle (e.g. Cramer et al., 2001; Liu et al., 2021). Historically, DGVMs have represented vegetation using the concept of plant functional types (PFTs) neglecting functional diversity. While tree PFTs are at least distinguished via different leaf types and phenology, grasslands are usually simulated using a single PFT for a specific climate. However, this implies the assumption that only environmental conditions and management control grassland productivity, neglecting the role of functional diversity.

Recently, the LPJmL model (Lutz et al., 2019; Schaphoff et al., 2018; von Bloh et al., 2018; Wirth et al., 2024a) has been extended to simulate grassland functional diversity based on CSR theory (Grime, 1974). The CSR theory distinguishes three main ecological strategies. The competitive (C) strategy is associated with efficient resource use, fast growth and low tolerance towards stress. The stress-tolerant (S) strategy is associated with investment into more expensive but robust tissue, slow growth and high stress tolerance. The ruderal (R) strategy is associated with a rapid growth in periods of favourable conditions between disturbances during which it completes its life cycle. As a consequence, it has a high disturbance tolerance but no stress tolerance. Intermediate strategies that show characteristics of several of the main strategies also exist. While the CSR theory by itself is not a representation of functional diversity, it has been connected to the global spectrum of plant form and function through functional traits (Pierce et al., 2013). Representing these functional traits as model parameters enables the LPJmL-CSR model to simulate key trade-offs present in the global spectrum of plant form and function (Díaz et al., 2016) reduced to the differences between strategies described by CSR theory. LPJmL-CSR was extended by a C-, S- and R-PFT to represent the three main strategies of the CSR theory. Intermediate strategies are not explicitly considered and are only reflected in the resulting mixture of the C-, S- and R-PFTs. LPJmL-CSR enables climate change impact assessments that explicitly consider grassland functional diversity to quantify its role for future grassland ecosystem services.

We limit our scope to two highly studied ecosystem services of grasslands, the gross primary productivity (GPP), which is important for the forage supply of grazing animals, and the soil organic carbon

(SOC) stock, which contributes to climate change mitigation. Environmental conditions and management are the key drivers of both productivity and SOC storage, but functional diversity is crucial as well (e.g. Cardinale et al., 2012; Tilman et al., 2001). Important factors controlling productivity and SOC dynamics are radiation, temperature, soil water and nutrient status and the atmospheric CO<sub>2</sub> concentration. All those factors will likely be altered by climate change. For example, a reduction of the ocean carbon sink as well as an increased risk of wildfires will likely contribute to increasing atmospheric CO<sub>2</sub> concentrations in addition to anthropogenic emissions (Di Virgilio et al., 2019; Le Quéré et al., 2010). The global average radiative forcing, and in turn, temperature, as well as annual precipitation over land, are projected to increase (Lee et al., 2021). However, spatial and temporal patterns will also change and precipitation will likely decrease over large parts of the subtropics while increasing over higher latitudes (Lee et al., 2021). These changes will also affect competitive and facilitative processes in managed grassland communities.

In managed grasslands, competition for light is usually reduced via the removal of biomass from grazing or mowing and light is not strongly limiting productivity. Atmospheric CO<sub>2</sub> concentrations are rising, potentially increasing productivity and SOC stocks (Sillen and Dieleman, 2012). While high grassland productivity can be achieved at moderate temperatures and sufficient water and nutrient supply, drought and nutrient stress can severely limit productivity. High productivity leads to high biomass input into the soil through litter fall which can lead to a high SOC storage. Especially since the formation of SOC-stabilising mineral surfaces and decomposition rates are also affected by precipitation. However, this depends on the temperature, since high temperatures lead to increased microbial activity and therefore decomposition. These mechanisms and their role for grassland productivity and SOC stocks have already been modelled at large scales (e.g. Chang et al., 2021; Chang et al., 2017). However, we believe that explicitly including the role of functional diversity in such assessments will improve projections of managed grassland productivity and SOC stocks under climate change.

Using the LPJmL-CSR model, we conducted the — to our knowledge — first global assessment of the role of functional diversity in grassland productivity and SOC storage in grasslands. In our assessment, we compare a world with high and low functional diversity against each other to quantify the role of functional diversity. We focus our assessment on trends and spatial patterns of productivity and SOC stocks globally and in exemplary regions that showcase prominent differences to answer the following research questions:

- To what extent does functional diversity contribute to the world's grassland productivity and SOC stocks under climate change?
- How does the presence or absence of functional diversity shape the main spatial patterns and regional differences of grassland productivity and SOC stocks?

- How do the model results compare to empirical findings on the role of functional diversity in different regions of the world?

## 5.2 Methods

To address our research questions, we used the global vegetation model LPJmL-CSR under different functional diversity settings. However, LPJmL-CSR has only been applied at the local scale so far (Wirth et al., 2024b). To enable LPJmL-CSR to run at the global scale, a calibration was necessary. After calibration to and evaluation against remote sensing data on GPP and C-, S- and R-PFT foliage projective cover (FPC), we simulated three different functional diversity scenarios using climate projections from five general circulation models (GCMs) for two forcing scenarios. Scenario names follow the conventions described in O'Neill et al. (2016) and are a combination of a shared socioeconomic pathway (SSP) and a radiative forcing. We use the SSP1-2.6 and SSP3-7.0 scenarios.

### 5.2.1 LPJmL-CSR

A detailed description of LPJmL is provided in previously published work. These include a detailed description of all model components with emphasis on the carbon cycle (Schaphoff et al., 2018), the description of the nitrogen cycle implementation (von Bloh et al., 2018; Wirth et al., 2024a), the livestock module (Heinke et al., 2023) and the representation of CSR strategies in managed grasslands (Wirth et al., 2024b). Therefore, we only give a brief qualitative overview of the relevant parts here.

LPJmL simulates the terrestrial carbon and nitrogen cycles of natural and managed vegetation. The daily computation of the gross primary production (GPP) from photosynthesis is at the core of the model. This computation accounts for the co-limitation of temperature, radiation, water and nutrient availability. Natural vegetation is represented by eight tree and three grass PFTs. While managed grasslands are represented using the same three grass PFTs in LPJmL (Schaphoff et al., 2018; von Bloh et al., 2018), in LPJmL-CSR additional grass PFTs were introduced (Wirth et al., 2024b). For this study, we calibrated parameters for three tropical, three temperate and three polar grass PFTs. These PFTs are allowed to be established within predefined bioclimatic limits to ensure that, for example, tropical PFTs do not grow in polar climates. Due to overlap of the bioclimatic limits, up to six PFTs can be established per grid cell. Together, the established PFTs form communities that differ in their functional diversity. We use the presence of different strategies and their community share to infer information on the role of functional diversity. If only one strategy is present, the functional diversity is low. In contrast, if all strategies are present, the functional diversity is high. When multiple strategies are present but one is strongly dominant, functional diversity is less important at that point in time. However, if multiple strategies are present, community composition may adapt over time, making functional diversity important for the

long-term performance of the community. In our simulation experiments (see 5.2.4), we aim to quantify such effects by artificially reducing functional diversity.

In LPJmL and LPJmL-CSR, grass PFTs are represented using leaf and root biomass stocks. The following daily processes determine the vegetation and soil biomass stocks of managed grasslands: (i) Carbon assimilation from photosynthesis to obtain GPP, (ii) autotrophic respiration to obtain the net primary productivity (NPP), (iii) transfer of leaf and root tissue to the litter layer, (iv) allocation of NPP to leaf and root biomass stocks and potentially (v) livestock grazing or mowing. The amount of photosynthesis, litter fall and grazing or harvest is determined depending on PFT-specific parameters – which are inferred from functional traits, environmental conditions and management. A full overview of PFT-specific parameters is given in the studies listed above. For LPJmL-CSR several parameters (Tab. 5.1) were adjusted during calibration (see 5.2.3).

For this study, we combined the implementation of CSR strategies (Wirth et al., 2024b) with the livestock module (Heinke et al., 2023) which required the introduction of a factor to account for grazing avoidance of the different strategies. This factor is used to adjust the carbon intake from each PFT so that the C-PFT, which follows a grazing tolerance and not an avoidance strategy (Briske, 1986; Stuart-Hill and Mentis, 1982), is grazed more heavily compared to the S- and R-PFT that follow a grazing avoidance strategy (Eq. 5.1).

$$f_{grazed,t,PFT} = \frac{C_{in,t} \cdot f_{avoid,PFT} \cdot C_{leaf,t,PFT}}{\sum_{p=1}^{NPFT} C_{leaf,t,PFT_p} \cdot f_{avoid,PFT_p}} \quad (5.1)$$

$f_{grazed,t,PFT}$  is the share of total carbon intake of a PFT at time step  $t$ ,  $C_{in}$  is the total carbon intake,  $f_{avoid,PFT}$  is the PFT-specific unitless avoidance factor,  $C_{leaf,PFT}$  is the PFT-specific leaf carbon in  $\text{gC m}^{-2}$  and  $NPFT$  is the number of established PFTs. This ensures that the total carbon intake remains as derived by Eq. 27 from Heinke et al., 2023. However, due to the different carbon-to-nitrogen ratios of the different PFTs, the total nitrogen intake may differ. As a consequence, the nitrogen allocated to faeces, carbon and nitrogen allocated to milk and urine and carbon respired are adjusted following Eqs. 42, 43, 48, 50 and 53 in Heinke et al., 2023.

## 5.2.2 Calibration and evaluation data

We calibrated the model using global data on grassland GPP and community share of C-, S- and R-PFTs, which had to be processed (Fig. 5.1).

### 5.2.2.1 GPP

We used a publicly available global remote sensing product for GPP (Zhang et al., 2017). This product contains total monthly GPP data ( $GPP_{tot}$ ) from 2000 to 2016 for  $0.05^\circ \times 0.05^\circ$  grid cells. To ob-

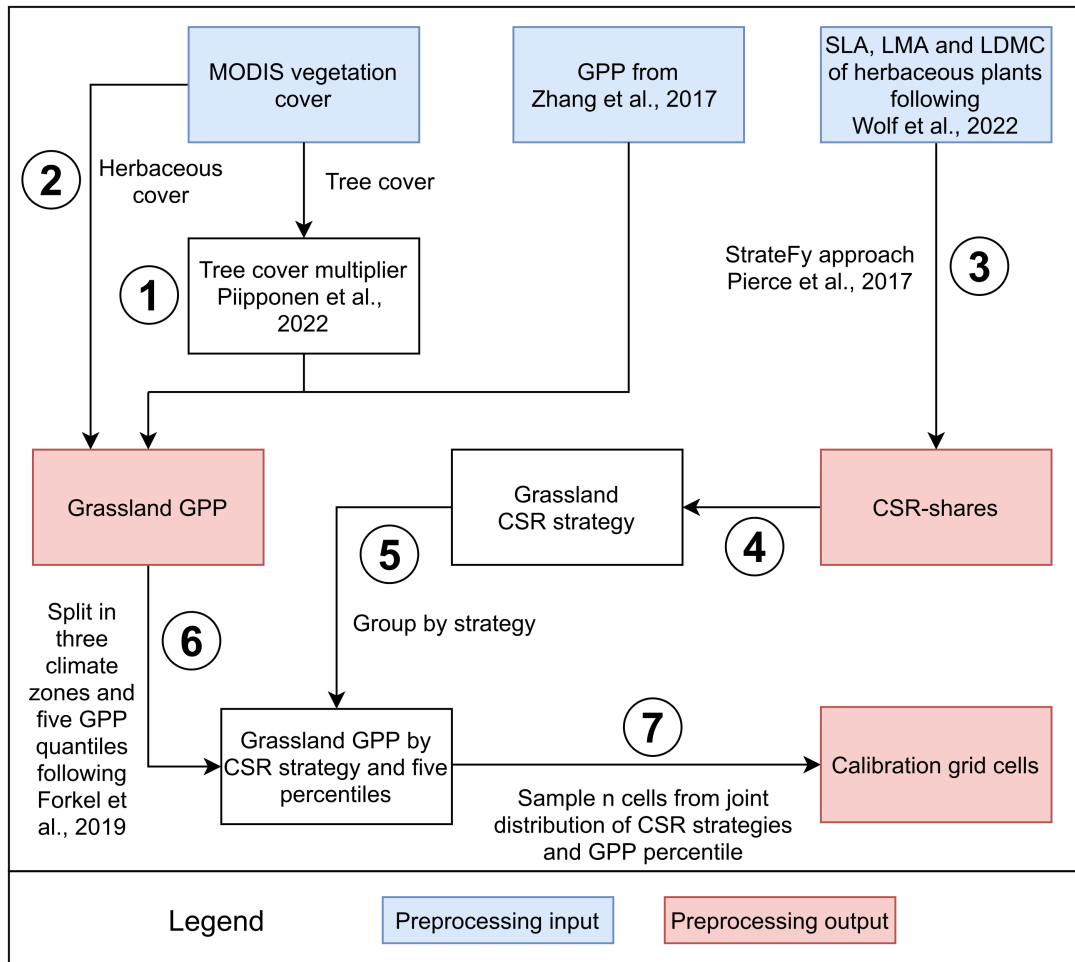


Figure 5.1: Overview of processing steps to prepare the calibration data and selection of grid cell subset for calibration. All data have a global coverage and a  $0.05^\circ$  by  $0.05^\circ$  resolution. Coloured boxes highlight preprocessing input (blue), temporal data of intermediate steps (white) and output data (red). Arrows show the information flow from input to output data and numbers reference specific steps described in 5.2.2 and 5.2.3

tain grassland GPP ( $GPP_{herb}$ ) we had to account for tree cover and scaled the resulting values to the grassland fraction for each grid cell (Eq. 5.2 and Fig. 5.1 1).

$$GPP_{herb} = GPP_{tot} \cdot s_{tree} / f_{grassland} \quad (5.2)$$

$s_{tree}$  is a tree cover multiplier (Eq. 5.3), calculated from annual MODIS MCD12C1 tree cover data from 2001 to 2016 at a spatial resolution of  $0.05^\circ$  by  $0.05^\circ$  (Friedl and Sulla-Menashe, Damien, 2015) following the approach of (Piipponen et al., 2022).

$$s_{tree} = \exp(-4.45521 \cdot f_{tree}) \quad (5.3)$$

Eq. (5.3) is an empirical relationship between tree cover ( $f_{tree}$ ) and the total productivity of this tree cover and needs to be used to account for the different productivity levels of woody and herbaceous vegetation.  $f_{grassland}$  is the fraction of the area not covered by trees from the same product and is used to scale herbaceous GPP to the entire grid cell to make it compatible with LPJmL (Fig. 5.1 2). We used the annual data to scale each monthly GPP value. Because data for 2000 were not available within MODIS MCD12C1, we assumed the tree cover of 2001 for 2000.

Afterwards, we aggregated  $GPP_{herb}$  to  $0.5^\circ$  by  $0.5^\circ$  because this is the resolution at which LPJmL-CSR was run. We weighted each  $0.5^\circ$  by  $0.5^\circ$  grid cell using its area fraction of the  $0.5^\circ$  by  $0.5^\circ$  grid cell (Eq. 5.4).

$$GPP_{herb,0.5,i} = \sum_{j=1}^{100} w_j \cdot GPP_{herb,j} \quad (5.4)$$

with  $w_j = A_j/A_i$ . Fig. D.1 show the time series average  $GPP_{herb}$  and the 5th to 95th percentile range.

### 5.2.2.2 Community share of the C-, S- and R-PFTs

To obtain the community share for C-, S- and R-PFTs, we combined global trait maps of SLA, leaf mass per area (LMA) and leaf dry matter content (LDMC) at a spatial resolution of  $0.5^\circ$  by  $0.5^\circ$  obtained from (Wolf et al., 2022) with the StrateFy approach (Pierce et al., 2017, Fig. 5.1 3). The StrateFy approach is described in detail in Pierce et al. (2017) and can be used to calculate the C, S and R shares of a species or community from SLA, LMA and LDMC data. Pierce et al. (2017) developed the StrateFy approach using TRY data (Kattge et al., 2020) which also provided the basis for the trait estimation of the algorithm used by Wolf et al., 2022. Global trait maps are obtained by combining citizen science data from iNaturalist provided by the Global Biodiversity Information Facility (GBIF) database (iNaturalist, 2024), with trait data from TRY using a convolutional neural network approach (Schiller et al., 2021; Wolf et al., 2022). The convolutional neural networks are trained to recognize

plant traits from morphological features present in photographic images of plants and the approach is described in detail in Schiller et al. (2021). Fig. D.2 shows the C, S and R share for each grid cell obtained using the median, average, 5th or 95th percentile trait estimates. We assumed the median estimates to represent the share of the C, S and R strategy. In LPJmL-CSR the community share is represented using the foliage projective cover (FPC).

### 5.2.3 Model calibration and evaluation

We calibrated LPJmL-CSR against the GPP and the community share of the C-, S- and R-PFT (5.2.2). For both variables we calculate a cost described in the following using simulation results from 2000 to 2016, matching the time period of the GPP data. Because the community share of the C-, S- and R-PFT data are only available for one year, we use the average from 2000 to 2016.

We calibrated LPJmL-CSR using a genetic optimization (GENOUD, Mebane Jr. and Sekhon, 2011) algorithm which is the basis for a model-data integration (MDI) approach for LPJmL implemented in the LPJmLMDI R package (Forkel et al., 2014). The approach is described in more detail in Forkel et al. (2014) and Forkel et al. (2019). LPJmLMDI calculates a cost based on the Kling-Gupta efficiency (KGE, Gupta and Kling, 2011) for each calibration variable  $d$  to evaluate the model fit compared to observations.

$$Cost = \sqrt{\sum_{d=1}^N \left( \left( \frac{\bar{s}_d}{\bar{o}_d} - 1 \right)^2 + \left( \frac{\sigma_{s,d}}{\sigma_{o,d}} - 1 \right)^2 + (r(s_d, o_d) - 1)^2 \right)} \quad (5.5)$$

$\bar{s}$  and  $\bar{o}$  are the spatial (grid cells) and temporal (years) mean values of the simulations  $s$  and the observations  $o$ , respectively, and represent the bias component in the KGE computation. The variance component is represented by  $\sigma$ , which is the variance, and the correlation component is represented by  $r$ , which is the Pearson correlation coefficient (both over space and time) (Forkel et al., 2014). Each of the components was weighted by the uncertainty of the observations to account for spatio-temporal uncertainty in the cost function. The algorithm is initialised by sampling a preset number (generation) of individual parameters sets (individuals) from a multivariate normal distribution reflecting the parameter space. After each individual parameter set has been evaluated, a new generation is initialised considering the divergence between simulation and observations of the previous generations. For details of how GENOUD derives the parameter sets for generations following the initial generation we refer to Sekhon and Jr, 1998. For each climate zone (tropical, temperate, polar), we sampled 64 grid cells from the joined distribution of grassland GPP and CSR strategy (Fig. 5.1 4 to 7). First, we grouped the community shares of the C-, S- and R-PFTs into 19 strategies (C, C/CR, C/CS, CR, C/CSR, CS, CR/CSR, CS/CSR, R/CR, CSR, S/CS, R/CSR, S/CSR, R, SR/CSR, S, R/SR, S/SR and SR), which are based on the thresholds for C, S, and R shares defined by Pierce et al. (2017, Fig. 5.1 4). Second, we assign each

GPP value the respective CSR strategy derived in Fig. 5.1 4 (Fig. 5.1 5). Third, we divide the GPP data into five equidistant intervals based on the level of productivity (very low, low, medium, high, very high) for each of the three climate zones (tropical, temperate and polar) (Fig.5.1 6). Finally, we sample 64 grid cells from each climate zone (Fig. 5.1 7). While we subset the data to only contain grid cells where the data on historical grassland fractions by Ostberg et al. (2023) contain managed grassland for the evaluation and our scenario analysis, for calibration, we sample from all grid cells. This results in a broader distribution of GPP and community shares of the C-, S- and R-PFTs for the sampled grid cells and maximises domain to which the calibration results are applicable. We included 16 PFT-specific parameters that relate to the difference between CSR strategies to calibrate three PFTs per climate zone (Tab. 5.1). The calibration of each climate zone comprised approximately 15 generations consisting of up to 2000 individuals each.

A subset of the data of the remaining grid cells that were not used for the calibration was used for the evaluation. This subset contains only grid cells in which the data on historical grassland fractions by Ostberg et al. (2023) contain managed grassland in at least one of the years used for calibration (2000-2016). In total, community-share data for 28,767 grid cells and GPP data for 37,742 grid cells for 204 time steps (17 years times 12 months) were used for the evaluation. For the evaluation, we used the differences between simulated and observed GPP and FPC. For GPP, we evaluate the model against the monthly data and annual sums but do not aggregate the data further. Similar to the calculation of the cost function, we average the community share of the C-, S- and R-PFT simulation results from 2000 to 2016 and compare these against the observations.

#### 5.2.4 Modelling protocol

For the calibration and evaluation simulations we used the climate data from the GSWP3-W5E5 dataset (Cucchi et al., 2020; Kim, 2017; Lange et al., 2022), historical atmospheric  $\text{NO}_3^-$  and  $\text{NH}_4^+$  deposition (Yang and Tian, 2020), historical atmospheric  $\text{CO}_2$  concentrations (Büchner and Reyer, 2022) and grazing management data (Heinke, 2025).

We used the optimised parameters to simulate three different functional diversity scenarios using climate data from five general circulation models (GFDL-ESM4 Dunne et al. 2020, IPSL-CM6A-LR Boucher et al. 2020, MPI-ESM1-2-HR Gutjahr et al. 2019, MRI-ESM2-0 Yukimoto et al. 2019 and UKESM1-0-LL Meinshausen et al. 2017) and two representative forcing scenarios provided by the inter-sectoral impact model intercomparison project (ISIMIP, Lange et al., 2022). The climate data have a daily temporal resolution and spatial resolution of  $0.5^\circ$  by  $0.5^\circ$  and include average, minimum and maximum temperature, precipitation, downward short wave radiation, long wave net radiation and wind speed. Data on  $\text{CO}_2$  concentration as well as deposition of  $\text{NO}_3^-$  and  $\text{NH}_4^+$  were also available

Table 5.1: PFT-specific minimum, maximum default and optimised values for calibrated parameters.

PFT	Value	$g_{min}$	SLA	Imro	LAI <sub>sapl</sub>	$E_{max}$	k <sub>light</sub>	mort <sub>t,max</sub>	k <sub>est</sub>	k <sub>root</sub>	$V_{max,up}$	$\beta_{root}$	$C_{max,BNF}$	$K_{store}$	$N_{max,BNF}$	$f_{avoid}$
C-TrH	Minimum	0.7	0.2	0.7	0.001	6	0.4	0.09	300	0.005	4	0.9	0.004	0.05	0.01	0.5
C-TrH	Maximum	2	0.4	1.5	0.03	12	0.8	0.4	3000	0.025	6	0.98	0.08	0.3	1	1.5
C-TrH	Default	0.8	0.3	0.8	0.01	7	0.5	0.1	365	0.01	5.51	0.972	0.03	0.05	0.5	1
C-TrH	Optimized	1.15	0.377828	1.49	0.027	7.13	0.55	0.17	2604	0.0076	5.844	0.928	0.038	0.11	0.97	1.38
S-TrH	Minimum	0.3	0.01	0.3	0.009	3.5	0.4	0.05	300	0.005	4	0.9	0.004	0.05	0.01	0.5
S-TrH	Maximum	1	0.2	1	0.05	8	0.8	0.2	3000	0.025	6	0.98	0.08	0.3	1	1.5
S-TrH	Default	0.8	0.0337936	0.8	0.01	7	0.5	0.1	365	0.01	5.51	0.972	0.03	0.05	0.5	1
S-TrH	Optimized	0.36	0.19654	0.53	0.03	6.91	0.7	0.15	1807	0.023	5.24	0.915	0.04	0.14	0.08	1.22
R-TrH	Minimum	0.6	0.4	0.3	0.005	6	0.2	0.05	3000	0.005	4	0.9	0.004	0.05	0.01	0.5
R-TrH	Maximum	2	0.8	1	0.02	12	0.5	1	6000	0.025	6	0.98	0.08	0.3	1	1.5
R-TrH	Default	0.8	0.5	0.8	0.01	7	0.4	0.2	3650	0.01	5.51	0.972	0.03	0.05	0.5	1
R-TrH	Optimized	1.42	0.739233	0.9	0.016	11.67	0.4	0.19	3034	0.0091	4.99	0.933	0.045	0.16	0.43	1.42
C-TeH	Minimum	0.7	0.04	0.7	0.001	6	0.4	0.09	300	0.005	4	0.9	0.004	0.05	0.01	1
C-TeH	Maximum	2	0.14	1.5	0.05	12	0.8	0.4	3000	0.025	6	0.95	0.08	0.3	1	1.5
C-TeH	Default	0.8	0.1	0.8	0.01	7	0.5	0.1	365	0.01	5.51	0.943	0.03	0.05	0.5	1
C-TeH	Optimized	1.57	0.118976	1.3	0.034	8.69	0.52	0.29	2207	0.0084	5.79	0.906	0.019	0.08	0.91	1.43
S-TeH	Minimum	0.3	0.01	0.3	0.009	3.5	0.4	0.05	300	0.005	4	0.93	0.004	0.05	0.01	0.5
S-TeH	Maximum	1	0.04	1	0.05	8	0.7	0.2	3000	0.025	6	0.98	0.08	0.3	1	1.5
S-TeH	Default	0.8	0.0337936	0.8	0.01	7	0.5	0.1	365	0.01	5.51	0.943	0.03	0.05	0.5	1
S-TeH	Optimized	0.48	0.010082	0.39	0.035	4.13	0.43	0.19	2933	0.0097	5.85	0.962	0.045	0.19	0.77	0.84
R-TeH	Minimum	0.7	0.14	0.3	0.005	6	0.2	0.05	3000	0.005	4	0.9	0.004	0.05	0.01	0.5
R-TeH	Maximum	2	0.35	1	0.03	12	0.5	1	6000	0.025	6	0.95	0.08	0.3	1	1.5
R-TeH	Default	0.8	0.3	0.8	0.01	7	0.4	0.2	3650	0.01	5.51	0.943	0.03	0.05	0.5	1
R-TeH	Optimized	0.86	0.344874	0.33	0.016	8.3	0.28	0.81	5418	0.021	5.25	0.919	0.022	0.16	0.38	0.68
C-PoH	Minimum	0.7	0.04	0.7	0.05	6	0.4	0.09	300	0.005	4	0.9	0.004	0.05	0.01	0.5
C-PoH	Maximum	2	0.14	1.5	0.3	12	0.8	0.4	3000	0.025	6	0.95	0.08	0.3	1	1.5
C-PoH	Default	0.8	0.1	0.8	0.1	7	0.5	0.1	365	0.01	5.51	0.943	0.03	0.05	0.5	1
C-PoH	Optimized	1.16	0.75055	0.94	0.226	10.75	0.49	0.34	2047	0.013	5.09	0.932	0.03	0.11	0.5	0.7
S-PoH	Minimum	0.3	0.01	0.3	0.05	3.5	0.4	0.05	300	0.005	4	0.93	0.004	0.05	0.01	0.5
S-PoH	Maximum	1	0.04	1	0.3	8	0.8	0.2	3000	0.025	6	0.98	0.08	0.3	1	1.5
S-PoH	Default	0.8	0.03	0.8	0.1	7	0.5	0.1	365	0.01	5.51	0.943	0.03	0.05	0.5	1
S-PoH	Optimized	0.63	0.589573	0.64	0.272	5.66	0.53	0.13	2576	0.011	5.18	0.946	0.03	0.21	0.5	0.7
R-PoH	Minimum	0.6	0.14	0.3	0.05	6	0.2	0.05	3000	0.005	4	0.9	0.004	0.05	0.01	0.5
R-PoH	Maximum	2	0.35	1	0.1	12	0.5	1	6000	0.025	6	0.95	0.08	0.3	1	1.5
R-PoH	Default	0.8	0.3	0.8	0.08	7	0.4	0.2	3650	0.01	5.51	0.943	0.03	0.05	0.5	1
R-PoH	Optimized	1.45	0.726572	0.74	0.075	9.02	0.45	0.4	4415	0.0137	5.36	0.919	0.03	0.27	0.5	0.7

from ISIMIP but not per GCM. All ISIMIP datasets distinguish a historical period from 1850 to 2014 and a future period from 2015 to 2100, for which simulated data were bias-corrected to observational data products. Additionally, we used data on historical grassland fractions (Ostberg et al., 2023) and grazing management data (Heinke, 2025). Grassland fractions were only available until 2017 and we assumed the fractions to be constant for the future periods using the values for 2014 i.e., the last year of the historical period. Grazing management was kept constant for the entire simulation period. These assumptions allow us to isolate the effect of climate change and eliminate other factors that influence global output variables such as grassland expansion or reduction as well as the impacts of management change.

For all scenarios, we conducted two spin-up simulations of 3500 years with natural vegetation only and a subsequent spinup of 420 years, gradually introducing historical land use patterns (Ostberg et al., 2023). During the spin-up, climatic forcing was a random permutation of the climate data from 1901 to 1930. The first spin-up simulation ensures that the C and N balances are in an equilibrium before the beginning of anthropogenic land-use change. The second spin-up simulation captures the effects of historical land-use change on the C and N cycle. Following the two spin-up simulations, the model is run from 1850 until 2100 using the transient input data.

For the historical period, we allow all PFTs to be established so that the community composition can evolve dependent upon environmental conditions and management. For the future period, we simulate the following three scenarios:

- **FD-**: where we remove all non-dominant PFTs in each grid cell at the end of the historical period and prohibit the establishment of new PFTs.
- **FD+**: where we maintain the PFTs established (non-zero FPC) at the end of the historical period but also allow establishment of new PFTs.

## 5.3 Results

### 5.3.1 Evaluation of model performance

We evaluate model performance before (prior) and after calibration (best) against observations to show whether the calibration was successful.

Comparing the observations of GPP and FPC for all grid cells not used in the calibration to simulations using the default (prior) and the optimised (best) parameter values showed minor changes for GPP but a substantial reduction of the difference to observations for FPC of C-, S- and R-PFTs. For GPP the median difference between observation and simulation was  $0.16 \text{ kgC m}^{-2} \text{ yr}^{-1}$  for the prior and  $0.18 \text{ kgC m}^{-2} \text{ yr}^{-1}$  for the best parameter set. Median values, the 25th and 75th percentiles, and the

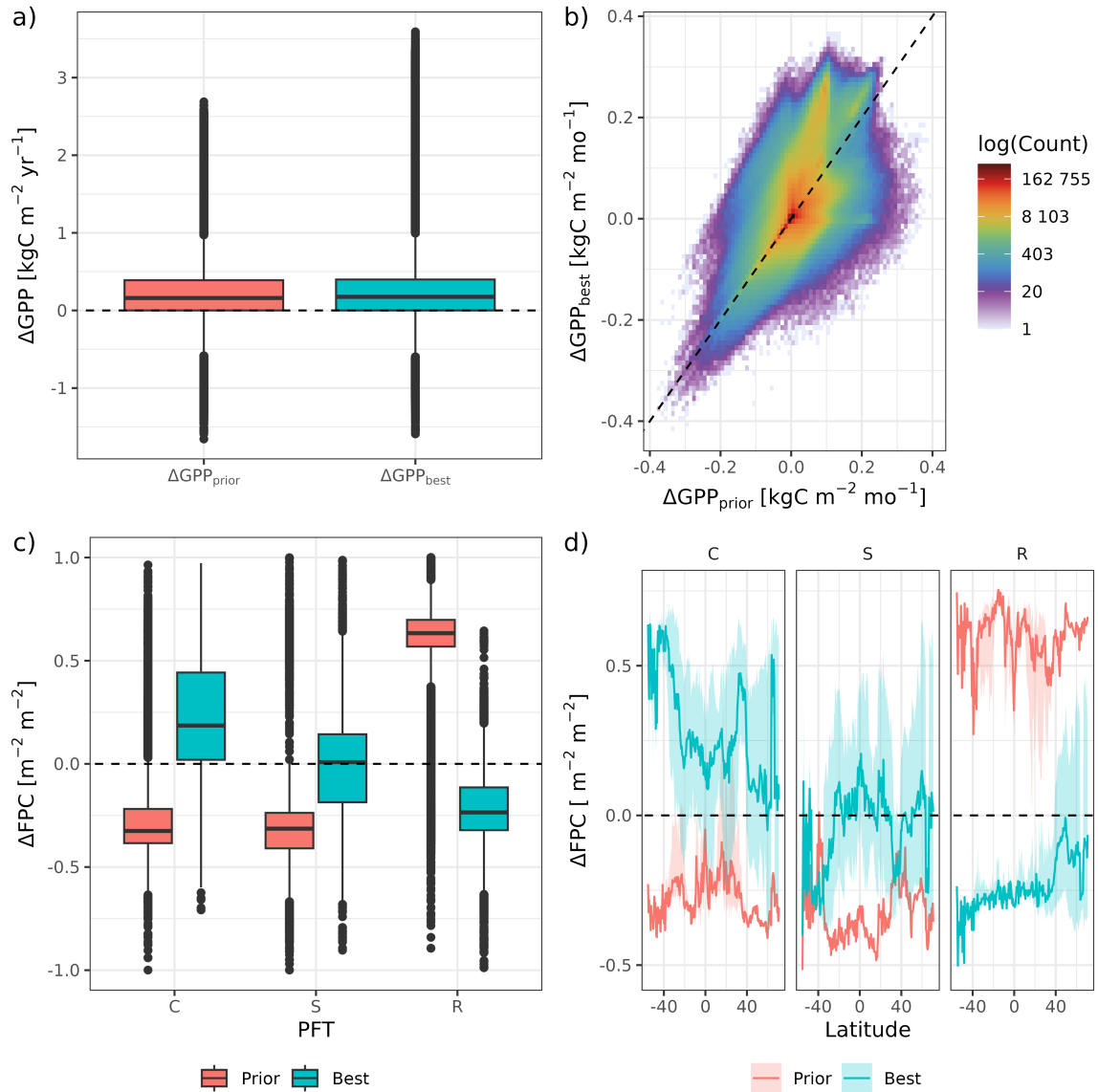


Figure 5.2: Boxplots (a,c), density plot (b) and latitudinal averages (d) of the difference between simulated and observed annual (a) and monthly (b) GPP between 2000 and 2016 and annual FPC (c,d) data for the parameter set before (prior, blue) and after (best, red) the calibration. For the latitude plot, lines show the differences to the 2000 to 2016 average of simulation results and shaded areas show the 5th to 95th percentiles.

interquartile range were similar between the prior and the best (Fig. 5.2 a). However, the best parameter set strongly overestimated annual GPP in more cases than the prior parameter set as indicated by the outlier values above the upper interquartile boundary. Monthly GPP was up to  $0.4 \text{ kgC m}^{-2} \text{ yr}^{-1}$  lower or higher than observations (Fig. 5.2 b) for both the prior and best parameter sets. Similar to the annual GPP, overestimations of the monthly GPP are more common using the best parameter set. However, the difference is small for a majority of data points as shown by the density plot in Fig. 5.2 b. The main increase in GPP between the prior and the best parameter set occurs in the tropics (Fig. D.3). For example, in the Congo basin, monthly GPP is up to  $0.3 \text{ kgC m}^{-2} \text{ yr}^{-1}$  higher using the best parameters (see Fig. D.3 a and c). However, here observations generally show a quite low grassland GPP potentially underestimating productivity. While we believe that representation of GPP observations can be improved, we are confident that the results using the best parameter set are sufficient to investigate the role of functional diversity in grassland ecosystem services.

FPC of the C-, S- and R-PFTs differed strongly between the prior and best parameter sets. Overall, the median difference to the observations was lower for the best parameter set. It was  $-0.33$ ,  $-0.31$ , and  $0.63 \text{ m}^2 \text{ m}^{-2}$  for the prior and  $0.18$ ,  $0.01$  and  $-0.23 \text{ m}^2 \text{ m}^{-2}$  for the best parameter set for the C-, S- and R-PFTs respectively (Fig. 5.2 c). Qualitatively, the FPC of the C-PFTs remains higher than the observations, while that of the R-PFTs is lower. The S-PFTs' FPC matches the observations best. However, for all three PFT types the difference to observations shows a wide range. Comparison by latitude showed that the FPC of the R-PFTs was strongly overestimated at the expense of the C- and S-PFTs using the prior parameter set (Fig. 5.2 d). In contrast, using the best parameter set, the FPC of the C-PFTs is overestimated at the expense of the other PFTs. In the high latitudes of the southern hemisphere overestimations were the largest and at the expense of both the S- and R-PFTs. At lower latitudes the FPC of the S-PFTs matches observations well while that of the C-PFTs is overestimated at the expense of the R-PFT. In the high latitudes of the northern hemisphere, differences are smaller and the FPCs mainly agree well with observations. The latitudes between  $60$  and  $66^\circ\text{N}$  are an exception. Here the share of managed grasslands is negligible except on Iceland which shows a strong overestimation of the FPC of C-PFTs (Fig. D.4 j).

Using the prior parameter set, the R-PFT was dominant across different climate zones except in India. The best parameter set results in regionally different FPC distributions (Fig. D.4). Using the best parameter set, the FPC of C-PFTs is close to 1 in Europe, south-eastern USA, Uruguay, southern Brazil, east Argentina as well as parts of South Africa, Australia and the Himalayas. These areas also correspond to the areas where LPJmL-CSR overestimates the observations for the FPC of the C-PFTs the most. Towards the tropics as well as the higher latitudes of the northern hemisphere, the share of C-PFTs decreases. Here, both the R- and S-PFTs have a substantial share of FPC with values up to approximately  $0.25$  and  $0.5$  respectively. However, the observations for the R-PFTs are still underestimated, while those

of the S-PFTs are overestimated. In the subtropics and tropics, the R-PFTs are barely present and the S-PFTs have an FPC of up to approximately 0.75 resulting in an overestimation of S- but also the C-PFTs and an underestimation of the R-PFTs.

### 5.3.2 Global productivity and SOC stocks under climate change

For the historical period, LPJmL-CSR simulates an increase of grassland GPP from approximately 8 PgC yr<sup>-1</sup> in 1901 to approximately 17.5 PgC yr<sup>-1</sup> in the 1990s (Fig. 5.3 a). This increase is predominantly caused by increasing grassland areas from approximately 16 Mkm<sup>2</sup> in 1901 to 33 Mkm<sup>2</sup> in 2001, other drivers are increasing atmospheric CO<sub>2</sub> concentration and N inputs from deposition.

Total global GPP and dry matter intake were substantially higher in the FD+ compared to FD- for both RCP 2.6 and 7.0 (Fig. 5.3 a and c). Historical GPP values peak around 17.5 PgC yr<sup>-1</sup> around 2000 and increased to approximately 20 PgC yr<sup>-1</sup> in 2100 for RCP 2.6 and 25 PgC yr<sup>-1</sup> for RCP 7.0 for the FD+ scenario (Fig. 5.3 a). Independent of the functional diversity scenario, LPJmL-CSR simulated a stronger GPP increase under RCP 7.0 compared to RCP 2.6, which is related to limitations of LPJmL in simulating drought effects (see 5.4.1). While this calls for additional analysis and future model development, we here focus on the differences between the scenario with functional diversity (FD+) and without functional diversity (FD-).

For FD-, GPP was substantially lower compared to FD+, which reproduces the well-established link between functional diversity and productivity. GPP reductions are reflected in lower dry matter intake and a decline in SOC (Fig. 5.3 c and d). PFT-specific GPP shows that the lower overall GPP in the FD- scenarios resulted from a stronger GPP decrease of the S- and R-PFT that outweighed the GPP increase of the C-PFT (Fig. 5.3 b). Essentially, the S- and R-PFTs were more often subordinate or marginal and therefore removed in the FD- scenario. However, while this made additional resources available for the dominant C-PFT, leading to an increase, this cannot compensate for the losses from removing the S- and R-PFTs.

We only show and describe the results for RCP 2.6 from here on but provide a figure for RCP 7.0 in the SI. We believe this is reasonable because the spatial patterns are similar (compare Fig. 5.4 and Fig. D.5), and results mainly differ only in the extent of the increases in GPP, SOC and other variables over time as well as the relative difference between FD+ and FD-. (Fig. 5.3 and Fig. D.5 and D.6). All maps only show data for MRI-ESM2-0 because the spatial pattern of an average or the median across GCMs is not meaningful. Generally, spatial patterns did not differ strongly between GCMs (data not shown) and showing only one GCM is representative.

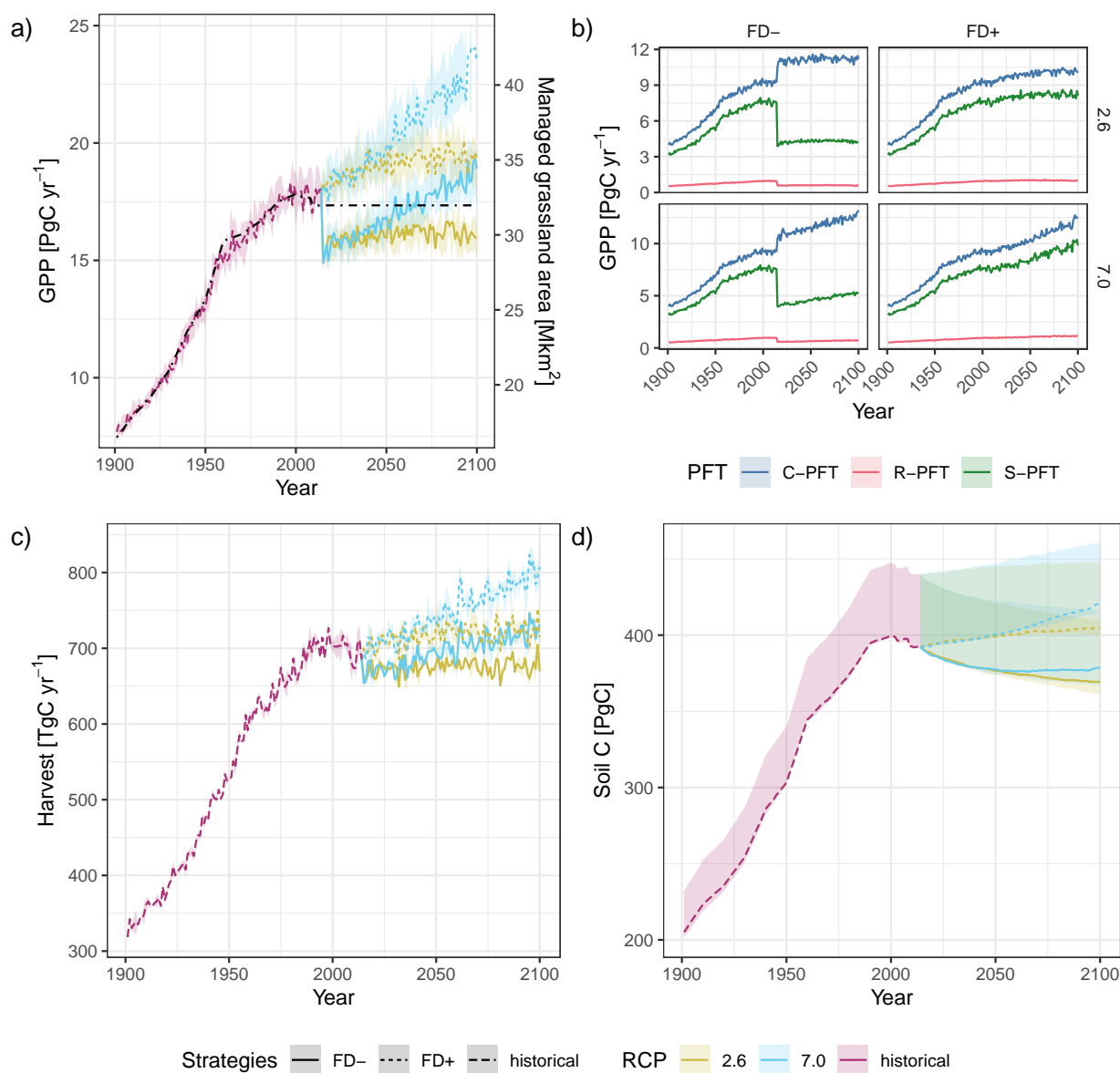


Figure 5.3: Time series of global total GPP (a), PFT-specific GPP (b), dry matter intake (c) and SOC stocks (d) from 1901 until 2100. Panels a,c and d show historical data (purple, dashed) and projections for RCP 2.6 (yellow) and 7.0 (lightblue) for the FD+ (solid) and FD- (dotted) scenarios. Grassland areas are shown in panel a (dot-dashed). For the PFT-specific GPP, different scenarios (FD- and FD+) and SSPs (2.6 and 7.0) are shown in separate panels and colors distinguish the C- (darkblue), S- (red) and R-PFT (darkgreen). Lines show the median and shaded areas the 5th to 95th percentile across five GCMs.

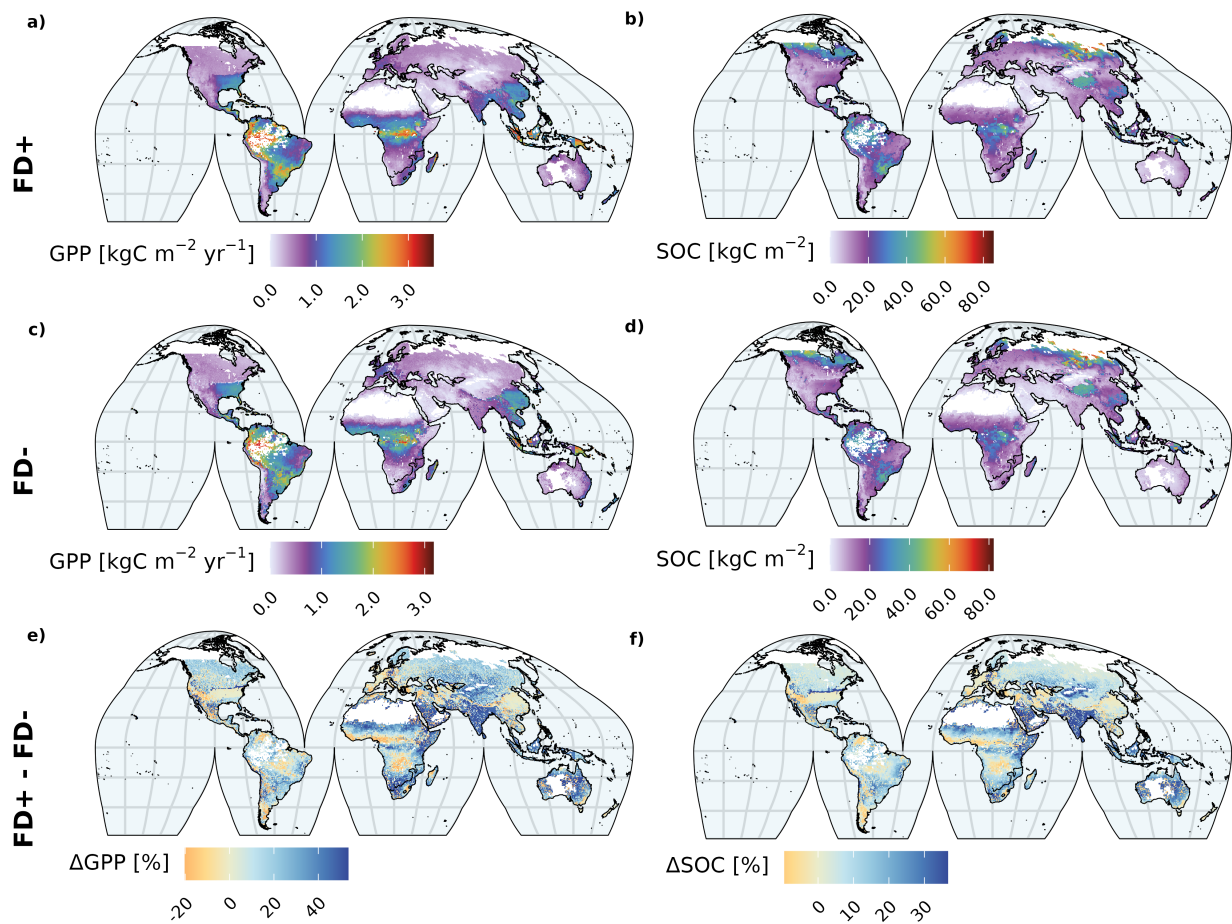


Figure 5.4: Global distribution of gross primary production (GPP) and soil organic carbon (SOC) dependent on functional diversity. Left panels show the average GPP for the scenarios (a) FD+, (b) FD- and (c) their difference, i.e. the net effect of a higher functional diversity. Right panels (b,d,f) show the respective results for SOC. All distributions show the 2091 to 2100 average of the respective output variable simulated using climate data from the MRI-ESM2-0.

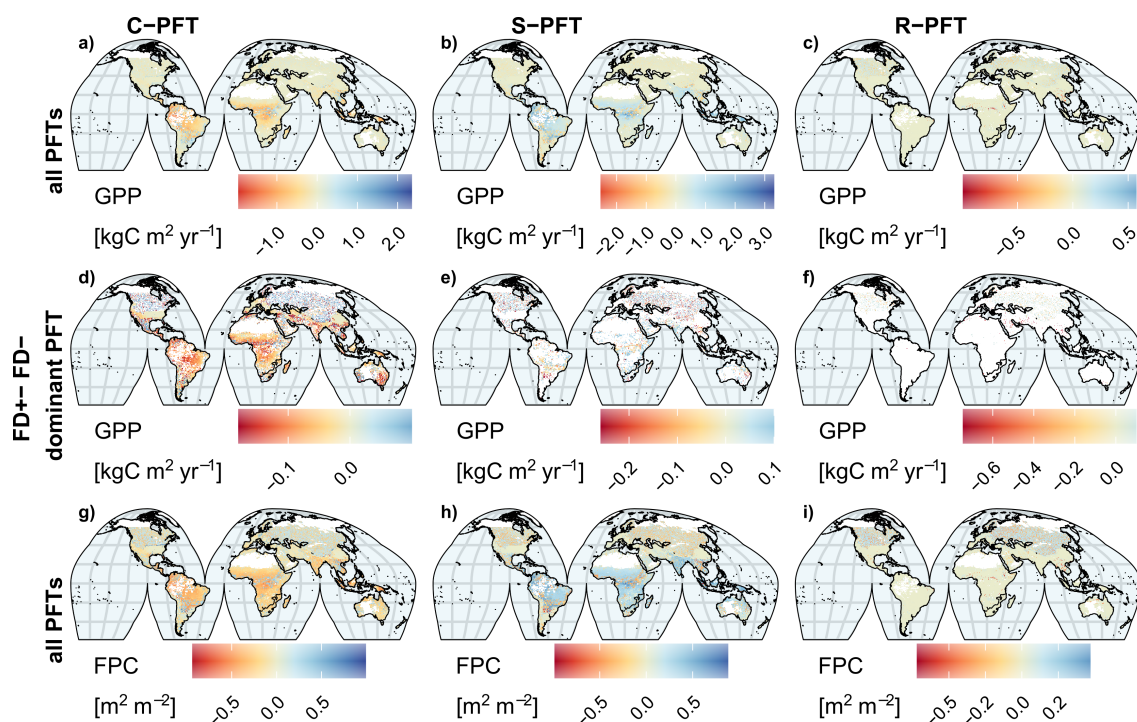


Figure 5.5: Global distribution of PFT-specific gross primary production (GPP) and foliage projective cover (FPC) dependent on functional diversity. All panels show the relative change between FD+ and FD- i.e. the net effect of a higher functional diversity. From left to right, panels show the distribution for the C- (a,d,g), S- (b,e,h) and R-PFTs (c,f,i). The first (a,b,c) and third (g,h,i) rows show the distribution using all PFTs present in FD+. The second row (d,e,f) shows the distribution using only the dominant PFT in FD+. Similar values (difference of 0) are shown in green, while white areas in d-f are grid cells in which the respective PFT is not dominant and no value is available. All distribution show the 2091 to 2100 average of the respective output variable simulated using climate data from the MRI-ESM2-0.

### 5.3.3 Spatial patterns of productivity and SOC stocks at the end of the century

Spatial patterns of GPP are similar between FD+ and FD- with the highest GPP in the inner tropics and the lowest GPP in semi-arid, arid and polar regions (Fig. 5.4 a and c). The strongest GPP reduction occurred around the equator, Paraguay and India where GPP is up to 50% lower for the FD- scenario (Fig. 5.4 e). GPP increased up to 20% in the African countries north and south of the equator and in Spain.

SOC patterns are also similar between FD+ and FD- with the highest values in polar regions where decay rates are low and lower values in drier and/or warmer climates (Fig. 5.4 b and d). Following the reduction of GPP, the highest SOC differences between FD+ and FD- were simulated around the equator, in Paraguay and in India (Fig. 5.4). Similarly, SOC slightly increased in areas where GPP increased.

Comparing the GPP of FD+ and FD- for the C-, S- and R-PFTs shows contrasting patterns for the C- and S-PFTs. In large areas, different PFTs are dominant at the end of the century compared to the end of the historical time period across all climates (Fig. D.7). For the C-PFTs, LPJmL-CSR simulated up

to approximately  $2 \text{ kgC m}^{-2} \text{ yr}^{-1}$  higher GPP in parts of the tropics, subtropics, the south-east USA, Portugal, Spain, France and north-west Germany and up to approximately  $2.5 \text{ kgC m}^{-2} \text{ yr}^{-1}$  lower GPP in lower latitudes for FD- compared to FD+ (Fig. 5.5 a). At the level of C-, S- and R-PFTs, the losses are likely caused by the removal of the respective PFT and do not have a high informational value. However, increases do not reflect the addition of a PFT but an increase in the productivity of the dominant PFT. In the tropics and subtropics, the C-PFT is dominant but the S- and/or R-PFT also make up a substantial share of the community (Fig. D.8 and D.9 a-c). Removing the subordinate PFTs frees up resources, which can be utilised by the dominant C-PFTs. This is not the case in areas where the C-PFTs were strongly dominant anyway such as the south-east of the USA, Uruguay, southern Brazil and east China (Fig. 5.5 g).

For the S-PFTs, GPP values are up to approximately  $3.5 \text{ kgC m}^{-2} \text{ yr}^{-1}$  lower in the tropics and subtropics and up to  $2.5 \text{ kgC m}^{-2} \text{ yr}^{-1}$  higher in higher latitudes (Fig. 5.5 b). The losses are mainly a reflection of areas where the C-PFT was dominant but the S-PFT also made up a substantial share of the community resulting in a large loss of GPP when the S-PFTs were removed (Fig. 5.5 h). As a consequence of the removal, the C-PFT can utilize additional resources and increase its GPP if the subordinate S-PFT is removed. However, as described above and shown in Fig. 5.4, the total GPP is lower in a majority of the subtropics and tropics in FD-.

For the R-PFTs, the differences are generally smaller and limited to latitudes above  $40^\circ\text{N}$  and west China (Fig. 5.5 c). However, the R-PFT is subordinate to the C- or S-PFT in the majority of grid cells (Fig. 5.5 i) resulting in a GPP loss of up to approximately  $0.5 \text{ kgC m}^{-2} \text{ yr}^{-1}$ . In the few grid cells in which the R-PFT is dominant, the GPP increases by up to approximately  $1 \text{ kgC m}^{-2} \text{ yr}^{-1}$  in FD- compared to FD+.

To assess if GPP losses could also be caused by a loss in productivity of the dominant PFT in FD- compared to FD+ and not only by the removal of subordinate and marginal PFTs, we additionally compared the GPP of the PFT of FD+ that was selected to simulate FD- (Fig. 5.5 d-f). For all strategies, the GPP of the PFT chosen for FD- was higher in FD- than in FD+ across large areas, meaning that this PFT was less productive in the high functional diversity scenario (FD+) than in the low functional diversity scenario (FD-). For the C-PFTs, GPP is up to approximately  $0.2 \text{ kgC m}^{-2} \text{ yr}^{-1}$  lower in FD+ except in large areas of the high latitudes of the northern hemisphere, where it is up to approximately  $0.1 \text{ kgC m}^{-2} \text{ yr}^{-1}$  higher. For the S- and R-PFTs, GPP is lower by up to approximately 0.25 (S-PFTs) and 0.7 (R-PFTs)  $\text{kgC m}^{-2} \text{ yr}^{-1}$  in FD+. While it can also be higher for the S-PFTs (up to  $0.1 \text{ kgC m}^{-2} \text{ yr}^{-1}$ ), for the R-PFTs, we did not find a substantial increase (values  $< 0.1 \text{ kgC m}^{-2} \text{ yr}^{-1}$ ). The described patterns can emerge for two reasons. First, the PFT remains dominant, but its resource access is limited by competitors in FD+. Second, considering that the dominant PFT changes over time in many areas, the PFT no longer has a competitive advantage any more and loses its dominance in FD+

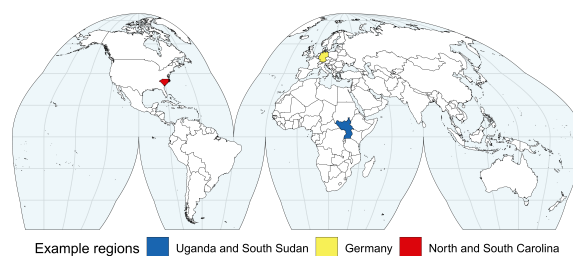


Figure 5.6: Locations of the three example regions Uganda and South Sudan (blue), Germany (yellow) and North and South Carolina (red).

until the end of the century (see also Fig. D.7). Still, because of the shifts in community composition until the end of the century, the disadvantage of this PFT in the community (FD+) is compensated by other PFTs.

### 5.3.4 Representative example regions

To highlight specific spatial features and prominent differences between scenarios, we present relative changes for GPP and SOC and the change in number of PFTs for three exemplary regions (Fig. 5.6): Uganda and South Sudan (Africa), Germany (Europe) and North and South Carolina (United States of America, North America). The lower GPP in FD- is related to a loss of subordinate PFTs that cannot be compensated in Uganda and South Sudan (5.3.4.1), to a loss in productivity of the dominant PFT in Germany (5.3.4.2) and to an increase in productivity in FD+ from the establishment of additional PFTs in North and South Carolina (5.3.4.3).

#### 5.3.4.1 Uganda and South Sudan, Africa

Across the entire region, only the tropical PFTs were established and the number of PFTs is reduced by two in FD- compared to FD+ where three PFTs were present (Fig. 5.7 c). However, this does not translate into a homogeneous reduction of GPP and SOC (Fig. 5.7 a,b). Generally, GPP is higher in Uganda than in South Sudan (Fig. D.10). This pattern is reflected by the relative changes in GPP from FD+ to FD-. In Uganda and the northern and eastern South Sudan, GPP is up to 50% higher in FD+ compared to FD- while it is up to 10% lower in the south-western part of South Sudan (Fig. 5.7 a). SOC storage shows a similar pattern but values are only up to 30% higher and less than 10% lower in FD+ (Fig. 5.7 b). This pattern results from the different plant community compositions. In Uganda, the FPC of the subordinate C-PFT is still substantial and its removal cannot be compensated by increased productivity of the dominant S-PFT. The pattern in South Sudan can be explained by the differently strong dominance of the C-PFT (Fig. D.11 a and b). The FPC of the C-PFT is higher in the south-west than in the north-east (Fig. D.11 a). A higher FPC of the C-PFT in FD+ means that its dominance is

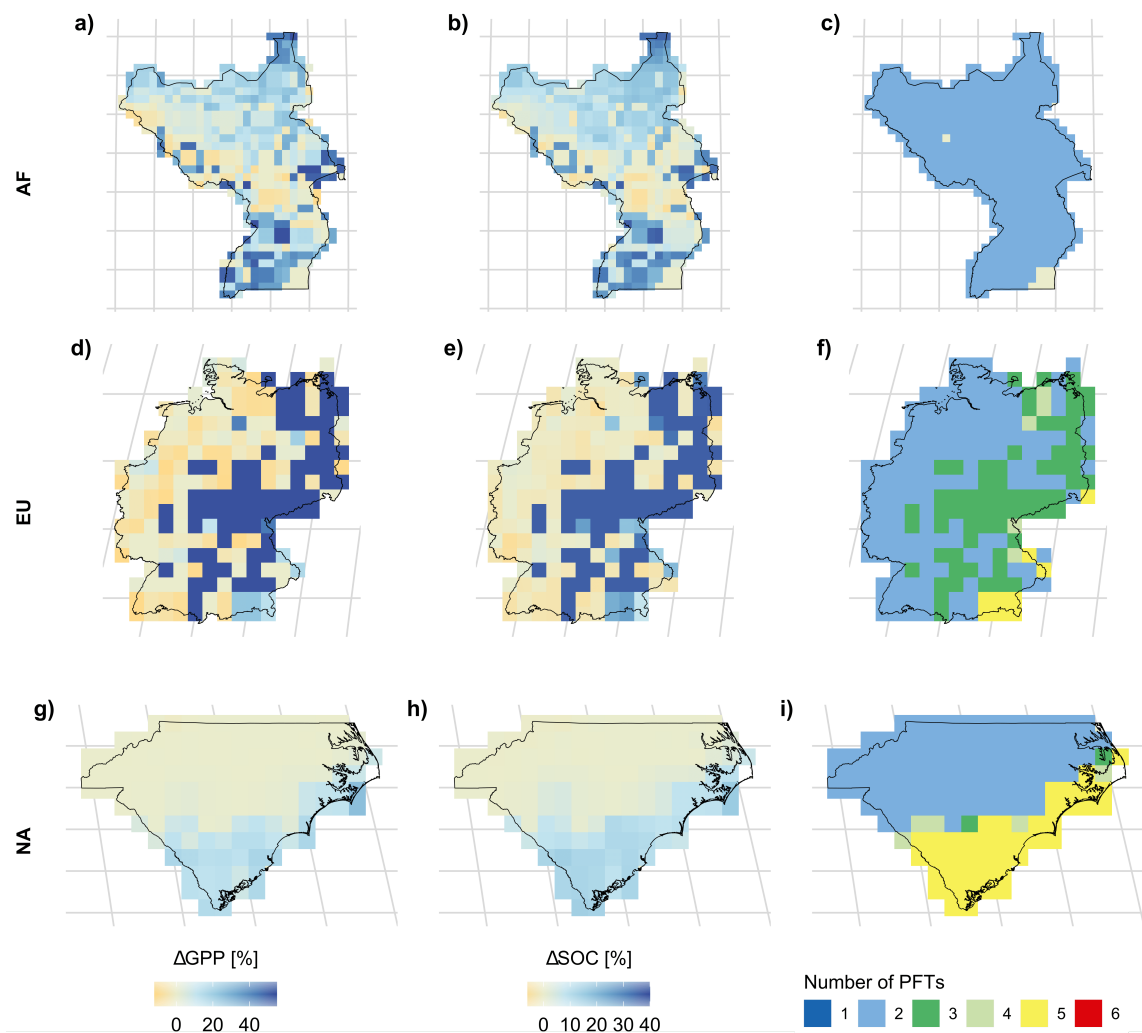


Figure 5.7: Distribution of the relative change between FD+ and FD- for gross primary production (GPP, a,d,g) and soil organic carbon (SOC, b,e,h) and the absolute change of the number of PFT present (c,f,i) dependent on functional diversity for the three example regions (Uganda and South Sudan, Germany and North and South Carolina). From top to bottom, the rows show the data for Uganda and South Sudan (a,b,c), Germany (d,e,f) and North and South Carolina (g,h,i). From left to right, columns show the relative change in GPP (a,d,g) and SOC (b,e,h) and the absolute change in the number of PFTs (c,f,i). All distributions are based on the 2091 to 2100 average of the respective output variable simulated using climate data from the MRI-ESM2-0.

stronger. If this was the case, it was able to utilise resources better in FD+ but also in FD- leading to a higher GPP and SOC in FD- (Fig. 5.7 a and b). Here, the C-PFT benefits from reduced competition because the subordinate PFTs were removed. In the areas where the C-PFT is less dominant in the north-east, this advantage from reduced competition is weaker, and having the S-PFT as part of the community in FD+ is advantageous, resulting in a higher GPP and SOC in FD+.

#### 5.3.4.2 Germany, Europe

In the second example region, Germany, absolute GPP is lower than in Uganda and South Sudan (compare Fig. D.10 a and d and D.12 a and d). However, the relative changes are similar with up to 50% higher and 10% lower GPP values in FD+ and up to 30% higher and less than 10% lower SOC values (Fig. 5.7 d and e). The spatial patterns show higher GPP and SOC values in the east and south-east of Germany and lower values in the remaining areas. The spatial patterns of changes in GPP and SOC correspond to those of the number of PFTs lost (Fig. 5.7 f). Three PFTs are lost in the areas where GPP and SOC are higher in FD+ and two PFTs in those in which FD+ values are lower. The strong loss of productivity in FD- in the south-east is caused by a complete loss of productivity of the historically dominant PFT (GPP of zero in south-east Germany in FD-, see Fig. D.12 d). This points towards a different mechanism than in Uganda and South Sudan where the dominant PFT was generally more productive in FD- but was still less productive compared to the mixture in FD+ in large areas. The community composition changes and PFTs are lost already in FD+ compared to the historical period, from which the dominant PFT was determined. (Fig S12 c and f) This is caused by increasing temperatures, which render the polar PFTs that were present in the past unsuitable in the future. Due to overlapping bioclimatic limits that control the areas in which PFTs can establish, the polar C-PFT was dominant at the end of the historical simulation period in the south-east of Germany. However under climate change, the temperatures in south-east Germany increase and are outside of the bioclimatic limits of the polar PFTs, resulting in their removal from the community and complete loss of productivity compared to the historical period (Fig. D.12 and D.14). Generally, we think that the polar PFTs should already not have been dominant in this region historically which suggests an adaptation of the bioclimatic limits. However, this nicely shows how climate change may lead to a loss of productivity if unsuitable PFTs cannot be replaced, leading to breakdown of GPP. In the west and north of Germany, the temperate C-PFT is dominant (Fig S13) and benefits from the removal of subordinate PFTs, allowing it to compensate for the loss of subordinate PFTs in FD-.

### 5.3.4.3 North and South Carolina, North America

Here, GPP increases from the north-west to the south-east and the values are between those of Uganda and South Sudan and Germany (compare Fig. D.10 a and d, D.12 a and d and D.15 a and d). Generally, GPP and SOC are higher or similar in FD+ with highest values of up to almost 20% for GPP and 15% for SOC in the south-east (Fig. 5.7 g and h). In the northern and north-western parts of the region, differences between FD+ and FD- are negligible. While the temperate C-PFT was strongly dominant across North and South Carolina except in the far south during the historical time period, in FD+, the tropical PFTs established under climate change, which is beneficial for productivity (Fig. D.16 a and d). In FD-, adaptation to the warmer climate by switching from a temperate C3 to a tropical C4 PFT is not possible. This is clearly shown by the similarity of the patterns for GPP, SOC and the number of PFTs, which are reduced by two in the north and north-western part and by 5 in the remaining example region (Fig. 5.7 i). In contrast to Germany, the higher productivity in FD+ is explained by the establishment of additional PFTs under climate change instead of a breakdown of the community. Historically, the temperate C-PFT is dominant in the entire example region and is therefore selected for FD-. Under climate change, the tropical C-PFT gains an advantage and becomes dominant in FD+ stabilising the community's productivity (Fig S16 d). In FD-, the temperate C-PFT benefits from decreased resource competition (Fig. D.17 d) but cannot compensate for the productivity gains of the mixture.

## 5.4 Discussion

We were able to demonstrate the role of functional diversity for the GPP and SOC stocks of managed grasslands at the global scale, making use of spatially explicit simulations of two functional diversity scenarios with LPJmL-CSR. Generally, we find the direction of change and the order of magnitude plausible because, despite our highly aggregated representation of functional diversity using CSR theory, the model was able to match historical observations well, and projected changes in community composition are rooted in important trade-offs between ecological strategies. This is a novel approach, with strengths and weaknesses regarding the LPJmL model in general, the CSR implementation (5.4.1) and its comparison to field experiments and ecological theory (5.4.2).

### 5.4.1 Highlights and limits of LPJmL-CSR

LPJmL-CSR is, to our knowledge, the only DGVM that includes a representation of the functional diversity of managed grasslands and neither follows an individual-based approach nor represents entire trait distributions. While LPJmL-CSR has previously been applied only at the local scale (Wirth et al., 2024b), we successfully calibrated it for a global application using only the three main CSR strategies.

While this is a major step, our evaluation highlighted the need for future model development because the representation of trade-offs between the different strategies is not sufficient to fully reproduce observational data (see 5.3.1). Our comparison showed that the R-PFT is generally at a disadvantage and underrepresented compared to the data, while the C-PFT is generally at an advantage and therefore overrepresented.

This is likely because the current version of LPJmL-CSR lacks a key feature of R strategies, the representation of reproduction and mortality (Wirth et al., 2024b). While LPJmL-CSR simulates a higher establishment rate — representative of more offspring — for the R-PFT, reproduction costs are not differentiated between strategies. However, the R strategy is characterised not only by a large number of offspring but also smaller seeds (Grime, 1977) and lower reproductive costs which correlate with plant size (Obeso, 2002). Additionally, the R strategy is successful in areas with a short growing season where the other strategies cannot survive due to factors like drought or cold mortality (Grime, 1977), which are not represented in LPJmL-CSR. Implementing additional processes to close these gaps will likely improve simulation results. To represent seed banks, the approach of the QUINCY model which includes the allocation of resources to fruits and a seedbed might serve as an inspiration (Thum et al., 2019). Different mortality types could be implemented following existing modelling approaches. For example, the FATES model represents frost death based on temperature and PFT-specific parameters (Lambert et al., 2023). Furthermore, we used only the three main strategies defined by the CSR theory. Therefore, communities in the model can follow intermediate strategies if they are mixtures of subsets of the main strategies. However, intermediate strategies could also be implemented at the PFT level, for example through the addition of a CS-PFT with traits lying between the C- and S-PFT. While this could improve model results further, it would also increase model complexity and, in turn, computation costs, necessary calibration efforts and data requirements.

Comparing historical GPP and projections for RCP2.6 and 7.0 showed an increase of grassland GPP under climate change. While higher atmospheric CO<sub>2</sub> concentrations and temperature facilitate productivity, these effects should be compensated by increased water limitation due to reduced precipitation and increasing number of drought events (Sheffield and Wood, 2008). We suspect that the water limitation and the effect of drought on vegetation are underestimated in the simulations as several related damage processes are not explicitly implemented in the model. Plant damage from drought as well as mortality, such as from embolism, are not represented in LPJmL enabling the PFTs to survive even severe droughts with only some biomass loss via litter fall. As a result, the amount of living biomass that can be used for photosynthesis is overestimated at the end of a dry period.

While additional model development will likely improve the fit to data, the existence of data on community share of the different strategies limit the calibration process and therefore the performance of the calibrated model substantially (5.4.2).

## 5.4.2 The role of functional diversity

We used data from Wolf et al., 2022 which provide a global map with almost full coverage for several plant traits combining TRY data and citizen science observations from iNaturalist. These data consist of photographs of plants taken by citizens and may contain a selection bias for rare or appealing species (Schiller et al., 2021). Resulting trait ranges might therefore not be representative of typical managed grassland species. Furthermore, we added another layer of pre-processing by applying the StrateFy approach. This approach can be used to calculate C, S and R shares of a community based on three plant traits. In the future, this approach could be refined by considering additional data sources, such as the sPlot-based traits maps from Wolf et al., 2022. Since sPlot is a database of scientific experiments, derived trait values are likely more representative of actual communities. However, it does not cover the same spatial extent as iNaturalist and is insufficient for a global evaluation. Still, the trait data derived from sPlot sites could potentially be used for a bias correction of the iNaturalist-based product in future research.

In line with the diversity productivity theory (Craven et al., 2016; Schulze and Mooney, 1993; Tilman et al., 2012), LPJmL-CSR simulated substantially lower GPP and SOC stocks if the non-dominant PFTs were removed. While this approach does not represent actual diversity loss, it can serve as a proxy to represent a very low biodiversity scenario comparable to the artificial communities of biodiversity experiments. Qualitatively, our results are in line with these experiments which show an increase in productivity with increasing species numbers (e.g. Tilman et al., 2001; Weisser et al., 2017). However, these experiments have been criticised for not being representative of natural systems due to the artificial removal of diversity through weeding, which affected soil fertility (Weisser et al., 2017) and in turn led to artificially low productivity in low-diversity plots (Jiang et al., 2009). In fact, other studies found a maximum productivity at low diversity levels (Schulze et al., 2018). In LPJmL-CSR, the loss of productivity is less severe because the model does not include pests, diseases and disturbances through repeated weeding. As such, the FD- scenario may be more comparable to the loss of some, but not all, functional diversity.

Our results show an increase in the productivity of the dominant PFT in FD- compared to FD+ due to increased resource availability and reduced competition. However, the communities with low functional diversity (FD-) rarely obtained a higher productivity than the functionally diverse communities (FD+). The differences between FD+ and FD- in our example regions highlight that the underlying reasons may differ. In large parts of Uganda and South Sudan and Germany, the increase in productivity of the dominant PFT in FD- could not compensate the loss of productivity from non-dominant PFTs. Only in communities where the dominant PFT could strongly increase its community share and therefore resource uptake, the increase in productivity of the dominant strategy could compensate the

effect of functional diversity. This aligns with recent findings that the diversity-productivity relationship is mediated by various factors such as climate, soil properties, management or landscape structures (e.g. Andrzejek et al., 2024; Lucie et al., 2023; Nie et al., 2024; Pan et al., 2022). In the south-east of Germany, FD- showed lower productivity because the historically dominant PFT became unsuitable in the future climate leading to the breakdown of the community. This shows that functional diversity can serve as insurance against climate change, which was also shown in multiple field experiments (e.g. Petermann and Buzhdygan, 2021). In North and South Carolina, however, the lower productivity in FD- was caused by the community's lack of adaptability to climate change. The temperature increase led to an advantage of tropical C4 PFTs not present in 2014 when the dominant PFT for FD- was determined, but present in 2100 in FD+. This is in line with field experiments and empirical modelling for North America showing an advantage of C4 species at higher temperatures and predicting an increase of C4 species in areas where C3 and C4 species are both abundant (Havrilla et al., 2023; von Fischer et al., 2008). This serves as an example of how the migration of plant species may help to adapt to climate change and lessen its impacts. While this is well researched (e.g. Twardek et al., 2023), the velocity of climate change and species migration are not the same, limiting the natural adaptation capacity of communities (Loarie et al., 2009; Pearson, 2006), which is not represented in LPJmL-CSR. Therefore, the effect of community adaptation simulated by LPJmL-CSR can only be interpreted as a potential effect.

## 5.5 Conclusions

Using the LPJmL-CSR DGVM, we conducted the, to our knowledge, first global-scale assessment of the role of functional diversity for GPP and SOC stocks of managed grasslands. In this first analysis, we compare two states: a scenario with functional diversity (FD+) to a scenario without functional diversity (FD-) quantifying the differences in GPP and SOC storage. However, the change in functional diversity is not a rapid state shift but long-term transition responding to climate change. In combination, climate change and functional adaptation of communities may encompass feedbacks and affect each other. For example, climate change is likely to outpace the natural adaptation capacity of managed grassland communities, accelerating the loss of functional diversity (Zhu et al., 2024), which may affect the land carbon sink via reduced SOC stocks (Bai and Cotrufo, 2022). While we see opportunities for further model improvement, our results are generally in line with observations and ecological theory. Therefore, LPJmL-CSR could serve as a tool to further investigate the aforementioned interactions at the global scale.

Furthermore, our results show once more that preventing the loss of functional diversity will help to maintain grassland productivity under climate change, which is crucial for many livelihoods, especially in the global south (Scollan et al., 2005; Wang et al., 2022a). The loss of SOC storage that goes

hand in hand with functional diversity loss reduces the terrestrial carbon sink, negatively affecting the remaining carbon budget. Further research is needed to better quantify productivity and SOC storage losses, and their feedbacks with other Earth system components. Our findings underpin the need for development and application of grassland management practices that support functional diversity to incentivise policymakers to assist farmers in the necessary transition.

**Author contributions:** SBW and SR designed the study in discussion with FT and CM. SBW conducted the model simulations and wrote the original draft of the manuscript. SBW, SR and FT discussed the simulation results and the original draft. All authors reviewed and edited the manuscript. SR and FT supervised this study.

**Acknowledgements:** SBW acknowledges financial support from the Evangelisches Studienwerk Villigst foundation, under the research program: "Third Ways of Feeding The World" and the German Federal Ministry for Education and Research (BMBF) within the project ABCDR (grant no. 01LS2105A). SR acknowledges financial support from the BMBF within the project ABCDR (grant no. 01LS2105A). The authors gratefully acknowledge the Ministry of Research, Science and Culture (MWFK) of Land Brandenburg for supporting this project by providing resources on the high performance computer system at the Potsdam Institute for Climate Impact Research.

## 5.6 References

- Andraczek, K., L. E. Dee, A. Weigelt, J. Hinderling, D. Prati, G. Le Provost, P. Manning, C. Wirth, and F. van der Plas (2024). "Weak Reciprocal Relationships between Productivity and Plant Biodiversity in Managed Grasslands". In: *J. Ecol.* 112.10, pp. 2359–2373. ISSN: 1365-2745. DOI: 10.1111/1365-2745.14400. (Visited on 11/13/2024).
- Bai, Y. and M. F. Cotrufo (2022). "Grassland Soil Carbon Sequestration: Current Understanding, Challenges, and Solutions". In: *Science* 377.6606, pp. 603–608. DOI: 10.1126/science.abo2380. (Visited on 02/13/2023).
- Boucher, O., J. Servonnat, A. L. Albright, O. Aumont, Y. Balkanski, V. Bastrikov, S. Bekki, R. Bonnet, S. Bony, L. Bopp, P. Braconnot, P. Brockmann, P. Cadule, A. Caubel, F. Cheruy, F. Codron, A. Cozic, D. Cugnet, F. D'Andrea, P. Davini, C. de Lavergne, S. Denvil, J. Deshayes, M. Devilliers, A. Ducharne, J.-L. Dufresne, E. Dupont, C. Éthé, L. Fairhead, L. Falletti, S. Flavoni, M.-A. Foujols, S. Gardoll, G. Gastineau, J. Ghattas, J.-Y. Grandpeix, B. Guenet, E. Guez Lionel, E. Guilyardi, M. Guimberteau, D. Hauglustaine, F. Hourdin, A. Idelkadi, S. Joussaume, M. Kageyama, M. Khodri, G. Krinner, N. Lebas, G. Levvasseur, C. Lévy, L. Li, F. Lott, T. Lurton, S. Luysaert, G. Madec, J.-B. Madeleine, F. Maignan, M. Marchand, O. Marti, L. Mellul, Y. Meurdesoif, J. Mignot, I. Musat, C. Ottlé, P. Peylin, Y. Planton, J. Polcher, C. Rio, N. Rochetin, C. Rousset, P. Sepulchre, A. Sima, D. Swingedouw, R. Thiéblemont, A. K. Traore, M. Vancoppenolle, J. Vial, J. Vialard, N. Viovy, and N. Vuichard (2020). "Presentation and Evaluation of the IPSL-CM6A-LR Climate Model". In: *J. Adv. Model. Earth Syst.* 12.7, e2019MS002010. ISSN: 1942-2466. DOI: 10.1029/2019MS002010. (Visited on 01/07/2025).
- Briske, D. D. (1986). "Plant Response to Defoliation: Morphological Considerations and Allocation Priorities". In: *Rangelands: A Resource under Siege*. Ed. by Joss, P. J., Lynch P. W., and Williams O. B. Canberra: Aust. Acad. Sci., pp. 425–427.
- Brose, U. and H. Hillebrand (2016). "Biodiversity and Ecosystem Functioning in Dynamic Landscapes". In: *Philos Trans R Soc Lond B Biol Sci* 371.1694, p. 20150267. ISSN: 0962-8436. DOI: 10.1098/rstb.2015.0267. (Visited on 10/01/2024).
- Büchner, M. and C. P. O. Reyer (2022). *ISIMIP3a Atmospheric Composition Input Data (v1.2)*. DOI: 10.48364/ISIMIP.664235.2. (Visited on 09/05/2023).
- Buzhdygan, O. Y., S. T. Meyer, W. W. Weisser, N. Eisenhauer, A. Ebeling, S. R. Borrett, N. Buchmann, R. Cortois, G. B. De Deyn, H. de Kroon, G. Gleixner, L. R. Hertzog, J. Hines, M. Lange, L. Mommer, J. Ravenek, C. Scherber, M. Scherer-Lorenzen, S. Scheu, B. Schmid, K. Steinauer, T. Strecker, B. Tietjen, A. Vogel, A. Weigelt, and J. S. Petermann (2020). "Biodiversity Increases Multitrophic Energy Use Efficiency, Flow and Storage in Grasslands". In: *Nat Ecol Evol* 4.3, pp. 393–405. ISSN: 2397-334X. DOI: 10.1038/s41559-020-1123-8. (Visited on 11/20/2023).
- Cardinale, B. J., J. E. Duffy, A. Gonzalez, D. U. Hooper, C. Perrings, P. Venail, A. Narwani, G. M. Mace, D. Tilman, D. A. Wardle, A. P. Kinzig, G. C. Daily, M. Loreau, J. B. Grace, A. Larigauderie, D. S. Srivastava, and S. Naeem (2012). "Biodiversity Loss and Its Impact on Humanity". In: *Nature* 486.7401, pp. 59–67. ISSN: 1476-4687. DOI: 10.1038/nature11148. (Visited on 01/29/2021).
- Chang, J., P. Ciais, T. Gasser, P. Smith, M. Herrero, P. Havlík, M. Obersteiner, B. Guenet, D. S. Goll, W. Li, V. Naipal, S. Peng, C. Qiu, H. Tian, N. Viovy, C. Yue, and D. Zhu (2021). "Climate Warming from Managed Grasslands Cancels the Cooling Effect of Carbon Sinks in Sparsely Grazed and Natural Grasslands". In: *Nat Commun* 12.1, p. 118. ISSN: 2041-1723. DOI: 10.1038/s41467-020-20406-7. (Visited on 04/17/2024).
- Chang, J., P. Ciais, N. Viovy, J.-F. Soussana, K. Klumpp, and B. Sultan (2017). "Future Productivity and Phenology Changes in European Grasslands for Different Warming Levels: Implications for Grassland Management and Carbon Balance". In: *Carbon Balance and Management* 12.1, p. 11. ISSN: 1750-0680. DOI: 10.1186/s13021-017-0079-8. (Visited on 04/17/2024).

- Cheng, C., Z. Liu, W. Song, X. Chen, Z. Zhang, B. Li, M. van Kleunen, and J. Wu (2024). “Biodiversity Increases Resistance of Grasslands against Plant Invasions under Multiple Environmental Changes”. In: *Nat Commun* 15.1, p. 4506. ISSN: 2041-1723. DOI: 10.1038/s41467-024-48876-z. (Visited on 10/01/2024).
- Conant, R. T., C. E. P. Cerri, B. B. Osborne, and K. Paustian (2017). “Grassland Management Impacts on Soil Carbon Stocks: A New Synthesis”. In: *Ecol. Appl.* 27.2, pp. 662–668. ISSN: 1939-5582. DOI: 10.1002/eap.1473. (Visited on 02/13/2023).
- Cramer, W., A. Bondeau, F. I. Woodward, I. C. Prentice, R. A. Betts, V. Brovkin, P. M. Cox, V. Fisher, J. A. Foley, A. D. Friend, C. Kucharik, M. R. Lomas, N. Ramankutty, S. Sitch, B. Smith, A. White, and C. Young-Molling (2001). “Global Response of Terrestrial Ecosystem Structure and Function to CO<sub>2</sub> and Climate Change: Results from Six Dynamic Global Vegetation Models”. In: *Glob. Change Biol.* 7.4, pp. 357–373. ISSN: 1365-2486. DOI: 10.1046/j.1365-2486.2001.00383.x. (Visited on 11/19/2024).
- Craven, D., F. Isbell, P. Manning, J. Connolly, H. Bruelheide, A. Ebeling, C. Roscher, J. van Ruijven, A. Weigelt, B. Wilsey, C. Beierkuhnlein, E. de Luca, J. N. Griffin, Y. Hautier, A. Hector, A. Jentsch, J. Kreyling, V. Lanta, M. Loreau, S. T. Meyer, A. S. Mori, S. Naeem, C. Palmberg, H. W. Polley, P. B. Reich, B. Schmid, A. Siebenkäs, E. Seabloom, M. P. Thakur, D. Tilman, A. Vogel, and N. Eisenhauer (2016). “Plant Diversity Effects on Grassland Productivity Are Robust to Both Nutrient Enrichment and Drought”. In: *Philos. Trans. R. Soc. B Biol. Sci.* 371.1694. ISSN: 0962-8436. DOI: 10.1098/rstb.2015.0277. (Visited on 12/09/2019).
- Crawford, M. S., K. E. Barry, A. T. Clark, C. E. Farrow, J. Hines, E. Ladouceur, J. W. Lichstein, I. Maréchaux, F. May, A. S. Mori, B. Reineking, L. A. Turnbull, C. Wirth, and N. Rüger (2021). “The Function-Dominance Correlation Drives the Direction and Strength of Biodiversity–Ecosystem Functioning Relationships”. In: *Ecol. Lett.* 00, pp. 1–14. ISSN: 1461-0248. DOI: 10.1111/ele.13776. (Visited on 06/23/2021).
- Cucchi, M., G. P. Weedon, A. Amici, N. Bellouin, S. Lange, H. Müller Schmied, H. Hersbach, and C. Buontempo (2020). “WFDE5: Bias-Adjusted ERA5 Reanalysis Data for Impact Studies”. In: *Earth Syst. Sci. Data* 12.3, pp. 2097–2120. ISSN: 1866-3508. DOI: 10.5194/essd-12-2097-2020. (Visited on 09/05/2023).
- Di Virgilio, G., J. P. Evans, S. A. P. Blake, M. Armstrong, A. J. Dowdy, J. Sharples, and R. McRae (2019). “Climate Change Increases the Potential for Extreme Wildfires”. In: *Geophys. Res. Lett.* 46.14, pp. 8517–8526. ISSN: 1944-8007. DOI: 10.1029/2019GL083699. (Visited on 01/06/2025).
- Díaz, S., J. Kattge, J. H. C. Cornelissen, I. J. Wright, S. Lavorel, S. Dray, B. Reu, M. Kleyer, C. Wirth, I. C. Prentice, E. Garnier, G. Bönisch, M. Westoby, H. Poorter, P. B. Reich, A. T. Moles, J. Dickie, A. N. Gillison, A. E. Zanne, J. Chave, S. J. Wright, S. N. Sheremet’ev, H. Jactel, C. Baraloto, B. Cerabolini, B. Shipley, D. Kirkup, F. Casanoves, J. S. Joswig, A. Günther, V. Falczuk, N. Rüger, M. D. Mahecha, and L. D. Gorné (2016). “The Global Spectrum of Plant Form and Function”. In: *Nature* 529.7585, pp. 167–171. ISSN: 1476-4687. DOI: 10.1038/nature16489. (Visited on 03/24/2020).
- Dunne, J. P., L. W. Horowitz, A. J. Adcroft, P. Ginoux, I. M. Held, J. G. John, J. P. Krasting, S. Malyshev, V. Naik, F. Paulot, E. Shevliakova, C. A. Stock, N. Zadeh, V. Balaji, C. Blanton, K. A. Dunne, C. Dupuis, J. Durachta, R. Dussin, P. P. G. Gauthier, S. M. Griffies, H. Guo, R. W. Hallberg, M. Harrison, J. He, W. Hurlin, C. McHugh, R. Menzel, P. C. D. Milly, S. Nikonov, D. J. Paynter, J. Ploshay, A. Radhakrishnan, K. Rand, B. G. Reichl, T. Robinson, D. M. Schwarzkopf, L. T. Sentman, S. Underwood, H. Vahlenkamp, M. Winton, A. T. Wittenberg, B. Wyman, Y. Zeng, and M. Zhao (2020). “The GFDL Earth System Model Version 4.1 (GFDL-ESM 4.1): Overall Coupled Model Description and Simulation Characteristics”. In: *J. Adv. Model. Earth Syst.* 12.11, e2019MS002015. ISSN: 1942-2466. DOI: 10.1029/2019MS002015. (Visited on 01/07/2025).
- Forkel, M., N. Carvalhais, S. Schaphoff, W. v. Bloh, M. Migliavacca, M. Thurner, and K. Thonicke (2014). “Identifying Environmental Controls on Vegetation Greenness Phenology through Model–Data Integration”. In: *Biogeosciences* 11.23, pp. 7025–7050. ISSN: 1726-4170. DOI: 10.5194/bg-11-7025-2014. (Visited on 06/29/2021).
- Forkel, M., M. Druke, M. Thurner, W. Dorigo, S. Schaphoff, K. Thonicke, W. von Bloh, and N. Carvalhais (2019). “Constraining Modelled Global Vegetation Dynamics and Carbon Turnover Using Multiple Satellite Observations”. In: *Sci Rep* 9.1, p. 18757. ISSN: 2045-2322. DOI: 10.1038/s41598-019-55187-7. (Visited on 06/29/2021).
- Friedl, M. and Sulla-Menashe, Damien (2015). *MCD12C1 MODIS/Terra+Aqua Land Cover Type Yearly L3 Global 0.05Deg CMG V006*. DOI: 10.5067/MODIS/MCD12C1.006. (Visited on 04/14/2023).
- Grime, J. P. (1974). “Vegetation Classification by Reference to Strategies”. In: *Nature* 250.5461, pp. 26–31. ISSN: 0028-0836, 1476-4687. DOI: 10.1038/250026a0. (Visited on 06/13/2022).
- Grime, J. P. (1977). “Evidence for the Existence of Three Primary Strategies in Plants and Its Relevance to Ecological and Evolutionary Theory”. In: *Am. Nat.* 111.982, pp. 1169–1194. ISSN: 0003-0147, 1537-5323. DOI: 10.1086/283244. (Visited on 10/28/2021).
- Gupta, H. V. and H. Kling (2011). “On Typical Range, Sensitivity, and Normalization of Mean Squared Error and Nash-Sutcliffe Efficiency Type Metrics”. In: *Water Resour. Res.* 47.10. ISSN: 1944-7973. DOI: 10.1029/2011WR010962. (Visited on 10/16/2024).
- Gutjahr, O., D. Putrasahan, K. Lohmann, J. H. Jungclaus, J.-S. von Storch, N. Brüggemann, H. Haak, and A. Stössel (2019). “Max Planck Institute Earth System Model (MPI-ESM1.2) for the High-Resolution Model Intercomparison Project (HighResMIP)”. In: *Geosci. Model Dev.* 12.7, pp. 3241–3281. ISSN: 1991-959X. DOI: 10.5194/gmd-12-3241-2019. (Visited on 01/07/2025).
- Havrilla, C. A., J. B. Bradford, C. Yackulic, and S. M. Munson (2023). “Divergent Climate Impacts on C<sub>3</sub> versus C<sub>4</sub> Grasses Imply Widespread 21st Century Shifts in Grassland Functional Composition”. In: *Divers. Distrib.* 29.3, pp. 379–394. DOI: 10.1111/ddi.13669. (Visited on 11/12/2024).
- Heinke, J. (2025). *A Livestock Density Input for LPJmL*. DOI: 10.5281/zenodo.14946695. (Visited on 03/05/2025).

- Heinke, J., S. Rolinski, and C. Müller (2023). “Modelling the Role of Livestock Grazing in C and N Cycling in Grasslands with LPJmL5.0-Grazing”. In: *Geosci. Model Dev.* 16.9, pp. 2455–2475. ISSN: 1991-959X. DOI: 10.5194/gmd-16-2455-2023. (Visited on 05/31/2023).
- Hoover, D. L., A. K. Knapp, and M. D. Smith (2014). “Resistance and Resilience of a Grassland Ecosystem to Climate Extremes”. In: *Ecology* 95.9, pp. 2646–2656. ISSN: 1939-9170. DOI: 10.1890/13-2186.1. (Visited on 01/13/2021).
- iNaturalist, i. contributors (2024). “iNaturalist Research-grade Observations”. In: *iNaturalistorg Occur. Dataset*. DOI: 10.15468/ab3s5x. (Visited on 10/16/2024).
- Isbell, F., D. Craven, J. Connolly, M. Loreau, B. Schmid, C. Beierkuhnlein, T. M. Bezemer, C. Bonin, H. Bruelheide, E. de Luca, A. Ebeling, J. N. Griffin, Q. Guo, Y. Hautier, A. Hector, A. Jentsch, J. Kreyling, V. Lanta, P. Manning, S. T. Meyer, A. S. Mori, S. Naeem, P. A. Niklaus, H. W. Polley, P. B. Reich, C. Roscher, E. W. Seabloom, M. D. Smith, M. P. Thakur, D. Tilman, B. F. Tracy, W. H. van der Putten, J. van Ruijven, A. Weigelt, W. W. Weisser, B. Wilsey, and N. Eisenhauer (2015). “Biodiversity Increases the Resistance of Ecosystem Productivity to Climate Extremes”. In: *Nature* 526.7574, pp. 574–577. ISSN: 1476-4687. DOI: 10.1038/nature15374. (Visited on 05/22/2019).
- Jiang, L., S. Wan, and L. Li (2009). “Species Diversity and Productivity: Why Do Results of Diversity-Manipulation Experiments Differ from Natural Patterns?” In: *J. Ecol.* 97.4, pp. 603–608. ISSN: 1365-2745. DOI: 10.1111/j.1365-2745.2009.01503.x. (Visited on 11/05/2024).
- Kattge, J., G. Bönisch, I. C. Díaz, S. Lavorel, I. C. Prentice, P. Leadley, S. Tautenhahn, G. D. A. Werner, T. Aakala, M. Abedi, A. T. R. Acosta, G. C. Adamidis, K. Adamson, M. Aiba, C. H. Albert, J. M. Alcántara, C. Alcázar, C. I. Aleixo, H. Ali, B. Amiaud, C. Ammer, M. M. Amoroso, M. Anand, C. Anderson, N. Anten, J. Antos, D. M. G. Apgaua, T.-L. Ashman, D. H. Asmara, G. P. Asner, M. Aspinwall, O. Atkin, I. Aubin, L. Baastrup-Spohr, K. Bahalkeh, M. Bahn, T. Baker, W. J. Baker, J. P. Bakker, D. Baldocchi, J. Baltzer, A. Banerjee, A. Baranger, J. Barlow, D. R. Barneche, Z. Baruch, D. Bastianelli, J. Battles, W. Bauerle, M. Bauters, E. Bazzato, M. Beckmann, H. Beeckman, C. Beierkuhnlein, R. Bekker, G. Belfry, M. Belluau, M. Beloiu, R. Benavides, L. Benomar, M. L. Berdugo-Lattke, E. Berenguer, R. Bergamin, J. Bergmann, M. Bergmann Carlucci, L. Berner, M. Bernhardt-Römermann, C. Bigler, A. D. Bjorkman, C. Blackman, C. Blanco, B. Blonder, D. Blumenthal, K. T. Bocanegra-González, P. Boeckx, S. Bohlman, K. Böhning-Gaese, L. Boisvert-Marsh, W. Bond, B. Bond-Lamberty, A. Boom, C. C. F. Boonman, K. Bordin, E. H. Boughton, V. Boukili, D. M. J. S. Bowman, S. Bravo, M. R. Brendel, M. R. Broadley, K. A. Brown, H. Bruelheide, F. Brunnich, H. H. Bruun, D. Bruy, S. W. Buchanan, S. F. Bucher, N. Buchmann, R. Buitenwerf, D. E. Bunker, J. Bürger, S. Burrascano, D. F. R. P. Burslem, B. J. Butterfield, C. Byun, M. Marques, M. C. Scalon, M. Caccianiga, M. Cadotte, M. Cailleret, J. Camac, J. J. Camarero, C. Company, G. Campetella, J. A. Campos, L. Cano-Arboleda, R. Canullo, M. Carbognani, F. Carvalho, F. Casanoves, B. Castagnyrol, J. A. Catford, J. Cavender-Bares, B. E. L. Cerabolini, M. Cervellini, E. Chacón-Madrigal, K. Chapin, F. S. Chapin, S. Chelli, S.-C. Chen, A. Chen, P. Cherubini, F. Chianucci, B. Choat, K.-S. Chung, M. Chytrý, D. Ciccarelli, L. Coll, C. G. Collins, L. Conti, D. Coomes, J. H. C. Cornelissen, W. K. Cornwell, P. Corona, M. Coyea, J. Craine, D. Craven, J. P. G. M. Crowsigt, A. Csecserits, K. Cufar, M. Cuntz, A. C. da Silva, K. M. Dahlin, M. Dainese, I. Dalke, M. Dalle Fratte, A. T. Dang-Le, J. Danihelka, M. Dannoura, S. Dawson, A. J. de Beer, A. De Frutos, J. R. De Long, B. Dechant, S. Delagrange, N. Delpierre, G. Derroire, A. S. Dias, M. H. Diaz-Toribio, P. G. Dimitrakopoulos, M. Dobrowolski, D. Doktor, P. Dřevojan, N. Dong, J. Dransfield, S. Dressler, L. Duarte, E. Ducouret, S. Dullinger, W. Durka, R. Duursma, O. Dymova, A. E-Vojtkó, R. L. Eckstein, H. Ejtehadi, J. Elser, T. Emilio, K. Engemann, M. B. Erfanian, A. Erfmeier, A. Esquivel-Muelbert, G. Esser, M. Estiarte, T. F. Domingues, W. F. Fagan, J. Fagúndez, D. S. Falster, Y. Fan, J. Fang, E. Farris, F. Fazlioglu, Y. Feng, F. Fernandez-Mendez, C. Ferrara, J. Ferreira, A. Fidelis, B. Finegan, J. Firn, T. J. Flowers, D. F. B. Flynn, V. Fontana, E. Forey, C. Forgiarini, L. François, M. Frangipani, D. Frank, C. Frenette-Dussault, G. T. Freschet, E. L. Fry, N. M. Fyllas, G. G. Mazzochini, S. Gachet, R. Gallagher, G. Ganade, F. Ganga, P. García-Palacios, V. Gargaglione, E. Garnier, J. L. Garrido, A. L. de Gasper, G. Gea-Izquierdo, D. Gibson, A. N. Gillison, A. Giroldo, M.-C. Glasenhardt, S. Gleason, M. Gliesch, E. Goldberg, B. Gödel, E. Gonzalez-Akre, J. L. Gonzalez-Andujar, A. González-Melo, A. González-Robles, B. J. Graae, E. Granda, S. Graves, W. A. Green, T. Gregor, N. Gross, G. R. Guerin, A. Günther, A. G. Gutiérrez, L. Haddock, A. Haines, J. Hall, A. Hambuckers, W. Han, S. P. Harrison, W. Hatingh, J. E. Hawes, T. He, P. He, J. M. Heberling, A. Helm, S. Hempel, J. Hentschel, B. Hérault, A.-M. Hereş, K. Herz, M. Heuertz, T. Hickler, P. Hietz, P. Higuchi, A. L. Hipp, A. Hirons, M. Hock, J. A. Hogan, K. Holl, O. Honnay, D. Hornstein, E. Hou, N. Hough-Snee, K. A. Hovstad, T. Ichie, B. Igić, E. Illa, M. Isaac, M. Ishihara, L. Ivanov, L. Ivanova, C. M. Iversen, J. Izquierdo, R. B. Jackson, B. Jackson, H. Jactel, A. M. Jagodzinski, U. Jandt, S. Jansen, T. Jenkins, A. Jentsch, J. R. P. Jaspersen, G.-F. Jiang, J. L. Johansen, D. Johnson, E. J. Jokela, C. A. Joly, G. J. Jordan, G. S. Joseph, D. Junaedi, R. R. Junker, E. Justes, R. Kabzems, J. Kane, Z. Kaplan, T. Kattenborn, L. Kavelenova, E. Kearsley, A. Kempel, T. Kenzo, A. Kerckhoff, M. I. Khalil, N. L. Kinlock, W. D. Kissling, K. Kitajima, T. Kitzberger, R. Kjølter, T. Klein, M. Kleyer, J. Klimešová, J. Klipel, B. Kloeppe, S. Klotz, J. M. H. Knops, T. Kohyama, F. Koike, J. Kollmann, B. Komac, K. Komatsu, C. König, N. J. B. Kraft, K. Kramer, H. Kreft, I. Kühn, D. Kumarathunge, J. Kuppler, H. Kurokawa, Y. Kurosawa, S. Kuyah, J.-P. Laclau, B. Lafleur, E. Lallai, E. Lamb, A. Lamprecht, D. J. Larkin, D. Laughlin, Y. Le Bagousse-Pinguet, G. le Maire, P. C. le Roux, E. le Roux, T. Lee, F. Lens, S. L. Lewis, B. Lhotsky, Y. Li, X. Li, J. W. Lichstein, M. Liebergesell, J. Y. Lim, Y.-S. Lin, J. C. Linares, C. Liu, D. Liu, U. Liu, S. Livingstone, J. Llusà, M. Lohbeck, Á. López-García, G. Lopez-Gonzalez, Z. Lososová, F. Louault, B. A. Lukács, P. Lukeš, Y. Luo, M. Lussu, S. Ma, C. Maciel Rabelo Pereira, M. Mack, V. Maire, A. Mäkelä, H. Mäkinen, A. C. M. Malhado, A. Mallik, P. Manning, S. Manzoni, Z. Marchetti, L. Marchino, V. Marcilio-Silva, E. Marcon, M. Marignani, L. Markesteijn, A. Martin, C. Martínez-Garza, J. Martínez-Vilalta, T. Mašková, K. Mason, N. Mason, T. J. Massad, J. Masse, I. Mayrose, J. McCarthy, M. L. McCormack, K. McCulloh, I. R. McFadden, B. J. McGill, M. Y. McPartland, J. S. Medeiros, B. Medlyn, P. Meerts, Z. Mehrabi, P. Meir, F. P. L. Melo, M. Mencuccini, C. Meredieu, J. Messier, I. Mészáros, J. Metsaranta, S. T.

- Michaletz, C. Michelaki, S. Migalina, R. Milla, J. E. D. Miller, V. Minden, R. Ming, K. Mokany, A. T. Moles, A. Molnár V, J. Molofsky, M. Molz, R. A. Montgomery, A. Monty, L. Moravcová, A. Moreno-Martínez, M. Moretti, A. S. Mori, S. Mori, D. Morris, J. Morrison, L. Mucina, S. Mueller, C. D. Muir, S. C. Müller, F. Munoz, I. H. Myers-Smith, R. W. Myster, M. Nagano, S. Naidu, A. Narayanan, B. Natesan, L. Negroita, A. S. Nelson, E. L. Neuschulz, J. Ni, G. Niedrist, J. Nieto, Ü. Niinemets, R. Nolan, H. Nottebrock, Y. Nouvellon, A. Novakovskiy, T. N. Network, K. O. Nystuen, A. O'Grady, K. O'Hara, A. O'Reilly-Nugent, S. Oakley, W. Oberhuber, T. Ohtsuka, R. Oliveira, K. Öllerer, M. E. Olson, V. Onipchenko, Y. Onoda, R. E. Onstein, J. C. Ordóñez, N. Osada, I. Ostonen, G. Ottaviani, S. Otto, G. E. Overbeck, W. A. Ozinga, A. T. Pahl, C. E. T. Paine, R. J. Pakeman, A. C. Papageorgiou, E. Parfionova, M. Pärtel, M. Patacca, S. Paula, J. Paule, H. Pauli, J. G. Pausas, B. Peco, J. Penuelas, A. Perea, P. L. Peri, A. C. Petisco-Souza, A. Petraglia, A. M. Petritan, O. L. Phillips, S. Pierce, V. D. Pillar, J. Pisek, A. Pomogaybin, H. Poorter, A. Portsmouth, P. Poschlod, C. Potvin, D. Pounds, A. S. Powell, S. A. Power, A. Prinzing, G. Puglielli, P. Pyšek, V. Raevel, A. Rammig, J. Ransijn, C. A. Ray, P. B. Reich, M. Reichstein, D. E. B. Reid, M. Réjou-Méchain, V. R. de Dios, S. Ribeiro, S. Richardson, K. Riibak, M. C. Rillig, F. Riviera, E. M. R. Robert, S. Roberts, B. Robroek, A. Roddy, A. V. Rodrigues, A. Rogers, E. Rollinson, V. Rolo, C. Römermann, D. Ronzhina, C. Roscher, J. A. Rosell, M. F. Rosenfield, C. Rossi, D. B. Roy, S. Royer-Tardif, N. Rüger, R. Ruiz-Peinado, S. B. Rumpf, G. M. Rusch, M. Ryo, L. Sack, A. Saldaña, B. Salgado-Negret, R. Salguero-Gomez, I. Santa-Regina, A. C. Santacruz-García, J. Santos, J. Sardans, B. Schamp, M. Scherer-Lorenzen, M. Schleuning, B. Schmid, M. Schmidt, S. Schmitt, J. V. Schneider, S. D. Schowaneck, J. Schrader, F. Schrod, B. Schuldt, F. Schurr, G. Selaya Garviza, M. Semchenko, C. Seymour, J. C. Sfair, J. M. Sharpe, C. S. Sheppard, S. Sheremetiev, S. Shiodera, B. Shipley, T. A. Shovon, A. Siebenkäs, C. Sierra, V. Silva, M. Silva, T. Sitzia, H. Sjöman, M. Slot, N. G. Smith, D. Sodhi, P. Soltis, D. Soltis, B. Somers, G. Sonnier, M. V. Sørensen, E. E. Sosinski Jr, N. A. Soudzilovskaia, A. F. Souza, M. Spasojevic, M. G. Sperandii, A. B. Stan, J. Stegen, K. Steinbauer, J. G. Stephan, F. Sterck, D. B. Stojanovic, T. Strydom, M. L. Suarez, J.-C. Svenning, I. Svitková, M. Svitok, M. Svoboda, E. Swaine, N. Swenson, M. Tabarelli, K. Takagi, U. Tappeiner, R. Tarifa, S. Tauougourdeau, C. Tavsanoğlu, M. te Beest, L. Tedersoo, N. Thiffault, D. Thom, E. Thomas, K. Thompson, P. E. Thornton, W. Thuiller, L. Tichý, D. Tissue, M. G. Tjoelker, D. Y. P. Tng, J. Tobias, P. Török, T. Tarin, J. M. Torres-Ruiz, B. Tóthmérész, M. Treurnicht, V. Trivellone, F. Trolliet, V. Trotsiuk, J. L. Tsakalos, I. Tsiropidis, N. Tysklind, T. Umehara, V. Usoltsev, M. Vadeboncoeur, J. Vaezi, F. Valladares, J. Vamosi, P. M. van Bodegom, M. van Breugel, E. Van Cleemput, M. van de Weg, S. van der Merwe, F. van der Plas, M. T. van der Sande, M. van Kleunen, K. Van Meerbeek, M. Vanderwel, K. A. Vanselow, A. Vårhammar, L. Varone, M. Y. Vasquez Valderrama, K. Vassilev, M. Vellend, E. J. Veneklaas, H. Verbeeck, K. Verheyen, A. Vibrans, I. Vieira, J. Villacís, C. Violle, P. Vivek, K. Wagner, M. Waldram, A. Waldron, A. P. Walker, M. Waller, G. Walther, H. Wang, F. Wang, W. Wang, H. Watkins, J. Watkins, U. Weber, J. T. Weedon, L. Wei, P. Weigelt, E. Weiher, A. W. Wells, C. Wellstein, E. Wenk, M. Westoby, A. Westwood, P. J. White, M. Whitten, M. Williams, D. E. Winkler, K. Winter, C. Womack, I. J. Wright, S. J. Wright, J. Wright, B. X. Pinho, F. Ximenes, T. Yamada, K. Yamaji, R. Yanai, N. Yankov, B. Yguel, K. J. Zanini, A. E. Zanne, D. Zelený, Y.-P. Zhao, J. Zheng, J. Zheng, K. Ziemińska, C. R. Zirbel, G. Zizka, I. C. Zo-Bi, G. Zotz, and C. Wirth (2020). "TRY Plant Trait Database – Enhanced Coverage and Open Access". In: *Glob. Change Biol.* 26.1, pp. 119–188. ISSN: 1365-2486. DOI: 10.1111/gcb.14904. (Visited on 04/19/2024).
- Kim, H. (2017). *Global Soil Wetness Project Phase 3 Atmospheric Boundary Conditions (Experiment 1), Data Integration and Analysis System (DIAS)*. DOI: 10.20783/DIAS.501.
- Lambert, M. S. A., H. Tang, K. S. Aas, F. Stordal, R. A. Fisher, J. W. Bjerke, J. A. Holm, and F.-J. W. Parmentier (2023). "Integration of a Frost Mortality Scheme Into the Demographic Vegetation Model FATES". In: *J. Adv. Model. Earth Syst.* 15.7, e2022MS003333. ISSN: 1942-2466. DOI: 10.1029/2022MS003333. (Visited on 11/05/2024).
- Lange, S., M. Mengel, S. Treu, and M. Büchner (2022). *ISIMIP3a Atmospheric Climate Input Data (v1.0)*. DOI: 10.48364/ISIMIP.982724. (Visited on 09/05/2023).
- Le Quéré, C., T. Takahashi, E. T. Buitenhuis, C. Rödenbeck, and S. C. Sutherland (2010). "Impact of Climate Change and Variability on the Global Oceanic Sink of CO<sub>2</sub>". In: *Glob. Biogeochem. Cycles* 24.4. ISSN: 1944-9224. DOI: 10.1029/2009GB003599. (Visited on 01/06/2025).
- Lee, J., J. Marotzke, G. Bala, L. Cao, S. Corti, J. Dunne, F. Engelbrecht, E. Fischer, J. Fyfe, C. Jones, A. Maycock, J. Mutemi, O. Ndiaye, S. Panickal, and T. Zhou (2021). "Future Global Climate: Scenario-Based Projections and Near-Term Information". In: *Climate Change 2021: The Physical Science Basis. Contribution of Working Group I to the Sixth Assessment Report of the Intergovernmental Panel on Climate Change*. Ed. by V. Masson-Delmotte, P. Zhai, A. Pirani, S. Connors, C. Péan, S. Berger, N. Caud, Y. Chen, L. Goldfarb, M. Gomis, M. Huang, K. Leitzell, E. Lonnoy, J. Matthews, T. Maycock, T. Waterfield, O. Yelekçi, R. Yu, and B. Zhou. Cambridge, United Kingdom and New York, NY, USA: Cambridge University Press, pp. 553–672.
- Liu, J., Y. You, J. Li, S. Sitch, X. Gu, J. E. Nabel, D. Lombardozzi, M. Luo, X. Feng, A. Arneeth, A. K. Jain, P. Friedlingstein, H. Tian, B. Poulter, and D. Kong (2021). "Response of Global Land Evapotranspiration to Climate Change, Elevated CO<sub>2</sub>, and Land Use Change". In: *Agricultural and Forest Meteorology* 311, p. 108663. ISSN: 01681923. DOI: 10.1016/j.agrformet.2021.108663. (Visited on 11/19/2024).
- Loarie, S. R., P. B. Duffy, H. Hamilton, G. P. Asner, C. B. Field, and D. D. Ackerly (2009). "The Velocity of Climate Change". In: *Nature* 462.7276, pp. 1052–1055. ISSN: 1476-4687. DOI: 10.1038/nature08649. (Visited on 11/05/2024).
- Lucie, L., E. Aude, F. Elodie, R. Sébastien, C. Benjamin, B. Maube, and M. Cendrine (2023). "Landscape Structure Influences Grassland Productivity through Plant Functional Diversity". In: *Agriculture, Ecosystems & Environment* 357, p. 108650. ISSN: 0167-8809. DOI: 10.1016/j.agee.2023.108650. (Visited on 01/13/2025).

- Lutz, F., T. Herzfeld, J. Heinke, S. Rolinski, S. Schaphoff, W. von Bloh, J. J. Stoorvogel, and C. Müller (2019). “Simulating the Effect of Tillage Practices with the Global Ecosystem Model LPJmL (Version 5.0-Tillage)”. In: *Geosci. Model Dev.* 12.6, pp. 2419–2440. ISSN: 1991-959X. DOI: 10.5194/gmd-12-2419-2019. (Visited on 05/31/2023).
- McSherry, M. E. and M. E. Ritchie (2013). “Effects of Grazing on Grassland Soil Carbon: A Global Review”. In: *Glob. Change Biol.* 19.5, pp. 1347–1357. ISSN: 1365-2486. DOI: 10.1111/gcb.12144. (Visited on 06/13/2022).
- Mebane Jr., W. R. and J. S. Sekhon (2011). “Genetic Optimization Using Derivatives: The Rgenoud Package for R”. In: *J. Stat. Softw.* 42, pp. 1–26. ISSN: 1548-7660. DOI: 10.18637/jss.v042.i11. (Visited on 10/16/2024).
- Meinshausen, M., E. Vogel, A. Nauels, K. Lorbacher, N. Meinshausen, D. M. Etheridge, P. J. Fraser, S. A. Montzka, P. J. Rayner, C. M. Trudinger, P. B. Krummel, U. Beyerle, J. G. Canadell, J. S. Daniel, I. G. Enting, R. M. Law, C. R. Lunder, S. O’Doherty, R. G. Prinn, S. Reimann, M. Rubino, G. J. M. Velders, M. K. Vollmer, R. H. J. Wang, and R. Weiss (2017). “Historical Greenhouse Gas Concentrations for Climate Modelling (CMIP6)”. In: *Geosci. Model Dev.* 10.5, pp. 2057–2116. ISSN: 1991-959X. DOI: 10.5194/gmd-10-2057-2017. (Visited on 01/07/2025).
- Nie, Y., L. Xu, X. Xin, and L. Ye (2024). “Long-Term Grassland Diversity-Productivity Relationship Regulated by Management Regimes in Northern China”. In: *Science of The Total Environment* 949, p. 175084. ISSN: 0048-9697. DOI: 10.1016/j.scitotenv.2024.175084. (Visited on 01/13/2025).
- O’Neill, B. C., C. Tebaldi, D. P. van Vuuren, V. Eyring, P. Friedlingstein, G. Hurtt, R. Knutti, E. Kriegler, J.-F. Lamarque, J. Lowe, G. A. Meehl, R. Moss, K. Riahi, and B. M. Sanderson (2016). “The Scenario Model Intercomparison Project (ScenarioMIP) for CMIP6”. In: *Geosci. Model Dev.* 9.9, pp. 3461–3482. ISSN: 1991-959X. DOI: 10.5194/gmd-9-3461-2016. (Visited on 01/06/2025).
- Obeso, J. R. (2002). “The Costs of Reproduction in Plants”. In: *New Phytol.* 155.3, pp. 321–348. ISSN: 1469-8137. DOI: 10.1046/j.1469-8137.2002.00477.x. (Visited on 01/22/2025).
- Ostberg, S., C. Müller, J. Heinke, and S. Schaphoff (2023). “LandInG 1.0: A Toolbox to Derive Input Datasets for Terrestrial Ecosystem Modelling at Variable Resolutions from Heterogeneous Sources”. In: *Geosci. Model Dev.* 16.11, pp. 3375–3406. ISSN: 1991-959X. DOI: 10.5194/gmd-16-3375-2023. (Visited on 09/05/2023).
- Pan, Q., A. J. Symstad, Y. Bai, J. Huang, J. Wu, S. Naem, D. Chen, D. Tian, Q. Wang, and X. Han (2022). “Biodiversity–Productivity Relationships in a Natural Grassland Community Vary under Diversity Loss Scenarios”. In: *J. Ecol.* 110.1, pp. 210–220. ISSN: 1365-2745. DOI: 10.1111/1365-2745.13797. (Visited on 01/13/2025).
- Pasari, J. R., T. Levi, E. S. Zavaleta, and D. Tilman (2013). “Several Scales of Biodiversity Affect Ecosystem Multifunctionality”. In: *Proc. Natl. Acad. Sci.* 110.25, pp. 10219–10222. DOI: 10.1073/pnas.1220333110. (Visited on 04/25/2024).
- Pearson, R. G. (2006). “Climate Change and the Migration Capacity of Species”. In: *Trends in Ecology & Evolution* 21.3, pp. 111–113. ISSN: 0169-5347. DOI: 10.1016/j.tree.2005.11.022. (Visited on 11/05/2024).
- Petermann, J. S. and O. Y. Buzhdygan (2021). “Grassland Biodiversity”. In: *Current Biology* 31.19, R1195–R1201. ISSN: 0960-9822. DOI: 10.1016/j.cub.2021.06.060. (Visited on 11/12/2024).
- Pfeiffer, M., L. Langan, A. Linstädter, C. Martens, C. Gaillard, J. C. Ruppert, S. I. Higgins, E. I. Mudongo, and S. Scheiter (2019). “Grazing and Aridity Reduce Perennial Grass Abundance in Semi-Arid Rangelands – Insights from a Trait-Based Dynamic Vegetation Model”. In: *Ecological Modelling* 395, pp. 11–22. ISSN: 0304-3800. DOI: 10.1016/j.ecolmodel.2018.12.013. (Visited on 02/13/2023).
- Pierce, S., G. Brusa, I. Vagge, and B. E. L. Cerabolini (2013). “Allocating CSR Plant Functional Types: The Use of Leaf Economics and Size Traits to Classify Woody and Herbaceous Vascular Plants”. In: *Funct. Ecol.* 27.4, pp. 1002–1010. ISSN: 1365-2435. DOI: 10.1111/1365-2435.12095. (Visited on 09/26/2018).
- Pierce, S., D. Negreiros, B. E. L. Cerabolini, J. Kattge, S. Díaz, M. Kleyer, B. Shipley, S. J. Wright, N. A. Soudzilovskaia, V. G. Onipchenko, P. M. van Bodegom, C. Frenette-Dussault, E. Weiher, B. X. Pinho, J. H. C. Cornelissen, J. P. Grime, K. Thompson, R. Hunt, P. J. Wilson, G. Buffa, O. C. Nyakunga, P. B. Reich, M. Caccianiga, F. Mangili, R. M. Ceriani, A. Luzzaro, G. Brusa, A. Siefert, N. P. U. Barbosa, F. S. Chapin, W. K. Cornwell, J. Fang, G. W. Fernandes, E. Garnier, S. L. Stradic, J. Peñuelas, F. P. L. Melo, A. Slaviero, M. Tabarelli, and D. Tampucci (2017). “A Global Method for Calculating Plant CSR Ecological Strategies Applied across Biomes World-Wide”. In: *Funct. Ecol.* 31.2, pp. 444–457. ISSN: 1365-2435. DOI: 10.1111/1365-2435.12722. (Visited on 11/26/2020).
- Piipponen, J., M. Jalava, J. de Leeuw, A. Rizayeva, C. Godde, G. Cramer, M. Herrero, and M. Kumm (2022). “Global Trends in Grassland Carrying Capacity and Relative Stocking Density of Livestock”. In: *Glob. Change Biol.* 28.12, pp. 3902–3919. ISSN: 1365-2486. DOI: 10.1111/gcb.16174. (Visited on 02/02/2023).
- Prangel, E., L. Kasari-Toussaint, L. Neuenkamp, N. Noreika, R. Karise, R. Marja, N. Ingerpuu, T. Kupper, L. Keerberg, E. Oja, M. Meriste, A. Tiitsaar, M. Ivask, and A. Helm (2023). “Afforestation and Abandonment of Semi-Natural Grasslands Lead to Biodiversity Loss and a Decline in Ecosystem Services and Functions”. In: *J. Appl. Ecol.* 60.5, pp. 825–836. ISSN: 1365-2664. DOI: 10.1111/1365-2664.14375. (Visited on 01/06/2025).
- Reeg, J., S. Heine, C. Mihan, S. McGee, T. G. Preuss, and F. Jeltsch (2018). “Simulation of Herbicide Impacts on a Plant Community: Comparing Model Predictions of the Plant Community Model IBC-grass to Empirical Data”. In: *Environmental Sciences Europe* 30.1, p. 44. ISSN: 2190-4715. DOI: 10.1186/s12302-018-0174-9. (Visited on 10/01/2024).
- Reeg, J., S. Heine, C. Mihan, S. McGee, T. G. Preuss, and F. Jeltsch (2020). “Herbicide Risk Assessments of Non-Target Terrestrial Plant Communities: A Graphical User Interface for the Plant Community Model IBC-grass”. In: *PLOS ONE* 15.3, e0230012. ISSN: 1932-6203. DOI: 10.1371/journal.pone.0230012. (Visited on 10/01/2024).
- Schaphoff, S., W. von Bloh, A. Rammig, K. Thonicke, H. Biemans, M. Forkel, D. Gerten, J. Heinke, J. Jägermeyr, J. Knauer, F. Langerwisch, W. Lucht, C. Müller, S. Rolinski, and K. Waha (2018). “LPJmL4 – a Dynamic Global Vegetation Model with Managed Land – Part 1: Model Description”. In: *Geosci. Model Dev.* 11.4, pp. 1343–1375. ISSN: 1991-959X. DOI: 10.5194/gmd-11-1343-2018. (Visited on 05/31/2023).

- Scheiter, S., M. Pfeiffer, K. Behn, K. K. Ayisi, F. Siebert, and A. Linstädter (2023). “Managing Southern African Rangeland Systems in the Face of Drought - a Synthesis of Observation, Experimentation, and Modelling for Policy and Decision Support”. In: *Sustainability of Southern African Ecosystems under Global Change*. Ed. by G. P. von Maltitz, G. F. Midgley, J. Veitch, C. Brümmer, R. P. Rötter, F. A. Viehberg, and M. Veste. Vol. 248. Ecological Studies. Springer.
- Schiller, C., S. Schmidlein, C. Boonman, A. Moreno-Martínez, and T. Kattenborn (2021). “Deep Learning and Citizen Science Enable Automated Plant Trait Predictions from Photographs”. In: *Sci Rep* 11.1, p. 16395. ISSN: 2045-2322. DOI: 10.1038/s41598-021-95616-0. (Visited on 01/10/2025).
- Schulze, E. D., O. Bouriaud, U. Weber, C. Roscher, D. Hessenmoeller, F. Kroiher, and P. Schall (2018). “Management Breaks the Natural Productivity-Biodiversity Relationship in Forests and Grassland: An Opinion”. In: *Forest Ecosystems* 5.1, p. 3. ISSN: 2197-5620. DOI: 10.1186/s40663-017-0122-y. (Visited on 01/13/2025).
- Schulze, E.-D. and H. A. Mooney, eds. (1993). *Biodiversity and Ecosystem Function*. Berlin, Heidelberg: Springer. ISBN: 978-3-540-58103-1 978-3-642-58001-7. DOI: 10.1007/978-3-642-58001-7. (Visited on 04/25/2024).
- Scollan, N. D., R. J. Dewhurst, A. P. Moloney, and J. J. Murphy (2005). “Improving the Quality of Products from Grassland”. In: *Grassland: A Global Resource*. Wageningen Academic, pp. 41–56. ISBN: 978-90-8686-551-2. (Visited on 01/27/2025).
- Sekhon, J. S. and W. R. M. Jr (1998). “Genetic Optimization Using Derivatives”. In: *Polit. Anal.* 7, pp. 187–210. ISSN: 1047-1987, 1476-4989. DOI: 10.1093/pan/7.1.187. (Visited on 10/16/2024).
- Sheffield, J. and E. F. Wood (2008). “Projected Changes in Drought Occurrence under Future Global Warming from Multi-Model, Multi-Scenario, IPCC AR4 Simulations”. In: *Clim Dyn* 31.1, pp. 79–105. ISSN: 1432-0894. DOI: 10.1007/s00382-007-0340-z. (Visited on 01/22/2025).
- Sillen, W. M. A. and W. I. J. Dieleman (2012). “Effects of Elevated CO<sub>2</sub> and N Fertilization on Plant and Soil Carbon Pools of Managed Grasslands: A Meta-Analysis”. In: *Biogeosciences* 9.6, pp. 2247–2258. ISSN: 1726-4170. DOI: 10.5194/bg-9-2247-2012. (Visited on 01/06/2025).
- Stuart-Hill, G. and M. Mentis (1982). “Coevolution of African Grasses and Large Herbivores”. In: *Proc. Annu. Congr. Grassl. Soc. South. Afr.* 17.1, pp. 122–128. ISSN: 0072-5560. DOI: 10.1080/00725560.1982.9648969. (Visited on 02/13/2023).
- Suttie, J., S. Reynolds, and C. Batello, eds. (2005). *Grasslands of the World*. Vol. No. 34. Plant Production and Protection Series. Rome: Food & Agriculture Organization of the United Nations. ISBN: 978-92-5-105337-9.
- Taubert, F., K. Frank, and A. Huth (2012). “A Review of Grassland Models in the Biofuel Context”. In: *Ecological Modelling*. 7th European Conference on Ecological Modelling (ECEM) 245, pp. 84–93. ISSN: 0304-3800. DOI: 10.1016/j.ecolmodel.2012.04.007. (Visited on 02/07/2019).
- Taubert, F., J. Hetzer, J. S. Schmid, and A. Huth (2020). “The Role of Species Traits for Grassland Productivity”. In: *Ecosphere* 11.7, e03205. ISSN: 2150-8925. DOI: 10.1002/ecs2.3205. (Visited on 02/09/2023).
- Thum, T., S. Caldararu, J. Engel, M. Kern, M. Pallandt, R. Schnur, L. Yu, and S. Zaehle (2019). “A New Model of the Coupled Carbon, Nitrogen, and Phosphorus Cycles in the Terrestrial Biosphere (QUINCY v1.0; Revision 1996)”. In: *Geosci. Model Dev.* 12.11, pp. 4781–4802. ISSN: 1991-959X. DOI: 10.5194/gmd-12-4781-2019. (Visited on 11/05/2024).
- Tilman, D., P. B. Reich, and F. Isbell (2012). “Biodiversity Impacts Ecosystem Productivity as Much as Resources, Disturbance, or Herbivory”. In: *PNAS* 109.26, pp. 10394–10397. ISSN: 0027-8424, 1091-6490. DOI: 10.1073/pnas.1208240109. (Visited on 12/16/2020).
- Tilman, D., P. B. Reich, J. Knops, D. Wedin, T. Mielke, and C. Lehman (2001). “Diversity and Productivity in a Long-Term Grassland Experiment”. In: *Science* 294.5543, pp. 843–845. DOI: 10.1126/science.1060391. (Visited on 01/06/2025).
- Twardek, W. M., J. J. Taylor, T. Rytwinski, S. N. Aitken, A. L. MacDonald, R. Van Bogaert, and S. J. Cooke (2023). “The Application of Assisted Migration as a Climate Change Adaptation Tactic: An Evidence Map and Synthesis”. In: *Biological Conservation* 280, p. 109932. ISSN: 0006-3207. DOI: 10.1016/j.biocon.2023.109932. (Visited on 11/05/2024).
- von Bloh, W., S. Schaphoff, C. Müller, S. Rolinski, K. Waha, and S. Zaehle (2018). “Implementing the Nitrogen Cycle into the Dynamic Global Vegetation, Hydrology, and Crop Growth Model LPJmL (Version 5.0)”. In: *Geosci. Model Dev.* 11.7, pp. 2789–2812. ISSN: 1991-959X. DOI: 10.5194/gmd-11-2789-2018. (Visited on 05/31/2023).
- von Fischer, J. C., L. L. Tieszen, and D. S. Schimel (2008). “Climate Controls on C3 vs. C4 Productivity in North American Grasslands from Carbon Isotope Composition of Soil Organic Matter”. In: *Glob. Change Biol.* 14.5, pp. 1141–1155. ISSN: 1365-2486. DOI: 10.1111/j.1365-2486.2008.01552.x. (Visited on 11/12/2024).
- Wang, B., H. Yan, and Q. Zhang (2022a). “Reciprocity of Grassland Conservation and Pastoralist Livelihoods: Evidence from Comparison between Developed and Developing Regions”. In: *Ecological Indicators* 144, p. 109517. ISSN: 1470-160X. DOI: 10.1016/j.ecolind.2022.109517. (Visited on 01/27/2025).
- Wang, Y., W. Pei, G. Cao, X. Guo, and Y. Du (2022b). “Response Characteristics of Grassland Ecosystem Biomass to Grazing Intensity in China”. In: *Grassl. Sci.* 68.2, pp. 193–201. ISSN: 1744-697X. DOI: 10.1111/grs.12346. (Visited on 10/16/2024).
- Weisser, W. W., C. Roscher, S. T. Meyer, A. Ebeling, G. Luo, E. Allan, H. Beßler, R. L. Barnard, N. Buchmann, F. Buscot, C. Engels, C. Fischer, M. Fischer, A. Gessler, G. Gleixner, S. Halle, A. Hildebrandt, H. Hillebrand, H. de Kroon, M. Lange, S. Leimer, X. Le Roux, A. Milcu, L. Mommer, P. A. Niklaus, Y. Oelmann, R. Proulx, J. Roy, C. Scherber, M. Scherer-Lorenzen, S. Scheu, T. Tschardtke, M. Wachendorf, C. Wagg, A. Weigelt, W. Wilcke, C. Wirth, E.-D. Schulze, B. Schmid, and N. Eisenhauer (2017). “Biodiversity Effects on Ecosystem Functioning in a 15-Year Grassland Experiment: Patterns, Mechanisms, and Open Questions”. In: *Basic Appl. Ecol.* Biodiversity Effects on Ecosystem Functioning: The Jena Experiment 23, pp. 1–73. ISSN: 1439-1791. DOI: 10.1016/j.baee.2017.06.002. (Visited on 01/27/2020).
- White, R. P., S. Murray, and M. Rohweder (2000). “Pilot Analysis of Global Ecosystems: Grassland Ecosystems.” In: *Pilot Anal. Glob. Ecosyst. Grassl. Ecosyst.* (Visited on 02/13/2023).

- Wirth, S. B., J. Braun, J. Heinke, S. Ostberg, S. Rolinski, S. Schaphoff, F. Stenzel, W. von Bloh, and C. Müller (2024a). “Biological Nitrogen Fixation of Natural and Agricultural Vegetation Simulated with LPJmL 5.7.9”. In: *EGUsphere*, pp. 1–29. DOI: 10.5194/egusphere-2023-2946. (Visited on 03/18/2024).
- Wirth, S. B., A. Poyda, F. Taube, B. Tietjen, C. Müller, K. Thonicke, A. Linstädter, K. Behn, S. Schaphoff, W. von Bloh, and S. Rolinski (2024b). “Connecting Competitor, Stress-Tolerator and Ruderal (CSR) Theory and Lund Potsdam Jena Managed Land 5 (LPJmL 5) to Assess the Role of Environmental Conditions, Management and Functional Diversity for Grassland Ecosystem Functions”. In: *Biogeosciences* 21.2, pp. 381–410. ISSN: 1726-4170. DOI: 10.5194/bg-21-381-2024. (Visited on 03/18/2024).
- Wolf, S., M. D. Mahecha, F. M. Sabatini, C. Wirth, H. Bruelheide, J. Kattge, Á. Moreno Martínez, K. Mora, and T. Kattenborn (2022). “Citizen Science Plant Observations Encode Global Trait Patterns”. In: *Nat Ecol Evol* 6.12, pp. 1850–1859. ISSN: 2397-334X. DOI: 10.1038/s41559-022-01904-x. (Visited on 09/18/2023).
- Yan, Z., Z. Gao, B. Sun, X. Ding, T. Gao, and Y. Li (2023). “Global Degradation Trends of Grassland and Their Driving Factors since 2000”. In: *Int. J. Digit. Earth* 16.1, pp. 1661–1684. ISSN: 1753-8947. DOI: 10.1080/17538947.2023.2207840. (Visited on 10/01/2024).
- Yang, J. and H. Tian (2020). *ISIMIP3b N-deposition Input Data (v1.0)*. DOI: 10.48364/ISIMIP.600567. (Visited on 09/05/2023).
- Yukimoto, S., H. Kawai, T. Koshiro, N. Oshima, K. Yoshida, S. Urakawa, H. Tsujino, M. Deushi, T. Tanaka, M. Hosaka, S. Yabu, H. Yoshimura, E. Shindo, R. Mizuta, A. Obata, Y. Adachi, and M. Ishii (2019). “The Meteorological Research Institute Earth System Model Version 2.0, MRI-ESM2.0: Description and Basic Evaluation of the Physical Component”. In: *J. Meteorol. Soc. Jpn. Ser II* 97.5, pp. 931–965. DOI: 10.2151/jmsj.2019-051.
- Zhang, Y., X. Xiao, X. Wu, S. Zhou, G. Zhang, Y. Qin, and J. Dong (2017). “A Global Moderate Resolution Dataset of Gross Primary Production of Vegetation for 2000–2016”. In: *Sci Data* 4.1, p. 170165. ISSN: 2052-4463. DOI: 10.1038/sdata.2017.165. (Visited on 02/02/2023).
- Zhu, K., Y. Song, J. C. Lesage, J. C. Luong, J. W. Bartolome, N. R. Chiariello, J. Dudley, C. B. Field, L. M. Hallett, M. Hammond, S. P. Harrison, G. F. Hayes, R. J. Hobbs, K. D. Holl, P. Hopkinson, L. Larios, M. E. Loik, and L. R. Prugh (2024). “Rapid Shifts in Grassland Communities Driven by Climate Change”. In: *Nat Ecol Evol*, pp. 1–13. ISSN: 2397-334X. DOI: 10.1038/s41559-024-02552-z. (Visited on 10/23/2024).

# Chapter 6

## General discussion

As outlined in 1.1, managed grasslands are complex systems and functional diversity is important for the ecosystem services they provide. In the past, field experiments and detailed modelling at small spatial scales have contributed to our understanding of the role of functional diversity in managed grasslands. Nevertheless, the role of functional diversity in grassland ecosystem services is still not fully resolved. Early empirical research suggested that the effect of functional diversity is generally positive for grassland productivity and functional diversity loss leads to a productivity decrease (Tilman et al., 2001). However, these findings were challenged because the effect was not observed in all field experiments (Adler et al., 2011). To date, functional ecologists are still disentangling the complex interplay of environmental conditions, management and functional diversity, trying to find universal relationships between functional diversity and ecosystem service provision. Especially the diversity-productivity (e.g., Craven et al., 2016; Tilman et al., 2012), diversity-stability (e.g., Buzhdygan et al., 2020; Isbell et al., 2015b) and diversity-invasion theories (Petermann et al., 2010; Zavaleta and Hulvey, 2004) are of interest beyond functional ecology because of their potential to contribute to ecosystem adaptation to climate change. Regardless of this debate, historically, dynamic global vegetation models (DGVMs) have not considered the role of functional diversity in their analyses. While this has been addressed for natural ecosystems in so-called next-generation DGVMs (Sakschewski et al., 2015; Scheiter et al., 2013), a representation of functional diversity in managed grasslands is still lacking.

Despite this gap, classic DGVMs — defined here as models that represent plant communities using only a small number of plant functional types (PFTs) and do not account for functional diversity beyond phenology and leaf type — are widely used to study managed grasslands under climate change. For example, Chang et al. (2017) project an increase in grassland yields and optimal stocking densities for warming levels between 1.5 and 3.5 °C (see also 1.1.2). However, their model considers only a C3 and C4 grass plant functional type (Chang et al., 2013) and their results do not account for the role of functional diversity. As a consequence, their projected increase in optimal stocking density does not consider the role of functional diversity in the ability of managed grasslands to adapt to climate change. Therefore they may have either over- or underestimated grassland productivity adaptation and projected optimal stocking densities under climate change. Additionally, animal stocking density also affects plant functional diversity and the relationship between functional diversity and ecosystem services (e.g., Chillo et al., 2017; Sanaei et al., 2023).

Rolinski et al. (2021) who also employed the Lund-Potsdam-Jena managed Land (LPJmL) model that was used in this thesis, studied the effects of climate and land-use change on grassland productivity

and soil organic carbon stocks. Similarly to Chang et al. (2017), functional diversity could not be considered by Rolinski et al. (2021) because it was not represented in LPJmL. While both examples provide important insights into the future of managed grasslands in different regions, future research would benefit from the explicit representation of functional diversity. Additionally, results would be more relevant — and potentially more informative for policymakers, farmers and other stakeholders — because functional diversity is an important side constraint of managed grassland productivity which is otherwise ignored.

Addressing this gap, this thesis provides an overview of the processes that are insufficiently represented or missing from DGVMs but are necessary for representing grassland functional diversity (Chapter 2). To identify these processes, I conducted a model comparison between the LPJmL DGVM and the Grassland Individual-based Dynamic Model (GRASSMIND) to investigate the capability of both models to simulate vegetation dynamics of monocultures and multi-species communities. Based on these findings, I developed an approach to represent the role of functional diversity in managed grassland ecosystem services (Chapter 3), as well as biological nitrogen fixation (Chapter 4) in the LPJmL DGVM. This approach incorporates the well-known competitor, stress-tolerator, ruderal (CSR) theory to represent the establishment of different ecological strategies depending on environmental conditions and management. The functional differences between the strategies described by the CSR theory are represented using several functional plant traits and trade-offs from the global spectrum of plant form and function (Díaz et al., 2016). Using the extended LPJmL-CSR model, I investigated the role of functional diversity in managed grassland productivity and soil organic carbon storage at the local scale in different climates and under different management (Chapter 3), as well as on the global scale under climate change (Chapter 5).

Chapters 2 to 5 provide a foundation to discuss the contribution of functional diversity to ecosystem services that support food security at the global scale (6.1), the implications for the challenges arising from the combination of biodiversity loss and climate change (6.2) and the advantages and disadvantages of using a classic DGVM to simulate functional diversity (6.3).

## **6.1 The contribution of grassland functional diversity to forage supply, soil organic carbon stocks and food security**

One of the main research questions of my thesis was to improve the understanding of functional diversity's role in the productivity and soil organic carbon (SOC) storage of managed grasslands. To address this, I analysed the results of several simulation experiments presented in Chapters 3 and 5. In Chapter 3, I assessed how different levels of management intensity affect forage offtake and SOC stocks across various climates. Using the new LPJmL-CSR model, I investigated three managed grasslands for which

data from field experiments were available to assess the validity of the approach and analyse the role of climate and management in community composition. Although my scenarios cover only a limited number of different management options, they highlight the system's complexity. For example, intensive management with high stocking densities leads to a loss of SOC and aboveground biomass at the cold steppe site in Inner Mongolia, which emphasizes the need to adapt — and often reduce — the stocking densities to prevent overgrazing.

However, simply reducing stocking densities is often not sufficient to restore grasslands because part of the native species pool has been lost (Török et al., 2021) or replaced by invasive or deliberately sown species. These native species pools co-developed with wild grazing animals over long periods resulting in a dynamic equilibrium of key ecosystem functions such as productivity and carbon storage. Restoration of the native species pool is complex and requires knowledge of the local seed bank, migration patterns and potential methods to suppress invasive species (Török et al., 2018). A recent study on grazing exclusion in Inner Mongolia showed that grazing exclusion for up to twenty years increases grassland productivity and SOC stocks, followed by a decline under prolonged exclusion (Liu et al., 2025). Hence, grassland restoration is complex and measures must be designed specific to the context of the respective grassland and the reference state against which restoration should be evaluated (see Török et al., 2021). While LPJmL-CSR is not a suitable tool to inform on grassland restoration practices at specific sites due to its resolution, the simulations still highlight that functional diversity underpins grassland productivity and SOC stocks and should be maintained or restored. Specifically, LPJmL-CSR enables studying management-dependent community compositions, which allows drawing conclusions on the effect of management changes not only on overall productivity and soil organic carbon stocks but also on the abundance of different strategies. For example, in Chapter 3, I investigated different resource limitations by conducting rainfed, irrigated or fertilised simulations. At the temperate grassland site in Germany, the comparison of these different scenarios showed that the simulated functional composition of the community was barely affected by manure application because nitrogen limitation was compensated by increased biological nitrogen fixation in the unfertilised simulations. However, at the hot steppe site in Namibia, irrigation increased the share of the competitive and ruderal strategies.

Considering the high complexity of factors that contribute to grassland ecosystem services in general, a broad set of research approaches is needed to improve knowledge, develop more sustainable management options and quantify sustainable stocking densities. As described in more detail in Chapters 3 and 5, productivity, and in turn, SOC stocks are controlled by temperature, water and nutrient availability, atmospheric carbon dioxide (CO<sub>2</sub>) concentration, irrigation, fertiliser application, defoliation intensity, trampling and fire. These factors influence productivity and SOC stocks directly but also indirectly via their control over functional diversity. For example, Weigelt et al. (2009) show that similar pro-

ductivity can be achieved in intensively managed low-diversity and extensively managed high-diversity systems, illustrating the importance of the interaction between functional diversity and management. It is therefore reasonable that a community with low resource stress and, as a result, a lower functional diversity and a community with somewhat higher resource stress and, in turn, functional diversity may have similar productivity and SOC stocks. However, if functional diversity is removed, the somewhat stressed community may lose some of its productivity and SOC stocks. Because plant communities that do not suffer from any stress are rare, maintaining functional diversity is crucial. This is in line with the results of Chapter 5, which show a substantial loss of simulated gross primary productivity (GPP) and SOC in many regions if functional diversity is reduced to the dominant strategy. Especially, GPP can directly be related to aboveground biomass and, in turn, the provision of forage and livestock products that contribute to food security.

With respect to food security research, LPJmL-CSR can only be used to assess the availability and stability dimensions of food security. My results indicate that functional diversity is important for both these dimensions of food security. As described in detail in Chapters 3 and 5, functional diversity supports productivity and SOC stocks in managed grasslands. Productivity largely determines the amount of ruminant meat or dairy that can be obtained and, therefore, food availability. SOC stocks are not only important for the terrestrial carbon sink but also for the nutrient balance (Gerke, 2022), preventing fertility loss and ensuring the stability and availability of grass-based food products. Furthermore, while I did not simulate scenarios to assess the capacity of functional diversity to increase community resilience against water stress, this has been established through field experiments across different environmental and management conditions (Isbell et al., 2015a; Walde et al., 2021). However, other studies did not find a benefit of functional diversity for drought resistance but rather a loss of functional diversity with decreasing precipitation (Miller et al., 2019). Considering that drought frequency and intensity will likely increase under climate change, the potential of functional diversity to reduce drought impacts and the risk of decreasing food security in regions of marginal productivity, where grass-based food products are most important for food security, should be a future research priority. Here, LPJmL-CSR could be used to conduct simulation experiments for various levels of drought stress as was already done with LPJmL and GRASSMIND in Chapter 2.

While field experiments provide important insights at the local scale and meta-analyses can synthesize these, using a global-scale model adds another perspective. It allows for the comparison of grasslands under different environmental conditions and management within one consistent framework, without additional harmonization that is necessary when comparing field experiments. This thesis showed that functional diversity is important for productivity in managed grasslands across the globe. However, the underlying reasons differed and, in some cases, were dependent on climate change (see also Chapter 6.2). While my results are similar to those of empirical research and highlight the importance of func-

tional diversity once more, I did not investigate the role of management intensity at the global scale. Here, sufficiently detailed datasets are not available. The dataset I used for stocking density (Heinke, 2025), based on Herrero et al. (2013), only contains estimates for one year and values for some countries are unrealistic. For example, stocking densities in India are unrealistically high as a result of high livestock numbers that are likely not all fed by reported grassland areas. Therefore, I did not include this in my research questions and refrained from giving detailed advice on how to adapt stocking densities and management practices but see this work as the basis for additional investigations and for providing a global-scale approximation of the importance of functional diversity (see Chapter 1.4).

Additionally, assessments based on one specific model can contain significant uncertainties. In modelling, multi-model ensembles are commonly applied to account for the uncertainties in different implementations of the same processes, making their results more robust than those of single models (Duan et al., 2019). For example, Sándor et al. (2020) and Sándor et al. (2023) compared the carbon and nitrogen fluxes of multiple grassland models, which vary in the range of processes represented and the complexity of their approaches. Using an ensemble, they were able to improve the representation of historical carbon fluxes (Sándor et al., 2023). However, Sándor et al. (2023) also highlight that ensembles may show deficiencies in the representation of underlying processes. Additionally, even if ensemble members produce similar results, there is no guarantee that the results are correct because all ensemble members might miss specific important processes or drivers potentially distorting their results (Parker, 2013). Unfortunately, I am also unaware of any other global vegetation models that can represent functional diversity in managed grasslands and a broad set of management options. However, such models would allow for providing an ensemble showing a range of changes for different variables at different grassland functional diversity levels.

## **6.2 Implications for the dual challenge: biodiversity loss and climate change**

I clearly demonstrated that functional diversity is important for grassland productivity and SOC stocks under climate change in Chapter 5. This analysis also presents the first global-scale assessment of the role of functional diversity in grassland productivity and SOC stocks. However, my evaluation showed that the representation of ecological strategies can be further improved and additional trade-offs and processes should be included in LPJmL-CSR. In this assessment, I compared a world where all represented ecological strategies could establish (high functional diversity) with one where communities only contain the dominant ecological strategy (low functional diversity). This comparison showed that the role of functional diversity for GPP and SOC stocks varied across different regions of the globe. These differences were related to different responses of the plant community to climate change and

the removal of subordinate PFTs. In some regions, the productivity of the dominant PFT increased if its competitors were removed. However, the increase was rarely sufficient to surpass the productivity of the diverse community. In other regions, the historically dominant PFT became unsuitable under climate change and grassland productivity either completely plummeted in the scenario without diversity or a shift in the community composition led to increased productivity in the scenario with a diverse community.

Generally, the results of Chapter 5 align well with ecological theory and functional diversity experiments. This is especially important, considering that currently functional diversity is continuously lost as a result of intensified management (Flynn et al., 2009; Wesche et al., 2012). Climate change has been discussed to accelerate functional diversity loss, which may, in turn, lead to a reduction in the natural carbon sink and the remaining CO<sub>2</sub> budget (Raven and Wagner, 2021; Warren et al., 2021; Zhu et al., 2024). Therefore, biodiversity loss and climate change cannot be treated as separate challenges but must be resolved together. While the large-scale interactions between functional diversity loss and climate change have been modelled for forests (e.g., Miles et al., 2004), for grasslands, only meta-analyses of empirical research (e.g., Borer et al., 2017) and local and regional studies exist (e.g., Moredi et al., 2023; Moredi et al., 2024). Nevertheless, these studies found a strong interaction effect and called for a change in management. In the future, LPJmL-CSR could be used to investigate a portfolio of management and functional diversity scenarios to project and inform on potential productivity and SOC stocks of managed grasslands. However, such scenarios should also consider projected land-use change. Especially since land-use allocation models project significant changes in the extent of managed grasslands (Popp et al., 2017).

At the global scale, land-use allocation models project a reduction in grassland areas until 2100 caused by large-scale afforestation/reforestation efforts to mitigate climate change (Bluwstein and Cavanagh, 2023; Weindl et al., 2024). However, Popp et al. (2017) show that the projected change in grassland area depends on socio-economic development and values for 2100 range from a reduction of up to 1000 Mha to an increase of 500 Mha. Considering that pasture areas will most easily become available for afforestation if the consumption of ruminant meat and dairy products is substantially reduced (Humpenöder et al., 2024), I observe a contrast to recent trends showing continuously high meat consumption in the global North and a catching up of the global South (Delgado et al., 2001), although I want to emphasize that livestock consumption remains minimal in many countries of the global South (Li et al., 2024). Regardless of the change in grassland area, whether these grasslands remain carbon sinks or become a source of carbon under climate change will largely depend on their management (Bai and Cotrufo, 2022; Bardgett et al., 2021; Conant et al., 2017). In Chapter 5, I showed that functional diversity provides a buffer against losses in productivity and SOC storage even under moderate climate change. It follows that functional diversity is important for both climate-change adaptation through

changes in communities as well as for climate change mitigation by supporting SOC stocks, which contribute to the land carbon sink. However, maintaining functional diversity in grasslands will also require the adaptation of production and consumption patterns, as management needs to be made less intensive. Even if diets shift and ruminant meat and dairy consumption is substantially reduced, large grassland areas will remain (Popp et al., 2010) and should be managed sustainably.

LPJmL-CSR could be used to assess different management intensities globally and compare the resulting productivity and SOC stocks to estimate sustainable management intensities. Providing such information to land-use allocation models or global land use modelling frameworks, such as the Model of Agricultural Production and its Impacts on the Environment (MAgPIE) (Dietrich et al., 2019), could improve their projections of future land-use change. These projections are based on socio-economic variables and projected agricultural productivity, which includes managed grassland productivity but currently does not explicitly quantify the role of functional diversity. The joint results of land-use allocation models and DGVMs could contribute to informing policies aimed at combating biodiversity loss and climate change while maintaining the role of grasslands in food security.

### **6.3 Advantages and disadvantages of using LPJmL-CSR to assess functional diversity**

DGVMs have long been criticized for their simplified representation of ecosystems using PFTs, which largely neglects functional diversity (Quillet et al., 2010). So-called next-generation or trait-based DGVMs have addressed this by including functional diversity, usually via trait distributions of well-known functional traits such as specific leaf area (SLA) (e.g., Pfeiffer et al., 2019; Sakschewski et al., 2015). Often, such models are individual-based models, where individuals represent single plants with different functional traits. While this is a substantial improvement in the representation of functional diversity and ecosystems, their application at the global scale is hindered by substantially higher computational costs compared to classic DGVMs. Therefore, DGVMs that follow a PFT approach are still widely used, either as parts of Earth system models (e.g., Drüke et al., 2023; Notaro et al., 2007) or stand-alone to assess climate change impacts (Friedlingstein et al., 2024; Liu et al., 2021). Additionally, next-generation DGVMs have mainly focused on forest ecosystems and natural vegetation but have so far not considered agricultural ecosystems such as managed grasslands. Considering the trade-offs between a detailed representation of important dynamics and computational costs, seeking a compromise that considers important dynamics in a simple way is required. One option is to develop a simple approach that aligns with the average individual philosophy of classic DGVMs.

The model inter-comparison of LPJmL and GRASSMIND in Chapter 2 highlights the advantages and disadvantages of both the average-individual and the individual-based approaches, providing guidance

on the level of complexity needed to represent functional diversity. While both models were able to moderately match observations of monoculture and multi-species communities, my comparison showed that neither model approach provides a definitive solution to represent all aspects of grassland ecosystems that were relevant at the Jena site well. In both models, the representation of multi-species communities required improvement, necessitating further model development. In particular, trade-offs between different ecological strategies were not well represented. For example, while species with a high specific leaf area were more competitive, consistent with empirical findings (Pierce et al., 2013), the trade-off with leaf longevity was not represented. Furthermore, in both models, competition for below-ground resources, such as water and nitrogen, was not sufficiently represented, limiting the number of potentially successful ecological strategies primarily to aboveground processes. I hypothesized that implementing trade-offs between different ecological strategies, along with a better representation of below-ground resource competition, would be a major step forward and, therefore, focused on these aspects during model development. This model development was conducted for the classic DGVM LPJmL, leading to advantages and disadvantages compared to a similar implementation in an individual-based next-generation DGVM.

While classic DGVMs are commonly used to investigate the carbon cycle (e.g., O’Sullivan et al., 2022; Teckentrup et al., 2021) and to quantify the terrestrial carbon sink (Friedlingstein et al., 2024), next-generation DGVMs — or, more generally individual-based vegetation models — focus more on ecological research questions, such as species interactions (Pfeiffer et al., 2019; Scheiter et al., 2020). Zakharova et al. (2019) conducted a review of trait-based models and found that they can contribute to a comprehensive understanding of global change effects on communities. However, considering that answering the research questions of this thesis requires an assessment of parts of the carbon cycle, I decided to use the classic DGVM LPJmL. LPJmL has a long-standing history of global-scale applications to assess different aspects of the carbon cycle (e.g., Herzfeld et al., 2021; Pugh et al., 2020; Rolinski et al., 2018; Xu et al., 2020); however, my comparison showed that trait trade-offs are not well represented. While I was able to improve this aspect through extensive model development (Chapter 3), continuous effort is needed to further enhance the representation of functional diversity (see 6.4).

To retain the PFT-based approach, I had to base the model development on a theory that allowed the aggregation of functional diversity into a limited set of ecological strategies. I decided to base the representation on CSR theory because it has been mapped to functional traits that were already present in LPJmL or could be added as new parameters. While CSR theory has been used in modelling at the local scale (e.g., Schippers et al., 2022), I was the first to apply it to represent functional diversity in a DGVM. The resulting model, LPJmL-CSR, was first tested at three sites in different climates and under various management conditions (Chapter 3) and subsequently calibrated and applied at the global scale (Chapter 5). The tests at the three sites showed that LPJmL-CSR could represent the annual average

CSR composition of the communities. However, the traits used to represent these communities differed depending on environmental conditions and management, illustrating that there is no one-size-fits-all parameter set to reproduce the results of local experiments in detail. However, this is not the main application of LPJmL, which was designed to reproduce large-scale patterns and trends and I therefore view the local-scale assessments in Chapters 2 and 3 as proof of concept that functional diversity can be represented in a DGVM if trade-offs between different ecological strategies are included. Chapter 5 contains a global-scale analysis in which I showed that total community GPP was well reproduced and that community composition varied across regions. However, I also identified the need for further model development to better distinguish ecological strategies and functional diversity. In the following paragraph, I compare some of the advantages and disadvantages identified in Chapters 2 and 3 to those of next-generation or trait-based DGVMs.

Considering that trait-based models are continuously being developed, they will likely always outperform classic DGVMs at representing functional diversity. However, they will also continue to have higher computational costs or become even more computationally expensive if additional functional traits are included, increasing the number of individuals required to represent the trait space adequately. Therefore, their ability to be applied to questions requiring large simulation ensembles using different inputs (e.g., climate or management scenarios) may remain limited. Ideally, the development of classic and trait-based DGVMs would become integrated, ensuring that general improvements of either are incorporated into the other. For example, the Lund-Potsdam-Jena General Ecosystem Simulator (LPJ-GUESS) model (Smith et al., 2001) can be applied as an individual-based and a classic DGVM which in theory promotes close interaction among developers of different model realisations. Similarly, LPJmL is developed in close collaboration with the trait-based Lund-Potsdam-Jena managed Land - Flexible Individual Traits (LPJmL-FIT) model (Sakschewski et al., 2015; Thonicke et al., 2020), fostering synergies between the different approaches. Such a setup also offers the opportunity to use a large-scale ensemble for an initial assessment, while a trait-based model can be used to investigate specific aspects in greater detail. This combination could lead to better results than using only one approach, increasing not only the informational value but also trust in the models.

## 6.4 Overall conclusion and future outlook

I successfully implemented a representation of functional diversity in managed grassland in a DGVM, making LPJmL-CSR the first DGVM capable of assessing a wide variety of management, climate and functional diversity scenarios. My assessments showed that the model was able to reproduce key effects of functional diversity on productivity and SOC stocks of managed grasslands at both the local and global scale, which have also been described in empirical research. While this represents a major

improvement, I found substantial potential for further model development. Future model development should focus on improving trade-offs and distinguishing the differences between ecological strategies. While LPJmL-CSR provides global-scale projections, it is limited by its coarse spatial resolution and numerous assumptions about grassland management. Future research would benefit from joint assessments with models at different scales especially for regions where LPJmL-CSR projects a strong role of functional diversity.

My results emphasize once again that functional diversity should be considered when designing sustainable management options and should be incorporated in corresponding policies. A multi-model ensemble would be useful for providing robust information to policymakers. However, this would require additional global-scale models to incorporate a variety of grassland management options and functional diversity. Furthermore, additional research is needed to improve the representation of key processes and in turn functional diversity. For example, the level of abstraction used to represent functional diversity strongly affects both model results and computational costs. Using additional trait data or a more fine-grained representation of functional diversity — one that covers a broader range of the trait space — may be necessary to balance computational efficiency and realistic ecosystem dynamics.

Especially, the dual challenge of biodiversity loss and climate change needs to be investigated more thoroughly to identify feedbacks and better quantify the role of functional diversity. My results provide a foundation for further research using additional data on management intensities as well as changes in grassland extent and allocation to broaden the scope of future scenarios. Initially, LPJmL-CSR could be used to generate projections of grassland productivity and SOC stocks along a management intensity gradient. These results could be integrated into land-use allocation models allowing them to account for the role of functional diversity and management intensity in their projections of future land use and land-use change. Finally, the scarcity of global-scale datasets on grassland management and productivity limits the comparability to real-world grasslands. However, at the regional scale, such datasets are available, for example, from field observations and remote sensing. Therefore, additional regional-scale assessments of large grassland biomes, where LPJmL-CSR is calibrated against regional datasets, would improve our understanding of the interactions between functional diversity, management intensity and climate. This approach would also contribute to developing sustainable management options to maintain agricultural production, preserve the land carbon sink and ensure food security.

## 6.5 References

Adler, P. B., E. W. Seabloom, E. T. Borer, H. Hillebrand, Y. Hautier, A. Hector, W. S. Harpole, L. R. O'Halloran, J. B. Grace, T. M. Anderson, J. D. Bakker, L. A. Biederman, C. S. Brown, Y. M. Buckley, L. B. Calabrese, C.-J. Chu, E. E. Cleland, S. L. Collins, K. L. Cottingham, M. J. Crawley, E. I. Damschen, K. F. Davies, N. M. DeCrappeo, P. A. Fay, J. Firn, P. Frater, E. I. Gasarch, D. S. Gruner, N. Hagenah, J. H. R. Lambers, H. Humphries, V. L. Jin, A. D. Kay, K. P. Kirkman, J. A. Klein, J. M. H. Knops, K. J. L. Pierre, J. G. Lambrinos, W. Li, A. S. MacDougall, R. L. McCulley, B. A. Melbourne, C. E. Mitchell, J. L. Moore, J. W. Morgan, B. Mortensen, J. L. Orrock, S. M. Prober, D. A. Pyke, A. C. Risch, M. Schuetz,

- M. D. Smith, C. J. Stevens, L. L. Sullivan, G. Wang, P. D. Wragg, J. P. Wright, and L. H. Yang (2011). “Productivity Is a Poor Predictor of Plant Species Richness”. In: *Science* 333.6050, pp. 1750–1753. ISSN: 0036-8075, 1095-9203. DOI: 10.1126/science.1204498. (Visited on 08/13/2018).
- Bai, Y. and M. F. Cotrufo (2022). “Grassland Soil Carbon Sequestration: Current Understanding, Challenges, and Solutions”. In: *Science* 377.6606, pp. 603–608. DOI: 10.1126/science.abo2380. (Visited on 02/13/2023).
- Bardgett, R. D., J. M. Bullock, S. Lavorel, P. Manning, U. Schaffner, N. Ostle, M. Chomel, G. Durigan, E. L. Fry, D. Johnson, J. M. Lavalley, G. Le Provost, S. Luo, K. Png, M. Sankaran, X. Hou, H. Zhou, L. Ma, W. Ren, X. Li, Y. Ding, Y. Li, and H. Shi (2021). “Combatting Global Grassland Degradation”. In: *Nat Rev Earth Environ* 2.10, pp. 720–735. ISSN: 2662-138X. DOI: 10.1038/s43017-021-00207-2. (Visited on 03/08/2022).
- Bluwstein, J. and C. Cavanagh (2023). “Rescaling the Land Rush? Global Political Ecologies of Land Use and Cover Change in Key Scenario Archetypes for Achieving the 1.5 °C Paris Agreement Target”. In: *J. Peasant Stud.* 50.1, pp. 262–294. ISSN: 0306-6150. DOI: 10.1080/03066150.2022.2125386. (Visited on 11/20/2024).
- Borer, E. T., J. B. Grace, W. S. Harpole, A. S. MacDougall, and E. W. Seabloom (2017). “A Decade of Insights into Grassland Ecosystem Responses to Global Environmental Change”. In: *Nat Ecol Evol* 1.5, pp. 1–7. ISSN: 2397-334X. DOI: 10.1038/s41559-017-0118. (Visited on 11/20/2024).
- Buzhdygan, O. Y., S. T. Meyer, W. W. Weisser, N. Eisenhauer, A. Ebeling, S. R. Borrett, N. Buchmann, R. Cortois, G. B. De Deyn, H. de Kroon, G. Gleixner, L. R. Hertzog, J. Hines, M. Lange, L. Mommer, J. Ravenek, C. Scherber, M. Scherer-Lorezen, S. Scheu, B. Schmid, K. Steinauer, T. Strecker, B. Tietjen, A. Vogel, A. Weigelt, and J. S. Petermann (2020). “Biodiversity Increases Multitrophic Energy Use Efficiency, Flow and Storage in Grasslands”. In: *Nat Ecol Evol* 4.3, pp. 393–405. ISSN: 2397-334X. DOI: 10.1038/s41559-020-1123-8. (Visited on 11/20/2023).
- Chang, J., P. Ciais, N. Viovy, J.-F. Soussana, K. Klumpp, and B. Sultan (2017). “Future Productivity and Phenology Changes in European Grasslands for Different Warming Levels: Implications for Grassland Management and Carbon Balance”. In: *Carbon Balance and Management* 12.1, p. 11. ISSN: 1750-0680. DOI: 10.1186/s13021-017-0079-8. (Visited on 04/17/2024).
- Chang, J., N. Viovy, N. Vuichard, P. Ciais, T. Wang, A. Cozic, R. Lardy, A.-I. Graux, K. Klumpp, R. Martin, and J.-F. Soussana (2013). “Incorporating Grassland Management in ORCHIDEE: Model Description and Evaluation at 11 Eddy-Covariance Sites in Europe”. In: *Geosci. Model Dev.* 6.6, pp. 2165–2181. ISSN: 1991-9603. DOI: 10.5194/gmd-6-2165-2013. (Visited on 08/13/2018).
- Chillo, V., R. A. Ojeda, V. Capmourteres, and M. Anand (2017). “Functional Diversity Loss with Increasing Livestock Grazing Intensity in Drylands: The Mechanisms and Their Consequences Depend on the Taxa”. In: *J. Appl. Ecol.* 54.3, pp. 986–996. ISSN: 1365-2664. DOI: 10.1111/1365-2664.12775. (Visited on 01/21/2025).
- Conant, R. T., C. E. P. Cerri, B. B. Osborne, and K. Paustian (2017). “Grassland Management Impacts on Soil Carbon Stocks: A New Synthesis”. In: *Ecol. Appl.* 27.2, pp. 662–668. ISSN: 1939-5582. DOI: 10.1002/eap.1473. (Visited on 02/13/2023).
- Craven, D., F. Isbell, P. Manning, J. Connolly, H. Bruelheide, A. Ebeling, C. Roscher, J. van Ruijven, A. Weigelt, B. Wilsey, C. Beierkuhnlein, E. de Luca, J. N. Griffin, Y. Hautier, A. Hector, A. Jentsch, J. Kreyling, V. Lanta, M. Loreau, S. T. Meyer, A. S. Mori, S. Naeem, C. Palmberg, H. W. Polley, P. B. Reich, B. Schmid, A. Siebenkäs, E. Seabloom, M. P. Thakur, D. Tilman, A. Vogel, and N. Eisenhauer (2016). “Plant Diversity Effects on Grassland Productivity Are Robust to Both Nutrient Enrichment and Drought”. In: *Philos. Trans. R. Soc. B Biol. Sci.* 371.1694. ISSN: 0962-8436. DOI: 10.1098/rstb.2015.0277. (Visited on 12/09/2019).
- Delgado, C., M. Rosegrant, H. Steinfeld, S. Ehui, and C. Courbois (2001). “Livestock to 2020: The Next Food Revolution”. In: *Outlook Agric* 30.1, pp. 27–29. ISSN: 0030-7270. DOI: 10.5367/00000001101293427. (Visited on 11/20/2024).
- Díaz, S., J. Kattge, J. H. C. Cornelissen, I. J. Wright, S. Lavorel, S. Dray, B. Reu, M. Kleyer, C. Wirth, I. C. Prentice, E. Garnier, G. Bönsch, M. Westoby, H. Poorter, P. B. Reich, A. T. Moles, J. Dickie, A. N. Gillison, A. E. Zanne, J. Chave, S. J. Wright, S. N. Sheremet’ev, H. Jactel, C. Baraloto, B. Cerabolini, S. Pierce, B. Shipley, D. Kirkup, F. Casanoves, J. S. Joswig, A. Günther, V. Falczuk, N. Rüger, M. D. Mahecha, and L. D. Gorné (2016). “The Global Spectrum of Plant Form and Function”. In: *Nature* 529.7585, pp. 167–171. ISSN: 1476-4687. DOI: 10.1038/nature16489. (Visited on 03/24/2020).
- Dietrich, J. P., B. L. Bodirsky, F. Humpenöder, I. Weindl, M. Stevanović, K. Karstens, U. Kreidenweis, X. Wang, A. Mishra, D. Klein, G. Ambrósio, E. Araujo, A. W. Yalew, L. Baumstark, S. Wirth, A. Giannousakis, F. Beier, D. M.-C. Chen, H. Lotze-Campen, and A. Popp (2019). “MAGPIE 4 – a Modular Open-Source Framework for Modeling Global Land Systems”. In: *Geosci. Model Dev.* 12.4, pp. 1299–1317. ISSN: 1991-9603. DOI: 10.5194/gmd-12-1299-2019. (Visited on 06/28/2019).
- Drüke, M., B. Sakschewski, W. von Bloh, M. Billing, W. Lucht, and K. Thonicke (2023). “Fire May Prevent Future Amazon Forest Recovery after Large-Scale Deforestation”. In: *Commun Earth Environ* 4.1, pp. 1–10. ISSN: 2662-4435. DOI: 10.1038/s43247-023-00911-5. (Visited on 11/19/2024).
- Duan, H., G. Zhang, S. Wang, and Y. Fan (2019). “Robust Climate Change Research: A Review on Multi-Model Analysis”. In: *Environ. Res. Lett.* 14.3, p. 033001. ISSN: 1748-9326. DOI: 10.1088/1748-9326/aaf8f9. (Visited on 11/20/2024).
- Flynn, D. F. B., M. Gogol-Prokurat, T. Nogeire, N. Molinari, B. T. Richers, B. B. Lin, N. Simpson, M. M. Mayfield, and F. DeClerck (2009). “Loss of Functional Diversity under Land Use Intensification across Multiple Taxa”. In: *Ecol. Lett.* 12.1, pp. 22–33. ISSN: 1461-0248. DOI: 10.1111/j.1461-0248.2008.01255.x. (Visited on 11/20/2024).
- Friedlingstein, P., M. O’Sullivan, M. W. Jones, R. M. Andrew, J. Hauck, P. Landschützer, C. Le Quééré, H. Li, I. T. Luijkx, A. Olsen, G. P. Peters, W. Peters, J. Pongratz, C. Schwingshackl, S. Sitch, J. G. Canadell, P. Ciais, R. B. Jackson, S. R. Alin, A. Arneeth, V. Arora, N. R. Bates, N. Bellouin, C. F. Berghoff, H. C. Bittig, L. Bopp, P. Cadule, K. Campbell, M. A. Chamberlain, N. Chandra, F. Chevallier, L. P. Chini, T. Colligan, J. Decayeux, L. Djeutchouang, X. Dou, C. Duran

- Rojas, K. Enyo, W. Evans, A. Fay, R. A. Feely, D. J. Ford, A. Foster, T. Gasser, M. Gehlen, T. Gkritzalis, G. Grassi, L. Gregor, N. Gruber, Ö. Gürses, I. Harris, M. Hefner, J. Heinke, G. C. Hurtt, Y. Iida, T. Ilyina, A. R. Jacobson, A. Jain, T. Jarníková, A. Jersild, F. Jiang, Z. Jin, E. Kato, R. F. Keeling, K. Klein Goldewijk, J. Knauer, J. I. Korsbakken, S. K. Lauvset, N. Lefèvre, Z. Liu, J. Liu, L. Ma, S. Maksyutov, G. Marland, N. Mayot, P. McGuire, N. Metz, N. M. Monacci, E. J. Morgan, S.-I. Nakaoka, C. Neill, Y. Niwa, T. Nützel, L. Olivier, T. Ono, P. I. Palmer, D. Pierrot, Z. Qin, L. Resplandy, A. Roobaert, T. M. Rosan, C. Rödenbeck, J. Schwinger, T. L. Smallman, S. Smith, R. Sospedra-Alfonso, T. Steinhoff, Q. Sun, A. J. Sutton, R. Séférian, S. Takao, H. Tatebe, H. Tian, B. Tilbrook, O. Torres, E. Tourigny, H. Tsujino, F. Tubiello, G. van der Werf, R. Wanninkhof, X. Wang, D. Yang, X. Yang, Z. Yu, W. Yuan, X. Yue, S. Zaehle, N. Zeng, and J. Zeng (2024). “Global Carbon Budget 2024”. In: *Earth Syst. Sci. Data Discuss.*, pp. 1–133. DOI: 10.5194/essd-2024-519. (Visited on 11/19/2024).
- Gerke, J. (2022). “The Central Role of Soil Organic Matter in Soil Fertility and Carbon Storage”. In: *Soil Syst.* 6.2, p. 33. ISSN: 2571-8789. DOI: 10.3390/soilsystems6020033. (Visited on 11/20/2024).
- Heinke, J. (2025). *A Livestock Density Input for LPJmL*. DOI: 10.5281/zenodo.14946695. (Visited on 03/05/2025).
- Herrero, M., P. Havlik, H. Valin, A. Notenbaert, M. C. Rufino, P. K. Thornton, M. Blummel, F. Weiss, D. Grace, and M. Obersteiner (2013). “Biomass Use, Production, Feed Efficiencies, and Greenhouse Gas Emissions from Global Livestock Systems”. In: *Proc. Natl. Acad. Sci.* 110.52, pp. 20888–20893. ISSN: 0027-8424, 1091-6490. DOI: 10.1073/pnas.1308149110. (Visited on 03/06/2019).
- Herzfeld, T., J. Heinke, S. Rolinski, and C. Müller (2021). “Soil Organic Carbon Dynamics from Agricultural Management Practices under Climate Change”. In: *Earth Syst. Dyn.* 12.4, pp. 1037–1055. ISSN: 2190-4979. DOI: 10.5194/esd-12-1037-2021. (Visited on 05/31/2023).
- Humpenöder, F., A. Popp, L. Merfort, G. Luderer, I. Weindl, B. L. Bodirsky, M. Stevanović, D. Klein, R. Rodrigues, N. Bauer, J. P. Dietrich, H. Lotze-Campen, and J. Rockström (2024). “Food Matters: Dietary Shifts Increase the Feasibility of 1.5°C Pathways in Line with the Paris Agreement”. In: *Sci. Adv.* 10.13, eadj3832. DOI: 10.1126/sciadv.adj3832. (Visited on 04/17/2024).
- Isbell, F., D. Craven, J. Connolly, M. Loreau, B. Schmid, C. Beierkuhnlein, T. M. Bezemer, C. Bonin, H. Bruelheide, E. de Luca, A. Ebeling, J. N. Griffin, Q. Guo, Y. Hautier, A. Hector, A. Jentsch, J. Kreyling, V. Lanta, P. Manning, S. T. Meyer, A. S. Mori, S. Naeem, P. A. Niklaus, H. W. Polley, P. B. Reich, C. Roscher, E. W. Seabloom, M. D. Smith, M. P. Thakur, D. Tilman, B. F. Tracy, W. H. van der Putten, J. van Ruijven, A. Weigelt, W. W. Weisser, B. Wilsey, and N. Eisenhauer (2015a). “Biodiversity Increases the Resistance of Ecosystem Productivity to Climate Extremes”. In: *Nature* 526.7574, pp. 574–577. ISSN: 1476-4687. DOI: 10.1038/nature15374. (Visited on 05/22/2019).
- Isbell, F., D. Tilman, S. Polasky, and M. Loreau (2015b). “The Biodiversity-Dependent Ecosystem Service Debt”. In: *Ecol. Lett.* 18.2, pp. 119–134. ISSN: 1461-0248. DOI: 10.1111/ele.12393. (Visited on 11/20/2024).
- Li, C., P. Pradhan, X. Wu, Z. Li, J. Liu, K. Hubacek, and G. Chen (2024). “Livestock Sector Can Threaten Planetary Boundaries without Regionally Differentiated Strategies”. In: *Journal of Environmental Management* 370, p. 122444. ISSN: 0301-4797. DOI: 10.1016/j.jenvman.2024.122444. (Visited on 10/18/2024).
- Liu, J., Y. You, J. Li, S. Sitch, X. Gu, J. E. Nabel, D. Lombardozzi, M. Luo, X. Feng, A. Arneeth, A. K. Jain, P. Friedlingstein, H. Tian, B. Poulter, and D. Kong (2021). “Response of Global Land Evapotranspiration to Climate Change, Elevated CO<sub>2</sub>, and Land Use Change”. In: *Agricultural and Forest Meteorology* 311, p. 108663. ISSN: 01681923. DOI: 10.1016/j.agrformet.2021.108663. (Visited on 11/19/2024).
- Liu, W., H. Zhang, X.-t. Lü, Y. Zhou, Y. Yang, Y. Lü, J. Yang, L. Wen, Q. Pan, and X. Han (2025). “Dynamics and Drivers of Primary Productivity along a 40-Year Grazing Exclusion Chronosequence in a Typical Steppe of Inner Mongolia”. In: *Restor. Ecol.* n/a.n/a, e14377. ISSN: 1061-2971. DOI: 10.1111/rec.14377. (Visited on 01/15/2025).
- Miles, L., A. Grainger, and O. Phillips (2004). “The Impact of Global Climate Change on Tropical Forest Biodiversity in Amazonia”. In: *Glob. Ecol. Biogeogr.* 13.6, pp. 553–565. ISSN: 1466-8238. DOI: 10.1111/j.1466-822X.2004.00105.x. (Visited on 11/20/2024).
- Miller, J. E. D., D. Li, M. LaForgia, and S. Harrison (2019). “Functional Diversity Is a Passenger but Not Driver of Drought-Related Plant Diversity Losses in Annual Grasslands”. In: *J. Ecol.* 107.5, pp. 2033–2039. ISSN: 1365-2745. DOI: 10.1111/1365-2745.13244. (Visited on 11/20/2024).
- Movedi, E., S. Bocchi, L. Paleari, F. M. Vesely, I. Vagge, and R. Confalonieri (2023). “Impacts of Climate Change on Semi-Natural Alpine Pastures Productivity and Floristic Composition”. In: *Reg Environ Change* 23.4, p. 159. ISSN: 1436-378X. DOI: 10.1007/s10113-023-02158-4. (Visited on 11/20/2024).
- Movedi, E., L. Paleari, G. Argenti, F. M. Vesely, N. Staglianò, S. Parrini, and R. Confalonieri (2024). “The Application of a Plant Community Model to Evaluate Adaptation Strategies for Alleviating Climate Change Impacts on Grassland Productivity, Biodiversity and Forage Quality”. In: *Ecological Modelling* 488, p. 110596. ISSN: 0304-3800. DOI: 10.1016/j.ecolmodel.2023.110596. (Visited on 11/20/2024).
- Notaro, M., S. Vavrus, and Z. Liu (2007). “Global Vegetation and Climate Change Due to Future Increases in CO<sub>2</sub> as Projected by a Fully Coupled Model with Dynamic Vegetation”. In: *J. Clim.* 20.1, pp. 70–90. ISSN: 0894-8755, 1520-0442. DOI: 10.1175/JCLI3989.1. (Visited on 11/19/2024).
- O’Sullivan, M., P. Friedlingstein, S. Sitch, P. Anthoni, A. Arneeth, V. K. Arora, V. Bastrikov, C. Delire, D. S. Goll, A. Jain, E. Kato, D. Kennedy, J. Knauer, S. Lienert, D. Lombardozzi, P. C. McGuire, J. R. Melton, J. E. M. S. Nabel, J. Pongratz, B. Poulter, R. Séférian, H. Tian, N. Vuichard, A. P. Walker, W. Yuan, X. Yue, and S. Zaehle (2022). “Process-Oriented Analysis of Dominant Sources of Uncertainty in the Land Carbon Sink”. In: *Nat Commun* 13.1, p. 4781. ISSN: 2041-1723. DOI: 10.1038/s41467-022-32416-8. (Visited on 11/19/2024).

- Parker, W. S. (2013). “Ensemble Modeling, Uncertainty and Robust Predictions”. In: *WIREs Clim. Change* 4.3, pp. 213–223. ISSN: 1757-7799. DOI: 10.1002/wcc.220. (Visited on 11/20/2024).
- Petermann, J. S., A. J. F. Fergus, C. Roscher, L. A. Turnbull, A. Weigelt, and B. Schmid (2010). “Biology, Chance, or History? The Predictable Reassembly of Temperate Grassland Communities”. In: *Ecology* 91.2, pp. 408–421. ISSN: 1939-9170. DOI: 10.1890/08-2304.1. (Visited on 04/25/2024).
- Pfeiffer, M., L. Langan, A. Linstädter, C. Martens, C. Gaillard, J. C. Ruppert, S. I. Higgins, E. I. Mudongo, and S. Scheiter (2019). “Grazing and Aridity Reduce Perennial Grass Abundance in Semi-Arid Rangelands – Insights from a Trait-Based Dynamic Vegetation Model”. In: *Ecological Modelling* 395, pp. 11–22. ISSN: 0304-3800. DOI: 10.1016/j.ecolmodel.2018.12.013. (Visited on 02/13/2023).
- Pierce, S., G. Brusa, I. Vagge, and B. E. L. Cerabolini (2013). “Allocating CSR Plant Functional Types: The Use of Leaf Economics and Size Traits to Classify Woody and Herbaceous Vascular Plants”. In: *Funct. Ecol.* 27.4, pp. 1002–1010. ISSN: 1365-2435. DOI: 10.1111/1365-2435.12095. (Visited on 09/26/2018).
- Popp, A., K. Calvin, S. Fujimori, P. Havlik, F. Humpenöder, E. Stehfest, B. L. Bodirsky, J. P. Dietrich, J. C. Doelmann, M. Gusti, T. Hasegawa, P. Kyle, M. Obersteiner, A. Tabreau, K. Takahashi, H. Valin, S. Waldhoff, I. Weindl, M. Wise, E. Kriegler, H. Lotze-Campen, O. Fricko, K. Riahi, and D. P. van Vuuren (2017). “Land-Use Futures in the Shared Socio-Economic Pathways”. In: *Global Environmental Change* 42, pp. 331–345. ISSN: 0959-3780. DOI: 10.1016/j.gloenvcha.2016.10.002. (Visited on 11/20/2024).
- Popp, A., H. Lotze-Campen, and B. Bodirsky (2010). “Food Consumption, Diet Shifts and Associated Non-CO2 Greenhouse Gases from Agricultural Production”. In: *Global Environmental Change. Governance, Complexity and Resilience* 20.3, pp. 451–462. ISSN: 0959-3780. DOI: 10.1016/j.gloenvcha.2010.02.001. (Visited on 04/17/2024).
- Pugh, T. A. M., T. Rademacher, S. L. Shafer, J. Steinkamp, J. Barichivich, B. Beckage, V. Haverd, A. Harper, J. Heinke, K. Nishina, A. Rammig, H. Sato, A. Arneith, S. Hantson, T. Hickler, M. Kautz, B. Quesada, B. Smith, and K. Thonicke (2020). “Understanding the Uncertainty in Global Forest Carbon Turnover”. In: *Biogeosciences* 17.15, pp. 3961–3989. ISSN: 1726-4170. DOI: 10.5194/bg-17-3961-2020. (Visited on 11/19/2024).
- Quillet, A., C. Peng, and M. Garneau (2010). “Toward Dynamic Global Vegetation Models for Simulating Vegetation–Climate Interactions and Feedbacks: Recent Developments, Limitations, and Future Challenges”. In: *Environ. Rev.* 18.NA, pp. 333–353. ISSN: 1181-8700, 1208-6053. DOI: 10.1139/A10-016. (Visited on 04/06/2018).
- Raven, P. H. and D. L. Wagner (2021). “Agricultural Intensification and Climate Change Are Rapidly Decreasing Insect Biodiversity”. In: *Proc. Natl. Acad. Sci.* 118.2, e2002548117. DOI: 10.1073/pnas.2002548117. (Visited on 11/20/2024).
- Rolinski, S., C. Müller, J. Heinke, I. Weindl, A. Biewald, B. L. Bodirsky, A. Bondeau, E. R. Boons-Prins, A. F. Bouwman, P. A. Leffelaar, J. A. te Roller, S. Schaphoff, and K. Thonicke (2018). “Modeling Vegetation and Carbon Dynamics of Managed Grasslands at the Global Scale with LPJmL 3.6”. In: *Geosci. Model Dev.* 11.1, pp. 429–451. ISSN: 1991-9603. DOI: 10.5194/gmd-11-429-2018. (Visited on 02/27/2018).
- Rolinski, S., A. V. Prishchepov, G. Guggenberger, N. Bischoff, I. Kurganova, F. Schierhorn, D. Müller, and C. Müller (2021). “Dynamics of Soil Organic Carbon in the Steppes of Russia and Kazakhstan under Past and Future Climate and Land Use”. In: *Reg Environ Change* 21.3, p. 73. ISSN: 1436-378X. DOI: 10.1007/s10113-021-01799-7. (Visited on 01/21/2025).
- Sakschewski, B., W. von Bloh, A. Boit, A. Rammig, J. Kattge, L. Poorter, J. Peñuelas, and K. Thonicke (2015). “Leaf and Stem Economics Spectra Drive Diversity of Functional Plant Traits in a Dynamic Global Vegetation Model”. In: *Glob. Change Biol.* 21.7, pp. 2711–2725. ISSN: 1365-2486. DOI: 10.1111/gcb.12870. (Visited on 10/15/2018).
- Sanaei, A., E. J. Sayer, Z. Yuan, H. Saiz, M. Delgado-Baquerizo, M. Sadeghinia, P. Ashouri, S. Ghafari, H. Kaboli, M. Kargar, E. W. Seabloom, and A. Ali (2023). “Grazing Intensity Alters the Plant Diversity–Ecosystem Carbon Storage Relationship in Rangelands across Topographic and Climatic Gradients”. In: *Funct. Ecol.* 37.3, pp. 703–718. ISSN: 1365-2435. DOI: 10.1111/1365-2435.14270. (Visited on 01/21/2025).
- Sándor, R., F. Ehrhardt, P. Grace, S. Recous, P. Smith, V. Snow, J.-F. Soussana, B. Basso, A. Bhatia, L. Brill, J. Doltra, C. D. Dorich, L. Doro, N. Fitton, B. Grant, M. T. Harrison, M. U. F. Kirschbaum, K. Klumpp, P. Laville, J. Léonard, R. Martin, R.-S. Massad, A. Moore, V. Myrriotis, E. Pattey, S. Rolinski, J. Sharp, U. Skiba, W. Smith, L. Wu, Q. Zhang, and G. Bellocchi (2020). “Ensemble Modelling of Carbon Fluxes in Grasslands and Croplands”. In: *Field Crops Res.* 252, p. 107791. ISSN: 0378-4290. DOI: 10.1016/j.fcr.2020.107791. (Visited on 11/23/2020).
- Sándor, R., F. Ehrhardt, P. Grace, S. Recous, P. Smith, V. Snow, J.-F. Soussana, B. Basso, A. Bhatia, L. Brill, J. Doltra, C. D. Dorich, L. Doro, N. Fitton, B. Grant, M. T. Harrison, U. Skiba, M. U. F. Kirschbaum, K. Klumpp, P. Laville, J. Léonard, R. Martin, R. S. Massad, A. D. Moore, V. Myrriotis, E. Pattey, S. Rolinski, J. Sharp, W. Smith, L. Wu, Q. Zhang, and G. Bellocchi (2023). “Residual Correlation and Ensemble Modelling to Improve Crop and Grassland Models”. In: *Environmental Modelling & Software* 161, p. 105625. ISSN: 1364-8152. DOI: 10.1016/j.envsoft.2023.105625. (Visited on 11/20/2024).
- Scheiter, S., D. Kumar, R. T. Corlett, C. Gaillard, L. Langan, R. S. Lapuz, C. Martens, M. Pfeiffer, and K. W. Tomlinson (2020). “Climate Change Promotes Transitions to Tall Evergreen Vegetation in Tropical Asia”. In: *Glob. Change Biol.* 26.9, pp. 5106–5124. ISSN: 1365-2486. DOI: 10.1111/gcb.15217. (Visited on 11/19/2024).
- Scheiter, S., L. Langan, and S. I. Higgins (2013). “Next-Generation Dynamic Global Vegetation Models: Learning from Community Ecology”. In: *New Phytol.* 198.3, pp. 957–969. ISSN: 1469-8137. DOI: 10.1111/nph.12210.
- Schippers, P., W. A. Ozinga, and R. Pouwels (2022). “Factors Affecting Functional Diversity of Grassland Vegetations”. In: *Ecological Modelling* 472, p. 110078. ISSN: 0304-3800. DOI: 10.1016/j.ecolmodel.2022.110078. (Visited on 11/20/2024).

- Smith, B., I. C. Prentice, and M. T. Sykes (2001). “Representation of Vegetation Dynamics in the Modelling of Terrestrial Ecosystems: Comparing Two Contrasting Approaches within European Climate Space”. In: *Glob. Ecol. Biogeogr.* 10.6, pp. 621–637. ISSN: 1466-8238. DOI: 10.1046/j.1466-822X.2001.t01-1-00256.x. (Visited on 06/28/2021).
- Teckenstrup, L., M. G. De Kauwe, A. J. Pitman, D. S. Goll, V. Haverd, A. K. Jain, E. Joetzjer, E. Kato, S. Lienert, D. Lombardozzi, P. C. McGuire, J. R. Melton, J. E. M. S. Nabel, J. Pongratz, S. Sitch, A. P. Walker, and S. Zaehle (2021). “Assessing the Representation of the Australian Carbon Cycle in Global Vegetation Models”. In: *Biogeosciences* 18.20, pp. 5639–5668. ISSN: 1726-4170. DOI: 10.5194/bg-18-5639-2021. (Visited on 11/19/2024).
- Thonicke, K., M. Billing, W. von Bloh, B. Sakschewski, Ü. Niinemets, J. Peñuelas, J. H. C. Cornelissen, Y. Onoda, P. van Bodegom, M. E. Schaepman, F. D. Schneider, and A. Walz (2020). “Simulating Functional Diversity of European Natural Forests along Climatic Gradients”. In: *J. Biogeogr.* 47.5, pp. 1069–1085. ISSN: 1365-2699. DOI: 10.1111/jbi.13809. (Visited on 06/23/2023).
- Tilman, D., P. B. Reich, and F. Isbell (2012). “Biodiversity Impacts Ecosystem Productivity as Much as Resources, Disturbance, or Herbivory”. In: *PNAS* 109.26, pp. 10394–10397. ISSN: 0027-8424, 1091-6490. DOI: 10.1073/pnas.1208240109. (Visited on 12/16/2020).
- Tilman, D., P. B. Reich, J. Knops, D. Wedin, T. Mielke, and C. Lehman (2001). “Diversity and Productivity in a Long-Term Grassland Experiment”. In: *Science* 294.5543, pp. 843–845. DOI: 10.1126/science.1060391. (Visited on 01/06/2025).
- Török, P., L. A. Brudvig, J. Kollmann, J. N. Price, and B. Tóthmérész (2021). “The Present and Future of Grassland Restoration”. In: *Restor. Ecol.* 29.S1, e13378. ISSN: 1526-100X. DOI: 10.1111/rec.13378. (Visited on 11/20/2024).
- Török, P., A. Helm, K. Kiehl, E. Buisson, and O. Valkó (2018). “Beyond the Species Pool: Modification of Species Dispersal, Establishment, and Assembly by Habitat Restoration”. In: *Restor. Ecol.* 26.S2, S65–S72. ISSN: 1526-100X. DOI: 10.1111/rec.12825. (Visited on 11/20/2024).
- Walde, M., E. Allan, S. L. Cappelli, M. Didion-Gency, A. Gessler, M. M. Lehmann, N. A. Pichon, and C. Grossiord (2021). “Both Diversity and Functional Composition Affect Productivity and Water Use Efficiency in Experimental Temperate Grasslands”. In: *J. Ecol.* 109.11, pp. 3877–3891. ISSN: 1365-2745. DOI: 10.1111/1365-2745.13765. (Visited on 11/20/2024).
- Warren, R., J. Price, and R. Jenkins (2021). “Chapter 4 - Climate Change and Terrestrial Biodiversity”. In: *The Impacts of Climate Change*. Ed. by T. M. Letcher. Elsevier, pp. 85–114. ISBN: 978-0-12-822373-4. DOI: 10.1016/B978-0-12-822373-4.00025-2. (Visited on 11/20/2024).
- Weigelt, A., W. W. Weisser, N. Buchmann, and M. Scherer-Lorenzen (2009). “Biodiversity for Multifunctional Grasslands: Equal Productivity in High-Diversity Low-Input and Low-Diversity High-Input Systems”. In: *Biogeosciences* 6.8, pp. 1695–1706. ISSN: 1726-4170. DOI: 10.5194/bg-6-1695-2009. (Visited on 11/20/2024).
- Weindl, I., B. Soergel, G. Ambrósio, V. Daioglou, J. C. Doelman, F. Beier, A. Beusen, B. L. Bodirsky, A. Bos, J. P. Dietrich, F. Humpenöder, P. J. v. von Jeetze, K. Karstens, S. Rauner, E. Stehfest, M. Stevanovic, W.-J. van Zeist, H. Lotze-Campen, D. P. van Vuuren, E. Kriegler, and A. Popp (2024). “Food and Land System Transformations under Different Societal Perspectives on Sustainable Development”. In: *Environ. Res. Lett.* ISSN: 1748-9326. DOI: 10.1088/1748-9326/ad8f46. (Visited on 11/20/2024).
- Wesche, K., B. Krause, H. Culmsee, and C. Leuschner (2012). “Fifty Years of Change in Central European Grassland Vegetation: Large Losses in Species Richness and Animal-Pollinated Plants”. In: *Biological Conservation* 150.1, pp. 76–85. ISSN: 0006-3207. DOI: 10.1016/j.biocon.2012.02.015. (Visited on 11/20/2024).
- Xu, W., J. Chang, P. Ciais, B. Guenet, N. Viovy, A. Ito, C. P. O. Reyer, H. Tian, H. Shi, K. Frieler, M. Forrest, S. Ostberg, S. Schaphoff, and T. Hickler (2020). “Reducing Uncertainties of Future Global Soil Carbon Responses to Climate and Land Use Change With Emergent Constraints”. In: *Glob. Biogeochem. Cycles* 34.10, e2020GB006589. ISSN: 1944-9224. DOI: 10.1029/2020GB006589. (Visited on 11/19/2024).
- Zakharova, L., K. M. Meyer, and M. Seifan (2019). “Trait-Based Modelling in Ecology: A Review of Two Decades of Research”. In: *Ecological Modelling* 407, p. 108703. ISSN: 0304-3800. DOI: 10.1016/j.ecolmodel.2019.05.008. (Visited on 11/19/2024).
- Zavaleta, E. S. and K. B. Hulvey (2004). “Realistic Species Losses Disproportionately Reduce Grassland Resistance to Biological Invaders”. In: *Science* 306.5699, pp. 1175–1177. DOI: 10.1126/science.1102643. (Visited on 04/25/2024).
- Zhu, K., Y. Song, J. C. Lesage, J. C. Luong, J. W. Bartolome, N. R. Chiariello, J. Dudley, C. B. Field, L. M. Hallett, M. Hammond, S. P. Harrison, G. F. Hayes, R. J. Hobbs, K. D. Holl, P. Hopkinson, L. Larios, M. E. Loik, and L. R. Prugh (2024). “Rapid Shifts in Grassland Communities Driven by Climate Change”. In: *Nat Ecol Evol*, pp. 1–13. ISSN: 2397-334X. DOI: 10.1038/s41559-024-02552-z. (Visited on 10/23/2024).

# Appendix A

Appendix A contains the supplementary information for Chapter 2 Do details matter? Disentangling the processes related to plant species interactions in two grassland models of different complexity.

## A.1 Information on empirical data, input parameter and calibration of the grassland models GRASSMIND and LPJmL

### A.1.0.1 Information on the field experiment

We used empirical observations of four species (*Festuca pratensis*, *Festuca rubra*, *Poa pratensis*, *Plantago lanceolata*) of the Jena Biodiversity Experiment (Weisser et al., 2017) for the parameterization of the two grassland models. For each species, a monoculture plot (20 m x 20 m) is available. Note that the following parameterizations for *Poa pratensis* and *Plantago lanceolata* do not include information of the respective two-species-mixture plot. For a comparison of calibrated parameters in GRASSMIND including this information, we refer to Taubert et al. (2020b). The two-species-mixture plot of *P. pratensis* and *P. lanceolata* (although available in the field experiment) was not used for calibration of the models because it was the only mixture-plot for which this information was available.

### A.1.1 Vegetation attributes

Measurements have been collected for seven consecutive years (starting in year 2002). Seeds of each plot were sown on bare field in the period 11-16 May 2002. From 2003 onwards, measurements were taken twice a year for (a) aboveground biomass (AGB), (b) leaf area index (LAI), (c) vegetation height, and (d) vegetation cover (Weigelt et al., 2010). Replicated measurements per census within the plot are available for aboveground biomass (3 to 4 replicates) and vegetation height (10 replicates). In both cases, we used the median value of all replicates for each of the biannual censuses. The field plots were mown twice a year to a height of 10 cm (Weigelt et al., 2010).

### A.1.2 Climate and soil properties

Climatic conditions for the local study site (precipitation, global radiation, relative humidity and air temperature) were measured daily at two weather stations located near the experiment. Data from January 2004 onwards are supplied by the weather station of the Max Planck Institute for Biogeochemistry (MPI, 2019) in Jena, Germany. Missing climate data for the years 2002 and 2003 were substituted by data from the weather station of the Ernst-Abbe-Fachhochschule Jena (FH Jena, 2020). Gaps of missing data at three days were filled with the mean value of the previous and following day.

For each plot, empirical data on (a) soil texture (silt, sand and clay content), (b) permanent wilting point (PWP), (c) field capacity (FC), (d) mineral nitrogen content and (e) dry bulk density was available (Kreutziger et al., 2018). Measurements are available in different soil layers (different for each property; down to 30 cm soil).

## **A.2 Model parameterization**

### **A.2.1 GRASSMIND**

#### **A.2.1.1 Climate data preparation**

Climate data were available on a daily basis and already ready-to-use for the grassland model. The additional required potential evapotranspiration was derived from air temperature, global radiation and relative humidity (Turc, 1961), while the required astronomic day length was calculated based on the latitude (Forsythe et al., 1995).

#### **A.2.1.2 Model parameter of plant attributes**

GRASSMIND simulations start from bare ground and seeds start to grow into the simulated plots at a specific point in time (here, we used 16 May 2002). In general, seeds can be sown once initially and seeds can disperse from plants present at the plots and from the surrounding landscape during the simulation time. Those different sources of seed ingrowth are summarized in GRASSMIND in one model parameter (similar for all simulated plots).

During the simulation, plots were mown twice a year to a height of 10 cm (similar to the field experiment). Mowing height is explicitly included in the GRASSMIND model as a day-specific parameter for each mowing event (and thus, yield is dependent on the plant height structure of the simulated community at that specific point in time). As mowing dates, we used in the model for all years 15 May and 15 August (except for the year 2002: 15 July and 15 September; year 2006: 15 June and 15 August). The growth of plants is simulated dependent on constant plant parameters (different parameters for each species), and describe demographic, physiological and geometric attributes of the respective plant species. Some parameters were measured at the field experiment or were available from independent literature (Table SI A.1). Unknown parameters have been determined by applying inverse calibration methods (see section on model calibration).

Sensitivity of parameters and processes have already been investigated in previous publications on simulation studies using GRASSMIND. For example, (Schmid et al., 2021) identified in a global sensitivity and robustness analysis for monocultures and multi-species mixtures (based on PFTs) the importance of specific plant parameters and competition processes in relation to grassland productivity

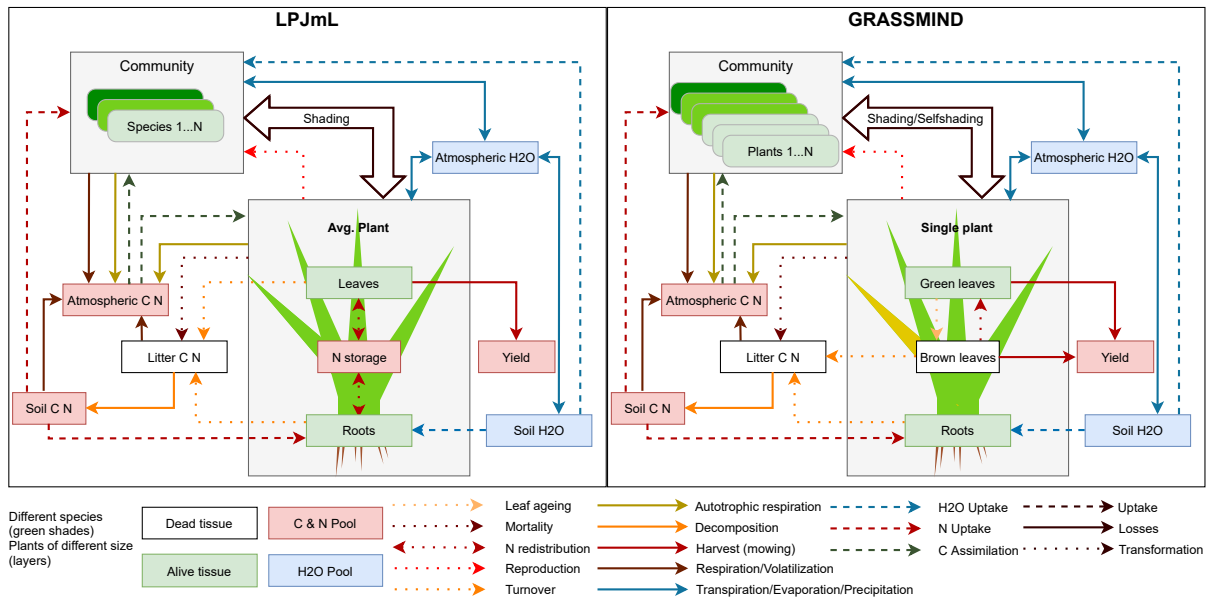


Figure A.1: Processes and plant compartments simulated in GRASSMIND and LPJmL

and species composition. The robustness analysis showed, for example, that space competition between plants has a greater influence than competition for light (shading) on the productivity of the simulated grassland (Schmid et al., 2021). Plant traits related to different processes such as reproduction, photosynthesis, or growth geometry play a major role in the species composition of grasslands (Hetzer et al., 2021; Schmid et al., 2021; Taubert et al., 2020a). For example, Hetzer et al. (2021) showed that grassland productivity was mostly influenced by plant traits related to photosynthesis and geometry, while other attributes (e.g., leaf area index and GPP) are more influenced by plant geometry and recruitment. A simulation study of Taubert et al. (2020a) on a local parameter sensitivity of the grassland model additionally highlighted that even small differences in characteristics of two plant species can promote the dominance of one species in the mixture.

### A.2.1.3 Soil dynamics parameter

In GRASSMIND, we modelled 20 soil layers (each 10 cm in height). Soil properties partly differ between the soil layers (Table SI A.2). In case of no available data, we used the same properties as for the soil layer above. We assumed as initial soil water content for each soil layer the respective field capacity of each plot (Table SI A.2).

## A.2.2 LPJmL

### A.2.2.1 Climate data preparation

Because LPJmL requires a time-series with 365 days per year, in the preprocessing leap years were identified and the data for December 31st were dropped. Afterwards the climate data were ready-to-use

Table A.1: Species parameter for the GRASSMIND model. The table provides details about GRASSMIND parameters, with their units of measurements and prescribed or inversely parameterized values.

Parameter	Unit	Description	F. pratensis	F. rubra	P. pratensis	P. lanceolata	Reference
$h_{max}$	cm	Maximum height of a plant	120	120	60	70	(Info Flora 2021, Abaye 2019, Weryszko-Chmielewska et al., 2012)
$hw$	-	Height-width ratio of a plant's encasing cylinder	1.0	1.0	4.4	1.0	Inversely parameterized
$f_s$	$\text{g cm}^{-3}$	Shoot correction factor	0.00089	0.00146	0.00142	0.00055	Inversely parameterized
$f_o$	-	Overlapping factor	1	1	1	1	Fixed <sup>1</sup>
$SLA$	$\text{cm}^2 \text{g}^{-1}$	Specific leaf area	159.0	121.0	139.0	203.0	Inversely parameterized
$SRL$	$\text{cm g}^{-1}$	Specific root length	50000	50000	50000	50000	Fixed <sup>1</sup>
$rd_1, rd_2$	-	Parameters of the rooting depth power-law relationship	3.506 0.301	3.506 0.301	3.506 0.301	5.777 0.365	(Schenk and Jackson 2002)
$sr$	-	Shoot-root ratio of plant biomass organs	2.6	2.2	3.6	10.9	(Heisse et al. 2007) <sup>2</sup>
$N_{seed}^{meta}$	$\text{m}^{-2} \text{d}^{-1}$	Seed rain from surrounding landscape	2541	2541	2541	2541	Inversely parameterized <sup>3</sup>
$t_{meta}$	Julian day	Julian day at which seed rain starts	136	136	136	136	(Weigelt et al. 2010)
$t_{em}$	d	Time between seed rain and seedling emergence	14	14	21	7	(Heisse et al. 2007)
$germ\%$	-	Seed germination rate	0.3	0.3	0.75	0.9	(Roscher et al. 2004)
$h_{min}$	m	Initial height of ingrowing seedlings	0.03	0.03	0.03	0.03	Fixed (technical parameter)
$age_{rep}$	yr	Age at which recruitment starts	0.70	0.50	0.54	0.06	Inversely parameterized
$LLS$	d	Leaf life span (start of yellowing leaves)	40	126	170	21	Inversely parameterized
$RLS$	d	Root life span	668	311	703	741	Inversely parameterized
$sen$	$\text{d}^{-1}$	Rate of litterfall of yellowed leaves to the litter pool	0.08	0.08	0.08	0.08	Inversely parameterized <sup>3</sup>
$m_{seed}$	$\text{d}^{-1}$	Mortality rate of established seedlings	0.057	0.052	0.137	0.137	Inversely parameterized
$m_{basic}$	$\text{yr}^{-1}$	Mortality rate of mature plants	0.093	0.104	0.123	0.011	Inversely parameterized
$life$	yr	Life span of plants	Perennial	Perennial	Perennial	Perennial	(Künn and Klotz 2002)
$p_{max}$	$\mu\text{mol CO}_2 \text{m}^{-2} \text{s}^{-1}$	Maximum gross leaf photosynthesis	43	45	15	29	Inversely parameterized
$\alpha$	$\mu\text{mol CO}_2 \mu\text{mol photons}^{-1}$	Initial slope of light response curve	0.21	0.29	0.27	0.15	Inversely parameterized
$k$	-	Light extinction coefficient	0.2	0.2	0.2	0.8	Fixed <sup>1</sup>
$m$	-	Transmission coefficient	0.1	0.1	0.1	0.1	(Thornley and France 2007)
$WUE$	$\text{gODM kgH}_2\text{O}^{-1}$	Water use efficiency coefficient	11.0	9.7	7.2	3.1	Inversely parameterized
$CN_{green}$	-	CN ratio of green leaves	24	19	19	10	Inversely parameterized

<sup>1</sup>Note that these parameters have been fixed in this project in order to reduce the number of calibrated.<sup>2</sup>Shoot-root ratios were used as measured for the first calibration step. In the second calibration step, shoot-root ratios were fine-tuned in a range of  $\pm 0.5$ .<sup>3</sup>Parameters were only calibrated in the first step and remained fixed in the second step of calibration. Note the difference of this calibration to previous parameterizations where  $N_{seed}^{meta}$  was allowed to be different for the different species plots, but  $m_{basic}$  was kept constant (Taubert et al., 2020b).

Table A.1: Species parameter for the GRASSMIND model. The table provides details about GRASS-MIND parameters, with their units of measurements and prescribed or inversely parameterized values (continued).

Parameter	Unit	Description	F. pratensis	F. rubra	P. pratensis	P. lanceolata	Reference
$CN_{sen}$	-	CN ratio of senescent leaves and roots	31	40	38	48	Inversely parameterized
$N_{fix}$	y/n	Symbiotic N fixation	No	No	No	No	(Kühn and Klotz 2002)
$alloc_{shoot}$	-	Allocation rate of NPP to shoot growth	0.51	0.25	0.73	0.69	Inversely parameterized
$r_m$	$d^{-1}$	Maintenance respiration rate	0.02	0.02	0.02	0.02	(Amthor, 1984)
$r_g$	-	Growth respiration factor	0.2	0.2	0.2	0.2	(Amthor, 1984)

<sup>1</sup>Note that these parameters have been fixed in this project in order to reduce the number of calibrated.

<sup>2</sup>Shoot-root ratios were used as measured for the first calibration step. In the second calibration step, shoot-root ratios were fine-tuned in a range of  $\pm 0.5$ .

<sup>3</sup>Parameters were only calibrated in the first step and remained fixed in the second step of calibration. Note the difference of this calibration to previous parameterizations where  $N_{seed}^{meta}$  was allowed to be different for the different species plots, but  $m_{basic}$  was kept constant (Taubert et al., 2020b).

Table A.2: Summary of soil properties in GRASSMIND per plot and soil layer

Monoculture plot (sown species)	F. pratensis			F. rubra			P. pratensis			P. lanceolata		
	1	2	3ff	1	2	3ff	1	2	3ff	1	2	3ff
Soil layers <sup>1</sup>												
Field capacity (V%)	30.1	30.2	32.3	33.6	33.3	31.6	33.2	33.3	33.4	30.9	31.7	32.2
Permanent wilting point (V%)	17.0	16.9	18.5	20.8	20.5	19.1	20.7	20.8	20.8	17.9	19.4	19.3
Initial mineral nitrogen content $g/m^2$ <sup>2</sup>	0.32	0.32	0.5	0.26	0.26	0.47	0.27	0.27	0.25	0.17	0.17	0.24
Soil texture (silt/sand/clay) <sup>3</sup> in %	56/22/22			59/16/25			69/8/23			56/22/22		
Porosity (V%)	45.6	45.6	45.6	52.1	52.1	52.1	46.5	46.5	46.5	46.3	46.3	46.3
Hydraulic conductivity (mm/d)	163.2	163.2	163.2	163.2	163.2	163.2	163.2	163.2	163.2	163.2	163.2	163.2

<sup>1</sup>Soil layers are: (1) 0 – 10 cm, (2) 10 – 20 cm, (3ff) 20 – 30 cm and similar for all following 10-cm soil layers down to 200 cm soil depth.

<sup>2</sup>To calculate mineral nitrogen content, the sum of measured nitrate and ammonium per unit sediment mass [ $\mu g/g$ ] of year 2002 is used. Measured values are given for soil depth 0 – 0.15 cm (used for first and second soil layer) and for soil depth 0.15 – 0.30 cm (used for third and following soil layers). Mineral nitrogen content in [ $g/m^2$ ] is then calculated by multiplying the sum of both measured values (nitrate and ammonium) with the measured dry bulk density (and with 10-cm soil layer depth) and converted to [ $g/m^2$ ]. Among the four monoculture plots, measured dry bulk density was only available for the F.pratensis-plot and assumed for the other monoculture plots (maximum value of  $1.46 g/cm^3$  was used)

<sup>3</sup>Values measured at 31 December 2002 were used

Table A.3: Species parameter for the LPJmL model. The table provides details about LPJmL parameters, with their units of measurements and default parameter values.

Parameter	Unit	Description	Temperate Herbaceous	Reference
$SLA$	$\text{mm}^2 \text{mg}^{-1}$	Specific leaf area	12.5328	(Reich et al., 1992)
$k_{beer}$	-	Light extinction coefficient	0.5	(Larcher, 1995)
$\rho_{veg}$	$\text{gCm}^{-2}$	Area density of stubble biomass	25	(Rolinski et al., 2018)
$l : r$	-	Leaf to root ratio	0.8	(Sitch et al., 2003)

for the LPJmL model.

### A.2.2.2 Model parameters of plant attributes

LPJmL simulations start from bare ground with the establishment of saplings. Additional saplings can establish each day provided sufficient space is available. During the simulation, plots were mown twice a year using the same mowing days as in GRASSMIND. However, since height is not explicitly simulated in LPJmL mowing reduces aboveground biomass to a residual amount that is associated with a certain cutting height. Since this amount is species-specific we included the respective parameter in our calibration.

Plant growth is simulated depending on the pedoclimatic conditions and the constant plant parameters which differ for each plant functional type and are derived from literature. We used the parameter values of the temperate herbaceous plant functional type as starting values for our calibration (Table SI A.3) and determined species-specific values for selected parameters using a Markov chain Monte Carlo method (see section on model calibration). We selected the parameters based on expert knowledge and results of already existing sensitivity analysis (Zaehle et al., 2005) which showed that  $k_{beer}$  was a highly sensitive parameter. Forkel et al. (2019) found leaf longevity, which was used to determine  $SLA$  to be a sensitive parameter. Instead of calibrating leaf longevity and calculating  $SLA$  we prescribe  $SLA$  directly. This is possible, because leaf longevity is only needed to calculate  $SLA$  in the model version we used. In the analysis of Zaehle et al. (2005) several tree specific parameters related to allocation of carbon were sensitive and we selected  $l : r$  which is a grass specific parameter that is used in the allocation similar to the tree specific parameters  $k_{(sa:la)}$ ,  $k_{allom1}$ ,  $k_{allom2}$ ,  $k_{allom3}$ , described in Schaphoff et al. (2018).

### A.2.2.3 Soil dynamics parameter

LPJmL simulates the soil partitioned into 6 layers, with widths of 20, 30, 50, 100, 100 and 1,000 cm. Soil properties are defined for all layers (Table SI A.4). We calculated weighted averages of the measured soil properties. Initial soil water content for each soil layer was determined in the natural vegetation spinup.

Table A.4: Summary of soil properties in LPJmL.

Monoculture Plot (Sown Species)	<i>F. pratensis</i>	<i>F. rubra</i>	<i>P. pratensis</i>	<i>P. lanceolata</i>
Field Capacity (V%)	31.9	32.0	33.4	32.0
Permanent Wilting Point (V%)	18.2	19.4	20.8	19.2
Soil Texture (Silt/Sand/Clay) in %	56/22/22	59/16/25	69/8/23	56/22/22
Porosity (V%)	45.6	52.1	46.5	46.3

## A.3 Model Calibration

### A.3.1 GRASSMIND

Unknown parameter per species (listed in Table SI A.1 as “inversely parameterized”) were determined by comparing observations of the monoculture plot and model simulations (with randomly chosen parameter sets in predefined ranges).

For the observations to compare, we selected the seven-year time series data (2002 to 2008) of bi-annual measurement information and additionally aggregated the median of each two censuses per year to derive annual averages. We included all observed vegetation attributes: (a) aboveground biomass (AGB in  $\text{g}/\text{m}^2$ ), (b) vegetation height (H in cm), (c) leaf area index (LAI in  $\text{cm}^2/\text{cm}^2$ ), (d) vegetation cover (C in %). Because weed cover was considerably high in some censuses (and the grassland model does not simulate weeding), we corrected the measured target species cover by adding the respective observed weed cover (assuming that weeds have not been present).

We applied a two-step calibration: (1) we calibrated all four monoculture plots in parallel including all unknown parameters listed in Table SI A.1, and (2) we calibrated each monoculture plot separately (with fixed  $N_{seed}^{meta}$  and senescence rate, but allowed a fine-tuning of the shoot-root ratio). For each step, we used the ‘dynamically dimensioned search’ optimization algorithm with 2,000 optimization steps (Lehmann and Huth, 2015), which searched for an optimal set of model parameters by minimizing the cost function. In each optimization step, the grassland model GRASSMIND was simulated on one  $\text{m}^2$  with the algorithmic chosen parameter set, starting from bare ground in 2002 (seeding year) and simulating until the end of 2008. Initial height of seedlings is predefined at 3 cm from which other state variables (e.g. shoot biomass) are derived dependent on the species traits (Table SI A.1).

The cost function for the optimization included the comparison of all vegetation attributes of time-series data between observation and simulation and includes three parts: (1) the arithmetic mean of absolute errors for yearly aggregated measurements (with equal weights for each year), (2) sum of absolute errors of all measurements (two censuses across all years), and (3) a vegetation height restriction to ensure yield at mowing events (with 10 cm mowing height). For a selected attribute k (AGB, LAI, H and C) and species i, we calculated the three parts as follows:

$$C_{k,i}^1 = \frac{1}{6} \sum_{j=1}^6 \left( \frac{|\hat{y}_{k,i,j} - \hat{x}_{k,i,j}|}{\sum_{j=1}^6 \hat{x}_{k,i,j}} \right) \quad (\text{A.1})$$

## Appendix A

$$C_{k,i}^2 = \frac{\sum_{j=1}^{T_n} |y_{k,i,j} - x_{k,i,j}|}{\sum_{j=1}^{T_n} x_{k,i,j}} \quad (\text{A.2})$$

$$C_{k,i}^3 = 100 \cdot \left( 1 - \frac{\sum_{j=1}^{T_n} \delta(y_{H,i,j})}{T_n} \right) \quad \text{with} \quad \delta(y_{H,i,j}) = \begin{cases} 0 & \text{if } y_{H,i,j} \leq 10 \text{ cm} \\ 1 & \text{if } y_{H,i,j} > 10 \text{ cm} \end{cases} \quad (\text{A.3})$$

where  $y_{k,i}$  is the simulated and  $x_{k,i}$  is the observed time-series data (of all measurement samples of size  $T_n$ ), and  $\hat{y}_{k,i}$  is the simulated and  $\hat{x}_{k,i}$  is the observed time-series data (aggregated to annual averages, only including year 2003 to 2008) for the respective vegetation attribute  $k$  and species  $i$ . For the final calibration, we received an optimized cost function value of  $C = 7.11$  (details are listed in Table SI A.5).

Table A.5: Species plots with attributes and corresponding values for C1, C2, and C3

Species Plot	Attribute	C1	C2	C3
F. pratensis	AGB ( $\text{g m}^{-2}$ )	0.089	0.62	-
	Height (cm)	0.069	0.48	0
	LAI (-)	0.049	0.32	-
	Cover (%)	0.075	0.46	-
	Sum	0.28	1.88	0
F. rubra	AGB ( $\text{g m}^{-2}$ )	0.089	0.61	-
	Height (cm)	0.047	0.29	0
	LAI (-)	0.032	0.28	-
	Cover (%)	0.040	0.22	-
	Sum	0.21	1.40	0
P. pratensis	AGB ( $\text{g m}^{-2}$ )	0.086	0.69	-
	Height (cm)	0.022	0.28	0
	LAI (-)	0.044	0.35	-
	Cover (%)	0.030	0.23	-
	Sum	0.18	1.55	0
P. lanceolata	AGB ( $\text{g m}^{-2}$ )	0.048	0.44	-
	Height (cm)	0.046	0.35	0
	LAI (-)	0.028	0.32	-
	Cover (%)	0.050	0.33	-
	Sum	0.17	1.44	0

### A.3.2 LPJmL

Selected parameters were calibrated using a Markov chain Monte Carlo method with a Metropolis Hastings algorithm (Van Oijen et al., 2005). In this procedure, probability distributions of the parameters are updated conditional on observations of selected outputs, while also considering the uncertainty of these observations. This does not only lead to the identification of the best parameter vector but a distribution representing the uncertainty of the parameters (Van Oijen et al., 2005). The procedure is based in Bayesian statistics. The criterion for acceptance of a chosen parameter is a likelihood function calculating the differences between simulations and observations. For a selected parameter, a value is chosen from a prior distribution, i.e. an expected distribution of the parameter based on existing knowledge including known parameter uncertainties. When one parameter is calibrated, the likelihood function is determined for repeated choices of parameter values which results in a posterior distribution for this parameter. Mostly, the prior distribution is assumed to be an almost flat beta distribution within the known

range of values for this parameter and the mode, i.e. the center of the distribution, is used to calculate the initial likelihood. The subsequent choice of parameter values from a normal distribution forms a chain and is used to calculate the likelihood. The resulting posterior distribution is updated iteratively when the likelihood is improving.

For a more detailed description of the procedure we refer to McElreath (2016) and Van Oijen et al. (2005) for an introduction to Bayesian statistics since we only describe the model specific implementation in the following. Parameter values are drawn from a probability distribution and the model results ( $y_{mod}$ ) are compared to observations ( $y_{obs}$ ) and their error ( $\sigma_{obs}$ ), to calculate the Likelihood (see Eq. 4 to 6) - the cost function of the Bayesian calibration (BC). This is an iterative procedure for which we used 10.000 iteration steps which equals the chain length.

$$\log L_J = f_{\log P} + \sum f_{\log L,j} \quad (\text{A.4})$$

with the likelihood for each dataset  $j$  (AGB, LAI and cover)

$$f_{\log L,j}(y_{mod,j}, y_{obs,j}, \sigma_{obs,j}) = -0.5 \cdot \left( \frac{y_{mod,j} - y_{obs,j}}{\sigma_{obs,j}} \right)^2 - 0.5 \cdot \log(2\pi) - \log(\sigma_{obs,j}) \quad (\text{A.5})$$

and the prior likelihood

$$f_{\log P} = \sum_{i=1}^n B(\theta_i, p, q) \quad (\text{A.6})$$

$B(\theta_i, p, q)$  is the value of a beta distribution at  $\theta_i$  with  $p = 1.0 + 4 \cdot \frac{\hat{\theta}_{start} - \hat{\theta}_{min}}{\hat{\theta}_{max} - \hat{\theta}_{min}}$  and  $q = 6.0 - p$ . Where each  $\theta_i$  is the parameter value of the current iteration step from the parameter vector  $\Theta = (\theta_1, \dots, \theta_n)$  used in the calibration and  $\hat{\theta} = \frac{\theta}{|\theta|}$ .

$\alpha_{\log} = \log P_{old} + \log L_{old} - (\log P + \log L)$  — the difference between the likelihood of the last accepted and the current parameter vector  $\Theta$  — is calculated and compared to  $\xi_{\log}$ , the logarithm of a random number between zero and one, to evaluate whether  $\Theta$  is accepted and can be used to update the prior distributions of the parameters. If  $\alpha_{\log} > \xi_{\log}$ ,  $\Theta$  is accepted. The randomness creates a chance that  $\Theta$ s, which do not improve the likelihood but are expected to improve the prior distributions, can also be accepted. Using the logarithm ensures that  $\Theta$ s with less bad likelihoods have a higher chance of being accepted. If  $\Theta$  is accepted, the multivariate Gaussian distribution is updated and the iteration step ends.

After the iteration, the parameter values with the maximum probability from the updated prior distributions (maximum a posteriori) are selected for the new species'. We preselected parameters that were expected to be sensitive to calibration (Table SI A.3) and used a range of  $\pm 50\%$  of the default value for the prior normal distributions.

For  $y_{obs,AGB}$  and  $\sigma_{obs,AGB}$ , we used the median of AGB replicates and the respective standard deviation

for each observation date. Since only one measurement was available per observation date for LAI and cover, we used these for  $y_{\text{obs}}$  of the two datasets and assumed an  $\sigma_{\text{obs}}$  of 30% of the mean over all observations as proposed by Van Oijen et al. (2005). We provide an evaluation of the procedure based on the RMSE, as well as the square errors and their decomposition into phase, variance, and bias for simulation results using default and calibrated parameter values.

During each iteration step the model simulates vegetation dynamics between 2002 and 2015. However, only data between 2002 and 2008 for the observation dates are used in the cost function. The initial water, carbon and nitrogen pools in the vegetation are the same for each iteration step and were obtained using a 10.000 year spinup run with natural vegetation. The natural vegetation is converted into grassland at the beginning of each iteration step.

## A.4 Model evaluation

### A.4.1 GRASSMIND

Model evaluation is based on the comparison of time-series data between observations and simulation for each species concerning AGB, LAI, vegetation height and cover (Table SI A.6). We calculated the root mean squared error (RMSE) and its normalized counterpart (NRMSE) based on each (bi-annually) measured and simulated data point (excluding year 2002) by using R (R Core Team, 2019) and the hydroGOF package (Zambrano-Bigiarini [aut et al., 2020]). Normalization for calculating the NRMSE was based on the range of maximum and minimum measured values.

Table A.6: RMSE (with NRMSE (%) normalized by range of observed values) of model calibration results

Species	<b>F. pratensis</b>	<b>F. rubra</b>	<b>P. pratensis</b>	<b>P. lanceol ata</b>
AGB (g/m <sup>2</sup> )	209.4 (29.3%)	236.6 (38.8%)	80.1 (38.8%)	34.0 (26.9%)
Height (cm)	21.8 (50%)	11.7 (33%)	7.6 (50.9%)	8.3 (37.5%)
LAI (-)	0.73 (27.6%)	0.60 (36.7%)	0.47 (39.3%)	0.51 (27.1%)
Cover (%)	40.2 (53.5%)	26.4 (47.5%)	22.0 (36.9%)	23.5 (32.1%)

The influence of model stochasticity in GRASSMIND is only minor for the simulation results. A single simulation run deviates from the average of 100 replicates by a maximum of 18% (median of absolute relative differences), dependent on species: (a) for *F. pratensis*: 17.5% (AGB, LAI), 6.7% (height), 7.6% (cover), (b) for *F. rubra*: 5.8% (AGB, LAI), 6.8% (height), 2.5% (cover), (c) for *P. pratensis*: 1.6% (AGB, LAI), 12.1% (height), 0.3% (cover), and (d) for *P. lanceolata*: 6.2% (AGB, LAI), 6.5% (height), 3.0% (cover).

### A.4.2 LPJmL

We evaluated the calibration procedure against the same observations we used for calibration (Figure SI A.1-3) and against a second set of observations from the monoculture experiments (see section 2.2.2). Comparing the RMSE values before and after calibration show strong improvements between 1.0 and  $1.9 \text{ m}^2\text{m}^{-2}$  for LAI (Table SI A.6). For AGB, the changes ranged from moderate improvements to similar but slightly worse with values between -6.1 and  $122.3\text{gDMm}^{-2}$  (Table SI A.7). For LAI and especially AGB, the majority of the remaining mismatch between data and simulations can be attributed to two observations (Figure SI A.4-5) while most of the observations were matched well. LPJmL simulated substantially lower cover than observed (Figure SI A.3) and similar or higher RMSEs between -36.2 and 4.5 % were not driven by a mismatch to a small subset of observations (Figure SI A.6). The underlying reasons and processes responsible are explained in detail in the main text (see section 3.1).

Table A.7: RMSE before and after calibration.

Species	F. pratensis		F. rubra		P. pratensis		P. lanceolata	
	Prior	Posterior	Prior	Posterior	Prior	Posterior	Prior	Posterior
AGB	239.7	245.8	238.6	225.4	162.6	82.7	168.7	46.4
LAI	2.2	1.2	2.2	0.5	2.5	0.6	2.7	0.9
FPC	36.0	40.0	17.4	24.0	23.8	60.0	44.5	40.0

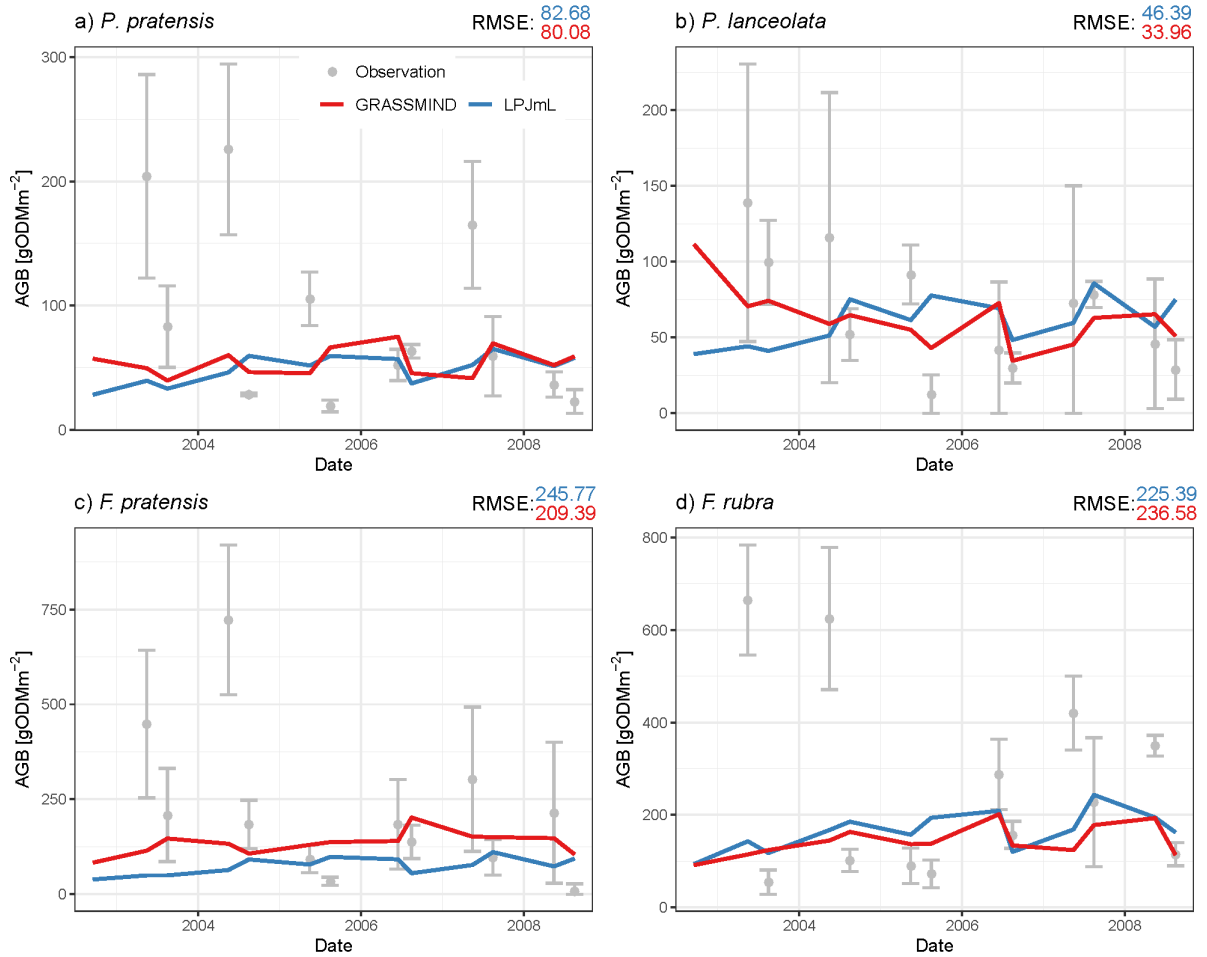


Figure A.2: Simulated and observed AGB in  $gDMm^{-2}$  for *P. pratensis* (a), *P. lanceolata* (b), *F. pratensis* (c) and *F. rubra* (d) for GRASSMIND (red) and LPJmL (blue). Coloured lines and labels show model results and RMSE, grey points show observations used for the validation. Observations are the median of samples for each date and error bars show one standard deviation.

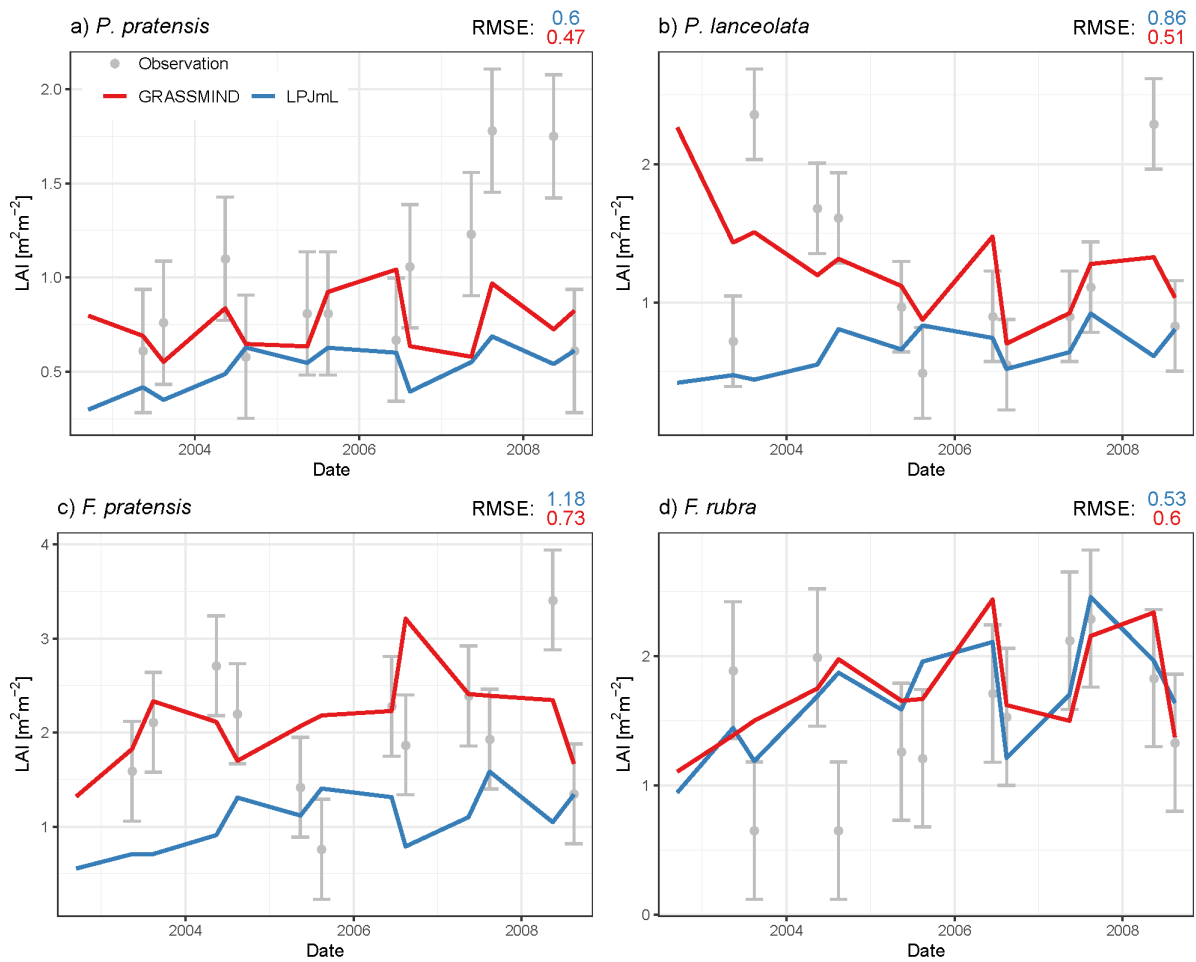


Figure A.3: Simulated and observed LAI in  $m^2 m^{-2}$  for *P. pratensis* (a), *P. lanceolata* (b), *F. pratensis* (c) and *F. rubra* (d) for GRASSMIND (red) and LPJmL (blue). Coloured lines and labels show model results and RMSE, grey points show observations used for the validation. Observations are the median of samples for each date and error bars show one standard deviation.

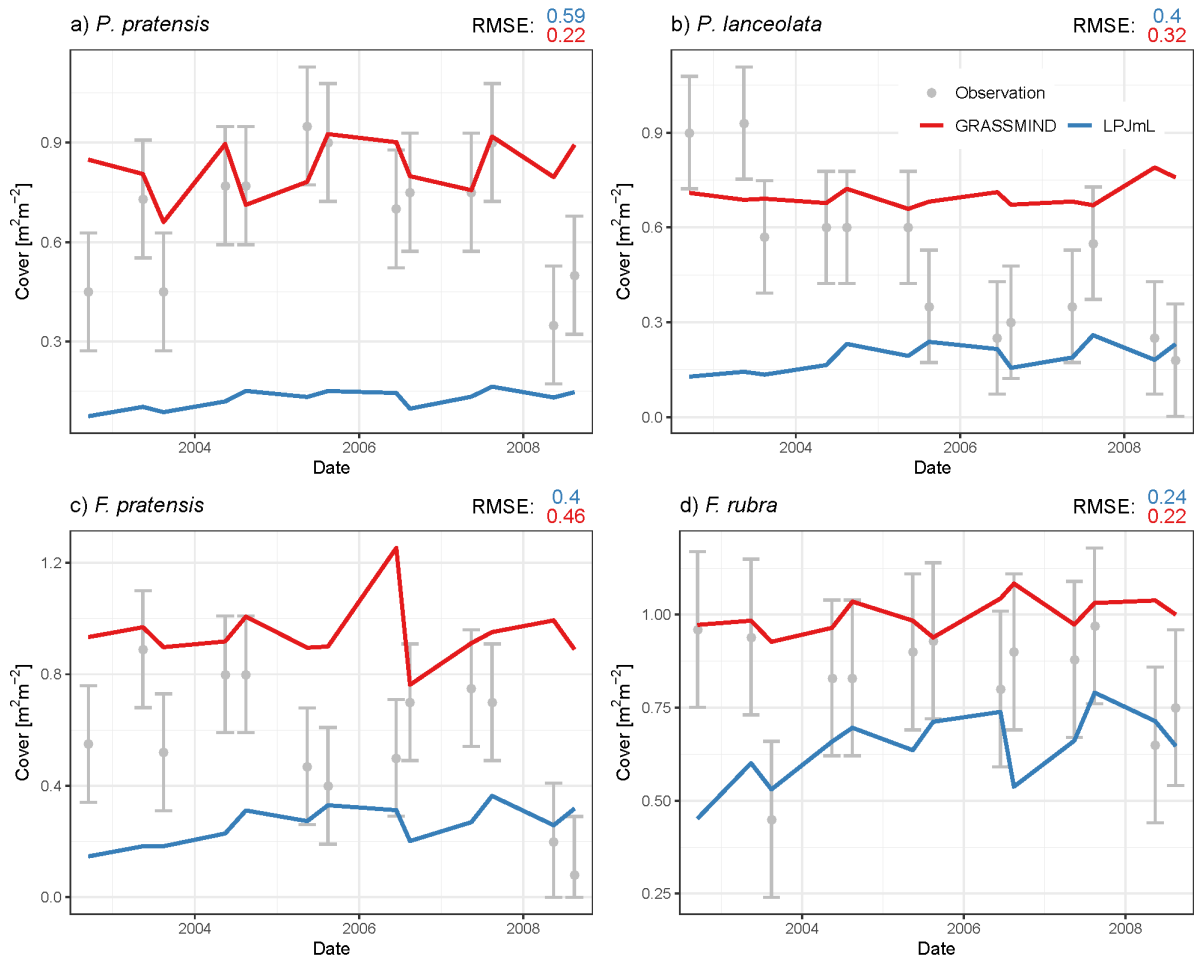


Figure A.4: Simulated and observed cover in % for *P. pratensis* (a), *P. lanceolata* (b), *F. pratensis* (c) and *F. rubra* (d) for GRASSMIND (red) and LPJmL (blue). Coloured lines and labels show model results and RMSE, grey points show observations used for the validation. Observations are the median of samples for each date and error bars show one standard deviation.

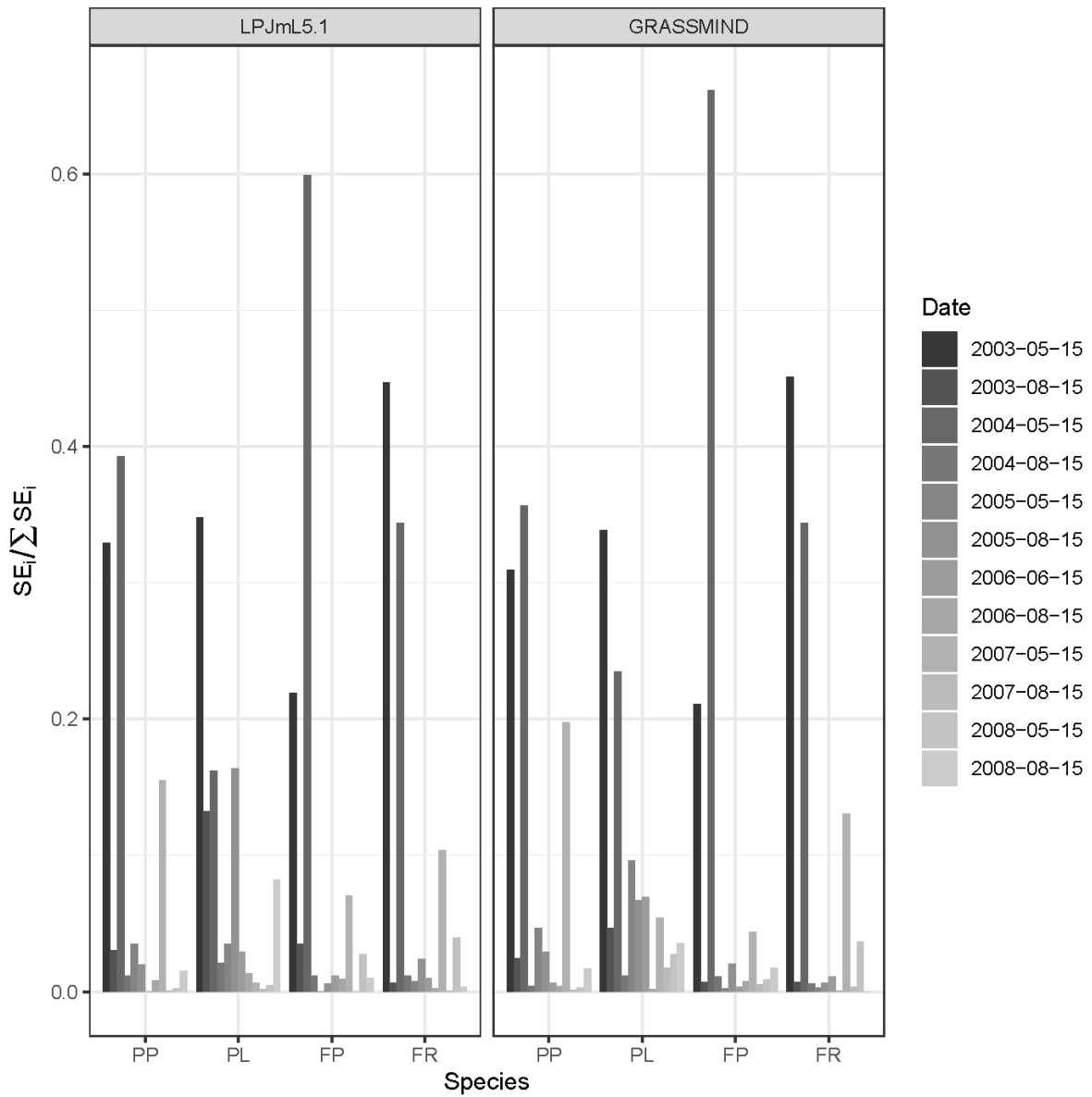


Figure A.5: Share of the SE of each observation date of the sum of all SE for AGB of the species *P. pratensis* (PP), *P. lanceolata* (PL), *F. pratensis* (FP) and *F. rubra* (FR) of the main experiment.

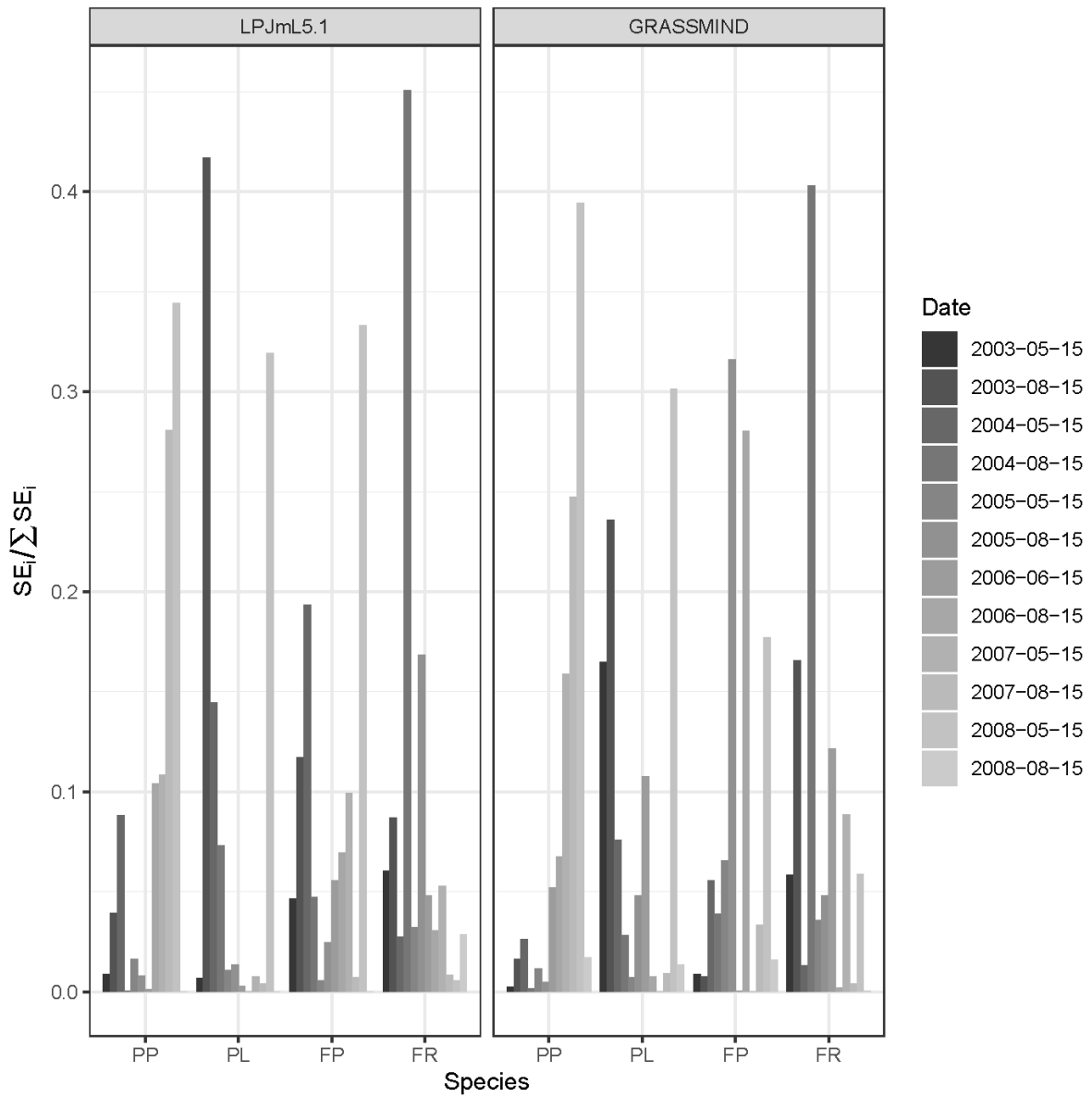


Figure A.6: Share of the SE of each observation date of the sum of all SE for LAI of the species *P. pratensis* (PP), *P. lanceolata* (PL), *F. pratensis* (FP) and *F. rubra* (FR) of the main experiment.

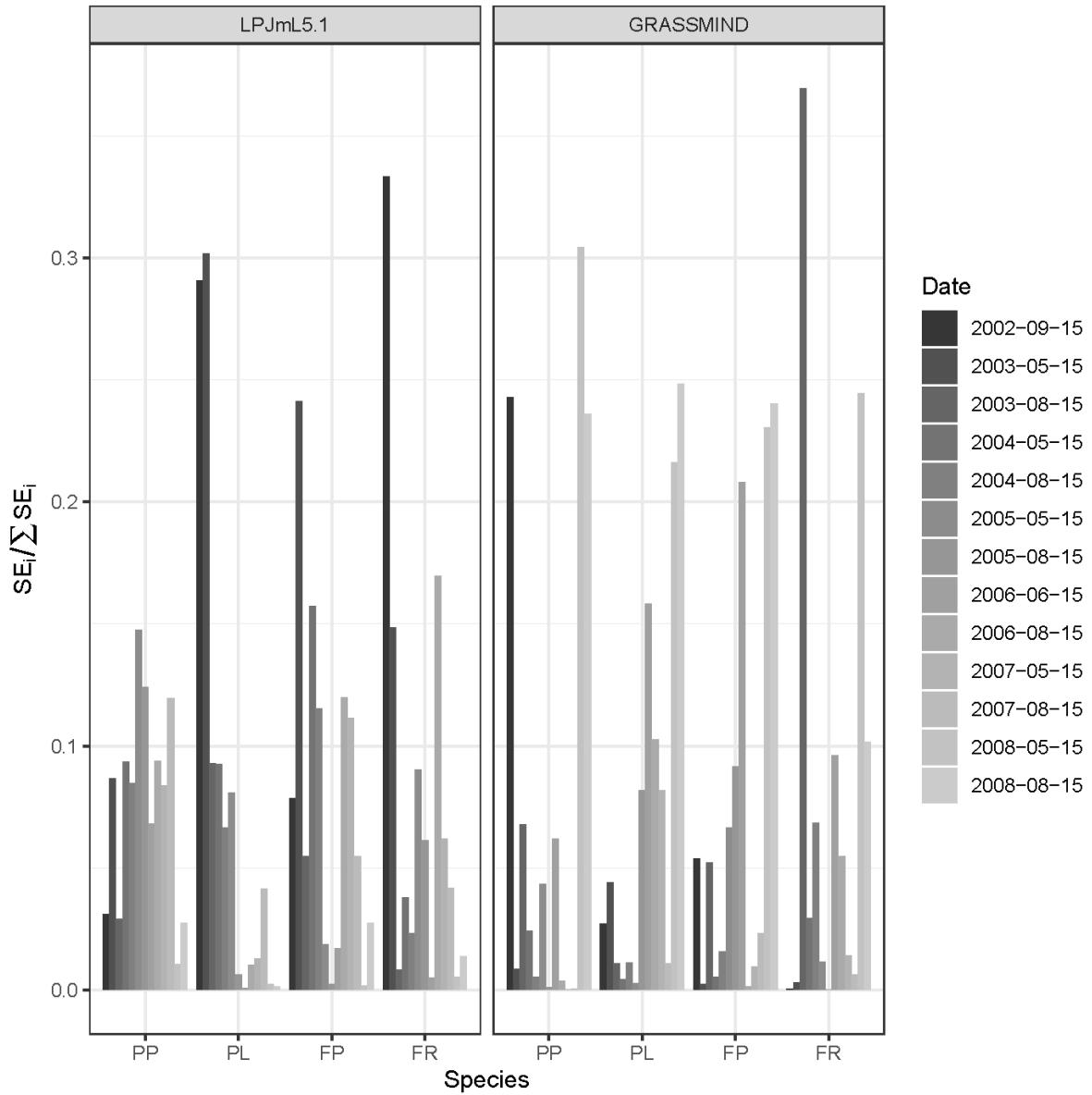


Figure A.7: Share of the SE of each observation date of the sum of all SE for Cover of the species *P. pratensis* (PP), *P. lanceolata* (PL), *F. pratensis* (FP) and *F. rubra* (FR) of the main experiment.

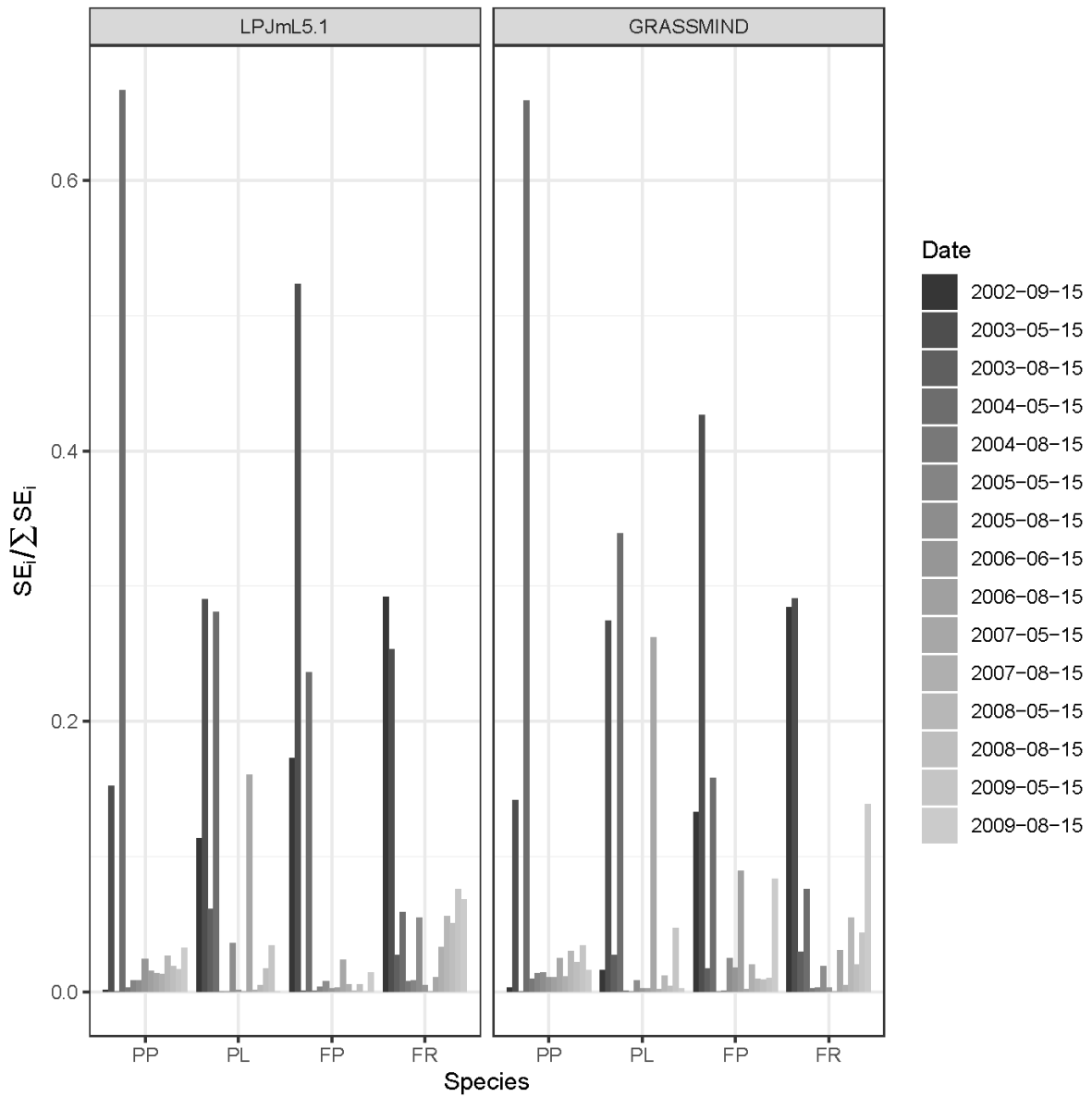


Figure A.8: Share of the SE of each observation date of the sum of all SE for AGB of the species *P. pratensis* (PP), *P. lanceolata* (PL), *F. pratensis* (FP) and *F. rubra* (FR) of the monoculture experiment.

## A.5 Competition related processes of GRASSMIND and LPJmL

Table A.8: Overview of important processes and their descriptions in GRASSMIND and LPJmL

Process	Resource	Inputs/Description	Equation	Effect
Crowding mortality	Space/light	Excess: Cover exceeding 1.0. (e.g.: Cover of 1.2 means an Excess of 0.2)	If $FPC > 1.0$ : $k = \frac{1}{\text{Excess}}$ else $k = 1$ Reduce biomass of all PFTs to the inverse value of total excess cover if cover is larger 1	
Cover distribution	Space/light	$\overline{LAI}$ , $k_{ext}$ : PFT specific leaf area and light extinction coefficients Examples: Weak Comp.: $LAI = 0.75$ ; $k_{ext} = 0.2$ Strong Comp.: $LAI = 7$ ; $k_{ext} = 0.8$	$FPC_i = w \cdot (1 - \exp(-k_{ext,i} \cdot LAI_i))$ $w = \frac{(1 - \exp(-k_{ext,i} \cdot \sum LAI))}{FPC_{sum}}$ $FPC_{sum} = \sum_j (1 - \exp(-k_{ext,j} \cdot LAI_j))$ Calculate cover of each PFT following a lambert beer law. If multiple PFTs are present in the stand, their cover is weighted using the cover it would occupy if it had the total stand LAI, divided by the sum of the covers of the other PFTs.	
Water uptake	Water, Carbon	$\beta_{root}$ : parameter for PFT specific root distribution $FPC_{PFT}$ : Foliage projective cover of the PFT $E_{max}$ : Maximum transpiration rate $w_i$ : rel. soil water content $S_{PFT}$ : PFT specific supply $z, z_{bottom}$ : lower soil layer boundary measured from top of the soil	$D_{PFT} = (1 - wet) \cdot E_{eq} \cdot \frac{\alpha_m}{(1 + \frac{\alpha_m \cdot g_m}{g_c})}$ $S_{PFT} = E_{max} \cdot w_r \cdot FPC_{PFT}$ $w_r = \sum_{l=1}^{N_{soil,layer}-1} w_l \cdot rootdist_l$ $rootdist_l = \frac{1 - \beta_{root}^z}{1 - \beta_{root}^{z_{bottom}}}$ If $S_{PFT} < D_{PFT}$ : $g_c = \frac{g_m \cdot \alpha_m \cdot S_{PFT}}{(1 - wet) \cdot E_{eq} \cdot \alpha_m - S_{PFT}}$ $g_c$ is used to calculate new gross photosynthesis $g_c, g_{min}$ : potential/actual and minimum canopy conductance $\alpha_m$ : maximum Priestley-Taylor coefficient describing the asymptotic transpiration rate $E_{eq}$ : Equilibrium evapotranspiration $wet$ : Fraction of $E_{eq}$ used to vaporize canopy	<div style="border: 1px solid black; padding: 5px; margin-bottom: 5px;">Calculate PFT specific water demand D using the potential canopy <math>g_c</math></div> <div style="border: 1px solid black; padding: 5px; margin-bottom: 5px;">Calculate PFT specific water supply S from <math>E_{max}</math> and root distribution</div> <div style="border: 1px solid black; padding: 5px; margin-bottom: 5px;">Calculate reduced <math>g_c</math> from S</div> <div style="border: 1px solid black; padding: 5px;">Calculate reduced photosynthesis rate and transpiration from <math>g_c</math></div>
Nitrogen uptake	Nitrogen, Carbon	$v_{max,PFT}$ $k_{N,min,PFT}$ $K_{N,min,PFT}$ $w_{sat}$ $z_i$ $\tau_{alloc}$ $f(t_{soil})$ $f(NC_{PFT})$ $rootdist_l$ $kn_{store}$	$potN_{uptake,PFT} = \sum_{l=1}^{N_{soil,layer}} \min \left( 2 \cdot v_{max,PFT} \cdot \left( k_{N,min,PFT} + \frac{N_{tot}}{N_{tot} + K_{N,min,PFT} \cdot w_{sat} \cdot \frac{z_l}{1000}} \right) \cdot f(t_{soil}) \cdot f(NC_{PFT}) \cdot (C_{root,PFT} + C_{inc} \cdot \tau_{alloc}) \cdot rootdist_l, N_{tot} \right)$ $actN_{uptake,PFT} = \min(potN_{uptake,PFT}, N_{demand,tot,PFT} - N_{PFT})$ $N_{demand,leaf,PFT} = p \cdot 0.02314815 \cdot \frac{v_{max}}{h_{day}} \cdot \exp(-k_{temp} \cdot (temp - 25)) \cdot f(LAI) + NC_{leaf,low} \cdot C_{leaf}$ $N_{demand,tot,PFT} = N_{demand,leaf,PFT} + C_{root}$ If $N_{demand,tot,PFT} > N_{PFT}$ $N_{demand,leaf,PFT}$ is adjusted and N limited $v_{max}$ is calculated and used for update gross photosynthesis.	<div style="border: 1px solid black; padding: 5px; margin-bottom: 5px;">Calculate <math>v_{max}</math> from water-stressed photosynthesis rate</div> <div style="border: 1px solid black; padding: 5px; margin-bottom: 5px;">Calculate nitrogen demand from <math>v_{max}</math></div> <div style="border: 1px solid black; padding: 5px; margin-bottom: 5px;">Calculate actual N uptake from soil <math>NO_3^-</math> and <math>NH_4^+</math></div> <div style="border: 1px solid black; padding: 5px; margin-bottom: 5px;">Calculate reduced <math>v_{max}</math> from available leaf N</div> <div style="border: 1px solid black; padding: 5px;">Calculate reduced photosynthesis rate and transpiration from <math>v_{max}</math></div>

Table A.8: Overview of important processes and their descriptions in GRASSMIND and LPJmL (continued)

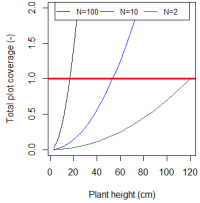
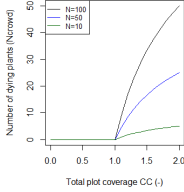
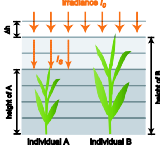
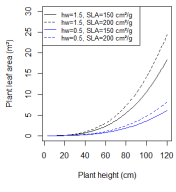
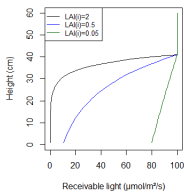
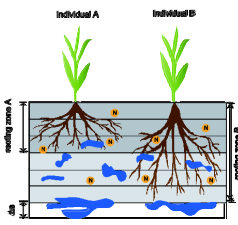
Process	Resource	Inputs/Description	Equation	Effect
Crowding mortality	Space	<p><b>1. Calculation of coverage CC</b> Inputs are CA being the circular ground area of a plant (width of circle dependent on plant height <math>H</math> and species parameter <math>hw</math>). Overlapping is allowed by the species parameter <math>fo</math> (no distinction between live and dead leaves)</p> <p><b>2. If too crowded (<math>CC &gt; 1</math>, i.e. <math>CC^{-1} &lt; 1</math>), then randomly selected plants die (<math>N_{crowd}</math>)</b></p>	<p><b>1. Calculation of coverage</b></p> $CC = \sum_{plant\ i=1}^N \frac{CA_i(H)}{A} \cdot f_{o_i}$ <p><math>CC</math> .. total cover on plot  <math>CA</math> .. plant's circular ground area (m<sup>2</sup>)  <math>H</math> .. plant height (m)  <math>hw</math> .. constant species parameter  <math>fo</math> .. constant species parameter  <math>A</math> .. constant plot area (1 m x 1 m)</p> <p><b>2. If <math>CC^{-1} &lt; 1</math></b></p> $N_{crowd} = N \cdot (1 - CC^{-1})$ <p><math>N_{crowd}</math> .. dying plants due to crowding</p>	<p>Example of one cohort of plants of same height</p>  <p><math>hw=1.5, fo=1</math> (the smaller <math>hw</math>, the larger <math>CC</math>) (the smaller <math>fo</math>, the smaller <math>CC</math>)</p>  <p>The less plants on the plot, the lower the number of dying plants due to crowding</p>
Light competition	Light	<p><b>1. Calculation of light climate</b> Aboveground canopy is discretized in several layers of width <math>\Delta h</math> (m). Leaf area of plants <math>L_i</math> is distributed among respective height layer (dependent on plant height <math>H</math>, biomass <math>B</math> and species parameter <math>SLA</math>).</p> <p><b>2. Limitation of light by shading</b> Smaller plants receive only attenuated light <math>I_s</math> (exponentially reduced by above cumulative leaf area; Beer-Lambert law) Asymmetric competition: larger plants receive more light than smaller ones</p>	<p><b>1. Light climate</b></p> <p><math>LAI_i</math> .. plot-level leaf area index (m<sup>2</sup>/m<sup>2</sup>) of a specific height layer</p> $LAI_i = \frac{1}{A} \cdot \sum_{plant\ i} k_i \cdot \tilde{L}_i$ <p><math>\tilde{L}_i</math> .. leaf area of a plant in a specific height layer  <math>k</math> .. constant species parameter</p> $\tilde{L}_i = \begin{cases} \frac{B \cdot SLA}{H} \cdot \Delta h, & 0 \leq i \leq H \\ 0, & i > H \end{cases}$ <p><math>B</math> .. plant shoot biomass (g)  <math>SLA</math> .. specific leaf area (m<sup>2</sup>/g)  <math>H</math> .. plant height (m)</p> $B = \frac{\pi}{4} \cdot H^3 \cdot \frac{f_s}{hw}$ <p><math>hw</math> .. constant species parameter  <math>f_s</math> .. constant species parameter</p> <p><b>2. Shading</b></p> $I_s = I_0 \cdot e^{-\sum_{i>H} (LAI_i)}$ <p><math>I_s</math> .. attenuated light a plant (of height <math>H</math>) receives  <math>I_0</math> .. light on top of the canopy</p>	  
Water competition	Soil water	<p><b>Limitation of GPP and transpiration (= water uptake) due to</b></p> <p><b>1. soil water content</b> If soil water content falls between permanent wilting point and minimal soil water content, limitation happens linearly. Below the PWP, reduction is zero. No direct interaction between plants. But, plants with deeper roots (dependent on root biomass and species parameter <math>r_{1,2}</math>) have more chance of larger soil water content.</p>	<p><b>1. Limited soil water</b></p> $R_w = \begin{cases} 0, & \theta_w^{plant} < \theta_{PWP}^{plant} \\ \frac{\theta_w^{plant} - \theta_{PWP}^{plant}}{\theta_{MSW}^{plant} - \theta_{PWP}^{plant}}, & \theta_{PWP}^{plant} \leq \theta_w^{plant} \leq \theta_{MSW}^{plant} \\ 1, & \theta_{MSW}^{plant} \leq \theta_w^{plant} \end{cases}$ <p><math>R_w</math> ... reduction of plants (factor between 0 and 1)  <math>\theta_{PWP}^{plant}</math> .. permanent wilting point (of plant-specific rooted soil layers, mm)  <math>\theta_w^{plant}</math> .. soil water content (of plant-specific rooted soil layers, mm)  <math>\theta_{MSW}^{plant}</math> .. minimal soil water content for reduction (40% between PWP and field capacity, dependent on plant-specific rooted layers, mm)</p>	

Table A.8: Overview of important processes and their descriptions in GRASSMIND and LPJmL (continued)

		<p>Gross productivity (GPP) and soil water uptake of plants is reduced by RW.</p> <p><b>2. Interception</b></p> <p>If the sum of interception and transpiration exceeds potential evapotranspiration, both – GPP and soil water uptake is reduced proportionally.</p> <p><b>3. Wilting point</b></p> <p>If the sum of soil water uptake by all plants would let soil water content fall below PWP in the entire soil, GPP and soil water uptake is reduced proportionally.</p>	$\theta_{uptake} = \frac{GPP \cdot R_W}{WUE}$ <p><math>\theta_{uptake}</math> .. soil water uptake of a plant (equals transpiration; mm/d)  <math>GPP</math> .. plant gross productivity (g/m<sup>2</sup>/d)  <math>WUE</math> .. constant species parameter (water use efficiency, g/kgH<sub>2</sub>O)</p> <p><b>2. Interception</b></p> $f_{PET} = \frac{PET - RI}{\sum_{plants} \theta_{uptake}}$ <p><math>PET</math> .. potential evapotranspiration (mm/d)  <math>RI</math> .. interception of rainfall by plants (mm/d)</p> <p><b>3. Wilting point</b></p> $f_{PWP} = \frac{\theta_{W}^{soil} - \theta_{PWP}^{soil}}{\sum_{plants} \theta_{uptake}}$ <p><math>\theta_{PWP}^{soil}</math> .. permanent wilting point (of entire soil down to 2 m depth, mm)  <math>\theta_{W}^{soil}</math> .. soil water content (of entire soil, mm)</p>	
Nitrogen competition	Soil nitrogen	<p><b>1. Nitrogen demand based on NPP</b></p> <p>Nitrogen demand of a plant is calculated based on the potential net productivity (NPP<sub>pot</sub>, possibly already reduced due to shading or soil water).          Dependent on <b>species parameter</b> (allocation rates to shoot, root and seed production), and species-specific <b>green and brown CN-ratios</b>.</p> <p><b>2. Nitrogen access based on rooting depth and root branch lengths</b></p> <p><b>Rooting depth and root branch length</b> is calculated based on <b>root biomass</b> (proportional to shoot biomass; constant species parameter) and <b>three constant species parameter</b> (<math>r_1, r_2, SRL</math>)</p> <p>Root branch lengths are therefore distributed among rooted soil layers and related to the total sum of all root branches of all plants in that layer (normalization).</p> <p><b>3. Nitrogen limitation</b></p> <p>The ratio between accessible and demanded nitrogen is used to reduce NPP<sub>pot</sub> and nitrogen uptake proportionally.</p>	<p><b>1. Nitrogen demand</b></p> $N_{demand} = alloc_{shoot} \cdot \frac{f_c \cdot NPP_{pot}}{CN_{green}} + (alloc_{root} + alloc_{seed}) \cdot \frac{f_c \cdot NPP_{pot}}{CN_{brown}}$ <p><math>f_c</math> .. biomass-carbon conversion factor 0.43  <math>alloc</math> .. allocation fraction of NPP to shoot, root or reproduction  <math>NPP_{pot}</math> .. potential net productivity  <math>CN_{green}</math> .. CN ratio of green leaves  <math>CN_{brown}</math> .. CN ratio of brown leaves/root branches/seed</p> <p><b>2. Nitrogen access</b></p> $N_{access} = \sum_{j < s_{max}} F_j \cdot N_j$ $F_j = \frac{\left( \frac{length_{shoot}}{s_{max}} \right)}{\left( \sum_{plants \text{ with } j < s_{max}} \left( \frac{length_{shoot}}{s_{max}} \right) \right)}$ <p><math>N_{access}</math> .. amount of nitrogen that can be accessed in soil layers until rooting depth (s<sub>max</sub>)  <math>F_j</math> .. percentage of root branch lengths of the plant in relation to total root branch length  <math>N_j</math> .. amount of soil nitrogen in a specific soil layer (g/m<sup>2</sup>)</p> <p><b>3. Nitrogen limitation</b></p> $R_N = \min \left( 1, \frac{N_{access}}{N_{demand}} \right)$	<p>The more is allocated to the aboveground shoot, the more nitrogen is demanded (solid lines: blue &gt; black). The smaller CN (esp. green) the more nitrogen is demanded (dashed lines &gt; solid lines)</p>

## A.6 Additional Figures Baseline\_Mow and NoMow

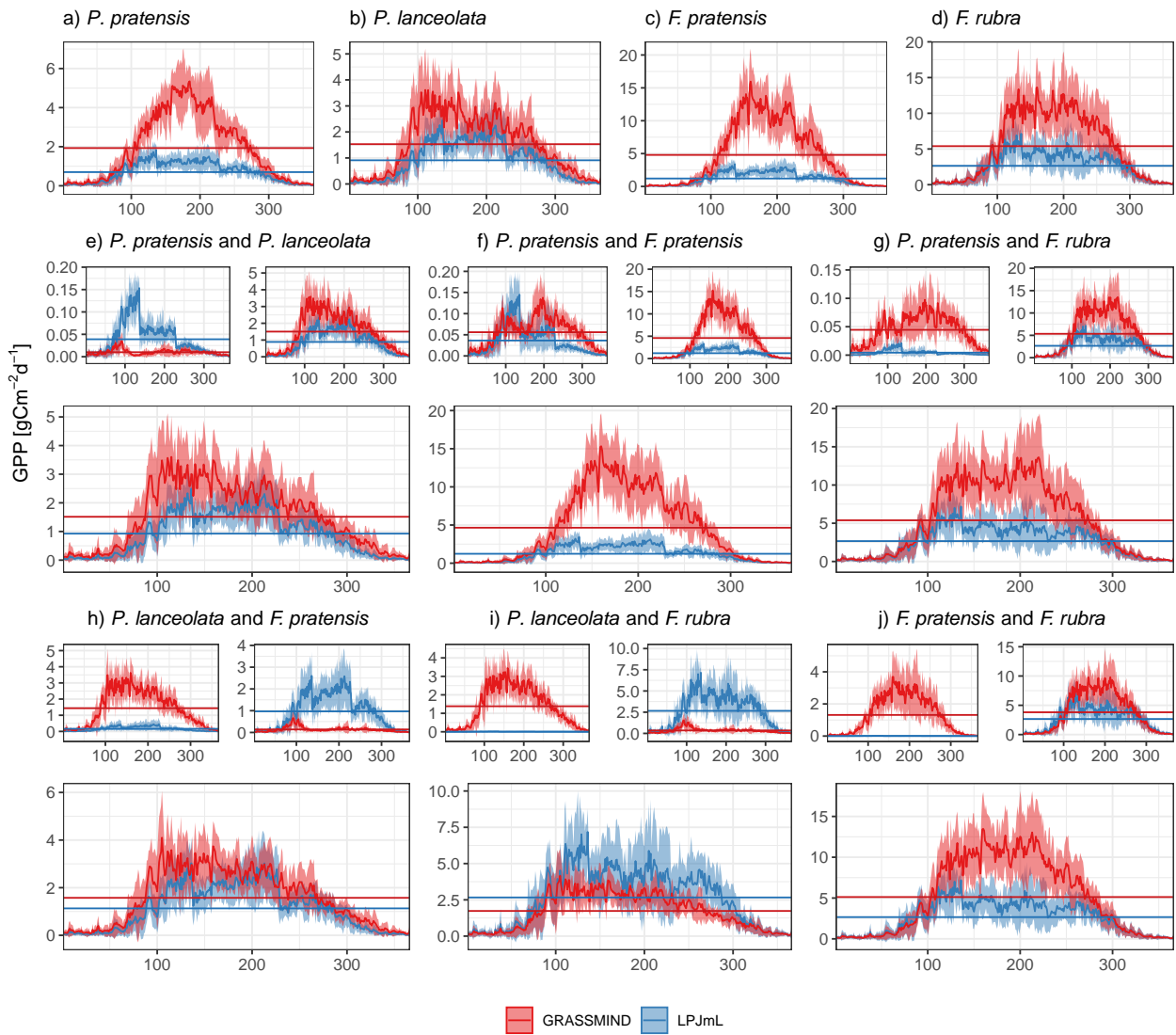


Figure A.9: Mean GPP in gC m<sup>-2</sup> (lines ± 1 standard deviation shaded) for Baseline\_Mow for GRASSMIND (red) and LPJmL (blue) averaged over all simulation years for each day of the year for monocultures (a,b,c,d) and two-species mixtures (e,f,g,h,i,j). For mixtures specie specific (top) and total GPP (bottom) are shown separately. Horizontal lines show the time series mean.

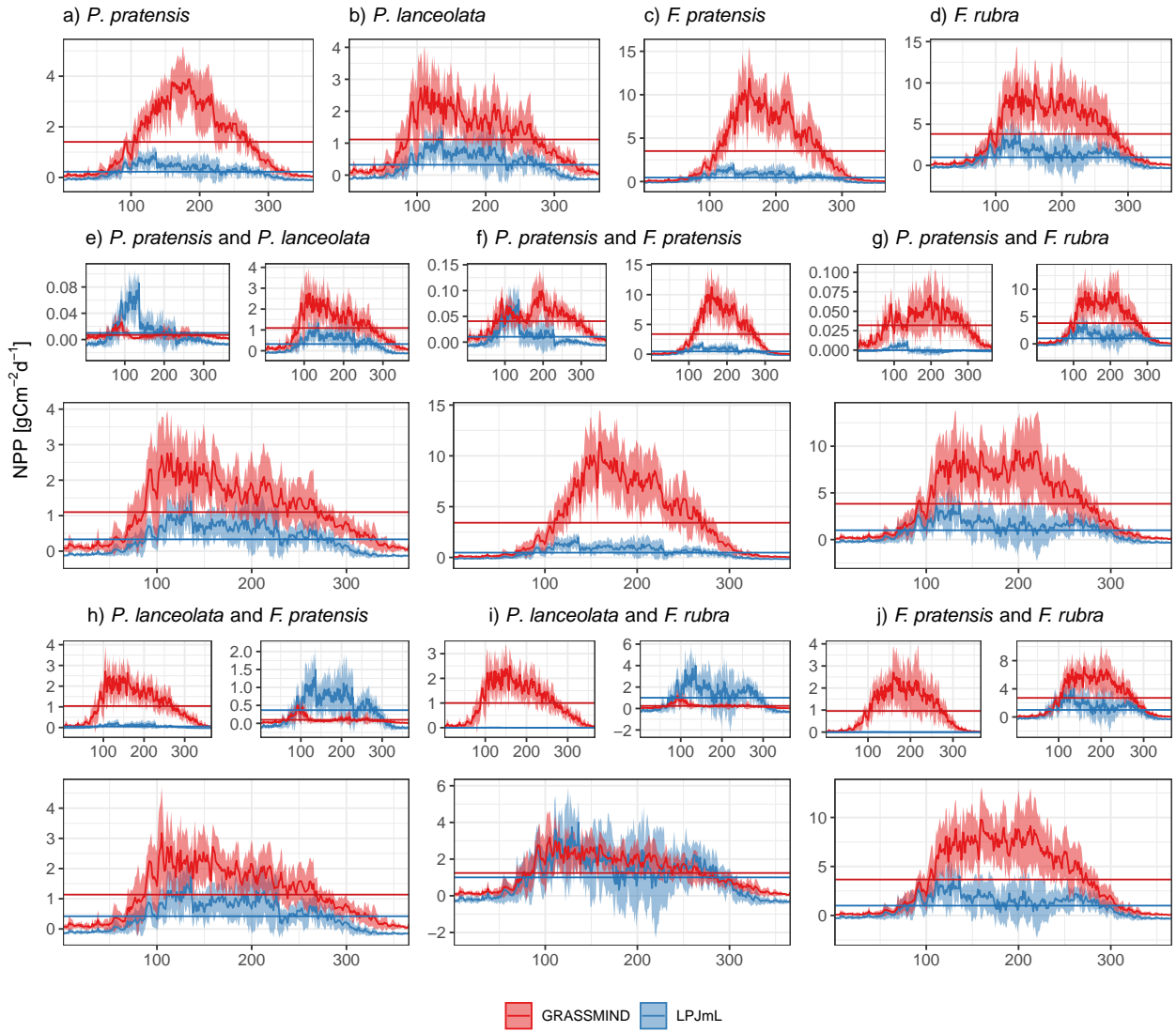


Figure A.10: Mean NPP in  $\text{gC m}^{-2}$  (lines  $\pm$  1 standard deviation shaded) for Baseline\_Mow for GRASSMIND (red) and LPJmL (blue) averaged over all simulation years for each day of the year for monocultures (a,b,c,d) and two-species mixtures (e,f,g,h,i,j). For mixtures specie specific (top) and total NPP (bottom) are shown separately. Horizontal lines show the time series mean.

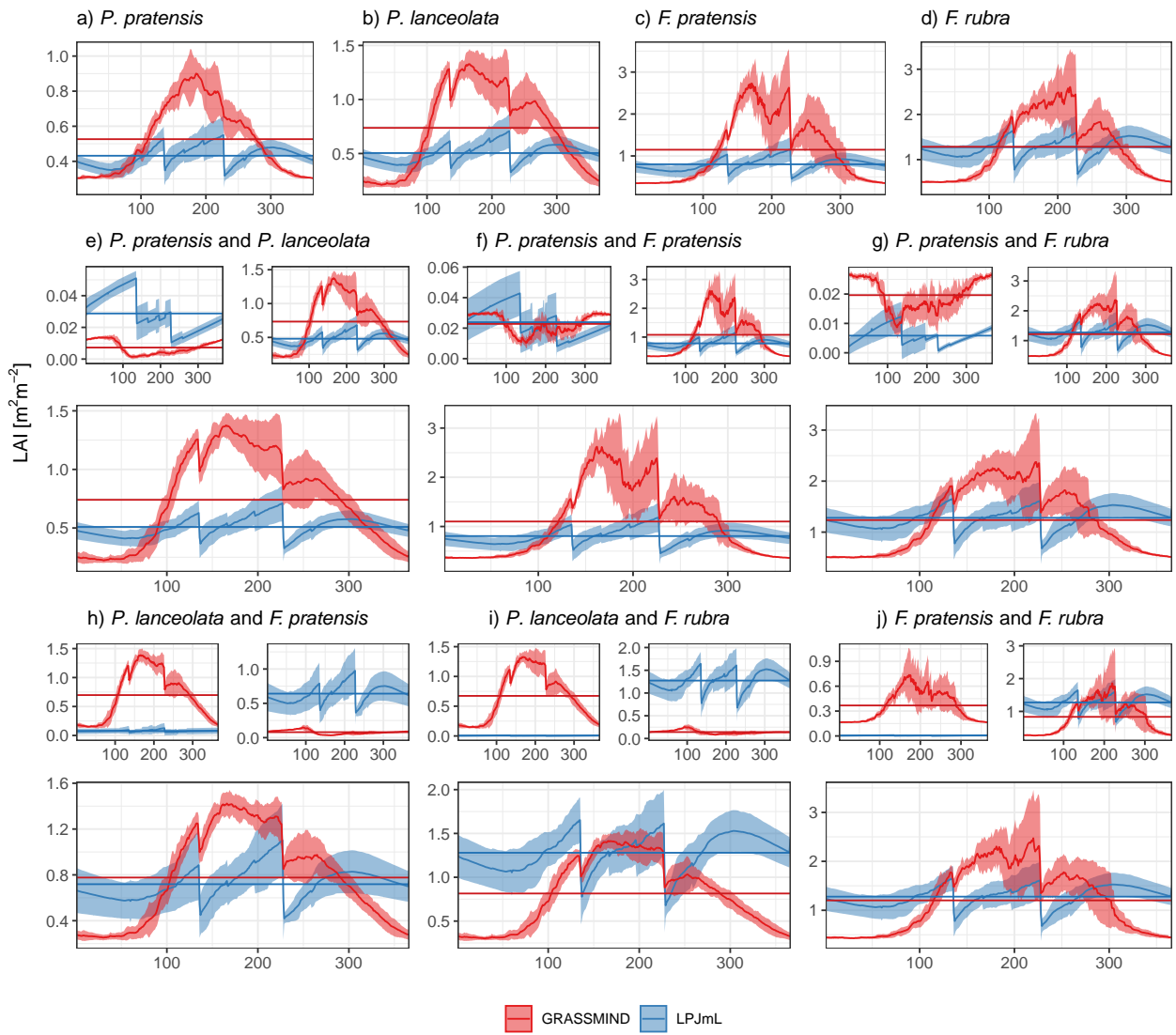


Figure A.11: Mean LAI in  $\text{m}^2 \text{m}^{-2}$  (lines  $\pm 1$  standard deviation shaded) for Baseline\_Mow for GRASSMIND (red) and LPJmL (blue) averaged over all simulation years for each day of the year for monocultures (a,b,c,d) and two-species mixtures (e,f,g,h,i,j). For mixtures specie specific (top) and total LAI (bottom) are shown separately. Horizontal lines show the time series mean.

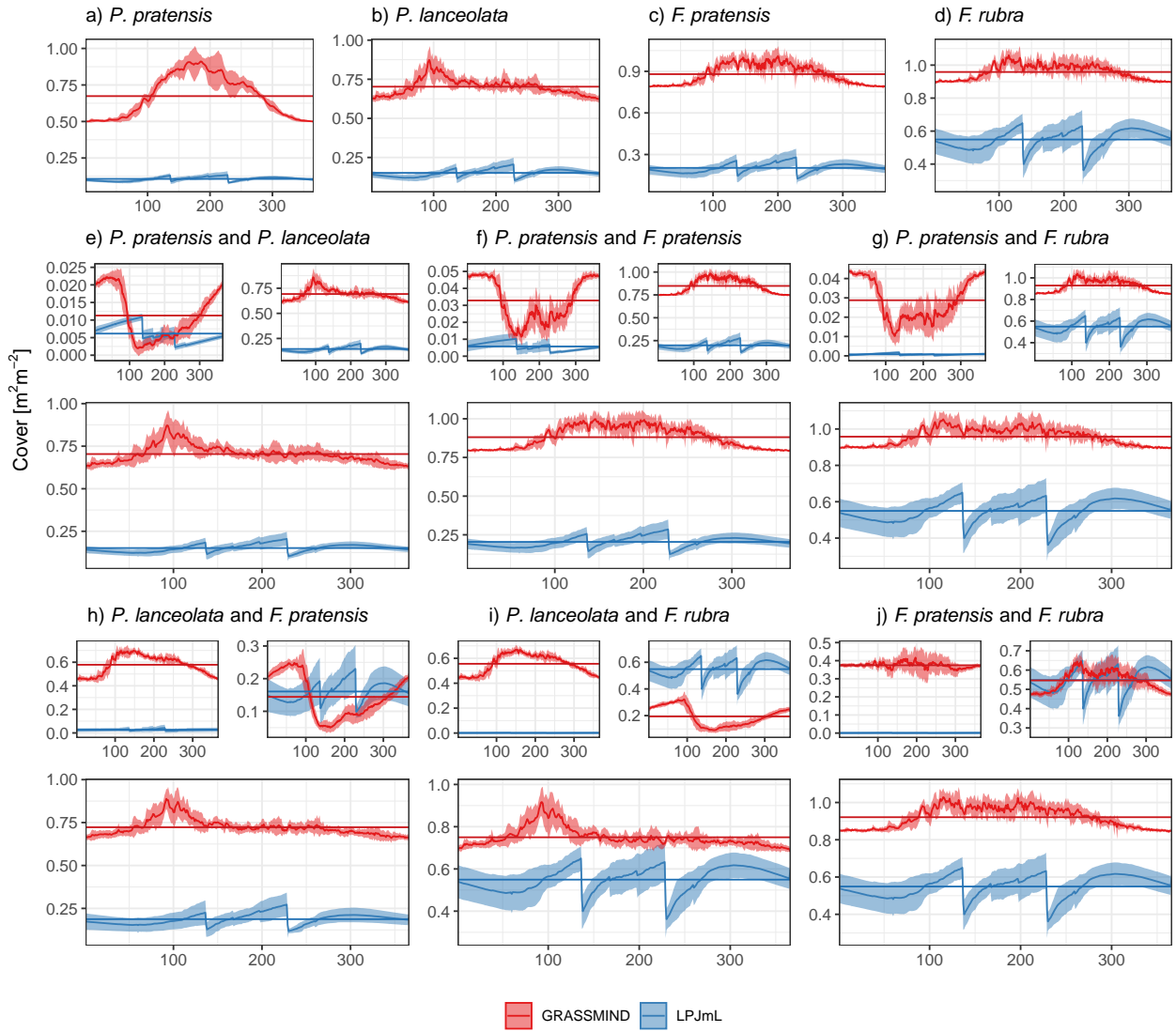


Figure A.12: Mean Cover in  $\text{m}^2 \text{m}^{-2}$  (lines  $\pm$  1 standard deviation shaded) for Baseline\_Mow for GRASSMIND (red) and LPJmL (blue) averaged over all simulation years for each day of the year for monocultures (a,b,c,d) and two-species mixtures (e,f,g,h,i,j). For mixtures specie specific (top) and total Cover (bottom) are shown separately. Horizontal lines show the time series mean.

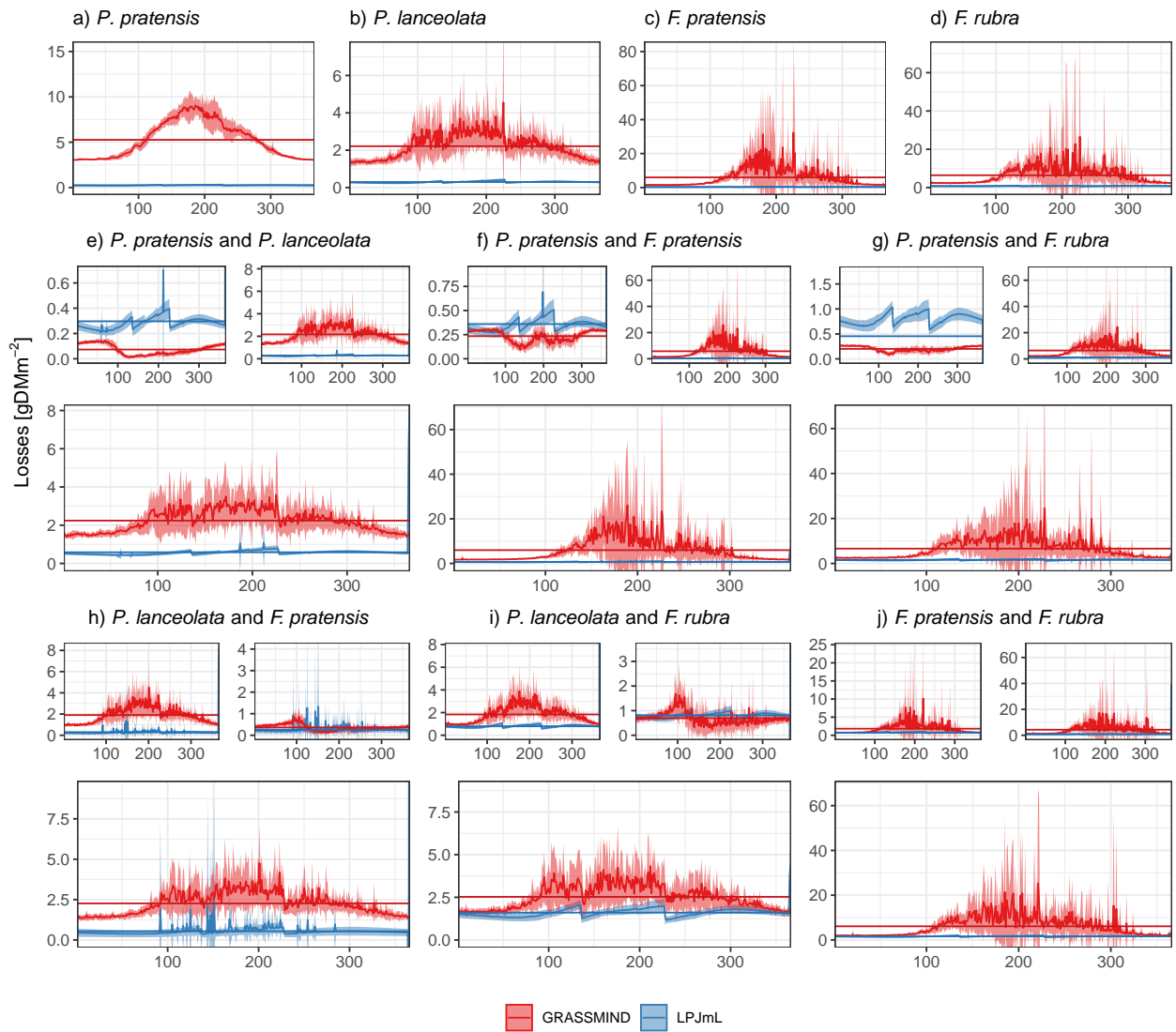


Figure A.13: Mean losses from mortality and litterfall in  $\text{gDM m}^{-2}$  (lines  $\pm 1$  standard deviation shaded) for Baseline\_Mow for GRASSMIND (red) and LPJmL (blue) averaged over all simulation years for each day of the year for monocultures (a,b,c,d) and two-species mixtures (e,f,g,h,i,j). For mixtures specie specific (top) and total losses (bottom) are shown separately. Horizontal lines show the time series mean.

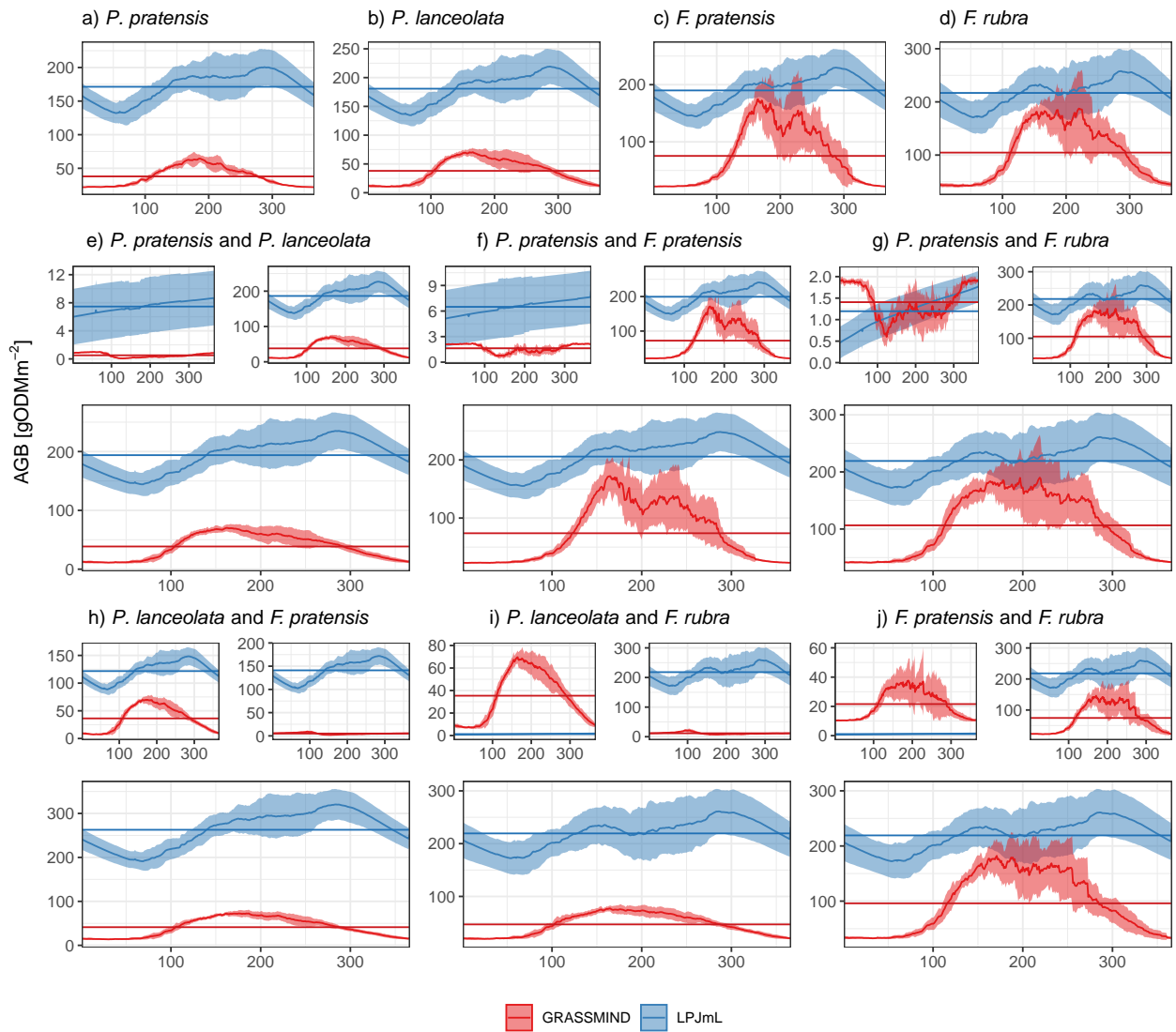


Figure A.14: Mean AGB in  $\text{gDM m}^{-2}$  (lines  $\pm$  1 standard deviation shaded) for Baseline\_NoMow for GRASSMIND (red) and LPJmL (blue) averaged over all simulation years for each day of the year for monocultures (a,b,c,d) and two-species mixtures (e,f,g,h,i,j). For mixtures specie specific (top) and total AGB (bottom) are shown separately. Horizontal lines show the time series mean.

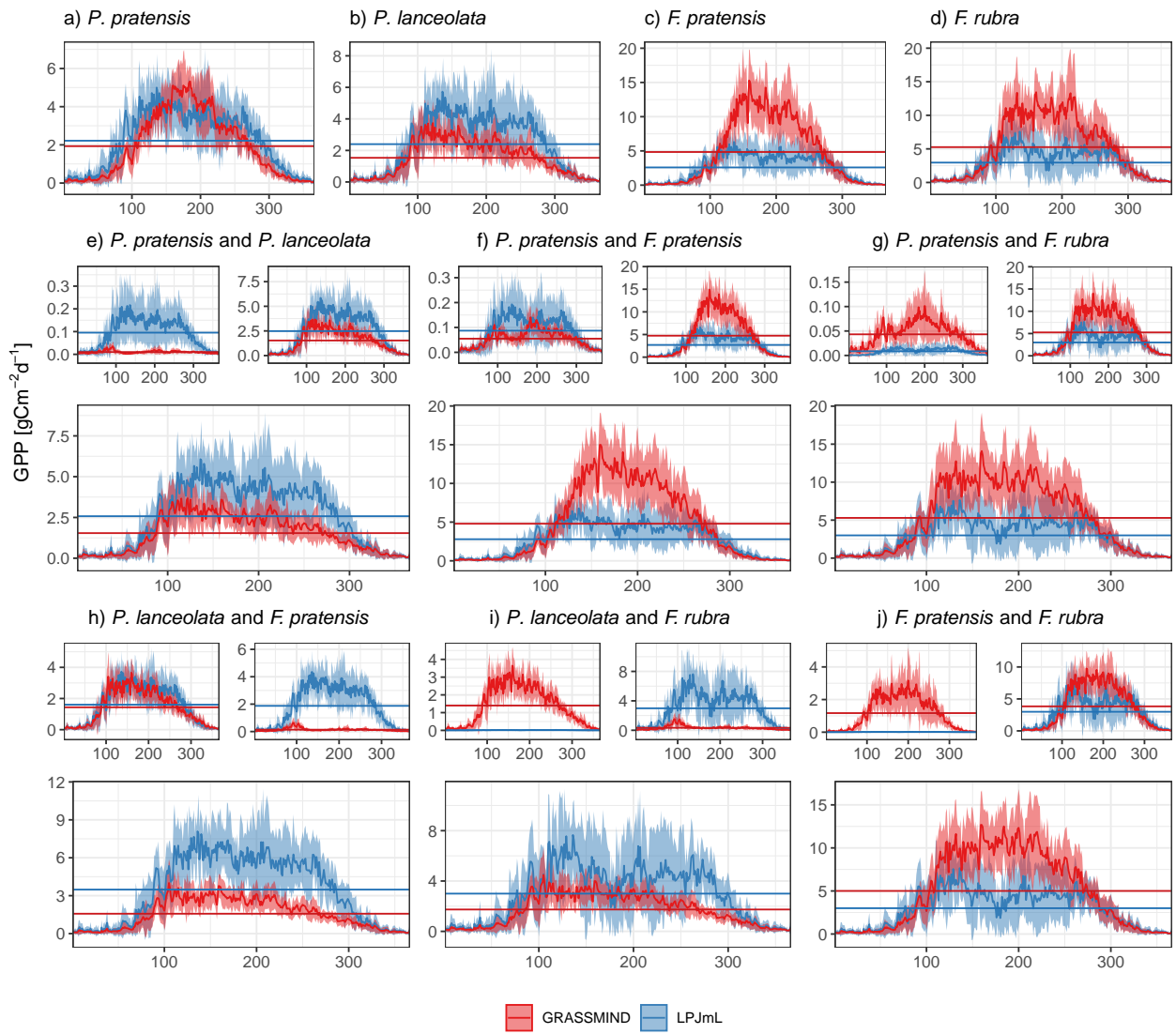


Figure A.15: Mean GPP in  $\text{gC m}^{-2}$  (lines  $\pm$  1 standard deviation shaded) for Baseline\_NoMow for GRASSMIND (red) and LPJmL (blue) averaged over all simulation years for each day of the year for monocultures (a,b,c,d) and two-species mixtures (e,f,g,h,i,j). For mixtures specie specific (top) and total GPP (bottom) are shown separately. Horizontal lines show the time series mean.

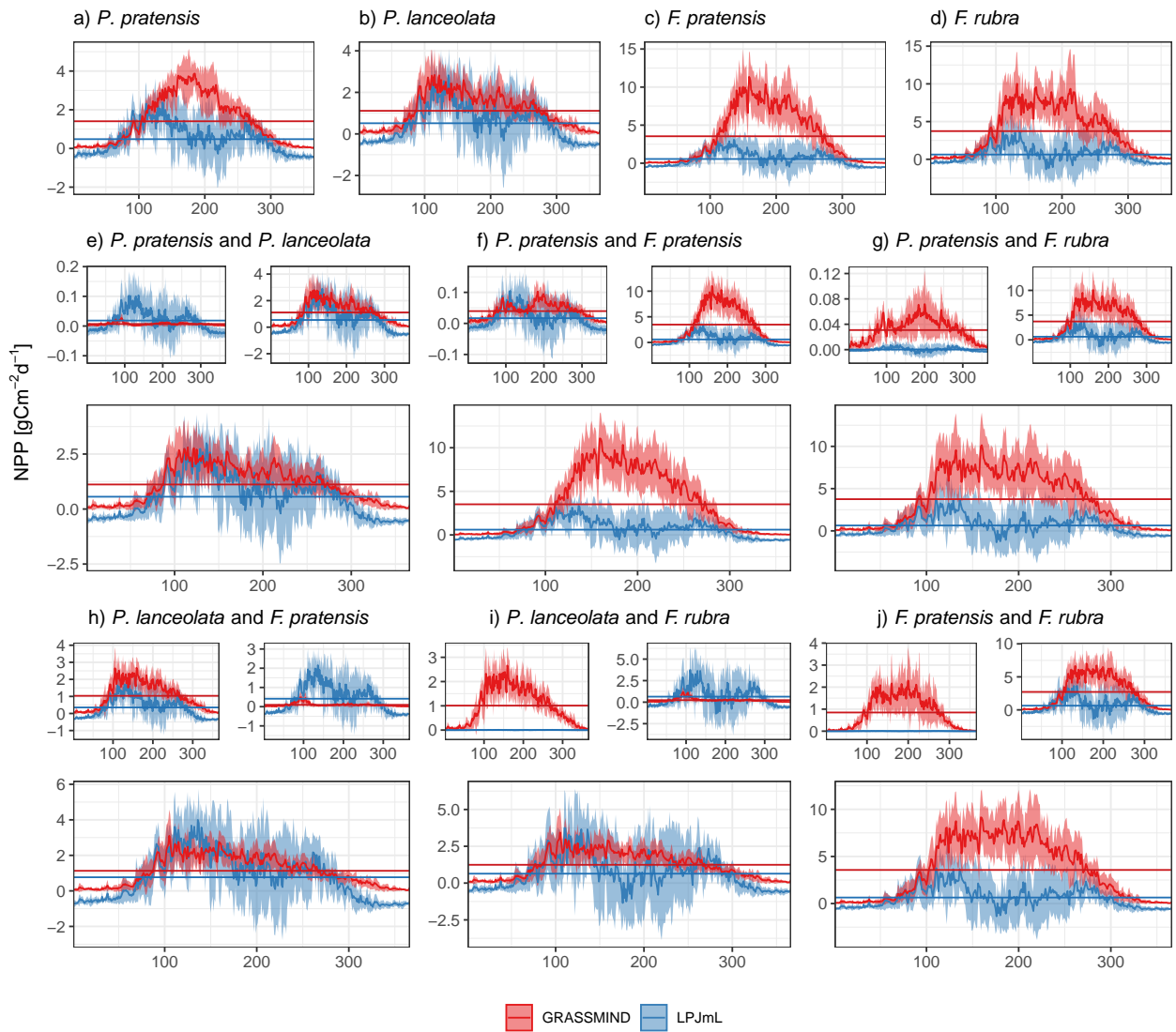


Figure A.16: Mean NPP in  $\text{gC m}^{-2}$  (lines  $\pm$  1 standard deviation shaded) for Baseline\_NoMow for GRASSMIND (red) and LPJmL (blue) averaged over all simulation years for each day of the year for monocultures (a,b,c,d) and two-species mixtures (e,f,g,h,i,j). For mixtures specie specific (top) and total NPP (bottom) are shown separately. Horizontal lines show the time series mean.

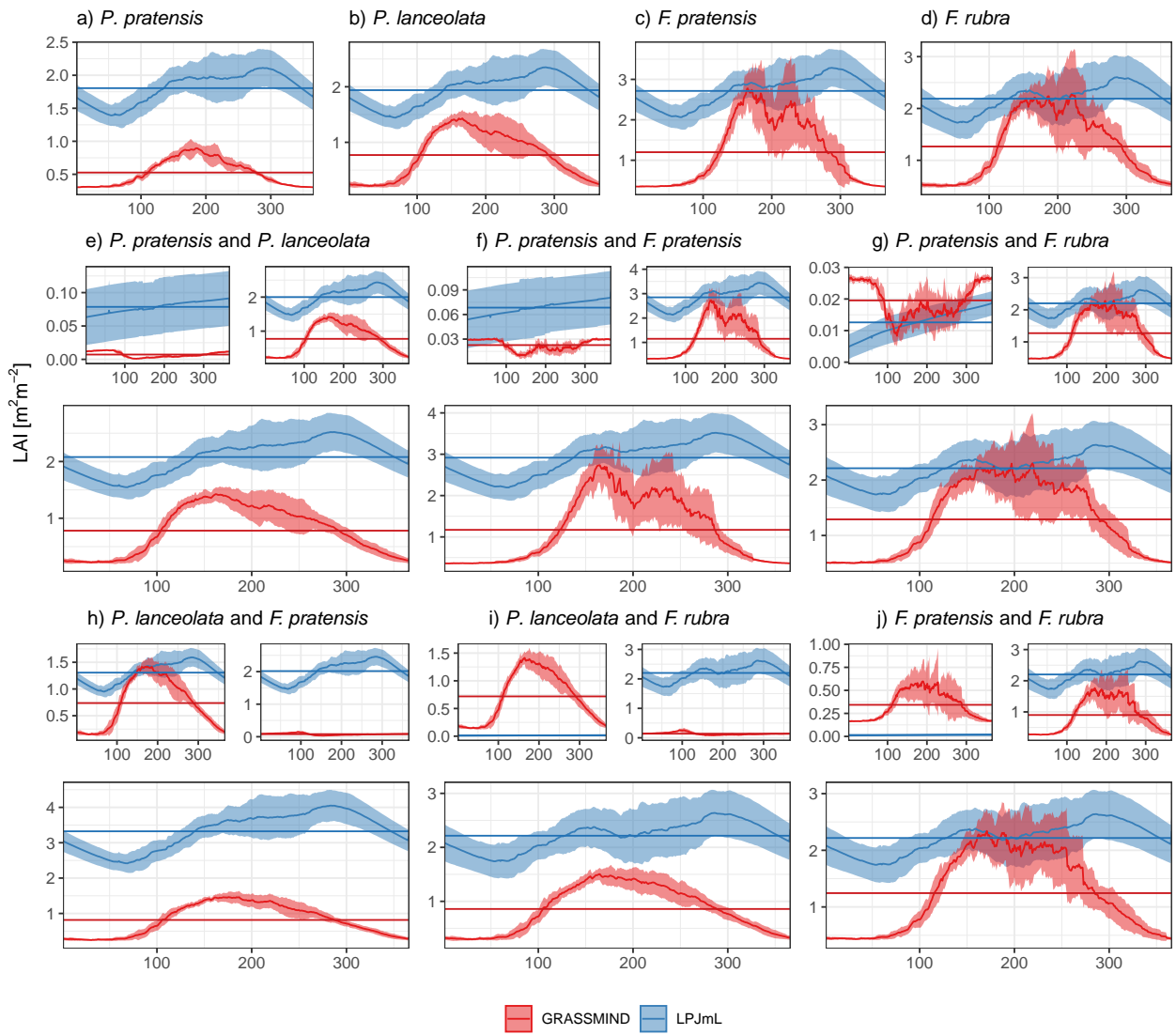


Figure A.17: Mean LAI in  $\text{m}^2 \text{m}^{-2}$  (lines  $\pm$  1 standard deviation shaded) for Baseline\_NoMow for GRASSMIND (red) and LPJmL (blue) averaged over all simulation years for each day of the year for monocultures (a,b,c,d) and two-species mixtures (e,f,g,h,i,j). For mixtures specie specific (top) and total LAI (bottom) are shown separately. Horizontal lines show the time series mean.

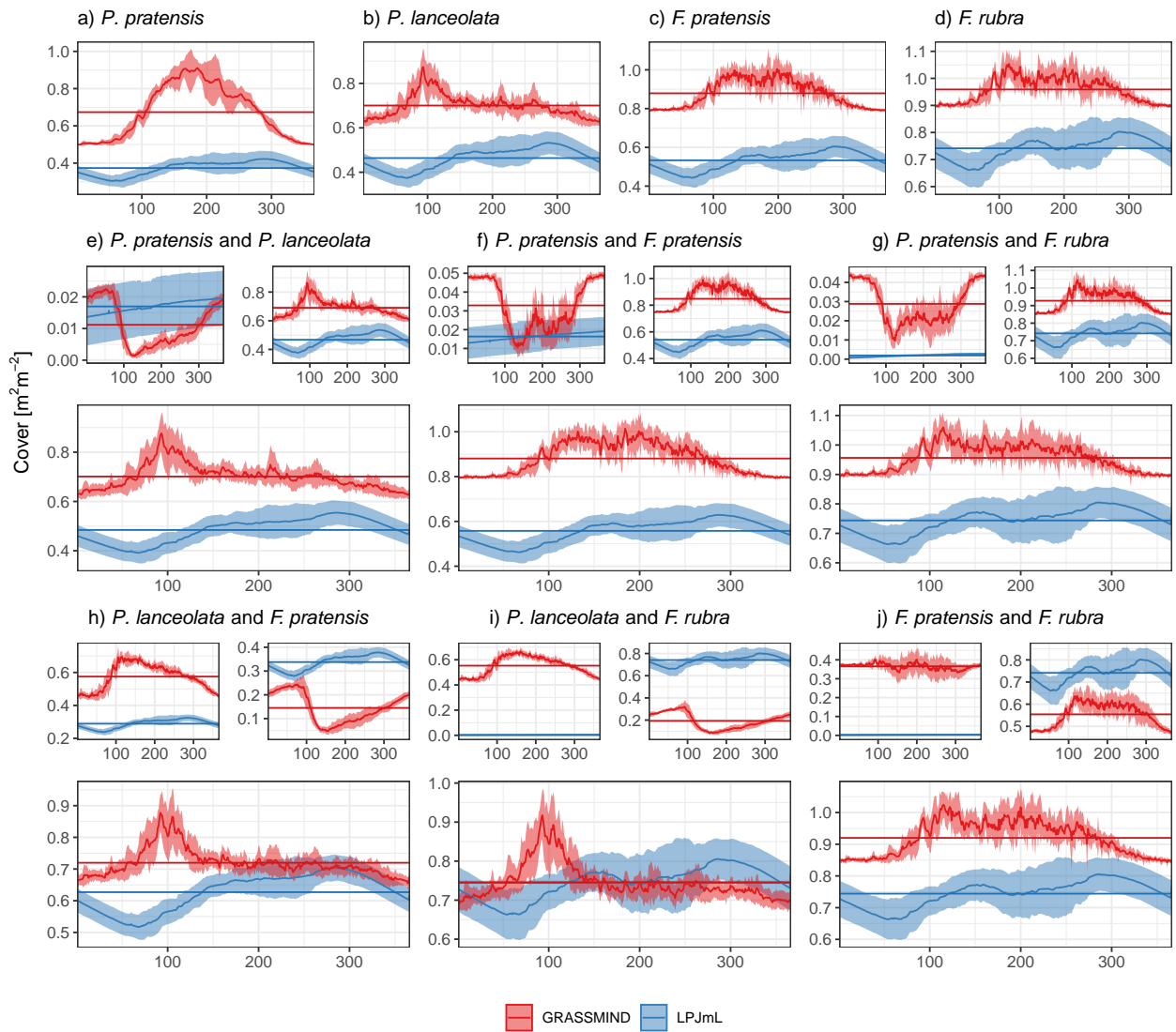


Figure A.18: Mean Cover in  $\text{m}^2 \text{m}^{-2}$  (lines  $\pm 1$  standard deviation shaded) for Baseline\_NoMow for GRASSMIND (red) and LPJmL (blue) averaged over all simulation years for each day of the year for monocultures (a,b,c,d) and two-species mixtures (e,f,g,h,i,j). For mixtures specie specific (top) and total Cover (bottom) are shown separately. Horizontal lines show the time series mean.

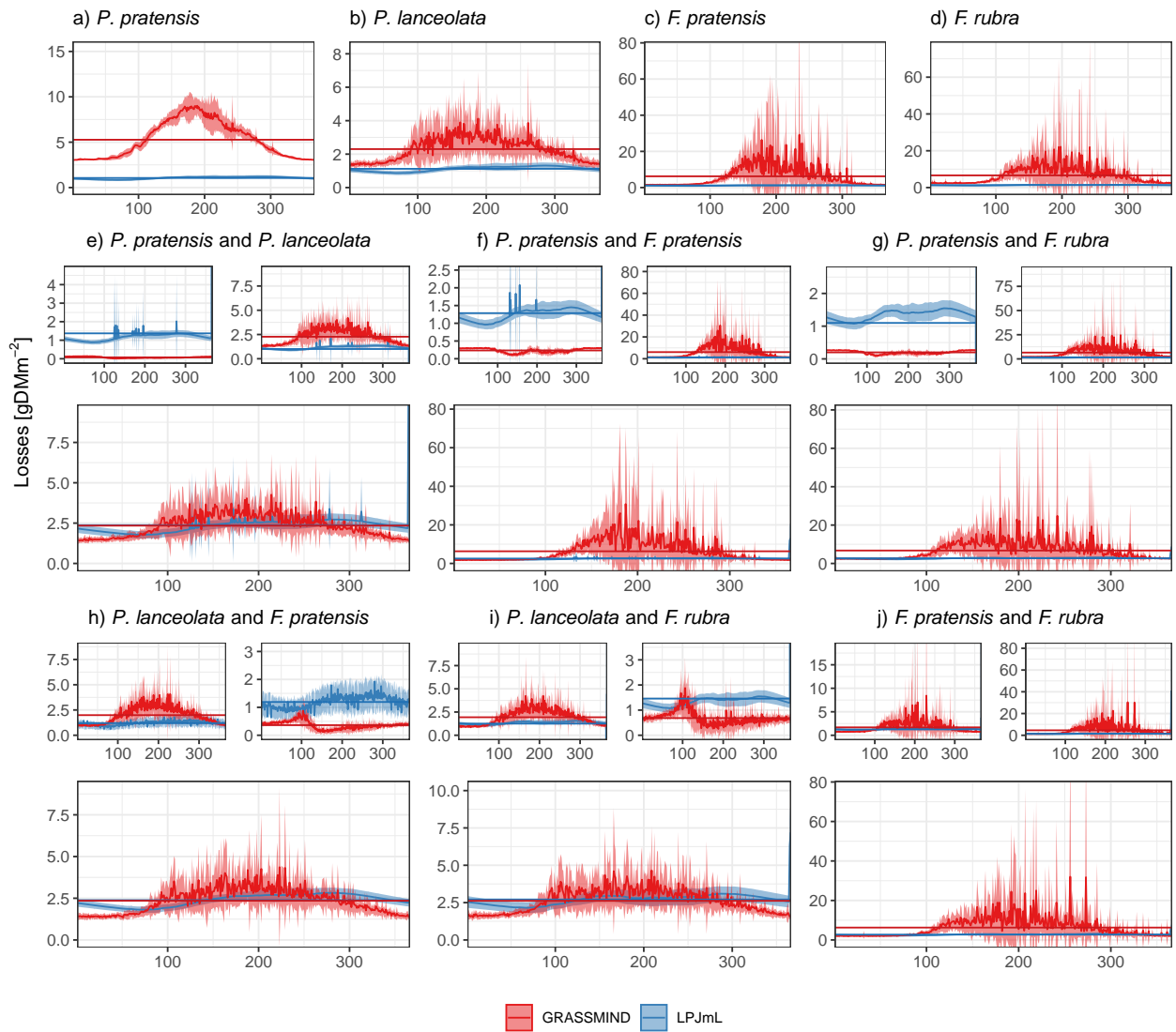


Figure A.19: Mean losses from mortality and litterfall in  $\text{gDM m}^{-2}$  (lines  $\pm 1$  standard deviation shaded) for Baseline\_NoMow for GRASSMIND (red) and LPJmL (blue) averaged over all simulation years for each day of the year for monocultures (a,b,c,d) and two-species mixtures (e,f,g,h,i,j). For mixtures specie specific (top) and total losses (bottom) are shown separately. Horizontal lines show the time series mean.

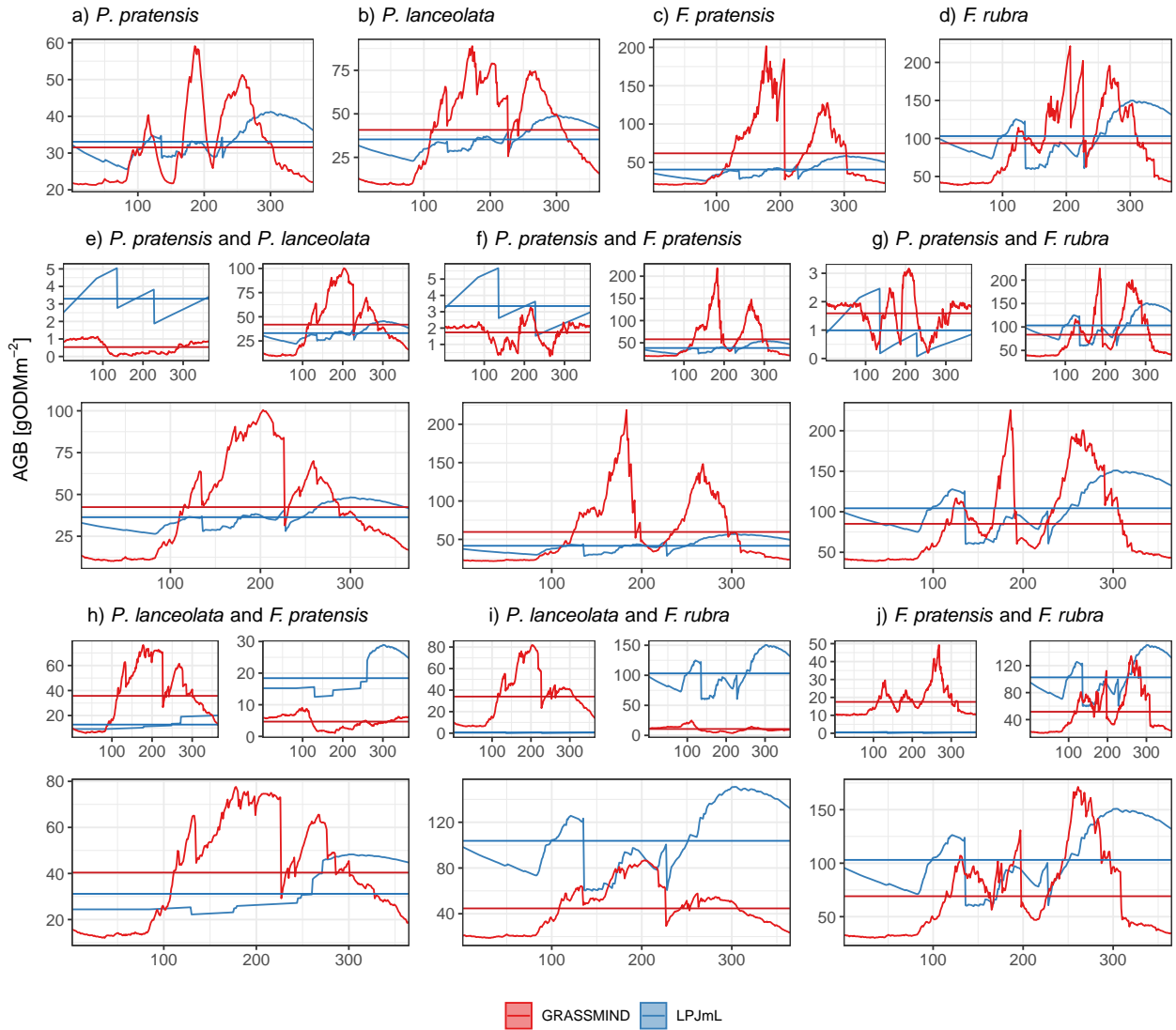


Figure A.20: AGB in  $\text{gDM m}^{-2}$  for ModD.Mow for GRASSMIND (red) and LPJmL (blue) for the year with reduced precipitation (2003) for monocultures (a,b,c,d) and two-species mixtures (e,f,g,h,i,j). For mixtures species specific (top) and total AGB (bottom) are shown separately. Horizontal lines show the annual mean.

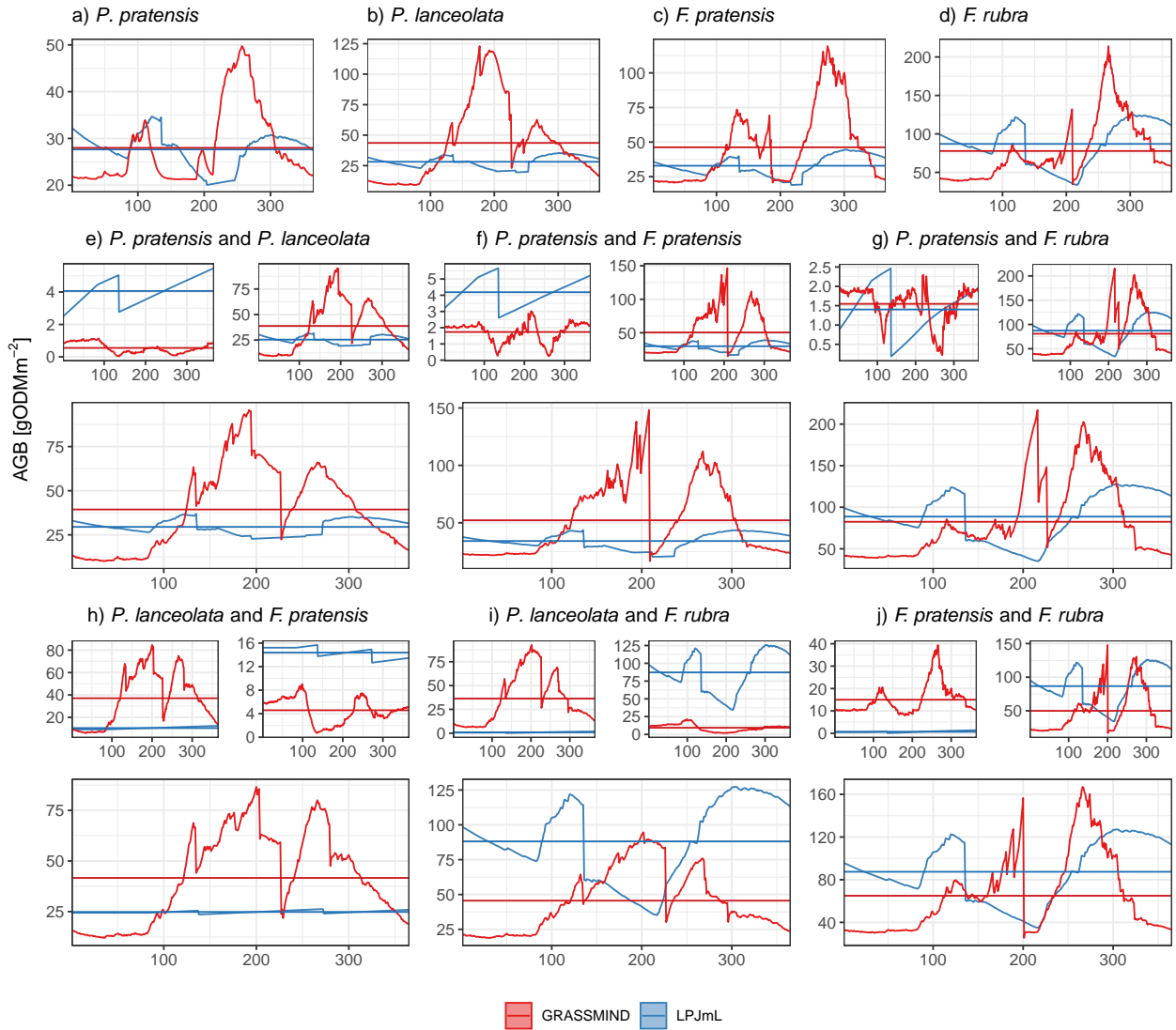


Figure A.21: AGB in  $\text{gDM m}^{-2}$  for ExtrD\_Mow for GRASSMIND (red) and LPJmL (blue) for the year with reduced precipitation (2003) for monocultures (a,b,c,d) and two-species mixtures (e,f,g,h,i,j). For mixtures species specific (top) and total AGB (bottom) are shown separately. Horizontal lines show the annual mean.

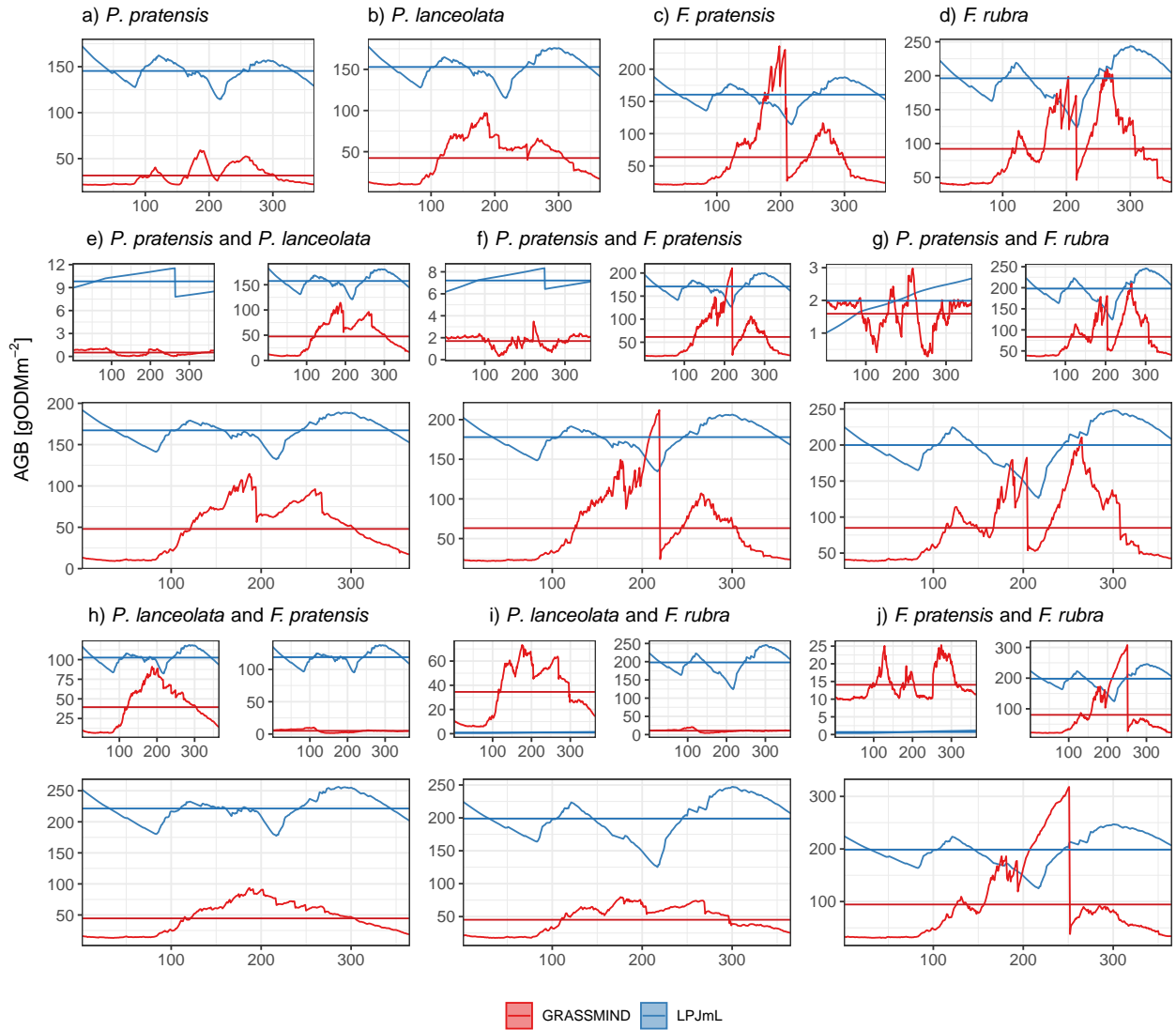


Figure A.22: AGB in  $\text{gDM m}^{-2}$  for ModD\_NoMow for GRASSMIND (red) and LPJmL (blue) for the year with reduced precipitation (2003) for monocultures (a,b,c,d) and two-species mixtures (e,f,g,h,i,j). For mixtures species specific (top) and total AGB (bottom) are shown separately. Horizontal lines show the annual mean.

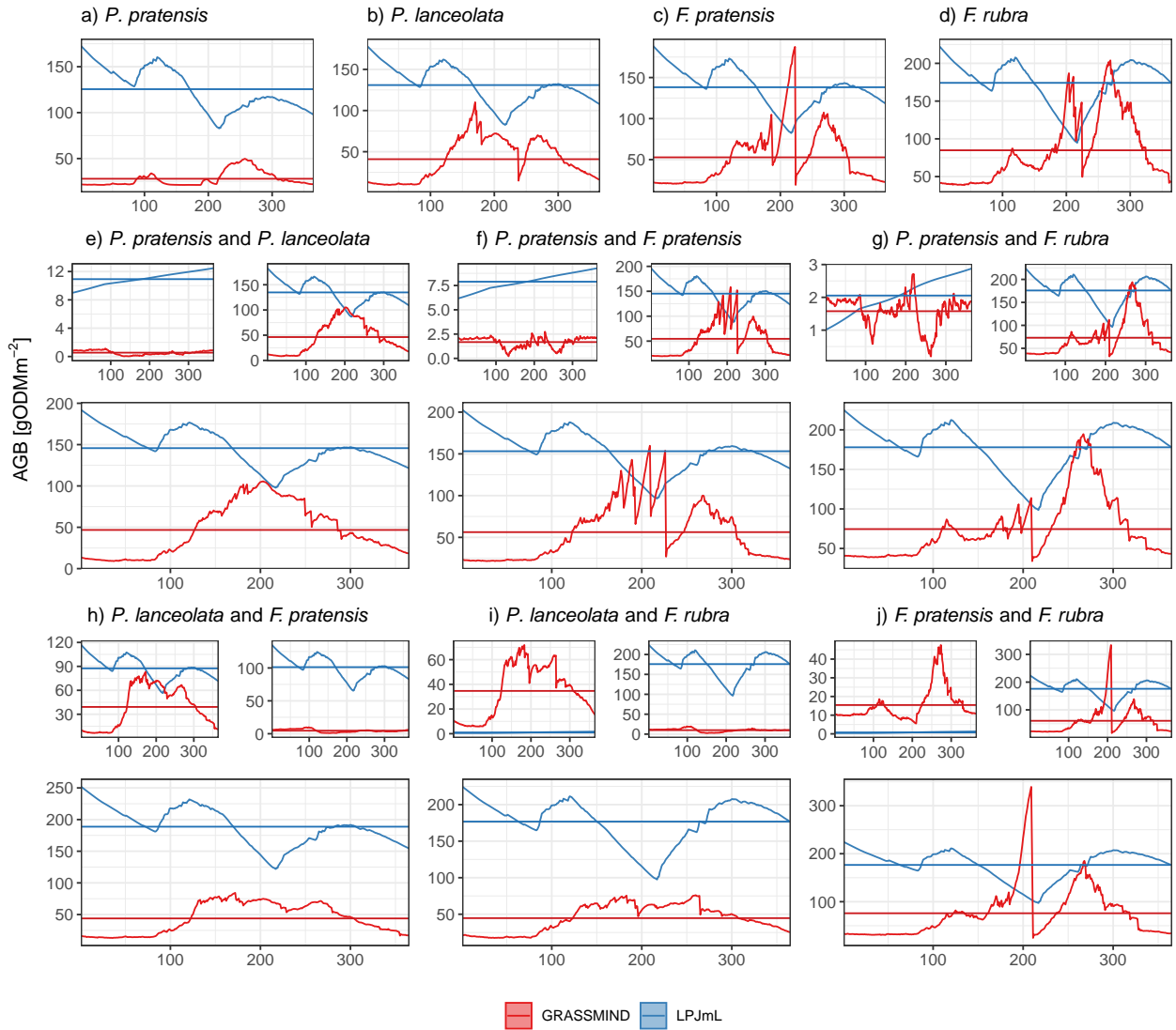


Figure A.23: AGB in  $\text{gDM m}^{-2}$  for ExtrD\_NoMow for GRASSMIND (red) and LPJmL (blue) for the year with reduced precipitation (2003) for monocultures (a,b,c,d) and two-species mixtures (e,f,g,h,i,j). For mixtures species specific (top) and total AGB (bottom) are shown separately. Horizontal lines show the annual mean.

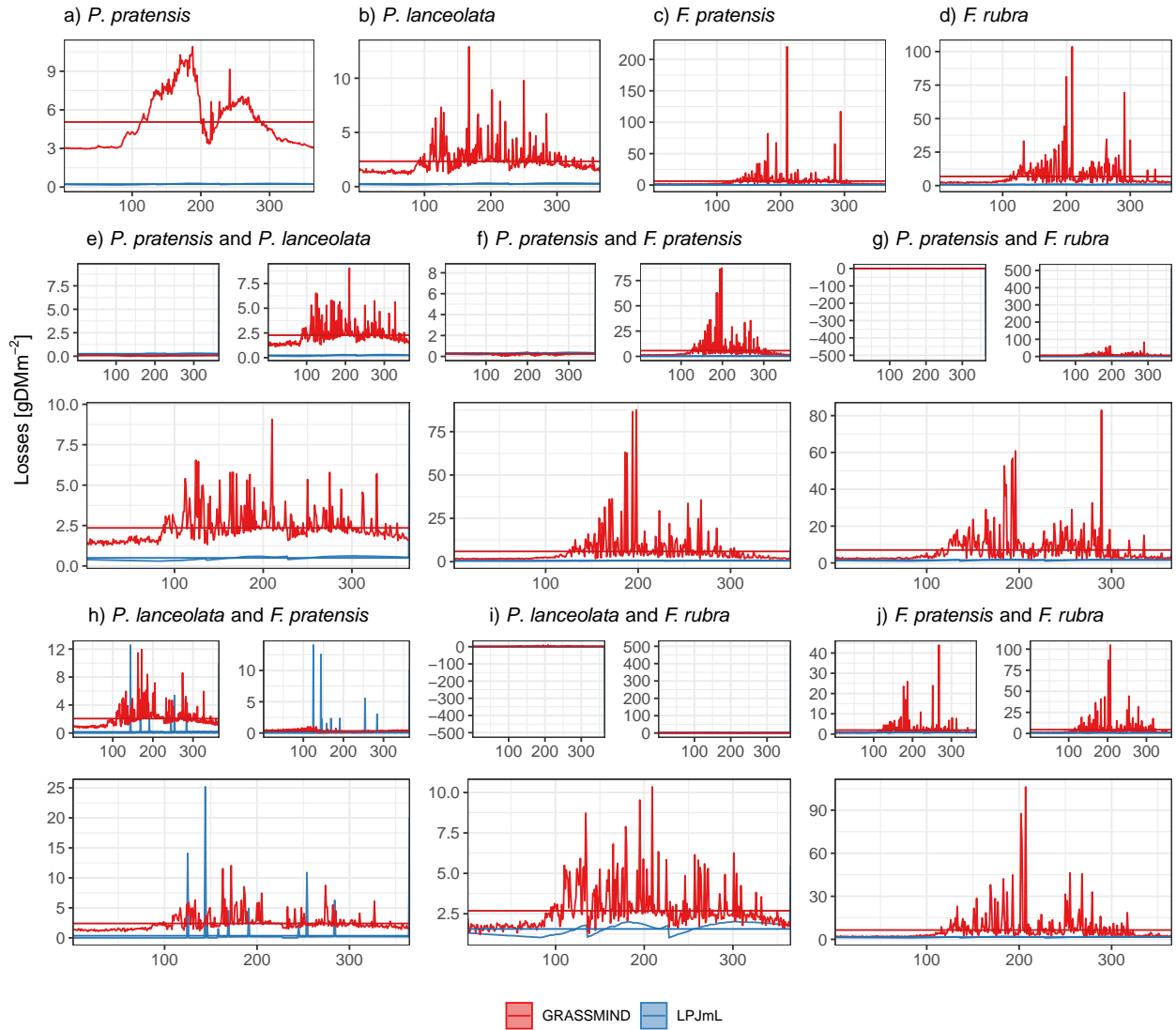


Figure A.24: Losses in  $\text{gDM m}^{-2}$  for Baseline\_Mow for GRASSMIND (red) and LPJmL (blue) for the year with reduced precipitation (2003) for monocultures (a,b,c,d) and two-species mixtures (e,f,g,h,i,j). For mixtures specie specific (top) and total losses (bottom) are shown separately. Horizontal lines show the annual mean.

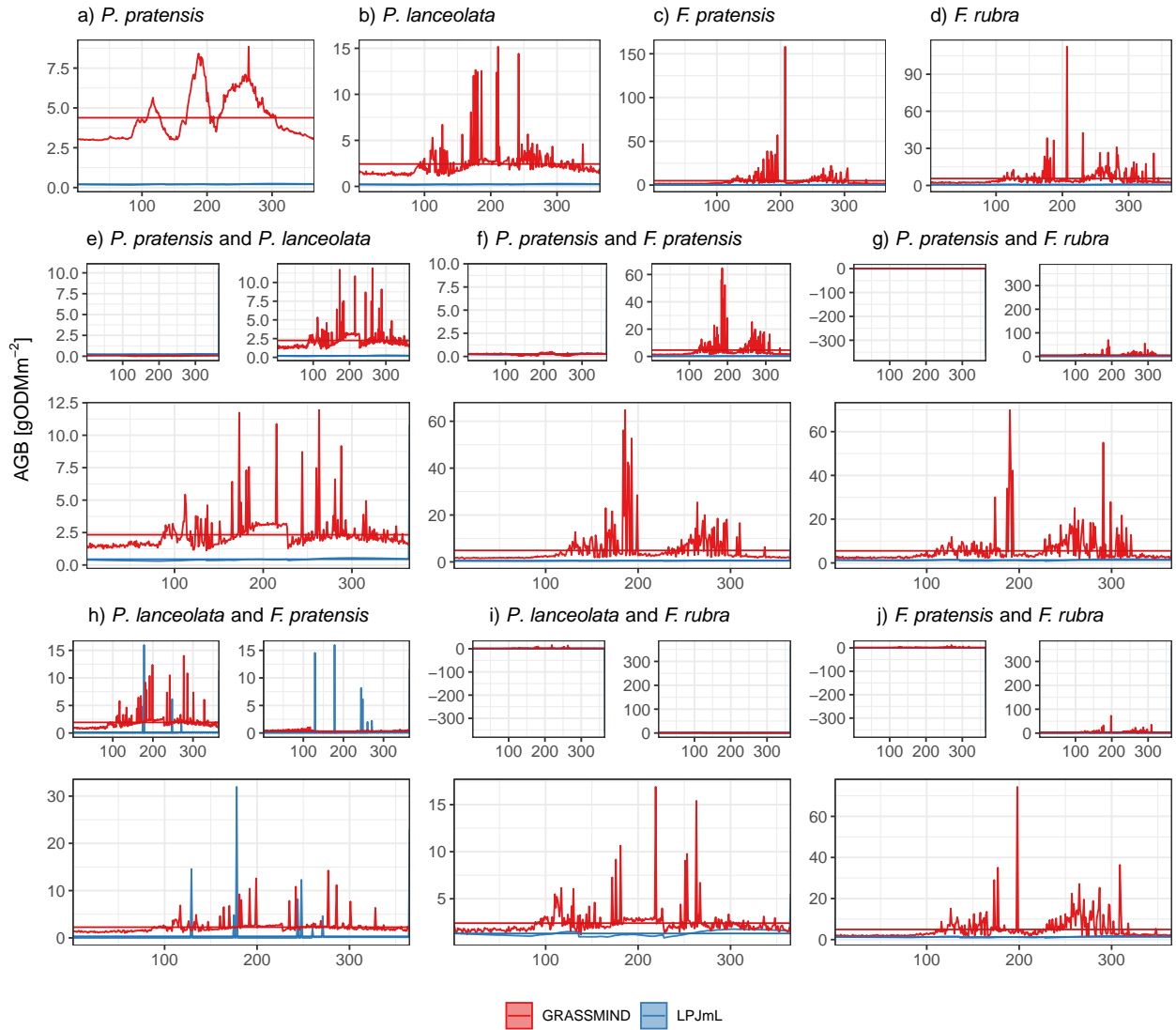


Figure A.25: Losses in  $\text{gDM m}^{-2}$  for ModD\_Mow for GRASSMIND (red) and LPJmL (blue) for the year with reduced precipitation (2003) for monocultures (a,b,c,d) and two-species mixtures (e,f,g,h,i,j). For mixtures specie specific (top) and total losses (bottom) are shown separately. Horizontal lines show the annual mean.

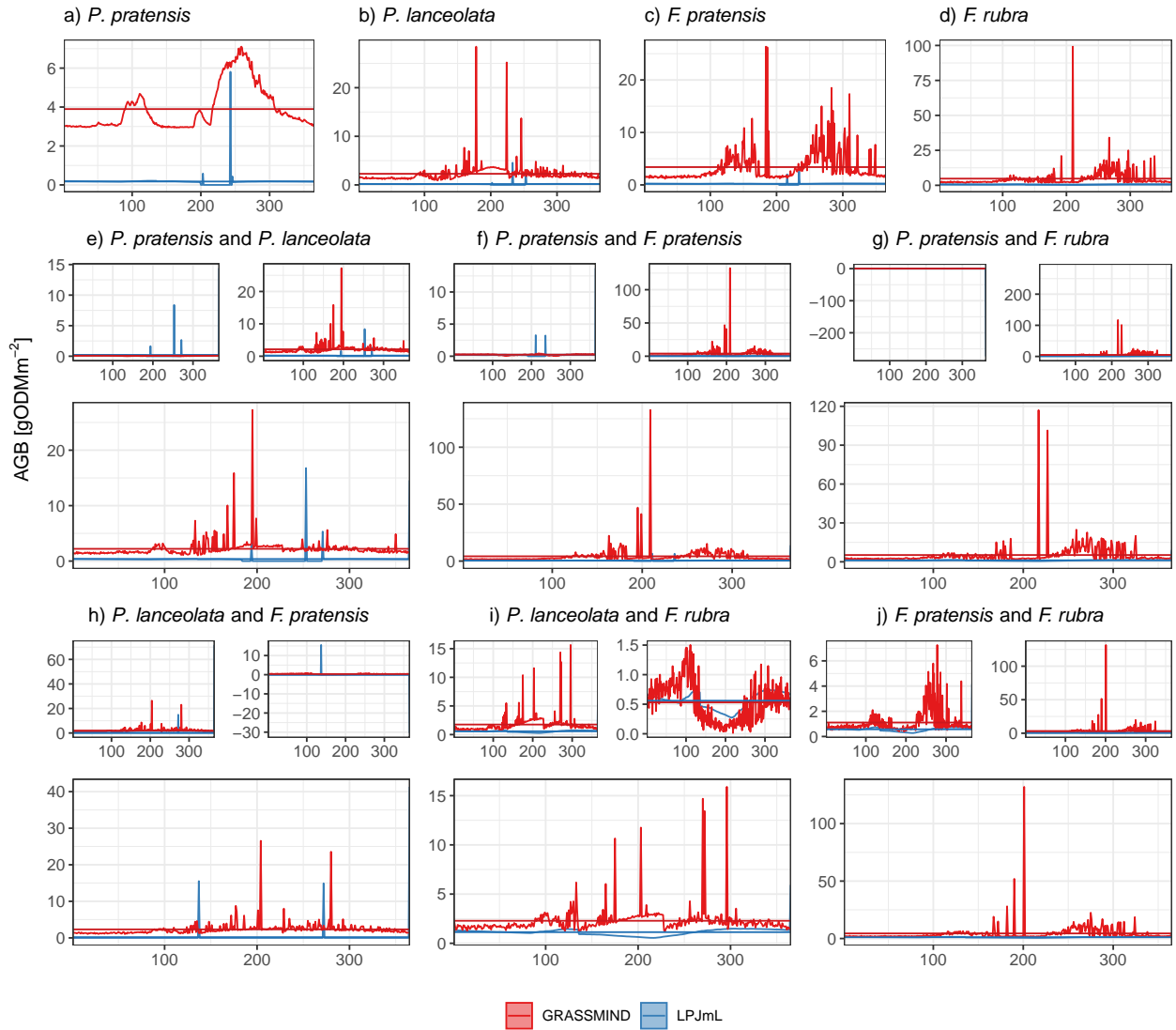


Figure A.26: Losses in  $\text{gDM m}^{-2}$  for ExtrD\_Mow for GRASSMIND (red) and LPJmL (blue) for the year with reduced precipitation (2003) for monocultures (a,b,c,d) and two-species mixtures (e,f,g,h,i,j). For mixtures specie specific (top) and total losses (bottom) are shown separately. Horizontal lines show the annual mean.

## A.7 Additional Figures ModD\_Mow and ExtrD\_Mow

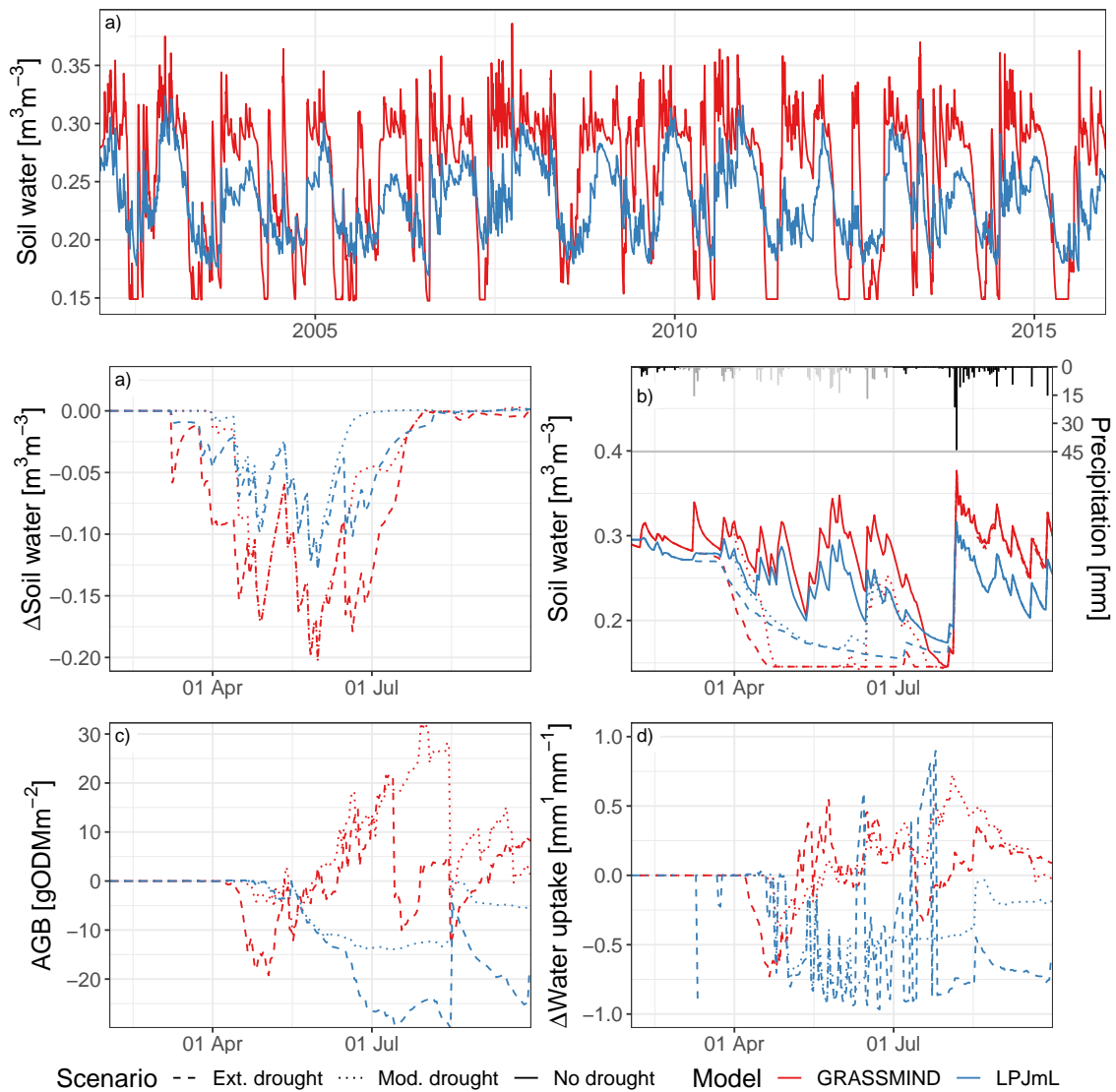


Figure A.27: Simulated fractional soil water content at the Jena Experiment site (a), relative changes of soil water content in  $\text{m}^3 \text{m}^{-3}$  (b), absolute changes of soil water content in  $\text{m}^3 \text{m}^{-3}$  as well as daily precipitation in mm with reduction for ModD (light grey) and ExtrD (light and dark grey) (c), absolute changes in AGB (d) in  $\text{gDM m}^{-2}$  and relative changes in water uptake (e)  $\text{mm mm}^{-1}$  caused by the moderate (dotted) and extreme (dashed) droughts for LPJmL (blue) and GRASSMIND (red). Simulation results of mixture of *P. pratensis* and *P. lanceolata* from LPJmL using observed weather data (a) and average climate (b-e).

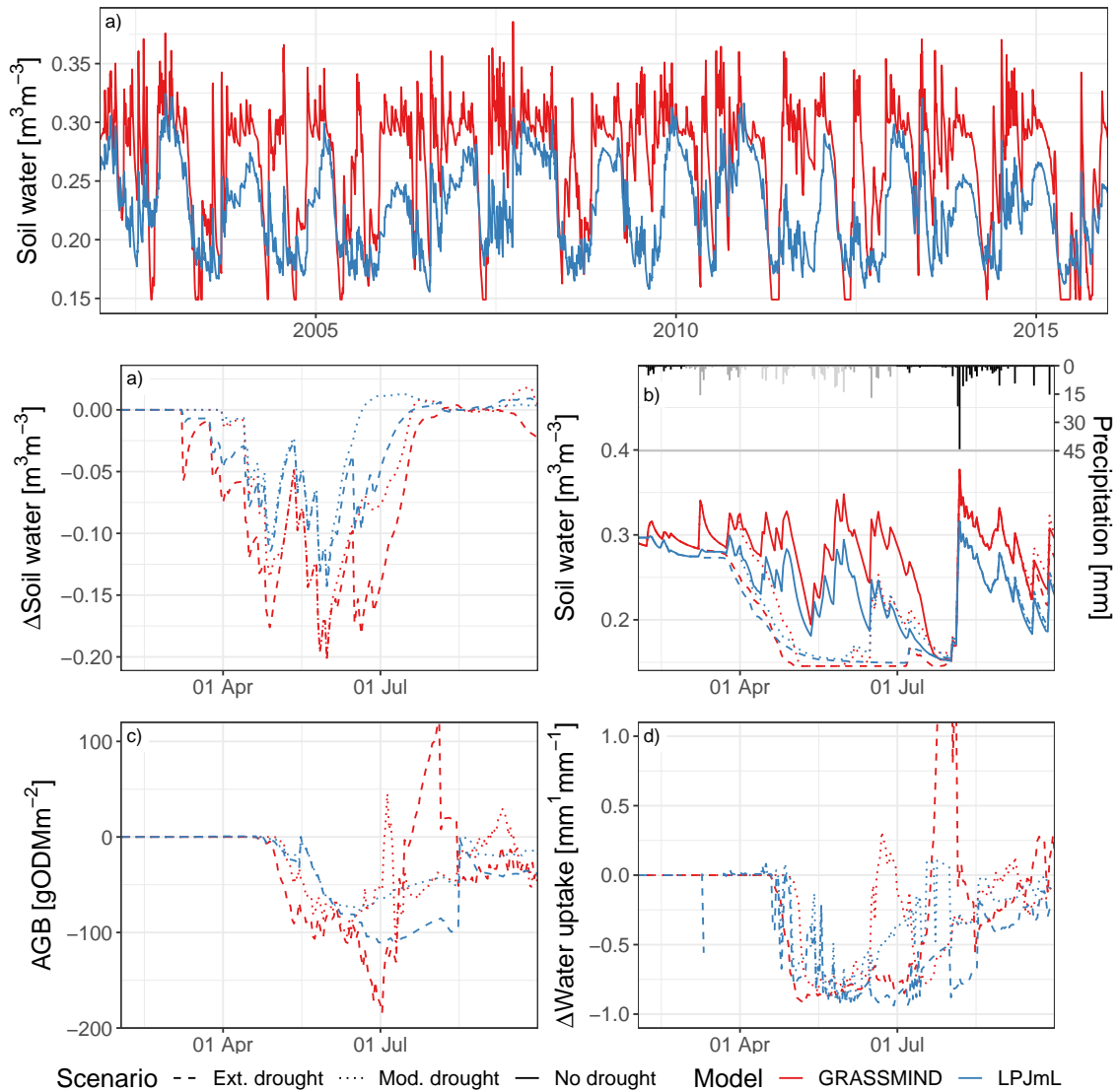


Figure A.28: Simulated fractional soil water content at the Jena Experiment site (a), relative changes of soil water content in  $\text{m}^3 \text{m}^{-3}$  (b), absolute changes of soil water content in  $\text{m}^3 \text{m}^{-3}$  as well as daily precipitation in mm with reduction for ModD (light grey) and ExtrD (light and dark grey) (c), absolute changes in AGB (d) in  $\text{gDM m}^{-2}$  and relative changes in water uptake (e)  $\text{mm mm}^{-1}$  caused by the moderate (dotted) and extreme (dashed) droughts for LPJmL (blue) and GRASSMIND (red). Simulation results of mixture of *P. pratensis* and *F. rubra* from LPJmL using observed weather data (a) and average climate (b-e).

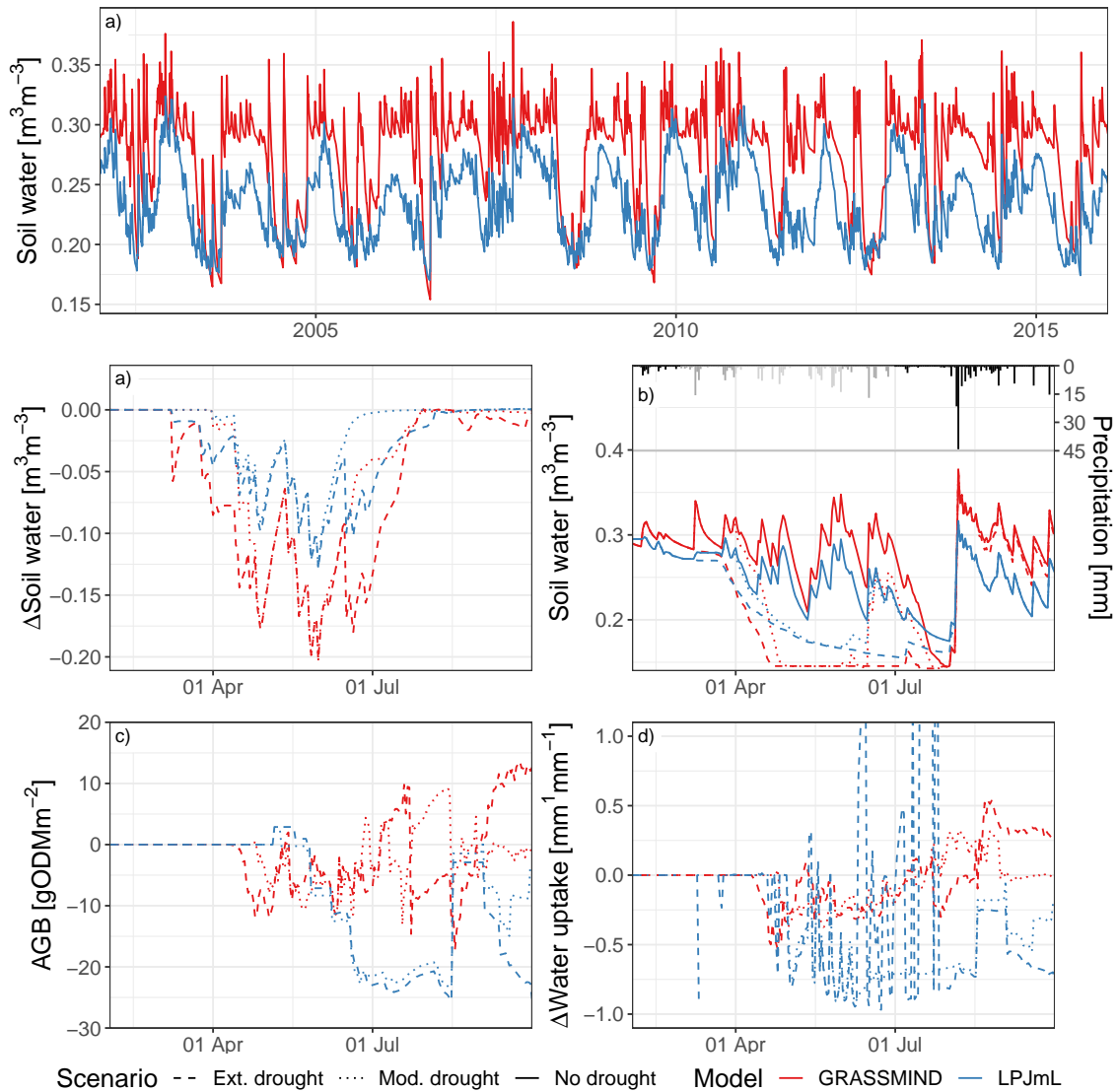


Figure A.29: Simulated fractional soil water content at the Jena Experiment site (a), relative changes of soil water content in  $\text{m}^3 \text{m}^{-3}$  (b), absolute changes of soil water content in  $\text{m}^3 \text{m}^{-3}$  as well as daily precipitation in mm with reduction for ModD (light grey) and ExtrD (light and dark grey) (c), absolute changes in AGB (d) in  $\text{gDM m}^{-2}$  and relative changes in water uptake (e)  $\text{mm mm}^{-1}$  caused by the moderate (dotted) and extreme (dashed) droughts for LPJmL (blue) and GRASSMIND (red). Simulation results of mixture of *P. lanceolata* and *F. pratensis* from LPJmL using observed weather data (a) and average climate (b-e).

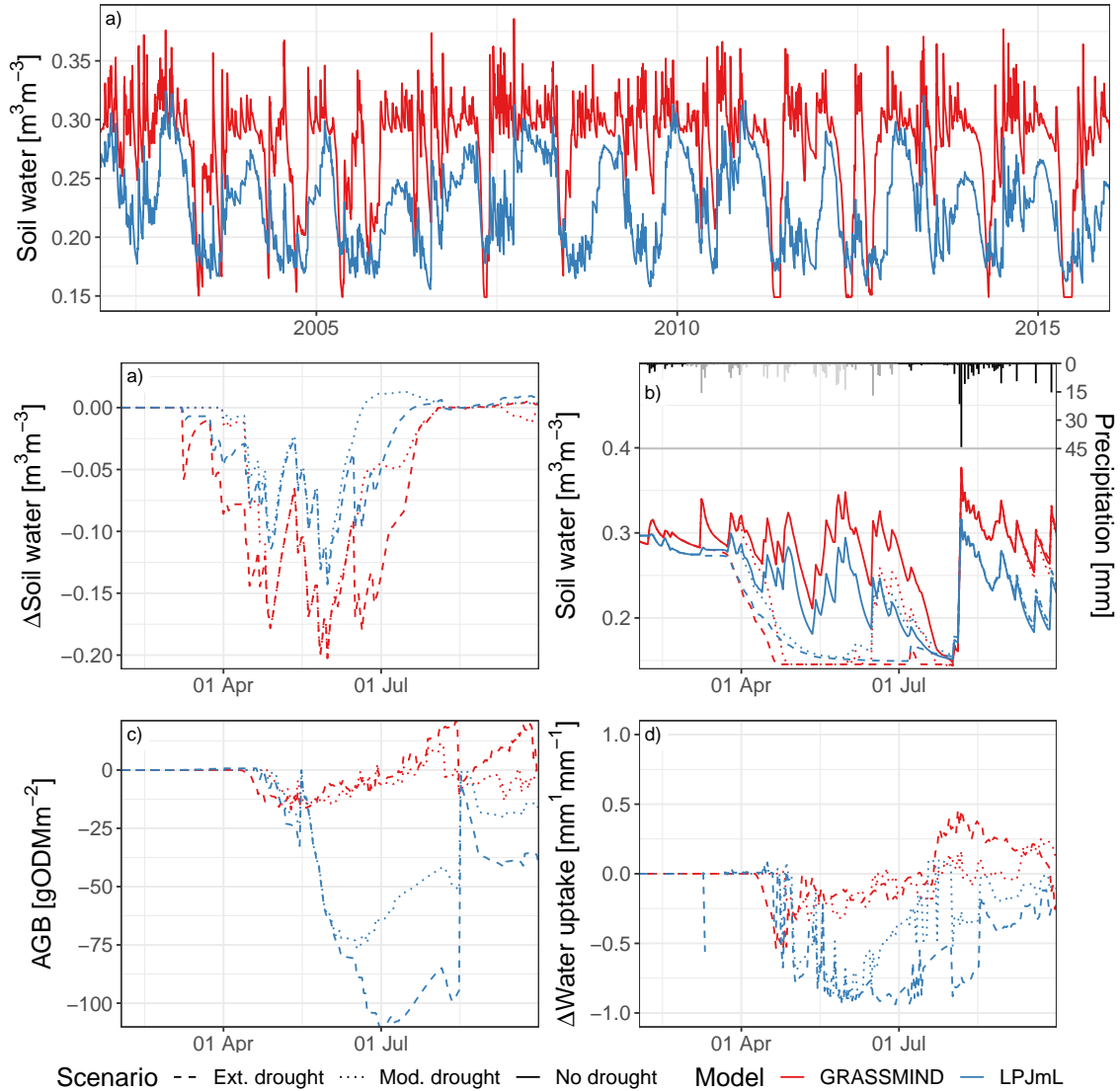


Figure A.30: Simulated fractional soil water content at the Jena Experiment site (a), relative changes of soil water content in  $\text{m}^3 \text{m}^{-3}$  (b), absolute changes of soil water content in  $\text{m}^3 \text{m}^{-3}$  as well as daily precipitation in mm with reduction for ModD (light grey) and ExtrD (light and dark grey) (c), absolute changes in AGB (d) in  $\text{gDM m}^{-2}$  and relative changes in water uptake (e)  $\text{mm mm}^{-1}$  caused by the moderate (dotted) and extreme (dashed) droughts for LPJmL (blue) and GRASSMIND (red). Simulation results of mixture of *P. lanceolata* and *F. rubra* from LPJmL using observed weather data (a) and average climate (b-e).

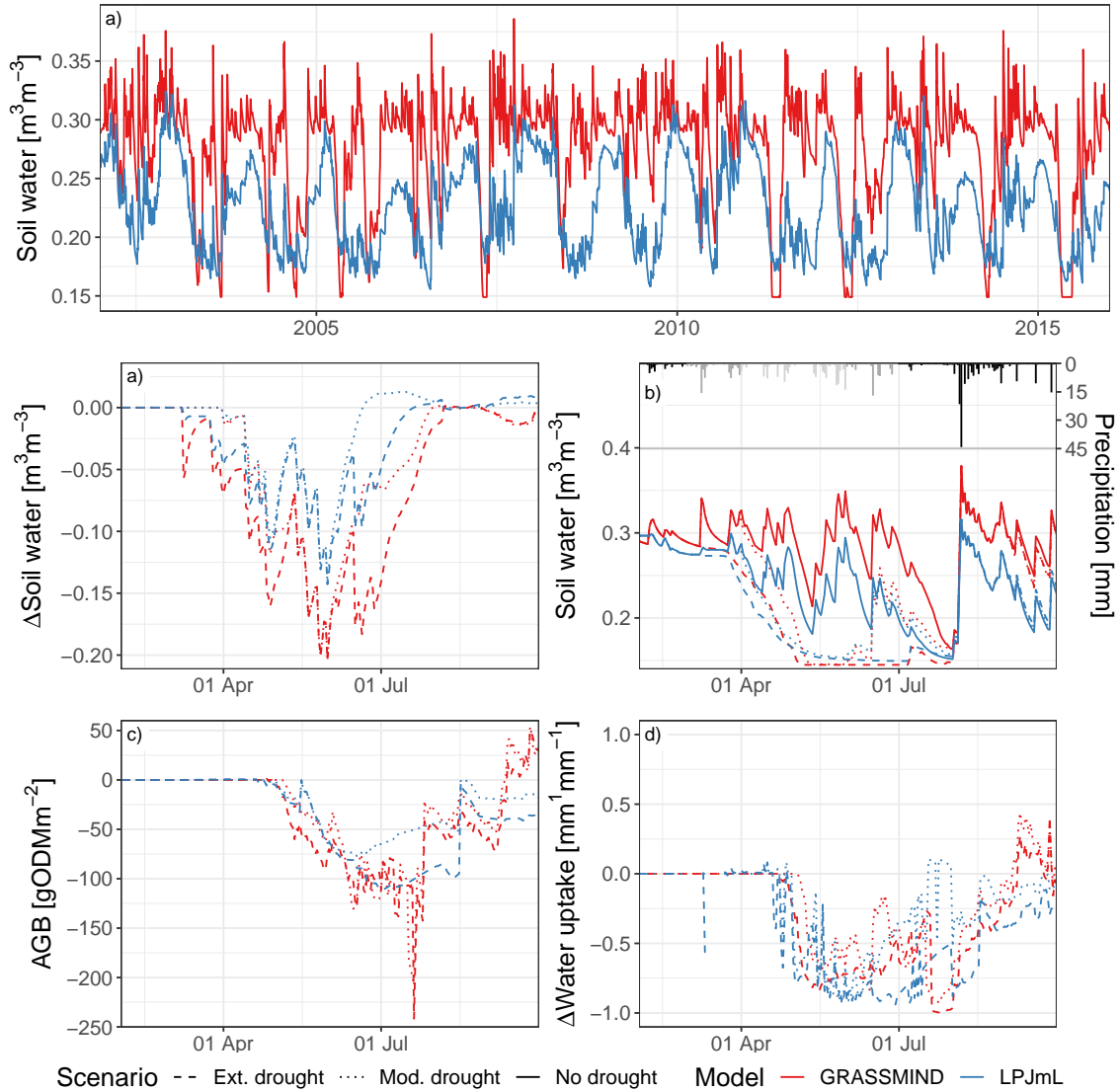


Figure A.31: Simulated fractional soil water content at the Jena Experiment site (a), relative changes of soil water content in  $\text{m}^3 \text{m}^{-3}$  (b), absolute changes of soil water content in  $\text{m}^3 \text{m}^{-3}$  as well as daily precipitation in mm with reduction for ModD (light grey) and ExtrD (light and dark grey) (c), absolute changes in AGB (d) in  $\text{gDM m}^{-2}$  and relative changes in water uptake (e)  $\text{mm mm}^{-1}$  caused by the moderate (dotted) and extreme (dashed) droughts for LPJmL (blue) and GRASSMIND (red). Simulation results of mixture of *F. pratensis* and *F. rubra* from LPJmL using observed weather data (a) and average climate (b-e).

## A.8 Additional Figures Baseline<sub>→</sub>, ModD<sub>→</sub> and ExtrD<sub>→</sub> Mow and NoMow

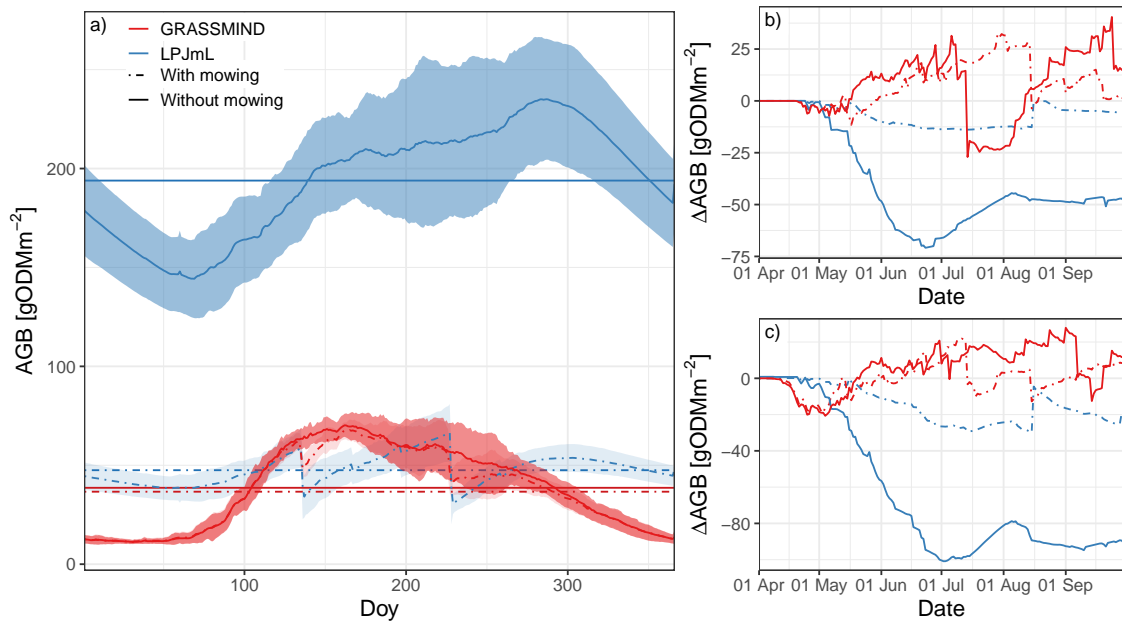


Figure A.32: Mean ( $\mu$ ) AGB in  $\text{gDM m}^{-2}$  (coloured lines  $\pm 1$  standard deviation) for GRASSMIND (red) and LPJmL (blue) for the sum of the two-species mixture of *P. pratensis* and *P. lanceolata* (a). Coloured ribbons show  $\mu \pm \sigma$ . Horizontal lines show overall mean for Baseline\_Mow (dot-dashed) and Baseline\_NoMow (solid). Difference between Baseline\_Mow and ModD\_Mow (dot-dashed) and ModD\_NoMow (solid, b) and ExtrD\_Mow (dot-dashed) and ExtrD\_NoMow (solid, c) between April and October of the drought year.

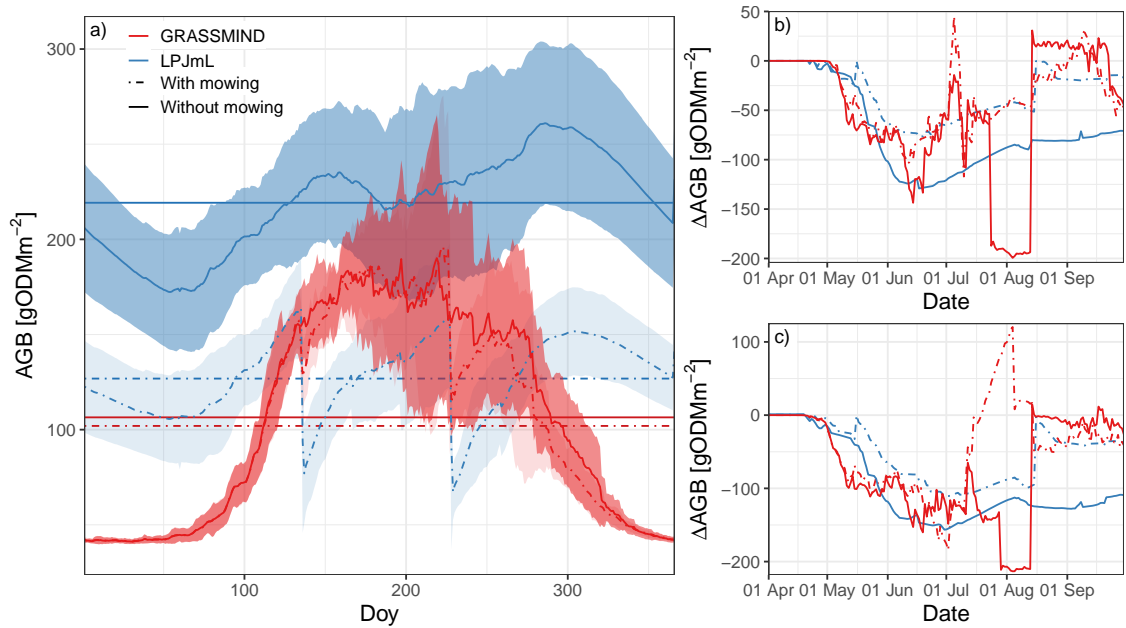


Figure A.33: Mean ( $\mu$ ) AGB in  $\text{gDM m}^{-2}$  (coloured lines  $\pm 1$  standard deviation) for GRASSMIND (red) and LPJmL (blue) for the sum of the two-species mixture of *P. pratensis* and *F. rubra* (a). Coloured ribbons show  $\mu \pm \sigma$ . Horizontal lines show overall mean for Baseline\_Mow (dot-dashed) and Baseline\_NoMow (solid). Difference between Baseline\_Mow and ModD\_Mow (dot-dashed) and ModD\_NoMow (solid, b) and ExtrD\_Mow (dot-dashed) and ExtrD\_NoMow (solid, c) between April and October of the drought year.

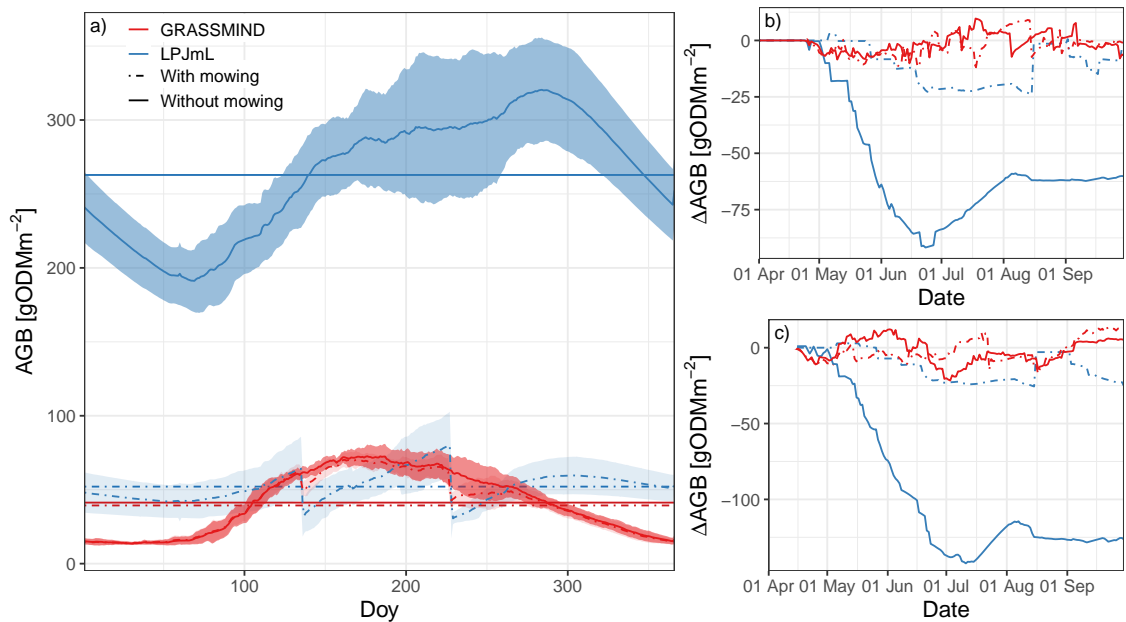


Figure A.34: Mean ( $\mu$ ) AGB in  $\text{gDM m}^{-2}$  (coloured lines  $\pm 1$  standard deviation) for GRASSMIND (red) and LPJmL (blue) for the sum of the two-species mixture of *P. lanceolata* and *F. pratensis* (a). Coloured ribbons show  $\mu \pm \sigma$ . Horizontal lines show overall mean for Baseline\_Mow (dot-dashed) and Baseline\_NoMow (solid). Difference between Baseline\_Mow and ModD\_Mow (dot-dashed) and ModD\_NoMow (solid, b) and ExtrD\_Mow (dot-dashed) and ExtrD\_NoMow (solid, c) between April and October of the drought year.

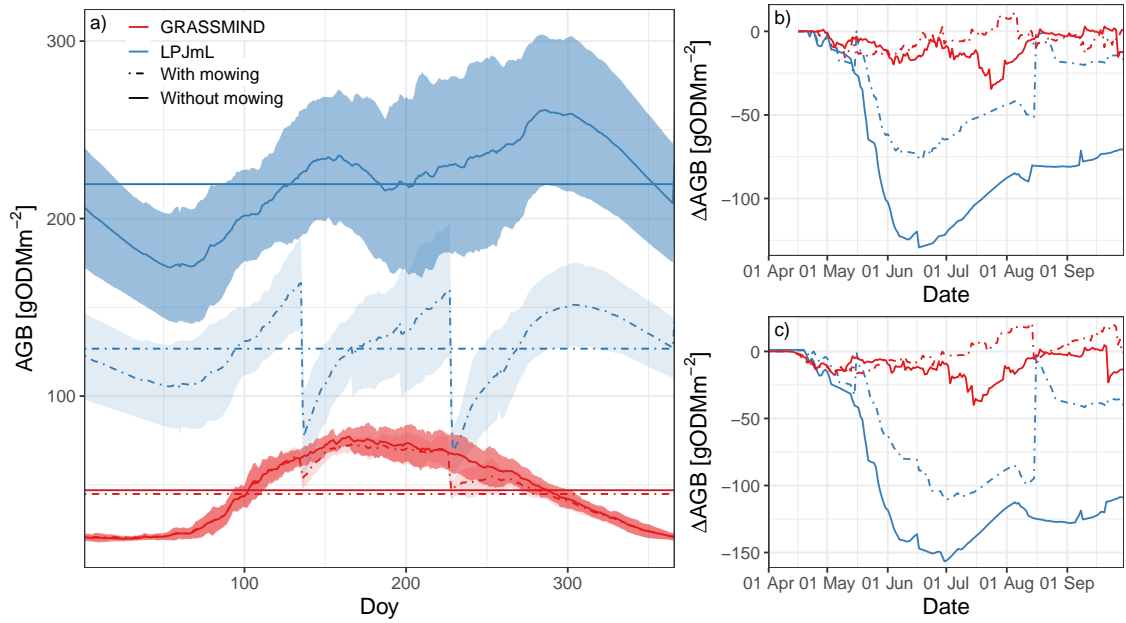


Figure A.35: Mean ( $\mu$ ) AGB in  $\text{gDM m}^{-2}$  (coloured lines  $\pm 1$  standard deviation) for GRASSMIND (red) and LPJmL (blue) for the sum of the two-species mixture of *P. lanceolata* and *F. rubra* (a). Coloured ribbons show  $\mu \pm \sigma$ . Horizontal lines show overall mean for Baseline\_Mow (dot-dashed) and Baseline\_NoMow (solid). Difference between Baseline\_Mow and ModD\_Mow (dot-dashed) and ModD\_NoMow (solid, b) and ExtrD\_Mow (dot-dashed) and ExtrD\_NoMow (solid, c) between April and October of the drought year.

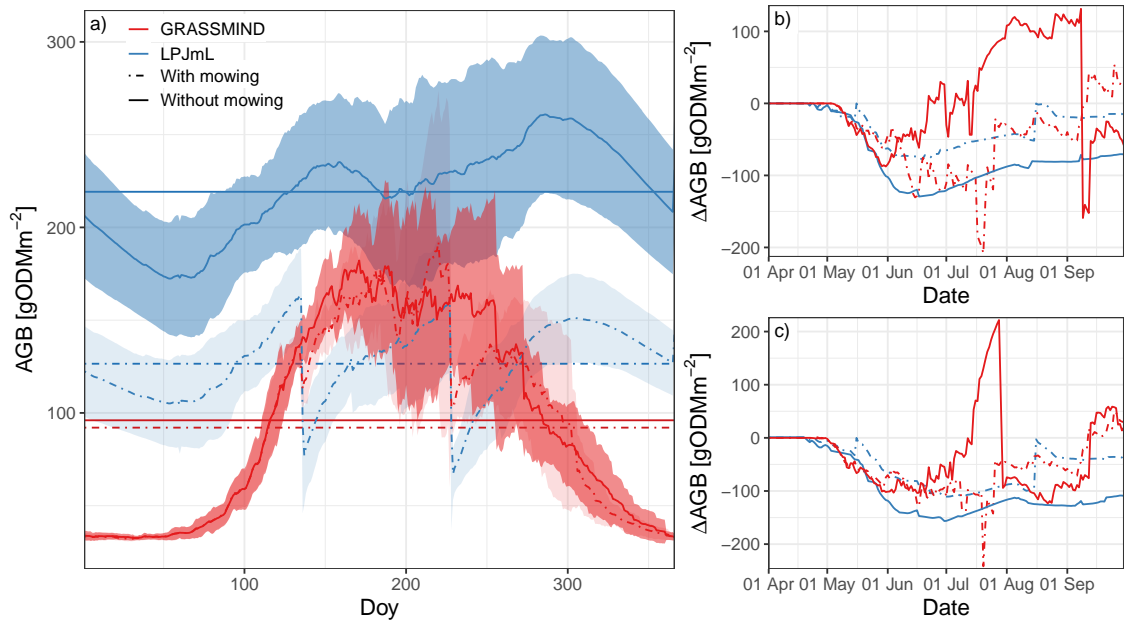


Figure A.36: Mean ( $\mu$ ) AGB in  $\text{gDM m}^{-2}$  (coloured lines  $\pm 1$  standard deviation) for GRASSMIND (red) and LPJmL (blue) for the sum of the two-species mixture of *F. pratensis* and *F. rubra* (a). Coloured ribbons show  $\mu \pm \sigma$ . Horizontal lines show overall mean for Baseline\_Mow (dot-dashed) and Baseline\_NoMow (solid). Difference between Baseline\_Mow and ModD\_Mow (dot-dashed) and ModD\_NoMow (solid, b) and ExtrD\_Mow (dot-dashed) and ExtrD\_NoMow (solid, c) between April and October of the drought year.

## A.9 References

- Abaye, A. O., ed. (2019). *Common Grasses, Legumes and Forbs of the Eastern United States*. Elsevier. ISBN: 978-0-12-813951-6. (Visited on 03/25/2021).
- Amthor, J. S. (1984). "The Role of Maintenance Respiration in Plant Growth". In: *Plant Cell Environ.* 7.8, pp. 561–569. ISSN: 1365-3040. DOI: 10.1111/1365-3040.ep11591833. (Visited on 03/25/2021).
- FH Jena (2020). *Ernst-Abbe Hochschule Jena, University of Applied Sciences, Climatological Monitoring Station*. <http://wetter.mb.eah-jena.de/station/>. (Visited on 12/22/2020).
- Forkel, M., M. Drüke, M. Thurner, W. Dorigo, S. Schaphoff, K. Thonicke, W. von Bloh, and N. Carvalhais (2019). "Constraining Modelled Global Vegetation Dynamics and Carbon Turnover Using Multiple Satellite Observations". In: *Sci Rep* 9.1, p. 18757. ISSN: 2045-2322. DOI: 10.1038/s41598-019-55187-7. (Visited on 06/29/2021).
- Forsythe, W. C., E. J. Rykiel, R. S. Stahl, H.-i. Wu, and R. M. Schoolfield (1995). "A Model Comparison for Daylength as a Function of Latitude and Day of Year". In: *Ecological Modelling* 80.1, pp. 87–95. ISSN: 0304-3800. DOI: 10.1016/0304-3800(94)00034-F. (Visited on 03/25/2021).
- Hesse, K., C. Roscher, J. Schumacher, and E.-D. Schulze (2007). "Establishment of Grassland Species in Monocultures: Different Strategies Lead to Success". In: *Oecologia* 152.3, pp. 435–447. ISSN: 1432-1939. DOI: 10.1007/s00442-007-0666-6. (Visited on 12/22/2020).
- Hetzer, J., A. Huth, and F. Taubert (2021). "The Importance of Plant Trait Variability in Grasslands: A Modelling Study". In: *Ecological Modelling* 453, p. 109606. ISSN: 0304-3800. DOI: 10.1016/j.ecolmodel.2021.109606. (Visited on 07/14/2021).
- Info Flora (2021). *Info Flora. The National Data and Information Centre on the Swiss Flora*. <https://www.infoflora.ch/de/flora/festuca-pratensis.html>. (Visited on 03/25/2021).
- Kreutziger, Y., J. Baade, G. Gleixner, M. Habekost, A. Hildebrandt, G. Schwichtenberg, S. Attinger, Y. Oelmann, W. Wilcke, R. Cortois, G. B. De Deyn, G. Luo, and S. T. Meyer (2018). *Collection of Data on Physical and Chemical Soil Properties in the Jena Experiment (Main Experiment)*. DOI: 10.1594/PANGAEA.885439. (Visited on 03/25/2021).
- Kühn, I. and S. Klotz (2002). "Systematik, Taxonomie und Nomenklatur". In: *BIOLFLOR - Eine Datenbank zu biologisch-ökologischen Merkmalen der Gefäßpflanzen in Deutschland*. Ed. by S. Klotz, I. Kühn, and W. Durka. Vol. 38. Schriftenreihe für Vegetationskunde. Bonn: Bundesamt für Naturschutz (BfN), pp. 41–46.
- Larcher, W. (1995). *Physiological Plant Ecology: Ecophysiology and Stress Physiology of Functional Groups*. 3rd ed. Berlin: Springer-Verlag. ISBN: 978-3-540-43516-7. (Visited on 03/25/2021).
- Lehmann, S. and A. Huth (2015). "Fast Calibration of a Dynamic Vegetation Model with Minimum Observation Data". In: *Ecological Modelling* 301, pp. 98–105. ISSN: 0304-3800. DOI: 10.1016/j.ecolmodel.2015.01.013. (Visited on 06/18/2020).
- McElreath, R. (2016). *Statistical Rethinking: A Bayesian Course with Examples in R and Stan*. Boca Raton FL: Chapman & Hall/CRC Press.
- MPI (2019). *Max-Planck-Institute for Biogeochemistry*. <https://www.bgc-jena.mpg.de/wetter/>. (Visited on 12/22/2020).
- R Core Team (2019). *A Language and Environment for Statistical Computing*. R Foundation for Statistical Computing, Vienna, Austria.
- Reich, P. B., M. B. Walters, and D. S. Ellsworth (1992). "Leaf Life-Span in Relation to Leaf, Plant, and Stand Characteristics among Diverse Ecosystems". In: *Ecol. Monogr.* 62.3, pp. 365–392. ISSN: 00129615. DOI: 10.2307/2937116. (Visited on 10/11/2018).
- Rolinski, S., C. Müller, J. Heinke, I. Weindl, A. Biewald, B. L. Bodirsky, A. Bondeau, E. R. Boons-Prins, A. F. Bouwman, P. A. Leffelaar, J. A. te Roller, S. Schaphoff, and K. Thonicke (2018). "Modeling Vegetation and Carbon Dynamics of Managed Grasslands at the Global Scale with LPJmL 3.6". In: *Geosci. Model Dev.* 11.1, pp. 429–451. ISSN: 1991-9603. DOI: 10.5194/gmd-11-429-2018. (Visited on 02/27/2018).
- Roscher, C., J. Schumacher, J. Baade, W. Wilcke, G. Gleixner, W. W. Weisser, B. Schmid, and E.-D. Schulze (2004). "The Role of Biodiversity for Element Cycling and Trophic Interactions: An Experimental Approach in a Grassland Community". In: *Basic Appl. Ecol.* 5.2, pp. 107–121. ISSN: 1439-1791. DOI: 10.1078/1439-1791-00216. (Visited on 02/06/2020).
- Schaphoff, S., W. von Bloh, A. Rammig, K. Thonicke, H. Biemans, M. Forkel, D. Gerten, J. Heinke, J. Jägermeyr, J. Knauer, F. Langerwisch, W. Lucht, C. Müller, S. Rolinski, and K. Waha (2018). "LPJmL4 – a Dynamic Global Vegetation Model with Managed Land – Part 1: Model Description". In: *Geosci. Model Dev.* 11.4, pp. 1343–1375. ISSN: 1991-959X. DOI: 10.5194/gmd-11-1343-2018. (Visited on 05/31/2023).
- Schenk, H. J. and R. B. Jackson (2002). "Rooting Depths, Lateral Root Spreads and below-Ground/above-Ground Allometries of Plants in Water-Limited Ecosystems". In: *J. Ecol.* 90.3, pp. 480–494. ISSN: 1365-2745. DOI: 10.1046/j.1365-2745.2002.00682.x. (Visited on 06/07/2018).
- Schmid, J. S., A. Huth, and F. Taubert (2021). "Influences of Traits and Processes on Productivity and Functional Composition in Grasslands: A Modeling Study". In: *Ecological Modelling* 440, p. 109395. ISSN: 0304-3800. DOI: 10.1016/j.ecolmodel.2020.109395. (Visited on 02/13/2023).
- Sitch, S., B. Smith, I. C. Prentice, A. Arneth, A. Bondeau, W. Cramer, J. O. Kaplan, S. Levis, W. Lucht, M. T. Sykes, K. Thonicke, and S. Venevsky (2003). "Evaluation of Ecosystem Dynamics, Plant Geography and Terrestrial Carbon Cycling in the LPJ Dynamic Global Vegetation Model". In: *Glob. Change Biol.* 9.2, pp. 161–185. ISSN: 1365-2486. DOI: 10.1046/j.1365-2486.2003.00569.x. (Visited on 03/03/2018).
- Taubert, F., J. Hetzer, J. S. Schmid, and A. Huth (2020a). "The Role of Species Traits for Grassland Productivity". In: *Ecosphere* 11.7, e03205. ISSN: 2150-8925. DOI: 10.1002/ecs2.3205. (Visited on 02/09/2023).

## Appendix A

- Taubert, F., J. Hetzer, J. S. Schmid, and A. Huth (2020b). “Confronting an Individual-Based Simulation Model with Empirical Community Patterns of Grasslands”. In: *PLOS ONE* 15.7, e0236546. ISSN: 1932-6203. DOI: 10.1371/journal.pone.0236546. (Visited on 02/09/2023).
- Thornley, J. H. M. and J. France (2007). *Mathematical Models in Agriculture: Quantitative Methods for the Plant, Animal and Ecological Sciences*. 2nd ed. Wallingford: CAB International. ISBN: 978-0-85199-010-1.
- Turc, L. (1961). “Water Requirements Assessment of Irrigation, Potential Evapotranspiration: Simplified and Updated Climatic Formula”. In: *Ann. Agron.* 12, pp. 13–49.
- Van Oijen, M., J. Rougier, and R. Smith (2005). “Bayesian Calibration of Process-Based Forest Models: Bridging the Gap between Models and Data”. In: *Tree Physiol* 25.7, pp. 915–927. ISSN: 0829-318X. DOI: 10.1093/treephys/25.7.915. (Visited on 02/04/2020).
- Weigelt, A., E. Marquard, V. M. Temperton, C. Roscher, C. Scherber, P. N. Mwangi, S. Felten, N. Buchmann, B. Schmid, E.-D. Schulze, and W. W. Weisser (2010). “The Jena Experiment: Six Years of Data from a Grassland Biodiversity Experiment”. In: *Ecology* 91.3, pp. 930–931. ISSN: 1939-9170. DOI: 10.1890/09-0863.1. (Visited on 12/22/2020).
- Weisser, W. W., C. Roscher, S. T. Meyer, A. Ebeling, G. Luo, E. Allan, H. Beßler, R. L. Barnard, N. Buchmann, F. Buscot, C. Engels, C. Fischer, M. Fischer, A. Gessler, G. Gleixner, S. Halle, A. Hildebrandt, H. Hillebrand, H. de Kroon, M. Lange, S. Leimer, X. Le Roux, A. Milcu, L. Mommer, P. A. Niklaus, Y. Oelmann, R. Proulx, J. Roy, C. Scherber, M. Scherer-Lorenzen, S. Scheu, T. Tschardtke, M. Wachendorf, C. Wagg, A. Weigelt, W. Wilcke, C. Wirth, E.-D. Schulze, B. Schmid, and N. Eisenhauer (2017). “Biodiversity Effects on Ecosystem Functioning in a 15-Year Grassland Experiment: Patterns, Mechanisms, and Open Questions”. In: *Basic Appl. Ecol. Biodiversity Effects on Ecosystem Functioning: The Jena Experiment* 23, pp. 1–73. ISSN: 1439-1791. DOI: 10.1016/j.baae.2017.06.002. (Visited on 01/27/2020).
- Weryszko-Chmielewska, E., A. Matysik-Woźniak, A. Sulborska, and R. Rejdak (2012). “Commercially Important Properties of Plants of the Genus *Plantago*”. In: *Acta Agrobot.* 65.1, pp. 11–20. ISSN: 0065-0951. DOI: 10.5586/aa.2012.038. (Visited on 03/25/2021).
- Zaehle, S., S. Sitch, B. Smith, and F. Hatterman (2005). “Effects of Parameter Uncertainties on the Modeling of Terrestrial Biosphere Dynamics”. In: *Glob. Biogeochem. Cycles* 19.3. ISSN: 1944-9224. DOI: 10.1029/2004GB002395. (Visited on 07/02/2021).
- Zambrano-Bigiarini [aut, M., cre, and cph (2020). *hydroGOF: Goodness-of-Fit Functions for Comparison of Simulated and Observed Hydrological Time Series*. (Visited on 03/25/2021).

# Appendix B

Appendix B contains the supplementary information for Chapter 3 Connecting competitor, stress-tolerator and ruderal (CSR) theory and Lund Potsdam Jena managed Land 5 (LPJmL 5) to assess the role of environmental conditions, management and functional diversity for grassland ecosystem functions.

## B.1 Model description

We provided a qualitative description of the new model development in the main text (Sect. 3.2.3), for which we supplement the underlying equations and additional minor developments here.

### Water uptake

To make resource uptake of different resources dependent on different plant traits, we adapted the water uptake routine of the LPJmL model. Available soil water is now distributed between PFTs dependent on their root carbon ( $C_{\text{root,PFT}}$ ) and a PFT-specific parameter ( $k_{\text{root,PFT}}$ ), which is used as a substitute for information on root functional traits (e.g. branching of the root network, amount of fine roots, number of root tips). These traits cannot directly be incorporated, because either the simplified representation of belowground plant organs hinders their representation or data are not sufficiently available.

$$f_{\text{root,PFT}} = w_{\text{PFT}} \cdot (1 - \exp(-k_{\text{root,PFT}} \cdot C_{\text{root,PFT}})) \quad (\text{B.1})$$

Equations (B.1)–(B.3) describe an exponential function which follows the approach used for the calculation of the foliage projective cover (FPC; see Schaphoff et al., 2018), which was used to distribute water between PFTs in previous model versions.

$$w_{\text{PFT}} = \left( 1 - \exp(-k_{\text{root,PFT}} \cdot \sum_i^{\text{Number of PFTs}} C_{\text{root},i}) \right) \cdot f_{\text{root,sum}}^{-1} \quad (\text{B.2})$$

Each PFT's access to plant-available soil water ( $f_{\text{root,PFT}}$ ) is weighted using Eq. (B.2). Here  $w_{\text{PFT}}$  is calculated as the fraction of the respective PFT's potential access to the plant-available soil water if the entire community root carbon would belong to it and the sum of all PFTs' access to plant-available soil water if now weighting would be applied (Eq. B.3).

$$f_{\text{root,sum}} = \sum_i^{\text{Number of PFTs}} 1 - \exp(-k_{\text{root},i} \cdot C_{\text{root},i}) \quad (\text{B.3})$$

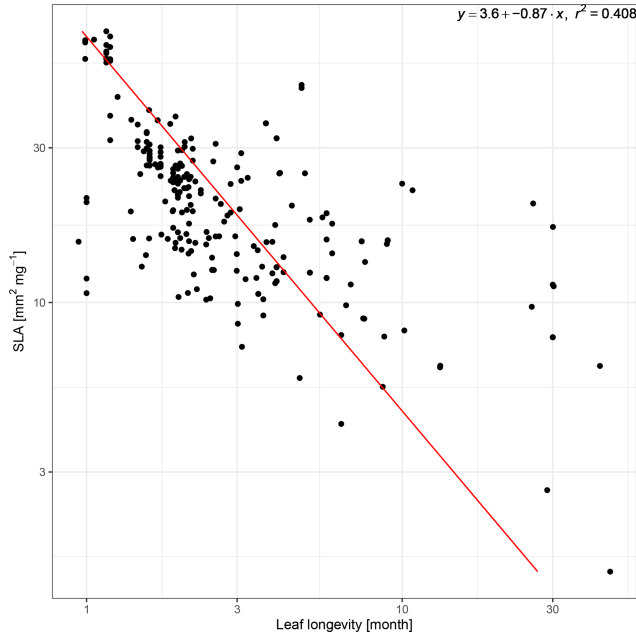


Figure B.1: Linear regression of log SLA and log LL using trait data for herbaceous species from the TRY database.

### B.1.1 The leaf economic spectrum

To incorporate the trade-offs associated with the LES, we implemented a power law relationship between SLA and leaf longevity (LL) described by Eq. (B.4)

$$LL = a \cdot SLA^b \cdot 12^{-1}, \quad (\text{B.4})$$

where  $a = 36.3753$  and  $b = -0.85384$ . Parameters  $a$  and  $b$  were derived from a regression (Fig. B.1) using trait data for SLA and LL retrieved from the TRY database (Boenisch and Kattge, 2018; Kattge et al., 2011). A detailed listing of the data sets used is provided in Table B.1 in the Supplement.

The leaf turnover rate is calculated as the inverse of the leaf longevity ( $\tau_{\text{leaf}} = 1/LL$ ) and is linearly related to root turnover ( $\tau_{\text{root}} = k \cdot \tau_{\text{leaf}}$  with  $k = 2$ ) assuming that the LES and the conservation gradient (Bergmann et al., 2020) of the root economic space are aligned (Weigelt et al., 2021). Plant biomass is transferred to the litter pools each day only if one of two conditions is met: under grazing, we assume that, depending on the stocking density, leaf tissue is grazed before it becomes senescent, and we define a threshold ( $\xi_{\text{leaf}} = 5 \text{ gC m}^{-2}$ ) for leaf biomass below which no senescent tissue for turnover is available; for mowing, we assume that senescent leaf biomass has to build up again after a mowing event, and we define a threshold for the leaf-to-root mass ratio ( $\xi_{\text{lmform}} = 0.7 \cdot \text{lmform}_{\text{opt}}$ ) beyond which senescent tissue is built up again.

### B.1.2 Reproduction and mortality

To improve the representation of different reproduction strategies and lifecycles, we adapted the establishment and mortality routine of the model. Both establishment and mortality are executed daily. In the new establishment routine, the number of average individuals ( $n_{ind}$ ) and the carbon ( $C_{ind,pool}$ ) and nitrogen ( $N_{ind,pool}$ ) pools of the leaves and roots for the average individuals are increased following Eqs. (B.5)–(B.7).

$$\Delta n_{ind,PFT} = k_{est,PFT} \cdot 365^{-2} \cdot (1 - \exp(-5 \cdot (1 - FPC_{sum}))) \cdot (1 - FPC_{sum}) \cdot \left( k_{est,PFT} \cdot \left( \sum_i^{\text{Number of PFTs}} k_{est,i} \right)^{-1} \right), \quad (B.5)$$

$$\Delta C_{ind,PFT} = (C_{seedling,leaf,PFT} + C_{seedling,root,PFT}) \cdot \Delta n_{ind,PFT}, \quad (B.6)$$

$$\Delta N_{ind,PFT} = \Delta C_{ind,PFT} \cdot NC_{ratio,leaf,PFT}. \quad (B.7)$$

Here,  $k_{est}$  is the PFT-specific establishment rate,  $FPC_{sum} = \sum_i^{\text{Number of PFTs}} FPC_i$  is the sum of the FPC of all PFTs,  $C_{seedling,pool}$  is the PFT-specific leaf and root pool size of a seedling and  $NC_{ratio,leaf,PFT}$  is the PFT-specific nitrogen-to-carbon ratio. The new individual properties are calculated following Eqs. (B.8) and (B.9).

$$C_{ind,pool,PFT} = (C_{ind,pool,PFT} \cdot n_{ind,PFT} + C_{seedling,pool,PFT} \cdot \Delta n_{ind,PFT}) \cdot (n_{ind,PFT} \cdot \Delta n_{ind,PFT})^{-1}, \quad (B.8)$$

$$N_{ind,pool,PFT} = (N_{ind,pool,PFT} \cdot n_{ind,PFT} + C_{seedling,pool,PFT} \cdot NC_{ratio,pool,PFT} \cdot \Delta n_{ind,PFT}) \cdot (n_{ind,PFT} \cdot \Delta n_{ind,PFT})^{-1}. \quad (B.9)$$

Mortality was implemented as an age mortality using the concept of growth efficiencies (Waring, 1983; Waring and Schlesinger, 1985) using Eq. (B.10)

$$mort_{PFT} = mort_{max,PFT} \cdot 365^{-1} \cdot (1 + k_{mort} \cdot \Delta bm \cdot C_{ind,leaf,PFT}^{-1} \cdot SLA_{PFT}^{-1})^{-1}, \quad (B.10)$$

with

$$\Delta bm = C_{inc,PFT} \cdot n_{ind,PFT}^{-1} - C_{turn,PFT}, \quad (B.11)$$

where  $C_{turn,PFT}$  is the amount of carbon that was transferred to the litter pool since the last allocation, and  $C_{inc,PFT}$  is the biomass increment from photosynthesis since the last allocation. The growth efficiency  $\Delta bm \cdot C_{ind,leaf,PFT}^{-1}$  is the ratio of the net carbon change and the carbon stock of the leaves, which is lower for old plants. The SLA influences the maximum age of the different strategies assuming that plants with a low SLA and faster metabolism reach a lower age compared to high SLA plants. The number of

average individuals is decreased following Eq. (B.12).

$$n_{\text{ind,PFT}} = n_{\text{ind,PFT}} \cdot (1 - \text{mort}_{\text{PFT}}) \quad (\text{B.12})$$

In grasslands with a high growth efficiency and frequent defoliation, establishment may lead to a continuous increase of the number of average individuals. To avoid numerical errors that could result from this, we prohibit the number of average individuals to exceed  $250 \text{ Ind. m}^{-2}$ .

### B.1.3 Biological nitrogen fixation

Symbiotic biological nitrogen fixation (BNF) is an important source, especially in unfertilised grassland systems. We implemented an approach adapted from published models of grain legumes (e.g. LPJ-GUESS, CROPGRO, EPIC, APSIM; see Liu et al., 2011; Ma et al., 2022), which considers the potential N fixation rate ( $N_{\text{fix,pot}}$ ), the soil temperature ( $f_T$ ) and the soil water ( $f_W$ ) status. The consideration of the growth stage had to be omitted, because LPJmL represents herbaceous vegetation using only leaves and roots, not allowing for a determination of growth stages. The nitrogen fixation rate  $N_{\text{fix}}$  is calculated using Eq. (B.13).

$$N_{\text{fix}} = N_{\text{fix,pot}} \cdot f_T \cdot f_W, \quad (\text{B.13})$$

with  $N_{\text{fix,pot}} = 0.1 \text{ gN m}^{-2} \text{ d}^{-1}$  (Yu and Zhuang, 2020). The soil temperature limitation is modelled linearly outside the optimal temperature range (Eq. B.14):

$$f_T = \begin{cases} 0, & \text{if } T_{\text{soil}} < T_{\text{min}} \text{ or } T_{\text{soil}} > T_{\text{max}} \\ \frac{T_{\text{soil}} - T_{\text{min}}}{T_{\text{opt,low}} - T_{\text{min}}}, & \text{if } T_{\text{min}} \leq T_{\text{soil}} < T_{\text{opt,low}} \\ 1, & \text{if } T_{\text{opt,low}} \leq T_{\text{soil}} \leq T_{\text{opt,high}} \\ \frac{T_{\text{max}} - T_{\text{soil}}}{T_{\text{max}} - T_{\text{opt,high}}}, & \text{if } T_{\text{opt,high}} < T_{\text{soil}} \leq T_{\text{max}} \end{cases} \quad (\text{B.14})$$

with  $T_{\text{min}} = 0.5$ ,  $T_{\text{opt,low}} = 18.0$ ,  $T_{\text{opt,high}} = 35.0$  and  $T_{\text{max}} = 45.0$  (Yu and Zhuang, 2020). The soil water limitation is linearly dependent on the relative soil water content (SWC) (Eq. B.15):

$$f_W = \begin{cases} 0, & \text{if } \text{SWC} \leq \text{SWC}_{\text{min}} \\ \varphi_1 + \text{SWC} \cdot \varphi_2, & \text{if } \text{SWC}_{\text{low}} < \text{SWC} < \text{SWC}_{\text{high}} \\ 1, & \text{if } \text{SWC} \geq \text{SWC}_{\text{high}} \end{cases} \quad (\text{B.15})$$

with  $\text{SWC}_{\text{low}} = 0$ ,  $\text{SWC}_{\text{high}} = 0.5$ ,  $\varphi_1 = 0$  and  $\varphi_2 = 2.0$  (Yu and Zhuang, 2020). BNF only happens if the nitrogen uptake from other sources is insufficient and the net primary productivity (NPP) is larger

than zero. The costs of BNF are set at a moderate constant value of  $6 \text{ gC gN}^{-1}$  (Boote et al., 2009; Kaschuk et al., 2009; Patterson and Larue, 1983; Ryle et al., 1979). If the costs exceed the maximum costs which are set at 50 % of the NPP (Kull, 2002), the nitrogen fixation is reduced to the amount achievable with the maximum costs. A full description of the original approach is provided in Ma et al. (2022). While in reality biological nitrogen fixation is a feature restricted to legume species, in LPJmL we decided to not distinguish between fixing and non-fixing PFTs to keep the number of PFTs as small as possible. This is reasonable because a PFT can be representative of multiple species and will only fix additional nitrogen if its demand cannot be fulfilled by other sources of nitrogen uptake and if its NPP is sufficient. One could say that the PFT has the ability to fix nitrogen only if needed comparable to a community containing legumes only if they are advantageous.

### B.1.4 Feed demand

We implemented a relationship between metabolic body weight (MBW) and feed demand following (Cordova et al., 1978). This is the same relationship used to calculate the feed demand in LPJmL 5, but we replaced the constant 650 kg per animal with a parameter BW (Eq. B.16) while preserving  $\text{intake}_{\text{MBW}} = 31.07$  (Rolinski et al., 2018).

$$\text{feed demand} = \text{BW}^{0.75} \cdot \text{intake}_{\text{MBW}}. \quad (\text{B.16})$$

## B.2 MSE components

We calculated the mean square error and its components (the bias, phase and variances) following Eqs. (B.17) to (B.20). Parameters  $x$  and  $y$  are the time series of simulated and observed values of a variable;  $\bar{x}$  and  $\bar{y}$  are the time series mean,  $\sigma_x$ ;  $\sigma_y$  is the time series standard deviation; and  $N$  is the number of values in the time series.

$$\text{MSE} = (\overline{x - y})^2, \quad (\text{B.17})$$

$$\text{MSE}_{\text{Bias}} = (\bar{x} - \bar{y})^2, \quad (\text{B.18})$$

$$\text{MSE}_{\text{Phase}} = 2 \cdot \left( \frac{N-1}{N} \right) \cdot \sigma_x \cdot \sigma_y \cdot (1 - \text{corr}(x, y))^2, \quad (\text{B.19})$$

$$\text{MSE}_{\text{Variance}} = \left( \left( \frac{N-1}{N} \right) \cdot (\sigma_x - \sigma_y) \right)^2. \quad (\text{B.20})$$

## B.3 Additional figures

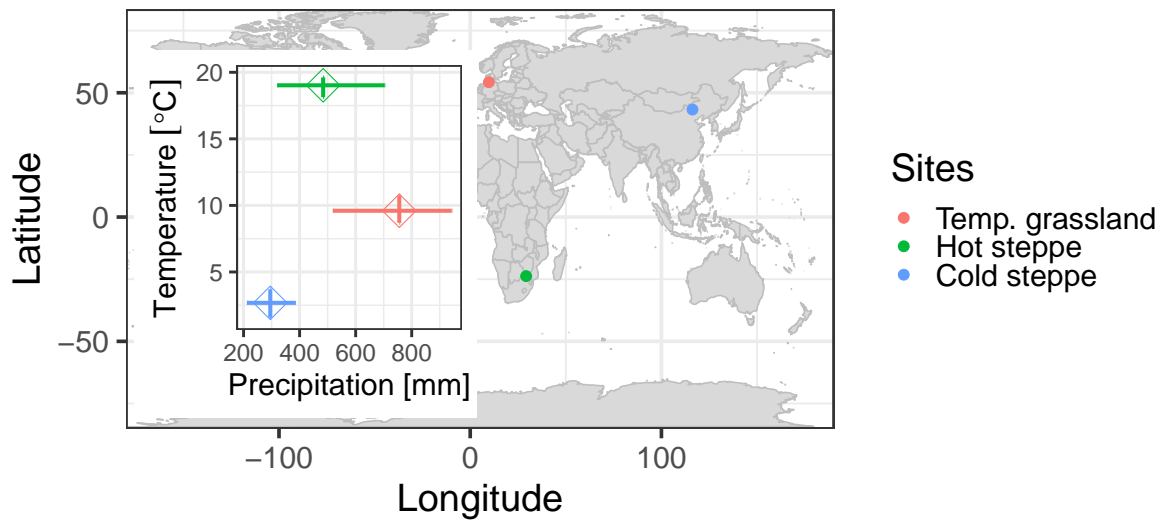


Figure B.2: Location (points) of the three grassland sites and their mean annual temperature and precipitation (squares). Lines show one standard deviation.

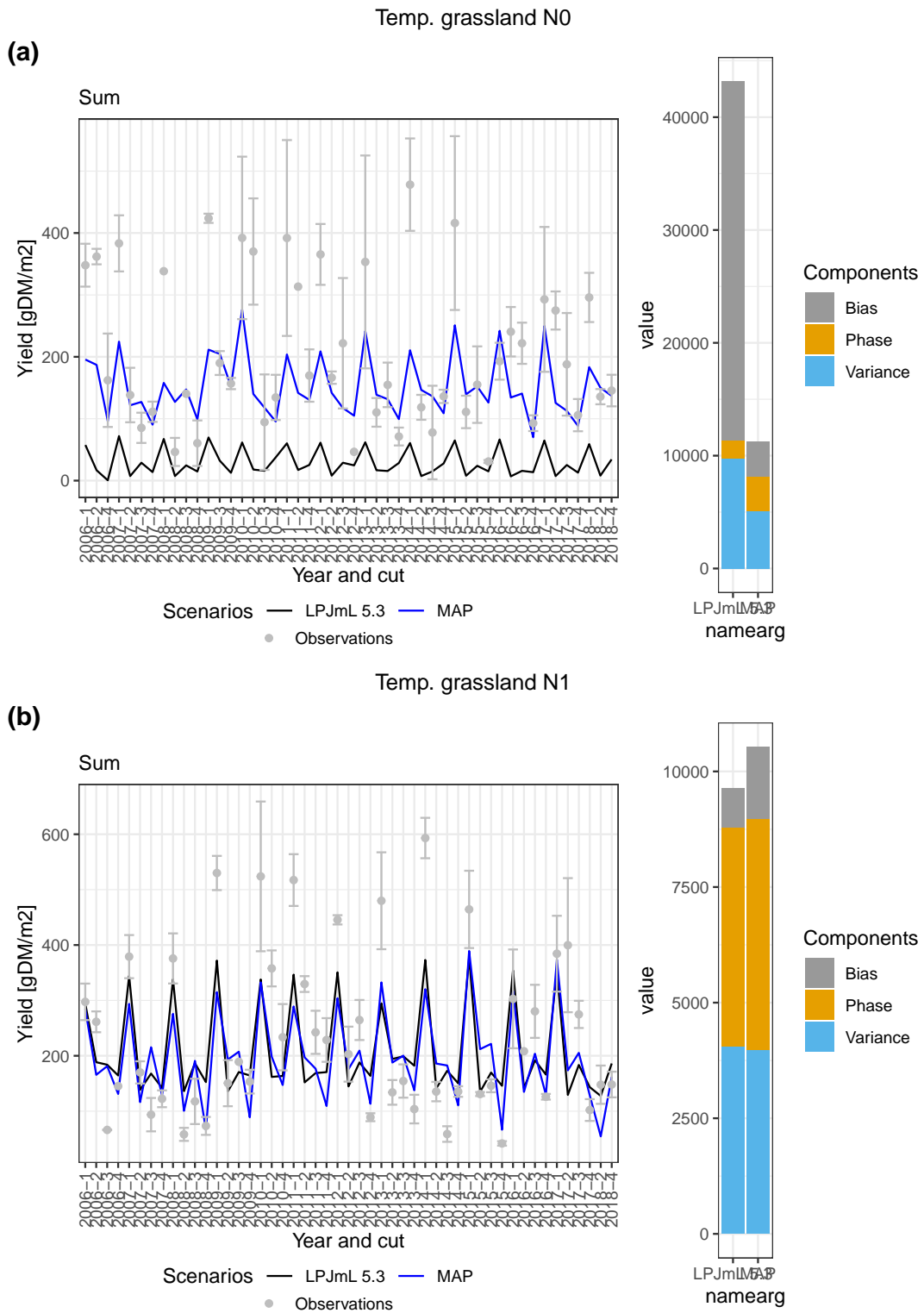


Figure B.3: Dry matter yields in  $\text{gDMm}^{-2}$  for the unfertilized (a) and fertilised (b) scenario for LPJmL 5.3 (black), the maximum a posteriori (MAP blue) and observations (grey) at the temperate grassland (left). Error bars are one standard deviation. MSE and its components bias (grey), phase (yellow) and variance (blue) for LPJmL 5.3 and the MAP.

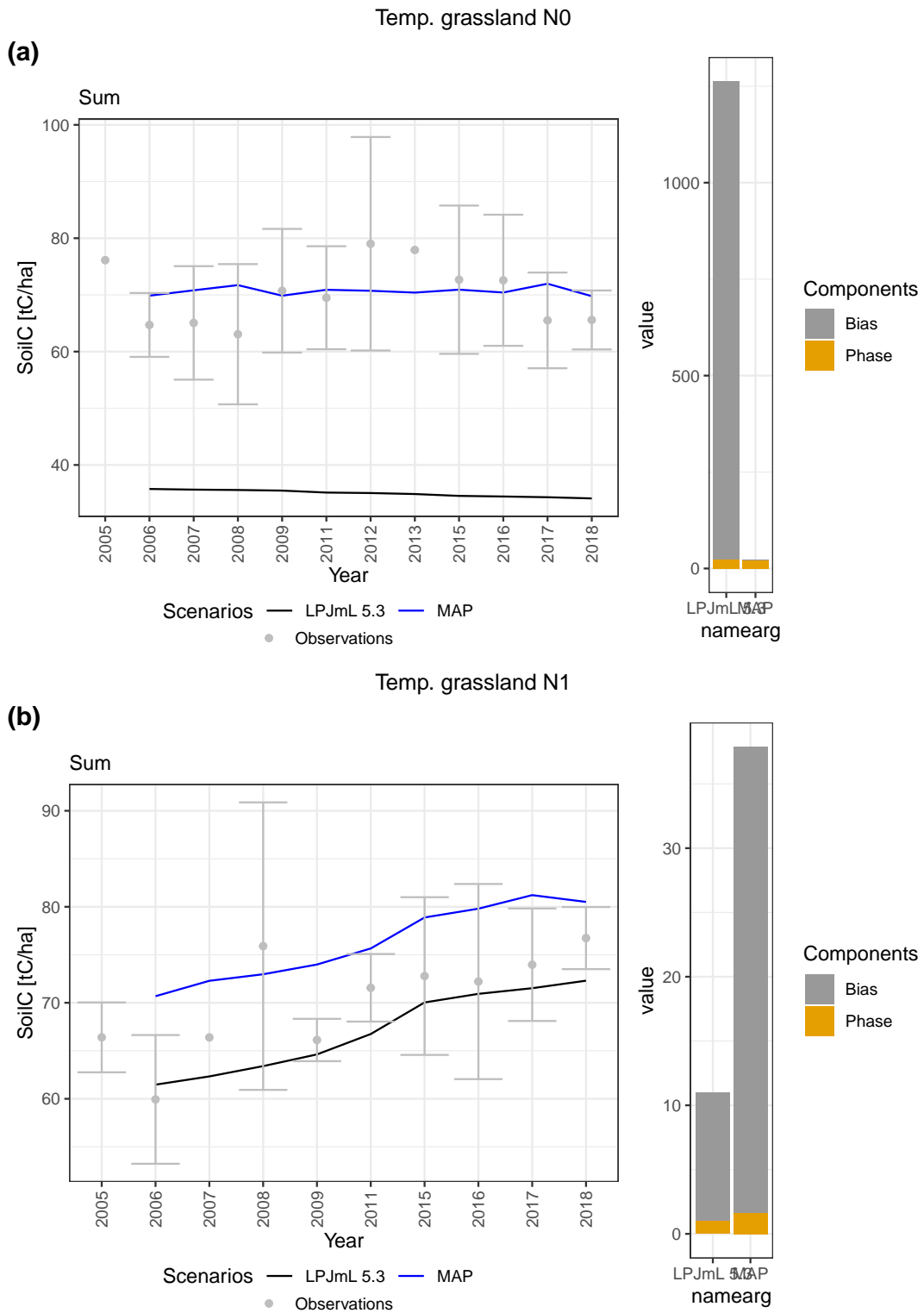
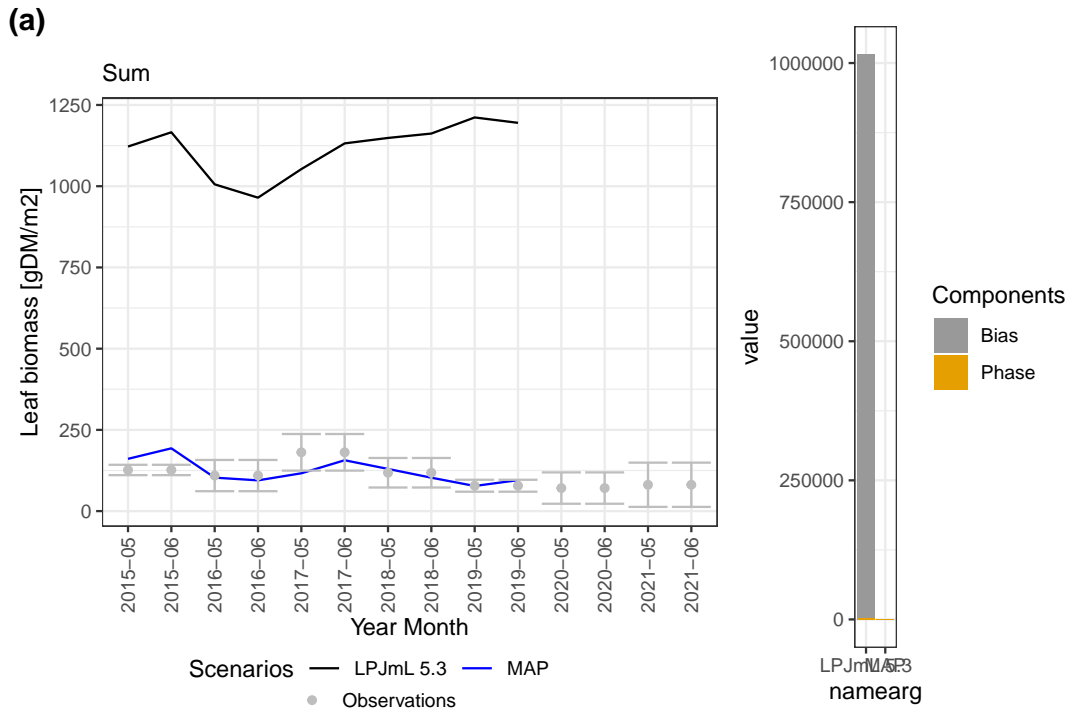


Figure B.4: Soil organic carbon in  $\text{tCha}^{-1}$  for the unfertilized (a) and fertilised (b) scenario for LPJmL 5.3 (black), the maximum a posteriori (MAP blue) and observations (grey) at the temperate grassland (left). Error bars are one standard deviation. MSE and its components bias (grey), phase (yellow) and variance (blue) for LPJmL 5.3 and the MAP.

Hot steppe 0C



Hot steppe 1C

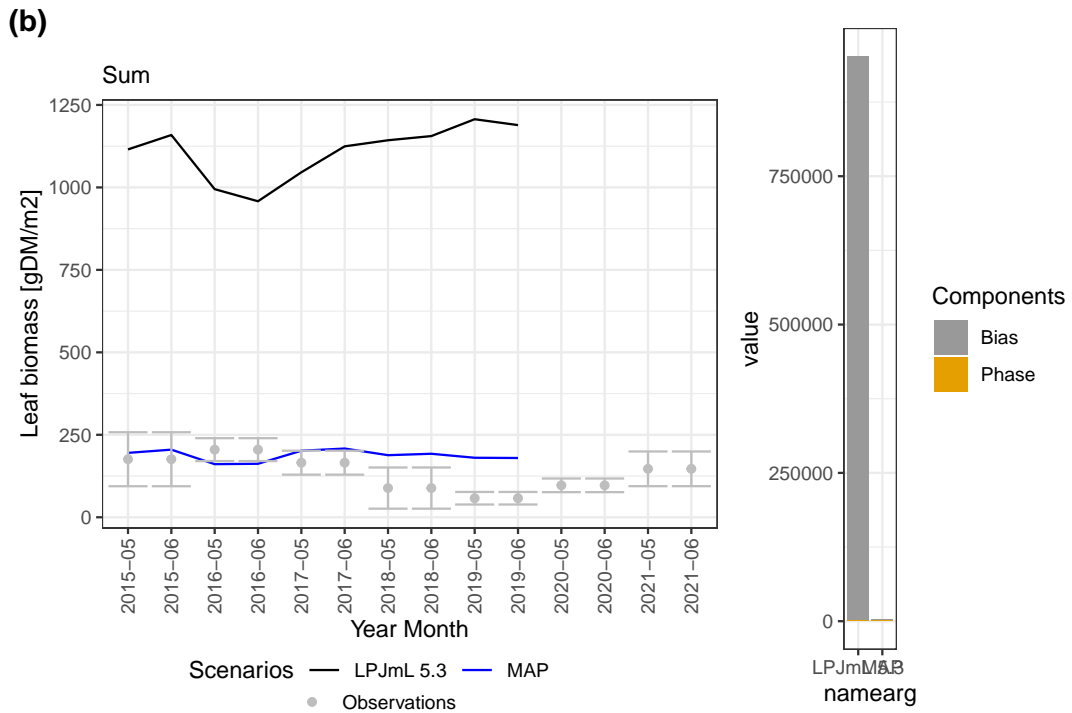


Figure B.5: Leaf biomass in  $\text{gDMm}^{-2}$  for the ungrazed (a) and grazed (b) scenario for LPJmL 5.3 (black), the maximum a posteriori (MAP blue) and observations (grey) at the hot steppe (left). Error bars are one standard deviation. MSE and its components bias (grey), phase (yellow) and variance (blue) for LPJmL 5.3 and the MAP.

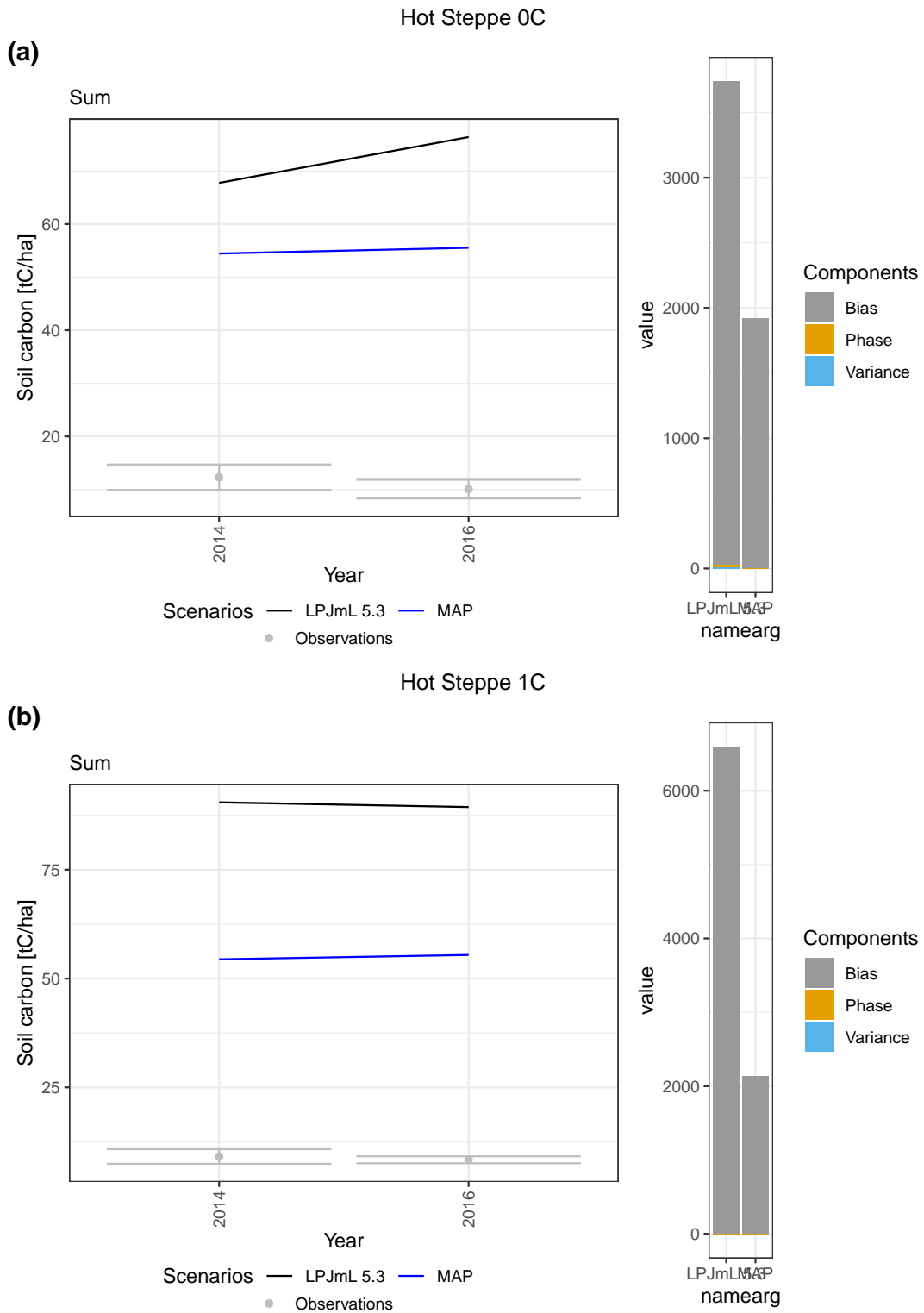


Figure B.6: Soil organic carbon in  $tCha^{-1}$  for the ungrazed (a) and grazed (b) scenario for LPJmL 5.3 (black), the maximum a posteriori (MAP blue) and observations (grey) at the hot steppe (left). Error bars are one standard deviation. MSE and its components bias (grey), phase (yellow) and variance (blue) for LPJmL 5.3 and the MAP.

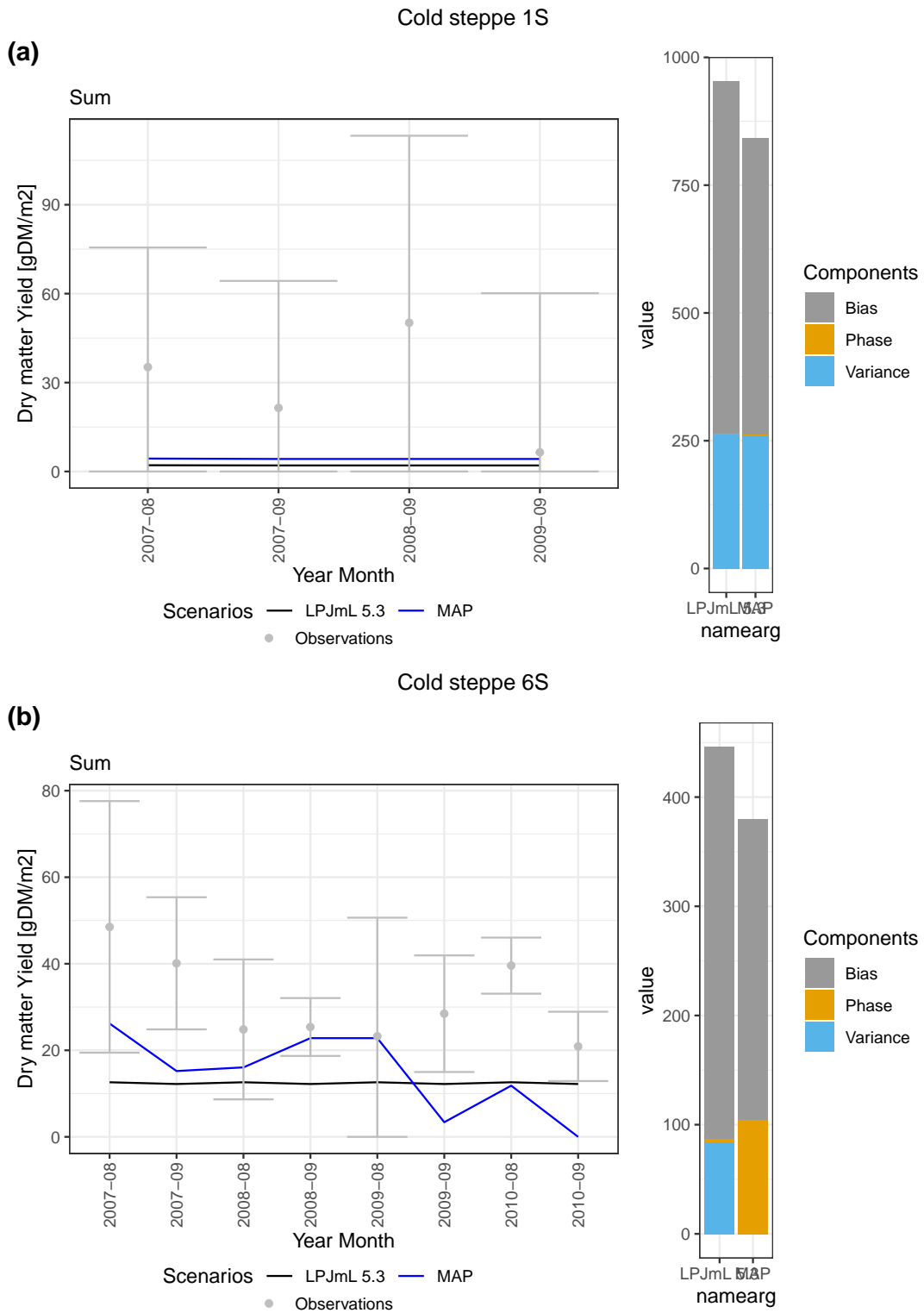


Figure B.7: Grazing offtake in  $\text{gDMm}^{-2}$  for the extensively (a) and intensively (b) grazed scenario for LPJmL 5.3 (black), the maximum a posteriori (MAP blue) and observations (grey) at the cold steppe (left). Error bars are one standard deviation. MSE and its components bias (grey), phase (yellow) and variance (blue) for LPJmL 5.3 and the MAP.

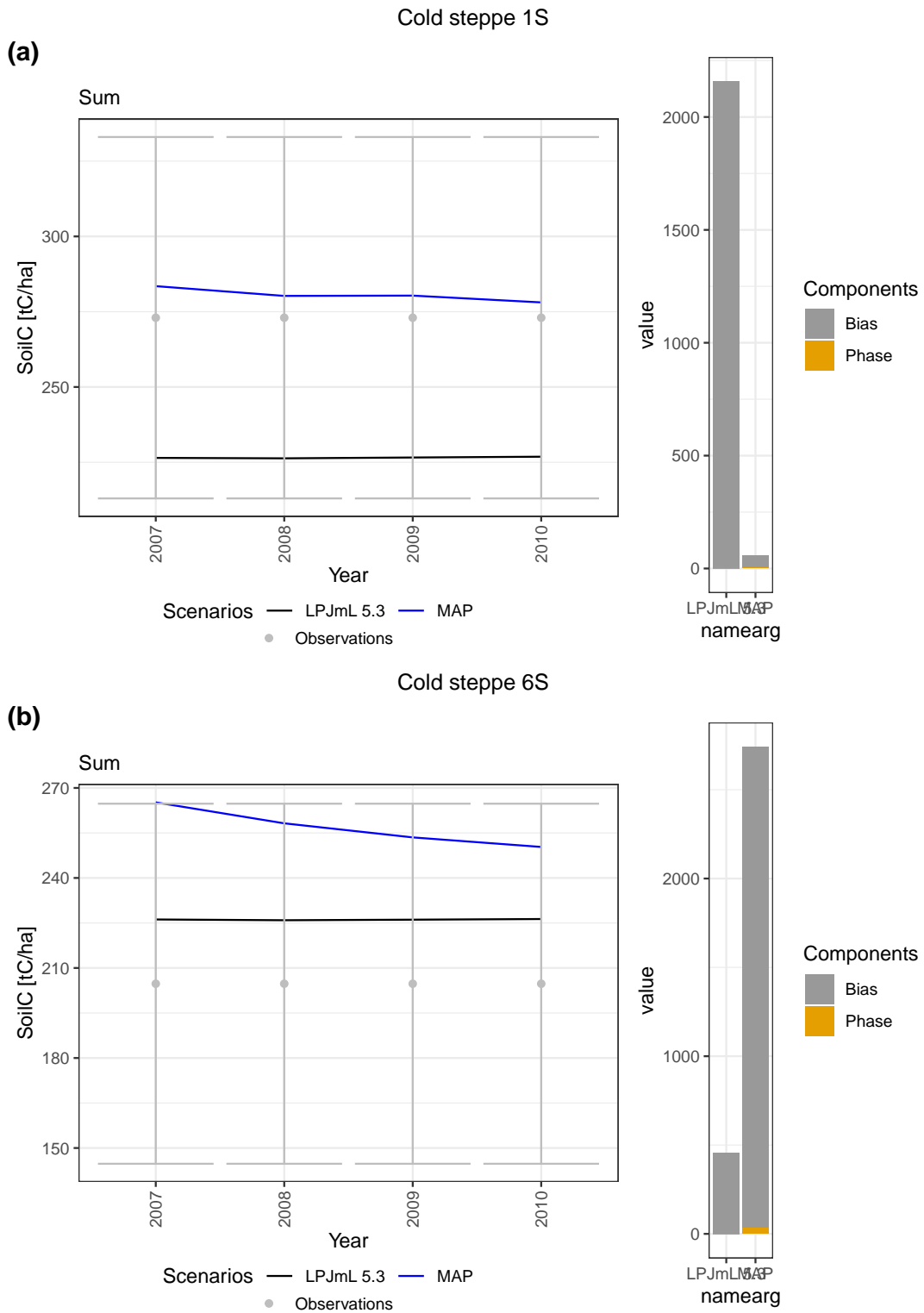


Figure B.8: Soil organic carbon in  $\text{tC ha}^{-1}$  for the extensively (a) and intensively (b) grazed scenario for LPJmL 5.3 (black), the maximum a posteriori (MAP blue) and observations (grey) at the cold steppe (left). Error bars are one standard deviation. MSE and its components bias (grey), phase (yellow) and variance (blue) for LPJmL 5.3 and the MAP.

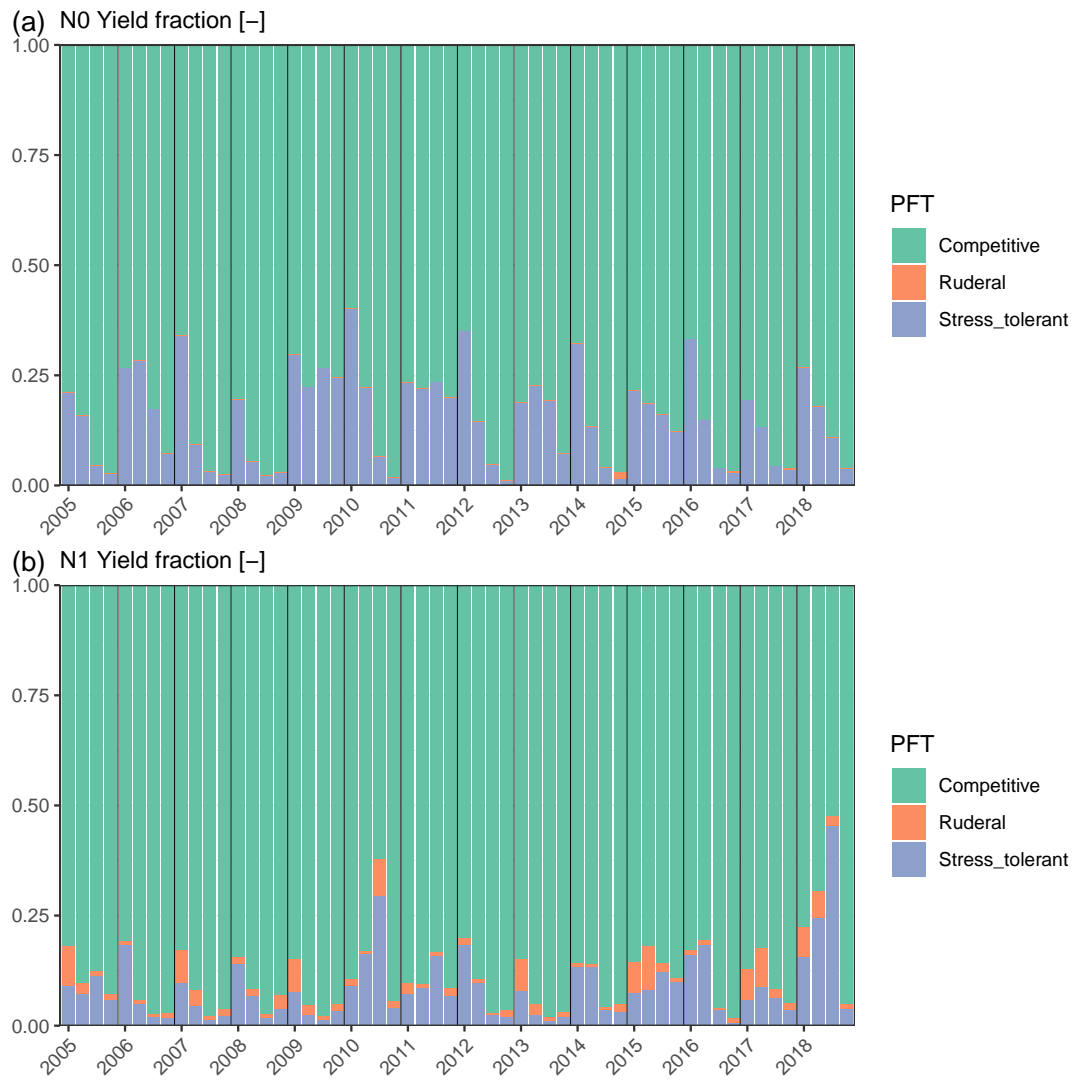


Figure B.9: PFT fractions (colours) of dry matter yield for each cut for the unfertilised (a) and fertilized (b) experiment at the temperate grassland.

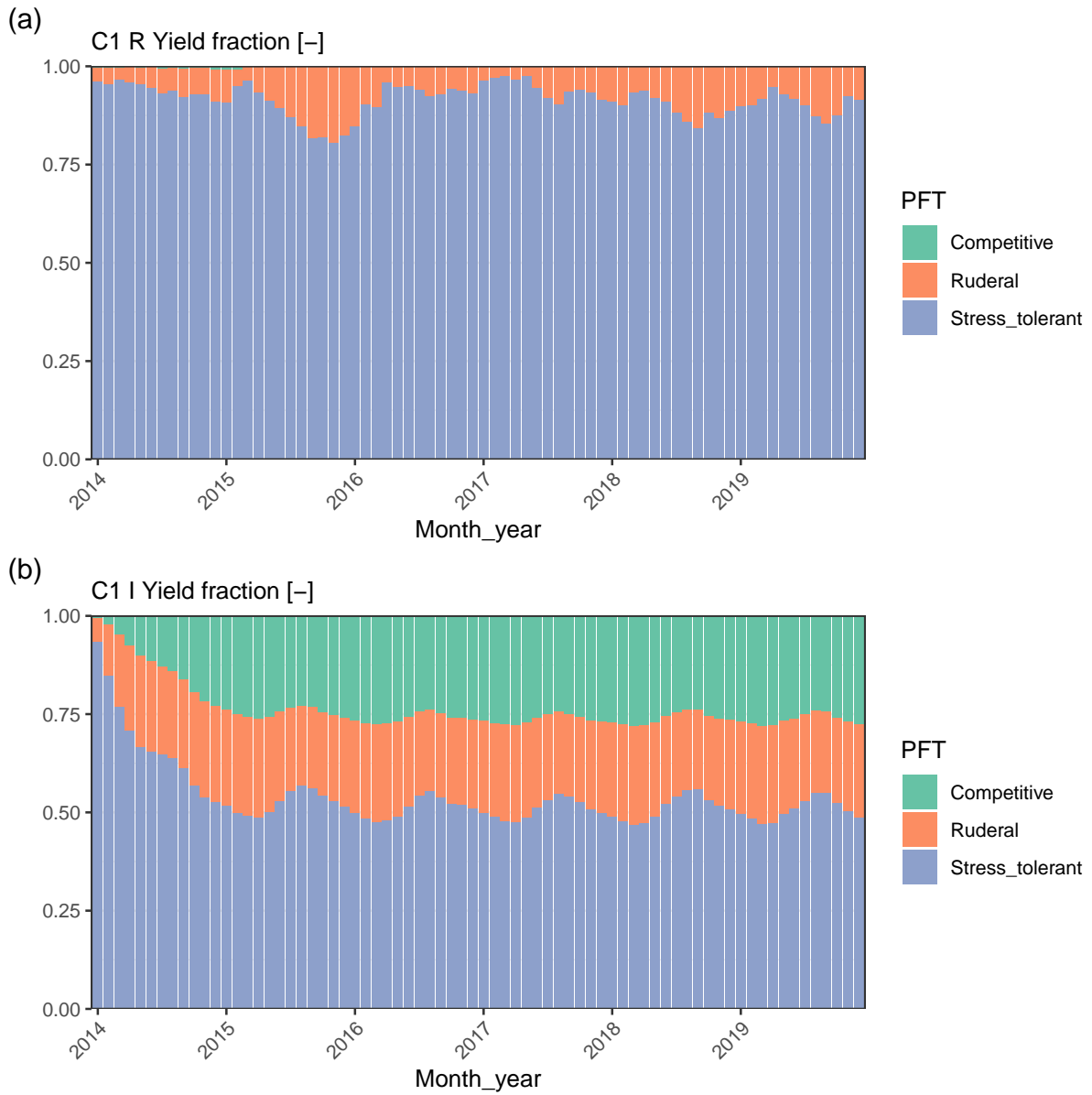


Figure B.10: PFT fractions (colours) of monthly grazing offtake for the rainfed (a) and irrigated (b) experiment at the hot steppe.

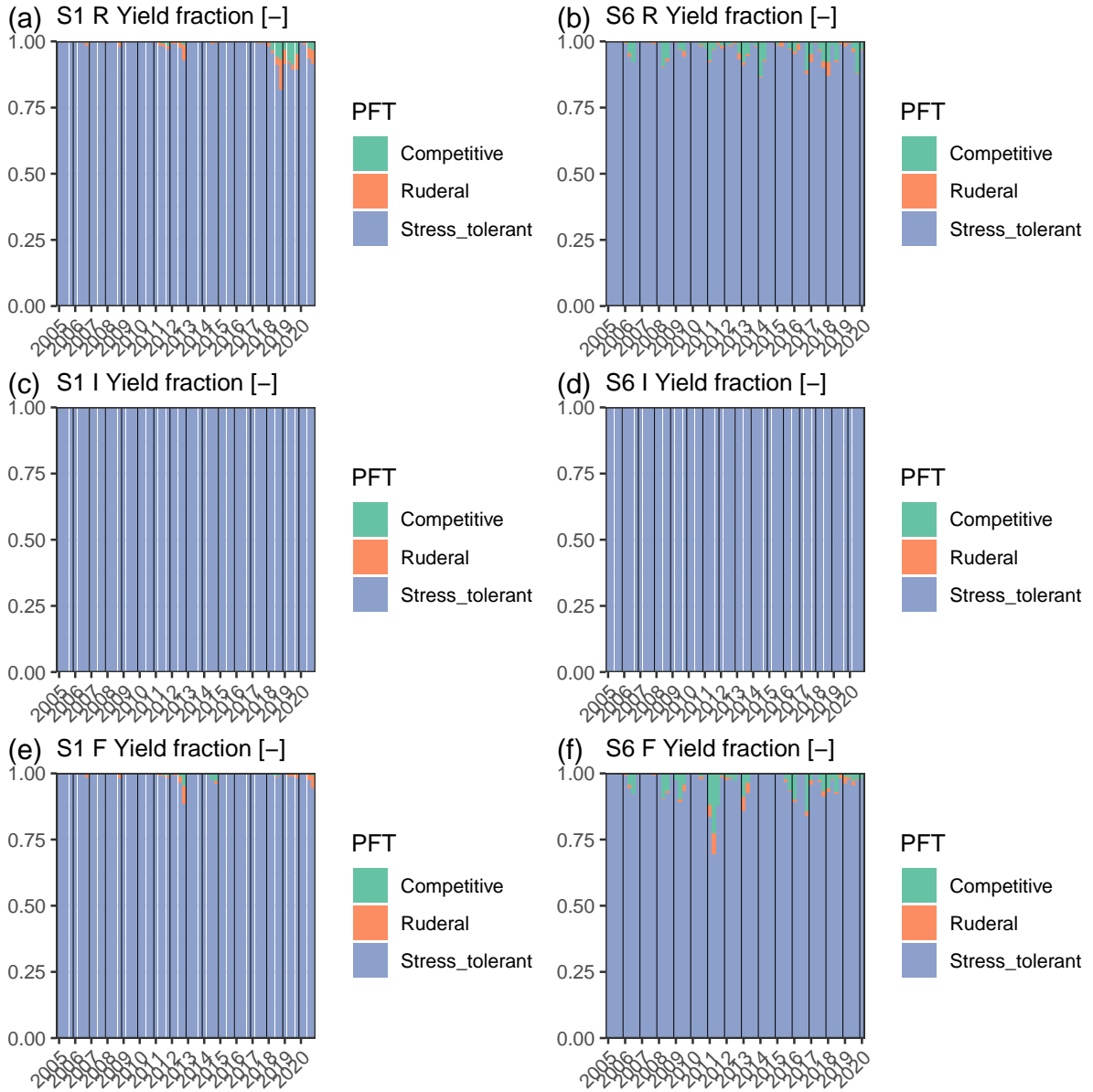


Figure B.11: PFT fractions (colours) of monthly grazing offtake for the extensively (a,c,e) and intensively (b,d,f) grazed experiment for the rainfed (a,b), fertilized (c,d) and irrigated (e,f) scenarios at the cold steppe.

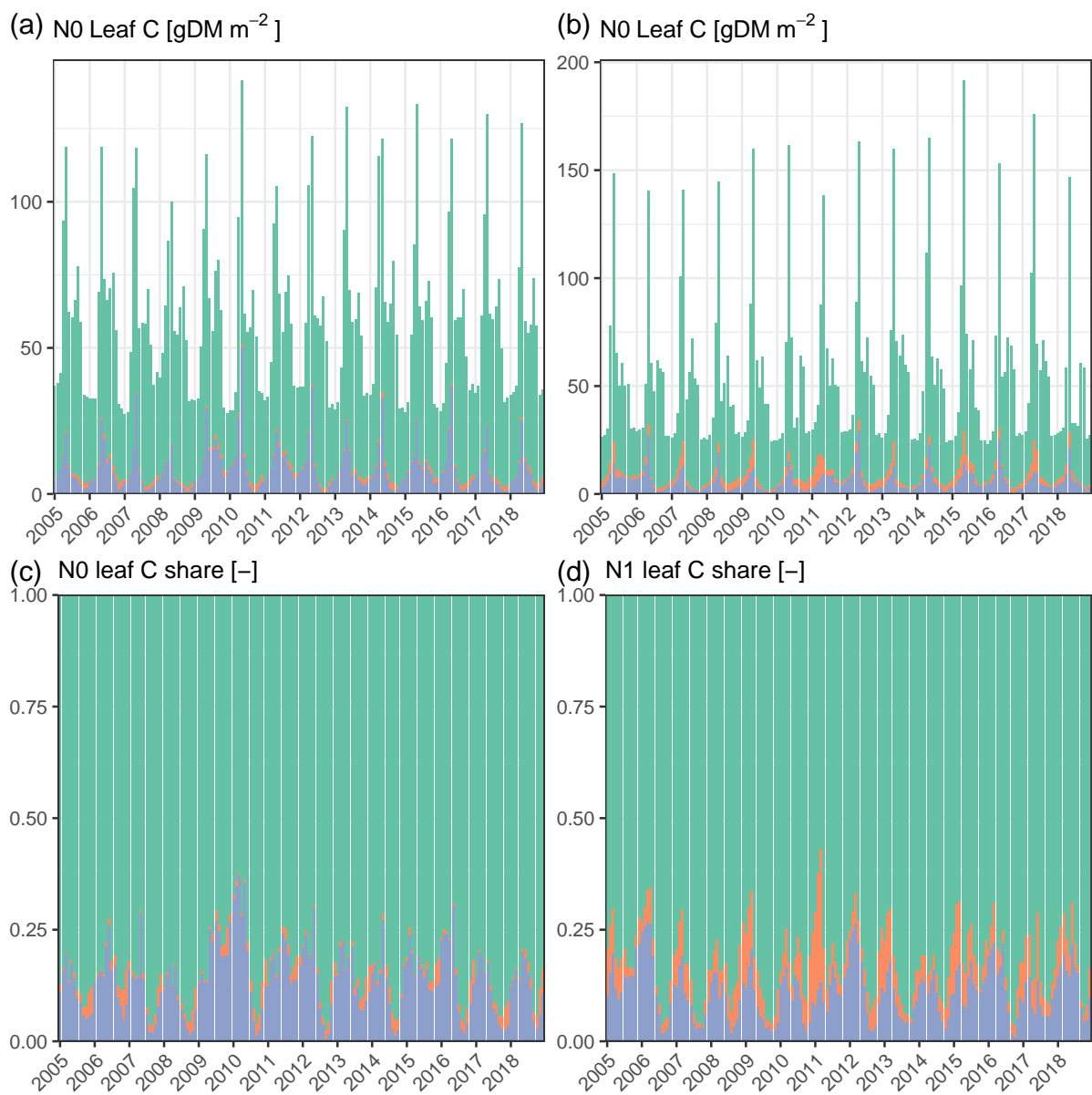


Figure B.12: Total (a,b) and fractional (c,d) monthly leaf carbon for the unfertilized (a,c) and fertilized (b,d) experiment for each PFT (colours).

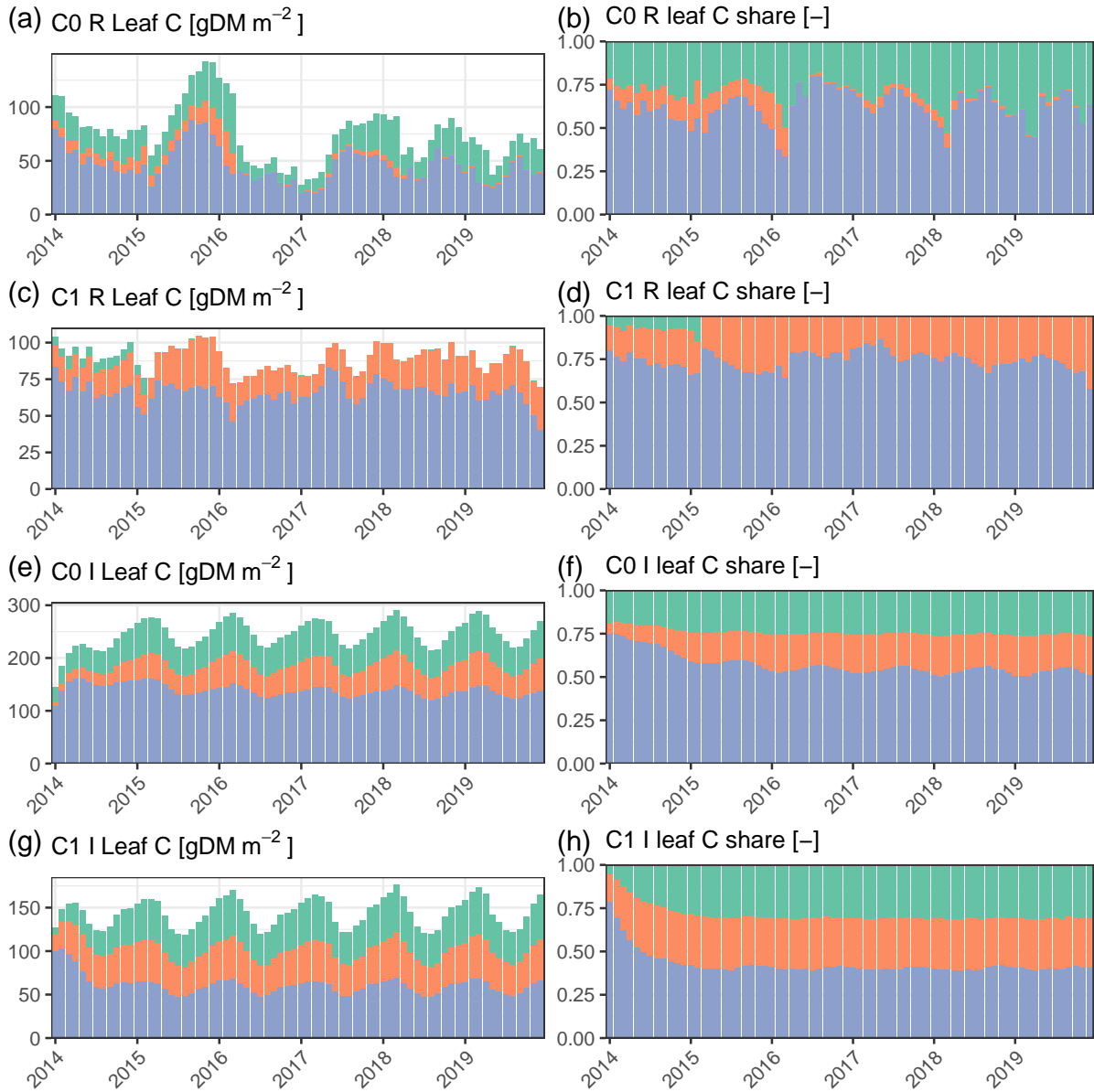


Figure B.13: Total (a,c,e,g) and fractional (b,d,f,h) monthly leaf carbon for the ungrazed (a,b,e,f) and grazed (c,d,g,h) experiment for the rainfed (a-d) and irrigated (e-h) scenarios for each PFT (colours).

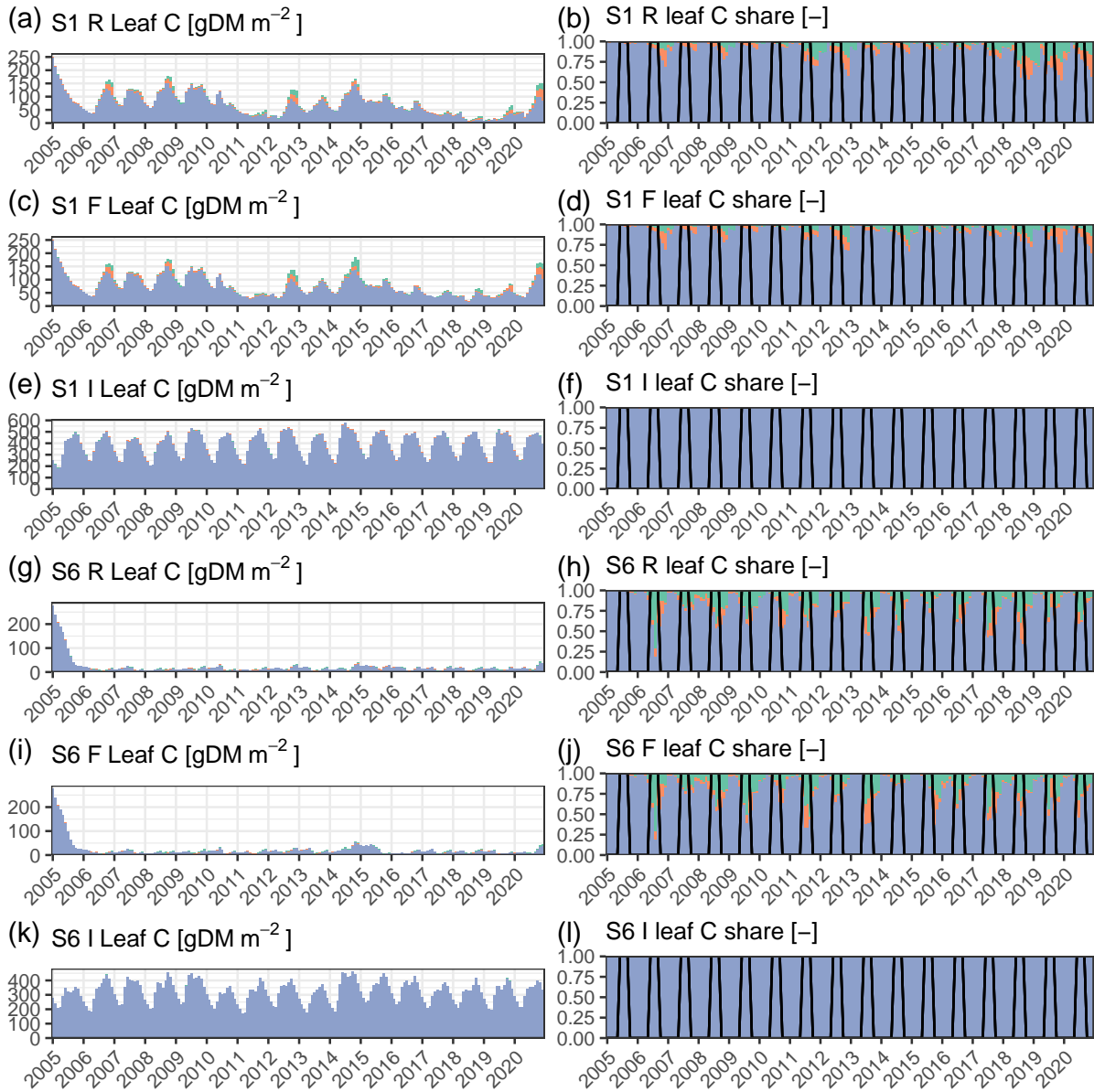


Figure B.14: Total (a,c,e,g,i,k) and fractional (b,d,f,h,j,l) monthly leaf carbon for the extensively (a-f) and intensively (g-l) grazed experiment for the rainfed (a,b,g,h), fertilized (c,d,i,j) and irrigated (e,f,k,l) scenarios for each PFT (colours).

## B.4 Additional tables

Table B.1: Overview of the SLA and leaf longevity data obtained from the TRY database.

Name	TRY Dataset ID	References
Abisko and Sheffield Database	1	(Cornelissen et al., 2004; Qusted et al., 2003)
GLOPNET-Global Plant Trait Network Database	20	(Wright et al., 2004)
Sheffield Database	37	(Cornelissen, 1996; Cornelissen et al., 2004; Diaz et al., 2004)
Leaf Physiology Database	67	(Kattge et al., 2009)
Global A, N, P, SLA Database	94	(Reich et al., 2009)
Tropical Traits from West Java Database	99	(Shiodera et al., 2008)
Functional Traits Explaining Variation in Plant Life History Strategies	285	(Adler et al., 2014)
Plant Traits of <i>Arabidopsis thaliana</i>	359	(Blonder et al., 2015)

## B.5 Model development

### B.5.1 Phenology dependent allocation

Based on the GSI phenology (Forkel et al., 2014) we calculate the allocation of net primary productivity to leaves and roots ( $LR$ ) dependent on changes in the temperature and light functions of the phenology ( $f$ ) as follows:

$$LR = LR_{\text{base}} \cdot s_{\text{light}} \cdot s_{\text{cold}} \quad (\text{B.21})$$

with

$$s_i = \begin{cases} 1 + f_i & \text{if } \Delta f_i > \epsilon_i, \\ 1 & \text{if } -\epsilon_i \leq \Delta f_i \leq \epsilon_i, \\ 1 - f_i & \text{if } \Delta f_i < -\epsilon_i. \end{cases} \quad (\text{B.22})$$

where  $i \in \{\text{light, cold}\}$ ,  $\Delta f_i = f_{i,t} - f_{i,t-1}$ ,  $\epsilon_{\text{light}} = 0.01$ , and  $\epsilon_{\text{cold}} = 0.001$ .

$LR_{\text{base}} = LR_{\text{PFT}} \cdot 0.5 + (0.5) \cdot \min(w_{\text{scal}}, v_{\text{scal}})$  where  $w_{\text{scal}}$  and  $v_{\text{scal}}$  are the water and nitrogen limitation factors from photosynthesis (Schaphoff et al., 2018; von Bloh et al., 2018).

### B.5.2 Manure application

Manure application was implemented as for the annual crops in LPJmL (Herzfeld et al., 2021). Manure is applied with a C:N ratio of 10 and a  $\text{NH}_4$  fraction of  $2/3$ . Manure is only applied if the mowing management option is used and  $24 \text{ g/m}^2$  is split across 4 applications of 8, 6, 6 and  $4 \text{ g/m}^2$  on April 1st, May 31st, July 1st and August 15th.  $\text{NH}_4$ , C and N from manure are added to the first soil layer following B.23-B.25.

$$\Delta \text{NH}_4 = \text{manure} \cdot \text{fraction}_{\text{NH}_4} \quad (\text{B.23})$$

$$\Delta C_{\text{soil}} = \text{manure} \cdot CN_{\text{manure}} \quad (\text{B.24})$$

$$\Delta N_{\text{soil}} = \text{manure} \cdot (1 - \text{fraction}_{NH_4}) \quad (\text{B.25})$$

## B.6 Input data and parameters

### B.6.1 Climate data and preparation

Data on temperature, precipitation and for the cold steppe also shortwave radiation were available for different time periods (Table B.2). For the cold steppe, data did not contain any gaps and we only had to identify and prune leap years. This is required to obtain 365 days per year time-series which are needed to run LPJmL. For pruning we dropped December 31st.

For the temperate grassland and the hot steppe, the data contained gaps that needed to be filled. Additionally, they did not contain a full calendar year at the end and/or the beginning of the time-series for which we had to extrapolate the data. We used two different procedures for the gap filling: A spline fitting (temperature) and a sampler (precipitation). With the spline fitting we aimed to capture the seasonality trends of the observed temperature (Fig. B.15 and B.16) but also account for day to day variation. First, we fitted a spline to the temperature data using the `smooth.spline` function from the `stats`-package (R Core Team, 2019). Second, to account for day to day variability we scattered the data by a random value we drew from a uniform distribution in the interval  $x_{min}$  to  $x_{max}$ . For the different sites, we used different percentiles of the difference between the fitted spline and the observed data for the values for  $x_{min}$  and  $x_{max}$  (Table B.2). For the extrapolation we calculated the average for each day of the year over the time-series for the fitted spline. The values of the respective day of the year were then then used for the extrapolation. This data were also scattered with the same approach as for the gap filling.

For the precipitation (Fig. B.17 and B.18) we used a sampler for gap filling and extrapolation because the spline fitting did overestimate the number of days with precipitation. We sampled the missing values directly from the observed data at randomly drawn percentiles. This ensures, that the gap-filled data have a similar distribution compared to the original data.

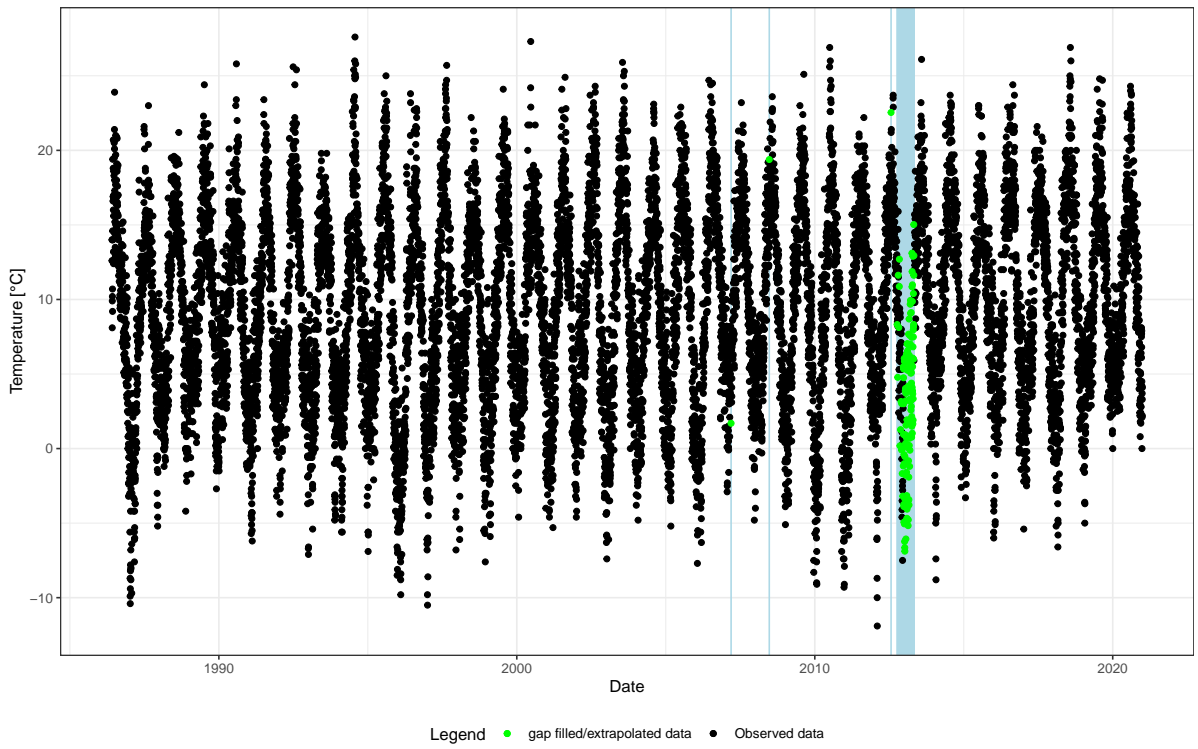


Figure B.15: Daily temperature at the temperate grassland. Colors show observed (black) and gap filled or extrapolated (green) data.

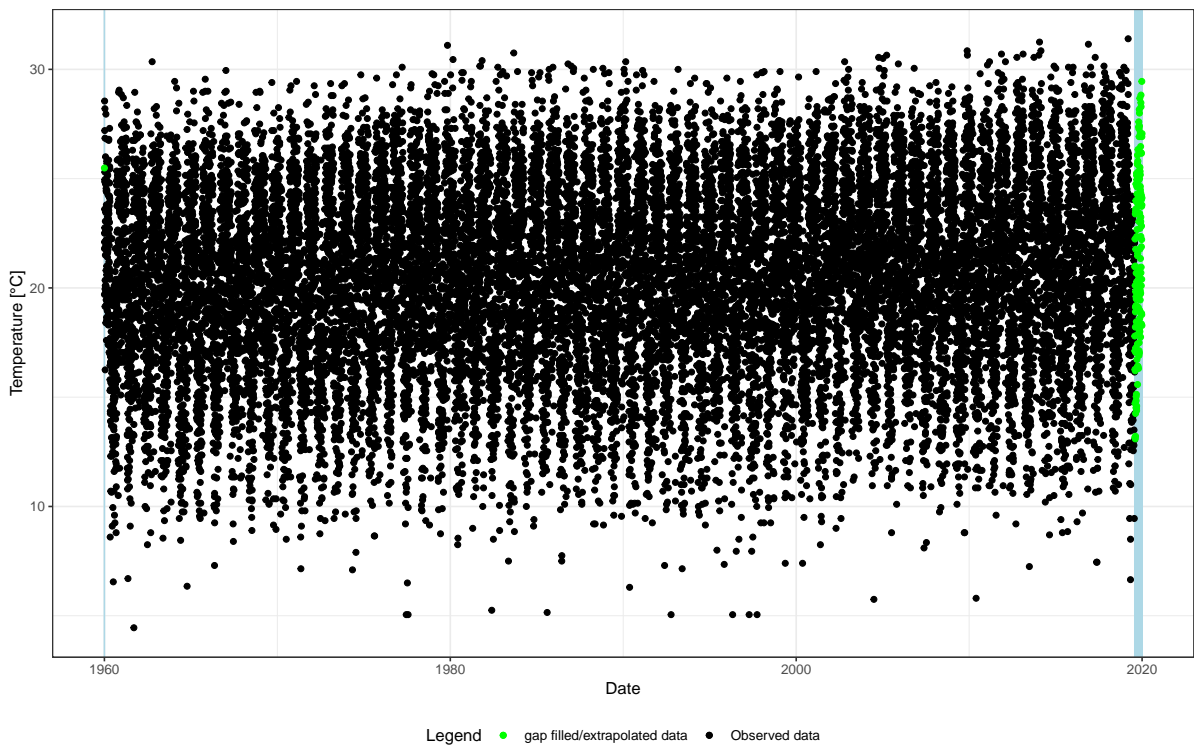


Figure B.16: Daily temperature at the hot steppe. Colors show observed (black) and gap filled or extrapolated (green) data.

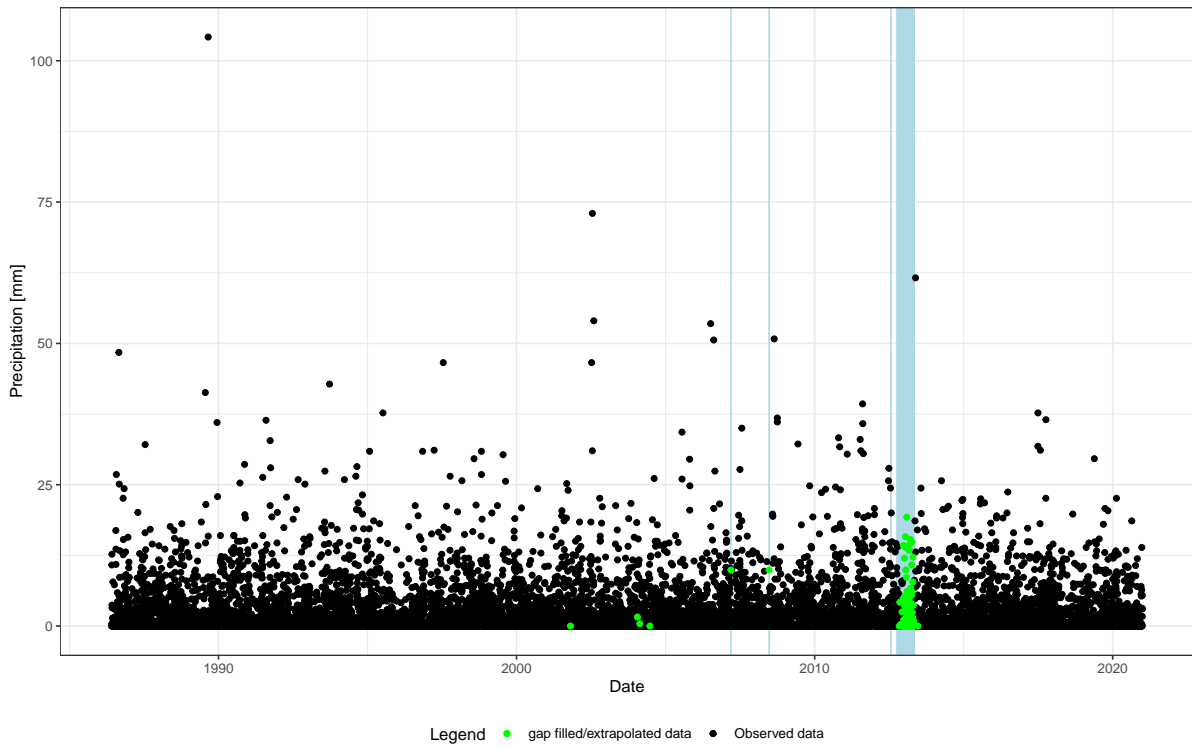


Figure B.17: Daily precipitation at the temperate grassland. Colors show observed (black) and gap filled or extrapolated (green) data.

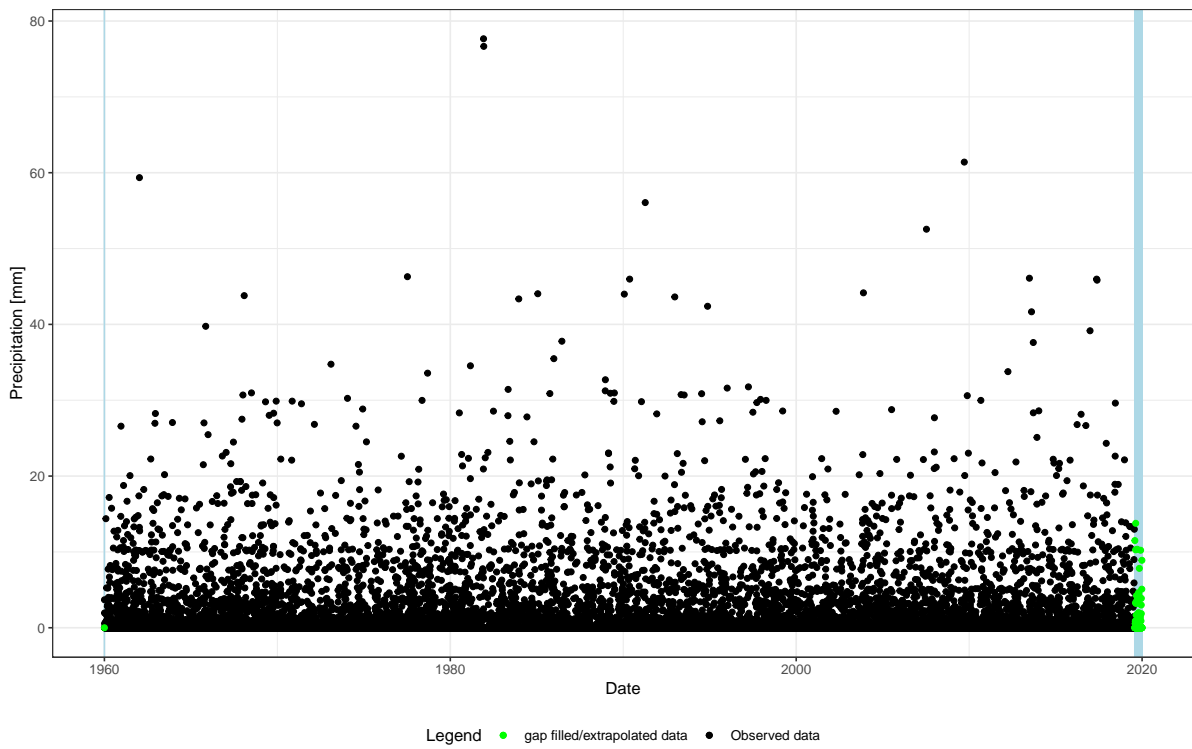


Figure B.18: Daily precipitation at the hot steppe. Colors show observed (black) and gap filled or extrapolated (green) data.

Table B.2: Overview of climate products used for the simulations.

Site	Variable	Gap-filling	$x_{\min}$ to $x_{\max}$	Extrapolation	$x_{\min}$ to $x_{\max}$	Source
Temperate grassland	Temperature	Yes	1st-99th percentile	Yes	1st-99th percentile	(DWD, 2021)
Temperate grassland	Precipitation	Yes	-	Yes	-	(DWD, 2021)
Temperate grassland	Radiation	No	-	No	-	-
Temperate grassland	Wind	No	-	No	-	-
Hot steppe	Temperature	No	1st-99th percentile	Yes	5th-95th percentile	(Munjonji et al., 2020)
Hot steppe	Precipitation	No	-	Yes	-	(Munjonji et al., 2020)
Hot steppe	Radiation	No	-	No	-	(Lange and Büchner, 2022)
Hot steppe	Wind	No	-	No	-	(Lange and Büchner, 2022)
Cold steppe	Temperature	No	-	No	-	(Hoffmann et al. 2016, Schönbach et al. 2012)
Cold steppe	Precipitation	No	-	No	-	(Hoffmann et al. 2016, Schönbach et al. 2012)
Cold steppe	Radiation	No	-	No	-	-
Cold steppe	Wind	No	-	No	-	(Lange and Büchner, 2022)

## B.6.2 Soil texture

Data on sand, silt and clay content of the soils were used to determine the texture class and hydraulic parameters. Data for each site were available and are listed in Table B.3.

Table B.3: Sand, silt and clay content of the soils at each site.

Site	Sand [%]	Silt [%]	Clay [%]	Source
Temperate grassland	61	24.2	14.8	(Reinsch et al., 2018a; Reinsch et al., 2018b)
Hot steppe	80	12	8	(Munjonji et al., 2020)
Cold steppe	62.7	16.8	20.5	(Wiesmeier et al., 2011)

## B.6.3 Fixed parameters

In addition to the PFT specific parameters we calibrated, we changed several parameters to capture sites specific management and history (Table B.4).

Table B.4: Adjusted global parameter values.

Parameter	Temperate grassland	Hot steppe	Cold steppe
lsuha_spinup	1.0	0.1	1.0
animal_bw	650	450	35
grazing_stubble	5	5	2
nfrac_grassharvest	1.0	-	-
first_irrig_year	-	2014	2005

## B.7 R packages

We used several R packages for data handling and plotting (Table B.5). The ggradar package was not loaded but the ggradar function was adapted to create ggradar\_expression.

Table B.5: R-packages used for pre/postprocessing and data visualization.

Package (version)	Source
ggplot2 (3.3.6), tidy (1.1.4), dplyr (1.0.7), purrr (0.3.4), readr (2.0.2), stringr (1.4.0), tibble (3.1.8)	(Wickham et al., 2019)
rlang (1.0.4)	(Henry and Wickham, 2022)
ggtern (3.3.5)	(Hamilton and Ferry, 2018)
magrittr (2.0.3)	(Bache and Wickham, 2022)
reshape2 (1.4.4)	(Wickham, 2007)
plyr (1.8.6)	(Wickham, 2011)
doParallel (1.0.16)	(Microsoft Corporation and Weston, 2020)
foreach (1.5.1)	(Microsoft and Weston, 2020)
lubridate (1.7.10)	(Grolemund and Wickham, 2011)
tidyselect (1.1.1)	(Henry and Wickham, 2021)
gridExtra (2.3)	(Auguie, 2017)
MASS (7.3-53.1)	(Venables and Ripley, 2002)
Kendall (2.2.1)	(McLeod, 2022)
cowplot (1.1.1)	(Wilke, 2020)
ggradar (0.2)	(Bion, 2022)
LandMark (1.2.0)	(Kowalewski et al., 2018)
PIKTools (1.6)	(Kowalewski and Breier, 2021)

## B.8 References

- Adler, P. B., R. Salguero-Gómez, A. Compagnoni, J. S. Hsu, J. Ray-Mukherjee, C. Mbeau-Ache, and M. Franco (2014). “Functional Traits Explain Variation in Plant Life History Strategies”. In: *Proc Natl Acad Sci U S A* 111.2, pp. 740–745. ISSN: 0027-8424. DOI: 10.1073/pnas.1315179111. (Visited on 06/01/2022).
- Auguie, B. (2017). *gridExtra: Miscellaneous Functions for “Grid” Graphics*.
- Bache, S. M. and H. Wickham (2022). *Magrittr: A Forward-Pipe Operator for R*.
- Bergmann, J., A. Weigelt, F. van der Plas, D. C. Laughlin, T. W. Kuyper, N. Guerrero-Ramirez, O. J. Valverde-Barrantes, H. Bruelheide, G. T. Freschet, C. M. Iversen, J. Kattge, M. L. McCormack, I. C. Meier, M. C. Rillig, C. Roumet, M. Semchenko, C. J. Sweeney, J. van Ruijven, L. M. York, and L. Mommer (2020). “The Fungal Collaboration Gradient Dominates the Root Economics Space in Plants”. In: *Sci. Adv.* 6.27, eaba3756. DOI: 10.1126/sciadv.aba3756. (Visited on 03/08/2022).
- Bion, R. (2022). *Ggradar: Create Radar Charts Using Ggplot2*.
- Blonder, B., F. Vasseur, C. Violle, B. Shipley, B. J. Enquist, and D. Vile (2015). “Testing Models for the Leaf Economics Spectrum with Leaf and Whole-Plant Traits in *Arabidopsis thaliana*”. In: *AoB PLANTS* 7, plv049. ISSN: 2041-2851. DOI: 10.1093/aobpla/plv049. (Visited on 06/01/2022).
- Boenisch, G. and J. Kattge (2018). *TRY Plant Trait Database*. <https://www.try-db.org/TryWeb/Home.php>. (Visited on 03/08/2018).
- Boote, K. J., G. Hoogenboom, J. W. Jones, and K. T. Ingram (2009). “Modeling Nitrogen Fixation and Its Relationship to Nitrogen Uptake in the CROPGRO Model”. In: *Quantifying and Understanding Plant Nitrogen Uptake for Systems Modeling*. CRC Press. ISBN: 978-0-429-14053-2.
- Cordova, F. J., J. D. Wallace, and R. D. Pieper (1978). “Forage Intake by Grazing Livestock: A Review”. In: *J. Range Manag.* 31.6, pp. 430–438. ISSN: 0022-409X. DOI: 10.2307/3897201. JSTOR: 3897201. (Visited on 06/14/2022).
- Cornelissen, J. H. C. (1996). “An Experimental Comparison of Leaf Decomposition Rates in a Wide Range of Temperate Plant Species and Types”. In: *J. Ecol.* 84.4, pp. 573–582. ISSN: 0022-0477. DOI: 10.2307/2261479. JSTOR: 2261479. (Visited on 03/09/2018).
- Cornelissen, J. H. C., H. M. Quested, D. Gwynn-Jones, R. S. P. Van Logtestijn, M. A. H. De Beus, A. Kondratchuk, T. V. Callaghan, and R. Aerts (2004). “Leaf Digestibility and Litter Decomposability Are Related in a Wide Range of Subarctic Plant Species and Types”. In: *Funct. Ecol.* 18.6, pp. 779–786. ISSN: 0269-8463. JSTOR: 3599104. (Visited on 06/01/2022).
- Díaz, S., J. G. Hodgson, K. Thompson, M. Cabido, J. H. C. Cornelissen, A. Jalili, G. Montserrat-Martí, J. P. Grime, F. Zarrinkamar, Y. Asri, S. R. Band, S. Basconcelo, P. Castro-Díez, G. Funes, B. Hamzehee, M. Khoshnevi, N. Pérez-Harguindeguy, M. C. Pérez-Rontomé, F. A. Shirvany, F. Vendramini, S. Yazdani, R. Abbas-Azimi, A. Bogaard, S. Boustani, M. Charles, M. Dehghan, L. de Torres-Espuny, V. Falczuk, J. Guerrero-Campo, A. Hynd, G. Jones, E. Kowsary, F. Kazemi-Saeed, M. Maestro-Martínez, A. Romo-Díez, S. Shaw, B. Siavash, P. Villar-Salvador, and M. R. Zak (2004). “The Plant Traits That Drive Ecosystems: Evidence from Three Continents”. In: *J. Veg. Sci.* 15.3, pp. 295–304. ISSN: 1654-1103. DOI: 10.1111/j.1654-1103.2004.tb02266.x. (Visited on 12/19/2018).
- DWD (2021). *Wetter Und Klima - Deutscher Wetterdienst - Leistungen - Klimadaten Deutschland - Monats- Und Tageswerte (Archiv)*. <https://www.dwd.de/DE/leistungen/klimadatendeutschland/klarchivtagmonat.html>. (Visited on 06/16/2022).
- Forkel, M., N. Carvalhais, S. Schaphoff, W. v. Bloh, M. Migliavacca, M. Thurner, and K. Thonicke (2014). “Identifying Environmental Controls on Vegetation Greenness Phenology through Model–Data Integration”. In: *Biogeosciences* 11.23, pp. 7025–7050. ISSN: 1726-4170. DOI: 10.5194/bg-11-7025-2014. (Visited on 06/29/2021).
- Grolemund, G. and H. Wickham (2011). “Dates and Times Made Easy with Lubridate”. In: *J. Stat. Softw.* 40.3, pp. 1–25.
- Hamilton, N. E. and M. Ferry (2018). *Ggtern: Ternary Diagrams Using Ggplot2*.

## Appendix B

- Henry, L. and H. Wickham (2021). *Tidyselect: Select from a Set of Strings*.
- Henry, L. and H. Wickham (2022). *Rlang: Functions for Base Types and Core R and 'tidyverse' Features*.
- Herzfeld, T., J. Heinke, S. Rolinski, and C. Müller (2021). "Soil Organic Carbon Dynamics from Agricultural Management Practices under Climate Change". In: *Earth Syst. Dyn.* 12.4, pp. 1037–1055. ISSN: 2190-4979. DOI: 10.5194/esd-12-1037-2021. (Visited on 05/31/2023).
- Hoffmann, C., M. Giese, U. Dickhoefer, H. Wan, Y. Bai, M. Steffens, C. Liu, K. Butterbach-Bahl, and X. Han (2016). "Effects of Grazing and Climate Variability on Grassland Ecosystem Functions in Inner Mongolia: Synthesis of a 6-Year Grazing Experiment". In: *Journal of Arid Environments* 135, pp. 50–63. ISSN: 0140-1963. DOI: 10.1016/j.jaridenv.2016.08.003. (Visited on 12/09/2021).
- Kaschuk, G., T. W. Kuyper, P. A. Leffelaar, M. Hungria, and K. E. Giller (2009). "Are the Rates of Photosynthesis Stimulated by the Carbon Sink Strength of Rhizobial and Arbuscular Mycorrhizal Symbioses?" In: *Soil Biology and Biochemistry* 41.6, pp. 1233–1244. ISSN: 0038-0717. DOI: 10.1016/j.soilbio.2009.03.005. (Visited on 03/07/2022).
- Katze, J., S. Díaz, S. Lavorel, I. C. Prentice, P. Leadley, G. Bönsch, E. Garnier, M. Westoby, P. B. Reich, I. J. Wright, J. H. C. Cornelissen, C. Violle, S. P. Harrison, P. M. Van Bodegom, M. Reichstein, B. J. Enquist, N. A. Soudzilovskaia, D. D. Ackerly, M. Anand, O. Atkin, M. Bahn, T. R. Baker, D. Baldocchi, R. Bekker, C. C. Blanco, B. Blonder, W. J. Bond, R. Bradstock, D. E. Bunker, F. Casanoves, J. Cavender-Bares, J. Q. Chambers, F. S. Chapin Iii, J. Chave, D. Coomes, W. K. Cornwell, J. M. Craine, B. H. Dobrin, L. Duarte, W. Durka, J. Elser, G. Esser, M. Estiarte, W. F. Fagan, J. Fang, F. Fernández-Méndez, A. Fidelis, B. Finegan, O. Flores, H. Ford, D. Frank, G. T. Freschet, N. M. Fyllas, R. V. Gallagher, W. A. Green, A. G. Gutierrez, T. Hickler, S. I. Higgins, J. G. Hodgson, A. Jalili, S. Jansen, C. A. Joly, A. J. Kerkhoff, D. Kirkup, K. Kitajima, M. Kleyer, S. Klotz, J. M. H. Knops, K. Kramer, I. Kühn, H. Kurokawa, D. Laughlin, T. D. Lee, M. Leishman, F. Lens, T. Lenz, S. L. Lewis, J. Lloyd, J. Llusà, F. Louault, S. Ma, M. D. Mahecha, P. Manning, T. Massad, B. E. Medlyn, J. Messier, A. T. Moles, S. C. Müller, K. Nadrowski, S. Naeem, Ü. Niinemets, S. Nöllert, A. Nüske, R. Ogaya, J. Oleksyn, V. G. Onipchenko, Y. Onoda, J. Ordoñez, G. Overbeck, W. A. Ozinga, S. Patiño, S. Paula, J. G. Pausas, J. Peñuelas, O. L. Phillips, V. Pillar, H. Poorter, L. Poorter, P. Poschlod, A. Prinzing, R. Proulx, A. Rammig, S. Reinsch, B. Reu, L. Sack, B. Salgado-Negret, J. Sardans, S. Shiodera, B. Shipley, A. Siefert, E. Sosinski, J.-F. Soussana, E. Swaine, N. Swenson, K. Thompson, P. Thornton, M. Waldram, E. Weiher, M. White, S. White, S. J. Wright, B. Yguel, S. Zaehle, A. E. Zanne, and C. Wirth (2011). "TRY – a Global Database of Plant Traits". In: *Glob. Change Biol.* 17.9, pp. 2905–2935. ISSN: 1365-2486. DOI: 10.1111/j.1365-2486.2011.02451.x. (Visited on 03/05/2018).
- Katze, J., W. Knorr, T. Raddatz, and C. Wirth (2009). "Quantifying Photosynthetic Capacity and Its Relationship to Leaf Nitrogen Content for Global-Scale Terrestrial Biosphere Models". In: *Glob. Change Biol.* 15.4, pp. 976–991. ISSN: 1365-2486. DOI: 10.1111/j.1365-2486.2008.01744.x. (Visited on 06/01/2022).
- Kowalewski, J. and J. Breier (2021). *PIKTools: Datasets and Functions and Data to Handle PIK-model Data*.
- Kowalewski, J., J. Breier, R. J. Hijmans, E. Pebesma, R. Bivand, O. Etteradossi, and J. Pasek (2018). *LandMark: Benchmarking Functionality for the Vegetation Model Community*.
- Kull, O. (2002). "Acclimation of Photosynthesis in Canopies: Models and Limitations". In: *Oecologia* 133.3, pp. 267–279. ISSN: 1432-1939. DOI: 10.1007/s00442-002-1042-1. (Visited on 03/07/2022).
- Lange, S. and M. Büchner (2022). *Secondary ISIMIP3b Bias-Adjusted Atmospheric Climate Input Data*. DOI: 10.48364/ISIMIP.581124.1. (Visited on 02/16/2023).
- Liu, Y., L. Wu, J. A. Baddeley, and C. A. Watson (2011). "Models of Biological Nitrogen Fixation of Legumes. A Review". In: *Agronomy Sust. Developm.* 31.1, pp. 155–172. ISSN: 1773-0155. DOI: 10.1051/agro/2010008. (Visited on 04/26/2024).
- Ma, J., S. Olin, P. Anthoni, S. S. Rabin, A. D. Bayer, S. S. Nyawira, and A. Arneith (2022). "Modeling Symbiotic Biological Nitrogen Fixation in Grain Legumes Globally with LPJ-GUESS (v4.0, R10285)". In: *Geosci. Model Dev.* 15.2, pp. 815–839. ISSN: 1991-959X. DOI: 10.5194/gmd-15-815-2022. (Visited on 02/18/2022).
- McLeod, A. I. (2022). *Kendall: Kendall Rank Correlation and Mann-Kendall Trend Test*. (Visited on 02/17/2023).
- Microsoft and S. Weston (2020). *Foreach: Provides Foreach Looping Construct*.
- Microsoft Corporation and S. Weston (2020). *doParallel: Foreach Parallel Adaptor for the 'parallel' Package*.
- Munjonji, L., K. K. Ayisi, E. I. Mudongo, T. P. Mafeo, K. Behn, M. V. Mokoka, and A. Linstädter (2020). "Disentangling Drought and Grazing Effects on Soil Carbon Stocks and CO<sub>2</sub> Fluxes in a Semi-Arid African Savanna". In: *Front. Environ. Sci.* 8. ISSN: 2296-665X. (Visited on 06/13/2022).
- Patterson, T. G. and T. A. Larue (1983). "Root Respiration Associated with Nitrogenase Activity (C<sub>2</sub>H<sub>2</sub>) of Soybean, and a Comparison of Estimates 1". In: *Plant Physiology* 72.3, pp. 701–705. ISSN: 0032-0889. DOI: 10.1104/pp.72.3.701. (Visited on 03/07/2022).
- Quested, H. M., J. H. C. Cornelissen, M. C. Press, T. V. Callaghan, R. Aerts, F. Trosien, P. Riemann, D. Gwynn-Jones, A. Kondratyuk, and S. E. Jonasson (2003). "Decomposition of Sub-Arctic Plants with Differing Nitrogen Economies: A Functional Role for Hemiparasites". In: *Ecology* 84.12, pp. 3209–3221. ISSN: 0012-9658. JSTOR: 3450065. (Visited on 06/01/2022).
- R Core Team (2019). *A Language and Environment for Statistical Computing*. R Foundation for Statistical Computing. Vienna, Austria.
- Reich, P. B., J. Oleksyn, and I. J. Wright (2009). "Leaf Phosphorus Influences the Photosynthesis–Nitrogen Relation: A Cross-Biome Analysis of 314 Species". In: *Oecologia* 160.2, pp. 207–212. ISSN: 1432-1939. DOI: 10.1007/s00442-009-1291-3. (Visited on 09/26/2018).
- Reinsch, T., R. Loges, C. Kluß, and F. Taube (2018a). "Effect of Grassland Ploughing and Reseeding on CO<sub>2</sub> Emissions and Soil Carbon Stocks". In: *Agriculture, Ecosystems & Environment* 265, pp. 374–383. ISSN: 0167-8809. DOI: 10.1016/j.agee.2018.06.020. (Visited on 06/24/2019).

## Appendix B

- Reinsch, T., R. Loges, C. Kluß, and F. Taube (2018b). “Renovation and Conversion of Permanent Grass-Clover Swards to Pasture or Crops: Effects on Annual N<sub>2</sub>O Emissions in the Year after Ploughing”. In: *Soil and Tillage Research* 175, pp. 119–129. ISSN: 0167-1987. DOI: 10.1016/j.still.2017.08.009. (Visited on 06/24/2019).
- Rolinski, S., C. Müller, J. Heinke, I. Weindl, A. Biewald, B. L. Bodirsky, A. Bondeau, E. R. Boons-Prins, A. F. Bouwman, P. A. Leffelaar, J. A. te Roller, S. Schaphoff, and K. Thonicke (2018). “Modeling Vegetation and Carbon Dynamics of Managed Grasslands at the Global Scale with LPJmL 3.6”. In: *Geosci. Model Dev.* 11.1, pp. 429–451. ISSN: 1991-9603. DOI: 10.5194/gmd-11-429-2018. (Visited on 02/27/2018).
- Ryle, G. J. A., C. E. Powell, and A. J. Gordon (1979). “The Respiratory Costs of Nitrogen Fixation in Soyabean, Cowpea, and White Clover: I. Nitrogen Fixation and the Respiration of the Nodulated Root”. In: *Journal of Experimental Botany* 30.1, pp. 135–144. ISSN: 0022-0957. DOI: 10.1093/jxb/30.1.135. (Visited on 03/07/2022).
- Schaphoff, S., W. von Bloh, A. Rammig, K. Thonicke, H. Biemans, M. Forkel, D. Gerten, J. Heinke, J. Jägermeyr, J. Knauer, F. Langerwisch, W. Lucht, C. Müller, S. Rolinski, and K. Waha (2018). “LPJmL4 – a Dynamic Global Vegetation Model with Managed Land – Part 1: Model Description”. In: *Geosci. Model Dev.* 11.4, pp. 1343–1375. ISSN: 1991-959X. DOI: 10.5194/gmd-11-1343-2018. (Visited on 05/31/2023).
- Schönbach, P., H. Wan, M. Gierus, R. Loges, K. Müller, L. Lin, A. Susenbeth, and F. Taube (2012). “Effects of Grazing and Precipitation on Herbage Production, Herbage Nutritive Value and Performance of Sheep in Continental Steppe”. In: *Grass Forage Sci.* 67.4, pp. 535–545. ISSN: 1365-2494. DOI: 10.1111/j.1365-2494.2012.00874.x. (Visited on 06/09/2022).
- Shiodera, S., J. S. Rahajoe, and T. Kohyama (2008). “Variation in Longevity and Traits of Leaves among Co-Occurring Understorey Plants in a Tropical Montane Forest”. In: *J. Trop. Ecol.* 24.2, pp. 121–133. ISSN: 1469-7831, 0266-4674. DOI: 10.1017/S0266467407004725. (Visited on 06/01/2022).
- Venables, W. N. and B. D. Ripley (2002). *Modern Applied Statistics with S*. 4th ed. New York: Springer.
- von Bloh, W., S. Schaphoff, C. Müller, S. Rolinski, K. Waha, and S. Zaehle (2018). “Implementing the Nitrogen Cycle into the Dynamic Global Vegetation, Hydrology, and Crop Growth Model LPJmL (Version 5.0)”. In: *Geosci. Model Dev.* 11.7, pp. 2789–2812. ISSN: 1991-959X. DOI: 10.5194/gmd-11-2789-2018. (Visited on 05/31/2023).
- Waring, R. H. (1983). “Estimating Forest Growth and Efficiency in Relation to Canopy Leaf Area”. In: *Advances in Ecological Research*. Ed. by A. MacFadyen and E. D. Ford. Vol. 13. Academic Press, pp. 327–354. DOI: 10.1016/S0065-2504(08)60111-7. (Visited on 06/13/2022).
- Waring, R. H. and W. H. Schlesinger (1985). *Forest Ecosystems: Concepts and Management*. Orlando, Florida: Academic Press.
- Weigelt, A., L. Mommer, K. Andrzejek, C. M. Iversen, J. Bergmann, H. Bruelheide, Y. Fan, G. T. Freschet, N. R. Guerrero-Ramírez, J. Kattge, T. W. Kuyper, D. C. Laughlin, I. C. Meier, F. van der Plas, H. Poorter, C. Roumet, J. van Ruijven, F. M. Sabatini, M. Semchenko, C. J. Sweeney, O. J. Valverde-Barrantes, L. M. York, and M. L. McCormack (2021). “An Integrated Framework of Plant Form and Function: The Belowground Perspective”. In: *New Phytol.* 232.1, pp. 42–59. ISSN: 1469-8137. DOI: 10.1111/nph.17590. (Visited on 11/23/2021).
- Wickham, H. (2007). *Reshaping Data with the reshape Package*.
- Wickham, H. (2011). “The Split-Apply-Combine Strategy for Data Analysis”. In: *J. Stat. Softw.* 40.1, pp. 1–29.
- Wickham, H., M. Averick, J. Bryan, W. Chang, L. D. McGowan, R. François, G. Grolemund, A. Hayes, L. Henry, J. Hester, M. Kuhn, T. L. Pedersen, E. Miller, S. M. Bache, K. Müller, J. Ooms, D. Robinson, D. P. Seidel, V. Spinu, K. Takahashi, D. Vaughan, C. Wilke, K. Woo, and H. Yutani (2019). “Welcome to the Tidyverse”. In: *J. Open Source Softw.* 4.43, p. 1686. ISSN: 2475-9066. DOI: 10.21105/joss.01686. (Visited on 02/17/2023).
- Wiesmeier, M., F. Barthold, B. Blank, and I. Kögel-Knabner (2011). “Digital Mapping of Soil Organic Matter Stocks Using Random Forest Modeling in a Semi-Arid Steppe Ecosystem”. In: *Plant Soil* 340.1, pp. 7–24. ISSN: 1573-5036. DOI: 10.1007/s11104-010-0425-z. (Visited on 02/16/2022).
- Wilke, C. O. (2020). *Cowplot: Streamlined Plot Theme and Plot Annotations for 'Ggplot2'*.
- Wright, I. J., P. B. Reich, M. Westoby, D. D. Ackerly, Z. Baruch, F. Bongers, J. Cavender-Bares, T. Chapin, J. H. C. Cornelissen, M. Diemer, J. Flexas, E. Garnier, P. K. Groom, J. Gulias, K. Hikosaka, B. B. Lamont, T. Lee, W. Lee, C. Lusk, J. J. Midgley, M.-L. Navas, U. Niinemets, J. Oleksyn, N. Osada, H. Poorter, P. Poot, L. Prior, V. I. Pyankov, C. Roumet, S. C. Thomas, M. G. Tjoelker, E. J. Veneklaas, and R. Villar (2004). “The Worldwide Leaf Economics Spectrum”. In: *Nature* 428.6985, pp. 821–827. ISSN: 1476-4687. DOI: 10.1038/nature02403.
- Yu, T. and Q. Zhuang (2020). “Modeling Biological Nitrogen Fixation in Global Natural Terrestrial Ecosystems”. In: *Biogeosciences* 17.13, pp. 3643–3657. ISSN: 1726-4170. DOI: 10.5194/bg-17-3643-2020. (Visited on 02/18/2022).

# Appendix C

Appendix C contains the supplementary information for Chapter 4 Biological nitrogen fixation of natural and agricultural vegetation simulated with LPJmL 5.7.9.

## C.1 Nitrogen demand and uptake

The total N demand ( $N_{\text{demand}}$  in  $\text{gN m}^{-2}$ ) at any time  $t$  is the sum of the leaf N demand for RuBisCo and structural components ( $N_{\text{demand,leaf}}$  in  $\text{gN m}^{-2}$ ) and the N demand for structural components of the other plant compartments.

$$N_{\text{demand,leaf}} = 25 \cdot 0.02314815 / \text{daylength} \cdot V_{\text{max}} \cdot \exp(-0.02 \cdot (T - 25)) \cdot f_{\text{LAI}}(\text{LAI}) + NC_{\text{leaf,median}} \cdot C_{\text{leaf},t}, \quad (\text{C.1})$$

where  $V_{\text{max}}$  ( $\text{g C m}^{-2}$ ) is the PFT-specific maximum carboxylation capacity computed based on absorbed photosynthetically active radiation (APAR) and canopy conductance (Schaphoff et al., 2018; Sitch et al., 2003).  $T$  is the average temperature ( $^{\circ}\text{C}$ ) of the current day, and daylength is the duration of daylight (h).  $f_{\text{LAI}}(\text{LAI})$  is a dimensionless modifier to account for the current leaf area index (von Bloh et al., 2018), and  $C_{\text{leaf}}$  ( $\text{g C m}^{-2}$ ) is the current leaf C content.

$$f_{\text{LAI}}(\text{LAI}) = \begin{cases} \max(0.1, \text{LAI}) & \text{for LAI} < 1 \\ \exp(0.08 \cdot \min(\text{LAI}, 7)) & \text{otherwise,} \end{cases} \quad (\text{C.2})$$

$$C_{\text{leaf},t} = C_{\text{leaf}} + f_{\text{leaf}} \cdot \sum_{t'=1}^t \text{NPP}_{t'} - \Delta \text{litter}_{t'}. \quad (\text{C.3})$$

LAI is the current leaf area index, and  $\sum_{t'=1}^t \text{NPP}_{t'} - \Delta \text{litter}_{t'}$  is the difference between the accumulated biomass increment and litterfall.

$$N_{\text{demand},t} = \left( N_{\text{demand,leaf}} + \sum_{m=1}^M N_m + NC_t \cdot \sum_{m=1}^M (f_m / R_m) \cdot \sum_{t'=1}^t \text{NPP}_{t'} - \Delta \text{litter}_{t'} \right) \cdot (1 + k_{\text{store}}), \quad (\text{C.4})$$

where  $M$  is one for grasses, two for trees and three for crops, equalling the number of the respective PFT plant compartments and excluding leaves,  $NC_t = \min(\max(N_{\text{leaf},t} / C_{\text{leaf},t}, NC_{\text{leaf,low}}), NC_{\text{leaf,high}})$ .  $f_m$  is the fraction of biomass allocated to the compartment  $m$ ,  $R_m$  is the C : N ratio of compartment  $m$  relative to the leaf C : N ratio, and  $k_{\text{store}}$  is a PFT-specific parameter to maintain the PFT labile N storage. Passive and active N uptake ( $N_{\text{uptake}}$ ) from each soil layer  $l$  ( $n_{\text{soillayer}} = 6$ ) is calculated as a

Table C.1: PFT-specific parameters used in N-demand and N-uptake calculations.

PFT	NC <sub>leaf</sub>			R <sub>m</sub>				k <sub>store</sub>	N <sub>up,root</sub>	β <sub>root</sub>	k <sub>N,min</sub>	K <sub>n,min</sub>
	Low	Median	High	Root	Sap-wood	Storage organ	Pool					
	–	–	–	–	–	–	–	–	gN gC <sup>-1</sup> d <sup>-1</sup>	–	–	gN m <sup>-2</sup> gN m <sup>-2</sup>
TrBE	15.6	26.8	46.2	1.16	13.5	–	–	0.1	2.8	0.952	0.05	1.48
TrBR	15.4	23.1	34.6	1.16	13.5	–	–	0.1	2.8	0.981	0.05	1.48
TeNE	31.8	45.0	63.8	1.16	13.5	–	–	0.1	2.8	0.976	0.05	1.48
TeBE	15.6	26.8	46.2	1.16	13.5	–	–	0.1	2.8	0.964	0.05	1.48
TeBS	15.4	23.1	34.6	1.16	13.5	–	–	0.1	2.8	0.966	0.05	1.48
BoNE	31.8	45.0	63.8	1.16	13.5	–	–	0.1	2.8	0.955	0.05	1.48
BoBS	15.4	23.1	34.6	1.16	13.5	–	–	0.1	2.8	0.955	0.05	1.48
BoNS	18.4	26.0	36.9	1.16	13.5	–	–	0.1	2.8	0.955	0.05	1.48
TrH	17.4	34.0	66.9	1.16	–	–	–	0.05	5.51	0.973	0.05	1.19
TeH	10.5	19.9	37.9	1.16	–	–	–	0.05	5.51	0.943	0.05	1.19
PoH	10.5	19.9	37.9	1.16	–	–	–	0.05	5.51	0.943	0.05	1.19
Soybean	14.3	25.0	58.8	1.16	–	0.42	3	0.1	5.51	0.969	0.05	1.48
Pulses	14.3	25.0	58.8	1.16	–	0.42	3	0.1	5.51	0.969	0.05	1.48

function of the potential N uptake of the root system.

$$N_{\text{uptake}} = \sum_{l=1}^{n_{\text{soil layer}}} 2 \cdot N_{\text{up,root}} \cdot C_{\text{root},t} \cdot \text{rootdist}_l \cdot f_N(N_{\text{avail},l}) \cdot f_T(T_{\text{soil},l}) \cdot f_{\text{NC}}(\text{NC}_{\text{plant}}), \quad (\text{C.5})$$

where  $N_{\text{up,root}}$  is the PFT-specific maximum N-uptake rate per unit of fine root mass in each layer,  $C_{\text{root},t}$  is the current root C,  $\text{rootdist}_l$  is the fraction of roots in layer  $l$ .  $f_N$ ,  $f_T$  and  $f_{\text{NC}}$  are dimensionless modifiers for the availability of mineral N, soil temperature and plant N : C ratio (von Bloh et al., 2018).  $C_{\text{root},t}$  is calculated as  $C_{\text{leaf},t}$  in Eq. (C.3). The root distribution can be calculated from the proportion of roots from the surface to soil depth  $z$ , following Jackson et al. (1996):

$$\text{rootdist}_z = \frac{1 - \beta_{\text{root}}^z}{1 - \beta_{\text{root}}^{z_{\text{bottom}}}}, \quad (\text{C.6})$$

where  $z_{\text{bottom}}$  is the lower boundary of the last soil layer and  $\beta_{\text{root}}$  is a PFT-specific parameter (Table C.1). The root proportion of one soil layer can be calculated as

$$\text{rootdist}_l = \text{rootdist}_{z(l)} - \text{rootdist}_{z(l-1)}. \quad (\text{C.7})$$

$f_N$  follows Michaelis–Menten kinetics,

$$f_N(N_{\text{avail},l}) = k_{N,\text{min}} + \frac{N_{\text{avail},l}}{N_{\text{avail},l} + K_{N,\text{min}} \cdot \Theta_{\text{max}} \cdot d_{\text{soil}}}, \quad (\text{C.8})$$

where  $N_{\text{avail},l} = \text{NO}_{3,\text{soil},l}^- + \text{NH}_{4,\text{soil},l}^+$ ,  $k_{N,\text{min}}$  and  $K_{N,\text{min}}$  are the PFT-specific parameters describing the Michaelis–Menten kinetics.  $\Theta_{\text{max}}$  is the soil-type-specific fractional pore space, and  $d_{\text{soil},l}$  (dimensionless) is the soil layer depth (m).

$f_T$  is the temperature function given by Thornley (1991)

$$f_T(T_{\text{soil},l}) = \max\left(\frac{(T_{\text{soil},l} - T_0) \cdot (2 \cdot T_m - T_0 - T_{\text{soil},l})}{(T_r - T_0) \cdot (2 \cdot T_m - T_0 - T_r)}, 0\right), \quad (\text{C.9})$$

where  $T_0 < T_r < 2 \cdot T_m - T_0$  has to be fulfilled. von Bloh et al. (2018) defined  $T_m = 15^\circ\text{C}$ ,  $T_r = 15^\circ\text{C}$  and  $T_0 = -25^\circ\text{C}$ , which leads to the maximum of one at temperatures of  $15^\circ\text{C}$  and higher and non-zero values above  $-25^\circ\text{C}$ .

$f_{\text{NC}}$  was taken from Zaehle et al. (2010),

$$f_{\text{NC}} = \min\left(\max\left(\frac{\text{NC}_{\text{plant}} - \text{NC}_{\text{leaf,high}}}{\text{NC}_{\text{leaf,low}} - \text{NC}_{\text{leaf,high}}}, 0\right), 1\right), \quad (\text{C.10})$$

where  $\text{NC}_{\text{plant}} = \frac{N_{\text{leaf}} + N_{\text{root}}}{C_{\text{leaf}} + C_{\text{root}}}$ ,  $\text{NC}_{\text{leaf,min}}$  and  $\text{NC}_{\text{leaf,max}}$  are PFT-specific parameters extracted from the TRY database (Kattge et al., 2020) (Table C.1).

The labile-N values  $N_{\text{labile},t}$  are the current reserves which have accumulated via N uptake and retranslocation.

$$N_{\text{labile},t} = N_{\text{labile}} + \sum_{t'=1}^t N_{\text{uptake},t'} - N_{\text{resorb},t'} \quad (\text{C.11})$$

## C.2 Spin-up simulation carbon stocks

With constant forcing (i.e. stable pre-industrial atmospheric  $\text{CO}_2$  concentration, atmospheric N deposition and climate), the global C stocks showed a residual trend of  $-0.0106 \text{ PgC yr}^{-1}$  for the Original approach and  $-0.0121 \text{ PgC yr}^{-1}$  for the C-costly approach. This is 8–10 times lower than the steady-state criterion of the  $0.1 \text{ PgC yr}^{-1}$  residual trend after spin-up, which is used by the Global Carbon Project to validate DGVMs for inclusion in their global C budget analysis (Friedlingstein et al., 2022). At the grid cell level, the vast majority of cells (94 % for the Original approach and 95 % for the C-costly approach) exhibited residual trends in total C stocks of less than  $\pm 1 \text{ gC m}^{-2} \text{ yr}^{-1}$ . The corresponding maps are shown in Fig. C.1.

## Appendix C

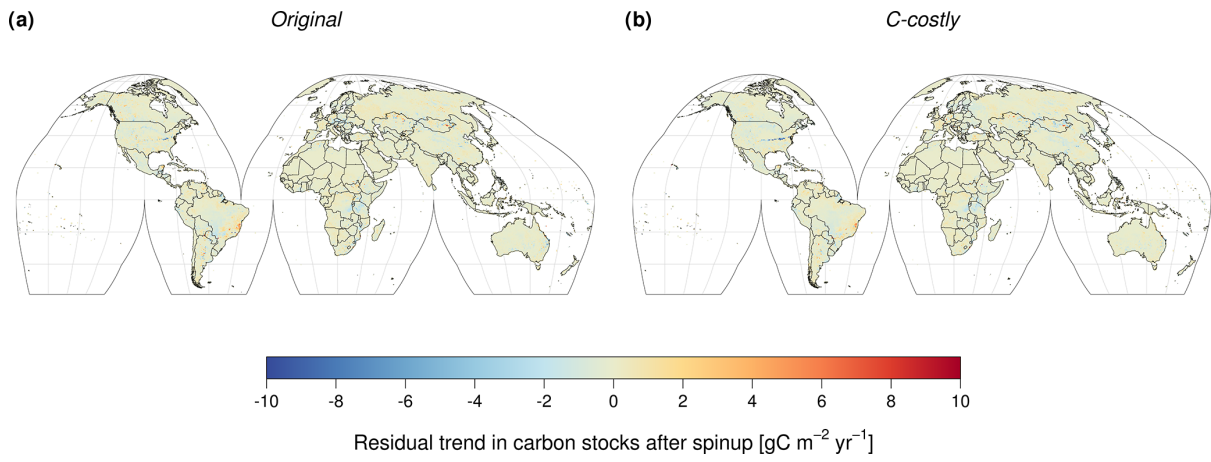


Figure C.1: Residual trends in C stocks after the spin-up simulation averaged over 1000 years for the Original approach (a) and the C-costly (b) approach.

### C.3 Additional figures and tables

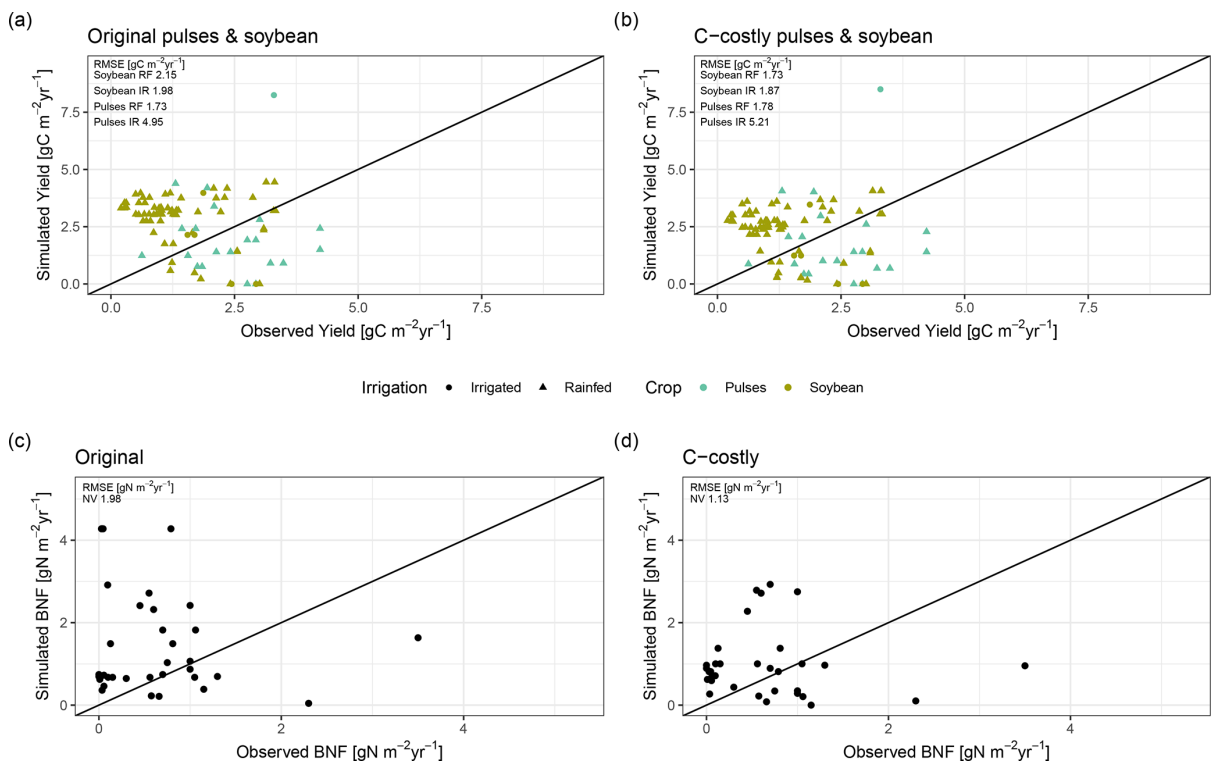


Figure C.2: Simulated and observed crop yields (a, b) for soybean (green) and pulses (blue) and BNF in natural vegetation (c, d).

## Appendix C

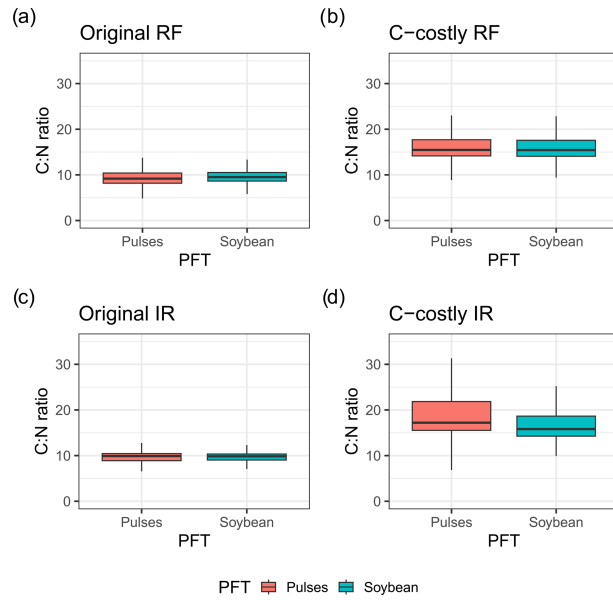


Figure C.3: Vegetation C : N ratio for the years 2001 to 2010 for rainfed (RF) and irrigated (IR) soybean (red) and pulses (blue) for the Original approach and C-costly approach.

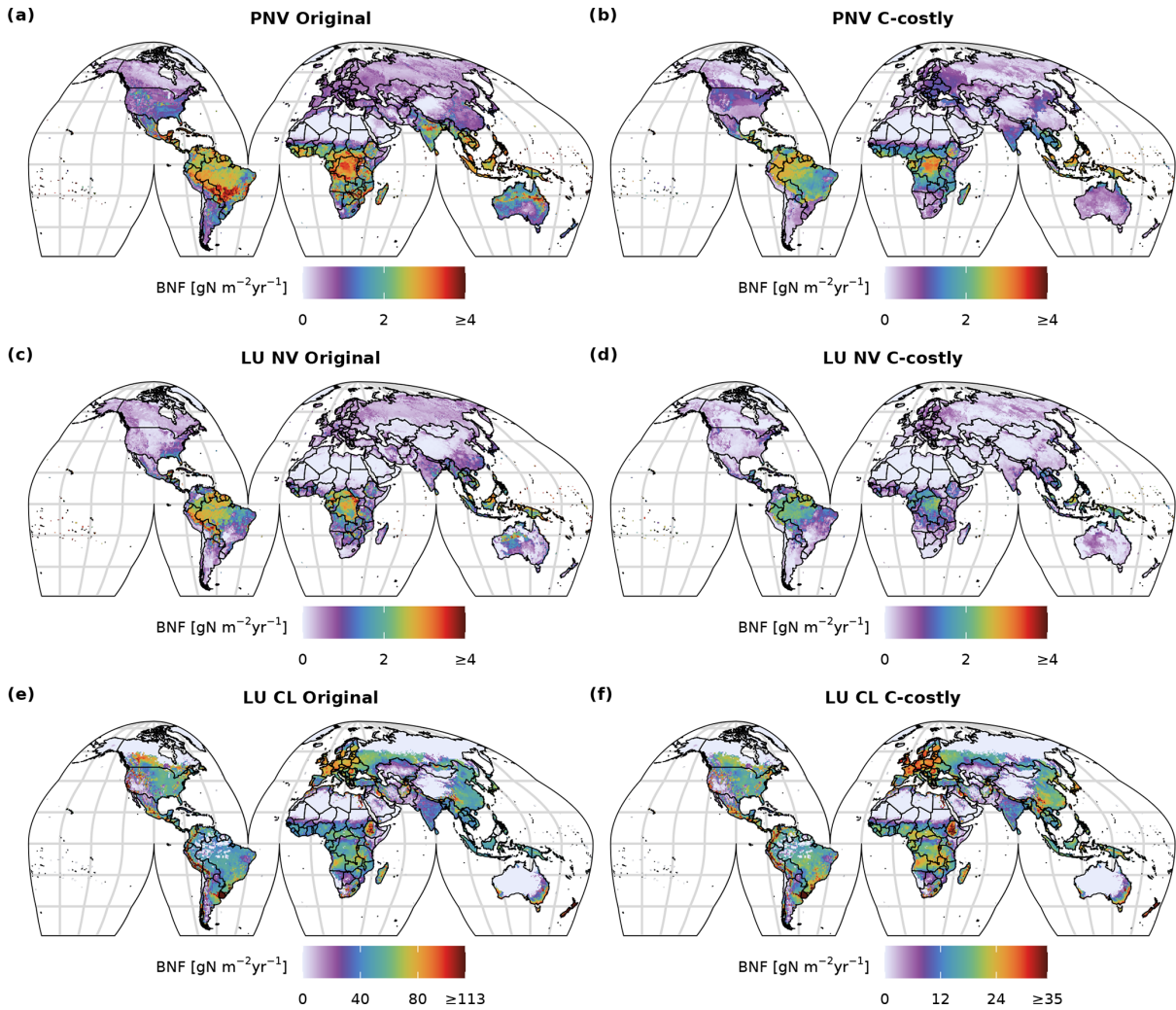


Figure C.4: The 2001 to 2010 average BNF (in gN m<sup>-2</sup> yr<sup>-1</sup>) of the potential natural vegetation (PNV) simulations (a, b), of the natural vegetation (NV) (c, d) and of the managed land (AG) (e, f) area fractions of the dynamic land-use (LU) simulations.

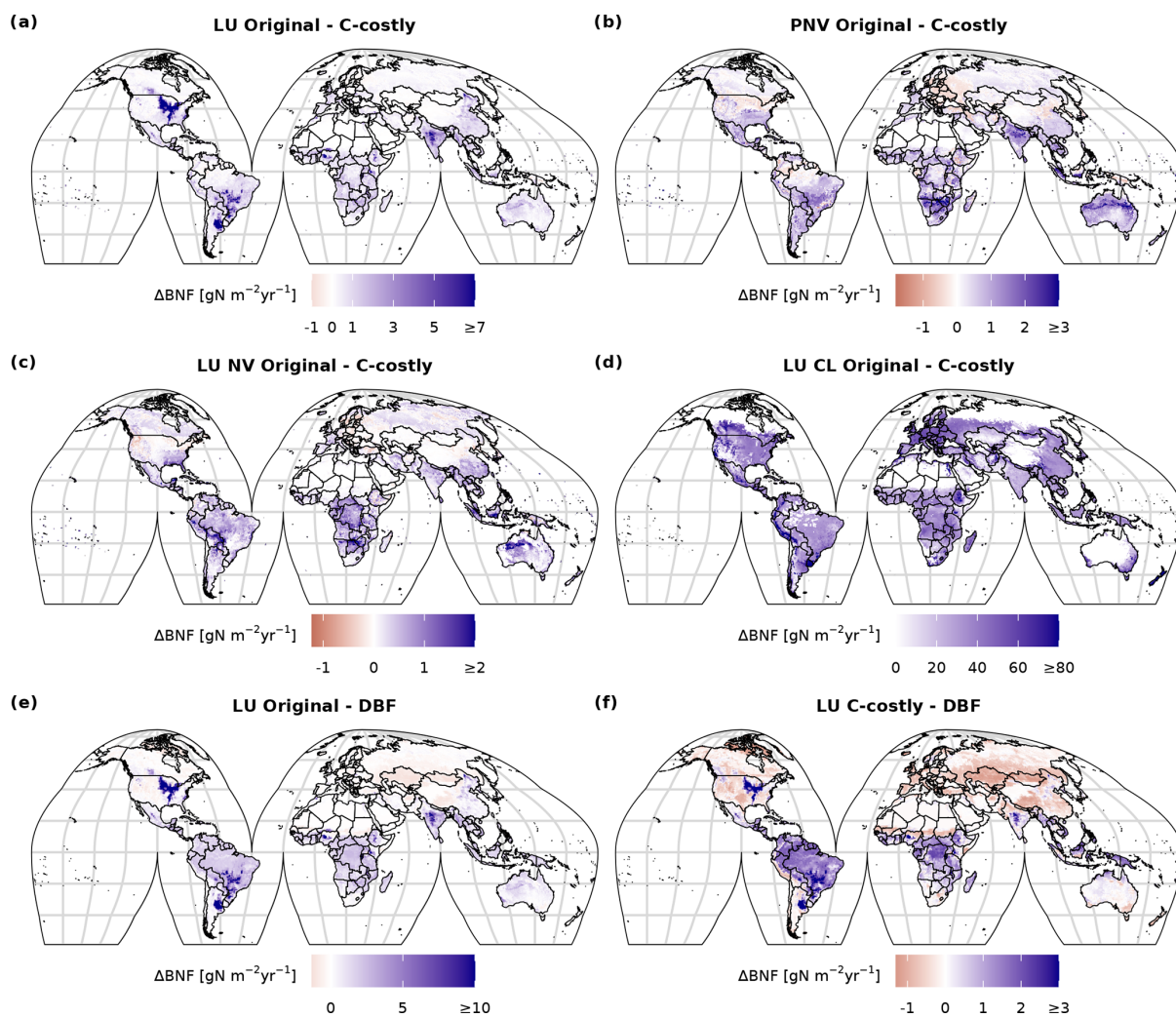


Figure C.5: Difference between 2001 to 2010 average BNF (in  $\text{gN m}^{-2}\text{yr}^{-1}$ ) between the two approaches (**a–d**) for the dynamic land-use (LU) simulations (**a**), for the potential natural vegetation (PNV) simulations (**b**), for the area fractions of natural vegetation (NV) (**c**) and for the managed land (AG) (**e**) of the dynamic land-use simulations and the difference compared to the data from Davies-Barnard and Friedlingstein (2020) (DBF) (**e, f**).

## Appendix C

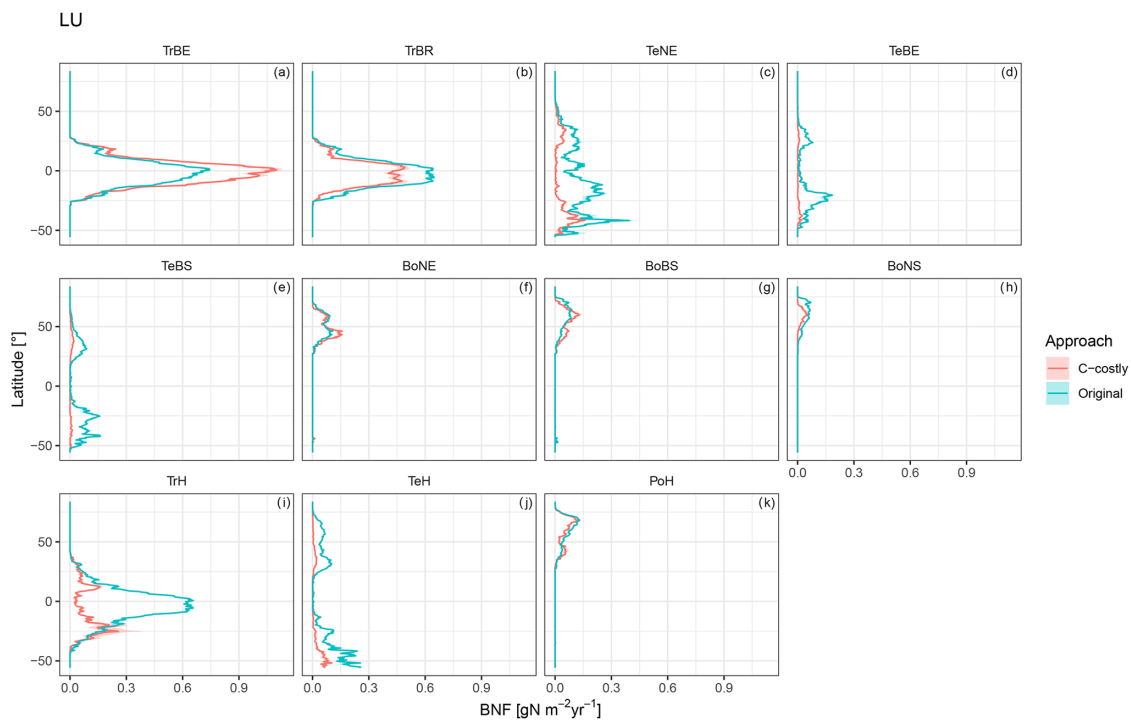


Figure C.6: Latitudinal distribution of BNF for each PFT for the dynamic land-use simulations for the Original approach (red) and C-costly approach (blue).

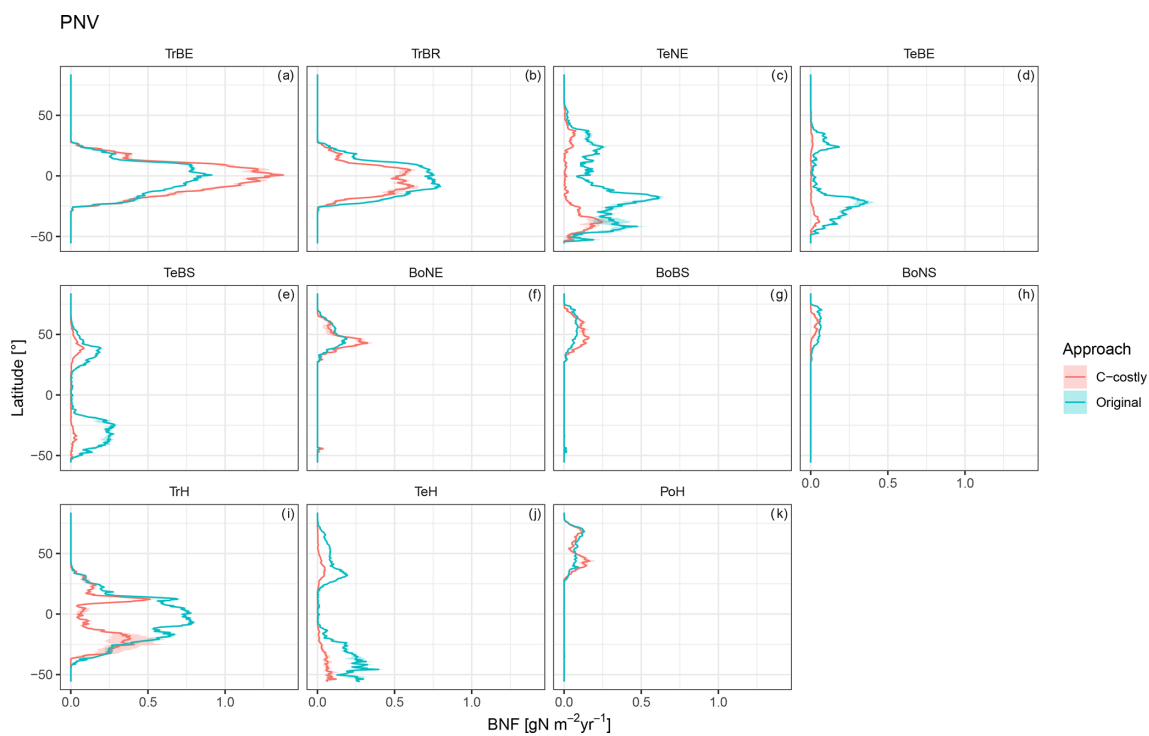


Figure C.7: Latitudinal distribution of BNF for each PFT for the potential natural vegetation simulations for the Original approach (red) and C-costly approach (blue).

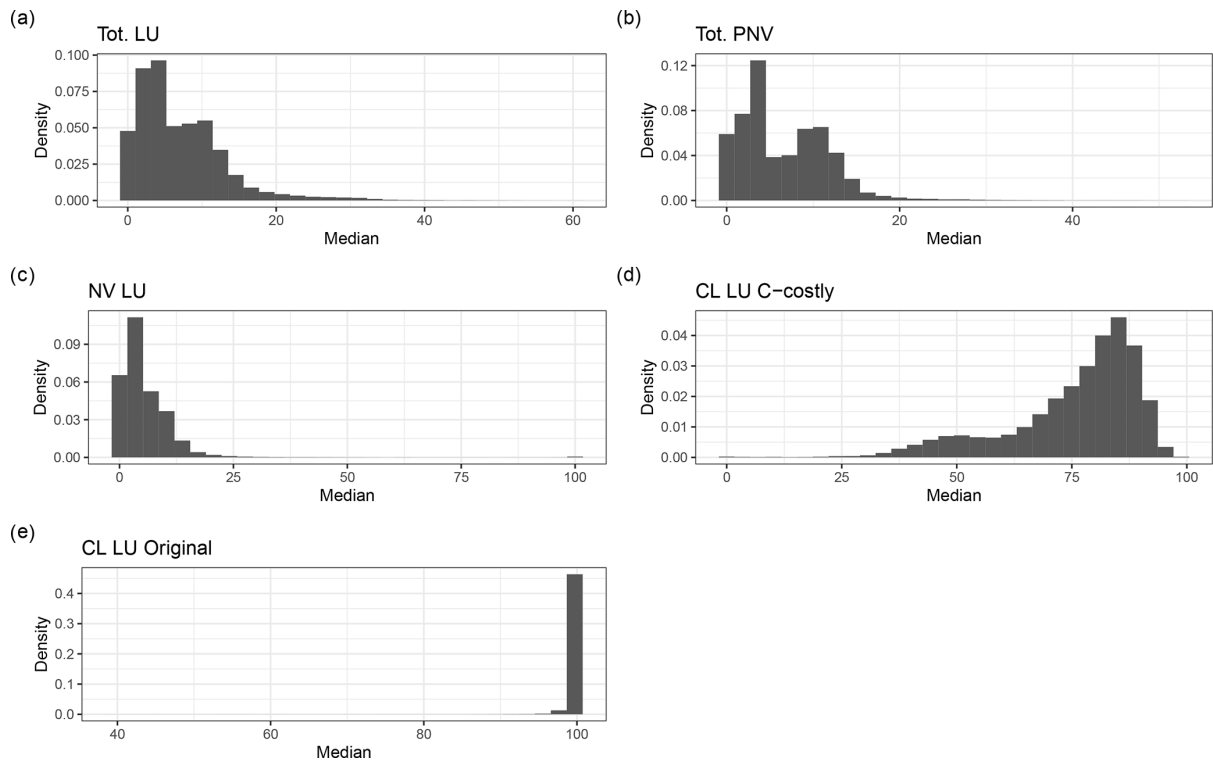


Figure C.8: Density distribution of the fraction of BNF of the total N uptake for the dynamic land-use simulations (a), for the potential natural vegetation (b) and for the area fractions of natural vegetation (NV) (c) and cropland (CL), using the C-costly approach (d) and the Original (e) approach for the dynamic land-use simulations.

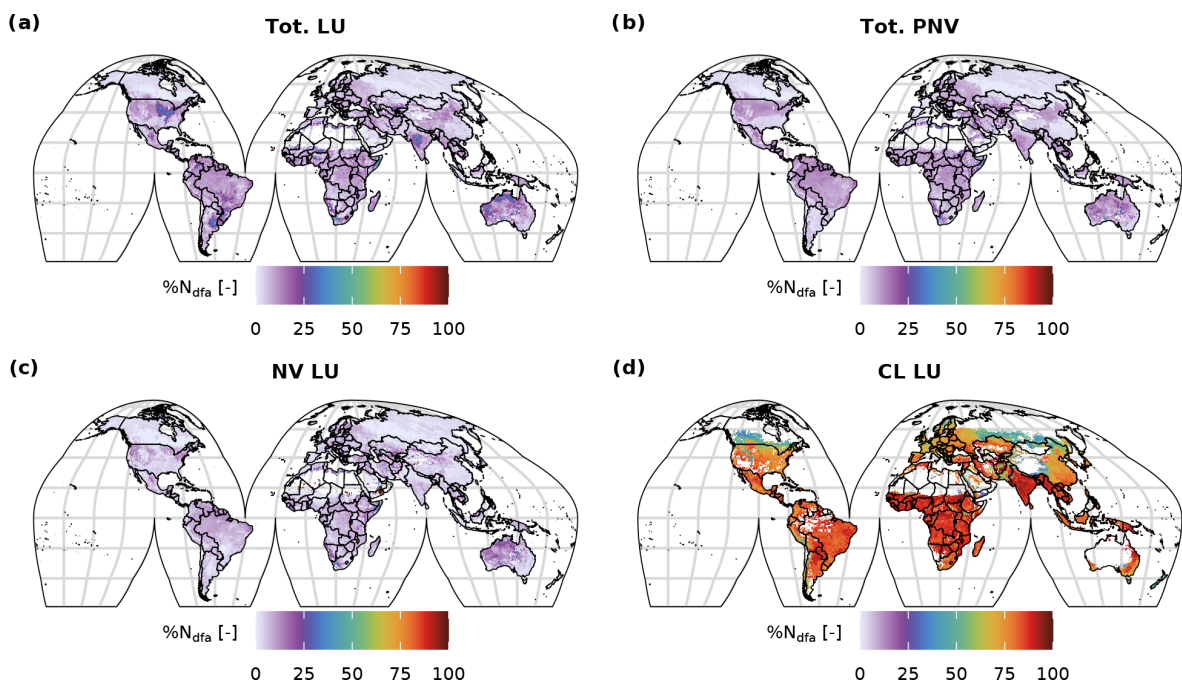


Figure C.9: Global distribution of the fraction of  $\%N_{dfa}$  for the dynamic land-use (a), for the potential natural vegetation simulations (b) and the natural vegetation (c) and cropland (d) fraction of the dynamic land-use simulation.

## Appendix C

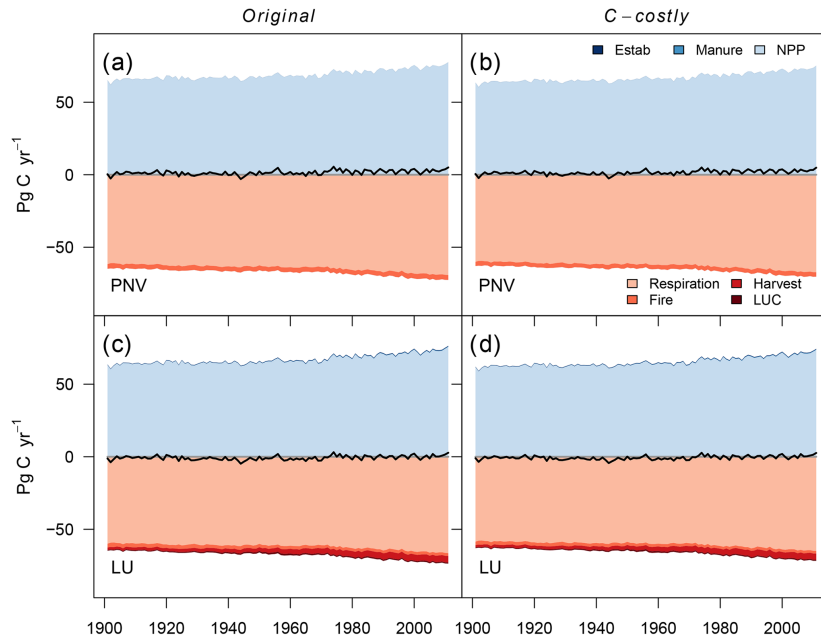


Figure C.10: Global terrestrial C balance. Scenarios include the Original approach and the C-costly approach for natural vegetation and actual land use. The net balance is denoted by the black line. C inputs include C from manure, PFT establishment (Estab) and NPP. C losses include heterotrophic respiration, fire emissions, harvested C and land-use change emissions (from deforestation and product turnover).

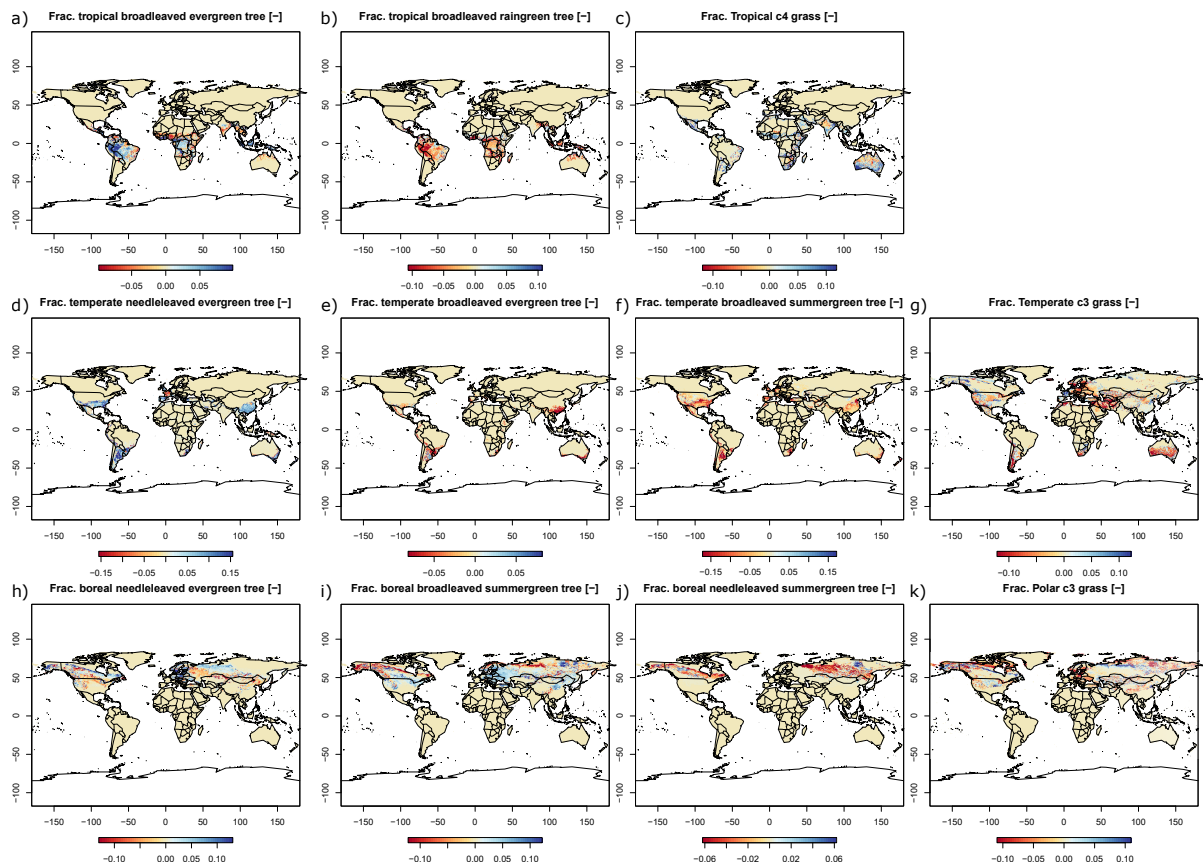


Figure C.11: Difference of foliage projective cover in  $\text{m}^2 \text{m}^{-2}$  between the C-costly and the Original BNF approach for dynamic land use simulation and each plant functional type (PFT).

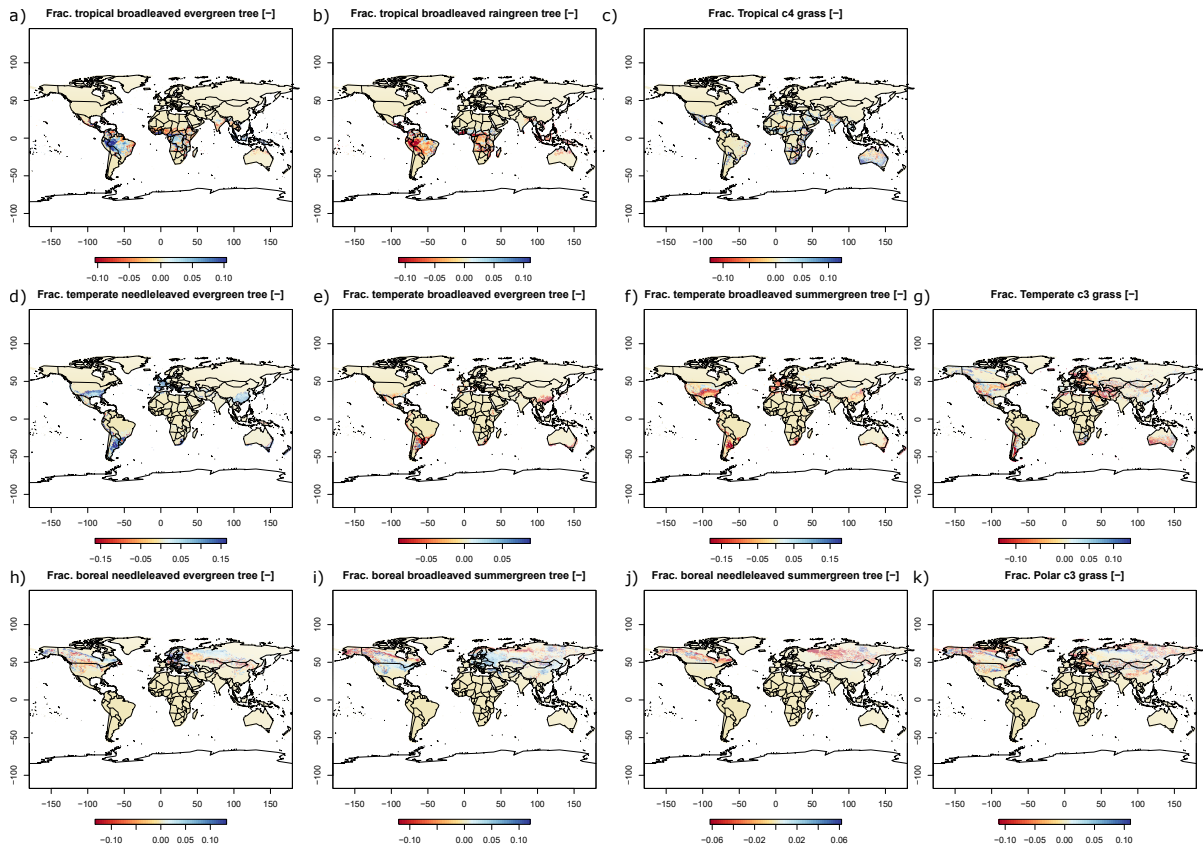


Figure C.12: Difference of foliage projective cover in  $\text{m}^2 \text{m}^{-2}$  between the C-costly and the Original BNF approach for potential natural vegetation simulation and each plant functional type (PFT).

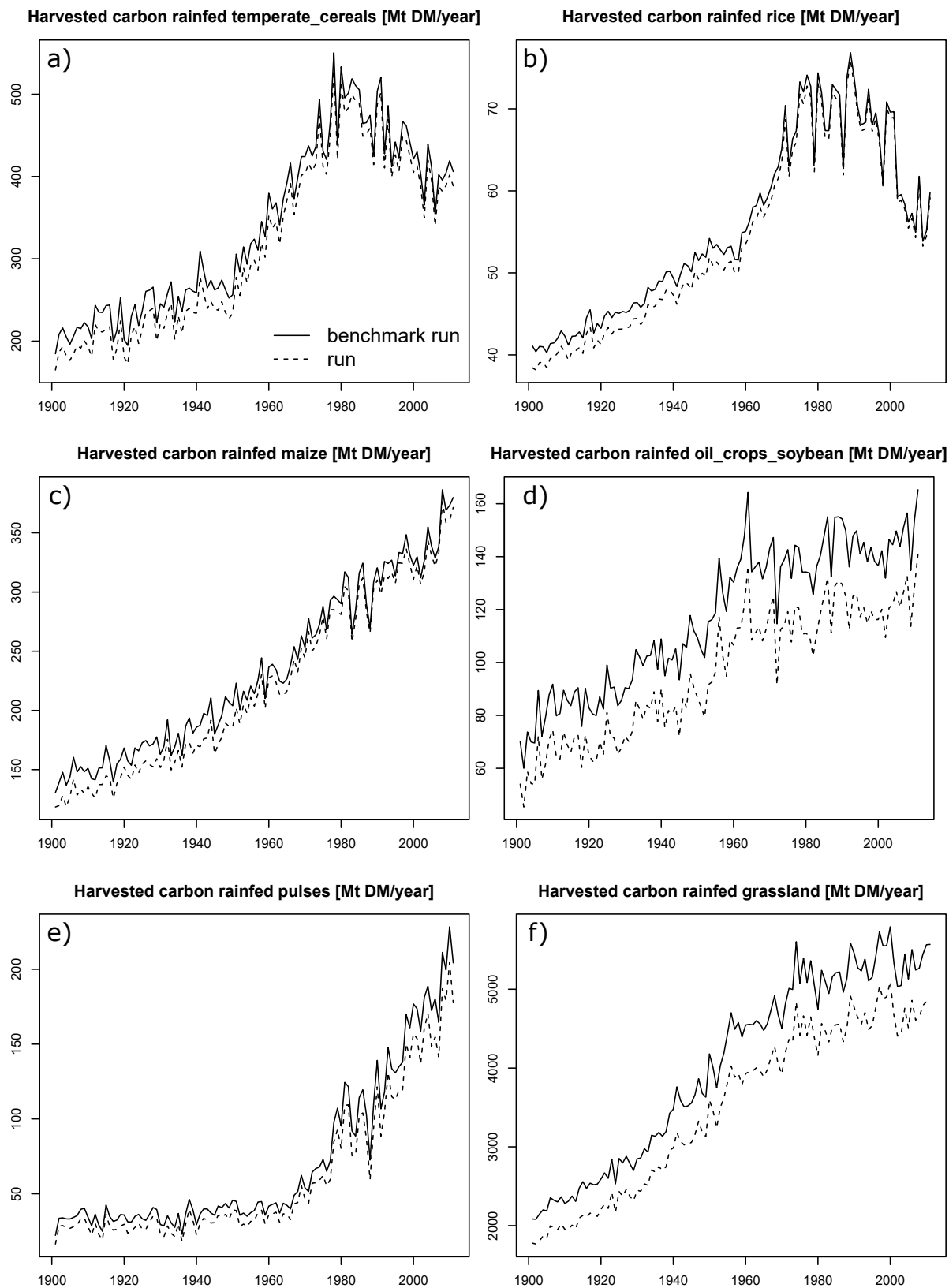


Figure C.13: Global sums of harvested carbon from 1901 to 2011 for rainfed temperate cereals (a), rice (b), maize (c), soybean (d), pulses (e) and managed grasslands (f)

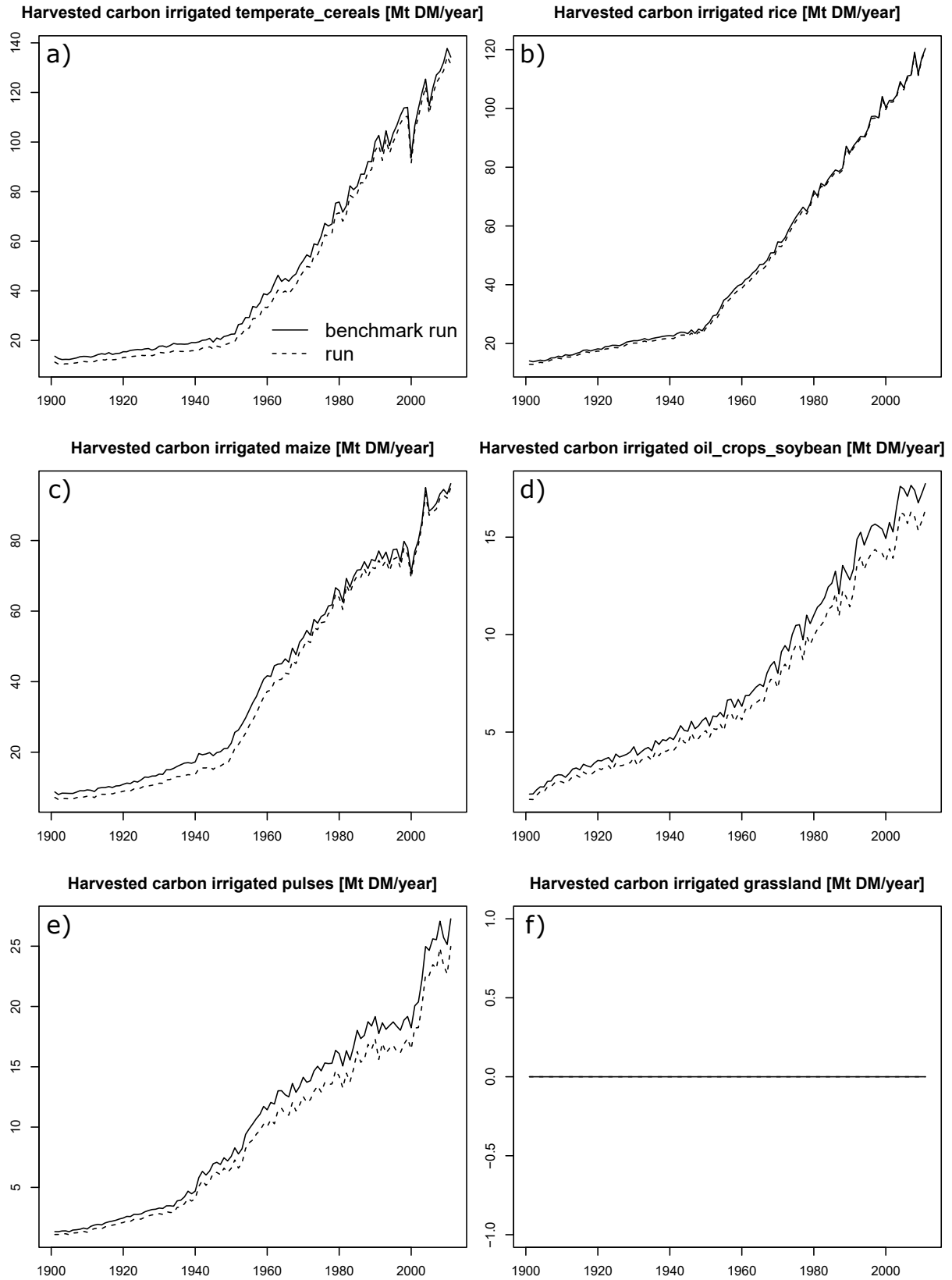


Figure C.14: Global sums of harvested carbon from 1901 to 2011 for irrigated temperate cereals (a), rice (b), maize (c), soybean (d), pulses (e) and managed grasslands (f)

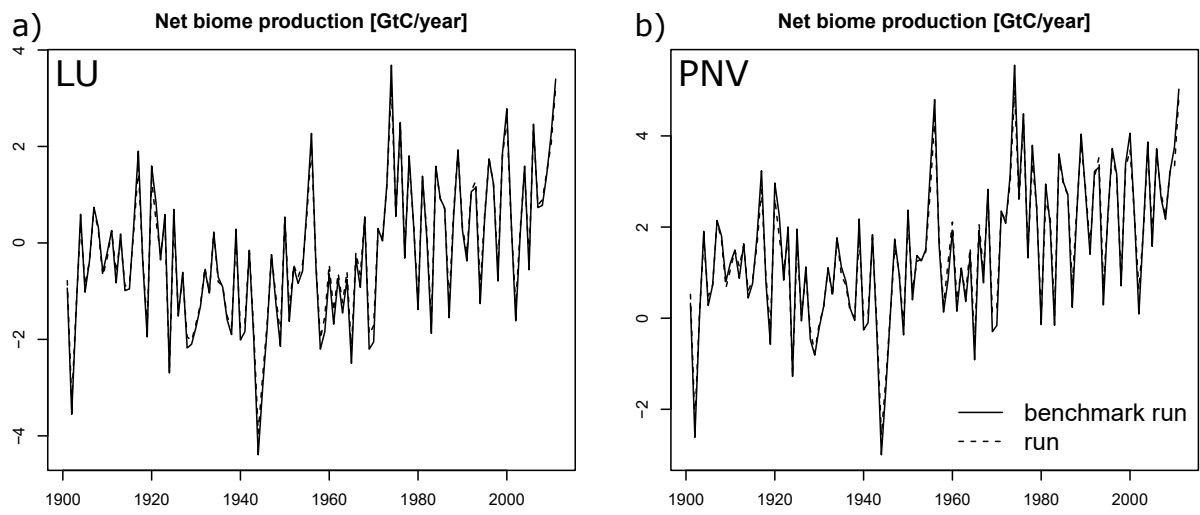


Figure C.15: Global sum of net biome production from 1901 until 2011 for the dynamic land use (LU) (a) and potential natural vegetation (PNV) simulation (b)

## C.4 References

- Davies-Barnard, T. and P. Friedlingstein (2020). *Data: The Global Distribution of Biological Nitrogen Fixation in Terrestrial Natural Ecosystems*. DOI: 10.24378/exe.2063. (Visited on 02/06/2023).
- Friedlingstein, P., M. O'Sullivan, M. W. Jones, R. M. Andrew, L. Gregor, J. Hauck, C. Le Quéré, I. T. Luijckx, A. Olsen, G. P. Peters, W. Peters, J. Pongratz, C. Schwingshackl, S. Sitch, J. G. Canadell, P. Ciais, R. B. Jackson, S. R. Alin, R. Alkama, A. Arneeth, V. K. Arora, N. R. Bates, M. Becker, N. Bellouin, H. C. Bittig, L. Bopp, F. Chevallier, L. P. Chini, M. Cronin, W. Evans, S. Falk, R. A. Feely, T. Gasser, M. Gehlen, T. Gkritzalis, L. Gloege, G. Grassi, N. Gruber, Ö. Gürses, I. Harris, M. Hefner, R. A. Houghton, G. C. Hurtt, Y. Iida, T. Ilyina, A. K. Jain, A. Jersild, K. Kadono, E. Kato, D. Kennedy, K. Klein Goldewijk, J. Knauer, J. I. Korsbakken, P. Landschützer, N. Lefèvre, K. Lindsay, J. Liu, Z. Liu, G. Marland, N. Mayot, M. J. McGrath, N. Metz, N. M. Monacci, D. R. Munro, S.-I. Nakaoka, Y. Niwa, K. O'Brien, T. Ono, P. I. Palmer, N. Pan, D. Pierrot, K. Pocock, B. Poulter, L. Resplandy, E. Robertson, C. Rödenbeck, C. Rodriguez, T. M. Rosan, J. Schwinger, R. Séférian, J. D. Shutler, I. Skjelvan, T. Steinhoff, Q. Sun, A. J. Sutton, C. Sweeney, S. Takao, T. Tanhua, P. P. Tans, X. Tian, H. Tian, B. Tilbrook, H. Tsujino, F. Tubiello, G. R. van der Werf, A. P. Walker, R. Wanninkhof, C. Whitehead, A. Willstrand Wranne, R. Wright, W. Yuan, C. Yue, X. Yue, S. Zaehle, J. Zeng, and B. Zheng (2022). "Global Carbon Budget 2022". In: *Earth Syst. Sci. Data* 14.11, pp. 4811–4900. ISSN: 1866-3508. DOI: 10.5194/essd-14-4811-2022. (Visited on 11/14/2023).
- Jackson, R. B., J. Canadell, J. R. Ehleringer, H. A. Mooney, O. E. Sala, and E. D. Schulze (1996). "A Global Analysis of Root Distributions for Terrestrial Biomes". In: *Oecologia* 108.3, pp. 389–411. ISSN: 0029-8549, 1432-1939. DOI: 10.1007/BF00333714. (Visited on 03/01/2018).
- Kattge, J., G. Bönisch, S. Díaz, S. Lavorel, I. C. Prentice, P. Leadley, S. Tautenhahn, G. D. A. Werner, T. Aakala, M. Abedi, A. T. R. Acosta, G. C. Adamidis, K. Adamson, M. Aiba, C. H. Albert, J. M. Alcántara, C. Alcázar C, I. Aleixo, H. Ali, B. Amiaud, C. Ammer, M. M. Amoroso, M. Anand, C. Anderson, N. Anten, J. Antos, D. M. G. Apgaua, T.-L. Ashman, D. H. Asmara, G. P. Asner, M. Aspinwall, O. Atkin, I. Aubin, L. Bastrup-Spohr, K. Bahalkeh, M. Bahn, T. Baker, W. J. Baker, J. P. Bakker, D. Baldocchi, J. Baltzer, A. Banerjee, A. Baranger, J. Barlow, D. R. Barneche, Z. Baruch, D. Bastianelli, J. Battles, W. Bauerle, M. Bauters, E. Bazzato, M. Beckmann, H. Beeckman, C. Beierkuhnlein, R. Bekker, G. Belfry, M. Belluau, M. Beloiu, R. Benavides, L. Benomar, M. L. Berdugo-Lattke, E. Berenguer, R. Bergamin, J. Bergmann, M. Bergmann Carlucci, L. Berner, M. Bernhardt-Römermann, C. Bigler, A. D. Bjorkman, C. Blackman, C. Blanco, B. Blonder, D. Blumenthal, K. T. Bocanegra-González, P. Boeckx, S. Bohlman, K. Böhning-Gaese, L. Boisvert-Marsh, W. Bond, B. Bond-Lamberty, A. Boom, C. C. F. Boonman, K. Bordin, E. H. Boughton, V. Boukili, D. M. J. S. Bowman, S. Bravo, M. R. Brendel, M. R. Broadley, K. A. Brown, H. Bruelheide, F. Brumlich, H. H. Bruun, D. Bruy, S. W. Buchanan, S. F. Bucher, N. Buchmann, R. Buitenwerf, D. E. Bunker, J. Bürger, S. Burrascano, D. F. R. P. Burslem, B. J. Butterfield, C. Byun, M. Marques, M. C. Scalon, M. Caccianiga, M. Cadotte, M. Cailleret, J. Camac, J. J. Camarero, C. Company, G. Campetella, J. A. Campos, L. Cano-Arboleda, R. Canullo, M. Carbognani, F. Carvalho, F. Casanoves, B. Castagneyrol, J. A. Catford, J. Cavender-Bares, B. E. L. Cerabolini, M. Cervellini, E. Chacón-Madrigal, K. Chapin, F. S. Chapin, S. Chelli, S.-C. Chen, A. Chen, P. Cherubini, F. Chianucci, B. Choat, K.-S. Chung, M. Chytrý, D. Ciccarelli, L. Coll, C. G. Collins, L. Conti, D. Coomes, J. H. C. Cornelissen, W. K. Cornwell, P. Corona, M. Coyea, J. Craine, D. Craven, J. P. G. M. Crowsigt, A. Csecserits, K. Cufar, M. Cuntz, A. C. da Silva, K. M. Dahlin, M. Dainese, I. Dalke, M. Dalle Fratte, A. T. Dang-Le, J. Danihelka, M. Dannoura, S. Dawson, A. J. de Beer, A. De Frutos, J. R. De Long, B. Dechant, S. Delagrangue, N. Delpierre, G. Derroire, A. S. Dias, M. H. Diaz-Toribio, P. G. Dimitrakopoulos, M. Dobrowolski, D. Doktor, P. Dřevojan, N. Dong, J. Dransfield, S. Dressler, L. Duarte, E. Ducouret, S. Dullinger, W. Durka, R. Duursma, O. Dymova, A. E-Vojtkó, R. L. Eckstein, H. Ejtehadi, J. Elser, T. Emilio, K. Engemann, M. B. Erfanian, A. Erfmeier, A. Esquivel-Muelbert, G. Esser, M. Estiarte, T. F. Domingues, W. F. Fagan, J. Fagúndez, D. S. Falster, Y. Fan, J. Fang, E. Farris, F. Fazlioglu, Y. Feng, F. Fernandez-Mendez, C. Ferrara, J. Ferreira, A. Fidelis, B. Finegan, J. Firn, T. J. Flowers, D. F. B. Flynn, V. Fontana, E. Forey, C. Forgiarini, L. François, M. Frangipani, D. Frank, C. Frenette-Dussault, G. T. Freschet, E. L. Fry, N. M. Fyllas, G. G. Mazzochini, S. Gachet, R. Gallagher, G. Ganade, F. Ganga, P. García-Palacios, V. Gargaglione, E. Garnier, J. L. Garrido, A. L. de Gasper, G. Gea-Izquierdo, D. Gibson, A. N. Gillison, A. Giroldo, M.-C. Glasenhardt, S. Gleason, M. Gliesch, E. Goldberg, B. Gödel, E. Gonzalez-Akre, J. L. Gonzalez-Andujar, A. González-Melo, A. González-Robles, B. J. Graae, E. Granda, S. Graves, W. A. Green, T. Gregor, N. Gross, G. R. Guerin, A. Günther, A. G. Gutiérrez, L. Haddock, A. Haines, J. Hall, A. Hambuckers, W. Han, S. P. Harrison, W. Hattingh, J. E. Hawes, T. He, P. He, J. M. Heberling, A. Helm, S. Hempel, J. Hentschel, B. Hérault, A.-M. Hereş, K. Herz, M. Heuertz, T. Hickler, P. Hietz, P. Higuchi, A. L. Hipp, A. Hirons, M. Hock, J. A. Hogan, K. Holl, O. Honnay, D. Hornstein, E. Hou, N. Hough-Snee, K. A. Hovstad, T. Ichie, B. Igić, E. Illa, M. Isaac, M. Ishihara, L. Ivanov, L. Ivanova, C. M. Iversen, J. Izquierdo, R. B. Jackson, B. Jackson, H. Jactel, A. M. Jagodzinski, U. Jandt, S. Jansen, T. Jenkins, A. Jentsch, J. R. P. Jaspersen, G.-F. Jiang, J. L. Johansen, D. Johnson, E. J. Jokela, C. A. Joly, G. J. Jordan, G. S. Joseph, D. Junaedi, R. R. Junker, E. Justes, R. Kabzems, J. Kane, Z. Kaplan, T. Kattenborn, L. Kavelenova, E. Kearsley, A. Kempel, T. Kenzo, A. Kerkhoff, M. I. Khalil, N. L. Kinlock, W. D. Kissling, K. Kitajima, T. Kitzberger, R. Kjeller, T. Klein, M. Kleyer, J. Klimešová, J. Klipel, B. Kloeppel, S. Klotz, J. M. H. Knops, T. Kohyama, F. Koike, J. Kollmann, B. Komac, K. Komatsu, C. König, N. J. B. Kraft, K. Kramer, H. Kreft, I. Kühn, D. Kumarathunge, J. Kuppler, H. Kurokawa, Y. Kurosawa, S. Kuyah, J.-P. Laclau, B. Laffleur, E. Lallai, E. Lamb, A. Lamprecht, D. J. Larkin, D. Laughlin, Y. Le Bagousse-Pinguet, G. le Maire, P. C. le Roux, E. le Roux, T. Lee, F. Lens, S. L. Lewis, B. Lhotsky, Y. Li, X. Li, J. W. Lichstein, M. Liebergesell, J. Y. Lim, Y.-S. Lin, J. C. Linares, C. Liu, D. Liu, U. Liu, S. Livingstone, J. Llusà, M. Lohbeck, Á. López-García, G. Lopez-Gonzalez, Z. Lososová, F. Louault, B. A. Lukács, P. Lukeš, Y. Luo, M. Lussu, S. Ma, C. Maciel Rabelo Pereira, M. Mack, V. Maire, A. Mäkelä, H. Mäkinen, A. C. M. Malhado, A. Mallik,

- P. Manning, S. Manzoni, Z. Marchetti, L. Marchino, V. Marcilio-Silva, E. Marcon, M. Marignani, L. Markesteijn, A. Martin, C. Martínez-Garza, J. Martínez-Vilalta, T. Mašková, K. Mason, N. Mason, T. J. Massad, J. Masse, I. Mayrose, J. McCarthy, M. L. McCormack, K. McCulloh, I. R. McFadden, B. J. McGill, M. Y. McPartland, J. S. Medeiros, B. Medlyn, P. Meerts, Z. Mehrabi, P. Meir, F. P. L. Melo, M. Mencuccini, C. Meredieu, J. Messier, I. Mészáros, J. Metsaranta, S. T. Michaletz, C. Michelaki, S. Migalina, R. Milla, J. E. D. Miller, V. Minden, R. Ming, K. Mokany, A. T. Moles, A. Molnár V, J. Molofsky, M. Molz, R. A. Montgomery, A. Monty, L. Moravcová, A. Moreno-Martínez, M. Moretti, A. S. Mori, S. Mori, D. Morris, J. Morrison, L. Mucina, S. Mueller, C. D. Muir, S. C. Müller, F. Munoz, I. H. Myers-Smith, R. W. Myster, M. Nagano, S. Naidu, A. Narayanan, B. Natesan, L. Negroita, A. S. Nelson, E. L. Neuschulz, J. Ni, G. Niedrist, J. Nieto, Ü. Niinemets, R. Nolan, H. Nottebrock, Y. Nouvellon, A. Novakovskiy, T. N. Network, K. O. Nystuen, A. O'Grady, K. O'Hara, A. O'Reilly-Nugent, S. Oakley, W. Oberhuber, T. Ohtsuka, R. Oliveira, K. Öllerer, M. E. Olson, V. Onipchenko, Y. Onoda, R. E. Onstein, J. C. Ordonez, N. Osada, I. Ostonen, G. Ottaviani, S. Otto, G. E. Overbeck, W. A. Ozinga, A. T. Pahl, C. E. T. Paine, R. J. Pakeman, A. C. Papageorgiou, E. Parfionova, M. Pärtel, M. Patacca, S. Paula, J. Paule, H. Pauli, J. G. Pausas, B. Peco, J. Penuelas, A. Perea, P. L. Peri, A. C. Petisco-Souza, A. Petraglia, A. M. Petritan, O. L. Phillips, S. Pierce, V. D. Pillar, J. Pisek, A. Pomogaybin, H. Poorter, A. Portsmouth, P. Poschlod, C. Potvin, D. Pounds, A. S. Powell, S. A. Power, A. Prinzing, G. Puglielli, P. Pyšek, V. Raavel, A. Rammig, J. Ransijn, C. A. Ray, P. B. Reich, M. Reichstein, D. E. B. Reid, M. Réjou-Méchain, V. R. de Dios, S. Ribeiro, S. Richardson, K. Riibak, M. C. Rillig, F. Riviera, E. M. R. Robert, S. Roberts, B. Robroek, A. Roddy, A. V. Rodrigues, A. Rogers, E. Rollinson, V. Rolo, C. Römermann, D. Ronzhina, C. Roscher, J. A. Rosell, M. F. Rosenfield, C. Rossi, D. B. Roy, S. Royer-Tardif, N. Rüger, R. Ruiz-Peinado, S. B. Rumpf, G. M. Rusch, M. Ryo, L. Sack, A. Saldaña, B. Salgado-Negret, R. Salguero-Gomez, I. Santa-Regina, A. C. Santacruz-García, J. Santos, J. Sardans, B. Schamp, M. Scherer-Lorenzen, M. Schleuning, B. Schmid, M. Schmidt, S. Schmitt, J. V. Schneider, S. D. Schowanek, J. Schrader, F. Schrod, B. Schuldt, F. Schurr, G. Selaya Garvizu, M. Semchenko, C. Seymour, J. C. Sfair, J. M. Sharpe, C. S. Sheppard, S. Sheremetiev, S. Shiodera, B. Shipley, T. A. Shovon, A. Siebenkäs, C. Sierra, V. Silva, M. Silva, T. Sitzia, H. Sjöman, M. Slot, N. G. Smith, D. Sodhi, P. Soltis, D. Soltis, B. Somers, G. Sonnier, M. V. Sørensen, E. E. Sosinski Jr, N. A. Soudzilovskaia, A. F. Souza, M. Spasojevic, M. G. Sperandii, A. B. Stan, J. Stegen, K. Steinbauer, J. G. Stephan, F. Sterck, D. B. Stojanovic, T. Strydom, M. L. Suarez, J.-C. Svenning, I. Svitková, M. Svitok, M. Svoboda, E. Swaine, N. Swenson, M. Tabarelli, K. Takagi, U. Tappeiner, R. Tarifa, S. Tauougourdeau, C. Tavsanoğlu, M. te Beest, L. Tedersoo, N. Thiffault, D. Thom, E. Thomas, K. Thompson, P. E. Thornton, W. Thuiller, L. Tichý, D. Tissue, M. G. Tjoelker, D. Y. P. Tng, J. Tobias, P. Török, T. Tarin, J. M. Torres-Ruiz, B. Tóthmérész, M. Treurnicht, V. Trivellone, F. Trolliet, V. Trotsiuk, J. L. Tsakalos, I. Tsiropidis, N. Tysklind, T. Umehara, V. Usoltsev, M. Vadeboncoeur, J. Vaezi, F. Valladares, J. Vamosi, P. M. van Bodegom, M. van Breugel, E. Van Cleemput, M. van de Weg, S. van der Merwe, F. van der Plas, M. T. van der Sande, M. van Kleunen, K. Van Meerbeek, M. Vanderwel, K. A. Vanselow, A. Vårhammar, L. Varone, M. Y. Vasquez Valderrama, K. Vassilev, M. Vellend, E. J. Veneklaas, H. Verbeeck, K. Verheyen, A. Vibrans, I. Vieira, J. Villacís, C. Violle, P. Vivek, K. Wagner, M. Waldram, A. Waldron, A. P. Walker, M. Waller, G. Walther, H. Wang, F. Wang, W. Wang, H. Watkins, J. Watkins, U. Weber, J. T. Weedon, L. Wei, P. Weigelt, E. Weiher, A. W. Wells, C. Wellstein, E. Wenk, M. Westoby, A. Westwood, P. J. White, M. Whitten, M. Williams, D. E. Winkler, K. Winter, C. Womack, I. J. Wright, S. J. Wright, J. Wright, B. X. Pinho, F. Ximenes, T. Yamada, K. Yamaji, R. Yanai, N. Yankov, B. Yguel, K. J. Zanini, A. E. Zanne, D. Zelený, Y.-P. Zhao, J. Zheng, J. Zheng, K. Ziemińska, C. R. Zirbel, G. Zizka, I. C. Zo-Bi, G. Zotz, and C. Wirth (2020). "TRY Plant Trait Database – Enhanced Coverage and Open Access". In: *Glob. Change Biol.* 26.1, pp. 119–188. ISSN: 1365-2486. DOI: 10.1111/gcb.14904. (Visited on 04/19/2024).
- Schaphoff, S., W. von Bloh, A. Rammig, K. Thonicke, H. Biemans, M. Forkel, D. Gerten, J. Heinke, J. Jägermeyr, J. Knauer, F. Langerwisch, W. Lucht, C. Müller, S. Rolinski, and K. Waha (2018). "LPJmL4 – a Dynamic Global Vegetation Model with Managed Land – Part 1: Model Description". In: *Geosci. Model Dev.* 11.4, pp. 1343–1375. ISSN: 1991-959X. DOI: 10.5194/gmd-11-1343-2018. (Visited on 05/31/2023).
- Sitch, S., B. Smith, I. C. Prentice, A. Arneth, A. Bondeau, W. Cramer, J. O. Kaplan, S. Levis, W. Lucht, M. T. Sykes, K. Thonicke, and S. Venevsky (2003). "Evaluation of Ecosystem Dynamics, Plant Geography and Terrestrial Carbon Cycling in the LPJ Dynamic Global Vegetation Model". In: *Glob. Change Biol.* 9.2, pp. 161–185. ISSN: 1365-2486. DOI: 10.1046/j.1365-2486.2003.00569.x. (Visited on 03/03/2018).
- Thornley, J. H. M. (1991). "A Transport-resistance Model of Forest Growth and Partitioning". In: *Ann. Bot.* 68.3, pp. 211–226. ISSN: 0305-7364. JSTOR: 42764399. (Visited on 06/04/2018).
- von Bloh, W., S. Schaphoff, C. Müller, S. Rolinski, K. Waha, and S. Zaehle (2018). "Implementing the Nitrogen Cycle into the Dynamic Global Vegetation, Hydrology, and Crop Growth Model LPJmL (Version 5.0)". In: *Geosci. Model Dev.* 11.7, pp. 2789–2812. ISSN: 1991-959X. DOI: 10.5194/gmd-11-2789-2018. (Visited on 05/31/2023).
- Zaehle, S., A. D. Friend, P. Friedlingstein, F. Dentener, P. Peylin, and M. Schulz (2010). "Carbon and Nitrogen Cycle Dynamics in the O-CN Land Surface Model: 2. Role of the Nitrogen Cycle in the Historical Terrestrial Carbon Balance". In: *Global Biogeochem. Cycles* 24.1, GB1006. ISSN: 1944-9224. DOI: 10.1029/2009GB003522. (Visited on 03/12/2018).

# Appendix D

Appendix D contains the supplementary information for Chapter 5 Global grassland productivity and carbon storage benefit from functional diversity already under moderate climate change.

## D.1 Additional figures

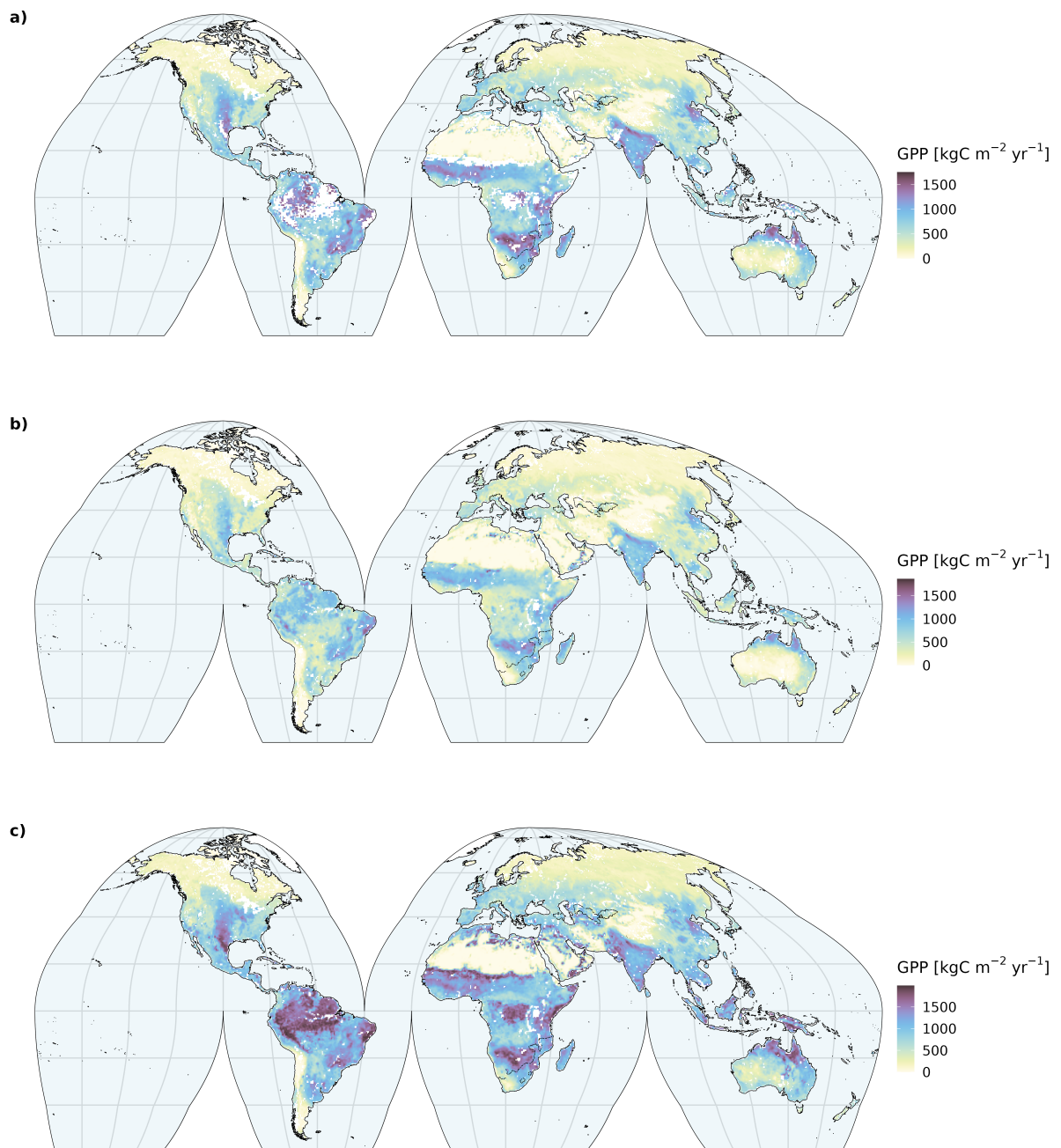


Figure D.1: Time series average (a), 5th (b) and 95th (c) percentiles of the annual herbaceous GPP calculated from Zhang et al. (2017).

Appendix D

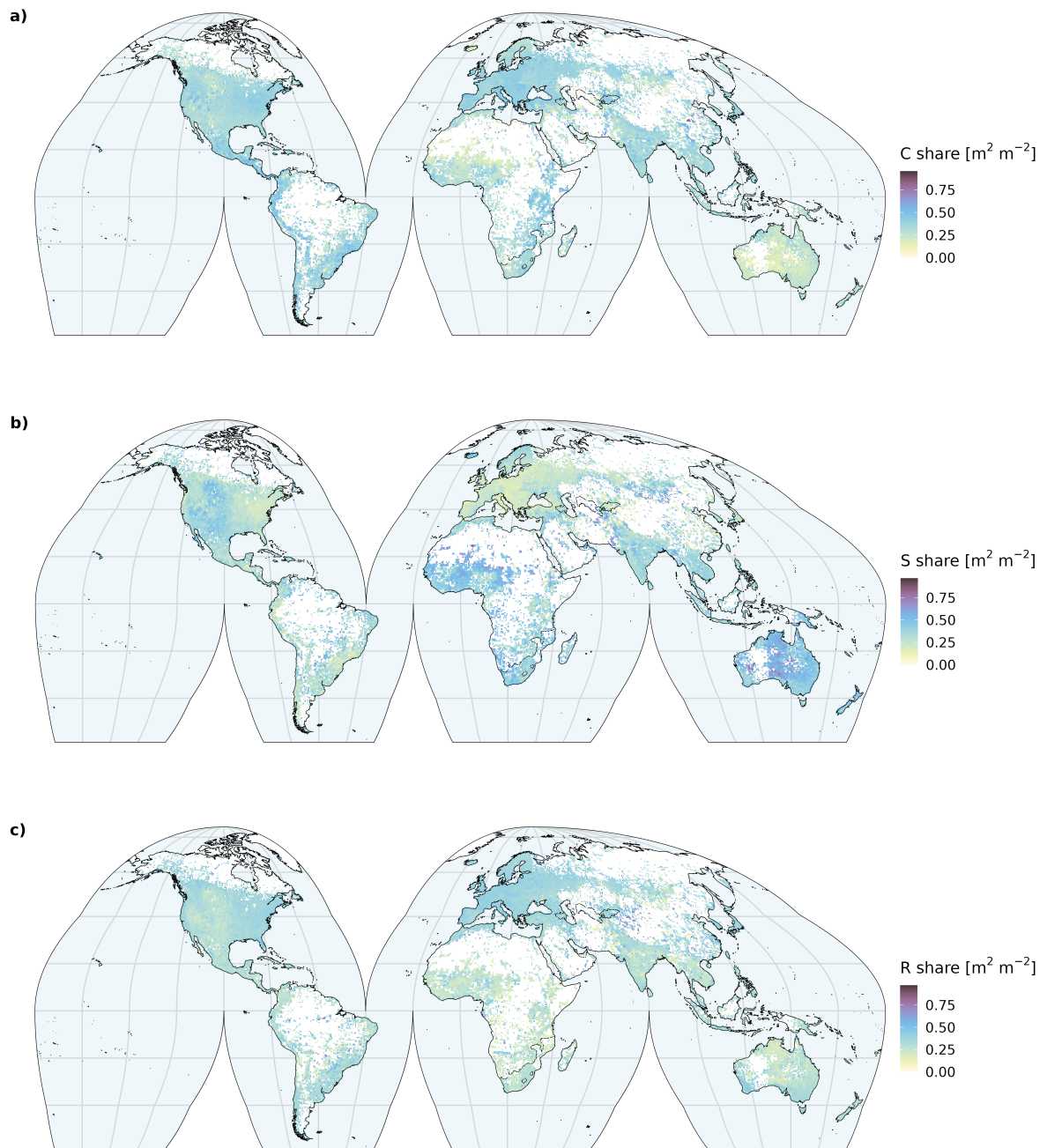


Figure D.2: Community share of the C- (a), S- (b) and R-PFT (c) calculated using the StrateFy approach and the Wolf et al. (2022) data.

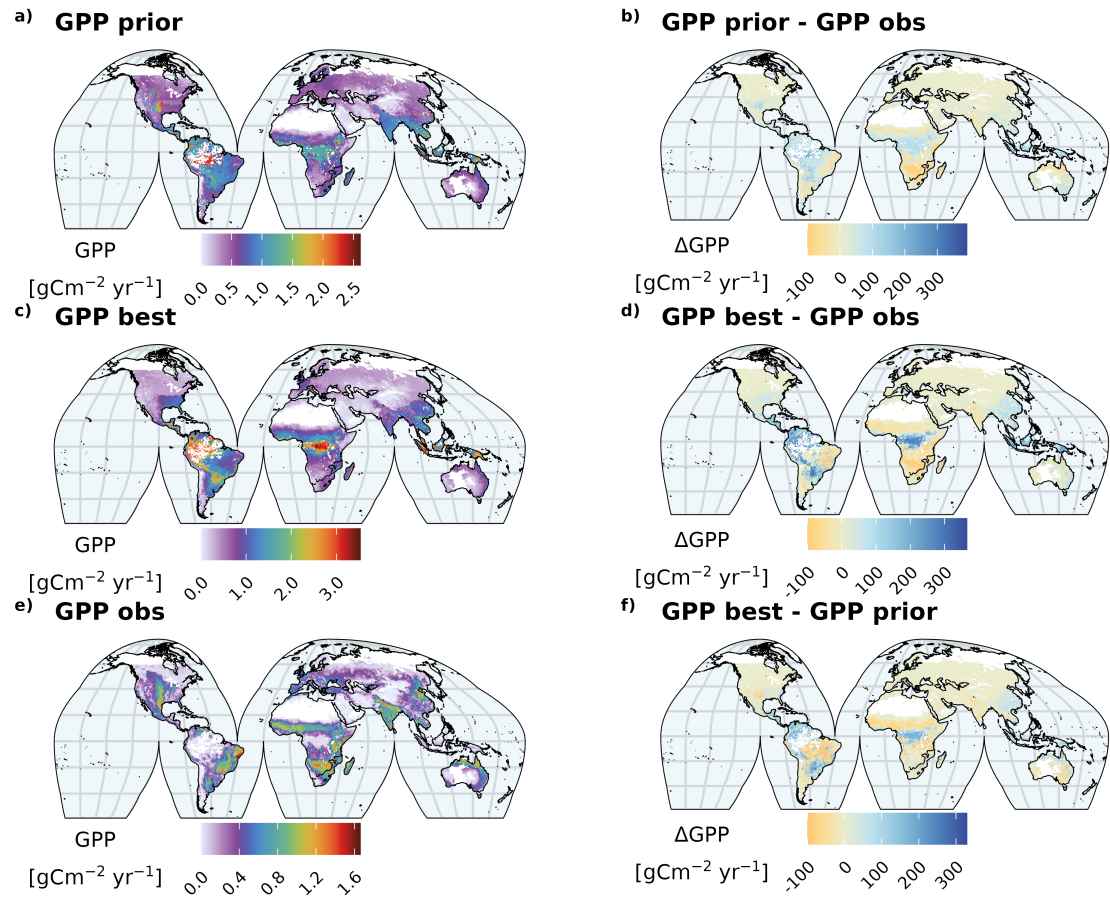


Figure D.3: 2000 to 2016 average GPP for the parameter sets before (a) and after (c) calibration and observations (e) as well as difference between the parameters before the calibration and observations (b), the parameter set after the calibration and observations (d) and the two parameter sets (f).

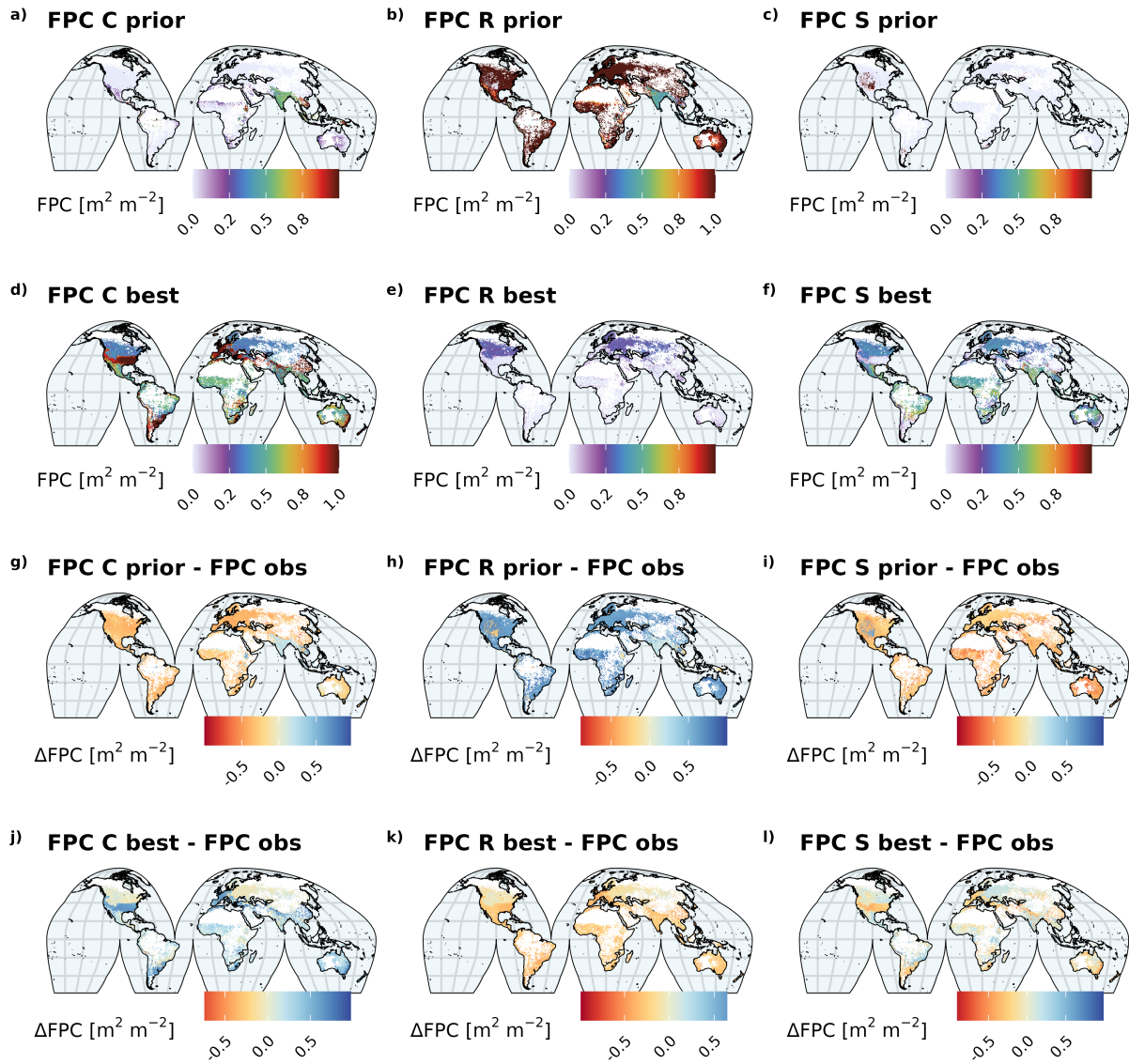


Figure D.4: FPC for each strategy for the parameter sets before (a, b, c) and after (d,e,f) calibration and difference to observations for the parameters before the calibration (g,h,i) and the parameter set after the calibration (j,k,l).

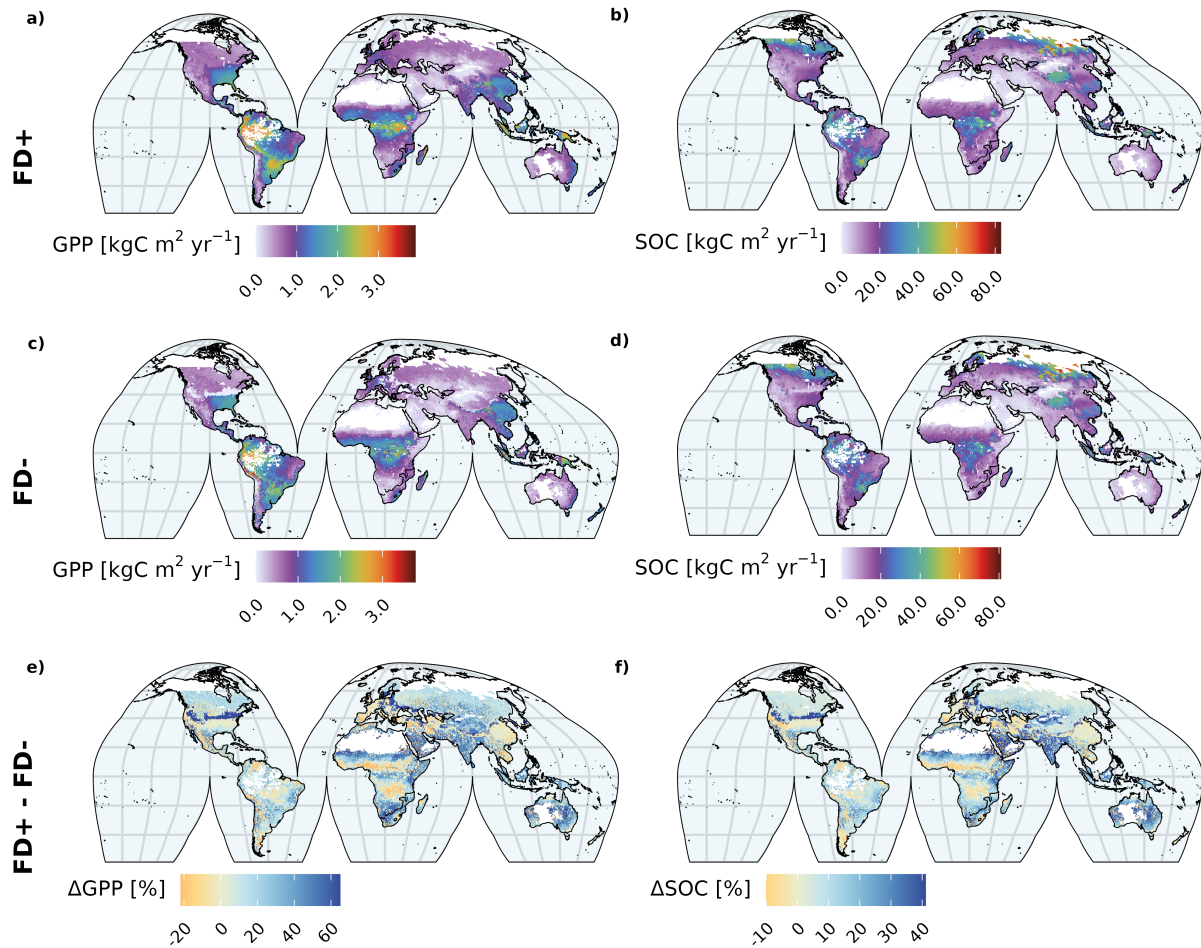


Figure D.5: Global distribution of GPP (a,c,e) and SOC (b,d,f) dependent on functional diversity for SSP3-7.0. Left panels show the average GPP for the scenarios (a) FD+, (b) FD- and (c) their difference, i.e. the net effect of a higher functional diversity. Right panels (b,d,f) show the respective results for SOC. All distributions show the 2091 to 2100 average of the respective output variable simulated using climate data from the MRI-ESM2-0.

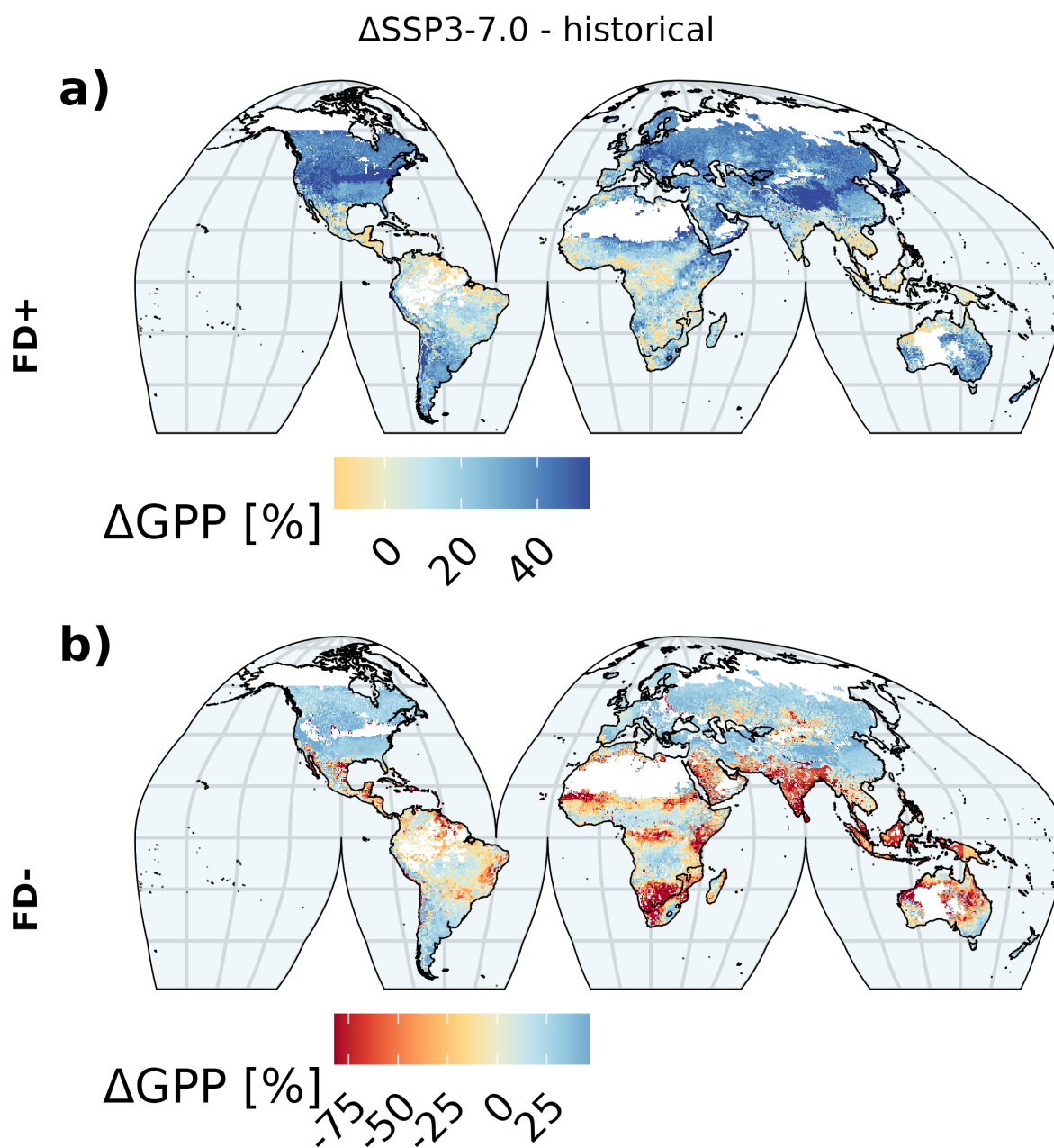


Figure D.6: Global distribution of the relative difference of GPP (a) and SOC (b) between the end of the historical time period (2005-2014) and the current century (2091-2100). All distributions show the time frame average of the respective output variable simulated using climate data from the MRI-ESM2-0.

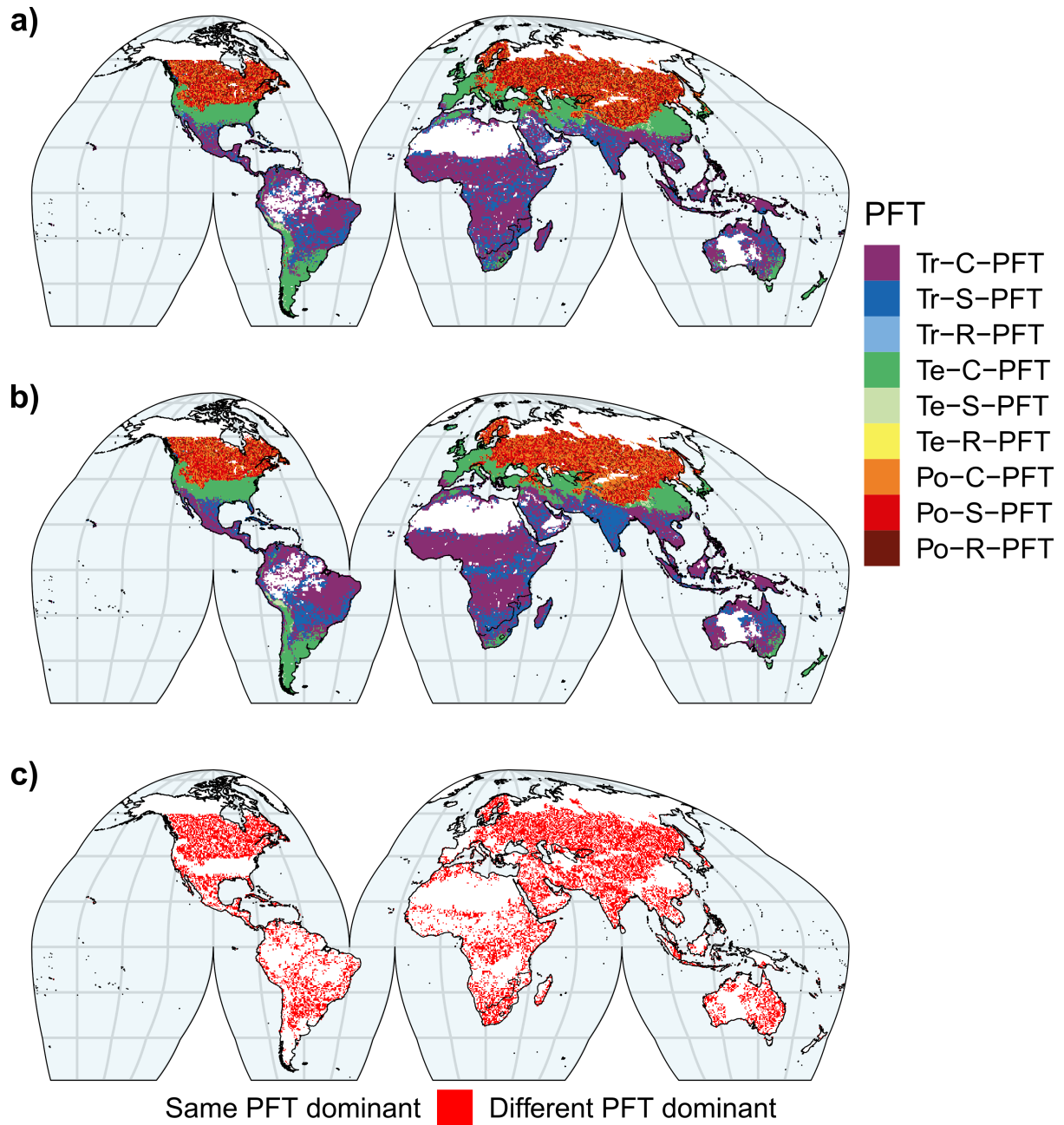


Figure D.7: Dominant PFT in FD+ at the end of the historical time period (2014, a), the current century (2091-2100 average, b) and change of the dominant PFT between the end of the historical time period and the current century (c). PFTs are the tropical (Tr), temperate (Te) and polar (Po), competitive (C), stress-tolerant (S) and ruderal (R).

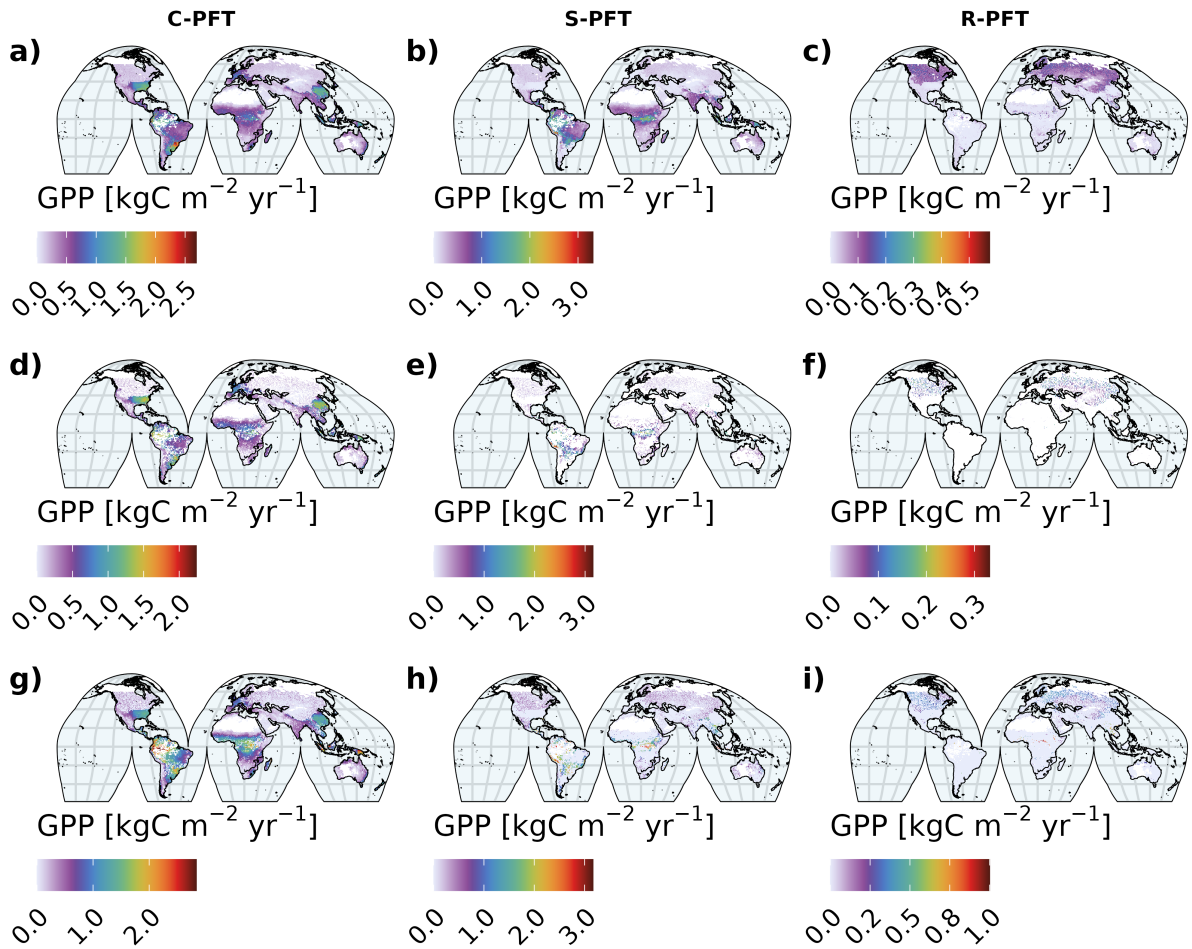


Figure D.8: Global distribution of PFT-specific GPP dependent on functional diversity. From left to right, panels show the distribution for the C- (a,d,g), S- (b,e,h) and R-PFTs (c,f,i). The first (a,b,c) and third (g,h,i) rows show the distribution using all PFTs present in FD+. The second row (d,e,f) shows the distribution using only the dominant PFT in FD+. The third row (g,h,i) shows the distribution for FD-. All distribution show the 2091 to 2100 average of the respective output variable simulated using climate data from the MRI-ESM2-0.

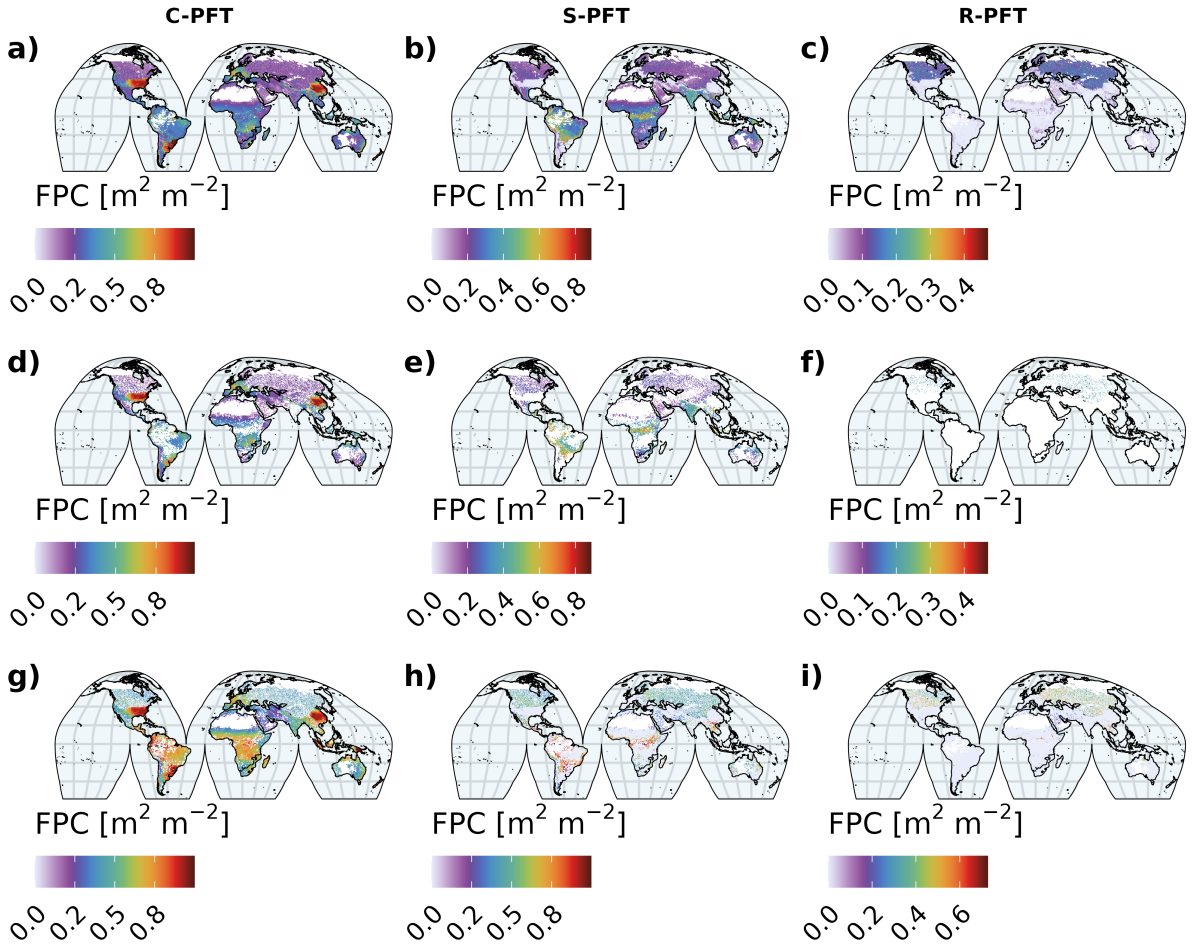


Figure D.9: Global distribution of PFT-specific FPC dependent on functional diversity. From left to right, panels show the distribution for the C- (a,d,g), S- (b,e,h) and R-PFTs (c,f,i). The first (a,b,c) and third (g,h,i) rows show the distribution using all PFTs present in FD+. The second row (d,e,f) shows the distribution using only the dominant PFT in FD+. The third row (g,h,i) shows the distribution for FD-. All distribution show the 2091 to 2100 average of the respective output variable simulated using climate data from the MRI-ESM2-0.

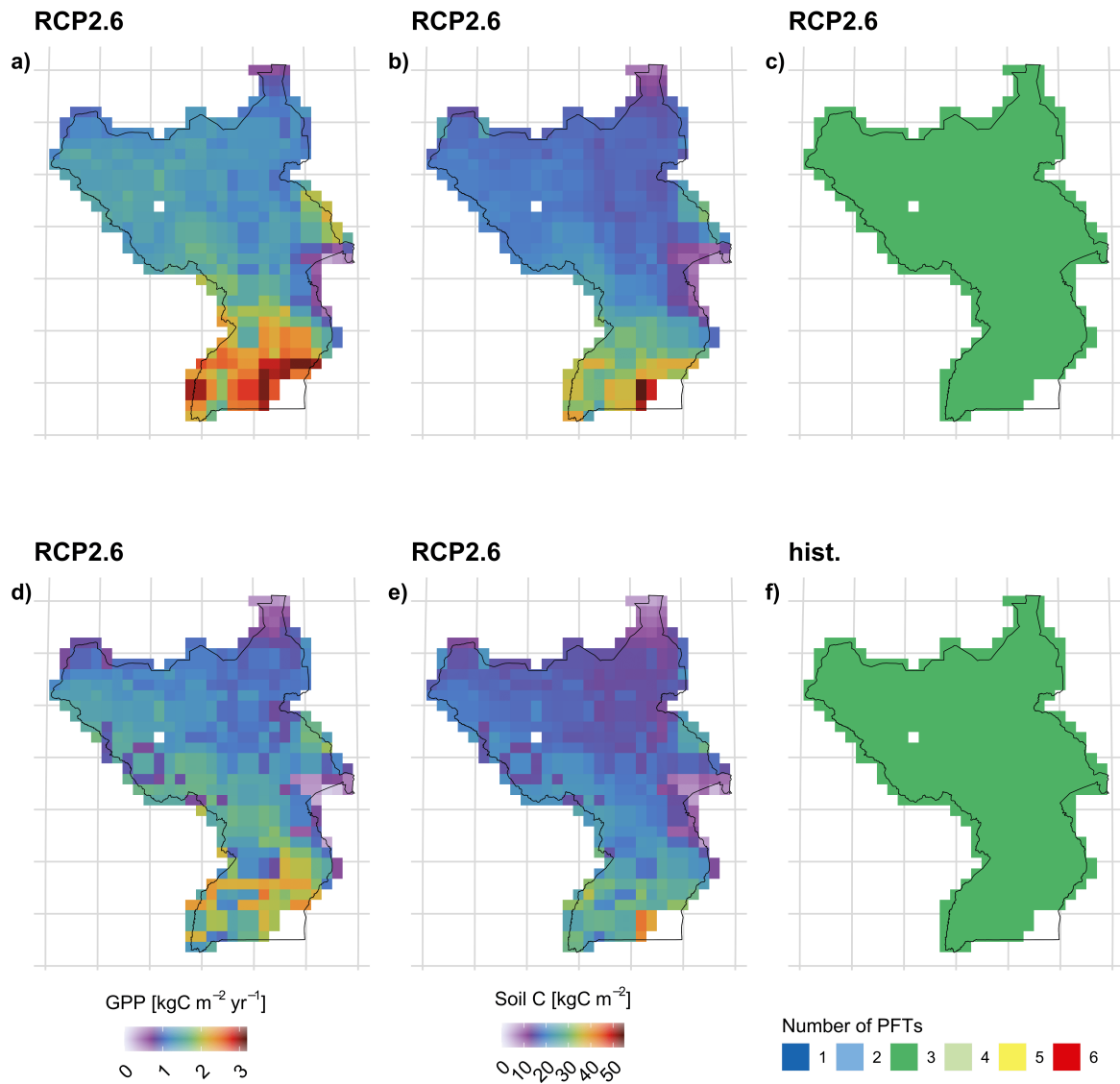


Figure D.10: Distribution of the absolute GPP (a,d), SOC (b,e) and the number of PFT present (c,f) dependent on functional diversity for Uganda and South Sudan. Panels show the data FD+ (a,b,c,f) and FD-(d,e). All distribution are based on the 2091 to 2100 average of the respective output variable simulated using climate data from the MRI-ESM2-0.

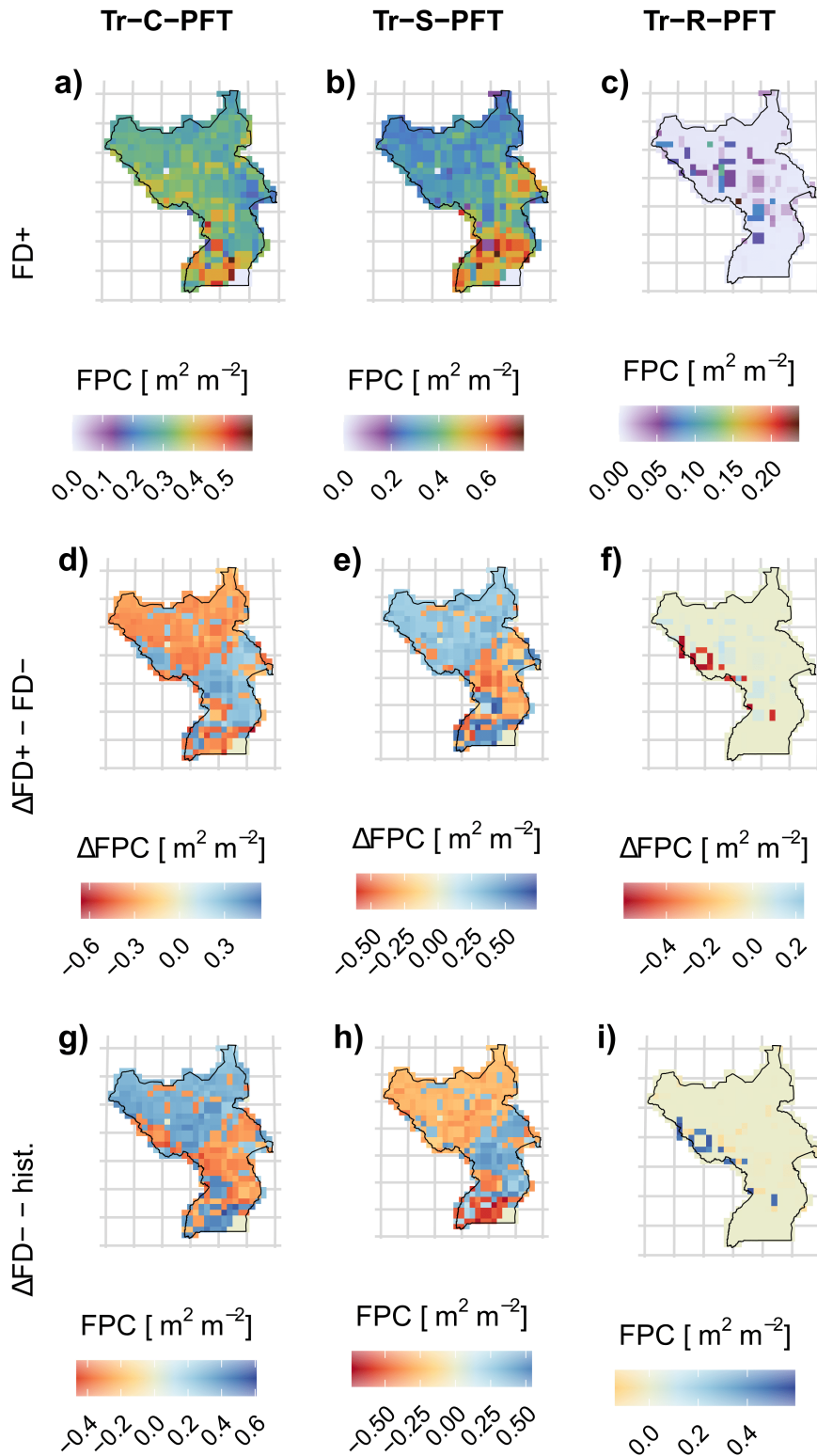


Figure D.11: Distribution of the absolute FPC (a,b,c) and relative difference between FD+ and FD- (c,d,e) and end of the historical time period (g,h,i) for the tropical C- (a,d,g), S- (b,e,h) and R-PFT (c,f,i) for Uganda and South Sudan. All distributions are based on the 2005 to 2014 and 2091 to 2100 average of the respective output variable simulated using climate data from the MRI-ESM2-0.

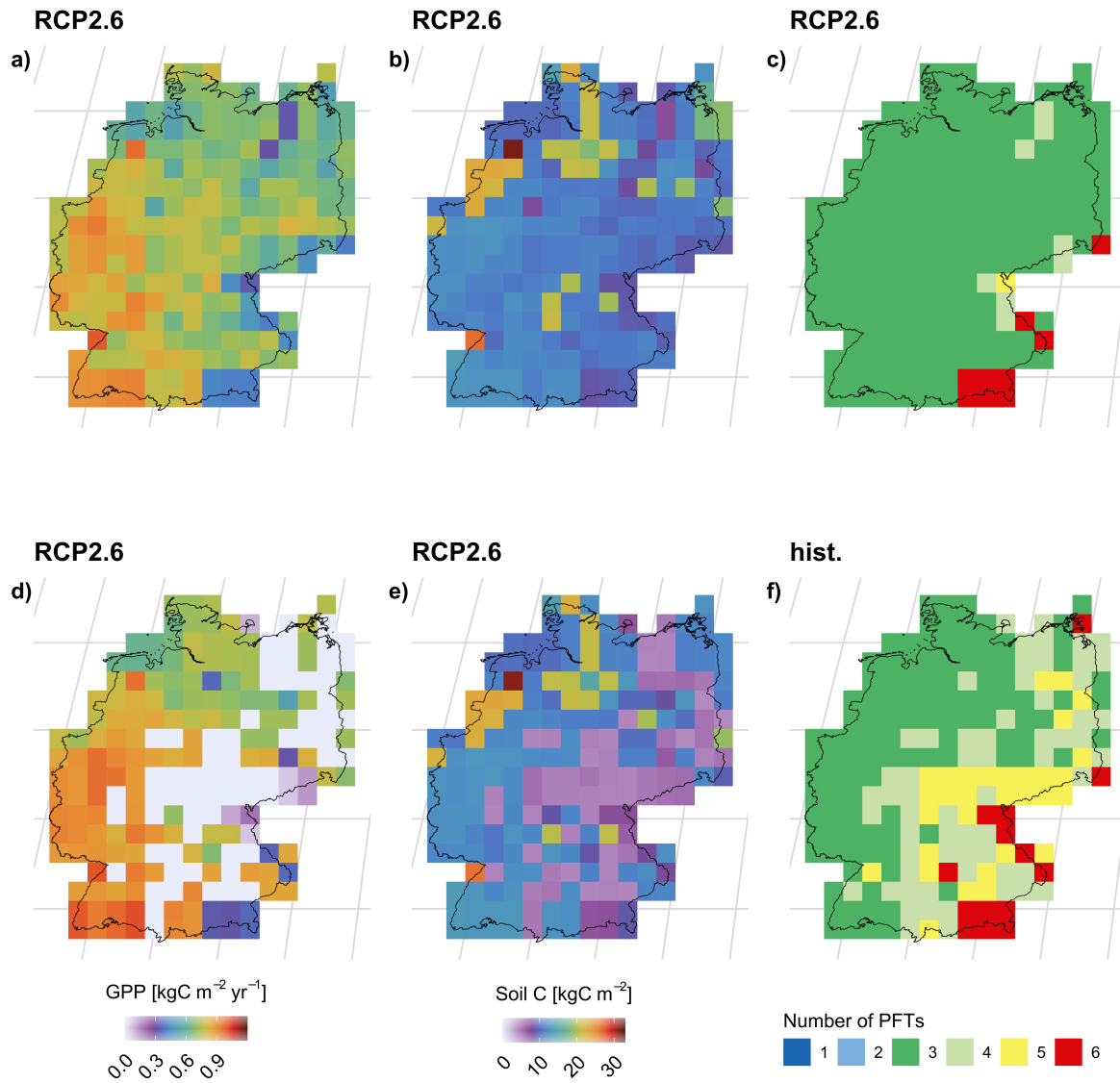


Figure D.12: Distribution of the absolute GPP (a,d), SOC (b,e) and the number of PFT present (c,f) dependent on functional diversity for Germany. Panels show the data FD+ (a,b,c,f) and FD- (d,e). All distribution are based on the 2091 to 2100 average of the respective output variable simulated using climate data from the MRI-ESM2-0.

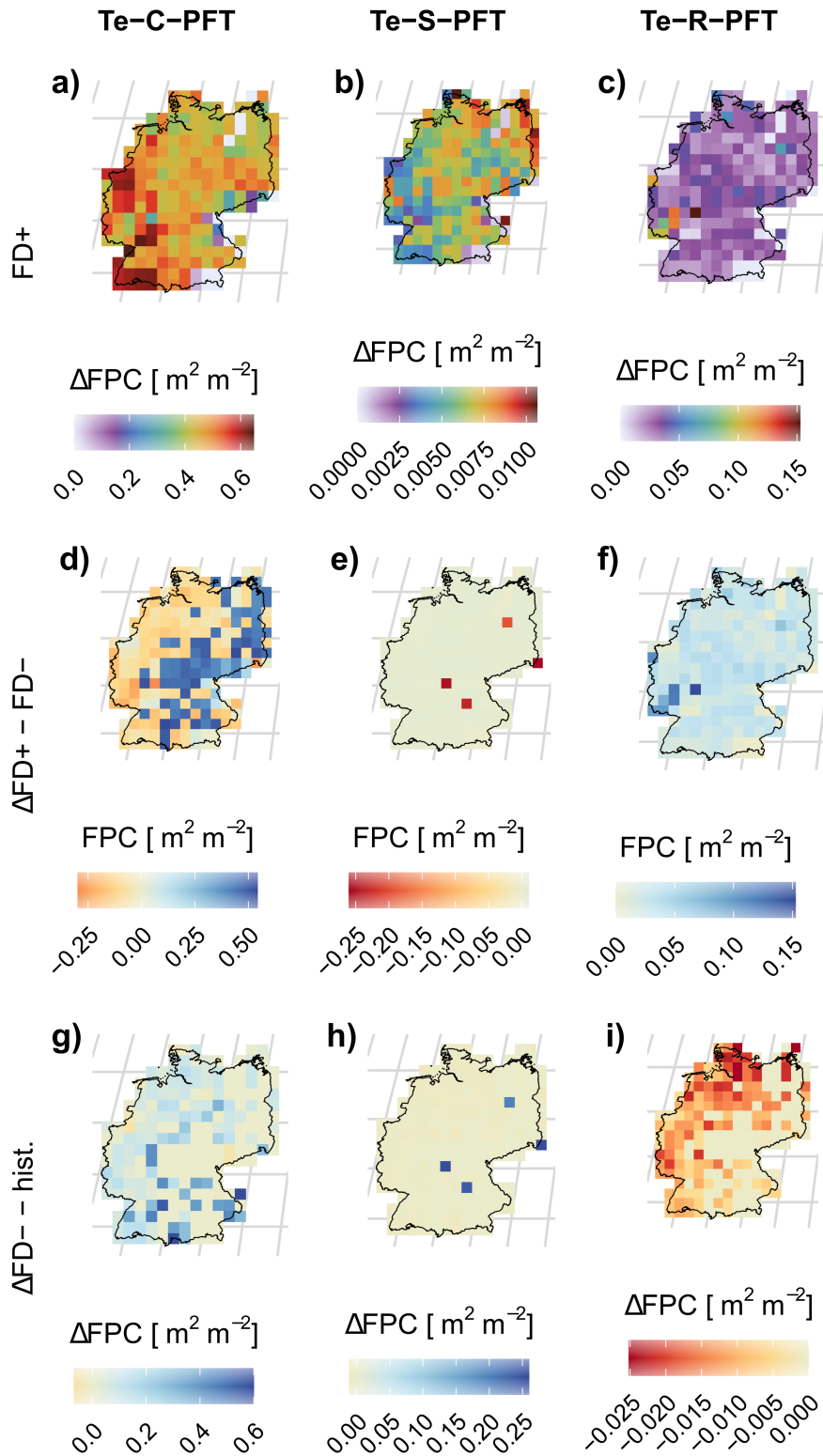


Figure D.13: Distribution of the absolute FPC (a,b,c) and relative difference between FD+ and FD- (c,d,e) and end of the historical time period (g,h,i) for the temperate C- (a,d,g), S- (b,e,h) and R-PFT (c,f,i) for Germany. All distribution are based on the 2005 to 2014 and 2091 to 2100 average of the respective output variable simulated using climate data from the MRI-ESM2-0.

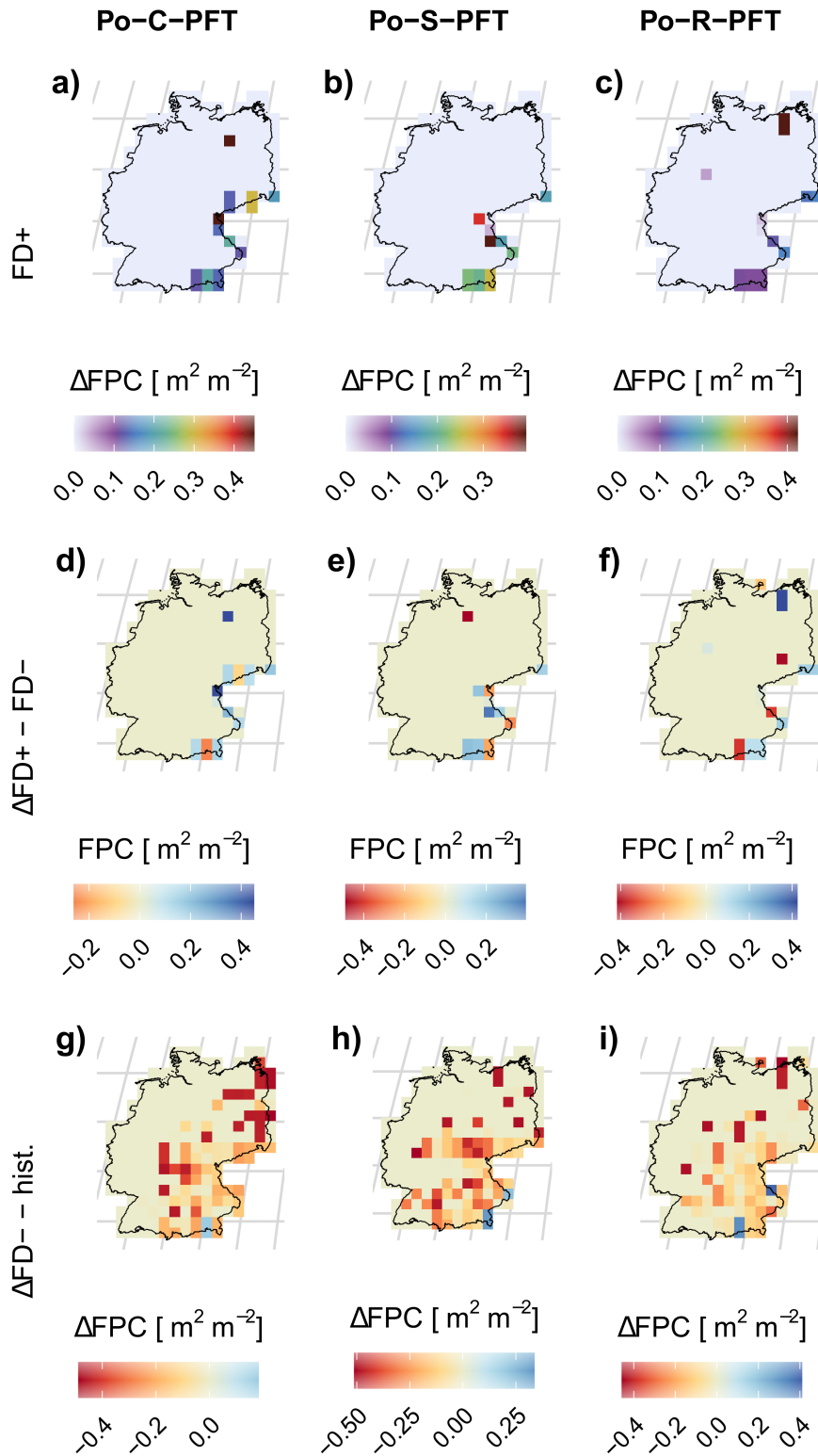


Figure D.14: Distribution of the absolute FPC (a,b,c) and relative difference between FD+ and FD- (c,d,e) and end of the historical time period (g,h,i) for the polar C- (a,d,g), S- (b,e,h) and R-PFT (c,f,i) for Germany. All distribution are based on the 2005 to 2014 and 2091 to 2100 average of the respective output variable simulated using climate data from the MRI-ESM2-0.

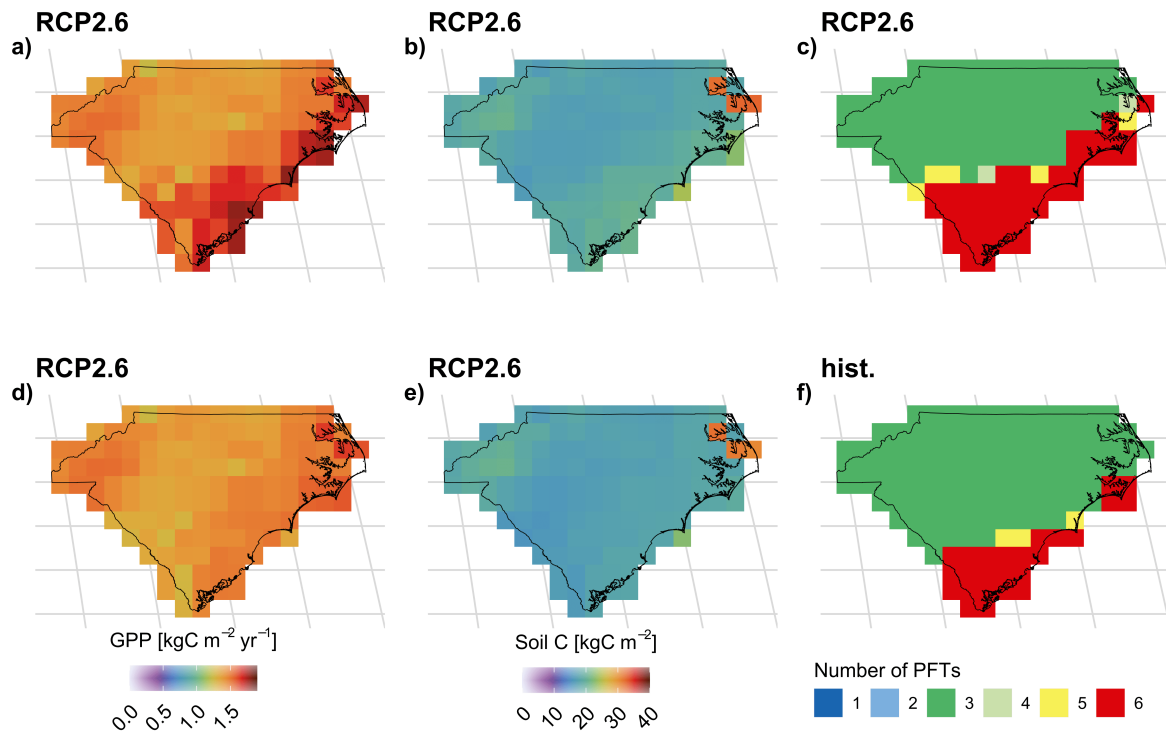


Figure D.15: Distribution of the absolute GPP (a,d), SOC (b,e) and the number of PFT present (c,f) dependent on functional diversity for North and South Carolina. Panels show the data FD+ (a,b,c,f) and FD-(d,e). All distribution are based on the 2091 to 2100 average of the respective output variable simulated using climate data from the MRI-ESM2-0.

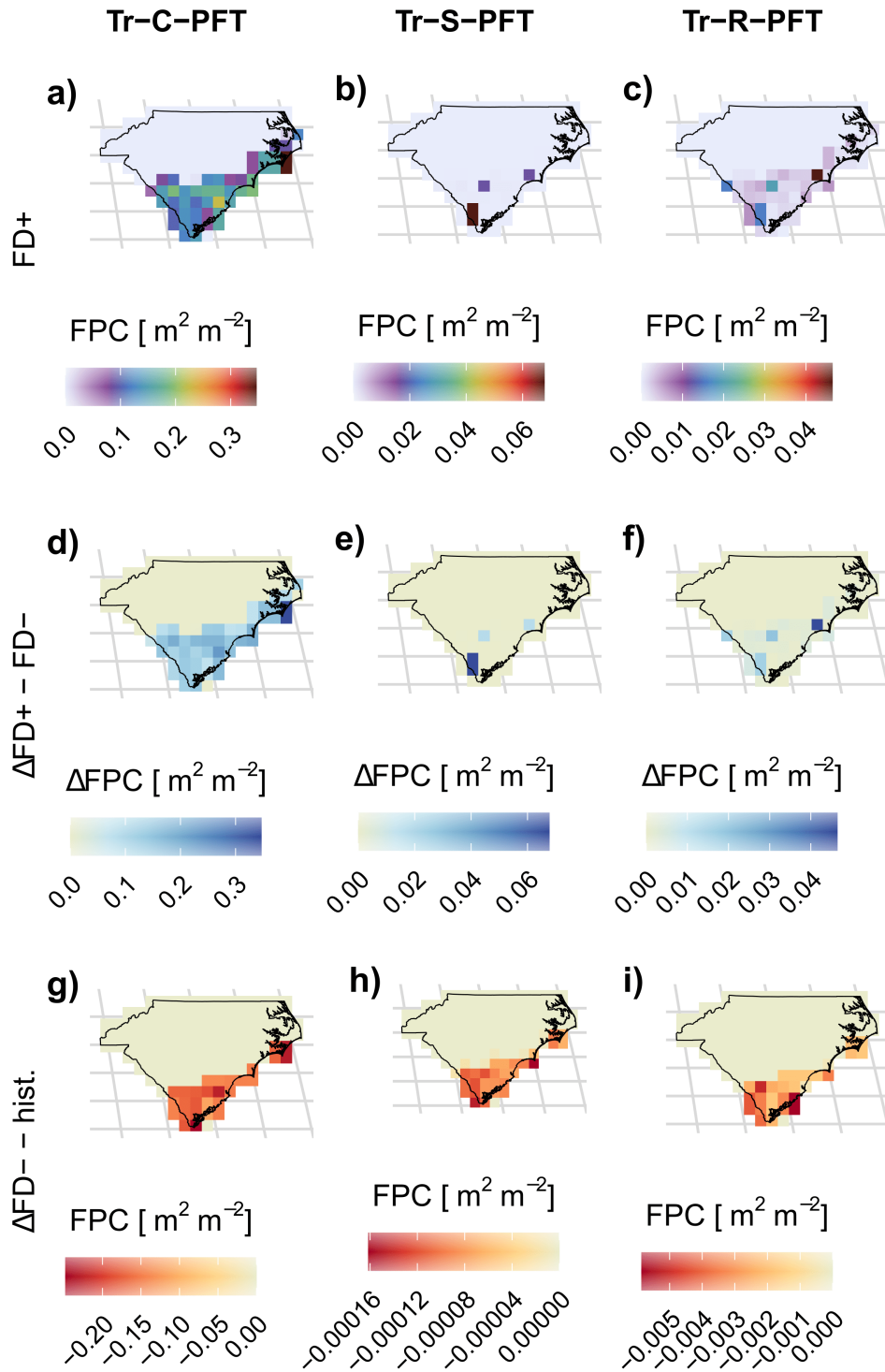


Figure D.16: Distribution of the absolute FPC (a,b,c) and relative difference between FD+ and FD- (c,d,e) and end of the historical time period (g,h,i) for the tropical C- (a,d,g), S- (b,e,h) and R-PFT (c,f,i) for North and South Carolina. All distribution are based on the 2005 to 2014 and 2091 to 2100 average of the respective output variable simulated using climate data from the MRI-ESM2-0.

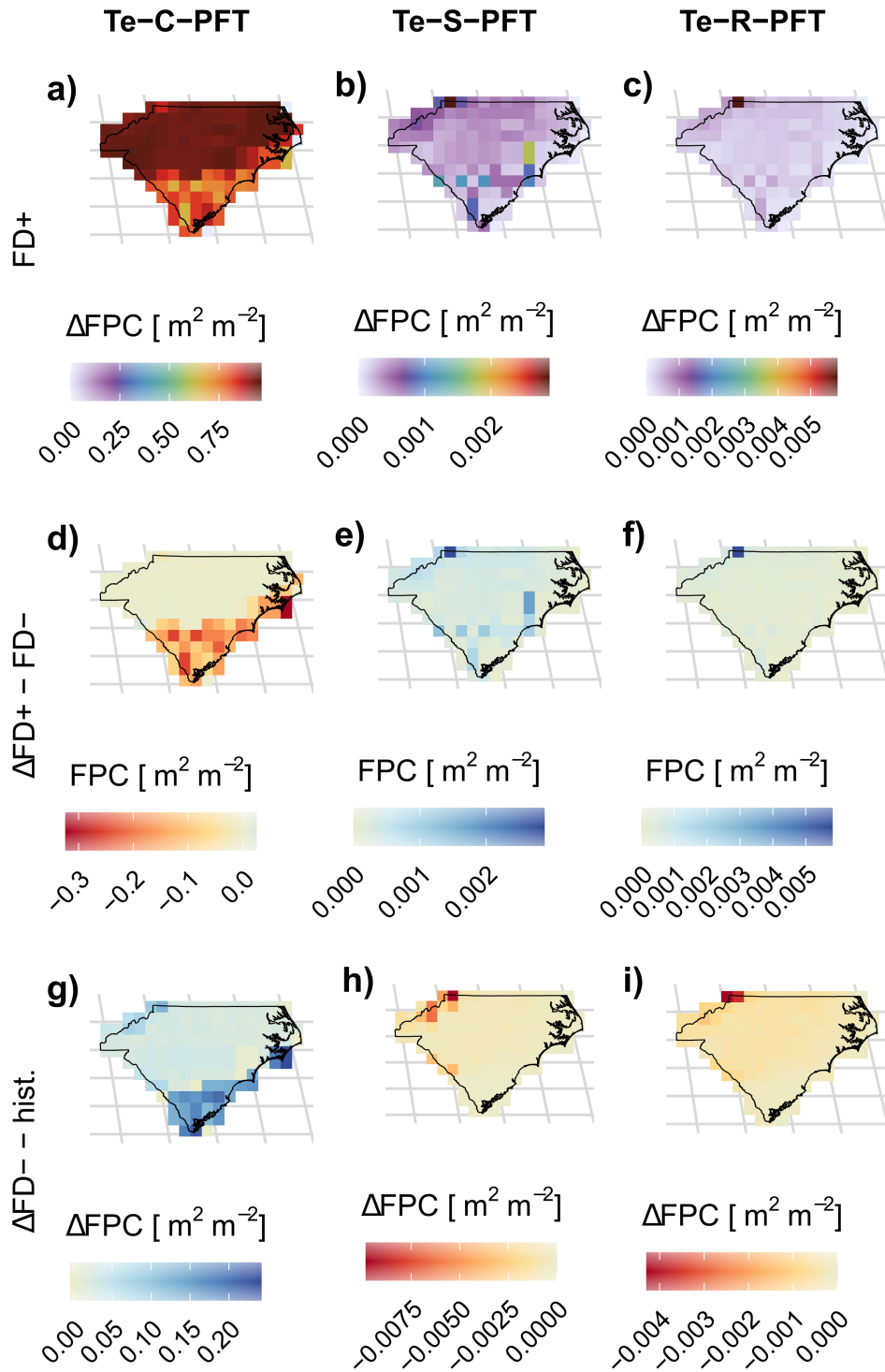


Figure D.17: Distribution of the absolute FPC (a,b,c) and relative difference between FD+ and FD- (c,d,e) and end of the historical time period (g,h,i) for the temperate C- (a,d,g), S- (b,e,h) and R-PFT (c,f,i) for North and South Carolina. All distributions are based on the 2005 to 2014 and 2091 to 2100 average of the respective output variable simulated using climate data from the MRI-ESM2-0.

## D.2 References

- Wolf, S., M. D. Mahecha, F. M. Sabatini, C. Wirth, H. Bruehlheide, J. Kattge, Á. Moreno Martínez, K. Mora, and T. Kattenborn (2022). “Citizen Science Plant Observations Encode Global Trait Patterns”. In: *Nat Ecol Evol* 6.12, pp. 1850–1859. ISSN: 2397-334X. DOI: 10.1038/s41559-022-01904-x. (Visited on 09/18/2023).
- Zhang, Y., X. Xiao, X. Wu, S. Zhou, G. Zhang, Y. Qin, and J. Dong (2017). “A Global Moderate Resolution Dataset of Gross Primary Production of Vegetation for 2000–2016”. In: *Sci Data* 4.1, p. 170165. ISSN: 2052-4463. DOI: 10.1038/sdata.2017.165. (Visited on 02/02/2023).

# Acknowledgements

My research was funded by Evangelisches Studienwerk Villigst within their doctoral program "Third Ways of Feeding the World". I gratefully acknowledge the Ministry of Research, Science and Culture (MWFK) of Land Brandenburg for supporting this project by providing resources on the high performance computer system at the Potsdam Institute for Climate Impact Research.

Many people have supported me during my time as a doctoral researcher and I would like to express my gratitude to all of them.

I am very grateful to Susanne Rolinski, Friedhelm Taube and Arne Poyda for providing guidance and motivation the entire time. All our fruitful discussions were important in reaching this point and were much appreciated. A special thank you goes to Friedhelm Taube for giving me the opportunity to apply for a scholarship within the doctoral program "Third Ways of Feeding the World" of the Evangelisches Studienwerk Villigst. I also extend my gratitude to Christoph Müller for trusting my ability to manage both my thesis and an entirely different research project simultaneously and providing the additional funding needed to cross the finish line.

The papers that compose a large part of this thesis are collaborative works and would not have been possible without the continuous interactions with my co-authors. I also want to thank past and present members of the land-use, the land biosphere dynamics group and the LPJmL groups at the Potsdam Institute for Climate Impact Research for welcoming me and engaging in many inspiring discussions on topics ranging from carbon and nitrogen cycling in terrestrial ecosystems to software development standards.

Outside of the work environment, there are also many people I want to thank. First, I want to thank the Baumi flat share for allowing me to spend so much time there when COVID-19 hit the hardest. Your support tremendously improved the uncertain times during which I started my PhD. Second, all my other friends with whom I enjoyed regular walks, bike trips and dinners among many other things. Third, my boulder group for the weekly sessions containing an entirely different type of problem-solving. Last, my family, who enabled me to undertake this journey in the first place.

Finally, I want to thank Paula, who always believed in me and was there for the entire journey, supporting me at my worst and best without hesitation.

# In der Schriftenreihe des Institutes für Pflanzenbau und Pflanzenzüchtung der Christian-Albrechts- Universität zu Kiel sind bisher erschienen:

Heft	Autor	Jahr	Titel
1	Heller, R.	1997	Die genetische Analyse nematodenresistenter Zuckerrüben mit molekularen Markern
2	Schröder, Heidi	1997	Untersuchungen zur Ertragsbildung und Stickstoffverwertung von Wintergerstenbeständen in verschiedenen Produktionssystemen
3	Kornher, Alois Wulfes, Rainer Wachendorf, Michael Taube, Friedhelm	1998	Untersuchungen zur Dynamik der Ertragsbildung und der Qualitätsentwicklung von Extensivgrünland
4	Richter, K.	1998	Die Lokalisation von Genen für die Resistenz gegen die Netzfleckenkrankheit ( <i>Drechslera teres</i> ) in der Gerste
5	Kifle, Sirak	1998	Das <i>hairy roots</i> -Transformationssystem zur Expression des Nematodenresistenzgens <i>HS1</i> in Zuckerrüben und <i>Arabidopsis thaliana</i>
6	Puzio, Stefanie	1998	Untersuchungen zur Überwinterung und zum jahreszeitlichen Verlauf der Ertragsbildung von Weißklee in Abhängigkeit von der Witterung und der Sorteneigenschaft
7	Christen, Olaf	1998	Untersuchungen zur Anbautechnik von Winterweizen nach unterschiedlichen Vorfruchtkombinationen
8	Schacht, Johannes	1998	Beiträge zur Nutzung von Wildformen zur Verbesserung quantitativ vererbter Merkmale am Beispiel Gerste
9	Loges, Ralf	1998	Ertrag, Futterqualität, N <sub>2</sub> -Fixierungsleistung und Vorfruchtwert von Rotklee- und Rotklee grasbeständen
10	Teebken, Tammo	1998	N-Dynamik unter der Fruchtfolge Winterraps-Winterweizen-Wintergerste bei mehrjähriger Rotationsdauer und unterschiedlichen Produktionsintensitäten sowie einfache Ansätze zur N-Bilanzierung
11	Winkelmann, Christoph	1999	Ertragsbildung von Winterweizen in Abhängigkeit von Fruchtfolgestellung, Anbautechnik und Bodenunterschieden
12	Setiawan, Asep	1999	Mapping quantitative trait loci (QTL) for resistance to leaf spot disease ( <i>Cercospora beticola</i> Sacc.) in sugar beet ( <i>Beta vulgaris</i> L.)
13	Ruhe, Iris	2000	Winterweizenanbau in stickstofflimitierten Produktionssystemen unter besonderer Berücksichtigung der Ertragsbildung, der organischen Düngung und der mechanischen Beikrautregulierung

---

- 
- |    |                                  |      |  |
|----|----------------------------------|------|--|
| 14 | Oberschmidt, Olaf                | 2000 | Anwendung der <i>differential display</i> -Technik zur Isolierung und Analyse von differenziell exprimierten Genen in nematodenresistenten Zuckerrüben ( <i>Beta vulgaris</i> L.)  |
| 15 | Hühn, Manfred                    | 2000 | Universität und Bildungsauftrag. Wirklichkeit oder Farce?  |
| 16 | Sieling, Klaus                   | 2000 | Untersuchungen zu den Auswirkungen unterschiedlicher Produktionssysteme auf einige Parameter des N-Haushaltes von Boden und Pflanze  |
| 17 | Kaske, Axel                      | 2000 | Leistungen unterschiedlich bewirtschafteter Futterleguminosenbestände und deren Auswirkungen auf Ertrag und ausgewählte Kenngrößen des Stickstoffhaushaltes der Folgefrucht Winterweizen   |
| 18 | El-Mezawy, Aliaa                 | 2001 | Fine mapping of the bolting gene from sugar beet ( <i>Beta vulgaris</i> L.) with molecular markers   |
| 19 | Gao, Dongjie                     | 2001 | Molecular and cytological characterization of a full set of monosomic addition lines from <i>Beta corolliflora</i> in <i>Beta vulgaris</i> and chromosomal localization of resistance genes to leaf spot ( <i>Cercospora beticola</i> ) and rhizomania disease from wild beets   |
| 20 | Jacobs, Gunnar                   | 2001 | Physikalische Kartierung der Region des Schossgens der Zuckerrübe ( <i>Beta vulgaris</i> L.)   |
| 21 | Ingwersen, Bernhard              | 2001 | Einfluss von Bewirtschaftungsmaßnahmen auf die Leistungsfähigkeit von leguminosenbasiertem Dauergrünland unter besonderer Berücksichtigung der Nährstoffbilanzierung   |
| 22 | Teebken, Tammo<br>Hanus, Herbert | 2001 | Landwirtschaftliche Produktion und Umweltaspekte – eine Literaturrecherche unter besonderer Berücksichtigung der Produktionsintensität   |
| 23 | Große-Herrenthey, Ute            | 2002 | Molekulare Analyse der genetischen Variabilität von <i>Cercospora beticola</i> Sacc., dem Erreger der Cercospora-Blattfleckenkrankheit bei Zuckerrüben, und Untersuchungen zur Resistenz von <i>Beta vulgaris</i> spp. <i>maritima</i> gegen <i>C. beticola</i> unter Anwendung unterschiedlicher Resistenztestsysteme |
| 24 | Tahir, Muhammand<br>Shafique     | 2002 | Reaction of different wheat ( <i>Triticum aestivum</i> L.) genotypes in response to salt stress and genetic mapping of OTL for salt tolerance using AFLP markers   |
| 25 | Thurau, Tim,                     | 2002 | Der Einfluss stromaufwärts gelegener regulatorischer Sequenzen auf die Transkriptionsintensität des <i>Hs1<sup>pro-1</sup></i> -Gens für Nematodenresistenz aus der Zuckerrübe   |
| 26 | Wegelin, Tanja                   | 2002 | Bestimmung von Funktion und Wirkungsweise des <i>Hs1<sup>pro-1</sup></i> Nematodenresistenzgens aus <i>Beta procumbens</i>   |
| 27 | Samuelian, Suren                 | 2002 | Identification of genes differentially expressed upon nematode infection by cDNA-AFLP analysis   |
| 28 | Trott, Hagen Theo                | 2003 | Mittelfristige Auswirkungen einer variierten Bewirtschaftungsform und N-Intensität auf Leistungsparameter und die Stickstoffbilanz von Dauergrünland   |

- 
- |    |                      |      |  |
|----|----------------------|------|--|
| 29 | Treue, Peter         | 2003 | Potenziale und Grenzen teilflächenspezifischer N-Düngung in Schleswig-Holstein/Precision Agriculture   |
| 30 | Büchter, Manfred     | 2003 | Nitratauswaschungen unter Grünland und Silomais in Monokultur auf sandigen Böden Norddeutschlands  |
| 31 | Tian, Yanyan         | 2003 | PCR-based cloning of the second nematode resistance gene <i>Hs1-1<sup>pro-1</sup></i> and resistance gene analogues form sugar beet ( <i>Beta vulgaris</i> L.)                             |
| 32 | Brase, Thorsten      | 2003 | Einfluss der N-Dynamik in unterschiedlichen Produktionssystemen auf die Ertragsbildung von Raps, Weizen und Gerste sowie die N-Auswaschung   |
| 33 | Jamsari, Ir.         | 2003 | Construction of high-density genetic and physical maps around the sex gene <i>M</i> of <i>Asparagus officinalis</i> L.   |
| 34 | Kelm, Michael        | 2004 | Strategies for sustainable agriculture with particular regard to productivity and fossil energy use in forage production and organic arable farming  |
| 35 | Wichmann, Stefan     | 2004 | Ertragsleistung, Futterqualitätsentwicklung, N <sub>2</sub> -Fixierungsleistung und Vorfruchtwirkung von verschiedenen Körnerleguminosenarten in Reinsaat und Gemenge mit Getreide         |
| 36 | Gaafar, Reda Mohamed | 2005 | Fine mapping of the bolting gene of sugar beet ( <i>Beta vulgaris</i> L) using BAC-derived sequences   |
| 37 | Lampe, Carola        | 2005 | Effect of nitrogen fertiliser and animal excrements on N <sub>2</sub> O emissions from permanent grassland using <sup>15</sup> N-labelling   |
| 38 | Beims, Sandra        | 2005 | Untersuchungen zur N-Effizienz und zum N-Mineralisationspotenzial in langjährig unterschiedlichen Düngungssystemen mit Hilfe von <sup>15</sup> N markiertem Mineraldünger                  |
| 39 | Baade, Julia         | 2005 | Untersuchungen zur Futteraufnahme, Futterqualität und -selektion auf Umtriebsweiden mittels einer pflanzenbaulichen Methode  |
| 40 | Volkers, Karen       | 2005 | Auswirkungen einer variierten Stickstoffintensität auf Leistung und Stickstoffbilanz von Silomais in Monokultur sowie einer Ackerfutterbau-Fruchtfolge auf sandigen Böden Norddeutschlands |
| 41 | Dreymann, Sonja      | 2005 | N-Haushalt unterschiedlich bewirtschafteter Rotklee-Bestände und deren Bedeutung für die Folgefrucht Weizen im Ökologischen Landbau  |
| 42 | Bobe, Janina         | 2005 | Nitratbelastung von Sickerwasser und Grundwasser in Futterbausystemen auf sandigen Böden Norddeutschlands  |
| 43 | Neumann, Helge       | 2005 | Optimierungsstrategien für den Getreideanbau im ökologischen Landbau: System "weite Reihe" und Direktsaat in ausdauernden Weißklee ("Bi-cropping")   |
| 44 | Hamwieh, Aladdin     | 2005 | Development of simple sequence repeat (SSR) and AFLP markers for linkage mapping in lentil ( <i>Lens culinaris</i> Medik)  |

- 
- |    |                                 |      |  |
|----|---------------------------------|------|--|
| 45 | Kruse, Sandra                   | 2006 | Charakterisierung und Modellierung des Abreifeverhaltens von Silomaisgenotypen mittels futterwertbestimmender Parameter                        |
| 46 | Schulte, Daniela                | 2006 | Physische Kartierung und Sequenzierung einer Translokation aus der Wildart <i>Beta procumbens</i> am Zuckerrüben-Chromosom 9                   |
| 47 | Werner, Susanne                 | 2007 | Genetische Kartierung von Kohlhernie ( <i>Plasmodiophora brassicae</i> ) - Resistenzgenen in Raps  |
| 48 | Telgmann-Rauber, Alexa          | 2007 | Untersuchungen zur Struktur des Spargel-Chromosoms L5 mit dem geschlechtsdeterminierten Locus M  |
| 49 | Treyse, Katharina               | 2007 | Indikatoren für eine nachhaltige intensive Grünlandbewirtschaftung   |
| 50 | Jung, Christian                 | 2007 | Ausgewählte Themen der Pflanzenzüchtung  |
| 51 | Schiborra, Anne                 | 2007 | Short-term effects of defoliation on herbage productivity and herbage quality in a semi-arid grassland ecosystem of Inner Mongolia, P.R. China |
| 52 | Endrigkeit, Jessica             | 2007 | Identifikation und Charakterisierung von Genen der Tocopherol-Biosynthese aus Raps ( <i>Brassica napus</i> L.)                                 |
| 53 | Nannen, David                   | 2008 | N fluxes in forage production systems as studied by <sup>15</sup> N and difference method  |
| 54 | Henke, Johannes                 | 2008 | Entwicklung und Bewertung von Strategien zur Verbesserung der Stickstoffeffizienz im Winterrapsanbau   |
| 55 | Lange, Tina                     | 2008 | Genetische Kartierung und molekulare Identifizierung von Genen für Speicherwurzelbildung in <i>Brassica napus</i> L.                           |
| 56 | Mauschering, Inken              | 2008 | Interseeding catch crops in organic wheat and rape seed production systems   |
| 57 | Kleen, Jana                     | 2008 | Ertragsleistung und Futterqualität verschiedener Leguminosen in binären Gemengen mit Deutschem Weidelgras ( <i>Lolium perenne</i> L.)          |
| 58 | Westphal, Derk                  | 2008 | Leistung und Vorfruchtwert von Leguminosen-Gras-Beständen im ökologischen Landbau unter Berücksichtigung der Winterbeweidung                   |
| 59 | Eickler, Birgit                 | 2008 | Nutritive value of forage legumes with special reference to polyphenol oxidase activity in red clover  |
| 60 | Keil, Tobias                    | 2008 | Selektion von Gerstenherkünften mit Resistenz gegen frei lebende Nematoden der Gattung <i>Pratylenchus</i>                                     |
| 61 | Müller, Karla                   | 2009 | Remote sensing and simulation modelling as tools for improving nitrogen efficiency for winter oilseed rape ( <i>Brassica napus</i> L.)         |
| 62 | Fittje, Susanne                 | 2009 | Wirkungen des Grünrodens auf Ertrag, Knollenbeschaffenheit und Virusbefall zur Erzeugung von Kartoffelpflanzgut im ökologischen Landbau        |
| 63 | Kage, Henning & Hollmann, Franz | 2009 | Norddeutsches Weizen-Forum 2009 – Kurzfassungen der Vorträge   |
| 64 | Schönbach, Philipp              | 2009 | Grazing effects on productivity and herbage quality of an Inner Mongolian steppe ecosystem – Results of a four-year grazing experiment         |

- 
- |    |                                 |      |  |
|----|---------------------------------|------|--|
| 65 | Gericke, Dirk                   | 2009 | Measurement and modelling of ammonia emissions after field application of biogas slurries  |
| 66 | Taube, Friedhelm                | 2009 | Modelling forage production systems<br>Dedicated to Prof. em. Alois Kornher's 75. birthday   |
| 67 | Salama, Heba                    | 2010 | Process-oriented evaluation of yield performance and nutritive value of perennial rye-grass ( <i>Lolium perenne</i> L.) genotypes  |
| 68 | Gong, Xiaoying                  | 2010 | Water and nitrogen co-limitation of plant primary production in a semiarid grassland of Inner Mongolia   |
| 69 | Capistrano, Gina                | 2010 | A candidate sequence for the nematode resistance gene <i>HS1-2</i> in sugar beet   |
| 70 | Lösche, Marc                    | 2010 | Nutritive value of perennial ryegrass ( <i>Lolium perenne</i> L.) with special reference to genotype- and ploidy-related effects   |
| 71 | Kage, Henning & Hollmann, Franz | 2011 | Norddeutsches Marktfruchtforum 2011 – Kurzfassungen der Vorträge   |
| 72 | Abou-Elwafa, Salah              | 2011 | Novel genetic factors affecting bolting and floral transition control in beta vulgaris   |
| 73 | Büttner, Bianca                 | 2011 | Genetic mapping of flowering time genes and functional characterisation of an <i>FVE</i> homologue from sugar beet.  |
| 74 | Bangemann, Lars                 | 2011 | Pathogen-nutrient interactions in potato: the case of nitrogen and late blight in organic farming.   |
| 75 | Krawutschke, Manuel             | 2011 | Qualitätsveränderungen im Zuwachsverlauf und bei der Gärfutterbereitung von Rotklee ( <i>Trifolium pratense</i> L.) unter besonderer Berücksichtigung der Rohproteinfraktionen                                       |
| 76 | Svoboda, Nikolai                | 2011 | Auswirkungen der Gärrestapplikation auf das Stickstoffauswaschungspotential von Anbausystemen zur Substratproduktion   |
| 77 | Wienforth, Babette              | 2011 | Cropping systems for biomethane production: a simulation based analysis of yield, yield potential and resource use efficiency  |
| 78 | Wan, Hongwei                    | 2011 | Impacts of grazing intensity, grazing system, mowing, and nitrogen fertilization on species dominance and coexistence in typical steppe of Inner Mongolia  |
| 79 | Weiher, Nina                    | 2011 | Variation in the nutritive value of red clover ( <i>Trifolium pratense</i> L.) with special reference to polyphenol oxidase activity   |
| 80 | Schmeer, Maria Susanne          | 2012 | Der Einfluss von Bodenverdichtung sowie Grünlanderneuerung auf Stickstoffemissionen und Ertragsleistungen von Futterbausystemen  |
| 81 | Fritsche, Steffi                | 2012 | Cloning and functional characterization of genes from the tocopherol biosynthesis pathway in rapeseed ( <i>Brassica napus</i> L.) and candidate gene based association studies of tocopherol content and composition |

- 
- |    |  |      |   |
|----|--|------|---|
| 82 | Ren, Haiyan  | 2013 | Impacts of grazing intensity, precipitation and temperature on productivity, forage quality, species composition and diversity in typical steppe of Inner Mongolia                            |
| 83 | Ratjen, Arne Markus                                | 2013 | Refined N fertilization of winter wheat: a model supported approach combining statistical and mechanistic components  |
| 84 | Kage, Henning<br>Sieling, Klaus<br>Hollmann, Franz | 2013 | Norddeutsches Marktfruchtforum 2013 – Kurzfassungen der Vorträge  |
| 85 | Pahlmann, Ingo                                     | 2013 | Entwicklung eines teilflächenspezifischen Düngealgorithmus als Beitrag zur Steigerung der Stickstoffeffizienz und Optimierung der Treibhausgasbilanz im Winterrapsanbau                       |
| 86 | Kardel, Marika                                     | 2013 | Charakterisierung von Tanninen aus Pflanzenextrakten und deren Einfluss auf pansenphysiologische Parameter  |
| 87 | Techow, Anna                                       | 2013 | Leistung und ökologische Effekte von Anbausystemen zur Biogas-/Futtererzeugung  |
| 88 | Lana, Marcos                                       | 2013 | Regionalization of climate change impacts and adaptation strategies for maize in Santa Catarina State, Brazil   |
| 89 | Chen, Shimeng                                      | 2014 | Sward age and nitrogen determine the quantity and quality of root growth in grass-clover swards   |
| 90 | Biegemann, Torsten                                 | 2014 | Grünlandumbruch und Neuansaat: Kurz- und langfristige Effekte auf Treibhausgasemissionen und Ertragsleistungen von Grünlandbeständen  |
| 91 | Stephan, Helge                                     | 2014 | Examining the yield potential of winter sugar beet with a process-orientated dynamic simulation model   |
| 92 | Quakernack, Robert                                 | 2014 | Biogas cropping systems at a calcareous coastal marsh: productivity, ammonia volatilization, nitrogen use efficiency and soil nitrogen dynamics after fertilization with anaerobic digestates |
| 93 | Galal, Ahmed<br>Abdelrahman                        | 2014 | Mapping root-lesion nematode resistance QTL in barley ( <i>Hordeum vulgare</i> L.)  |
| 94 | Poyda, Arne  | 2015 | Klimarelevanz futterbaulich genutzter Niedermoorböden in Schleswig-Holstein   |
| 95 | Rath, Jürgen                                       | 2015 | Maisgenotypen zur Biogasnutzung: Übersicht, Entwicklung und Validierung eines Modells zur Potenzialabschätzung der Biogasausbeute   |
| 96 | Weymann, Wiebke                                    | 2015 | Model-based analysis of weather, soil and management effects on yield formation of winter oilseed rape  |
| 97 | Ullmann, Ines                                      | 2016 | The critical phase of stem elongation in perennial ryegrass: a new plant functional trait for understanding yield and forage quality performance  |
| 98 | Neukam, Dorothee                                   | 2016 | Modelling wheat canopy temperature: A key to identify plant traits for drought tolerance and to quantify heat stress  |

- 
- |     |                                 |      |  |
|-----|---------------------------------|------|--|
| 99  | Biernat, Lars                   | 2016 | Ökoeffizienz im ökologischen und konventionellen Marktfruchtbau Schleswig-Holsteins – ein konzeptioneller Ansatz zur Bewertung von Landnutzungssystemen                        |
| 100 | Hamacher, Maike                 | 2016 | Potentiale sekundärer Pflanzeninhaltsstoffe in Futterleguminosen und Wiesenkräutern für eine verbesserte N-Verwertung beim Wiederkäuer   |
| 101 | Komainda, Martin                | 2017 | Catch cropping in silage maize ( <i>Zea mays</i> L.) – potential with respect to yield and environmental performance under the climatic conditions of northern Germany         |
| 102 | Schoo, Burkhard<br>Clemens      | 2017 | Comparative eco-physiological analyses in cup plant, maize and lucerne-grass   |
| 103 | Struck, Inga                    | 2018 | No-tillage silage maize ( <i>Zea mays</i> L.) in ley-arable systems - Crop performance and environmental effects under maritime climates                                       |
| 104 | Räbiger, Thomas                 | 2020 | Direct and indirect nitrous oxide emissions in oilseed rape production systems: Measurement and simulation   |
| 105 | Graß, Rikard                    | 2020 | High-throughput phenotyping of drought stress resistance in mapping populations of rye: Canopy temperature, radiation interception and stay-green                              |
| 106 | Loza, Cecilia                   | 2021 | Examining the impact of different grass-legume mixtures on milk quality and methane emission in pasture-based milk production systems  |
| 107 | Nyameasem, John<br>Kormla       | 2021 | Diverse forage production systems and their potential for greenhouse gas mitigation  |
| 108 | Smit, Hendrik Petrus<br>Jordaan | 2021 | Mitigation strategies to reduce greenhouse gas emissions and nitrogen losses from pasture-based dairy systems  |
| 109 | Lorenz, Heike                   | 2021 | Towards eco-efficiency in dairy farming: the role of pasturing and grass-clover leys   |
| 110 | Rose, Till                      | 2022 | The contribution of functional traits to breeding progress of central European winter wheat  |
| 111 | Bukowiecki, Josephine           | 2022 | Site-specific yield formation of winter wheat: combining remotely sensed crop data with simulation modeling  |
| 112 | Verma                           | 2022 | Examining the inter- and intraspecies variability in the polyphenolic profile and in vitro antimethanogenic potential of forage species  |
| 113 | Kemmann, Björn                  | 2022 | Assessment of field-derived greenhouse gas mitigation potential in biomass production by replacing maize with cup plant ( <i>Silphium perfoliatum</i> ) in low mountain ranges |
| 114 | Peters, Tammo                   | 2023 | Plant functional trait analysis and dynamic growth modelling of perennial ryegrass dominated pastures in north-west Europe   |
| 115 | Rothardt, Steffen               | 2023 | Mitigating N losses and improving N transfer in cropping systems by residue management   |
| 116 | De Los Rios Mera, Josue         | 2023 | Effects of land use and land use change in agricultural systems on soil carbon sequestration in north-west Europe  |

- |            |                     |      |   |
|------------|---------------------|------|---|
| <b>117</b> | Brigitte Köhler     | 2024 | Untersuchungen zur quantitativen Erfassung von Masse- und Stoffströmen im Futterbaubetrieb  |
| <b>118</b> | Katja Holzhauser    | 2025 | Cover crops for sustainable silage-maize production: Enhancing resource use efficiency through modelling and remote sensing                                       |
| <b>119</b> | Stephen Björn Wirth | 2025 | The Role of Plant Functional Diversity in Productivity and Soil Organic Carbon Stocks of Managed Grasslands: Advancements Using a Dynamic Global Vegetation Model |

